PROCEEDINGS OF PAPERS

UNIVERSITY OF NIŠ
FACULTY OF OCCUPATIONAL SAFETY OF NIŠ
Department of Preventive Engineering
Noise and Vibration Laboratory

"POLYTECHNICA" UNIVERSITY OF TIMISOARA
FACULTY OF MECHANICAL ENGINEERING
Department of Mechanics and Vibration
Noise and Vibration Laboratory

24th International Conference

Noise and Vibration

Niš, 29 - 31, October 2014.
SERBIA

24th INTERNATINAL CONFERENCE

NOISE AND VIBRATION

PROCEEDING OF PAPERS

Niš, October 29 - 31, 2014.

Publisher: *University of Niš, Faculty of Occupational Safety*
For the publisher: *Prof. Ljiljana Živković, Ph. D.*
dean

Editors of proceeding of papers:
Prof. Dragan Cvetković, Ph. D.
Prof. Vasile Marinca, Ph. D.
Prof. Nicolae Herisanu, Ph. D.
Prof. Momir Praščević, Ph. D.

Graphic design and prepress:
Ass. Darko Mihajlov, M. Sc.
Rodoljub Avramović

Printout: "M Kops Center" Niš

No. of copies: 150

ISBN: 978-86-6093-062-2

REVIEWS:
All papers have been reviewed by following members of scientific committee:

ORGANIZER

University of Niš
Faculty of Occupational Safety of Niš
Department of Preventive Engineering
Noise and Vibration Laboratory
www.znrfak.ni.ac.rs

"Politechnica" University of Timisoara
Faculty of Mechanical Engineering
Department of Mechanical Engineering
Noise and Vibration Laboratory
http://www.mec.upt.ro

AUSPICE

Ministry of Education, Science and Technological Development Republic Serbia
www.mpn.gov.rs

GENERAL SPONSOR

Brüel & Kjær

www. bksv.com

CONFERENCE REVIEW

1st Yugoslav Conference	Belgrade	1978
2nd Yugoslav Conference	Belgrade	1979
3rd Yugoslav Conference	Belgrade	1980
4th Yugoslav Conference	Belgrade	1981
5th Yugoslav Conference	Belgrade	1982
6th Yugoslav Conference	Belgrade	1983
7th Yugoslav Conference	Belgrade	1984
8th Yugoslav Conference	Belgrade	1985
9th Yugoslav Conference	Belgrade	1986
10th Yugoslav Conference	Belgrade	1987
11th Yugoslav Conference & 1st International Conference	Belgrade	1988
12th Yugoslav Conference	Belgrade	1989
13th Yugoslav Conference	Niš	1991
14th Yugoslav Conference & 2nd International Conference	Niš	1993
15th Yugoslav Conference & 3rd International Conference	Niš	1995
16th Yugoslav Conference with international participation	Niš	1998
17th Yugoslav Conference with international participation	Niš	2000
18th Yugoslav Conference with international participation	Niš	2002
19th Conference with international participation	Niš	2004
20th Conference with international participation	Tara	2006
21st Conference with international participation	Tara	2008
22nd Conference with international participation	Niš	2010
23rd Conference and 4th International Conference	Niš	2012
24th International Conference	Niš	2014

PROGRAM COMMITTEE

Prof. Dragan Cvetković, Ph. D.,
University of Niš, Faculty of Occupational Safety – chairman
Prof. Vasile Marinca, Ph. D.,
"Politehnica" University of Timişoara, Romania – co-chairman
Prof. Petar Pravica, Ph. D.,
University of Belgrade, Faculty of Electrical Engineering
Prof. Giangiacomo Minak, Ph. D.,
University of Bologna, Italy
Prof. Marek Grzybowski, Ph. D.,
Gdynia Maritime University, Poland
Assoc. Prof. Miloš Manić, Ph. D.,
University of Idaho, USA
Prof. Pantele Chelu, Ph. D.,
"Politehnica" University of Timişoara, Romania
Prof. Nicolae Herisanu, Ph. D.,
"Politehnica" University of Timişoara, Romania
Prof. Vasile Bacria, Ph. D.,
"Politehnica" University of Timişoara, Romania
Prof. Liviu Bereteu, Ph. D.,
"Politehnica" University of Timişoara, Romania
Prof. Gheorghe Draganescu, Ph. D.,
"Politehnica" University of Timişoara, Romania
Prof. Tihomir Trifunov, Ph. D.,
National Military University „Vassil Levski“ of Veliko Turnovo, Bulgaria
Prof. Koleta Zafirova, Ph. D.,
Faculty of Technology and Metallurgy, Skopje, Macedonia
Ass. prof. Nikola Holeček,
Environmental Protection College, Velenje, Slovenia
Ass. prof. Valentina Golubović-Bugarski,
Faculty of Mechanical Engineering, Banja Luak, Rep. of Srpska
Ratko Uzunović, Ph. D.,
VIBEX system
Prof. Ljiljana Živković , Ph. D.,
University of Niš, Faculty of Occupational Safety
Prof. Nenad Živković, Ph. D.,
University of Niš, Faculty of Occupational Safety
Prof. Predrag Kozić, Ph. D.,
University of Niš, Faculty of Mechanical Engineering
Prof. Nikola Lilić, Ph. D.,
University of Belgrade, Faculty of Minig and Geology
Prof. Slobodan Gajin, Ph. D.,
University of Novi Sad, Faculty of Civil Engineering in Subotica
Prof. Zoran Perić, Ph. D.,
University of Niš, Faculty of Electronic Engineering
Assoc. prof. Zoran Petrović, Ph. D.,
University of Kragujevac, Faculty of Civil and Mechanical Engineering in Kraljevo
Assoc. prof. Zlatan Šoškić, Ph. D.,
University of Kragujevac, Faculty of Civil and Mechanical Engineering in Kraljevo
Assoc. prof. Dejan Ćirić, Ph. D.,
University of Niš, Faculty of Electronic Engineering
Ass. prof. Aleksandar Cvjetić, Ph. D.,
University of Belgrade, Faculty of Minig and Geology

ORGANISITION COMMITTEE

Assoc. prof. Momir Praščević, Ph. D.
University of Niš, Faculty of Occupational Safety – chairman
Prof. Nicolae Herisanu, Ph. D. - co-chairman
"Politehnica" University of Timişoara, Romania – co-chairman
Prof. Vasile Marinca, Ph. D.
"Politehnica" University of Timişoara, Romania
Prof. Dragica Milenković, Ph. D.
University of Niš, Faculty of Mechanical Engineering
Prof. Jasmina Radosavljević, Ph. D.
University of Niš, Faculty of Occupational
Assoc. prof. Miomir Raos, Ph. D.
University of Niš, Faculty of Occupational Safety
Ass. Branko Radičević, MSc
University of Kragujevac, Faculty of Civil and mechanical Engineering in Kraljevo
Ass. Nebojša Bogojević, M. Sc.
University of Kragujevac, Faculty of Civil and mechanical Engineering in Kraljevo
Ass. Darko Mihajlov, M. Sc.
University of Niš, Faculty of Occupational Safety

CONTENT

3RD SESSION

4TH SESSION

5TH SESSION

6TH SESSION

University of Nis
Faculty of Occupational Safety
„Politechnica“ University of Timisoara
Faculty of Mechanical Engineering
24th International Conference
NOISE AND VIBRATION
Niš, 29 - 31. 10. 2014.

ACTION PLANS FOR PREVENT AND REDUCE THE NOISE IN THE CITY OF TIMISOARA

Vasile Bacria[1], Nicolae Herisanu[2]

[1] ”Politehnica” University of Timisoara, Faculty of Mechanical Engineering, Romania, vasile.bacria@upt.ro
[2] ”Politehnica” University of Timisoara, Faculty of Mechanical Engineering, Romania, nicolae.herisanu@upt.ro

Abstract - *The noise generated by transportation means and industrial activities is present also in the city of Timisoara influencing the comfort and the health of habitants. The EU Environmental Noise Directive 2002/49/EC, which Romania should comply with, obliges the local authorities to elaborate action plans for management of urban noise, whose implementation will lead to solving the problems identified after noise mapping. In this paper we present the action plans designed in order to reduce the noise in the city of Timisoara, taking into account the noise map of the city last updated in 2013. Elaboration of action plans was performed taking into account the requirements of the Directive 2002/49/EC.*

1. INTRODUCTION

As it is known, the European Parliament and the European Council have adopted in 25 June 2002 the Directive 2002/49/EC whose main goal is to create a common basis for all the states of the European Union concerning the assessement and management of urban noise. This common basis includes:

- Monitoring some environmental problems by imposing local authorities to develop strategic noise maps for roads, railways, airports, industrial zones and main urban areas, using the noise indicators L_{den} and L_n. These maps will be used for evaluating the number of persons exposed to noise in the whole European Union, Romania being a member state.
- Informing and consulting habitants on noise exposure and its effects as well as on the measures which can be adopted to fight against noise.
- Elaboration of action plans for noise management in order to prevent and reduce the urban noise with the aim to protect habitant’s health and to preserve quiet zones.
- Ensuring an active involvement of habitants to the whole process of planning activities related to noise management

In the first stage, member states of the European Union reported on 30 June 2007 strategic noise maps for all urban zones having more than 250.000 habitants, as well as for main roads having more than 6.000.000 passings per year, railways with more than 60.000 passing per years and airoports located near main urban zones. Following these strategic noise maps, member states reported on 18 July 2008 action plans intended to reduce the noise where the noise maps have identified exceedings of admissible limits.

The city of Timisoara takes place on the list of urban zones who must comply with the rules described above, due to the presence of more than 250.000 habitants, so that local authorities were concerned with the problems related to noise management.

According to the noise Directive, the strategic noise map and consequent action plans for prevent and reduce the urban noise should be renewed every 5 years, and therefore, the strategic noise map of Timisoara city has been updated in 2013. Based on the data resulting from this renewed noise map, the authors of the present paper elaborated the action plans to prevent and reduce the noise in the city of Timisoara, which is the subject of this paper. The noise Directive 2002/49/EC clearly states the requirements for the content of action plans and starting from this fact, action plans for Timisoara city were built up taking into account all these requirements.

2. GENERAL REQUIREMENTS FOR ACTION PLANS

As it is known an action plan must contain at least the following elements:

- A short description of the urban area, major roads, major railways and airports, as well as and other noise sources taken into account by the responsible authority
- Legal context and values taken into account to apply Art.5 from the Directive 2002/49/EC
- A brief summary of the results of strategic noise maps
- An evaluation of the number of habitants exposed to noise
- Identification of problems and situations which request attention from the point of view of the noise
- Information concerning public consultations on noise reduction problems
- Measures already taken to reduce the noise and other projects envisaged to reduce the noise
- Actions which local authorities intend to perform within the next 5 years, including measures intended to preserve quiet zones and the long term strategy
- Financial information (if available)
- Measures intended to evaluate the implementation of action plans and the obtained results.

3. DESCRIPTION OF THE AGGLOMERATION, RESPONSIBLE AUTHORITY AND LEGAL CONTEXT

Timisoara, the capital of Timis county, is located at $45^{o}47'$N and $21^{0}17'$E. The town is extended on a surface of 130.5 km^2 having a population of 306.466 habitants and therefore is the largest agglomeration from the West part of Romania and also a very important industrial, historical, social and cultural centre. Timisoara is an important economic and industrial pole of Romania, where many national and European road, rail and air transportation routes are intersecting.

The authority responsible for realizing noise mapping and action plans for reducing the environmental noise in the city of Timisoara is the Primaria Municipiului Timisoara.

In the frame of the action plans, based on the results of noise mapping, there were identified the zones strongly affected by noise generated in road, rail and air traffic, as well as by industrial activity. Besides, there were identified solutions to reduce the environmental noise in these critical points.

In the process of noise mapping as well as to the elaboration of action plans, there were taken into consideration the legal requirements adopted by the following legal documents: HG 321/2005 re-published, concerning assessement and management of environmental noise; OM 1830/2007 concerning approving the Gide to realize, analyse and asses the noise maps; OM 152/558/1119/1532/2008 for approving the Guide concerning adopting the limit values of L_{den} and L_n, and their application when elaborating action plans, for the road traffic, rail, air and industrial noise.

According to OM MMDD no. 152/13.02.2008, the maximum values allowed for the noise indicators L_{den} and L_n are presented in Table 1.

Table 1 *Admissible values for noise indicators L_{den} and L_n*

L_{den} [dB(A)]			L_n [dB(A)]		
Source of noise	Target 2012	Max. value	Source of noise	Target 2012	Max. value
Roads	65	70	Roads	50	60
Railways	65	70	Railways	50	60
Airports	65	70	Airports	50	60
Industrial	60	65	Industrial	50	55

4. SINTHESIS OF INFORMATION OBTAINED BY NOISE MAPPING

In the following we present the data revealed by the strategic noise maps updated in 2013 for the city of Timisoara, related to the noise generated by roads, railways and industrial activities, using harmonised noise indicators L_{den} and L_{night}.

In this respect, the main results of the noise mapping process, for both L_{den} and L_{night} noise indicators are available at the addresses:

http://www.dmmt.ro/uploads/files/harta_zgomot_ziua.pdf

http://www.dmmt.ro/uploads/files/harta_zgomot_noapte.pdf

The number of people annoyed from the point of view of both L_{den} and L_{night} indicators is presented in tables 2 and 3, while in tables 4 and 5 is presented the number of buildings exposed to noise from the point of view of the same harmonized noise indicators.

Table 2 *Number of people exposed to noise-L_{den}*

Source of noise	55-59 dB	60-64 dB	65-69 dB	70-74 dB	>75 dB
Roads	28363	17839	14580	8349	1365
Rails-CFR	686	158	5	0	0
Rails-trams	0	0	0	0	0
Airports	0	0	0	0	0
Industrial	140	10	0	0	0

Table 3 *Number of people exposed to noise-L_{night}*

Source of noise	45-49 dB	50-54 dB	55-59 dB	60-64 dB	65-69 dB	>70 dB
Roads	22531	18540	15288	9600	1808	326
Rails-CFR	850	520	12	3	0	0
Rails-trams	0	0	0	0	0	0
Airports	0	0	0	0	0	0
Industrial	184	98	1	0	0	0

Table 4 *Number of buildings exposed to noise-L_{den}*

Source of noise	55-59 dB	60-64 dB	65-69 dB	70-74 dB	>75 dB
Roads	8539	7335	6890	3651	600
Rails-CFR	237	59	1	0	0
Rails-trams	0	0	0	0	0
Airports	0	0	0	0	0
Industrial	64	4	0	0	0

Table 5 *Number of buildings exposed to noise-L_{night}*

Source of noise	45-49 dB	50-54 dB	55-59 dB	60-64 dB	65-69 dB	>70 dB
Roads	22531	18540	15288	9600	1808	326
Rails-CFR	850	520	12	3	0	0
Rails-trams	0	0	0	0	0	0
Airports	0	0	0	0	0	0
Industrial	184	98	1	0	0	0

Analysing the obtained results one can be observed that, concerning the road traffic noise, there exists a number of 24294 people exposed to noise levels which exceed 65 dB from the point of view of L_{den} indicator and 45562 people exposed to a noise level which exceeds 50dB from the point of view of L_{night} indicator.

As regards the noise generated by the rail traffic, one can be identified 5 people exposed to a noise level which exceeds the limit of 65 dBfrom the point of view of L_{den} indicator and

535 people exposed to noise levels which exceed 50 dB from the point of view of L_{night} indicator.

Concerning the noise generated by the industrial activity, there are 10 people exposed to a noise level beyond the admissible limit of 60 dB for the L_{den} indicator, and 99 people exposed to more than 50 dB, which is the limit for the L_{night} indicator.

According to the strategic noise maps of Timisoara city, in what concerns the noise generated by tramways and air traffic, there are not people exposed to a noise level which exceed the limit of 65 dB admissible for L_{den} indicator, respectively 50dB admissible for L_{night} indicator.

Starting from the data offered by the strategic noise maps, there were identified the roads with the most important impact on the exposure of people to noise: on 24 roads, on some sections, the L_{den} equivalent noise level exceeds 75 dB and on 29 roads, this noise indicator rages between 70-75 dB. On other 19 roads from the city, the noise indicator L_{den} ranges between 65-70 dB.

These exceedings of the noise limits are mainly due to the condition of the roads' superstructure, to the intensity of the road traffic and also to the presence in the traffic of some heavy vehicles on some of the roads.

People affected by the rail traffic reside near the railway route and those affected by the industrial noise reside in the vicinity of the city thermal station CET Centru and near a beer factory.

This actual relatively good situation of the phonic pollution in Timisoara city is due to the fact that the local administration were very much concerned in the last decades with reducing the noise in Timisoara, since as early as 1996, based on a collaboration with the research team from the Mecanics and Vibration Department, Faculty of Mechanical Engineering from "Politehnica" University of Timisoara, started an intensive program aimed at identification of noise sources and reducing the noise level in Timisoara city. Moreover, responding to the requirements of EU policy on environmental noise, in 2007 was realised the first strategic noise map of the city and consequent action plans, whose stipulations were already implemented.

5. SYNTHESIS OF ACTIONS AIMED AT INFROMING AND CONSULTING THE PUBLIC

The stipulations of the Environmental Noise Directive 2002/49/EC concerning the action plans include organizing actions aimed at informing and consulting the public about noise exposure, its effects, and the measures considered to address noise problems and possible solutions.

In this respect, at a first stage of public consultations, the public opinion on noise exposure was revealed by some questionnaires filled in by various people which reside in Timisoara near the most affected zones. These questionnaires contain questions related to the position to the roads, the degree of annoy produced by the urban noise, possible health disturbances, possible proposals to reduce the urban noise, etc.

Synthesizing the responses obtained by means of these questionnaires, one can draw some important conclusions:

- 72.4% of the buildings are placed frontal to the roads
- 34.5% of the habitants are disturbed by the street noise during displacement within the town, 24.2% are disturbed by the noise in buildings, 34.5% are disturbed by both street and building noise, and 6.9% are not disturbed.
- the noise has affected the health of 17.2% of the questioned habitants causing stress and headaches.

The questioned habitants have made different proposals for reducing the noise generated by transportation means and other sources, such as: public transportation be free, in order to encouraged it and discouraging individual transportation by individual cars; finalizing the road-ring of the town in order to eliminate a part of transitory traffic; building noise screens and improving the superstructure of the roads; increasing the greea areas; replacing old and noisy transportation means with a new and silent generation.

These proposals collected from the participants were used in designing the action plans along with the data resulting from the noise maps.

In order to inform the habitants, the action plans were published on the website of the municipality.

6. MEASURES IMPLEMENTED FOR REDUCING THE NOISE

Before the elaboration of the action plan to prevent and reduce the noise, the municipality implemented a set of measures intended to reduce the environmental noise in Timisoara, such as: building a ring-road in the Northeast part of the city; improvement of infrastructure and superstructure of the railway for trams on a significant length; improvement of the state of an important number of roads from the city; acquisition of new and more silent trams and buses for local transportation; modernization of some crossings and roads; imposing some speed limitations on some roads; imposing one-way traffic on some routes; banning the acces of heavy traffic in the central area of the city; encouragement of phonic and thermal insulation of buildings; enlargement of greea areas and green screens; building of an acoustic screen in a critical point; investigation of sound absorbing effects of rubberized asphalt in order to used at large scale as a solution to reduce traffic noise; construction of bicycle lanes, and so on.

Even if these measures were implemented, noise mapping revealed zones where the admissible limits are exceeded. That is why identification of noise sources is a very important task which must be accomplished.

7. IDENTIFICATION OF NOISE SOURCES

The main sources of noise in the urban environment are the road, rail and air transportation means as well as industrial activities. Concerning transportation means, the noise and vibration are generated by the engine, transmission system, braking system, air resistance and rolling. The noise generated by transportation means are significantly influenced by the intensity and composition of traffic, speed of

displacement, the technical state of vehicles, as well as rolling and state of the superstructure of roads.

In case of rail transportation means, noise and vibrations are due to variation of speed, imperfection and elasticity of railway, joints of railways, guiding of rolling wheels, etc.

In case of air transportation means, the sources are represented by the engines, propulsion propellers, cooling and oil pumps, turbochargers, etc. Due to the noise produced by airplanes, the functioning of an airport represents an important problem for the personnel and neighbor residential areas.

In case of industrial activities, noise is due to collisions of rigid bodies, friction on contact surfaces, aerodynamic turbulences, forced oscillations of rigid bodies, vibration of membrane-shaped parts, hydraulic operated devices, deployment of mechanical, electromagnetical, aerodynamical hydrostatic processes.

The presence of noise affect a large number of inhabitants which are disturbed. Thus, in the case of a noise having an equivalent level of 75 dB(A) during the day, 80% of the population is disturbed [6].

Having an action upon the human body, the noise can affect the auditory system, different internal organs and systems of the body, reduce the work productivity and speech intelligibility. The noise also affect the nervous system producing psychophysiological modifications, blood circulation problems and sleep disturbances, influences the visual function and the functioning of endocrine glands, producing biochemical disturbances. The noise can produce auditory fatigue, sonorous trauma and a general fatigue of the body. All these affect physical activity, especially for individuals which need focus of attention, mainly in the intellectual work.

Having in view detrimental effects of the noise, in order to ensure proper conditions for human life and activity, there were established levels of noise which should not be exceeded. In order to characterize admissible limits of the environmental noise, specific noise indicators are used, such as those presented in Table 1, where L_{den} is defined by

$$L_{den} = 10\lg\frac{1}{24}\left[12\cdot 10^{\frac{L_d}{10}} + 4\cdot 10^{\frac{L_e+5}{10}} + 8\cdot\frac{L_n+10}{10}\right] \qquad (1)$$

where L_d is the long term noise measured in the day during 12 hours, between 7.00 and 19.00; L_e is the long term noise level measured during 4 hours between 19.00-23.00; L_n is the long term noise level in the night during 8 hours, between 23.00 and 07.00.

In case when the admissible limits are exceeded, some measures aimed at reducing the noise are needed for each particular case.

8. METHODS FOR NOISE REDUCING

Establishing the methods for noise reducing is done taking into account the causes of noise generation, which are in our case the presence and positioning of roads, railways, airports and industrial areas.

In what concerns the noise generated by the road traffic, one can introduce restrictions regarding traffic composition and speed limitations.

The way in which one can obtain noise reduction by reducing the percentage of trucks for different speeds of displacement, by improving the state of the superstructure of roads, by imposing speed limitations, can be observed in diagrams presented in [5].

Reducing the noise generated by tyre-road contact can be achieved by replacing normal asphalt with a rubberized one, obtained by combining normal asphalt with crumbled rubber. This will ensure a reducing of the rolling noise of 1 up to 6 dB, depending on the speed of displacement, the most important reducing being obtained in the frequency bands corresponding to 1 kHz and 2 kHz. It was proved that sound absorption properties of rubberized asphalt are more important at high speeds of displacements [12].

In order to reduce the noise generated by vehicles, trains, trams and industrial activities, one can resort to acoustic screens and protective zones (green zones) between residential areas and these sources.

Such screens were mounted in a zone located at the entering in Timisoara city with the aim to protect a school against noise generated by the road traffic and in another place located near the railway which cross the city in order to protect residents from neighborhood against rail traffic noise. Attenuation achieved by these screens depend on the relative position of sources and receivers, dimensions, wavelength, acoustic transparency of the screens and so on [14].

Attenuation of the noise generated by tyre-road contact in rolling of cars can be achieved in an ecological way by mounting a hedgerow of shrubs and trees. Moreover, the noise generated by rolling of trams can be attenuated by employing an insulation system for the railway using modern technologies. Taking into account that significant noise levels are identified in Timisoara city due to transitory heavy traffic, it is necessary to finalize a complete ring-road of the city, so that the heavy traffic will be completely eliminated and a noise source disappear.

In what concerns reducing the noise produced by rail traffic, it is necessary to extend green protected areas, reflective or absorbent acoustic screens or green screens between railways and residential areas, along with ensuring a proper technical state of rolling stock.

Concerning the industrial noise, it is necessary to apply a complex of measures comprising both attenuation at source and attenuation on the transmission way. In this way, within each industrial unit should be applied adequate reducing methods envisaging the noise generated by the main mechanical parts, machine-tools, industrial equipment and installations used in technological processes.

Taking into account the above mentioned principial measures, one can identify the best possible solutions applicable in order to reduce the noise in Timisoara city.

9. ACTION PLANS

The problem of road traffic noise is still unsolved in Timisoara, even if it was diminished by inaugurating a part of the ring-road.

The configuration of the street network of Timisoara city has a radial-annular shape, better structured in northern part of the city and less contoured in southern part.

A lack of sufficient passages over the Bega river which cross the city and the railway which cross the central zone of the town are some major dysfunctions of traffic organization, which do not allow a proper connection between different parts of the city. The existing bridges are very congested.

Bega channel and the railway constitute two major obstacle which substantially affect the continuity of street network, the low number of bridges being confirmed also by the values of the noise indicators registered on 24 involved streets.

In order to improve the circulation in the city, with direct benefit on noise reduction, it is necessary the deviation of heavy traffic to the ring-road, eliminating the transit traffic from the city. development of public transportation system including employment of silent transportation means.

The proposals to attenuate the noise on the roads in Timisoara city where admissible limits of the noise indicators are exceeded, were established taking into account the study concerning the circulation in Timisoara.

Analysing the results obtained after noise mapping of Timisoara city, there were established the objectives of the activities which which should be developed in order to reduce the noise. Thus, there were designed six action plans aimed at reducing the road traffic noise, rail traffic noise and industrial noise. These provide modernization of some important crossings, mounting acoustic screens on 14 roads, finalizing the ring-road in the Southwestern part of the city an opening a fourth circulation ring, replacing normal asphalt with rubberized asphalt on six roads, realizing some green protective areas on 60 roads, envelopment of residential buildings (with sound-absorption effects), and so on.

Table 6 *Number of people exposed to noise-L_{den}*

Source of noise	55-59 dB	60-64 dB	65-69 dB	70-74 dB	>75 dB
Road	17674	14465	8105	1889	0
Rail	149	14	0	0	0
Industrial	10	0	0	0	0

Table 7 *Number of people exposed to noise-L_n*

Source of noise	45-49 dB	50-54 dB	55-59 dB	60-64 dB	65-69 dB	>70 dB
Road	18290	15161	9395	2390	326	0
Rail	508	23	4	0	0	0
Industrial	94	5	0	0	0	0

The number of people exposed to noise after the implementation of these action plans taking into account the indicators L_{den} and L_n is presented in Tables 6 and 7.

The difference between the initial total number of persons exposed to noise and the number of persons exposed after the implementation of action plans in terms of L_{den} and L_n, respectively, is presented in Tables 8 and 9.

Table 8 *Difference between the number of exposed persons in terms of L_{den}*

Source of noise	55-59 dB	60-64 dB	65-69 dB	70-74 dB	>75 dB
Road	-	-	6475	6460	1365
Rail	-	144	5	0	0
Industrial	130	10	0	0	0

Table 7 *Difference between the number of exposed persons in terms of L_n*

Source of noise	45-49 dB	50-54 dB	55-59 dB	60-64 dB	65-69 dB	>70 dB
Road	-	3379	5893	7210	1482	326
Rail	-	497	8	3	0	0
Industrial	90	93	1	0	0	0

From Tables 8 and 9 we can see that after the application of action plans, 14459 persons benefit of a reduction of noise exposure in terms of Lden, while in terms of Ln the number persons which benefit is 18892.

These action plans contain also a section concerned with delineation of quiet zones from the city of Timisoara and actions intended to be performed in the next 5 years by the municipality in order to protect these zones.

10. LONG TERM STRATEGY

The action plan for the next 5 years must be completed with a long term strategy which should include the long term vision regarding noise reduction. In this way, more of the ideas developed in the elaboration of action plans will be solutioned better in a longer term, especially for measures which have expensive solutions. Prevention of noise problems on long term is ensured based on a a good planning.

Based on the strategic noise maps, one can adjust urban development plans so that to ensure that new buildings will not be constructed in areas with a high impact of noise and new noisy industrial units will not be placed near residential areas or quiet zones.

According to the development strategy "Vision Timisoara 2030"elaborated by the municipality in collaboration with "Politehnica" university of Timisoara and Fraunhofer Institute Stuttgart, it is envisaged that environmental issues be integrated with all other aspects as much as possible.

In the frame of this action plan are found some specific politics and projects. Synthesizing the objectives of the projects considered in the long term strategy, one can be emphasized the main measures for noise reduction which will be applied: building a closed ring-road (deadline for completion 2020); closing the other rings of circulation (deadline 2019); making some uneven circulation nodes

(deadline 2021); building of 5 new bridges over Bega river (deadline 2020); developing the network of bicycle lanes (deadline 2025); applying a layer of rubberized asphalt on an important number of roads (deadline 2025); mounting acoustic screens to protect hospitals, schools, universities and other buildings (deadline 2020); improvement of technical state of the superstructure of roads (deadline 2025); preserving and extending green areas and green screens along the roads (deadline 2022); replacing the railway which cross the city with an underground line (deadline 2020); expansion of subway network (deadline 2030); rehabilitation and reconversion of industrial units placed near residential zones (deadline 2019); finalizing the program of thermal rehabilitation and phonic insulation of buildings (deadline 2020); rehabilitation of Timisoara rail station and Timisoara airport (deadline 2022); extension of parking places (deadline 2025); rehabilitation of Bega channel in order to develop naval transportation (deadline 2020); replacing old public transportation means with 100 new trams and 100 new silent electric buses (deadline 2020); rehabilitation of the old tram's railways on 3 roads and extension with new lines (deadline 2020); modernization of an important number of streets and boulevards (deadline 2020).

After the application of the measures from the long term strategy it is estimated an important number of persons which will benefit of the noise reduction: 8349 persons in terms of L_{den} and 15288 persons in terms of L_n. In the same time, the municipality will be concerned about conservation of quiet zones identified in Timisoara city by applying specific measures.

11. FORECASTS CONCERNING IMPLEMENTING ACTION PLANS

By implementing the results of action plans, an important reduction of the number of people and buildings affected by noise will be achieved, and a healthier environment will be ensured. This will lead to an increase of their work capacity and to decrease the costs caused by medical treatments.

The implementation of noise reduction measures should be continued until persons or buildings are not exposed to noise which exceed the admissible limits. Reduction of noise in residential buildings will indirectly lead to an increase of the people's work productivity since they will live in a more quiet environment.

After the implementation of action plans, a set of real measurements should be developed in order to assess the efficiency the measures and the effect of their implementation.

REFERENCES

[1] S.C. Enviro Consult SRL Bucuresti, "Protocol privind actualizarea hărţii strategice de zgomot în Municipiul Timişoara" April, 2013

[2] M. Grumăzescu, A. Stan, N. Wegener, Combaterea zgomotului şi vibraţiilor, Ed. Tehnică, Bucureşti, 1964

[3] E.Ia. Iudin, Izolarea împotriva zgomotului, Ed. Tehnică, Bucureşti, 1968

[4] Vibrocomp KFT Budapest, "Harta strategică de zgomot a Timişoarei", Budapest-Cluj Napoca, 2008

[5] *** Stadtbauliche Laermfild. Hinweise fur die Bauleitplanung, Baden Wurtenberg, Innenminist., 1991

[6] *** Larmbekamfung in Wien, Enwichlung Stand Tendenzen Magistratsabteilung 22 Umweltschutz

[7] Directive 2002/49/EC of European Parlaiment and European Council

[8] N.Herişanu, V.Bacria, M.Toader, S. Popa Radovan, Investigation of noise pollution in an urban area, *WSEAS Transaction on Systems*, vol. 7(5), pp.1648-1653, 2006.

[9] N.Herisanu, V.Bacria, M.Toader, S.Popa Radovan, Investigation and reduction of ambient noise in urban area, *7-th WSEAS Int. Conf. on Acoustics, Theory and Apllications*, Cavtat, Croatia, pp. 48-53, 2006

[10] V. Bacria, M. Toader, N. Herisanu, S. Popa Radovan, C. Opritescu, Noise investigation in the penetration zones of an urban area, MECSOL 2006, Constanta Maritime University, vol.9, pp.69-72, 2006

[11] V. Bacria, M. Toader, N. Herisanu, C. Opritescu, V. Ciupa, C. Fiat, Considerations concerning noise attenuation in urban environment, Proc. of the IX-th Symposium AVMS Timişoara, pp.7-12, May 2007

[12] N. Herisanu, V. Bacria, The effect of rubberized asphalt on decreasing the phonic pollution, Applied Mechanics and Materials, vol.430, pp.257-261, 2013

[13] V. Bacria, N. Herisanu, Noise control in an industrial hall, Applied Mechanics and Materials, pp.251-256, 2013

[14] V. Bacria, N. Herisanu, Phonic attenuation due to screen barriers, Analele Univ. Resita, pp. 35-42, 2011

[15] *** Vision 2030 Timişoara metropolă europeană, Ed. Brumei, Timişoara, 2009

[16] *** Studiu de circulaţie pentru municipiul Timişoara, Primăria Timişoara, Search Corporation, 2012

University of Nis
Faculty of Occupational Safety
„Politechnica“ University of Timisoara
Faculty of Mechanical Engineering
24th International Conference
NOISE AND VIBRATION
Niš, 29 - 31. 10. 2014.

STRATEGIC NOISE MAPPING AND ACTION PLANNING. EXPERIENCE, PRACTICAL CONCLUSIONS

Boris Mihaylov[1]

[1] SPECTRI LTD. (www.spectri.net), Bulgaria, spectri@spectri.net
[1] Bulgarian Association for Public Noise control and Management (www.nonoise-bg.com), bmihaylov@nonoise-bg.com

Abstract – *Based on EU Noise Directive (END – Directive 2002/49/EC) since 2005 started an intensive noise mapping process in EU member states. Some of the countries had a significant tradition in creating noise maps in the past. The END set a new path, and aimed a harmonized global strategic approach to reduce the increasing environmental noise from major sources (causing heavy health impact to EU population).*

The author has a broad experience in last more than 5 years – creating noise maps and strategic noise plans, mainly in Bulgaria.

In the recent paper is presented a short overview of obtained experience and related practical conclusions.

The final aim is to determine exact dedicated action plans - based on the strategic noise management (restriction and reduction of the environmental noise impact), and applying set of measures and acoustical planning in short, middle and long terms.

Key Words*: - Strategic noise map(s), action plan(s), environmental noise.*

1. INTRODUCTION

The END defines EU Member States obligations towards overall strategic approach on Environmental Noise Protection.

The aim of END is **“to define a common approach intended to avoid, prevent or reduce on a prioritized basis the harmful effects, including annoyance, due to exposure to environmental noise”.**

One can quote as well the definition from EU technical document “Common Noise Assessment Methods in Europe (CNOSSOS-EU)”, i. e.:

Europe is acting to to determine the exposure to environmental noise through strategic noise mapping and elaborate action plans to reduce noise pollution. Since June 2007, EU countries are obliged to produce strategic noise maps for all major roads, railways, airports and agglomerations, on a five- year basis. These noise maps are used by national competent authorities to identify priorities for action planning and by the European Commission to globally assess noise exposure across the EU. This information also serves to inform the general public about the levels of noise to which they are exposed, and about actions undertaken to reduce noise pollution to a level not harmful to public health and the environment.

An interesting quote from the official World Health Organization paper “Burden of disease from environmental noise”

DALYs (disability-adjusted life-years) lost from environmental noise are 61 000 years for ischemic heart disease, 45 000 years for cognitive impairment of children, 903 000 years for sleep disturbance, 22 000 years for tinnitus and 654 000 years for annoyance in the European Union Member States and other western European countries. These results indicate that at least one million healthy life years are lost every year from traffic related noise in the western part of Europe.

The last more than 5 years the author of recent paper, through company SPECTRI Ltd. – Bulgaria successfully finalized directly and indirectly 8 (six) SNM (Strategic Noise Maps), and 10 (ten) AP (Action Plans). Thus we collected vast experience not only re. the process of END noise mapping, but as well re. the on going process of sustainable follow up, and expected publicly available strategic approach for reducing the environment noise impact, combined with dedicated protection of quite zones in the agglomerations.

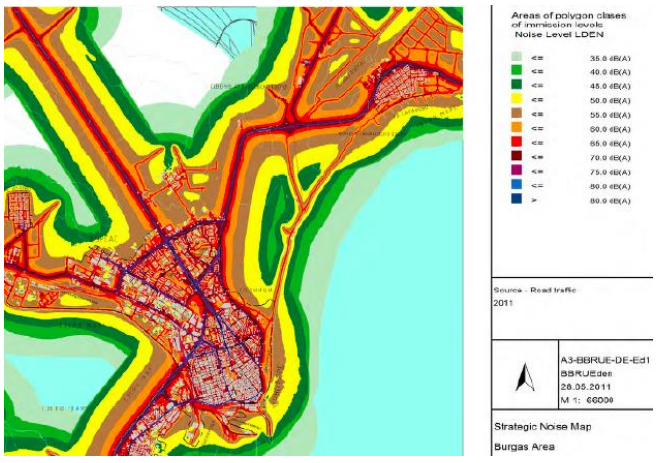

Fig. 1 *SNM from SPECTRI extract from Burgas city*

2. METHODOLOGY, EXPERIENCE

Until 2017 shall be used the recommended by END harmonized assessment methods (see Appendix II - 2.2., recommended methods).

From 2017 is mandatory to generate next stage SNM via the defined by CNOSSOS-EU New Noise Assessment Methods.

Based on his experience SPECTRI Ltd. can recommend and advise the total project's algorithm, shown in Fig. 2.

2.1. SNM (Strategic Noise Maps):

The quality of SNM is defined by several main requisites:

- quality of input GIS model, and its subsequent dedicated adaptation;
- data for main sources (own collection required)
- verification procedure (procedure needed)
- Used toolkits from EC Good Practice Guide (EC expert noise group paper – WG-AEN)

EXAMLE OF ROAD TRAFFIC CATEGORIZATION FOR SOFIA CITY:

Roads categories (as per own study & GPS tools)	Light Vehicles traffic (per hour) D/E/N	Heavy Vehicles traffic (relative) D/E/N
G (EndNoTraffic**) 6,**13,14,16	12/4/8	12/4/8
F (Dead roads**)** 11,15	128/37/18	0.01/0.01/0.00
E (Service roads**)** 10,17	256/73/37	0.03/0.01/0.01
D (Collecting roads**)** 9,12	511/146/73	0.05/0.03/0.02
C (Small main roads**)** 4,5	1023/292/146	0.08/0.05/0.03
B (Main roads**)** 3,8	2045/584/292/45	0.10/0.08/0.05
A (Major main roads) 1,2,7	3535/1010/505	0.10/0.08/0.05
A0 (Major extra roads) 0	8703/2487/1243	0.25/0.35/0.45

EXAMLE OF RAIL TRAFFIC CATEGORIZATION FOR SOFIA CITY:

TRAIN	**Type**	**N** day	**N** evening	**N** night	**N** vagons
---	---	**day**	**evening**	**night**	**Pcs.**
P_xx	passenger	136	48	41	4
F_xx	freight	57	26	87	20

EXAMLE OF TRAMS TRAFFIC CATEGORIZATION FOR SOFIA CITY:

ITEM	**TRAFFIC**		
TRAM	**N_TR_D**	**N_TR_V**	**N_TR_N**
lines	**DAY**	**EVENING**	**NIGHT**
32	1591	1591	556

An acceptable SNM accuracy of 3dB is to be achieved.

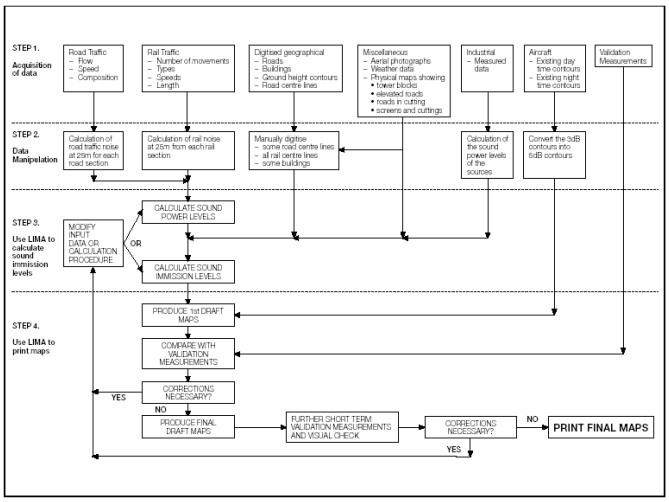

Fig. 2 *Main steps re. Strategic noise mapping*

Special attention shall be taken re. methodology of using existing, or organizing new measurements and/or monitoring of noise. A direct ISO1996 measurement and/or monitoring results cannot be implemented in SNM process directly, without careful consideration and undertaken corrections.

Some of the commercially available calculation tools for SNM are offering the so-called "reverse engineering" (correcting the acoustical model with introduced real noise level results). This tool is recommended to use rarely and with big care.

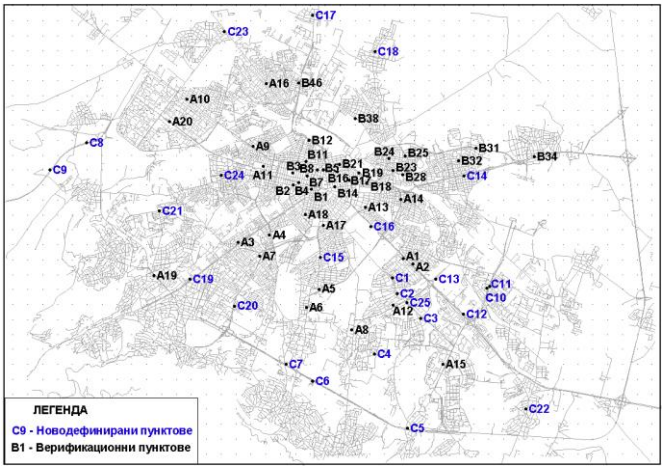

Fig. 3.1 *Verification points for Sofia city*

For rough verification purpose can be used available measurement and monitoring data base (see Fig. 3.1.-3.2).

Point ID	**Address**	Laeq, dB	Laeq-LIMA	**L24H/LIMA/ -LEQ /EV.M/**
C 1	bul.Makedoniya i ul.20-ti april	64.5	68.89	**-4.39**
C 20	ul.Zhitnitsa i ul.Kyustendzha	71.5	73.79	**-2.29**
C 21	bul.Gotse Delchev 31	74.5	76.28	**-1.78**
C 25	bul. Aleksandar Stamboliyski i ul.Lavele	63	65.34	**-2.34**
C 3	gara Poduyane	75.3	72.64	**2.66**
C 31	ul.Tsvetan Radoslavov i ul.Galileo Galiley	58.5	57.71	**0.79**
C 35	II MBAL bul.Hristo Botev	68	67.14	**0.86**
C 36	II SAGBAL, ul.Sheynovo 19	62	64.07	**-2.07**
C 44	zh.k. Druzhba, bl.96	55.5	58.36	**-2.86**
C 45	ul.Kievska i ul.Novo selo	56.9	59.56	**-2.66**
C 46	ul.Georgi izmerliev 24 DKTS	66	63.06	**2.94**
C 5	bul.Konstantin Velichkov i ul.Pirotska	71.5	73.62	**-2.12**
C 8	bul.Tsarigradsko shose i ul.Latinka	77.5	75.92	**1.58**

Fig. 3.2 *Example for verification calculations in selected monitoring points in Sofia city*

SNM performer has to provide, even for verification purposes own argumented methodology for obtaining main END indexes – Lden & Lnight.

$$L_{den} = 10\lg\frac{1}{24}\left(12*10^{\frac{L_{day}}{10}} + 4*10^{\frac{L_{evening}+5}{10}} + 8*10^{\frac{L_{night}+10}{10}}\right)$$

Fig. 4 *L_{den} calculation*

2.2. AP (Action Plans)

For all direct and concrete noise reduction measures shall be provided calculation of prognostic effect – using the recommended by END harmonized assessment methods (see Appendix II - 2.2., recommended methods)., and from 2017 the defined by CNOSSOS-EU New Noise Assessment Methods.

Fig. 5 *Real action measure calculation quote*

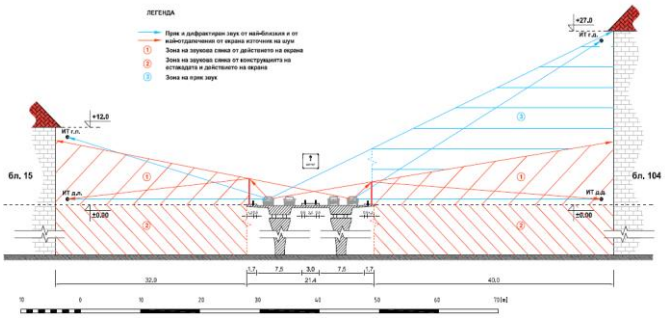

Fig. 6 *Acoustical measure – noise barrier, design phase*

Fig. 7 *Acoustical measure – noise barrier, real set-up*

In a final AP document, one shall include variety of measures, i. e.:

- organizatorical global measures, with overall acoustical impact
- investment environmental projects, with overall acoustical impact
- public campaigns and measures with indirect acoustical impact
- measures on state and even cross border measures - with direct and indirect acoustical impact
- measures with direct acoustical impact (such as barriers, large green zones, traffic improvement, etc.)

3. CONCLUSIONS

Main practical advises, and conclusions from SPECTRI experience and Non Governmental involvement in Environmental Prediction process (through Bulgarian Acoustical Association):

3.1. Collection of maximum possibly correct input data is achieved either through available sources, or collecting via different institutions' collaboration, or using own collective procedure and argumented methodology.

3.2. Using measurement and monitoring data (available ones), and further organizing of own measurements and traffic counts. Needed own argumented methodology for introducing measurement data into SNM process, and for verification procedure.

SPECTRI www.WEBNOISE.eu.

Fig. 8 *SPECTRI WEBNOISE.eu portal*

3.3. Producing reliable, accurate and trustful tool for professional strategic noise impact reduction and noise protection – the END defined Action Plans, organized and created with care.

3.4. Important practical conclusion is that the SNM and AP are to be created with same methodology, and possibly by the same performer.

3.5. Publicly available data in a clear, attractive, and easy understood format. One example is the maintained by SPECTRI own environmental on-line protection portal - seem http://www.webnoise.eu – See Fig. 8.

REFERENCES

[1] European Noise Directive (END) 2002/49/EC;

[2] EC Good practice guide for strategic noise mapping (EC expert noise group paper – WG-AEN);

[3] "Common Noise Assessment Methods in Europe (CNOSSOS-EU)", 2012

[4] World Health Organization paper "Burden of disease from environmental noise"

[5] Strategic Noise Map of Sofia City (project by SPECTRI Ltd.), 2009 – see city's official web page.

[6] Action Plan on Environmental Noise of Sofia City (project by SPECTRI Ltd.), 2010 – see city's official web page.

[7] Strategic Noise Map of Plovdiv City (project by SPECTRI Ltd.), 2009 – see city's official web page.

[8] Action Plan on Environmental Noise of Plovdiv City (project by SPECTRI Ltd.), 2010 – see city's official web page.

[9] Strategic Noise Map of Bourgas City (project by SPECTRI Ltd.), 2012 – see city's official web page.

[10] Action Plan on Environmental Noise of Bourgas City (project by SPECTRI Ltd.), 2013 – see city's official web page.

[11] Strategic Noise Map of Rousse City (project by SPECTRI Ltd.), 2012 – see city's official web page.

[12] Action Plan on Environmental Noise of Rousse City (project by SPECTRI Ltd.), 2013 – see city's official web page.

[13] Strategic Noise Map of Pleven City (project by SPECTRI Ltd.), 2012 – see city's official web page.

[14] Action Plan on Environmental Noise of Pleven City (project by SPECTRI Ltd.), 2013 – see city's official web page.

[15] Strategic Noise Map of Major Roads (project by SPECTRI Ltd.), 2009-2011 – see official Roads' Agency web page.

[16] Action Plan on Environmental Noise of Major Roads (project by SPECTRI Ltd.), 2010-2012 – see Roads' Agency official web page.

[17] H. Jonasson et al., Source modeling of road vehicles, EU- FP5 project HARMONOISE deliverable report no D09 (HAR11TR- 041210- SP10), SP, 2004.

[18] Guidelines for the use of traffic models for noise mapping and noise action planning, EU- FP6 project IMAGINE deliverable report no 7 (IMA02DR7- 060531- TNO10), TNO, 2006.

University of Nis
Faculty of Occupational Safety
„Politechnica“ University of Timisoara
Faculty of Mechanical Engineering
24th International Conference
NOISE AND VIBRATION
Niš, 29 - 31. 10. 2014.

STRATEGIC NOISE MAPS FOR MAJOR ROADS - FIRST RESULTS IN SERBIA

Aleksandar Gajicki[1], Vladimir Babić[2], Momir Praščević[3], Darko Mihajlov[4]

[1] Institute of transportation CIP, Serbia, aleksandar@gajicki.com
PhD student at University of Nis, Faculty of Occupational Safety, Serbia
[2] The Highway Institute, Serbia, babic.vladimir@gmail.com
[3] University of Nis, Faculty of Occupational Safety, Serbia, momir.prascevic@znrfak.ni.ac.rs
[4] University of Nis, Faculty of Occupational Safety, Serbia, darko.mihajlov@znrfak.ni.ac.rs

Abstract – *The Republic of Serbia through the Law on environmental noise protection (2009), and related by-laws (2010) started with implementation of Directive 2002/49/EC and set deadline for the first round of strategic noise mapping to June 30, 2015. Strategic noise maps for four section of major roads in Serbia have been produced in the first half of 2014 and have included 45.4 km of roads with the average annual traffic flow higher than 6,000,000 vehicles. This paper shows experiences in production of the strategic noise maps, description of the used methodology, identification of the problems that have appeared and presentation of the results.*

1. INTRODUCTION

In 2002, the European Parliament adopted the Directive 2002/49/EC [1] as a principal document for assessment and management of environmental noise. The purpose of the Directive was to define a common approach intended to avoid, prevent or reduce, on a prioritized basis, the harmful effects including annoyance, due to the exposure to environmental noise. Serbia started with implementation of the Directive attitudes adopting the Law on Environmental Noise Protection in 2009 [2] and the by-laws in 2010 [3-6].

Environmental noise regulation in the field of strategic noise mapping in Serbia includes the following documents:

- Law on environmental noise protection, “Official Gazette RS”, No. 36/2009 and 88/2010 [2];
- Regulation on noise indicators, limit values, assessment methods for indicators of noise, disturbance and harmful effects of noise in the environment, “Official Gazette RS”, No. 75/2010 [3];
- Rulebook on the methods of development and contents of the strategic noise maps and the manner of presentation of the strategic noise maps to the public, “Official Gazette RS”, No. 80/2010 [4];
- Rulebook on the methodology for action plans development, "Official Gazette of RS", No. 72/2010 [5];
- Rulebook on Methodology of Acoustic Zoning, “Official Gazette RS”, No. 72, 2010 [6].

The Directive and the noise legislation of the Republic of Serbia have prescribed reporting obligation about the state and the impact of noise on population through the strategic noise maps. Reporting will provide information about noise exposure in local, national and international level and development of action plans in order to manage and reduce the negative impact of the noise. All information from strategic noise maps shall be communicated to the public on most understandable and accessible way using the appropriate information technologies.

EU member states have done two rounds of strategic noise mapping for major roads. The first round has been done in 2007 and covered 63,902 km of main roads, while the second round has been done in 2012 and covered 151,676 km of main roads [7]. According to the Directive, member states have an obligation to complete the third round of mapping by the end of June 2017.

In accordance with the legal obligation the procurement of strategic noise mapping for major roads was announced in early 2014. The subject of public procurement was divided into four parties, namely:

- Lot 1: The strategic noise maps for major road I-A class (A3), section: Dobanovci – airport „Nikola Tesla“ (L = 5,3 km);
- Lot 2: The strategic noise maps for major road I-A class (A1), section: Vrčin – Mali Požarevac (L = 14,3 km);
- Lot 3: The strategic noise maps for major road I-A class (A1), section: Mali Požarevac – Umčari – Vodanj – Kolari (L = 12,4 km), and
- Lot 4: The strategic noise maps for major road I-A class (A1), section: Kolari – Ralja (Smederevo) – Ralja (Požarevac) (L = 13,4 km).

Strategic noise maps from the procurement were completed in early July 2014. In this paper the basic definitions of strategic noise mapping with a methodological approach to their production will be present, as well as an identification of problems which have appeared during the production of noise maps. The results of the strategic noise mapping for section Vrčin – Mali Požarevac are shown as an illustrative example.

2. STRATEGIC NOISE MAPS

Basic notions about strategic noise mapping are defined by the Law [2]:

- Strategic noise map is a map representing data about level of noise in certain area and serves for the assessment of total noise exposure of certain area to different noise sources or prediction of total noise in certain area;
- Development of strategic noise maps is a presentation of data on existing or assessed noise levels, including exceeding of prescribed limit values, number of people exposed to noise in certain area or number of households exposed to certain values of noise indicators in certain area
- Strategic maps shall be mandatory for agglomerations with more than 100,000 inhabitants, for major roads with average annual traffic flow higher than 3,000,000 vehicles, for major railroads with average annual traffic flow higher than 30,000 trains, for major airports, as well for plants and activities for which integrated permit is issued.

It is prescribed obligation in the Republic of Serbia that the first round of strategic noise map shall be done no later than June 30, 2015 and must include agglomerations with more than 250,000 inhabitants, major roads with average annual traffic flow of more than 6,000,000 vehicles, main railway lines with the average annual traffic flow of more than 60,000 trains and major airports with more than 50,000 operations (take-off and landing operations) annually.

The second round of strategic noise maps shall be done no later than December 31, 2020 and must include agglomerations with more than 100,000 inhabitants, major roads with average annual traffic flow of more than 3,000,000 vehicles, main railway lines with the average annual flow traffic of more than 30,000 trains and airports that were not included in the first round of mapping.

3. STRATEGIC NOISE MAPPPING PROCESS

The process of producing strategic noise map for major roads is very similar to the methodologies used within noise modeling for environmental impact assessments for road development and reconstruction. The key difference is in covered area which is significantly greater for strategic noise mapping.

Strategic noise mapping process may be divided into seven stages. Each stage of the process is defined by preceding stages such that requirements and specifications are captured ahead of the datasets. Strategic noise mapping process can be defined through [8]:

- Stage 1 - Define areas to be mapped
- Stage 2 - Define noise calculation methods
- Stage 3 - Develop dataset specification
- Stage 4 - Produce dataset
- Stage 5 - Develop noise model dataset
- Stage 6 - Noise level calculation
- Stage 7 - Post processing and analysis

Prior to the adoption of the strategic noise mapping process and their producing, an analysis of literature in this area have been done. In this way it was attempted to look at what was good and what was bad in their production in Europe in the last two rounds. It was one of the ways not to repeat the perceived mistakes, to optimize some methods or to omit unnecessary things. Of particular importance were papers [9] and [10] which describes sensitivity of strategic noise maps to the change of input data and uncertainties that may occur during their producing. The report [11] summarized the European experience in the strategic noise mapping for major roads.

3.1. Define areas to be mapped

Strategic noise maps produced for major roads must cover all areas exposed to noise levels greater than 45 dB(A) for noise indicator L_{night} and greater than 55 dB(A) for noise indicator L_{den}.

Area which should be included in strategic noise mapping of major road was determined on the basis of the preliminary calculation in open condition (i.e. without ground terrain, objects, etc.). The estimated calculations boundaries are increased multiplying by safety factor of 1.5.

3.2. Define noise calculation methods

Road noise indicators were calculated using French method NMPB-Routes-96 (Bruit des Infrastructures Routiers Methode de calcul incluant les effets météorologiques) [12] and French standard "XPS 31-133" [13] in accordance with the recommendations of Directive [1] and Law [2]. For input data with respect to emissions, these documents refer to "Guide du bruit des transports terrestres, fascicule prévision des niveaux sonores, CETUR 1980".

3.3. Develop dataset specification

Dataset specification development for the road noise calculation was performed on the basis of the noise indicator calculation method specification, noise mapping process, as well as area on which the strategic noise mapping is carried out. Systematized overview of basic data required for strategic noise mapping of main roads is shown below:

- 3D Model Environment:
  - DTM – 3D surface model;
  - DEM – 3D building heights.
- Road as noise source:
  - Carriageway centerline;
  - Technical and technological characteristics of road;
  - Traffic flow;
  - Traffic speed;
  - Percentage of heavy vehicles.
- Meteorological parameters:
  - Speed and wind frequency;
  - Average air temperature;
  - Average humidity;
  - Average atmospheric pressure.
- Demographics data:
  - Number of people in the strategic noise mapping area;
  - Distribution of population in the strategic noise mapping area.

If actual data required for strategic noise mapping is missing as a source of data for replacements can be used the last edition of the European Commission Working Group Assessment of Exposure to Noise - Position Paper - Good Practice Guide for Strategic Noise Mapping and the Production of Associated Data on Noise Exposure [14] .

Procuring entity of strategic noise maps must be informed and must agree for using data from this document. Used data must be clearly indicated.

3.4. Produce dataset

For strategic noise mapping it is necessary to use data from the year proceeding the year of their producing. In the case of strategic noise maps for main roads it is supposed to be the data from 2013. Also, it is necessary to use only data from authorized organizations.

It was not possible to provide all relevant data from 2013. Instead of them 2012 data were mainly used for the calculation. Demographic data were taken from the last census in the Republic of Serbia which was held in 2011. Part of the topographic maps that have been used as the basis for the creation of 3D terrain models were from the period from 1959 to 1972.

All the maps to the scale of 1:25,000 meet the required accuracy of the topographic surface defined by the relative relationship of height points which cannot be less than 1.5 meters. However, this large-scale maps are not detailed enough to produce precise strategic noise maps. This issue should be further defined in terms that maximum scale of topographic maps should be set. Otherwise we may be in a position that details of generated 3D terrain model, which affects the results of the noise indicators calculations, can vary significantly depending on the used topographic map.

Population data were available at level of the settlement, or census units. Their allocation to individual residential buildings for the calculation and assessment of noise annoyance was left to the knowledge and experience of each individual maker of strategic noise maps.

3.5. Develop noise model dataset

All collected data were analyzed and customized in accordance with the requirements for their use in the software package for the noise indicators calculation and analysis of population exposure.

All spatial data were georeferenced according to the new geodetic reference system of the Republic of Serbia, which is consistent with ETRS89 (European Terrestrial Reference System 1989).

3.6. Noise level calculation

Software package which is used for the noise indicators calculation must be in accordance with the requirements of Nordtest Method "Framework for the Verification of Environmental Noise Calculation Software", ACOU 107 (Nordtest, Finland, 2001) and DIN 45687 "Acoustics - Software products for the calculation of the sound propagation outdoors - Quality requirements and test conditions", Beuth Verlag GmbH (Germany, 2006).

The first round of strategic noise mapping for major roads has been done using software packages Predictor-Lima, SoundPLAN and CadnA.

3.7. Post processing and analysis

Post processing and analysis of the strategic noise mapping results for each individual section was performed by using already prepared templates for displaying numerical data to the public [15-17]. All necessary templates are given by the Regulations [4]. The number of noise-affected people and the degree of their affection was determinated using the LarmKennZiffer - LKZ Method (Noise-Evaluation-Index-Method).

The Serbian noise legislation requires the calculation of noise indicators at 4 meters height above the ground. Accordingly, only the population living in residential buildings that are taller than 4 meters were taken in consideration during annoyance analyses. In settlements along section of major roads, for which strategic maps were done, almost half of residential buildings is lower than 4 meters, or at this height are attics and roofs.

During the noise exposure calculation there were several input parameters whose sizes are not specified, but it was left to each individual strategic noise map maker to determine their values. This primarily refers to the distance of measuring points with respect to the façade, the mutual spacing between the measurement points and minimal length of the façade which will be taken into the consideration. Their size can range in certain ranges, but these differences are sufficient that there may be some discrepancies in the final results.

Graphical representation of strategic noise maps for the night period (L_{night}) and the period of the day-evening-night (L_{den}) have been prepared in accordance with the Regulations [4] which defines the colors for each noise level bands. In order to correctly display color on the screen and print properly, it was necessary to calibrate monitor and printer. In practice this means, no matter how much care was taken during preparation for the press, when the same strategic noise map printed on various printers that are not calibrated the difference in the presented colors will appear.

As part of the strategic noise maps it is necessary to analyze the impact of noise to kindergartens, schools, hospitals and other facilities sensitive to noise. If we literally implement legislation which provides that the strategic noise map are made for periods of "day-evening-night" and "night" it would be unusable results in the post processing and analysis. Analyzing noise exposure of kindergarten, school, or community-health center using L_{den} and L_{night} we cannot get any concrete conclusions. First, the Serbian legislation does not recognize the noise indicator L_{den} and cannot be compared with threshold limit values. On the other hand, these institutions do not work at night so in that sense the noise exposure indicator L_{night} does not mean anything.

4. RESULTS

As an illustrative example of the strategic noise mapping for major roads in the paper are presented obtained result for the section Vrčin - Mali Požarevac [15].

Section length is 14.2 km, and the calculation boundaries were set at 1000 m on the left and right from the axis of the highway. Total covered area for analysis was 29.1 km^2.

Mapping area partially or fully encompass seven settlements whose demographics data are shown in table 1.

Table 1 *Settlements with demographics data*

Settlements	Population	Households	Average population per household
Vrčin	9088	2397	3,8
Zaklopača	2297	709	3,2
Grocka	8441	2911	2,9
Begaljica	3029	942	3,2
Mala Ivanča	1769	642	2,8
Mali Požarevac	1391	441	3,2
Senaja	405	139	2,9

Data from noise exposure analyses, the number of inhabitants and dwellings as well as the area exposed ranges of noise indicators L_{den} and L_{night}, are shown in Tables 2, 3, 4, 5, 6 and 7. The shown data are rounded to hundreds in accordance with the legislation but the exact values are given in parentheses.

Table 2 *Population exposure analysis related to L_{den}*

Noise indicator L_{den} [dB(A)]	Number of people
< 55	2700 (2736)
55 - 59	800 (842)
60 - 64	400 (433)
65 - 69	200 (150)
70 - 74	0 (40)
> 75	0 (7)

Table 3 *Population exposure analysis related to L_{night}*

Noise indicator L_{night} [dB(A)]	Number of people
< 45	2400 (2365)
45 - 49	900 (896)
50 - 54	600 (646)
55 - 59	200 (222)
60 - 64	100 (65)
65 - 69	0 (14)
> 70	0 (1)

Table 4 *Area exposure analysis related to L_{den}*

Noise indicator L_{den} [dB(A)]	Exposed area [km^2]
< 55	9,5
55 - 64	13,2
65 - 74	4,9
> 75	1,5

Table 5 *Dwellings exposure analysis related to L_{den}*

Noise indicator L_{den} [dB(A)]	Estimated numbers of dwellings
< 55	900 (921)
55 - 64	400 (434)
65 - 74	100 (66)
> 75	0 (2)

Table 6 *Population exposure analysis in dwellings with quiet facade related to L_{den}*

Noise indicator L_{den} [dB(A)]	Number of people
< 55	0 (46)
55 - 59	0 (16)
60 - 64	0 (9)
65 - 69	0 (5)
70 - 74	0 (4)
> 75	0 (2)

Table 7 *Population exposure analysis in dwellings with quiet facade related to L_{night}*

Noise indicator L_{night} [dB(A)]	Number of people
< 45	0 (36)
45 - 49	0 (23)
50 - 54	0 (9)
55 - 59	0 (6)
60 - 64	0 (5)
65 - 69	0 (3)
> 70	0 (0)

There is no dwellings with special insulation against noise in the settlements which were included in the strategic noise mapping.

Part of the graphical presentation of strategic noise maps for the period day-evening-night (noise indicator L_{den}) for the settlements Mali Požarevac is shown in Figure 1.

CONCLUSION

Strategic noise mapping is a complex and demanding process which has to be done in several phases.

A strategic noise maps are accurate and precise as much as data upon which they are made are accurate and precise.

Many parts of the strategic noise mapping process are not clearly and unambiguously defined, including the required quality of the input data. This may lead to different approaches which are all within the law, but we can get a lot of different outputs.

In order to avoid certain arbitrariness in the production of strategic noise maps it is necessary to define appropriate guideline, which will contain a methodology, as well as all other necessary information in order to get uniformly strategic noise maps.

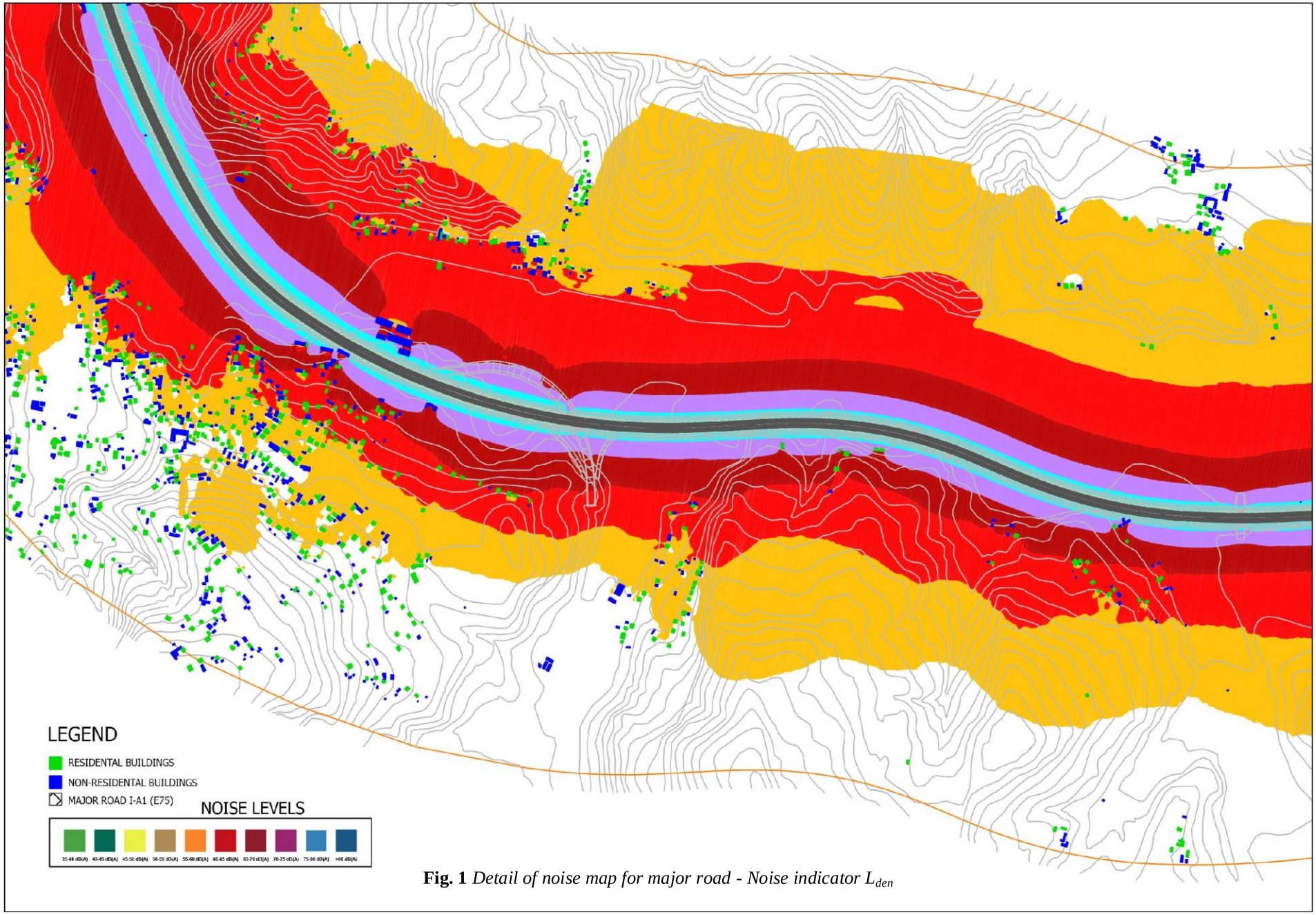

Fig. 1 *Detail of noise map for major road - Noise indicator* L_{den}

Noise legislation of the Republic of Serbia does not prescribe the obligation and procedures for validation and verification of input data or strategic noise maps.

REFERENCES

[1] DIRECTIVE 2002/49/EC OF THE EUROPEAN PARLIAMENT AND OF THE COUNCIL of 25 June 2002 relating to the assessment and management of environmental noise, Official Journal of the European Communities, vol. L189, pp. 12-26, 2002.

[2] Law on environmental noise protection, "Official Gazette RS", No. 36, 2009 and No.88, 2010. (In Serbian)

[3] Regulation on noise indicators, limit values, assessment methods for indicators of noise, disturbance and harmful effects of noise in the environment, "Official Gazette RS", No. 75, 2010. (In Serbian)

[4] Rulebook on the methods of development and contents of the strategic noise maps and the manner of presentation of the strategic noise maps to the public, "Official Gazette RS", No. 72, 2010. (In Serbian)

[5] Rulebook on the methodology for action plans development, "Official Gazette RS", No. 72, 2010. (In Serbian)

[6] Rulebook on Methodology of Acoustic Zoning, "Official Gazette RS", No. 72, 2010. (In Serbian)

[7] European Environment Agency, Population exposure to noise from different sources in Europe, Available on: http://forum.eionet.europa.eu/etc-sia-consortium/library/noise_database/end_df4_8_results_2012.xls (accessed September 17, 2014).

[8] Environmental Protection Agency, Guidance Note for Strategic Noise Mapping For the Environmental Noise Regulations 2006 - Version 2, Wexford: EPA, 2011.

[9] S.Shilton et al, WG-AEN's Good Practice Guide and The Implications for Acoustic Accuracy - Final Report: Sensitivity Analysis for Noise Mapping, Warrington: Hepworth Acoustics, 2005.

[10] C.Popp, Noise prediction method uncertainties, in Environmental control of physical agents: new perspectives and emerging issues, 2009.

[11] J.R.Alférez et al, Best Practice in Strategic Noise Mapping, Paris: CEDR, 2013.

[12] NMPB-Routes-96 "Road Traffic Noise New French calculation method including meteorological effects", Arrété du 15 mai 1995 relatif au bruit des infrastructures routiéres, Official Gazette from May 10, 1995, Article 6

[13] French standard XP S31-133 (norme experimentale) "Acoustic - Road and railway traffic noise – Calculation of sound attenuation during outdoor propagation, including meteorological effects"

[14] European Commission Working Group Assessment of Exposure to Noise (WG-AEN), Position Paper, Good Practice Guide for Strategic Noise Mapping and the Production of Associated Data on Noise Exposure, Version 2, 13th August 2007

[15] A.Gajicki et al, The strategic noise maps for major road I-A class (A1), section: Vrčin – Mali Požarevac, Belgrade: Institute of transportation CIP, 2014. (In Serbian)

[16] A.Gajicki et al, The strategic noise maps for major road I-A class (A1), section: Mali Požarevac – Umčari – Vodanj – Kolari, Belgrade: Institute of transportation CIP, 2014. (In Serbian)

[17] V.Babić et al, The strategic noise maps for major road I-A class (A3), section: Dobanovci – airport „Nikola Tesla", Belgrade: The Highway Institute, 2014. (In Serbian)

University of Nis
Faculty of Occupational Safety
„Politechnica“ University of Timisoara
Faculty of Mechanical Engineering
24th International Conference
NOISE AND VIBRATION
Niš, 29 - 31. 10. 2014.

METHODOLOGY FOR VERIFICATION OF SOFTWARE FOR NOISE ATTENUATION CALCULATION ACCORDING TO ISO 9613-2 STANDARD

Jelena Tomić, Slobodan Todosijević, Nebojša Bogojević, Zlatan Šoškić

Faculty of Mechanical and Civil Engineering, University of Kragujevac, tomic.j@mfkv.rs

Abstract - *One of the goals of the project "Development of methodologies and means for noise protection of urban areas" is development of software tools for local noise mappings. For the purposes of software verification, we developed method for testing of software for noise mapping and prediction according to ISO 9613-2 standard. This method tests modeling of the all physical effects covered by the standard. The paper presents proposed tests for noise mapping software verification with reference mapping results, i.e. sound pressure levels calculated according to ISO 9613- 2 standard for the each of proposed tests.*

1. INTRODUCTION

For the purpose of urban planning and development of action plans for managing noise issues and effects, it is necessary to produce strategic noise maps. This maps are intended to describe the environmental noise levels and to assess the total number of seriously annoyed residents. In accordance with Environmental Noise Directive (2002/49/EC) [1], noise mapping and drawing of Noise Action Plans became mandatory for major cities of the European Union.

Noise maps can be created on the basis of experimental measurements of noise levels or by applying appropriate calculation methods. As calculation methods enable prediction of noise levels at large number of receiver points, and also prediction of future noise, they are significantly more used. Software packages for noise mapping are numerous, but their price is usually high. The best-known software packages for noise mapping are LIMA Predictor [2], Cadnam [3], IMMI [4], SoundPlan [5], Olive Tree Lab [6], SPM9613 [7].

As Serbia is in accession process to the European Union, Serbian legislation related to noise protection is in accordance to Environmental Noise Directive. As there is no commercial software tool for noise mapping at this moment in Serbia, and only representatives of foreign companies offer software solutions, Faculty of Mechanical and Civil Engineering Kraljevo has been developing software tools for local noise mapping in course of the project "Development of methodologies and means for noise protection of urban environment" [8] funded by Serbian Ministry of Education and Science.

Since the testing of software for noise mapping is usually done by comparing estimated noise levels with experimental results, in order to verify and validate developed software solution, there is a need to develop a plan for noise mapping software testing. Software verification should provide an answer to the question of whether the software meets the desired functionality and requirements, while validation should answer to the question of whether the software meets the real needs of users. To obtain the answers on these questions, it is necessary to execute unitary testing, i.e. independent testing of each program component, integration testing, which checks whether the connections between components are well defined and implemented, and the system (final) testing. Within the system testing, so-called reference tests are generated. Reference tests present the common conditions under which the system should perform when it is installed.

Therefore, for the purposes of software verification and validation, test plan should be defined according to project requirements, system model and project documentation. A separate specification should be made for each of the tests and should define purpose of the test, criteria for determining whether the requirements are met, as well as necessary data for testing.

In this paper are presented proposed tests for noise mapping software verification. For each of the proposed tests, necessary data for creating a noise map are given, as well as the reference mapping results, i.e. the sound levels calculated using the ISO 9613- 2 standard..

2. ISO 9613-2 STANDARD

ISO 9613-2 standard [9] specifies a method for calculating attenuation of sound during outdoors downwind propagation. The application of defined method enables prediction of the equivalent continuous A-weighted sound pressure level and also calculation of a long-term average A-weighted sound pressure level.

ISO 9613-2 standard defines octave-band algorithms for calculating the attenuation of sound emitted by point sound source or an assembly of point sources. Line and area sources may be divided into line and area sections, respectively, and each section represented by a point source with certain sound power and directivity at the center of the section. Also, when only A-weighted sound power levels of the sound sources are known, the attenuation for 500 Hz may be used for estimation of the resulting attenuation.

Standard defines algorithms for the following physical effects:

- geometrical divergence,
- atmospheric absorption,
- ground effect,
- reflection from surfaces,
- screening by obstacles.

The method for calculating attenuation of sound during propagation through foliage, industrial sites and housing is also specified by the ISO 9613-2 standard. Propagation over water surfaces is not covered by this standard. Also, standard is not applicable to sound from aircraft in flight and to blast waves from mining, military and similar operations.

3. METHODOLOGY FOR SOFTWARE VERIFICATION

The developed method for the verification of noise mapping and prediction software consists of set of tests for comparing noise maps obtained by tested software and by using methodology defined by ISO 9613-2 standard. Proposed method tests modeling of the all physical effects covered by the standard. For the purpose of the software testing, functions for calculating the sound attenuation and A-weighted sound power levels according to ISO 9613-2 standard were developed by using MATLAB software package.

For each of the proposed tests the ambient temperature has value 30^0C, while relative humidity of the air is equal 70%, in order to decrease high-frequency atmospheric absorption which, under these conditions, has value 59.3 dB/km for the octave band with 8000 Hz midband frequency. As the attenuation of the sound pressure level due to atmospheric absorption is approximately $(\Delta L_{eq})_{atm} = d/100$ [dB] under defined conditions (temperature and air humidity), distance between the sound source and the receiver d should be less than 100 m so that the atmospheric absorption influence becomes less than 1 dB. Also, in each test, noise sources are assumed to produce 100 dB sound pressure level with flat octave band spectrum.

Further in the paper are described proposed tests for noise mapping software verification and validation. Also, reference noise mapping results, i.e. the sound levels calculated according to ISO 9613- 2 standards, are given for each of the tests.

3.1 Horizontal propagation

In order to test modeling of the sound propagation in horizontal plane and calculating the sound attenuation due to geometrical divergence, omnidirectional point source is assumed to emit sound into free space with no physical obstacles to sound propagation. Equivalent continuous A-weighted sound pressure levels should be calculated for the network of receivers whose positions are defined by the coordinates [5i 5j 0] m, where i=1,...,9 and j=1,...,9. In order to results be symmetric, sound source is located in the center of the network of receivers, so its position is given by the coordinates [25 25 0] m. Defined network provides sufficient receiver points for verifying the symmetry of the sound field. A-weighted sound pressure levels calculated in accordance with ISO 9613-2 standard are given in the Table 1.

3.2 Vertical propagation

This test is designed to check sound propagation modeling in vertical plane. The point source is assumed to emit sound equally in all directions in free space with no physical obstacles to sound propagation. Equivalent continuous A-weighted sound pressure levels should be calculated for five receivers distributed along vertical line, i.e. line parallel to z-axes of the coordinate system. The position of the first receiver point is defined by the coordinates [10 10 10] m, while the distance between neighboring points is equal 10 m. In order to study the symmetry, sound source is located at position of the middle receiver, so its position is given by the coordinates [10 10 30] m. Table 2 contains A-weighted sound pressure levels calculated in accordance with ISO 9613-2 standard.

Table 1 Horizontal propagation test

x[m] / y[m]	5	10	15	20	25	30	35	40	45
5	57.4	58.5	59.5	60.3	60.6	60.3	59.5	58.5	57.4
10	58.5	60	61.5	62.7	63.1	62.7	61.5	60	58.5
15	59.5	61.5	63.7	65.8	66.8	65.8	63.7	61.5	59.5
20	60.3	62.7	65.8	69.8	72.9	69.8	65.8	62.7	60.3
25	60.6	63.1	66.8	72.9	98	72.9	66.8	63.1	60.6
30	60.3	62.7	65.8	69.8	72.9	69.8	65.8	62.7	60.3
35	59.5	61.5	63.7	65.8	66.8	65.8	63.7	61.5	59.5
40	58.5	60	61.5	62.7	63.1	62.7	61.5	60	58.5
45	57.4	58.5	59.5	60.3	60.6	60.3	59.5	58.5	57.4

Table 2 Vertical propagation test

z [m]	10	20	30	40	50
Leq [dBA]	60.6	66.8	98	66.8	60.6

Table 3 Anisotropic source test

x[m] / y[m]	5	10	15	20	25	30	35	40	45
5	0	0	0	0	0	0	0	0	0
10	0	0	0	0	104	0	0	0	0
15	0	0	0	75.9	78.9	75.9	0	0	0
20	0	0	69.7	71.8	72.8	71.8	69.7	0	0
25	0	66	67.5	68.7	69.2	68.7	67.5	66	0
30	63.4	64.5	65.6	66.3	66.6	66.3	65.6	64.5	63.4

Table 4 Multiple sources test

x[m] / y[m]	5	10	15	20	25	30	35	40	45
5	98	73	67.2	64.4	63.6	64.4	67.2	73	98
10	72.9	70	66.3	64	63.3	64	66.3	70	72.9
15	67	66.1	64.4	63.1	62.6	63.1	64.4	66.1	67
20	63.6	63.3	62.5	61.8	61.5	61.8	62.5	63.3	63.6
25	61.3	61.2	60.9	60.5	60.4	60.5	60.9	61.2	61.3
30	59.5	59.6	59.5	59.3	59.3	59.3	59.5	59.6	59.5
35	58.1	58.2	58.2	58.2	58.2	58.2	58.2	58.2	58.1
40	56.9	57	57.1	57.1	57.1	57.1	57.1	57	56.9
45	55.8	56	56.1	56.1	56.1	56.1	56.1	56	55.8

3.3 Anisotropic source

In order to test calculation of the sound field of an anisotropic source, a sound source is assumed to emit energy into solid angle $\Delta\theta = 90^0$, $\Delta\varphi = 180^0$, i.e. into an angle of 90^0 around y-axes direction in free space. Equivalent continuous A-weighted sound pressure levels should be calculated for the network of receivers whose positions are defined by the coordinates [5*i* 5*j* 0] m, where *i*=1,...,9 and *j*=1,...,6. This network provides sufficient points for examining the distribution of the sound radiation. In order to enable symmetry of the sound field testing, sound source is located at position given by [25 10 0] m. In the region of sound radiation sound pressure level should be 6 dB higher than the sound pressure level due to omnidirectional source, while outside of this region sound pressure level has value 0 dB. The reference noise mapping results are given in the Table 3.

3.4 Multiple sources

This test enables examining calculation of the sound field of multiple sound sources in horizontal plane in free space. Equivalent continuous A-weighted sound pressure levels should be calculated for the network of receivers whose positions are defined by the coordinates [5*i* 5*j* 0] m, where *i*=1,...,9 and *j*=1,...,9. In order to results be symmetric, positions of the sound sources are given by [5 5 0] m and [45 5 0] m. Each noise source is assumed to produce 100 dB sound pressure level with flat octave band spectrum. Table 4 contains noise mapping results obtained in accordance with ISO 9613-2 standard.

3.5 Ground effect

In order to check the prediction of the influence of the terrain hardness on sound propagation in the near and far field, calculation of the sound field in a horizontal plane above the hard, flat ground and, also, above the porous, flat ground, should be tested. Except the ground factor, both tests have the same testing parameters.

Equivalent continuous A-weighted sound pressure levels should be calculated for the network of receivers whose positions are defined by the coordinates [10*i* 10*j* 1] m, where *i*=1,...,9 and *j*=1,...,9. Position of the omnidirectional sound source is given by the coordinates [50 10 1] m. There are no physical obstacles to sound propagation in horizontal plane.

Table 5 Hard ground test

x[m] / y[m]	10	20	30	40	50	60	70	80	90
10	57.2	59.8	63.6	69.8	101	69.8	63.6	59.8	57.2
20	56.9	59.4	62.5	66.7	69.8	66.7	62.5	59.4	56.9
30	56.1	58.1	60.4	62.5	63.6	62.5	60.4	58.1	56.1
40	55.1	56.6	58.1	59.4	59.8	59.4	58.1	56.6	55.1
50	53.9	55.1	56.1	56.9	57.2	56.9	56.1	55.1	53.9
60	52.9	53.6	54.4	54.9	55.1	54.9	54.4	53.6	52.9
70	52	52.5	53	53.2	53.3	53.2	53	52.5	52
80	51.2	51.6	52	52.2	52.2	52.2	52	51.6	51.2
90	50.4	50.7	51	51.2	51.2	51.2	51	50.7	50.4

Table 6 Porous ground test

x[m] / y[m]	10	20	30	40	50	60	70	80	90
10	53.1	55.9	59.8	66.3	98	66.3	59.8	55.9	53.1
20	52.8	55.4	58.8	63.1	66.3	63.1	58.8	55.4	52.8
30	52	54.1	56.5	58.8	59.8	58.8	56.5	54.1	52
40	50.9	52.5	54.1	55.4	55.9	55.4	54.1	52.5	50.9
50	49.6	50.9	52	52.8	53.1	52.8	52	50.9	49.6
60	48.4	49.3	50.1	50.7	50.9	50.7	50.1	49.3	48.4
70	47.1	47.9	48.5	48.9	49	48.9	48.5	47.9	47.1
80	46	46.6	47	47.3	47.4	47.3	47	46.6	46
90	44.9	45.4	45.7	46	46.1	46	45.7	45.4	44.9

Choice of these parameters enables verification of calculation of sound pressure level in the near and far field, because it is achieved that the distance between the source and the receiver in some cases cases meets, while in other cases does not meet the condition $d<30\cdot(h_s+h_r)$, where h_s represents height of the source above ground and h_r is height of receiver above ground ($h_s=h_r$ =1m). Also, defined network provides enough receiver points for testing the symmetry of the sound field.

Reference noise mapping results for flat, hard ground are given in the Table 5, while the sound pressure levels for flat, porous ground are given in the Table 6.

3.6 Sound barrier

This test is designed to check the calculation of the sound pressure levels when the screening obstacle (sound barrier) is positioned between the sound source and the receiver. Sound barrier is modeled as a thin, flat object with a rectangular vertical cross-section, whose vertices are given by [5 -150 0] m, [5 150 0] m, [5 -150 3] m, [5 150 3] m. Hence, the barrier is parallel to the yz-plane, and its height is 3 m. Omnidirectional sound source is located at position [0 0 1.5] m, while the receivers are positioned on the other side of the sound barrier, and their positions are given by [5i 5j 1.5] m, where i=2, ...,6 and j=-2,...,2, so the symmetry of the sound field testing is possible. Since the distance between the receiver and the vertical edges of the barrier is more than four times larger than the distance between the barrier and the receiver, the influence of the diffraction around the vertical edges of the barrier may be neglected, so the prediction of the influence of diffraction over the top edge of the barrier on the sound pressure level may be tested. Also, horizontal dimension of the barrier normal to the source-receiver line is larger than the acoustic wavelength at the nominal midband frequency for each of the eight octave bands of interest, so that defined barrier may be considered as screening obstacle and taken into account when calculating the sound pressure level for each of the octave bands.

As, according to ISO 9613-2 standard, barrier attenuation for more than two barriers may be calculated approximately by choosing the two most effective obstacles and neglecting the effects of the others, verification of the calculation of the attenuation due to two parallel sound barriers is proposed, too. Testing parameters are the same as in previous test, except that another sound barrier, given by [3 -150 0] m, [3 150 0] m, [3 -150 2.5] m, [3 150 2.5] m, is added between the sound source and the noise barrier defined in previous test.

Table 7 and Table 8 contain A-weighted sound pressure levels at receiver points when one or two barriers, respectively, are positioned between the sound source and the receiver points.

Table 7 One sound barrier test

x[m] / y[m]	10	15	20	25	30
-10	49.1	47.4	45.6	44.1	42.8
-5	50.3	48.1	46.1	44.4	43
0	51	48.4	46.2	44.5	43
5	50.3	48.1	46.1	44.4	43
10	49.1	47.4	45.6	44.1	42.8

Table 8 Two sound barriers test

x[m] / y[m]	10	15	20	25	30
-10	47.2	45.5	43.8	42.3	41
-5	48.5	46.3	44.3	42.6	41.2
0	49.1	46.5	44.4	42.7	41.2
5	48.5	46.3	44.3	42.6	41.2
10	47.2	45.5	43.8	42.3	41

3.7 Reflections

This test enables examining calculation of the sound field consisting of direct and reflected sounds. A-weighted sound pressure level should be calculated for the network of receivers whose positions given by the coordinates [5i 5j 1.5] m, where i = 1,...,9 and j = 1,...,9. The proposed location of the omnidirectional source is defined by coordinates [25 25 1.5] m. Terrain is flat and hard, and the distance between source and receiver $d<30\cdot(h_s+h_r)$, so the attenuation due to ground effect is Ag = -3 dB. The reflecting obstacle is modeled as a flat object with a rectangular cross-section, whose vertices are given by [50 0 0] m, [50 50 0] m, [50 0 10] m, [50 50 10] m. Hence, the obstacle is parallel to the yz-plane, and its height is 10 m. Reflection coefficient has value 0.8 and, therefore, corresponds to walls of building with windows. A-weighted sound pressure levels calculated in accordance with ISO 9613-2 standard are given in the Table 9.

Table 9 Reflections test

x[m] / y[m]	5	10	15	20	25	30	35	40	45
5	60.8	61.9	62.9	63.6	64	63.8	63.3	62.6	62.1
10	61.9	63.3	64.7	65.9	66.4	66	65	63.9	63.1
15	62.8	64.7	66.8	68.9	69.9	68.9	67	65.2	64
20	63.5	65.8	68.9	72.9	75.9	72.9	69	66.3	64.6
25	63.8	66.3	69.8	75.9	101	75.9	70	66.7	64.8
30	63.5	65.8	68.9	72.9	75.9	72.9	69	66.3	64.6
35	62.8	64.7	66.8	68.9	69.9	68.9	67	65.2	64
40	61.9	63.3	64.7	65.9	66.4	66	65	63.9	63.1
45	60.8	61.9	62.9	63.6	64	63.8	63.3	62.6	62.1

Table 10 Foliage test

x[m] / y[m]	5	10	15	20	25	30	35
5	62.3	61.1	58.1	56.5	54.6	52.9	51.7
10	65.5	63.3	59.6	57.6	55.5	53.6	52.3
15	69.6	65.5	60.8	58.4	56.2	54.1	52.6
20	72.7	66.5	61.3	58.6	56.4	54.2	52.7
25	69.6	65.5	60.8	58.4	56.2	54.1	52.6
30	65.5	63.3	59.6	57.6	55.5	53.6	52.3
35	62.3	61.1	58.1	56.5	54.6	52.9	51.7

3.8 Foliage

This test is designed to check the calculation of attenuation due to sound propagation through foliage of trees. The terrain is assumed to be flat and soft. The position of the sound source is given by [0 20 1.5] m. The source is assumed to emit sound equally in all directions. A-weighted sound pressure levels should be calculated for the network of receivers whose positions are given by [5i 5j 1.5] m, where i=1,...,7 and j=1,...,7. Height of the trees is 3 m and the area with vegetation may be represented by a rectangle in xy-plane whose vertices are given by [4.5 0 0] m, [30.5 0 0] m, [30.5 40 0], m [4.5 40 0] m. Thus, the source is outside the area with vegetation, while some of the receivers are within this area, but to each receiver sound propagates through foliage of trees. In some cases the total path length through the foliage d_f is less than 10 m, so there is no additional attenuation due to foliage A_{fol}, while in other cases d_f is between 10m and 20 m and A_{fol} = [0 0 1 1 1 1 2 3] dB, or between 20 m and 200 m, when A_{fol} attenuation depends on the length of propagation distance through the foliage d_f, and has value $d_f \cdot$[0.02 0.03 0.04 0.05 0.06 0.08 0.09 0.12] dB (d_f is in meters). Table 10 contains desired noise mapping results obtained in accordance with ISO 9613-2 standard.

3.9 Housing

This test is designed to check the calculation of attenuation due to sound propagation through the built-up region of houses. The terrain is assumed to be flat and hard. Region with houses may be represented by a rectangle in xy-plane whose vertices are given by [4.5 0 0] m, [24.5 0 0] m, [24.5 40 0] m, [4.5 40 0] m. Buildings height is 6 m, and the density of the buildings is 0.7. The location of the omnidirectional sound source is given by the coordinates [0 25 1.5] m. A-weighted sound pressure levels should be calculated for the network of receivers whose positions are given by the coordinates [5i 5j 1.5] m, where i = 5,...,9 and j = 3,…,7. Desired noise mapping results are given in the Table 11.

Table 11 Housing test

x[m] / y[m]	25	30	35	40	45
15	59.3	57.9	56.6	55.4	54.4
20	59.9	58.3	56.9	55.7	54.6
25	60.1	58.4	57	55.8	54.7
30	59.9	58.3	56.9	55.7	54.6
35	59.3	57.9	56.6	55.4	54.4

4. CONCLUSIONS

This paper presented developed methodology for testing of software for noise prediction according to ISO 9613-2 standard. Designed tests enable examining calculation of the sound attenuation due to geometrical divergence, atmospheric absorption, ground effect and sound barriers. Also is enabled testing of the calculation of sound field of an anisotropic source or multiple sound sources, as well as examining prediction of the sound field consisting of direct and reflected sounds or even checking the calculation of attenuation due to sound propagation through foliage or built-up region of houses. As developed testing methodology does not cover propagation above uneven terrain and diffraction around vertical edges of barrier, it should be improved and expanded by adding corresponding tests.

ACKNOWLEDGEMENT

The authors wish to express their gratitude to Serbian Ministry of Education and Science for support through project TR37020.

REFERENCES

[1] "Directive 2002/49/EC of the European Parliament and the Council of June 2002", Official Journal of the European Communities, 2002.

[2] http://www.softnoise.com/predictor.htm

[3] http://www.datakustik.com

[4] http://www.woelfel.de/produkte/immissionsschutz.html

[5] http://www.soundplan.eu

[6] http://www.otlterrain.com

[7] http://poweracoustics.com/Software.html

[8] http://www.mfkv.rs/urbaNoise

[9] ISO 9613-2:1996, Acoustics - Attenuation of sound during propagation outdoors – Part 2: General method of calculation

University of Nis
Faculty of Occupational Safety
„Politechnica“ University of Timisoara
Faculty of Mechanical Engineering
24th International Conference
NOISE AND VIBRATION
Niš, 29 - 31. 10. 2014.

PERMANENT AND SEMI-PERMANENT NOISE MONITORING - FIRST RESULTS IN THE CITY OF NIS

Momir Praščević[1], Darko Mihajlov[2], Dragan Cvetković[3]

[1] University of Nis, Faculty of Occupational Safety, Serbia, momir.prascevic@znrfak.ni.ac.rs
[2] University of Nis, Faculty of Occupational Safety, Serbia, darko.mihajlov@znrfak.ni.ac.rs
[3] University of Nis, Faculty of Occupational Safety, Serbia, dragan.cvetkovic@znrfak.ni.ac.rs

Abstract – *Environmental Noise Directive and the Serbian regulations introduce the new noise indicators for environmental noise assessment. For the purposes of strategic noise mapping and assessment of noise harmfull effects it is necessary to determine the annual value of these indicators. Two measurement principles were developed for determination of noise indicators by long-term or short-term measurements. The long-term measurements can be realized as permanent noise monitoring or semi-permanent noise monitoring. Permanent monitoring can indicate environmental noise trends and help produce noise maps. Semi-permanent monitoring, typically ranging from a few days up to several weeks or months, is also used for cost-effective monitoring of environmental noise trends, limit compliance, public awareness, the improved knowledge of dose-response relationships and the calibration of noise maps. The procedure of permanent and semi-permanent environmental noise measurements at three locations in the city of Niš has been carried out starting from January 1, 2014. The first results of these measurements will be presented in this paper.*

1. INTRODUCTION

Regarding the state of the used noise indicators in European countries, there was a need to harmonize ones. By adopting the Directive on the Assessment and Management of Environmental Noise, 2002/49/EC [1], the basic principles of a harmonized European noise policy were defined. One of the key elements of the Environmental Noise Directive is the assessment of environmental noise by common noise indicators and common assessment methods.

The Environmental Noise Directive has been transposed in Serbian legislation by the adoptaion of the Law on Environmental Noise Protection in 2009 (revised in 2010) [2] and several national sub-laws adopted in 2010. Regulation on noise indicators, limit values, assessment methods, noise annoyance, noise effects, impact on health, collecting data for noise assessment [3] introduce the noise indicators defined in the Environmental Noise Directive.

Directive [1] and Serbian legislation [2,3] require the use the common and supplement noise indicators. The common noise indicators are:

- the day-evening-night noise indicator, L_{den}[dB(A)] - indicator describing the overall annoyance caused by noise within 24 hours, i.e. for the day-evening-night;
- the daily noise indicator, L_d [dB(A)] - indicator describing the annoyance caused by noise within the day (from 6 a.m. to 6 p.m.);
- the evening noise indicator, L_e [dB(A)] - indicator describing the annoyance caused by noise during the evening (from 6 p.m. to 10 p.m.);
- the night-time noise indicator, L_n [dB(A)] - indicator describing the sleep distrubance caused by noise at night (from 10 p.m. to 6 a.m.).

The day-evening-night noise indicator is defined by the following formula:

$$L_{den} = 10\log\frac{1}{24}\left(12\cdot 10^{0.1\cdot L_d} + 4\cdot 10^{0.1\cdot (L_e+5)} + 4\cdot 10^{0.1\cdot (L_n+10)}\right) \quad (1)$$

where:

- L_d - the A-weighted long-term average sound level determined over all the day periods of a year,
- L_e - the A-weighted long-term average sound level determined over all the evening periods of a year,
- L_n - the A-weighted long-term average sound level determined over all the night periods of a year.

A year is a relevant year as regards the emission of sound and an average year as regards the meteorological circumstances [1].

The A-weighted long-term average sound levels for different day periods of a year are defined by the following formula:

$$L_{d(e,n)} = 10\log\left[\frac{1}{N}\sum_{i=1}^{N} 10^{0.1\cdot L_{d(e,n),i}}\right] \quad (2)$$

where N is the number of days in a year, $N = 365$.

The values of noise indicators for i-th day in year are determined based on the continuous measurement of the equivalent noise level in day periods, or by sampling techniques during day periods.

2. NOISE MONITORING STRATEGIES

IMAGINE document [4] describes how to determine L_{den} and L_n by direct measurement or by extrapolation of measurement

results by means of calculation. The measurement method is intended to be used outdoors as a basis for assessing environmental noise and verifying the quality of predictions. Also, the revision of ISO 1996-2 standard that will provide the guidelines for noise indicators determination is in progress.

Two measurement principles were developed for determination of noise indicators. First, the long-term measurements involve measurements during a time long enough to include all variations in operating and meteorological conditions of noise source. Second, the short-term measurements involve measurements under specified operating and meteorological conditions of noise source and the use of relevant prediction method in order to determine the noise indicators value.

For long-term measurements, measurement time interval shall be some significant fraction of a year (e.g. 3 months, 6 months, 1 year), while for the short-term measurements, the minimal time interval shall be 10 minutes but 30 minute measurement is recommended in order to average weather induced variations.

The results of long-term measurements are more accurate and can be used with fewer corrections than those of short-term measurements.

The long-term measurements can be realized using two measurement strategies:

- permanent noise monitoring or
- semi-permanent noise monitoring.

The permanent noise monitoring includes 24 hour a day, 365 days a year, noise measurements using a permanently installed noise monitoring terminal (NMT). The permanent monitoring can indicate environmental noise trends and help produce noise maps.

The semi-permanent monitoring, typically ranging from a few days up to several weeks or months, is also used for cost-effective monitoring of environmental noise trends, limit compliance, public awareness, the improved knowledge of dose-response relationships and calibration of noise maps. The quickly and easily moved noise monitoring terminal are used for the semi-permanent monitoring.

The optimal duration of semi-permanent monitoring cannot be easily determined. Noise source operating conditions, e.g. traffic composition and vehicle flow conditions, shall be as representative as possible to minimize later corrections. If propagation conditions or emission conditions vary strongly between the different seasons of the year, e.g. because of winter tires and snow cover, it might be necessary to perform measurement during several different seasons in order to achieve a low measurement uncertainty.

3. SHORT REVIEW OF NOISE MONITORING IN THE SERBIA

Environmental noise level monitoring in Serbia is performed in several cities and it is pursuant to the Law of environmental noise protection and the accompanying regulations. Although these regulations are in accordance with the national standards [5,6], the methodology of noise monitoring varies in different cities. The issues which differ include as follows: the number of measurement spots; the number of daily, weekly, and monthly measurement intervals, the duration of measurement intervals, measurement parameters and noise indicators used for noise evaluation [7]. Different measurement procedures result from different city configurations, the traffic structure, the traffic flow, the arrangement of noise-sensitive objects, and different shares of noise sources.

The current practice of noise monitoring and assessment in Serbia usually implies short-time measurements with 15-min time interval together with recording general traffic and site information [7]. The measurement period is extended to 1 h in some cases. Continuous twenty-four hours noise level measurements have lately taken place in some cities (for example: Novi Sad, Belgrade, and Pancevo), while the long-term noise measurements by semi-permanent noise monitoring have been carried out lately only in Novi Sad [8].

The environmental noise level monitoring in the city of Niš has been organized on a monthly basis, for the reference time intervals since 1995 until today. The daytime measurement interval is divided into 3 or 5 periods, whereas the night time measurement interval is divided into 2 periods. Within one cycle/month interval there is one 15 minute measurement at each determined measurement spot and for each mentioned period. The values of noise indicators are calculated based on these short-term measurements. The results of calculation are shown in [9].

The two newly purchased noise monitoring terminals by Noise and Vibration Laboratory of the Faculty of Occupational Safety in Nis, enabled the long-term noise measurements. The procedure of permanent and semi-permanent environmental noise measurements at three locations in the city of Nis is being carried out starting from January 1, 2014

The research has been conducted with the aim of determination of the optimal duration of semi-permanent monitoring that would enables the cost-effective monitoring of environmental noise and the determination of the noise indicators at multiple locations with only two noise monitoring stations.

4. METHODOLOGY OF PERMANENT AND SEMI-PERMANENT NOISE MONITORING IN THE CITY OF NIS

Brüel&Kjær's Environmental Noise Management System (Fig. 1) used to permanent noise monitoring consists of:

- Environmental Noise Management System Software Type 7843
- Two Noise Monitoring Terminals Type 3639B

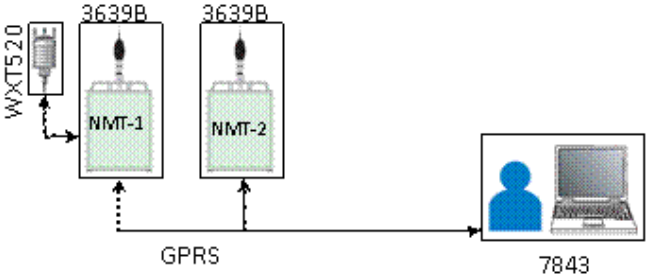

Fig. 1 *Environmental Noise Management System*

The Environmental Noise Management System (ENMS) is built around a server and a set of clients with a professional Microsoft® SQL Server® database as the central server component [10]. The ENMS server provides the basic data storage and business logic for accessing objects in the ENMS database. The server receives data from two noise monitoring terminals (NMT) that provides the server with noise and weather data and stores data and measurement setups as templates.

Environmental Noise Management System Software Type 7843, the central part of the ENM makes it a powerful noise data management tool. It offers real-time communication with NMTs ensuring continuous data storage in both the NMTs and the system's central database. The software ensures data retrieval, analysis, reporting and export of noise, weather, and geographic data through its configurable user interface with built-in GIS functionality.

Noise Monitoring Terminal Type 3639-B is a self-calibrating NMT optimized for remote, unattended, environmental noise measurements [11]. It can measure, record, process, store, and transmit noise information as part of a noise monitoring system. The NMT consists of a weatherproof cabinet containing a noise level analyzer and a battery, a GPRS router, GPS receiver and an outdoor microphone, all of which can be mounted on a mast, pole, tripod or wall. Noise monitoring and analysis is performed by the included analyzer Type 2250 protected inside the cabinet which measures data coming from the outdoor microphone and logs it onto its on-board memory, including broadband and 1/3-octave L_{Aeq} or SPL, continuously at half- or one second intervals. The NMT can also identify, record and analyze noise events. Analyses produced include: hourly reports, short reports (from 1 to 30 minutes), calibration check reports, noise events and instrument health reports.

The procedure of permanent environmental noise monitoring, starting from January 1, 2014 according to guidelines given in standards SRPS ISO 1996-1 [5] and SRPS ISO 1996-2 [6] and IMAGINE document [4] has been carried out at location near the intersection of two roads (marked as NMT-1). The procedure of semi-permanent monitoring starting from July 1, 2014 has been carried out at location near a faculty (marked as NMT-2.2). Location of noise monitoring terminals is shown on Fig. 2 and the coordinates are shown in Table 1.

Table 1 *The coordinates of noise monitoring terminals*

	NMT-1	NMT-2.1	NMT-2.2
Latitude	43° 19' 12.8"	43° 19' 13"	43° 19' 12"
Longitude	21° 53' 27.6"	21° 54' 13.2"	21° 53' 27"
Altitude	195.3 m	196.8 m	197.1 m
Microphone height	4 m	4 m	4 m

The NMTs were mounted on the lighting pole at location NMT-1 (Fig. 3) and NMT-2.1, while the NMT was mounted on the separate pole at location NMT-2.2 (Fig. 4).

Fig. 2 *Location of noise monitoring terminals on GIS plan of the city of Nis*

Fig. 3 *NMT mounted on the lighting pole (location NMT-1: Intersection of two roads)*

Fig. 4 *NMT mounted on the separate pole (location NMT-2.2: Faculty of Medicine)*

The NMTs were connected to constant supply during all day at location NMT-1 and NMT-2.2, while the NMT was connected to constant external AC power supply during night at location NMT-2.1. If long-term monitoring is required, constant AC power from an external mains source is the most reliable and convenient than occasional external AC power.

Both NMTs are equipped with GPRS router and GPS receiver. One of the terminals (marked as NMT-1) is equipped with Weather Station Type WXT520 manufactured by Vaisala, which enable measurement of the following meteorological parameters: temperature, humidity, air pressure, wind velocity, wind direction and rainfall.

The measurement settings of NMTs is shown in Fig. 5. The weather paramenters are valid only for NMT-1. The time for performing charge injection calibration (CIC) was defined for checking system. CIC has been perfomed one time every 24 hours.

The system generates four default period reports based on the noise data: hour, day, month and year reports. It can be defined twelve additional periodical reports. Three additional reports were defined for purpose of this research: working day, weekend and week.

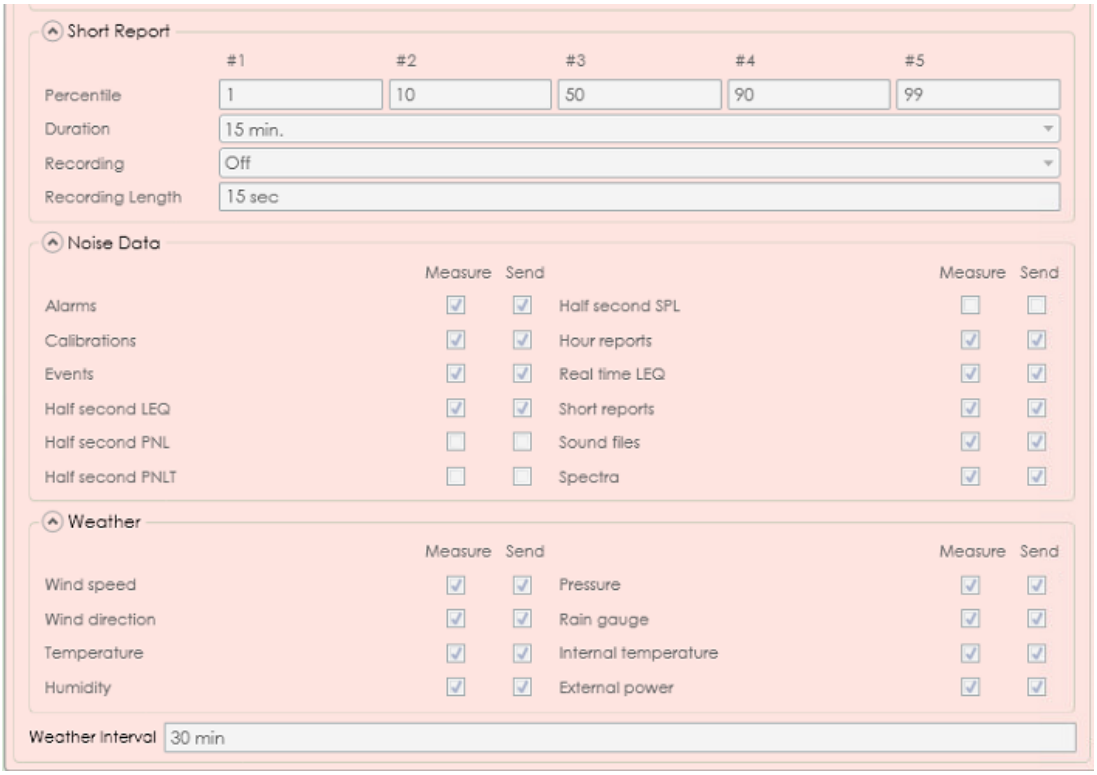

Fig. 5 *Parameter settings of NMTs*

5. RESULTS OF NOISE MONITORING

The monthly values of the noise indicators for NMT-1, NMT-2.1 and NMT2.2 are shown in Table 2, Table 3 and Table 4, respectively, as well as the results of statistical analysis (mean value and standard deviation).

Table 2 *The monthly noise indicators in dB(A) for NMT-1*

	L_d	L_e	L_n	L_{den}	$L_{eq,total}$
January	73.1	71.9	67.9	75.9	71.7
February	73.1	71.9	67.7	75.8	71.7
March	73.3	72.1	67.9	76.0	71.9
April	73.4	72.4	68.3	76.3	72.0
May	73.3	72.3	68.1	76.2	71.9
June	73.0	72.0	68.1	76.0	71.7
July	72.8	72.2	67.8	75.8	71.5
August	72.7	71.9	68.2	76.0	71.5
September	73.1	72.0	67.9	75.9	71.7
mean value	**73.1**	**72.1**	**68.0**	**76.0**	**71.7**
σ	**0.21**	**0.16**	**0.19**	**0.15**	**0.17**

Table 3 *The monthly noise indicators in dB(A) for NMT-2.1*

	L_d	L_e	L_n	L_{den}	$L_{eq,total}$
January	70.3	69.9	67.4	74.7	69.4
February	70.2	69.7	66.7	74.1	69.2
March	70.6	69.8	66.7	74.2	69.5
April	70.5	70.2	67.2	74.6	69.6
May	70.6	70.3	66.8	74.4	69.6
June	70.1	69.7	66.6	74.0	69.1
mean value	**70.4**	**69.9**	**66.9**	**74.3**	**69.4**
σ	**0.17**	**0.24**	**0.32**	**0.24**	**0.16**

Table 4 *The monthly noise indicators in dB(A) for NMT-2.2*

	L_d	L_e	L_n	L_{den}	$L_{eq,total}$
July	63.5	63.0	57.6	66.1	62.2
August	62.2	62.0	57.5	65.5	61.1
September	63.1	62.5	57.9	66.0	61.8
mean value	**62.9**	**62.5**	**57.7**	**65.9**	**61.7**
σ	**0.54**	**0.41**	**0.17**	**0.26**	**0.45**

The daily values of the noise indicators for NMT-1, NMT-2.1 and NMT-2.2 are shown in Fig. 6, Fig. 7 and Fig. 8, respectively. The values of L_e noise indicator are omitted due to clarity of figure. Otherwise, the values of L_d noise indicator and L_e noise indicator are mainly very similar. The results of statistical analysis (mean value, standard deviation, maximum and minimum value) of daily values for NMT-1, NMT-2.2 and NMT-2.1 are shown in Table 5, Table 6 and Table 7, respectively. The results of statistical analysis of all daily values are shown in column 1, while the results of statistical analysis of daily values excluding weekend values are shown in column 2. The results of statistical analysis of daily values excluding value for January, 1 are marked with "*". The value of L_{den} noise indicator for January, 1 was much higher than other values due to the fireworks and the New Year celebration.

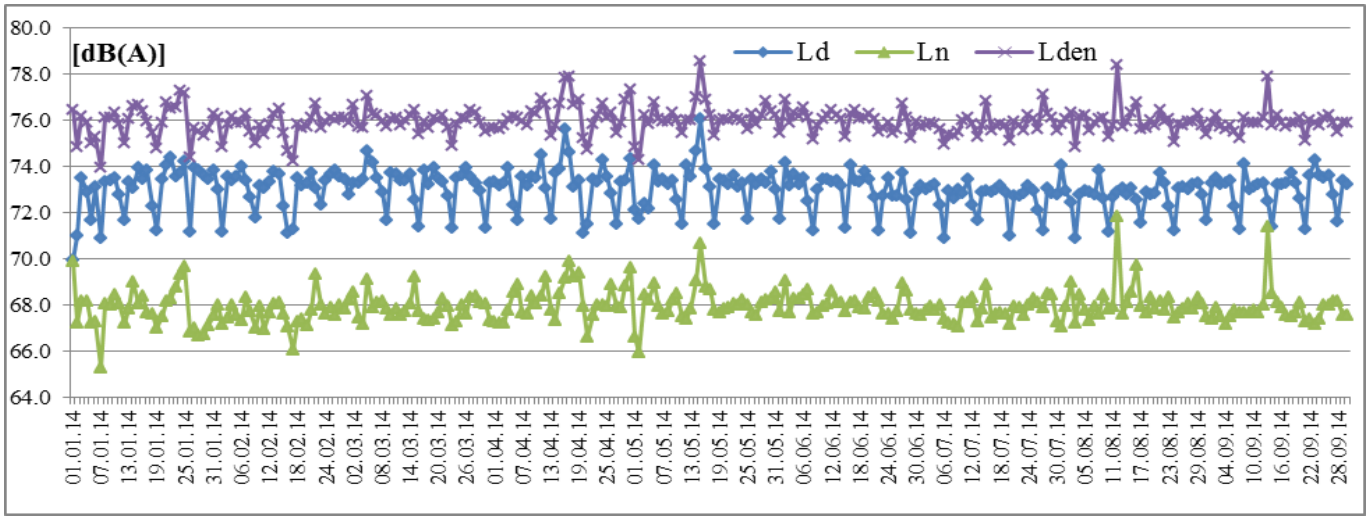

Fig. 6 *The daily values of noise indicators for NMT-1 for January-September 2014*

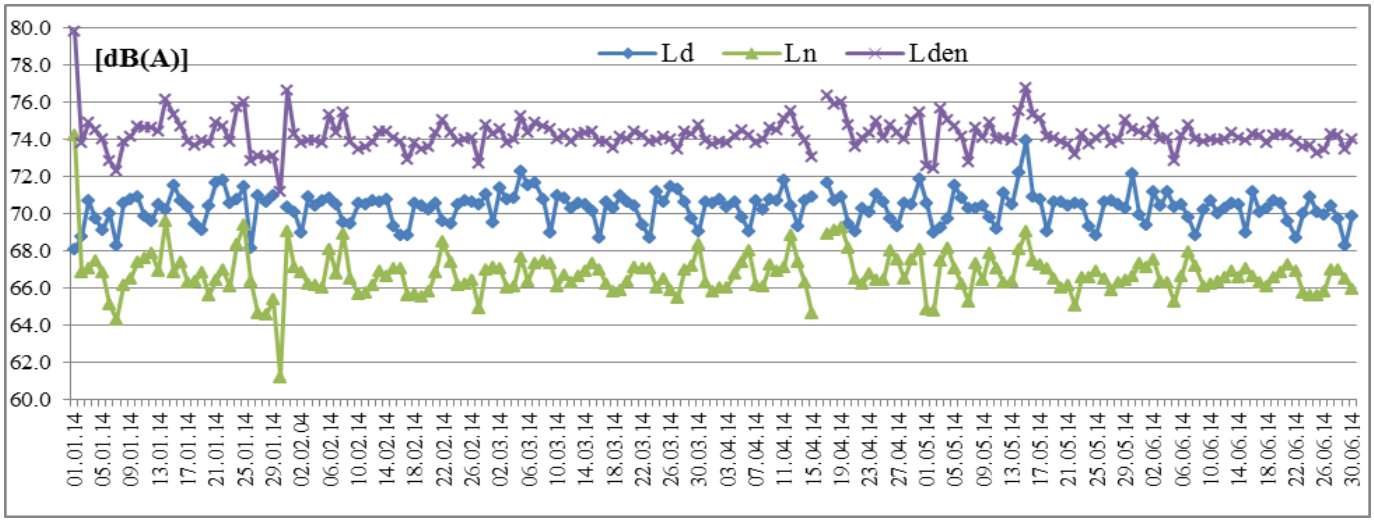

Fig. 7 *The daily values of noise indicators for NMT-2.1 for January-June 2014*

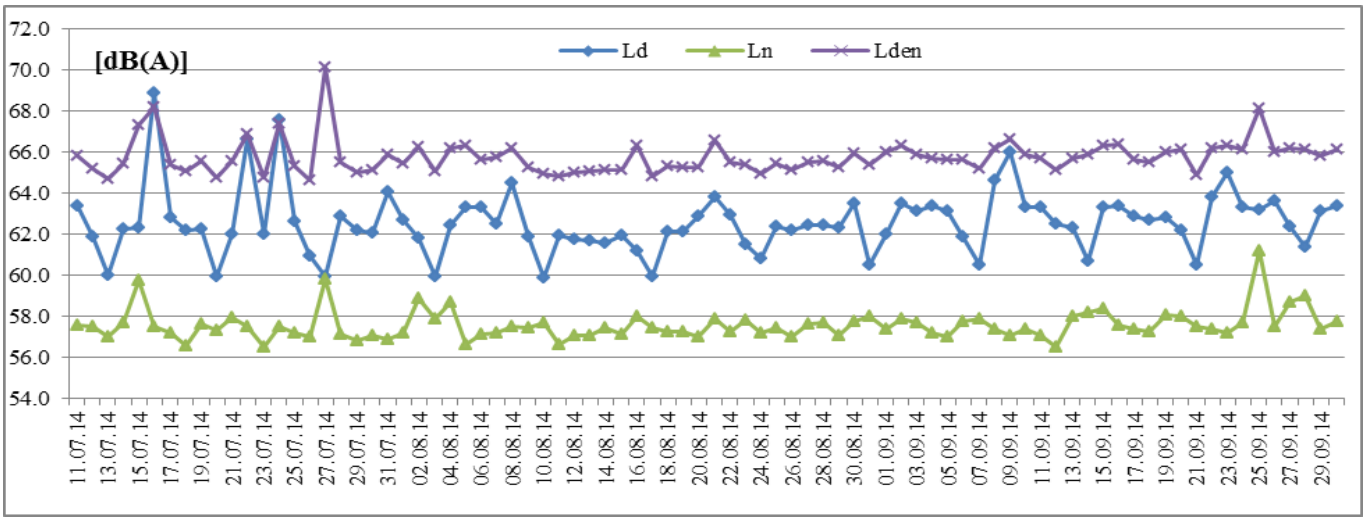

Fig. 8 *The daily values of noise indicators for NMT-2.2 for July-September 2014*

Table 5 *Statistical parameters of daily L_{den}, in dB(A), for NMT-1*

month	mean value		σ		max value		min value	
	1	2	1	2	1	2	1	2
I	75.9	76.0	0.77	0.69	77.3	77.3	74.0	74.0
II	75.8	75.9	0.54	0.45	76.7	76.5	74.2	74.2
III	76.0	76.1	0.39	0.31	77.0	77.0	74.9	75.7
IV	76.2	76.3	0.71	0.74	77.9	77.9	74.7	74.7
V	76.1	76.2	0.70	0.78	78.5	78.5	74.3	74.3
VI	76.0	76.2	0.43	0.33	76.9	76.9	75.2	75.5
VII	75.8	75.8	0.43	0.32	77.1	76.8	74.9	72.3
VIII	76.0	76.1	0.59	0.55	78.4	78.4	74.8	75.6
IX	75.9	75.9	0.45	0.16	77.9	76.2	75.1	75.6
I-IX	**76.0**	**76.1**	**0.59**	**0.55**	**78.5**	**78.5**	**74.0**	**74.0**

Table 6 *Statistical parameters of daily L_{den}, in dB(A), for NMT-2.2*

month	mean value		σ		max value		min value	
	1	2	1	2	1	2	1	2
VII	65.9	65.9	1.33	0.99	70.1	68.2	64.6	64.8
VIII	65.5	65.5	0.47	0.45	66.5	66.5	64.8	64.8
IX	66.0	66.1	0.55	0.56	68.1	68.1	63.9	65.1
VII-IX	**65.8**	**65.8**	**0.84**	**0.71**	**70.1**	**68.2**	**64.6**	**64.8**

Table 7 *Statistical parameters of daily L_{den}, in dB(A), for NMT-2.1*

month	mean value		σ		max value		min value	
	1	2	1	2	1	2	1	2
I	74.3	74.5	1.51	1.56	79.8	79.8	71.2	72.3
I*	74.2	74.3	1.15	1.08	76.6	76.6	71.2	72.3
II	74.0	73.9	0.60	0.59	75.4	75.3	72.7	72.7
III	74.2	74.1	0.37	0.39	75.2	75.2	73.5	73.5
IV	74.5	74.4	0.76	0.79	76.3	76.3	73.0	73.0
V	74.3	74.2	0.90	0.97	76.8	76.8	72.4	72.4
VI	74.0	74.0	0.41	0.42	74.9	74.9	72.8	72.8
I-VI	**74.2**	**74.2**	**0.87**	**0.95**	**79.8**	**79.8**	**71.2**	**71.2**
I-VI*	**74.2**	**74.1**	**0.77**	**0.81**	**76.8**	**76.8**	**71.2**	**71.2**

In addition to monthly and daily values of the noise indicators, the periodical values of the noise indicators for workdays, weekends and weeks were determined, i.e. five-day, two-day and seven-day values, respectively. The results of these noise indicators are shown in Fig. 9 and Fig. 10, for NMT-1 and NMT-2.1, respectively.

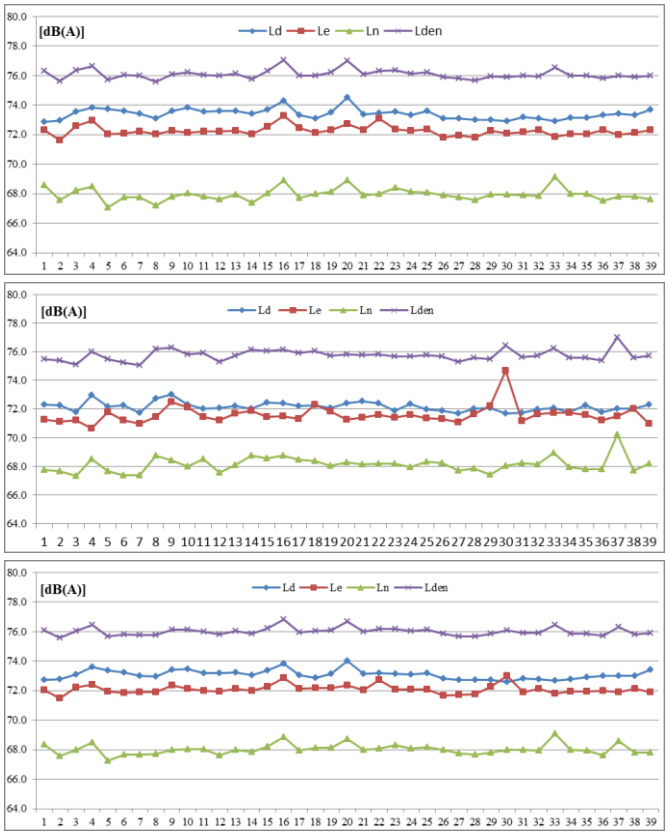

Fig. 9 *The periodical values of noise indicators for NMT-1 for January-Septembeer 2014 (upper graph – workday values, middle graph – weekend values, lower graph – week values)*

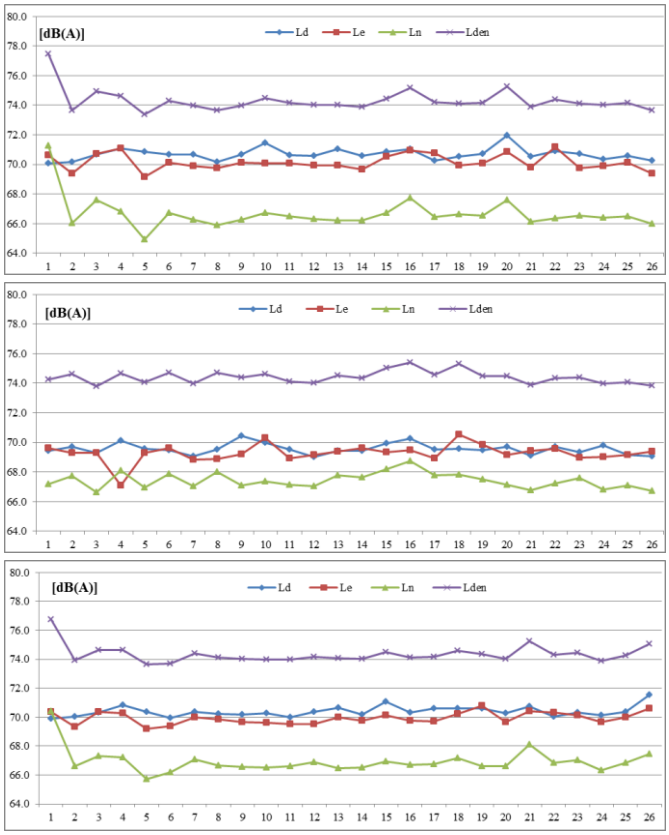

Fig. 10 *The periodical values of noise indicators for NMT-2.1 for January-June 2014 (upper graph – workday values, middle graph – weekend values, lower graph – week values*

The statistical parameters (mean value, standard deviation, maximum and minimum value) as the results of statistical analysis of the noise indicators for different monitoring periods (day, weekend, workday, week, month) were compared and the results of comparison are shown in Table 8 and Table 9, for NMT-1 and NMT-2.1, respectively.

Table 8 *Comparison of statistical parameters of noise indicators for different monitoring periods, in dB(A), for NMT-1*

		L_d	L_e	L_n	L_{den}	$L_{eq,total}$
month	mean value	73.1	72.1	68.0	76.0	71.7
	σ	0.21	0.16	0.19	0.15	0.17
	max value	73.4	72.4	68.3	76.3	72.0
	min value	72.7	71.9	67.7	75.8	71.5
day	mean value	73.0	72.0	68.0	76.0	71.7
	σ	0.88	0.75	0.71	0.59	0.70
	max value	76.0	76.7	71.8	78.5	74.4
	min value	70.0	69.5	65.3	74.0	69.8
week	mean value	73.1	72.1	68.0	76.0	71.8
	σ	0.31	0.29	0.36	0.27	0.26
	max value	74.0	73.0	69.1	76.8	72.5
	min value	72.6	71.5	67.2	75.6	71.4
work day	mean value	73.4	72.2	67.9	76.1	72.0
	σ	0.36	0.33	0.42	0.32	0.31
	max value	74.5	73.3	69.1	77.0	73.0
	min value	72.9	71.6	67.1	75.6	71.5
weekend	mean value	72.2	71.6	68.1	75.8	71.1
	σ	0.31	0.63	0.53	0.37	0.27
	max value	73.0	74.7	70.2	77.0	71.9
	min value	71.7	70.6	67.3	75.1	70.6

Table 9 *Comparison of statistical parameters of noise indicators for different monitoring periods, in dB(A), for NMT-2.1*

		L_d	L_e	L_n	L_{den}	$L_{eq,total}$
month	mean value	70.4	69.9	66.9	74.3	69.4
	σ	0.17	0.24	0.32	0.24	0.16
	max value	70.6	70.3	67.4	74.7	69.6
	min value	70.1	69.7	66.6	74.0	69.1
day	mean value	70.3	69.8	66.7	74.2	69.3
	σ	0.86	0.98	1.18	0.87	0.91
	max value	73.9	73.5	74.2	79.8	72.5
	min value	68.1	65.1	61.2	71.2	61.2
week	mean value	70.4	69.9	66.9	74.4	69.4
	σ	0.35	0.85	0.85	0.62	0.36
	max value	71.5	70.8	70.4	76.8	70.3
	min value	69.9	69.2	65.7	73.6	68.9
work day	mean value	70.7	70.1	66.7	74.3	69.6
	σ	0.39	0.53	1.07	0.76	0.42
	max value	71.9	71.2	71.3	77.5	70.7
	min value	70.1	69.2	64.9	73.4	69.0
weekend	mean value	69.6	69.3	67.4	74.4	68.9
	σ	0.36	0.59	0.51	0.41	0.30
	max value	70.5	70.5	68.7	75.4	69.7
	min value	69.0	67.1	66.6	73.8	68.5

CONCLUSION

Brüel&Kjær's Environmental Noise Management System described in this paper can be successfully used for long-term noise measurements. The results obtained by permanent and semi-permanent noise monitoring are very accurate and repeatable. The semi-permanent monitoring enables the cost-effective monitoring of environmental noise and the determination of the noise indicators at multiple locations with only few noise monitoring stations.

Based on the results of permanent and semi-permanent noise monitoring and the noise indicator determination by long-term measurements which are shown in this paper, the following conclusions can be derived:

- the monthly values of noise indicators for all three locations are slightly different from mean values of noise indicators for observation interval; the standard deviation for NMT-1 ranges from 0.15 dB(A) to 0.21 dB(A), for NMT-2.1 from 0.17 to 0.32 and for NMT-2.2 from 0.17 dB(A) to 0.54 dB(A);
- 95% of daily values of noise indicators are in the acceptable range of values; the value of daily and evening noise indicator are very similar;
- shorter monitoring periods (work days or week) give the very similar values to the monthly values; the mean values of week values and monthly values are almost identical, while the standard deviations of week values have acceptable value; the mean values of work day values and monthly values are very similar;

Generally, it can be concluded that the noise monitoring with duration of one month gives very accurate and repeatable values. Also, the noise monitoring with duration of one week or only work days gives very usable values but this conclusion should be confirmed for more locations, especially where the traffic conditions and the traffic noise are more variable.

ACKNOWLEDGEMENT

This research is part of the project "Development of methodology and means for noise protection from urban areas" (No. TR-037020) and "Improvement of the monitoring system and the assessment of a long-term population exposure to pollutant substances in the environment using neural networks" (No. III-43014. The authors gratefully acknowledge the financial support of the Serbian Ministry for Education, Science and Technological Development for this work.

REFERENCES

[1] Directive 2002/49/EC of the European Parliament and the Council relating to the assessment and management of environmental noise, Official Journal of the European Communities, L 189, Vol. 45, 2002. [Online]. Available: http://eur-lex.europa.eu/legal-content/EN/TXT/?uri= CELEX:32002L0049

[2] Law on Environmental Noise Protection, Official Gazette of the Republic of Serbia, No. 36/09 and No. 88/2010, 2010. In Serbian.

[3] Regulation on noise indicators, limit values, assessment methods, noise annoyance, noise effects, impact on health, collecting data for noise assessment, (Official Gazette of the Republic of Serbia, No. 75/10.2010. In Serbian.

[4] IMAGINE Project, Deliverable 5, "Determination of L_{den} and L_{night} using measurements", 2011. [Online]. Available: http://www.certificacioacustica.cat/Documents/Articles/ D5_IMA32TR-040510-SP08.pdf

[5] SRPS ISO 1996-1: 2010, Acoustics - Description, measurement and assessment of environmental noise - Part 1: Basic quantities and assessment procedures.

[6] SRPS ISO 1996-2: 2010, Acoustics - Description, measurement and assessment of environmental noise - Part 2: Determination of environmental noise levels.

[7] M. Pljakić, B. Radičević, J. Tomić, Z. Petrović, "Analysis of systematic measurements of noise in cities", in *Proceedings of 23rd Conference with International Conference "Noise and Vibration"*, Niš, Serbia, pp. 59-62, 2012.

[8] S. Milošević, S. Bijelović, E. Živadinović, M. Jevtić, M. Popović, "Continuous environmental noise measurement in the city of Novi Sad in April 2010", in Proceedings of 22nd Conference with International Conference "Noise and Vibration", Niš, Serbia, pp. 49-52, 2010. In Serbian.

[9] M. Praščević, D. Cvetković, D. Mihajlov, "Measurement and evaluation of the environmental noise levels in the urban areas of the city of Nis (Serbia)", Environmental Monitoring and Assessment, Vol. 186, pp. 1157-1165, 2014. [Online]. Available: http://dx.doi.org/10.1007/ s10661-013-3446-2.

[10] Technical documentation – Environmental Noise Management System Software Type 7843, version 2.8.1, Bruel&Kjaer, BE 1767-15, 2010.

[11] Technical documentation – Noise Monitoring terminal Types 3639-A, 3639-B and 3639-C with Hand-held Analyzer Type 2250-N or Hand-held Analyzer Type 2250-N-D00, version 4.1.1, Bruel&Kjaer, BE 1818-17, 2013.

University of Nis
Faculty of Occupational Safety
„Politechnica“ University of Timisoara
Faculty of Mechanical Engineering
24th International Conference
NOISE AND VIBRATION
Niš, 29 - 31. 10. 2014.

NOISE AS AN INDICATOR OF ENVIRONMENTAL QUALITY - PRE-MEASUREMENTS IN SELECTED AREAS IN THE MUNICIPALITY OF VELENJE

Nikola Holeček[1,2] , Natalija Špeh[2]

[1]Gorenje d.d., Slovenia, [2] Environmental Protection College Velenje, natalija.speh@vsvo.si

Abstract - *The noise in the living and working environment significantly reduces the quality of the environment. With the expansion of cities and consequently increase of traffic, the problem of noise increases significantly. The study was performed in Velenje, a large employment centre in Šaleška valley. In terms of population it is the fifth largest city in Slovenia. In recent years, Velenje is faced with the deterioration of environmental quality and increased noise, particularly around the city's main roads. In the last decade, this area is very active in investments (thermal power plant, Gorenje), and thus the living and working environment situation worsens. The longitudinal axis of the city is the concentration of traffic and industrial activity. The aim of the project was to create a professional basis and assess the degree of exposure of certain areas and its population to different sources of noise. The study is intended to prepare a quick and effective corrective measures for protection against the influence of noise.*

1. INTRODUCTION

This paper discusses the municipal noise, which refers to the external noise environment in the municipality of Velenje. The noise inside the accommodation and service spaces (buildings, workplaces, industrial plants etc.) does not belong to municipal noise. In the urban environment, transport is by far the most troublesome noise source. With the increase of traffic and spread of urban places the problem of noise also increases.

The solution to the problems with noise can be found in considered (sustainable) spatial planning of urban development that takes into account spacial and general city maps, detailed maps of urban planning and anticipating projects. Sustainable urban development planning must include the living habits of the population living in urban areas, the development of industrial, commercial and trading areas and areas for relaxation, fun and recreation as well as the transport needs of the city.

In the measurement of urban noise we measured the total of sound pressure level on the site of immisions, which means superposition of all noise sources, the close and distant, primary and secondary as well as parasitic ones. Measurements were carried out to: determine the noise impact of the measuring area (the city) with noise, compare with permitted limit values, determine the possible measures for protection against noise and identify the noise sources and their influential area, [1,2] .

2. CURRENT LEGISLATION IN THE FIELD OF ENVIRONMENTAL NOISE

Environmental noise is governed by two regulations in accordance with the Directive of European Parliament and Council 2002/49/EC of June 25, 2002. The basic law of protection against noise is the decree of noise in natural and living environment, its amendments and other regulations, [3]. Also important, is the »Regulation of noise from road and rail transport«. Both decrees define the evaluation of noise, its limits and measures to reduce and prevent excessive noise emissions or immissions. When planning the measurements we comply with the »Regulation on evaluation and regulation of environmental noise, OJ RS, no. 121/04. This regulation specifies, in accordance with the Directive of European Parliament and Council 2002/49/EC of June 25, 2002, concerning the assessment and regulation of environmental noise (UL L no. 189 of July 18, 2002, p. 12–26) and in order to avoid, prevent or reduce harmful effects, including interference caused by noise in the environment, measures to reduce the congestion of environment with noise, particularly in relation to methods of evaluation of environmental noise, the determination of noise exposure with mapping the congestion of populated areas with noise, providing access to information on environmental noise and its effects to the public, preparation of the operational programme for protection against noise pollution, which is based on the results of mapping the areas with noise congestion, with a view to prevent and reduce it, and the preparation of a programme of action in the areas of population, which are in the class of highest level of noise congestion and are because of the exposure defined as a degraded environment. The regulation on the limit values of environmental noise indicators, Gazette RS no. 105/2005 of November 23, 2005 and no. 105/ of November 7, 2008. The regulation on the limit values of environmental noise indicators, Gazette RS, in accordance with the Directive of European Parliament and Council 2002/49/ES of June 25, 2002, on the assessment and management of environmental noise, provides for, [4-14]:

- Rate of reduction of environmental pollution by noise,
- The limit values of indicators of noise in the environment,
- The critical values of indicators of noise in the environment,

- The provisional methods for assessment noise indicators,
- Adjustments that need to be taken in account for the calculation of the value of noise indicators in the use of the provisional methods for the assessment of noise indicators,
- Measures to reduce noise emissions in the environment,
- Taxpayers to ensure operational monitoring of noise for noise sources (herein after referred to as: operating monitoring) and
- The contents of environmental licence and situations, for which environmental authorisation does not need to be obtained.

The natural and living environment is divided into four levels of protection against noise, in which they allow different noise levels (limit, critical, taper) in the day and night time.

The regulation of protection concerning noise from road and rail traffic also classifies the environment in four different levels of protection; where individual noise level must not exceed the prescribed day and night noise level.

Policy on the first measurements and operational noise monitoring for noise sources and on conditions for their implementation and changes, Gazette RS, no. 70/96 specifies the kinds of quantities of the noise that need to be measured, and monitoring of the area laded with noise.

Experts who deal with planning of interventions in the environment are, in the context of their duty, required to make an assessment of impacts on the environment, which mostly include the following activities,:

- Carry out measurements in the field;
- Assess the specific origin of noise (the noise source);
- Calculate the expected noise levels;
- Produce a simulation of the load of the environment as a result of interference in the space (noise map);
- Informing the affected residents and wider community;
- Create databases for regular and later use;
- Participating in professional discussions about possible solutions.

3. AREA OF RESEARCH

Measurements were carried out on the territory of KS Gorica. It's a sloppy compact settlement of terraced single-family houses, placed next to and above of Goriška street, the main local vein, which leads to the Eastern city and suburban areas of Velenje. Main feature of the area is residential with the providers of various services. The hill side is rising up to 480 meters above sea level.

Next to the local traffic road a green belt is planted (a barrier) with the function of noise protection. In order to determine its effectiveness, we performed the measurements next to the road, and right after the green planting. We were also wondering, how the noise level varies with height and the distance from the noise source (the traffic), so we repeated the measurements one street higher (Splitska Street). The lowest measurement point on the Goriška Street was located at 397 metres above sea level, and the highest measurements were done on Splitska Street at 413 metres above sea level.

Fig. 1 *The distribution of monitoring sights (Mapping basis: Google Earth, content: N. Špeh)*

All measurements were carried out in the open. The noise next to traffic was measures 2 metres from the edge of the road at height of 1.5 metres. Measurement of noise was carried out on working days during the week from 12:30 to 14:30. The measuring site and the results of measurements are displayed in the web application Google Earth or Google Maps and with geographic information tool ArcMap 10.2.

4. RESULTS OF MEASURMENTS

Noise immissions are highly dependent on the micro location. The noise strongly varies with distance from the source (e.g. road), but the possible presence of physical barriers (e.g. buildings) between the source and the location of observation is also important. At the same time, temporal fluctuations are also important, [15, 16].

We structured the data into five categories: 1) 0 to 40 dB, 2) 41 to 55 dB, 3) 56 - 60 dB, 4) 61- 65 dB and 5) above 65 dB.

Base line measurements point (19) was pinned 2 meters from the edge of the road (on the map 1, they are marked with no. 1-19). The value of the measurement fluctuated from 54.2 dB (min) to 75.3 dB (max). The calculated average value of sound directly at the road was 67.5 dB

Followed by a parallel line of measurement (18 monitoring stations), which we did behind the green barrier (map 1, marks 20-37). In some parts, the measured values of noise clashed with three categories lower than those of roadside (2nd category: 41-55 dB). Values ranged between the absolute lowest 51.7 dB to highest 73.2 dB. The calculated average value for noise, measured behind the barrier, was 61.6 dB, which meant almost 6 dB less than the average values measured directly next to the lane of Goriška street. With the repetition of measurements in 2013, we find a greater influence of the green barrier; the difference in average values between road line and behind the barrier amounted to 10 dB.

Green barrier in the width of about two metres represents the planting of shrubs and pine trees. Less commonly planted shrubs affected the results of measurements, because there the instrument detected higher values, in some cases even of same category as directly to the Goriška Street. The data advocate the positive influence of green barrier usage. Additional (thicker, wider) planting might achieve even more effective anti-noise protection.

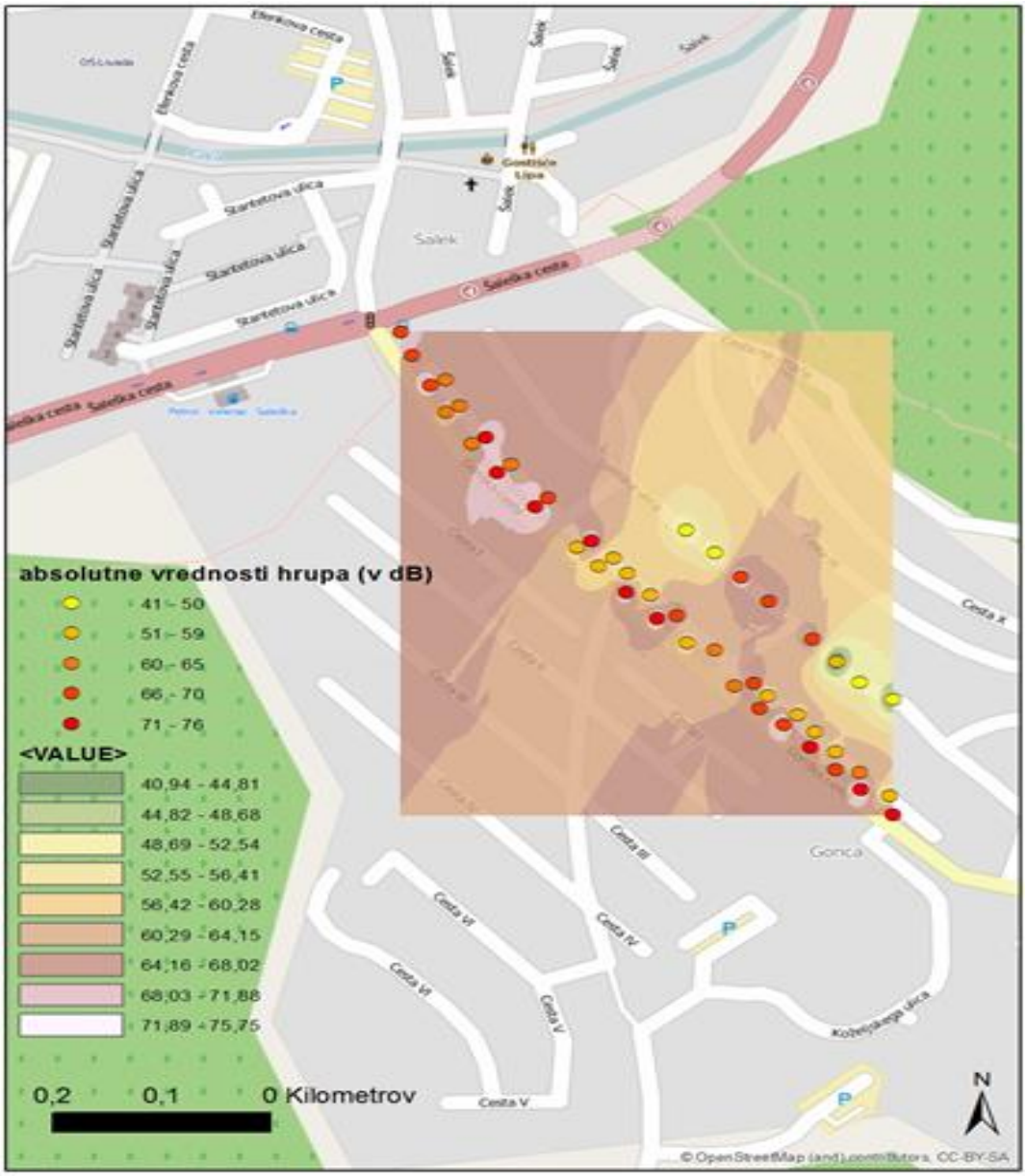

Fig. 2 *The level of noise in certain measuring points*

5. CONCLUSION

Noise in the living and working environment represents an important disturbance for a human and may significantly lower the quality of the living environment. In the urban environment transport (road) noise is by far the most troublesome. However, the problem of noise increases with the increase of traffic.

Velenje, the fifth largest city by population in Slovenia (25.329, municipality of Velenje 32.973, SURS, 2014), is an important employment centre, but at the same time it also has a transit role. In recent years, it is faced with a deterioration of the quality in the living environment, that is with transgression of burden with noise, in particular at the cities arteries. The negative impact is also reflected next to the valley axis in the direction to the neighbouring municipal centres, Šoštanj and Šmartno ob Paki. This valley axis represents the concentration of traffic and industrial activity in connection to settlement function of the space. In the last decade, this area is very investment active (TEŠ, Gorenje), which additionally worsens the situation of living and working environment and these parts of Savinja statistical region. Similarly, the traffic congestion increases beyond the urban area of the valley. There is an increasing pressure of transport activity on rural areas in the Šaleška valley, which represent a strong hinterland in terms of daily migration.

The results are represented by preliminary measurements that need to be upgraded (repetition in different times of day), if we were to use them for making the expertise with which we would determine the degree of exposure of individual areas (and the population) to various sources of noise. This is the only way we could have prepared a detailed spatial presentation and a set of necessary measures. The results of further studies could also be used for: a) creation of proposals on anti-noise measurements throughout the area with a special treatment for noise-critical parts of the municipality Velenje and b) with data, we would complement the spatial basis

(plans) and define the conditions for purposive use of space (OPN municipalities) and to determine the levels of protection against noise.

The purpose of solving the noise problem, its prevalence and spatial distribution on a wide range Šaleška valley originated from the need to update the basis for municipal spatial plans of the discussed municipalities, where for decades pressures of various anthropogenic activities come in line.

REFERENCES

[1] Prascevic M., Cvetkovic D., Environmental noise (book), University of Nis, Faculty of occupational safety of Nis, 2005.

[2] Brüel&Kjaer Sound & Vibration Measurement A/S. Prevod: IMS Industrijski merilni sistemi d.o.o., Ljubljana, Različica 2.0, leto 2009.

[3] Pravilnik o prvih meritvah in obratovalnem monitoringu hrupa z vire hrupa ter o pogojih za njegovo izvajanje, Uradni list RS št 70/1996 in 45/2002

[4] Ramšak M. 2005. 24 - urne meritve skupne obremenitve s hrupom na izbrani lokaciji ob avtocestnem odseku Krška vas – Obrežje. Ljubljana, ZAG

[5] SILENCE (Suistinable Development Global Change and Ecosystems), Practionitioner Handbook for Local Noise Action Plans, 2008

[6] SMILE (Sustainable Mobility Intitatoves for Local Environment), Guidlines for Rod Traffic Noise Abatment, 2004

[7] Uredba o mejnih vrednostih kazalcev hrupa v okolju, Uradni list RS št. 105/2005

[8] Uredba o ocenjevanju in urejanju hrupa v okolju, Uradni list RS št. 121/04

[9] [9] Uredba o spremembah in dopolnitvah Uredbe o mejnih vrednostih kazalcev hrupa v okolju, Uradni list RS, št. 34/2008 z dne 07.04.2008

[10] Zakon o varstvu okolja UL RS, št.41/2004: Uredba o hrupu v naravnem in življenskem okolju

[11] Zakon o varstvu okolja UL RS, št.41/2004: Uredba o hrupu zaradi cestnega in železniškega prometa

[12] Guiding Principles for Sustainable Spatial Development of the European Continent, 2010

[13] Čudina, M. 2001. Tehnična akustika, Ljubljana, UL FS

[14] Kang J., Urban sound environment, (Taylor & Francis, London and New York, 2007).

[15] Cigale, D., Lampič, B., 2002. Razširjenost hrupa v Ljubljani. GIS v Sloveniji 2001-2002, str. 175-184 .

[16] Cueto J. L. at all, Decision-making tools for action plans based on GIS: A case study of a Spanich agglomeration", Proceedings of Inter-noise, Lisabon, 2010

University of Nis
Faculty of Occupational Safety
„Politechnica“ University of Timisoara
Faculty of Mechanical Engineering
24th International Conference
NOISE AND VIBRATION
Niš, 29 - 31. 10. 2014.

IMPORTANCE OF MONITORING OF TRAFFIC NOISE FOR THE ACOUSTIC ZONING OF ZRENJANIN

Ivana Lakatus[1], Zivoslav Adamovic[1], Ljiljana Radovanovic[1]

[1] University of Novi Sad, Technical Faculty " Mihajlo Pupin " Zrenjanin, Serbia, vlakatus@gmail.com

Abstract - *This paper present monitoring of noise as a product of traffic in Zrenjanin. The purpose of this research is to point out the problems caused by the traffic noise. Measurements of sound levels were performed at several locations in Zrenjanin, along the main road: The corner of Nikola Pašić street near the shopping centre, Mala Varoš“.*

Milutin Milankovic Boulevard next to the Special hospital for pulmonary diseases „ Dr Vasa Savic“.

The paper gives an example of how to perform measurement in the field when determining the level of noise. In practice, for relevant datas measurement results are obtained by authorized accredited institutions that deal with measurement noise. In accordance with regulations, this research can serve as basis for future measurements and monitoring for the purpose of acoustic zoning of Zrenjanin, easier urban planning and controlling of noise level. Acoustic zoning and making zoning maps are of great importance for many urban and strategic planning.

1. INTRODUCTION

Noise is a loud, unpleasant or unexpected sound and it can be continual, uneven or impulse. It can have different levels, durations and time distribution. It has no proper definition, therefore it has to be accepted as subjective evaluation and feeling. Main sources of noise in human environment are traffic, industry, civil and construction works, recreation, sports and entertainment. Levels of noise are increasing as the life tempo is rapidly accelerating in large urban environments [1], [2].

The problem of environmental pollution has inflicted itself on us in the last decade of the last and at the beginning of current century which alarmed the whole human race and especially the developed countries to make greater steps in sustainment and protection of the environment from further degradation. Since noise is one of the problems of above mentioned pollution, more or less, this paper presents basic theoretical phenomena of noise and some of its physical characteristics and given measurement results make a solid base for evaluation of impact of traffic noise on environment in specific locations in Zrenjanin [3].

2. MEASUREMENT AND EVALUATION OF NOISE

Relevant acoustic data on noise characteristics which are obtained by measuring of acoustic amplitude and frequency are necessary for the control and evaluation of noise. Results of the measurement must have attribute of repeatability. Therefore, it is necessary to choose the appropriate instruments. In this paper, due to the large amount of data , it will only show data for one measurement (in one day) for day, evening and night. Basic attributes of noise which determine the choice of the measuring instrument are:

- Levels of noise
- Time-dependency of noise:
- Invariable noise - (up to 5 dB)
- variable noise - (above 5 dB)
- Incoherent noise – source of noise has cycles, such as passing by of one car or a plan; the level of noise decreases and increases very fast
- Impulse noise – explosive or impulse noise is a noise consisting of single bursts with a duration of less than 1s
- Frequency of noise:
- Broadband noise – a noise with even distribution of sound energy in broad frequency interval (several contiguous octaves)
- Narrowband noise – noise which energy is in limited frequency band (an octave or third of an octave)
- Tonal noise – noise which sound energy is in discreet frequencies [4], [5].

According to European Environment and Health Committee, in Serbia there are several difficulties with regard to noise such as inadequate legislation and lack of standards for levels of noise, inappropriate monitoring of noise in city areas, poor zoning of noise in urban planning, poor locations for industrial areas, limited projects for noise protection, insufficient traffic noise control, as well as inadequate traffic management [6].

In Table 1 are given appropriate sound levels.

Table 1 *From Protocol on highest appropriate levels of noise in working and living environment [7]*

Zones of noise	Purpose	The highest approved levels of noise (dB) Outdoor / indoor Day/night day/night
1.	Recreational	50 40 30 25
2.	Residential	55 40 35 25
3.	Predominantly residential	55 45 35 25
4.	Predominantly business	65 40 30
5.	Industrial	limit≤ 80 40 30

In Table 2 are given levels of traffic noise.

Table 2 *Levels of traffic noise [7]*

Main city roads (high traffic)	75 dB
Crossroads in the city centre (high traffic)	75 dB
Local roads (65% truck traffic)	70 dB
Local main roads	55 dB
Residential area streets	55 dB

3. LOCATIONS OF MEASUREMENT

Location 1 is situated next at Zitni trg to the business building „Mala Varoš“ where several city owned companies are situated and 50 meters from the building is a residential building which has several businesses in the ground floor. Picture in Fig.1 is taken during measurement.

Fig. 1 *The corner of Nikola Pašić street, Žitni square - view from the other corner [3]*

Location 2 is situated at Milutin Milankovic boulevard on part of the main city road next to a wall approximately 50 meters from the building of the hospital for pulmonary diseases „Dr Vasa Savić“. Picture in Figure 2 is taken during measurement.

Fig. 2 *Part of the city main road near the hospital for pulmonary diseases [3]*

The Fig.3 shows measurer of noise level.

Fig. 3 *Measurer of noise level [3]*

The following equipment was used during measurement:

- *Sound Level Meter with associated microphone:*
  Manufacturer: Voltcraft
  Type: SL - 400
  Class 2 according to IEC 61672-1

- *The acoustic calibrator*
  Manufacturer: Bruel & Kjaer , Denmark
  Type: 4231
  Sound level : (94 ± 0.2) dB and (114 ± 0.2) dB
  Frequency : (1,000 ± 1) Hz
  Calibration of the measuring chain, measuring noise levels and a condenser microphone made acoustic calibrator is listed on: 30.03.2014.year.

  Comparison of characteristics of the measuring chain was carried out internal audits using the following equipment :
- *A measurer of the noise level*
  Manufacturer: Bruel & Kjaer, Denmark
  Type: BK 2250
  Serial number: 2506333
  Measuring range (20 - 140) dB

Measurement of the levels of noise for the purposes of this paper was held on March 31st, 2014 [3].

For both locations instrument was 5m from the road and altitude on which the instrument was: 1,5 m.

Time frame for each measument (day, evening and night): 30 minutes.

Hourly measurements for Location 1:

Day: 09:39 h – 10:09 h

Evening: 18:33 h – 19:03 h

Night: 22:19 h – 22:49 h

Hourly measurements for Location 2:

Day: 10:26 h – 10:56 h

Evening: 19:25 h – 19:55 h

Night: 23:01 h – 23:31 h

4. RESULTS

When the measurement is performed, in the set time intervals, values measure by the instrument are methodised, sorted, and analysed. Process for the equipment used for this paper is following: computer is connected to the instrument by the cable which is the part of the equipment, and the previously installed software on the computer processes the data that instrument measures. Measured values for every second of the process are entered in Microsoft Excel table, which displays all measured values. Programme then calculates mean value for every measurement and makes a graphical chart of measured values. At Figure 4 is present only an example of how the table looks after the Microsoft Excel program read data from the instrument for easy insight into the process of calculating (every table has approximately 1700 rows) [3].

Clipboard | Font | Alignment | Numbe

Chart 1

	A	B	C	D	E	F	G
1							
2	1	9:39:01	65,2	3311311	1		68,74764
3	2	9:39:02	65,5	3548134	3		
4	3	9:39:03	64,6	2884032	5		
5	4	9:39:04	64	2511886	7		
6	5	9:39:05	68,5	7079458	9		
7	6	9:39:06	64,1	2570396	11		
8	7	9:39:07	66,6	4570882	13		
9	8	9:39:08	64,2	2630268	15		
10	9	9:39:09	65,4	3467369	17		
11	10	9:39:10	64,3	2691535	19		
12	11	9:39:11	64,8	3019952	21		
13	12	9:39:12	66,1	4073803	23		
14	13	9:39:13	68,2	6606934	25		
15	14	9:39:14	65,9	3890451	27		
16	15	9:39:15	75,5	35481339	29		
17	16	9:39:16	70,8	12022644	31		
18	17	9:39:17	65,3	3388442	33		
19	18	9:39:18	65,2	3311311	35		
20	19	9:39:19	65,5	3548134	37		
21	20	9:39:20	65	3162278	39		
22	21	9:39:21	66	3981072	41		
23	22	9:39:22	68,2	6606934	43		
24	23	9:39:23	67,7	5888437	45		

Fig. 4 *Microsoft Excel table with measured values [3]*

X -axis of the graphs indicates measurement time in seconds and the y axis indicates the measured sound pressure level in decibels . Amplitude show oscillation between the maximum and minimum values of the sound pressure, while for analytical calculation taking the average value.
Results for daily, evening and nightly interval measurements for location 1 are given in Figures 5-7 [3].

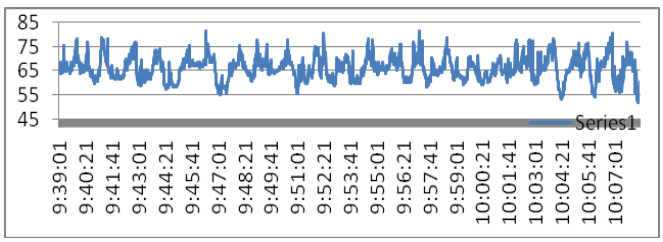

Fig. 5 *Graphic chart of results for daily interval measurements for location 1*

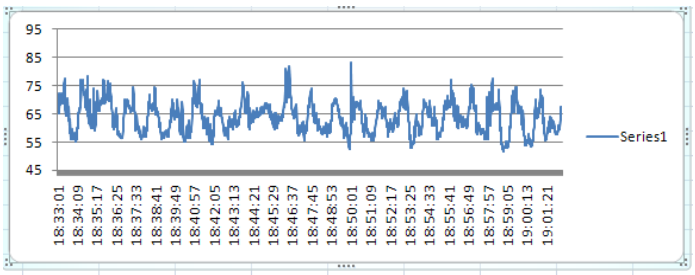

Fig. 6 *Graphic chart of results for evening interval measurements for location 1*

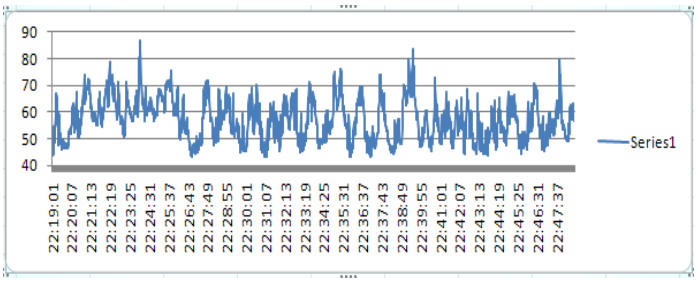

Fig. 7 *Graphic chart of results for nightly interval measurements for location 1*

All representative data are for location 1 – Žitni square, Nikola Pašić street corner. Calculation for practical measured values will be presents later in the paper after data for Location 2, for clarity of data and better analysis of calculated values of both locations.

Results for daily, evening and nightly interval measurements for location 2 are given in Figures 8-10 [3].

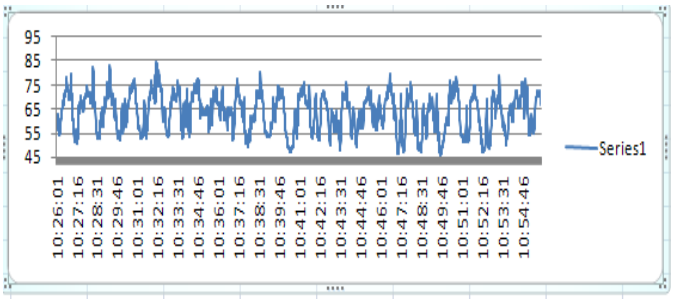

Fig. 8 *Graphic chart of results for daily interval measurements for location 2*

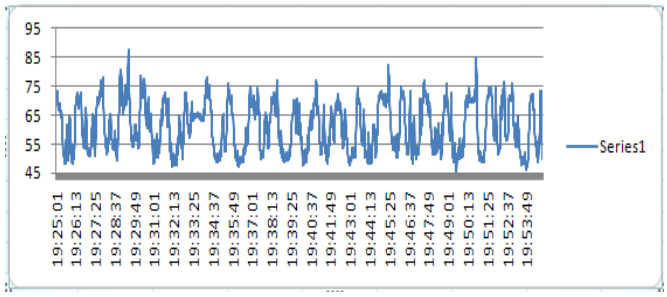

Fig. 9 *Graphic chart of results for evening interval measurements for location 2*

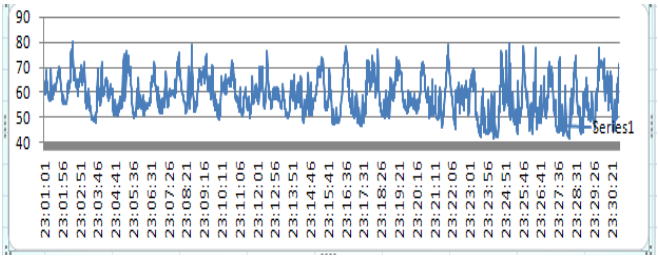

Fig. 10 *Graphic chart of results for nightly interval measurements for location 2*

5. ANALYTICAL CALCULATION OF NOISE

Level of noise for day-evening-night $\mathbf{L_{den}}$ (d – day , e – evening, n – night) in decibels dB(A) is defined by the equation below [8], [2]:

$$L_{den} = 10\ log\ \frac{1}{24}\left(12 \cdot 10^{\frac{L_{day}}{10}} + 4 \cdot 10^{\frac{L_{evening}+5}{10}} + 8 \cdot 10^{\frac{L_{night}+10}{10}}\right) \quad (1)$$

A - Weighted average for long-term levels of noise for specific periods of day is defined by the equation (2).

$$L_{Aeq,T} = 10log\left[\frac{1}{N}\sum_{i=1}^{N} 10^{0,1(L_{Aeq,T})i}\right] \quad (2)$$

In Table 3 are shown the values which are read off for all three periods of the measurement for location 1 [3].

Table 3 *Datas for calculation of L_{den} for location 1*

Measurement period	Ruling period	Measured value [dB(A)]
Day	12h	**65,97**
Evening	4h	**63,66**
Night	8h	**56,93**

Based on the previously presented equations 1 and 2 and datas from Table 3, it is calculated :

L_{DEN} = **64,03dB (A)**

In Table 4 are shown the values which are read off for all three periods of the measurement for location 2 [3].

Table 4 *Datas for calculation of L_{den} for location 2*

Measurement period	Standard period	Measured value [dB(A)]
Day	12h	**63,68**
Evening	4h	**60,8**
Night	8h	**58,41**

Based on the previously presented equations 1 and 2 and datas from Table 4, it is calculated:

L_{DEN} = **62,04 dB(A)**

Standard period is a period of 24 hours and it refers to daytime lasting from 6 till 18h , evening lasting from 18 till 22h and night lasting from 22 till 6h. In the table thre are number of hours for every period.

Note: Parameter L_{den} was calculated based on 1,5 h measurement. This was calculated by summing 30 minute intervals for every period of measurement – day, evening and night.

Table 5 shows the values read from the graphs of appropriate measurement - day, evening and night for the minimum and maximum values of the sound pressure for location 1 [3].

Table 5 *Measured values for location 1*

	L_{Aeq} [dB(A)]	$L_{AF\ max}$ [dB(A)]	$L_{AF\ min}$ [dB(A)]
Day	65,97	81,5	51,7
Evening	63,66	83,2	51,7
Night	56,93	86,6	43,1

L_{AFmax} [dB (A)] are maximum measured values of sound pressure

L_{AFmin} [dB(A)] are minimum measured values of sound pressure

Table 6 shows the values read from the graphs of appropriate measurement - day, evening and night for the minimum and maximum values of the sound pressure for location 2 [3].

Table 6 *Measured values for location 1*

	LAeq [dB(A)]	LAF max [dB(A)]	LAF min[dB(A)]
Day	63,68	84,7	45,7
Evening	60,8	87,7	45,5
Night	58,41	80,3	42,1

LAF max [dB(A)] are maximum measured values of sound pressure

LAF min[dB(A)] are minimum measured values of sound pressure

Noise measurement and result analysis were performed in accordance with standards SRPS ISO 1996 – 1 Acoustics -- Description and measurement of environmental noise -- Part 1: Basic quantities and procedure and SRPS ISO 1996 – 2 Acoustics -- Description, measurement and assessment of environmental noise -- Part 2: Determination of environmental noise levels. Calculation of results was also performed in accordance to the above standards above [4], [5].

6. ACOUSTIC ZONING IN ZRENJANIN

Traffic parameters that are taken into account while discerning levels of noise are: Car frequency, tractor frequency, heavy vehicle frequency, bus frequency, motorcycle frequency.

Bypass zone – bypass is one the most important traffic corridors in Zrenjanin, Fig.11. Realisation of the road connecting southeast entrance to the city from the Belgrade-Zrenjanin main road, following east and north border of the General urban planning project to the Novi Sad-Zrenjanin main road, will allow transferring transit traffic outside of the city and direct it towards the corridor.

Planning of the bypass area (petrol station, gas station etc.), will completely adapt this traffic corridor to the planned activities. Corridor is connected to the city streets by means of existing feeding roads exiting the town. There are no plans for connecting other streets to the corridor.

The measured values impose a conclusion that we should have necessary measures in order to decrease those values. Systematic monitoring of levels of noise determines acoustic pressure thus creating condition for acknowledging the problem of noise and incorporating it in the urban planning of new and reconstruction of existing residential areas. Construction and certificates of acceptance for residential, investment, industrial, small business buildings, and city infrastructure should comply with determined technical regulations which guarantee with quality of acoustic insulation. In this specific case, for Zrenjanin, based on measured values and levels of traffic noise and in opinion of the authors the best solution for the city would be finishing the bypass around the city, especially for the heavy vehicles that should not be allowed to use main city road, albeit city centre [3], [9] and [10].

7. CONCLUSION

In order to determine acoustic zones in the city, it is necessary to measure all sources of noise– traffic, industry etc. on the referent locations where results can reflect the level of noise in that zone. This way, certain areas of the city can be organised and planned, noise can be easily monitored, and inspections and supervising authorities can have better overview of the natural or legal person or persons who produce noise of the certain level, especially those who breach appropriate limits. This would establish a system of monitoring of noise within the city territory with purpose of long-term solution to the problems caused by noise, especially a problem of noise as health hazard.

Therefore, there is a possibility to perform acoustic zoning in Zrenjanin (which haven't been done before), give greater significance to noise monitoring, finish the bypass around the city which was mentioned in this paper.

There are excellent solution which could be applied in the shortest period, of course with appropriate funding and engagement of experts and institutions.

In Serbia, in addition to compliance with the European legislation and limit values for noise, it should be worked on noise monitoring in urban areas, the activities of the zoning noise in the spatial planning process.

Fig. 11 *Bypass zone – the most important traffic corridors in Zrenjanin (mark red and blue lines) [9]*

REFERENCES

[1] Adamovic, Z., Bursac, Z., Eric, S., Vibration and Noise Causes - Diagnosis - protection, Serbian academic Center, Novi Sad, 2014.

[2] Cvetkovic, D., Prascevic, M., Noise and Vibrations, University of Nis, Faculty of Occupational Safety, 2005.

[3] Lakatus, I, Importance of monitoring road traffic noise in the city of Zrenjanin, thesis, Technical faculty „Mihajlo Pupin" Zrenjanin, 2014.

[4] ISO 1996-1 Acoustics - Description, measurement and assessment of environmental noise - Part 1: Basic quantities and assessment procedures

[5] ISO 1996-2 Acoustics - Description, measurement and assessment of environmental noise - Part 2: Determine the level of environmental noise

[6] European Environment and Health Committee, Source: http://www.euro.who.int

[7] The Law on the Protection of environmental noise ("Off. Gazette of RS", no. 36/2009 and 88/2010)

[8] Bruel & Kjaer, Noise and Vibrations, 1998.

[9] Ljubojev, N., Bjelajac, Z., Mijatovic, MD., Kozar, V., Radovanovic, Lj., Implementation of the European Legislation on Protection of Noise Emissions in Republic of Serbia with a Particular View on Noise from Motor Vehicles, JOURNAL OF THE BALKAN TRIBOLOGICAL ASSOCIATION, (2014), vol. 20 br. 2, p. 300-308

[10] http://www.zrenjanin.rs

BRÜEL & KJÆR
SOUND & VIBRATION
MEASUREMENTS

We help our partners and customers
measure and manage
the quality of sound and vibration
in products and enviroment

With more than 90 sales offices or local agents,
we provide immediate and comprehensive
customer support

Contact your local
sales representative:

RMS d.o.o.
Partizanske avijacije 12/3
11070 Novi Beograd, Srbija
Tel.: +381(0)11 2280 951
Fax: +381(0)11 2280 751
www.rms.rs

Brüel & Kjær

University of Nis
Faculty of Occupational Safety
„Politechnica“ University of Timisoara
Faculty of Mechanical Engineering
24th International Conference
NOISE AND VIBRATION
Niš, 29 - 31. 10. 2014.

ASSESSMENT OF HARMFUL HEALTH IMPACT OF ENVIRONMENTAL NOISE

Darko Mihajlov[1], *Momir Praščević*[1], *Aleksandar Gajicki*[2]

[1] University of Nis, Faculty of Occupational Safety, Serbia, darko.mihajlov@znrfak.ni.ac.rs
[2] Institute of transportation CIP, Belgrade, Serbia

Abstract – *Environmental noise is an unavoidable phenomenon in urban environments. Even though efforts are continuously being made to reduce exposure to environmental noise, it still presents a problem, mostly due to rapid development of urbanization and transportation. Road, railway, and aircraft traffic are the main contributors to the overall environmental noise load. The ever-decreasing quiet zones in urban areas impact the health and well-being of urban population. Excessive exposure to noise can potentially cause a number of physical or psychological health effects, such as sleep disturbance, restricted communication, annoyance, cognitive impairment, and stress. The cardiovascular system can also be affected by prolonged exposure to traffic noise. Nevertheless, the precise impact of environmental noise has to be determined through risk assessment.*

Keywords: environmental noise, burden of disease, DALYs

1. INTRODUCTION

The scope of disease burden on a population is disease-specific. Over the past few decades, the disease burden has been systematically measured across many countries for the purpose of comparison. A burden of disease (BD) can be defined as the impact of a specific disease over a specific area as indicated by financial cost, mortality, or morbidity. BD is quantified by the WHO-developed summary measures of population health.

Summary measures of population health combine information on mortality and non-fatal health outcomes to provide a single-number representation of the health of a specific population. To that end, several indicators have been developed during the last 30 or so years to adjust mortality to reflect the impact of morbidity or disability. Based on the object of quantification, the measures are divided into two main categories: health expectancies and health gaps [2,7,11].

Health expectancies measure life years gained or years of improved quality of life. The following are some of the indicators included in this group:

- active life expectancy (ALE),
- disability-free life expectancy (DFLE),
- disability-adjusted life expectancy (DALE),
- healthy-adjusted life expectancy (HALE),
- quality-adjusted life expectancy (QALE).

Health gaps measure lost years of full health as compared to an “ideal” health status or the accepted standard. This group includes the following indicators:

- years of potential life lost (YPLL),
- years of healthy life lost (YHLL),
- quality-adjusted life years (QALY),
- disability-adjusted life years (DALY).

Both categories use time and multiply the number of years lived (or not lived, in the event of premature death) by the “quality” of those years. The adjustment of the years of healthy life lived is called “quality adjustment” (expressed as QALYs), whereas the adjustment of the years of healthy life lost is called “disability adjustment” (expressed as DALYs) [1,13]. Accordingly, QALYs represent a gain that is to be maximized, whereas DALYs represent a loss that is to be minimized. The QALY approach weights the quality (also called “utility”, as this falls within cost-utility analyses) on a scale from 1, indicating perfect health and the highest quality of life, to 0, indicating no quality of life, i.e. death. The DALY approach reverses the scale goes: a weighted 0 indicates perfect health (no disability), while a weighted 1 indicates death. The disability weighting in the DALY approach proved to be its most difficult aspect and has even sparked some controversy [1]. Figure 1 shows a typology of summary measures of population health.

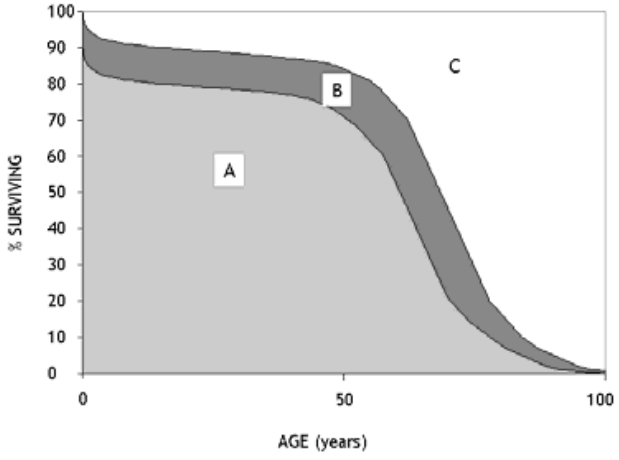

Figure 1. *A typology of summary measures* [11]
LEGEND: A = time lived in optimal health,
B = time lived in suboptimal health,
C = time lost due to mortality

2. BURDEN OF DISEASE FROM ENVIRONMENTAL NOISE

Noise is a major issue in urban environments, as it affects a large section of the population. So far, most environmental noise assessments have been focused on the annoyance it causes for humans or on the extent to which it affects daily human activities. Earlier assessments of the potential health impact of noise exposure have been insufficiently comprehensive [3].

There is a consensus among public health experts that environmental risks constitute 24% of the burden of disease. Such percentage is to a large extent due to widespread exposure to environmental noise from road and rail infrastructure, airports, and industrial sites. Every third individual experiences diurnal annoyance and every fifth individual suffers from nocturnal sleep disturbance due to traffic noise. Epidemiological evidence suggests that chronical exposure to high levels of environmental noise increases the risk of cardiovascular diseases such as myocardial infarction. Therefore, noise pollution is regarded as both an environmental nuisance and a public health threat.

Risk assessment of environmental noise requires knowledge of the following parameters:

- the nature of the health effects of noise;
- the exposure levels that instigate the health effects and the changes in the extent of the effects caused by increased noise levels; and
- the number of people exposed to hazardous levels of noise.

The WHO has developed and implemented quantitative risk assessments based on EBD (Environmental Burden of Disease) methodology to help the Member States quantify several environment-related health problems [14].

The specific health manifestations of environmental noise included:

- cardiovascular diseases,
- cognitive impairment,
- sleep disturbance,
- tinnitus, and
- annoyance.

Estimating the environmental burden of disease (EBD) due to environmental noise requires a quantitative risk assessment approach. Risk assessment involves hazard identification, population exposure assessment, and determination of the corresponding exposure-response relationships. The EBD is expressed as DALYs.

2.1 Exposure assessment

Noise exposure assessment requires that several factors be considered, such as

- the measured or calculated/predicted exposure, described in terms of an adequate noise metric; or
- the distribution of noise exposure of the population.

Population noise exposure is based on the noise mapping mandated by the Environmental Noise Directive (END), using the annual average metrics of L_{den} (day-evening-night equivalent level) and L_{night} (night equivalent level) proposed by the Directive:

$$L_{den} = 10 \cdot \log\left[\frac{1}{24}\left(12 \cdot 10^{\frac{L_{day}}{10}} + 4 \cdot 10^{\frac{L_{evening}+5}{10}} + 8 \cdot 10^{\frac{L_{night}+10}{10}}\right)\right] \quad (1)$$

with $L_{day} = L_{eq,12h}$, $L_{evening} = L_{eq,4h}$, $L_{night} = L_{eq,8h}$, and $L_{Aeq,th}$ the A-weighted equivalent sound pressure level over *t* hours outside at the most exposed facade.

Synthesis curves for the exposure-response relationships between L_{den} and %HA (proportion of highly annoyed persons) or %A (proportion of annoyed persons) are presented in the EC "Position paper on dose response relationships between transportation noise and annoyance" [4]. The curves follow from a comprehensive set of data from 46 studies on traffic noise and annoyance (20 on aircraft, 18 on road traffic, and 8 on railway noise) conducted in Europe, North America, and Australia between 1971 and 1993 [9,10]. Table 1 and Figure 2 show the proportion of highly annoyed and annoyed persons as a function of the L_{den} exposure for each traffic noise source. The data unequivocally shows that air traffic noise causes more annoyance than road traffic for any given noise level, just as road traffic causes more annoyance than railway traffic.

Table 1. *Percentage of annoyed (%A) and highly annoyed (%HA) persons for various noise exposure levels (L_{den}) for aircraft, road traffic, and rail traffic* [4]

L_{den}	Aircraft		Road traffic		Rail traffic	
[dB(A)]	%A	%HA	%A	%HA	%A	%HA
45	11	1	6	1	3	0
50	19	5	11	4	5	1
55	28	10	18	6	10	2
60	38	17	26	10	15	5
65	48	26	35	16	23	9
70	60	37	47	25	34	14
74	73	49	61	37	47	23

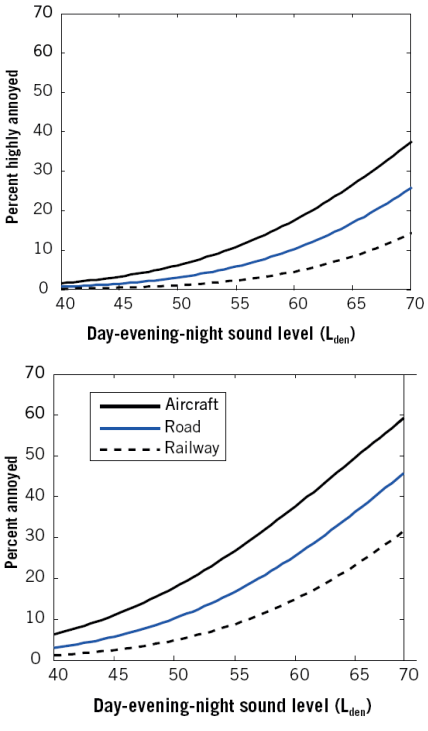

Figure 2. *Percentage of highly annoyed (top) and annoyed (bottom) persons as a function of exposure to aircraft, road, and railway noise (L_{den})*

2.2 Estimation by means of disability-adjusted life years (DALY)

DALYs represent the sum of potential years of life lost due to premature death and the equivalent years of "healthy" life lost due to ill health or disability.

The burden of disease in the general population is expressed in terms of DALYs through the equation

$$DALY = YLL + YLD. \quad (2)$$

YLL denotes the number of "Years of Life Lost" calculated by the equation

$$YLL = \sum_i \left(N_i^m \cdot L_i^m + N_i^f \cdot L_i^f\right), \quad (3)$$

where $N_i^m \left(N_i^f\right)$ is the number of deaths of males/females in age group *i* multiplied by the standard life expectancy $L_i^m \left(L_i^f\right)$ of males/females at their age of death.

The YLLs constitute the mortality component of the DALYs and they are proportional to the number of deaths and the average age of death:

$$YLL = \text{Number of Deaths} \cdot \text{Life expectancy at age of death}$$

YLD denotes the number of "Years Lived with Disability" calculated by the equation

$$YLD = I \cdot DW \cdot D, \quad (4)$$

where I is the number of incident cases multiplied by a disability weight (DW) and an average duration D of disability in years. DW applies to every health condition and ranges between 0 (full health) and 1 (death).

The YLDs constitute the morbidity component of the DALYs.

Disability weights are essential for DALY calculation, as they enable direct comparison of morbidity and mortality. DW reveals the severity of a disease on a scale from 0 (perfect health) to 1 (the worst possible health). The disease severity is inversely proportional to the length of healthy life of afflicted persons.

With the use of DWs, non-fatal health outcomes and deaths can be measured under a common unit [6]. DWs quantify time lived in various health states to be valued on a scale that factors societal preferences in. The DWs commonly used for calculating DALYs are measured on a scale from 0 (full health) to 1 (death) (see Table 2.).

DW values for various disease states have been heavily discussed among researchers. They are typically extracted from expert panels. WHO provides a fairly comprehensive list of DWs [8] recommended for use. If an appropriate DW is not included in the list, an expert committee may be formed to determine the appropriate DW by analogy with other known DWs.

Table 2. *Disability weight vs health condition* [5]

Health condition	Disability weight
Mortality	1.000
Non-fatal acute myocardial infarction	0.406 (WHO)
Ischaemic heart disease	0.350 (de Hollander, 1999)
High blood pressure	0.352 (Mathers, 1999)
Primary insomnia	0.100 (WHO, 2007)
Sleep disturbance	0.070 (WHO, 2009)
Annoyance	0.020 (WHO, preliminary) 0.010 (Stassen, 2008) 0.033 (Müller-Wenk, 2005)
Cognitive impairment	0.006 (Hygge, 2009)

These examples reveal the issue of data evaluation. The number of people suffering from myocardial infarction is relatively low, whereas the number of people experiencing sleep disturbance and annoyance is high.

Estimation of the total burden of disease requires another approach, which involves the following steps:

a) estimation of the exposure distribution in a population;
b) selection of one or more relevant relative risk estimates from the literature, usually from a newer meta-analysis;
c) estimation of the population-attributable fraction using the formula for population-attributable fraction.

This approach is called the exposure-based approach. Likewise, the number of cases can sometimes be directly estimated based on exposure (the outcome-based approach).

The attributable fraction is the proportion of noise-related disease in the population. The attributable fraction (also known as impact fraction or population-attributable risk) refers to the hypothetical reduction in disease incidence if the population were completely unexposed compared with the actual exposure pattern. It may also be difficult to specify the accuracy of the fraction of the outcome attributable to environmental noise. In order to estimate the population-attributable risk percentage for a population, the exposure distribution and the exposure-response relationship have to be known. To calculate the attributable risk percentage (AR%), the population-attributable risk percentage (PAR%), and the population-attributable risk (PAR) for each noise category [12], the following formulae can be used:

$$AR\% = (RR-1) / RR \cdot 100\ [\%]$$

$$PAR\% = P_e/100 \cdot (RR-1) / (P_e/100 \cdot (RR-1) + 1) \cdot 100\ [\%]$$

$$PAR = PAR\% / 100 \cdot N_d \quad (5)$$

RR = relative risk,
P_e = percentage of the exposed population [%],
N_d = number of subjects with disease (disease incidence).

It is also possible to use a generalized formula for calculating the population-attributable fraction (PAF). This formula is better suited to multiple comparisons for large relative risks.

$$PAF = \{\Sigma(P_i \cdot RR_i) - 1\} / \{\Sigma(P_i \cdot RR_i)\} \quad (6)$$

P_i = proportion of the population in exposure category *i*

RR_i = relative risk in exposure category *i* compared to reference level $P_i = 1$

$$PAR = PAF \cdot N_d \quad (7)$$

The above estimates of disease burden from environmental noise rely on the available information on exposure distributions in the population and exposure-response

relationships for each specific health outcome. In addition, the estimates are heavily dependent on the selected disability weight. However, the calculations of DALYs cannot be completely accurate because the information about various environmental aspects is somewhat limited and frequently relies on assumptions and guesswork (see Figure 3). Consequently, the estimates are to be taken provisionally, especially for cognitive effects and ischaemic heart disease, for which no reliable exposure-response relationships are available. Nevertheless, such calculations could provide valuable information for risk assessment, as well as for assessments of noise-related economic cost. Hence, it is recommended that the estimates of disease burden from environmental noise should be frequently updated.

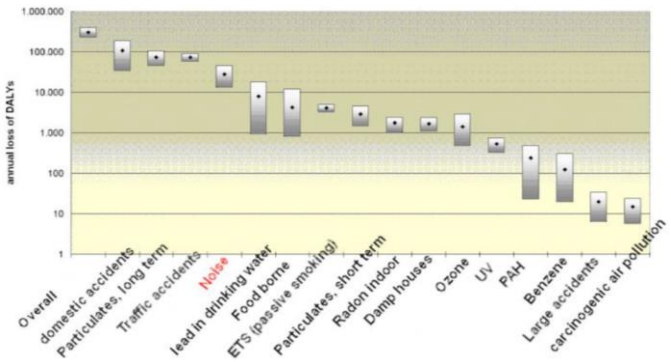

Figure 3. *Estimate of DALYs from different environmental aspects* [5]

CONCLUSION

Environmental noise represents not only a source of nuisance but also a threat to both public and environmental health. The estimation of DALYs lost due to environmental noise in the Western European countries is 61,000 years for ischaemic heart disease, 45,000 for cognitive impairment in children, 903,000 for sleep disturbance, 22,000 years for tinnitus, and 654,000 years for annoyance. When considered together, the disease burden would range from 1.0 to 1.6 million DALYs. This implies that no less than 1 million healthy life years in the Western European countries, including the EU Member States, are lost annually due to traffic-related noise [15]. Sleep disturbance and annoyance due to road traffic noise are prevalent in the disease burden from environmental noise in Western Europe. Unavailability of exposure data for South-eastern Europe and the Newly Independent States prevents estimations of the disease burden to be made for the whole WHO European Region.

ACKNOWLEDGEMENT

This research is part of the project "Development of methodology and means for noise protection from urban areas" (No. TR-037020) and "Improvement of the monitoring system and the assessment of a long-term population exposure to pollutant substances in the environment using neural networks" (No. III-43014. The authors gratefully acknowledge the financial support of the Serbian Ministry for Education, Science and Technological Development for this work.

REFERENCES

[1] Arnesen TM, Norheim OF. *Disability Adjusted Life Years - possibilities and problems*. National Institute of Public Health, Oslo, Norway. Available from URL: http://iier.isciii.es/supercourse/lecture/lec2911/index.htm. Accessed: April 8, 2009.

[2] Atanackovic-Markovic Z, Bjegovic V, Jankovic S, et al. *The burden of disease and injury in Serbia*. Serbian Burden of Disease study - an EU funded project managed by the European Agency for Reconstruction. Belgrade: Ministry of Health of the Republic of Serbia; 2003.

[3] de Hollander AE et al. *An aggregate public health indicator to represent the impact of multiple environmental exposures*. Epidemiology, 1999, 10:606–617.

[4] EC. *Position paper on dose response relationships between transportation noise and annoyance*. 2002, European Commission, Office for Official Publications of the European Communities: Luxembourg.

[5] European Environment Agency, *Good practice guide on noise exposure and potential health effects*, ISBN 978-92-9213-140-1, doi:10.2800/54080, 2010

[6] International Organization for Standardization. *Description and measurement of environmental noise. Part 2. Guide to the acquisition of data pertinent to land use*. Geneva, 1991 (ISO 1996-2).

[7] Jankovic S. *Summary measures of population health and their relevance for health policy*. In: Galan A, Scintee G, editors. Public Health Strategies. A handbook for teachers, researchers, health professionals and decision makers. Lage: Hans Jacobs Publishing Company; 2005. p.190-207. Available from URL: http://www.snz.hr/phsee/publications.htm. Accessed: August 14, 2009.

[8] Mathers CD et al. *Global burden of disease in 2002: data sources, methods and results*. Geneva, World Health Organization, 2003 (Global Programme on Evidence for Health Policy Discussion Paper No. 54).

[9] Miedema, H.M. and C.G. Oudshoorn. *Annoyance from transportation noise: relationships with exposure metrics DNL and DENL and their confidence intervals*. Environ. Health Perspect., 2001. 109(4): pp. 409–16.

[10] Miedema, H.M. and H. Vos. *Exposure-response relationships for transportation noise*. J Acoust Soc Am, 1998. 104(6): pp. 3432–45.

[11] Murray CJL, Lopez AD. *Assessing health needs: the Global Burden of Disease Study*. In: Detels R, McEwen J, Beaglehole R, Tanaka H, editors. Oxford Textbook of Public Health - Fourth edition. New York: Oxford University Press Inc.; 2004. pp. 243-54.

[12] Prüss-Üstün A et al. *Introduction and methods: assessing the environmental burden of disease at national and local levels*. Geneva, World Health Organization, 2003.

[13] Tulchinsky TH, Varavikova EA. *Measuring and evaluating the health of a population*. In: Tulchinsky TH, Varavikova EA. The New Public Health. An Introduction for the 21st century. San Diego: Academic Press; 2000. pp. 113-68.

[14] WHO, *Quantifying environmental health impacts* [web site], Geneva, 2010 (http://www.who.int/quantifying_ehimpacts/en/, accessed 21 July 2010).

[15] WHO Regional Office for Europe, *Burden of disease from environmental noise - Quantification of healthy life years lost in Europe*, ISBN: 978 92 890 0229 5, 2011

University of Nis
Faculty of Occupational Safety
„Politechnica“ University of Timisoara
Faculty of Mechanical Engineering
24th International Conference
NOISE AND VIBRATION
Niš, 29 - 31. 10. 2014.

SELF EXCITED VIBRATION OF A LINE ELEMENT OF BUILDING LINES STRUCTURE

Livija Cveticanin[1]

[1] ANKUV, Novi Sad, cveticanin@uns.ac.rs

Abstract - *Structure element of a building connected with the ground in a line is usually modeled as a beam with the Winkler type support. The elastic property of the support is assumed to be linear or with cubic nonlinearity. Unfortunately, the experiments do not prove such an assumption. It is evident that the nonlinearity is with the order which is a real positive number which need not to be an integer. In this paper the generalization of the beam with Winkler support is done by introducing the nonlinearity of any non-integer order. The line structure, i.e., beam has transversal vibrations. The mathematical description of these vibrations is a nonlinear partial differential equation. To solve the equation, we suggest an analytic procedure. The solution is assumed as a product of a time and a displacement function. After averaging, the problem transforms into a second order nonlinear differential equation. The approximate solution has the form of a cosine (ca) Ateb function. Analyzing the obtained results the influence of support properties on the system behavior is considered. The attention is given to the influence of the Winkler-Pasternak foundation, too.*

1. INTRODUCTION

The problem of beam vibration continually supported with elasticfounadtion is not a new one. Winkler was the first to introduce a continualy distributed linear support [1] which was assumed to model the connection between the beam and the foundation. The elastic property is supposed to be a linear one. The vibrations of the beam on the linear elastic foundation is modeled with a liner partial differential equation. Depending on the boundary conditions of the supproted beam, the solution of the equation are obtained. Further investigation in beam vibration required the improvement of the mathematical model due to improvement of foundation modelling. Thus, two types of models appear: one which includes the – Pasternak type of foundation [2] and the other which takes into consideration of the nonlinear properties of the foundament. Usually, instead of linear elastic function a weak nonlinear cubic order elastic force is considered [3]. The nonlinearity is assumed to weak in comparison to the linear terms. A significant number of papers is published where various mathematical models for solving partial differential equations with small nonlinearity are developed [4,5]. Recently, also the equation with strong cubic nonlinearity is considered. Results obtained by solving this equation are more appropriate than for the small cubic nonlinearity. Experimetnal investigation show that nonlinearity in foundation need not to be of cubic type. Usually, the nonlinearity is a deflection function with the order which may be any positive rational number (integer or non-integer) not smaller than 1. In this paper the self-excited vibration of a simply supported uniform beam on such strong nonlinear foundation is considered.

2. MATHEMATICAL MODEL OF THE SYSTEM

Mathematical model of vibration of a uniform beam on a nonlinear foundation is as follows

$$EI\left(\frac{\partial^4 u}{\partial x^4}\right)+\rho A\left(\frac{\partial^2 u}{\partial t^2}\right)+c_\beta u|u|^{\beta-1}=0, \quad (1)$$

where EI is the rigidity of beam, ρA is the elementary mass, c_β is the coefficient of rigidity of foundation and $\beta \geq 1$ is the order of nonlinearity. For the simply supported beam the boundary conditions are

$$\left(\frac{\partial^2 u}{\partial x^2}\right)_l=\left(\frac{\partial^2 u}{\partial x^2}\right)_0=0, \quad u(0)=u(l)=0, \quad (2)$$

where l is the length of the beam.

Let us assume the solution of (1) in the simple form [6]

$$u(x,t)=X(t)\sin(n\pi x/l) \quad (3)$$

where X(t) is an unknown time variable function, l is the length of the beam and n=1,2,... The solution (3) satisfies initial conditions (2). Substituting (3) into (1) it is

$$\left(\ddot{X}\rho A-XEI\left(\frac{n\pi}{l}\right)^4\right)\sin\left(\frac{n\pi x}{l}\right)+c_\beta X|X|^{\beta-1}\left(\sin\left(\frac{n\pi x}{l}\right)\right)^\beta=0. \quad (4)$$

Due to (4) it is evident that (3) is not an exact solution of (1). It represents only an approximate solution. Besides, the equation (4) depends on two variables x and t. The aim is to eliminate from (4) the functions with variable x. Let us divide the relation (4) with sin(nπx/l). We have

$$\left(\ddot{X}\rho A+XEI\left(\frac{n\pi}{l}\right)^4\right)+c_\beta X|X|^{\beta-1}\left(\sin\left(\frac{n\pi x}{l}\right)\right)^{\beta-1}=0. \quad (5)$$

This is at this point where the averaging procedure is introduced. Integrating the sinus function over its period of 2π, we obtain

$$\ddot{X}\rho A + XEI\left(\frac{n\pi}{l}\right)^4 + c_\beta C_\beta X\left|X\right|^{\beta-1} = 0, \quad (6)$$

where

$$\varphi = \frac{n\pi x}{l}, \quad C_\beta = \frac{1}{2\pi}\int_0^{2\pi} \left|\sin(\varphi)\right|^{\beta-1} d\varphi. \quad (7)$$

The equation (6) is a strongly non-linear. Namely, the linear terms are much more smaller than the last term in (6). It requires the equation to be treated as a strong nonlinear one, i.e.,

$$\ddot{X} + k_\beta^2 X\left|X\right|^{\beta-1} = -\varepsilon k_1^2 X, \quad (8)$$

where $\varepsilon<<1$ is a parameter of the linear term, while k_β is the coefficient of the nonlinear term, i.e.,

$$k_\beta^2 = \frac{c_\beta C_\beta}{\rho A}, \quad \varepsilon k_1^2 = \frac{EI}{\rho A}\left(\frac{n\pi}{l}\right)^4. \quad (9)$$

Now, the main task is to obtain the frequency properties of the system. It requires to find the solution of the strong nonlinear differential equaiton (8). Unfortunately, it is not an easy task.

3. SOLVING OF THE EQUATION

Let us assume a procedure for obtaining approximate solution of (8). The suggested method is based on the exact solution of the pure nonlinear differential equation ($\varepsilon=0$). As is supposed that the equation (8) is the perturbed version of the pure nonlinera equation, the approximate solution is assumed in the form of the exact solution but with time variable parameters.

For $\varepsilon=0$, the equation (8) transforms into a pure nonlinear equation

$$\ddot{X} + k_\beta^2 X\left|X\right|^{\beta-1} = 0. \quad (10)$$

For this equation the exact analytical solution has the form of an Ateb function [7]:

$$X = X_0 ca(\beta, 1, \psi), \quad (11)$$

where the phase angle of the cosine-Ateb function *ca* is

$$\psi = \Omega t + \theta, \quad (12)$$

with θ=const., X_0 is the amplitude of the oscillatory function and Ω is the frequency of the function which depends on the amplitude of vibration X_0 as

$$\Omega = \sqrt{\frac{k_\beta^2\left|X_0\right|^{\beta-1}(\beta+1)}{2}}. \quad (13)$$

The first time derivative of (11) is

$$\dot{X} = -\frac{2X_0\Omega}{\beta+1} sa(1, \beta, \psi), \quad (14)$$

where *sa* is the sine-Ateb function [7].

3.1 Approximate solution

We assume the solution of (8) and its time derivative in the form (11) and (14) but with time variable parameters:

$$X = X_0(t) ca(\beta, 1, \psi(t)), \quad (15)$$

$$\dot{X} = -\frac{2X_0(t)\Omega(X_0)}{\beta+1} sa(1, \beta, \psi(t)), \quad (16)$$

where

$$\dot{\psi}(t) = \Omega(X_0) + \dot{\theta}(t), \Omega(X_0) = \sqrt{\frac{k_\beta^2\left|X_0(t)\right|^{\beta-1}(\beta+1)}{2}} \quad (17)$$

and $X_0(t)$ and $\theta(t)$ are unknown functions. Substituting the assumed solution into (8) it is

$$\dot{X}_0 sa + \frac{2X_0\dot{\theta}}{\beta+1} ca^\beta = \varepsilon k_1^2 X_0\left|X_0\right|^{(1-\beta)/2}\sqrt{\frac{2}{(\beta+1)k_\beta^2}} ca. \quad (18)$$

Let us calculated the first time derivative of (15)

$$\dot{X} = \dot{X}_0 ca - \frac{2X_0\Omega}{\beta+1} sa - \frac{2X_0\dot{\theta}}{\beta+1} sa, \quad (19)$$

where $X_0 = X_0(t)$, $\Omega=\Omega(t)$, $sa=sa(1,\beta,\psi(t))$, $ca=ca(\beta,1,\psi(t))$. Equating the relations (16) and (18), it is evident that the assumption (16) is regular only if the following relation is satisfied:

$$\dot{X}_0 ca - \frac{2X_0\dot{\theta}}{\beta+1} sa = 0. \quad (20)$$

Using (18) and (20), after some transformation it is

$$\dot{X}_0 = \varepsilon k_1^2 X_0\left|X_0\right|^{(1-\beta)/2}\sqrt{\frac{2}{(\beta+1)k_\beta^2}} sa\, ca, \quad (21)$$

$$X_0\dot{\theta} = \varepsilon k_1^2 X_0\left|X_0\right|^{(1-\beta)/2}\sqrt{\frac{\beta+1}{2k_\beta^2}} ca^2. \quad (22)$$

Relations (21) and (22) represent the two first order differential equations which correspond to the second order equation (8). Solving coupled equations (21) and (22) is very unconvenient, and the approximate procedure is introduced. Using the periodical property of the Ateb functions, they are averaged over the period

$$\Pi_\beta = B\left(\frac{1}{\beta+1}, \frac{1}{2}\right), \quad (23)$$

and B is the Beta function [7]. For

$$\left\langle sa\, ca\right\rangle = \frac{1}{2\Pi_\beta}\int_0^{2\Pi_\beta} sa\, ca\, d\psi = 0, \quad (24)$$

$$C = \left\langle ca^2 \right\rangle = \frac{1}{2\Pi_\beta} \int_0^{2\Pi_\beta} ca^2 \, d\psi = \left(\frac{2}{3+\beta} \right)^{2/(\beta+1)}, \quad (25)$$

the averaged equations (21) and (22) are

$$\dot{X}_0 = 0, \quad X_0 \dot{\theta} = \varepsilon k_1^2 C X_0 \left| X_0 \right|^{(1-\beta)/2} \sqrt{\frac{\beta+1}{2k_\beta^2}}. \quad (26,27)$$

As the solution of (26) is X_0=const., we integrate (27) and obtain

$$\theta = \varepsilon k_1^2 C t \left| X_0 \right|^{(1-\beta)/2} \sqrt{\frac{\beta+1}{2k_\beta^2}} + \theta_0, \quad (28)$$

where θ_0 is a constant of integration. Substituting the result (28) into (17), the phase of the Ateb function is obtained

$$\psi = \theta_0 + t \sqrt{\frac{k_\beta^2 \left| X_0 \right|^{\beta-1} (\beta+1)}{2}} \left(1 + \frac{\varepsilon k_1^2 C}{k_\beta^2 \left| X_0 \right|^{\beta-1}}\right). \quad (29)$$

Based on (29) and the periodic property of the Ateb function, the frequency of (8) follows as

$$\Omega_1 = \frac{\pi}{\Pi_\beta} \sqrt{\frac{\beta+1}{2}} \left(\sqrt{k_\beta^2 \left| X_0 \right|^{\beta-1}} + \frac{\varepsilon k_1^2 C}{\sqrt{k_\beta^2 \left| X_0 \right|^{\beta-1}}} \right). \quad (30)$$

Substituting (29) into (11) and (17) it is

$$u = X_0 \sin\left(\frac{n\pi x}{l}\right) ca\left(\beta, 1, \theta_0 + t \sqrt{\frac{k_\beta^2 \left| X_0 \right|^{\beta-1} (\beta+1)}{2}} \left(1 + \frac{\varepsilon k_1^2 C}{k_\beta^2 \left| X_0 \right|^{\beta-1}}\right)\right).$$

For initial conditions

$$u(0,x) = f(x), \quad \frac{\partial u(0,x)}{\partial t} = 0, \quad (31)$$

and the time derivative of (31)

$$\frac{\partial u}{\partial t} = X_0 \sqrt{\frac{k_\beta^2 \left| X_0 \right|^{\beta-1} (\beta+1)}{2}} \left(1 + \frac{\varepsilon k_1^2 C}{k_\beta^2 \left| X_0 \right|^{\beta-1}}\right) \sin\left(\frac{n\pi x}{l}\right) sa\left(1, \beta, \theta_0 + t \sqrt{\frac{k_\beta^2 \left| X_0 \right|^{\beta-1} (\beta+1)}{2}} \left(1 + \frac{\varepsilon k_1^2 C}{k_\beta^2 \left| X_0 \right|^{\beta-1}}\right)\right). \quad (32)$$

we have

$$\theta_0 = 0, \quad f(x) = X_0 \sin\left(\frac{n\pi x}{l}\right). \quad (33)$$

Multiplying $(33)_2$ with $\sin(n\pi x/l)$ and integrating the equation over the period of this function the initial values for X_{0n} follow as

$$\theta_0 = 0, \quad X_{0n} = \frac{n}{l} \int_0^l f(x) \sin\left(\frac{n\pi x}{l}\right) dx. \quad (34)$$

Finally, the approximate solution of (8) is

$$u = \sum_{n=1}^{\infty} X_{0n} \sin\left(\frac{n\pi x}{l}\right) ca\left(\beta, 1, t \sqrt{\frac{k_\beta^2 \left| X_{0n} \right|^{\beta-1} (\beta+1)}{2}} \left(1 + \frac{\varepsilon k_1^2 C}{k_\beta^2 \left| X_{0n} \right|^{\beta-1}}\right)\right). \quad (35)$$

It can be concluded that in spite of the assumption that the form of vibration correspond to the linear oscillator the solution of (8) is quite complex. Nevertheless, the most important parameter of the system is its frequency of vibration.

3.2 Frequency of vibration

According to (30) and (34) the frequency of vibration of the n-th mode is

$$\Omega_{1n} = \frac{\pi}{\Pi_\beta} \sqrt{\frac{\beta+1}{2}} \left(\sqrt{k_\beta^2 \left| X_{0n} \right|^{\beta-1}} + \frac{\varepsilon k_1^2 C}{\sqrt{k_\beta^2 \left| X_{0n} \right|^{\beta-1}}} \right), \quad (36)$$

i.e.,

$$\Omega_{1n} = \frac{\pi}{B\left(\frac{1}{\beta+1}, \frac{1}{2}\right)} \sqrt{\frac{c_\beta C_\beta (\beta+1)}{2\rho A} \left| X_{0n} \right|^{\beta-1}} \left(1 + \frac{EI\left(\frac{n\pi}{l}\right)^4 \left(\frac{2}{3+\beta}\right)^{2/(\beta+1)}}{c_\beta C_\beta \left| X_{0n} \right|^{\beta-1}}\right). \quad (37)$$

Analyzing the relation (37) it can be seen that the dependance of the frequency on the properties of foundation is very complex. For simplicity, let us rewritten (37) in the form

$$\Omega_{1n} \approx \left(\frac{c_\beta \left| X_{0n} \right|^{\beta-1}}{\rho A} \frac{\pi^2 C_\beta (\beta+1)}{2B^2} + \frac{EI\left(\frac{n\pi}{l}\right)^4}{\rho A} \frac{\pi^2 (\beta+1)}{B^2} \left(\frac{2}{3+\beta}\right)^{2/(\beta+1)} \right)^{1/2}. \quad (38)$$

From the second term of (38) it is seen that the rigidity coefficient of the Winkler foundation has no affects to the frequency of the free beam. The frequency of the free beam vibration is multiplied with parameters which depend on the order of nonlinearity β. It is the reason that the influence of the order of the foundation nonlinearity on the frequency of vibration is discussed.

To prove the correctness of the relation (38), the special case when the elasticity of foundation is linear will be considered. For that case the approximate frequency of vibration is approximately

$$\Omega_{1nl} = \sqrt{\frac{c_1}{\rho A} + \frac{EI\left(\frac{n\pi}{l}\right)^4}{\rho A}}). \quad (39)$$

The relation (39) corresponds to the well known one, where the quadratic value of the frequency is a sum of quadratic frequencies of the free beam and of a hamonic oscillator with a mass ρA and elasticity c_1.

If the nonlinearity of Winkler foundation is of cubic order, the relation (37) gives the approximate frequency as

$$\Omega_{1n3} \approx 0.91\sqrt{0.4330\frac{c_3}{\rho A}\left|X_{0n}\right|^2 + \frac{EI\left(\frac{n\pi}{l}\right)^4}{\rho A}}. \quad (40)$$

Comparing (40) with the value given in [3]

$$\Omega^*_{1n3} = \sqrt{0.5625\frac{c_3}{\rho A}\left|X_{0n}\right|^2 + \frac{EI}{\rho A}\left(\frac{n\pi}{l}\right)^4}, \quad (41)$$

where the nonlinearity of Winkler type is small, it is obvious that the form of the solutions is the same, but the coefficients differ. It is due to the fact that in (40) the linear term is considered as a small one.

4. EXAMPLE

Let us consider the frequency of the first mode of vibration. For that case the approximate frequency of vibration is

$$\Omega_{11} \approx (\frac{c_\beta\left|X_{01}\right|^{\beta-1}}{\rho A}\frac{\pi^2 C_\beta(\beta+1)}{2B^2} + \frac{EI}{\rho A}\left(\frac{\pi}{l}\right)^4\frac{\pi^2(\beta+1)}{B^2}\left(\frac{2}{3+\beta}\right)^{2/(\beta+1)})^{1/2}. \quad (42)$$

To examine the influence of the order of nonlinearity of the Winkler foundation, we introduce the following numerical data into (42): c_β=1, X_{01}=0.5, l=π, EI/ρA=1. According to (42) the frequency of vibration is calculated. The parameter β is varied. The obtained values are shown in the Table 1.

Table 1.

β	Ω_{11}
1	1.06066
5/3	0.84145
2	0.80609
3	0.84514
10/3	0.88590

Analysing the calculated values it is obvious that for the given values the frequancy of vibration is smaller for the nonlinear than for the linear Winkler foundation. Besides, for the order of nonlinearity in the interval [1,2] the frequency decreases with increasing the order, while in the interval [2,4] the frequency increases with β.

4. EXAMPLE

In this paper the influence of the order of the Winkler type nonlinearity on self-excited vibrations of a line structure (beam) is investigated. A Bernouli-Euler beam is settled on the nonlinear foundation. Vibration is described with a partial differential equation. An approximate method for obtaining of the solution is developed. The motion is described in the form of two multipled functions: one, the exact temporal function and second, an approximate space function which satisfies the boundary conditions. It is shown that the beam on a linear Winkler foundation has higher frequencies than others on nonlinear one. A general conclusion about tendency of frequency of a beam on nonlinear fundation can not be given a'priori, as the frequency - β parameter function is implicit.

Acknowledgement

This work was partially supported by the Secretariat for Science and Technological Development, Autonomous Province of Vojvodina (Proj. No 114-451-2094/2011 and Proj. ANKUV 2014) and Ministry of Science of Serbia (Proj. No. ON 174028 and IT 41007).

REFERENCES

[1] S. Lenci, A.M. Tarantino, "Chaotic dynamics of an elastic beam resting on a Winkler-type soil", *Chaos, Solitons and Fractals*, vol. 7, pp. 1601-1614, 1996.

[2] X.-F. Li, G.-J. Tang, Z.-B., K.Y. Lee, "Vibration of nonclassical shear beams with Winkler-Pasternak-type restraint", *Acta Mechanica*, vol. 223, pp. 953-966, 2012.

[3] T.D. Burton and M.N. Hamdan, "On the calculation of non-linear normal modes in continuos systems", *Journal of Sound and Vibration*, vol. 197, pp. 117-130, 1996.

[4] L. Cveticanin and T. Atanackovic, "Non-linear vibration of an extensible elastic beam", *Journal of Sound and Vibration*, vol. 177, pp. 159-171, 1994.

[5] T.M. Atanackovic and L.J. Cveticanin, "Dynamics of plane motion of an elastic rod", Journal of Applied Mechanics, Trans. ASME, vol. 63, March, pp. 392-398, 1996.

[6] S.W. Shaw and C. Pierre, "Normal modes of vibration for non-linear continuous systems", *Journal of Sound and Vibration*, vol. 169, pp. 319-347, 1994.

[7] L.Cveticanin and T. Pogany, "Oscillator with a sum of noninteger-order nonlinearities", *Journal of Applied Mathematics*, vol. 2012, Article ID 649050, 20 pages, 2012.

University of Nis
Faculty of Occupational Safety
„Politechnica“ University of Timisoara
Faculty of Mechanical Engineering
24th International Conference
NOISE AND VIBRATION
Niš, 29 - 31. 10. 2014.

DUFFING OSCILLATOR WITH NON-VISCOUS EXPONENTIAL DAMPING

Vasile Marinca[1, 2], Remus-Daniel Ene[3]

[1.] Department of Mechanics and Vibration, "Politehnica" University of Timişoara,
Bd. M. Viteazul, No.1, 300222, Timişoara, Romania.

[2.] Department of Electromechanics and Vibration, Center for Advanced and Fundamental Technical Research Romania Academy, Timisoara Branch, Bd.Mihai Viteazul, Nr.24, 300223, Timişoara, Romania.

[3.] Department of Math., "Politehnica" University of Timişoara,
Pta Victoriei, No.2, 300006, Timisoara, Romania, E-mail: eneremus@gmail.com

***Abstract**: This paper studies the interaction between non-viscous exponential damping and nonlinearity for Duffing oscillator. The non-viscous damping function is an exponential damping model which adds a decaying memory property to the damping of the oscillator. An approximate analytical solution is obtained using Optimal Homotopy Asymptotic Method (OHAM) for hard nonlinearity. A very good agreement is found between our approximate results and numerical results, after only one iteration and two steps.*

1. INTRODUCTION

The systems with nonlinear restoring force, a method of successive approximations are subsequently named after Georg Wilhelm Christian Caspar Duffing (1861-1944). Duffing was the author of nine publications including books, book chapters and journal articles. We emphasize several systems which can be represented by various forms of the Duffing equation: the pendulum (the series of the trigonometric function sinus is truncated to third order), geometrical nonlinearities (for example systems consisting of two linear spring and a mass), large deflection of a pinned-pinned beam with nonlinear stiffness, nonlinear oscillators, nonlinear cable vibrations, beam with nonlinear stiffness due to inplane tension, nonlinear electrical circuits, and so on [1].

There exists a wide body of literature dealing with the problem of approximate solutions of Duffing equation with various methodologies. Many different approaches have been proposed such as: modified Lindstedt-Poincare method [2], modified variational iteration method [3], modified Mickens procedure [4], incremental harmonic balance method [5], Jacobi elliptic functions [6], and so on [7-9]. In many cases, the damping is nearly always assumed to be viscous.

Replacing viscous damping by the exponential damping force, the governing equation for the Duffing oscillator can be expressed as

$$m\frac{d^2x}{d\bar{t}^2}+\bar{c}\int_0^{\bar{t}}\bar{\mu}e^{-\bar{\mu}(\bar{t}-\bar{\tau})}\frac{dx}{d\bar{\tau}}d\bar{\tau}+kx+\alpha kx^3=0 \qquad (1)$$

where x represents the displacement of the oscillator of mass m, the linear stiffness is given by parameter k, the coefficient α represents the form of the cubic stiffness nonlinearity, $\bar{t}$ is the time, $\bar{\tau}$ is the integration variable. The viscous damping coefficient is $\bar{c}$ and the non-viscous damping effects are represent by the parameter $\bar{\mu}$. The initial conditions for Eq. (1) are

$$x(0)=A, \qquad \frac{dx}{d\bar{t}}(0)=\sqrt{\frac{k}{m}}v_0. \qquad (2)$$

Introducing the dimensionless variables

$$t=\sqrt{\frac{m}{k}}\,\bar{t}, \qquad \tau=\sqrt{\frac{m}{k}}\,\bar{\tau} \qquad (3)$$

Eq. (1) becomes

$$\ddot{x}(t)+2c\int_0^t\mu e^{-\mu(t-\tau)}\dot{x}(\tau)d\tau+x(t)+\alpha x^3(t)=0 \qquad (4)$$

and the initial conditions (2) are

$$x(0)=A, \qquad \dot{x}(0)=v_0 \qquad (5)$$

where $c=\frac{\bar{c}}{\sqrt{km}}$, $\mu=\sqrt{\frac{m}{k}}\,\bar{\mu}$ and an overdot represents differentiation with respect to dimensionless time. The model for the damping force expressed as

$$F(t)=2c\int_0^t\mu e^{-\mu(t-\tau)}\dot{x}(\tau)d\tau \qquad (6)$$

was originally proposed by Biot [10] and later used by several authors. For more details see [11]. In the limiting case when $\mu\to\infty$, the exponential kernel function approaches the Dirac delta function $\delta(t)$. For this special case, damping force given by Eq. (6) reduces to the case of viscous damping.

The objective of the present paper is to propose an accurate procedure to nonlinear differential equation of Duffing oscillator with non-viscous exponential damping given by Eqs. (4) and (5) using OHAM. A version of the OHAM is applied in

this work to derive highly accurate analytical expressions of the solutions using only one iteration and a small number of steps. The main advantage of this approach is the control of the convergence of approximate solutions in a very rigorous way. A very good agreement was found between our approximate solutions and numerical results, which proves that our method is very efficient and accurate.

2. BASIC IDEAS OF THE OHAM

Let us consider the following nonlinear differential equation

$$L(x(t)) + N(x(t)) = 0 \tag{7}$$

where L and N are linear and nonlinear operators repectively. If $p \in [0,1]$ denotes an embedding parameter and X is an analytic function in the form

$$X(t,p) = x_0(t) + p x_1(t, C_i) \tag{8}$$

then we construct a homotopy [12-17]

$$\begin{aligned} \mathrm{H}[L(X(t,p)), H(t,C_i), N(X(t,p))] &= L(x_0(t)) + \\ &+ p[L(x_1(t,C_i)) - H(t,C_i) N(x_0(t))] = 0 \end{aligned} \tag{9}$$

where $H(t,C_i) \neq 0$ is an arbitrary auxiliary convergence-control function depending on variable t and on s arbitrary parameters C_1, C_2, ..., C_s.

From Eq. (9), we obtain the governing equation of $x_0(t)$ and $x_1(t,C_i)$, i.e.:

$$L(x_0(t)) = 0 \tag{10}$$

$$L(x_1(t,C_i)) = H(t,C_i) N(x_0(t)) \tag{11}$$

where we find the following expression for the nonlinear operator into Eq. (11)

$$N(x_0(t)) = \sum_{i=1}^{m} h_i(t) g_i(t) \tag{12}$$

In the Eq. (12) the functions h_i and g_i are known and depend on the initial approximation $x_0(t)$ and also on the nonlinear operator, m being a known integer number.

In what follows we do not solve Eq. (11), but is more convenient to consider the unknown function $x_1(t,C_i)$ in the form:

$$x_1(t,C_j) = \sum_{i=1}^{n} H_i(t, h_j(t), C_j) g_i(t), \quad j = 1,2,\ldots,s \tag{13}$$

where within expression of $H_i(t,h_j(t),C_j)$ appear combinations of some functions h_j, the some terms which are given by the corresponding homogeneous equation and the unknown parameters C_j, $j = 1,2,\ldots,s$. In the sum given by Eq. (13) appear an arbitrary number of n of the such terms. This is underlying idea of our method. The convergence of the approximate solution obtained from Eq. (8) for $p = 1$:

$$\bar{x}(t,C_j) = x_0(t) + x_1(t,C_j) \tag{14}$$

depend on the parameters C_j, $j = 1,2,...,s$. The values of these parameters can be optimally identified via various methods, such as: the least-square method, the Galerkin method, the collocation method, the Ritz method or minimizing the square residual error. With these parameters known (called optimal convergence-control parameters), the first-order approximate solution given by Eq. (14) is well-known. It should be emphasized that our procedure contains the auxiliary functions $H_i(t, h_j(t), C_j)$ which provides us with a simple way to adjust and control the convergence of the approximate solutions.

3. APPLICATION OF OHAM TO DUFFING OSCILLATOR GIVEN BY EQS. (4) AND (5)

For the nonlinear differential equation (4), we choose the linear operator in the form

$$L(x(t)) = \ddot{x} + 2\lambda\dot{x} + (\lambda^2 + \omega^2)x \tag{15}$$

where λ and ω are unknown parameters.

The nonlinear operator corresponding to Eq. (4) is:

$$N(x(t)) = -2\lambda\dot{x} + (1 - \lambda^2 - \omega^2)x + 2\mu c \int_0^t e^{-\mu(t-\tau)} \dot{x}(\tau) d\tau + \alpha x^3$$

The initial approximation $x_0(t)$ can be obtained from Eq. (10) and has the form

$$x_0(t) = A e^{-\lambda t} \cos \omega t \tag{16}$$

The nonlinear operator corresponding to Eq. (16) it holds that

$$\begin{aligned} N(x_0(t)) = &\left[\left(1 + \lambda^2 - \omega^2 + \right.\right. \\ &\left. + \frac{2c(\lambda^2 + \omega^2 - \mu\lambda)}{\omega^2 + (\mu - \lambda)^2}\right) \cos \omega t + (2\lambda\omega - \\ &\left. - \frac{2\mu c\omega}{\omega^2 + (\mu - \lambda)^2}\right) \sin \omega t \Bigg] A e^{-\lambda t} + \\ &+ (\cos 3\omega t + 3\cos \omega t) \frac{\alpha A^3}{4} e^{-3\lambda t} + \\ &+ \frac{2Ac(\mu\lambda - \omega^2 - \lambda^2)}{\omega^2 + (\mu - \lambda)^2} e^{-\mu t} \end{aligned} \tag{17}$$

Comparing Eqs. (12) and (17) we find that:

$$\begin{aligned} h_1(t) = &\left(1 + \lambda^2 - \omega^2 + \right. \\ &\left. + \frac{2c(\lambda^2 + \omega^2 - \mu\lambda)}{\omega^2 + (\mu - \lambda)^2}\right) \cos \omega t + (2\lambda\omega - \\ &\left. - \frac{2\mu c\omega}{\omega^2 + (\mu - \lambda)^2}\right) \sin \omega t; \quad g_1(t) = A e^{-\lambda t}; \\ h_2(t) = &\frac{\alpha A^3}{4} (\cos 3\omega t + 3\cos \omega t); \\ &g_2(t) = e^{-3\lambda t}; \\ h_3(t) = &\frac{2Ac(\mu\lambda - \omega^2 - \lambda^2)}{\omega^2 + (\mu - \lambda)^2}; \quad g_3(t) = e^{-\mu t} \end{aligned} \tag{18}$$

The initial conditions from Eq. (16) are $x_0(0)=A,\ \dot{x}_0(0)=-\lambda A,$ such that from Eqs. (5) and (14) we have

$$x_1(0)=0,\quad \dot{x}_1(0)=v_0+\lambda A \tag{19}$$

From Eqs. (18), (13) and (19) we choose have

$$\begin{aligned} x_1(t)=&\left[(C_1t+C_2)\cos\omega t+(C3_1t+C_4)\sin\omega t\right]e^{-\lambda t}+\\ &+\left[\left(\frac{C_1+\omega C_4+(\mu-\lambda)C_2}{3\lambda-\mu}-\frac{v_0+\lambda A}{A(3\lambda-\mu)}-\right.\right.\\ &\left.\left.-C_5\right)\cos\omega t+C_5\cos 3\omega t\right]Ae^{-3\lambda t}+\\ &+\left[\frac{v_0+\lambda A}{A(3\lambda-\mu)}-\frac{C_1+\omega C_4+2\lambda C_2}{3\lambda-\mu}\right]Ae^{-\mu t} \end{aligned} \tag{20}$$

The first-order approximate solution of Eqs. (4) and (5) is given by Eq. (14) where $x_0(t)$ and $x_1(t)$ are given by Eqs. (16) and (20) respectively.

4. NUMERICAL EXAMPLES

We illustrate the accuracy of our procedure for the following values of the parameters:

Case 4.1 $A=1, k=1, c=0.1, \alpha=1, \mu=2, v_0=0.$ The optimal convergence-control parameters are determined by means of the least-square method in the two steps as follows:

For $t\in[0,15]$ we obtain

$$\begin{aligned} &C_1=-0.1894732806,\quad C_2=0.9932726810,\\ &C_3=-0.2944761127,\quad C_4=0.0599446760,\\ &C_5=0.0192507903,\quad \lambda=0.1745219520,\\ &\omega=1.0645662531 \end{aligned}$$

The first-order approximate solution given by Eq. (14) becomes for this first step:

$$\begin{aligned} \bar{x}(t)=&\left[(1.9932726810-0.1894732806\ t)\cos\omega t+\right.\\ &\left.+(0.0599446760-0.2944761127\ t)\sin\omega t\right]e^{-\lambda t}+\\ &+0.0315053815\,e^{-2t}+(0.0192507903\cos 3\omega t-\\ &-1.0440288529\cos\omega t)e^{-3\lambda t} \end{aligned} \tag{21}$$

For $t\in[15,30]$ the first-order approximate solution is given by:

$$\begin{aligned} \bar{x}(t)=&0.1421181924\left[(1.2105000919-\right.\\ &-0.6927427068\ t)\cos\omega t+(-11.7272117269+\\ &\left.+0.1599877579\ t)\sin\omega t\right]e^{-\lambda t}-1.2786938227\,e^{-2t}+\\ &+0.1421181924(6.4102019440\cos\omega t+\\ &+2.3766951370\cos 3\omega t)e^{-3\lambda t} \end{aligned} \tag{22}$$

where $\lambda=0.1134303730,\ \omega=1.0263621174.$

Case 4.2 $A=1, k=1, c=0.1, \alpha=1, \mu=20, v_0=0.$ and for $t\in[0,15]$ the first-order approximate solution of the Eqs. (4) and (5) is

$$\begin{aligned} \bar{x}(t)=&\left[(1.7761031086-0.1652946546\ t)\cos\omega t+\right.\\ &\left.+(0.0170154066-0.2988538309\ t)\sin\omega t\right]e^{-\lambda t}-\\ &-0.0020116055\,e^{-20t}+(0.0065110082\cos 3\omega t-\\ &-0.7806025112\cos\omega t)e^{-3\lambda t} \end{aligned} \tag{23}$$

where $\lambda=0.1977720251,\ \omega=1.0017462475.$

For $t\in[15,30]$ we obtain:

$$\begin{aligned} \bar{x}(t)=&-0.1166766794\left[(-2.8855125931+\right.\\ &+0.5582082220\ t)\cos\omega t+(10.9080343600+\\ &\left.+0.1134784335\ t)\sin\omega t\right]e^{-\lambda t}-0.0719185235\,e^{-20t}-\\ &-0.1166766794(4.0511796701\cos\omega t-\\ &-0.7820586635\cos 3\omega t)e^{-3\lambda t} \end{aligned} \tag{24}$$

where $\lambda=0.1246335189,\ \omega=0.9838871643.$

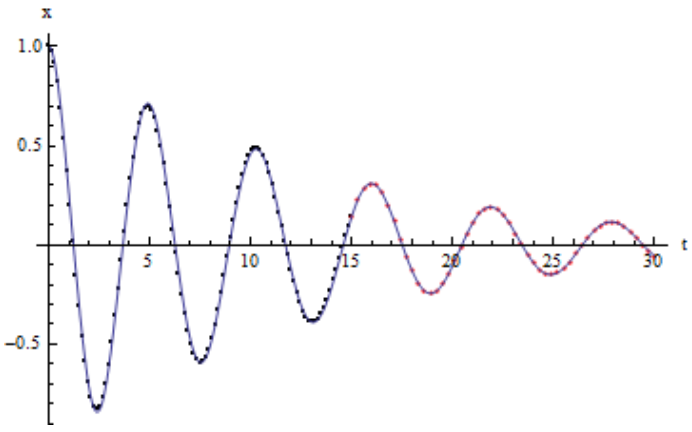

Fig.1 *Comparison between the approximate solution and numerical solution for* $A=k=\alpha=1,\ c=0.1,\ \mu=2$**:** _____ *numerical solution;* …… *approximate solution*

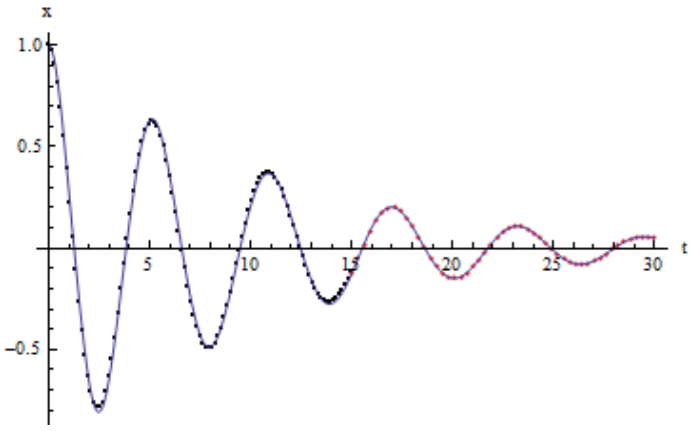

Fig.2 *Comparison between the approximate solution and numerical solution for* $A=k=\alpha=1,\ c=0.1,\ \mu=20$**:** _____ *numerical solution;* …… *approximate solution*

In Figs. 1 and 2 are plotted a comparison between the first-order approximate solution of Eqs. (4) and (5) and numerical results for the cases 4.1 and 4.2, respectively.

It can be seen that the solutions obtained by the proposed procedure are nearly identical with the numerical solutions obtained using a fourth-order Runge-Kutta method.

5. CONCLUSIONS

The Optimal Homotopy Asymptotic Method is employed to propose an analytic approximate solutions for Duffing oscillator with non-viscous exponential damping. Our procedure is valid even if the nonlinear differential equation does not contain any small or large parameters. In construction of the homotopy appear some distinctive concepts as: the linear operator, the nonlinear operator, the auxiliary functions $H_i(t, C_j)$ and several optimal convergence-control parameters $\lambda, \omega, C_1, C_2, \ldots$ which ensure a fast convergence of the solutions. The examples presented in this work, lead to the conclusion that the obtained results are of very accurate using only one iteration and two steps. The OHAM provides us with a simple and rigorous way to control and adjust the convergence of the solutions through the auxiliary functions $H_i(t, C_j)$ involving several parameters $\lambda, \omega, C_1, C_2, \ldots$ which are optimally determined. The capital strength of OHAM is its fast convergence, which proves that our procedure is very efficient in practice.

REFERENCES

[1] M. J. Brennan and I. Kovacic, *Examples of physical systems described by the Duffing equation*, In: The Duffing Equation: Nonlinear Oscillators and their Behavior, Edited by I. Kovacic and M. J. Brennan, New York: John Willey and Sons, 2011.

[2] J. H. He, "Modified Linstedt-Poincare methods for some strongly non-linear oscillations. Part I, expansion of a constant", *Int. J. Non-Linear Mech.*, vol. 37(2), pp. 309-314, 2002.

[3] V. Marinca and N. Herisanu, "Periodic solutions of Duffing equation with strong nonlinearity", *Chaos Solitons and Fractals*, vol. 37, pp. 144-149, 2008.

[4] C.W. Lim and B.S. Wu, "A modified Mickens procedure for certain non-linear oscillations", *J. Sound and Vibr.*, vol. 257, pp. 202-206, 2002.

[5] Y.K. Cheung, S.H. Chen and S.L. Lau, "Application of incremental harmonic balance method to cubic nonlinearity systems", *J. Sound and Vibr.*, vol. 140, pp. 273-286, 1990.

[6] L. Cveticanin, "The approximate solving methods for the cubic Duffing equation based on Jacobi elliptic functions", *Int.J. Nonlinear Sci. Numer. Simulat.*, vol. 10, pp. 1491-1516, 2009.

[7] J. Guckenheimer and P. Holmes, *Nonlinear Oscillations, Dynamical Systems and Bifurcations of Vector Field*, Springer N. Y., 1983.

[8] F.C. Moon, *Chaotic Vibrations: An Introduction for Applied Scientists and Engineers*, New York: John Willey, 1987.

[9] A. N. Nayfeh and D.T. Mook, *Nonlinear oscillations*, New York: John Willey and Sons, 1979.

[10] M. A. Biot, "Linear Thermodynamics and the mechanics of solids", *Proceedings of the Third US National Congress on Applied Mechanics*, pp. 1-18, 1958.

[11] S. Adhikari, *Structural Dynamic Analysis with Generalized Damping Models*, New York: John Willey, 2014.

[12] V. Marinca, N. Herisanu, C. Bota and B. Marinca, "An optimal homotopy asymptotic method applied to the steady flow of a fourth grade fluid past a porous plate", *Applied Mathematics Letters*, vol. 22, pp. 245-251, 2009.

[13] V. Marinca and N. Herisanu, *Nonlinear Dynamical Systems in Engineering – Some Approximate Approaches*, Springer Verlag, Heidelberg, 2011.

[14] V. Marinca and R.-D. Ene, "Analytical approximate solutions to the Thomas-Fermi equation", *Central Eur. J. of Physics*, vol. 12(7), pp. 503-510, 2014.

[15] V. Marinca and R.-D. Ene, "Dual approximate solutions of the unsteady viscous flow over a shrinking cylinder with Optimal Homotopy Asymptotic Method", *Advances in Mathematical Physics*, Article ID 417643, 2014, 11 pages.

[16] V. Marinca, R.-D. Ene and B. Marinca, "Analytic approximate solution for Falkner-Skan equation", *The Scientific World Journal*, Article ID 617453, 2014, 22 pages.

[17] V. Marinca, R.-D. Ene, B. Marinca and R. Negrea, "Different approximations to the solution of upper-convected Maxwell fluid over a porous stretching plate", *Abstract and Applied Analysis*, Article ID 139314, 2014, 13 pages.

University of Nis
Faculty of Occupational Safety
„Politechnica“ University of Timisoara
Faculty of Mechanical Engineering
24th International Conference
NOISE AND VIBRATION
Niš, 29 - 31. 10. 2014.

NONLINEAR OSCILLATIONS OF A POINT MASS ON A PARABOLA WHICH ROTATES

Vasile Marinca[1], *Nicolae Herisanu*[2]

[1] "Politehnica" University of Timisoara, Romania, vasile.marinca@upt.ro
[2] "Politehnica" University of Timisoara, Romania, nicolae.herisanu@upt.ro

Abstract *- In this paper we investigate the nonlinear behaviour of a point mass, which is a ring of mass m sliding freely on the wire describing a parabola which rotates with a constant angular velocity about the vertical axis. A version of the Optimal Homotopy Asymptotic Method is employed in order to find accurate analytical solutions to this problem. Analytical solutions are validated through numerical simulations which reveal an excellent agreement between the analytical and numerical integration results. Several meaningful cases are analyzed showing the effectiveness of the proposed method.*

1. INTRODUCTION

In this paper we consider the motion of a ring of mass m sliding freely on the wire described by the parabola $z=qx^2$ which rotates with a constant angular velocity ω about the z-axis as shown in Fig. 1 [1-3].

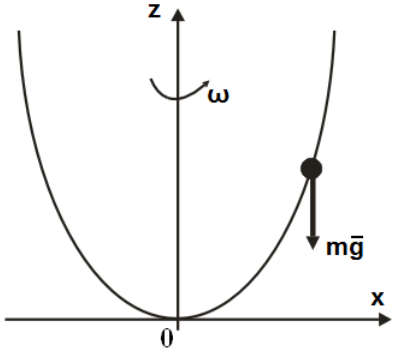

Fig. 1 *Particle on a rotating parabola*

Using the Euler-Lagrange equations, the motion of this particle is given by the equation:

$$\left(1+4q^2u^2\right)\frac{\mathrm{d}^2u}{\mathrm{d}t^2}+\Lambda u+4q^2\left(\frac{\mathrm{du}}{\mathrm{d}t}\right)^2 u=0 \qquad (1)$$

with the boundary conditions:

$$u(0)=A\ ,\ \frac{\mathrm{du}}{\mathrm{d}t}(0)=0 \qquad (2)$$

where q, Λ and A are known constants and need not to be small. Under the transformations

$$\tau=\Omega t,\quad u(t)=Ax(\tau) \qquad (3)$$

equations (1) and (2) become

$$\Omega^2x''+\omega^2x+4q^2A^2\Omega^2(x^2x''+xx'^2)=0 \qquad (4)$$

respectively

$$x(0)=1\ ,\ \mathrm{x}'(0)=0 \qquad (5)$$

where $\Lambda=\omega^2$ and $'=\frac{\mathrm{d}}{\mathrm{d}\tau}$.

2. METHOD OF SOLUTION

In order to apply the optimal homotopy asymptotic method (OHAM), we consider the following differential equation

$$\Omega^2x''(\tau)+\omega^2x(\tau)+\\+\frac{1}{A}f(Ax(\tau),A\Omega x'(\tau),A\Omega^2x''(\tau))=0 \qquad (6)$$

with the initial conditions

$$x(0)=1\ ,\ \mathrm{x}'(0)=0 \qquad (7)$$

where the prime denotes the derivative with respect to τ.

By means of OHAM one first construct a family of equations

$$(1-p)L(X(\tau,p))=H(\tau,C_i,p)[N(X(\tau,p),\Omega(\lambda,p))] \qquad (8)$$

where L is a linear operator

$$\mathrm{L}(\mathrm{X}(\tau,\mathrm{p})=\Omega_0^2\left[\frac{\partial^2X(\tau,p)}{\partial\tau^2}+X(\tau,p)\right] \qquad (9)$$

while N is a nonlinear operator

$$N(X(\tau,p),\Omega(\lambda,p))=\Omega^2(\lambda,p)\frac{\partial^2X(\tau,p)}{\partial\tau^2}+\\+(\omega^2+\lambda^2)X(\tau,p)+\frac{1}{A}f(AX(\tau,p),A\Omega(\lambda,p)\frac{\partial X(\tau,p)}{\partial\tau}, \qquad (10)$$
$$A\Omega^2(\lambda,p)\frac{\partial^2X(\tau,p)}{\partial\tau^2})-p\lambda X(\tau,p)$$

where λ is an arbitrary unknown parameter and Ω_0 will be given later. The initial conditions (7) can be written in the form

$$X(0,p)=1\ ,\ \left.\frac{\partial \mathrm{X}(\tau,\mathrm{p})}{\partial\tau}\right|_{\tau=0}=0 \tag{11}$$

Therefore it holds

$$X(\tau,0)=\mathrm{x}_0(\tau),\ X(\tau,1)=x(\tau),\ \Omega(0)=\Omega_0,\ \Omega(1)=\Omega \tag{12}$$

where $\mathrm{x}_0(\tau)$ is an initial approximation of $\mathrm{x}(\tau)$. As the embedding parameter p increases from 0 to 1, $\mathrm{X}(\tau,p)$ varies from the initial approximation $\mathrm{x}_0(\tau)$ to the solution $\mathrm{x}(\tau)$, so does $\Omega(\lambda,p)$ from the initial approximation Ω_0 to the exact frequency Ω.

Expanding $\mathrm{X}(\tau,p)$ and $\Omega(\lambda,p)$ in series with respect to the parameter p, one has respectively

$$X(\tau,\mathrm{p})=x_0(\tau)+px_1(\tau)+p^2x_2(\tau)+\ldots \tag{13}$$

$$\Omega(\lambda,\mathrm{p})=\Omega_0+p\Omega_1(\lambda)+p^2\Omega_2(\lambda)+\ldots \tag{14}$$

If the initial approximation $\mathrm{x}_0(\tau)$ and the auxiliary function $\mathrm{H}(\tau,C_i,p)$ are properly chosen so that the above series converges at p=1, one has

$$x(\tau)=x_0(\tau)+x_1(\tau)+x_2(\tau)+\ldots \tag{15}$$

$$\Omega=\Omega_0+\Omega_1+\Omega_2+\ldots \tag{16}$$

The Eqs. (15) and (16) contain the auxiliary function $\mathrm{H}(\tau,C_i,p)$. The results of the m th-order approximations are given by

$$\bar{x}(\tau)\approx x_0(\tau)+x_1(\tau)+\ldots+x_m(\tau) \tag{17}$$

$$\overline{\Omega}=\Omega_0+\Omega_1+\ldots+\Omega_{m-1} \tag{18}$$

If we substitute Eqs.(17) and (18) into Eq.(8) and if we equate to zero the coefficients of various powers of p we obtain the following linear equations:

$$L(x_0(\tau))=0,x_0(0)=1,x_0'(0)=0 \tag{19}$$

$$\begin{aligned}&L(x_i(\tau)-L(x_{i-1}(\tau))=\sum_{j=1}^{i}H_j(\tau,C_i,p)[L(x_{i-j}(\tau)+\\&+N_{i-j}(x_0,x_1,\ldots,x_{i-j},\Omega_0,\Omega_1,\ldots,\Omega_{i-j},A,\lambda)],\\&x_i(0)=x_i'(0)=0,i=1,2,..m-1\end{aligned} \tag{20}$$

$$\begin{aligned}&L(x_m)-L(x_{m-1})=\sum_{j=1}^{m-1}H_j(\tau,C_i,p)[L(x_{m-1-j}(\tau)+\\&+N_{m-1-j}]+H_mN_0(x_0)\end{aligned} \tag{21}$$

where $\mathrm{N_k}$ and $\mathrm{H_k}$ are obtained from the equations

$$\begin{aligned}&N(X,\Omega)=N_0(x_0,\Omega_0,A,\lambda)+pN_1(x_0,x_1,\Omega_0,\Omega_1,A,\lambda)\\&+p^2N_2(x_0,x_1,x_2,\Omega_0,\Omega_1,\Omega_2,A,\lambda)+\ldots\end{aligned} \tag{22}$$

$$\mathrm{H}(\tau,C_i,p)=H_1(\tau,C_i)+pH_2(\tau,C_i)+p^2H_3(\tau,C_i)+\ldots \tag{23}$$

Note that Ω_k can be determined avoiding the presence of secular terms into Eqs. (20) and (21). The frequency Ω depends upon the arbitrary parameter λ and we apply the so-called principle of minimal sensitivity [4] in order to fix the value of λ. We do this imposing that

$$\frac{\mathrm{d}\Omega}{\mathrm{d}\lambda}=0 \tag{24}$$

In this work we consider m=2 in Eq.(21) such that we obtain the second-order approximate solution in the form

$$\bar{x}(\tau,C_i)=x_0(\tau)+x_1(\tau,C_i)+x_2(\tau,C_i) \tag{25}$$

where the terms $\mathrm{x_0}$, $\mathrm{x_1}$ and $\mathrm{x_2}$ are given by the linear differential equations (19), (20) and (21), or more precisely, by the following linear equations:

$$L(x_0(\tau))=0,x_0(0)=1,x_0'(0)=0 \tag{26}$$

$$\begin{aligned}&L(x_1(\tau,C_i))=H_1(\tau,C_i)N_0(x_0(\tau),\Omega_0),\\&x_1(0)=x_1'(0)=0\end{aligned} \tag{27}$$

$$\begin{aligned}&L(x_2(\tau,C_i))-L(x_1(\tau,C_i))=H_1(\tau,C_i)[L(x_1(\tau,C_i)+\\&+N_1(x_0,x_1,\Omega_{0,}\Omega_1)]+H_2(\tau,C_i)N_0(x_0(\tau)),\\&x_2(0)=x_2'(0)=0\end{aligned} \tag{28}$$

The auxiliary functions $\mathrm{H_i}(\tau,C_i)$ are chosen so that in Eq.(20) the product

$$H_j[L_{i-j}(\tau)+N_{i-j}(x_0,x_1,\ldots,x_{i-j},\Omega_0,\Omega_1,\ldots\Omega_{i-1},A,\lambda)]$$

be of the same shape with other terms which appear into Eq.(20).

3. SOLUTION BY OHAM

In what follows we illustrate the efficiency of the presented procedure [5,6,7,8]. The linear and nonlinear operators are respectively:

$$L(x(\tau))=\Omega_0^2\left[x''(\tau)+x(\tau)\right] \tag{29}$$

$$\begin{aligned}&N\left[x(\tau),\Omega(p)\right]=\Omega^2(p)x''(\tau)+(\omega_0^2+\lambda)x(\tau)+\\&+4q^2A^2\Omega^2(p)\left[x^2(\tau)x''(\tau)+x(\tau)x'^2(\tau)\right]-\\&-p\lambda x(\tau)-\Omega_0^2[x''(\tau)+x(\tau)]\end{aligned} \tag{30}$$

where x and Ω are given by Eq. (17) and (18), respectively, and λ is an unknown parameter. From Eqs. (26), (27) and (28), we obtain the following three equations:

(20) $\Omega_0^2(x_0''+x_0)=0\ ,\ x_0(0)=1\ ,\ x'(0)=0$ (31)

$$\begin{aligned}&\Omega_0^2(x_1''+x_1)-H_1(\tau,C_i)\left[\Omega_0^2x_0''+(\omega_0^2+\lambda)x_0+\right.\\&\left.+4q^2A^2\Omega_0^2(x_0x_0''+x'_0{}^2x_0)\right]=0,\ \mathrm{x}_1(0)=x_1'(0)=0\end{aligned} \tag{32}$$

(20)

$$\begin{aligned}&\Omega_0^2(x_2''+x_2)-\Omega_0^2(x_1''+x_1)-H_1(\tau,C_i)\{2\Omega_0\Omega_1x_0''+\Omega_0^2x_1''+\\&+(\omega_0^2+\lambda)x_1+4q^2A^2[\Omega_0^2(2x_0x_0''x_1+x_0^2x_1''+2x_0x_0'x_1'+\\&+2x_0x_0'x_1'+x_0'^2x_1)+2\Omega_0\Omega_1(x_0^2x_0''+x_0'^2x_0)]-\lambda x_0\}-\\&-H_2(\tau,C_j)[\Omega_0^2x_0''+(\omega_0^2+\lambda)x_0+\\&+4q^2A^2\Omega_0^2(x_0^2x_0''+x_0'^2x_0)]=0\ ,\ \mathrm{x}_2(0)=x_2'(0)=0\end{aligned} \tag{33}$$

Equation (31) has the following solution:

$$x_0(\tau)=\cos\tau \tag{34}$$

If this result is substituted into Eq.(32) and assuming that $H_1=C_1$=constant, we obtain the following equation:

$$\Omega_0^2(x_1''+x_1)-C_1[(\omega_0^2+\lambda-\Omega_0^2-2q^2A^2\Omega_0^2)\cos\tau- \\ -2q^2A^2\Omega_0^2\cos 3\tau]=0\ ,\quad x_1(0)=x_1'(0)=0 \tag{35}$$

where C_1 is an unknown parameter at this moment. Avoiding the presence of a secular term needs:

$$\Omega_0^2=\frac{\omega_0^2+\lambda}{1+2q^2A^2} \tag{36}$$

With this requirement, the solution of Eq. (35) is:

$$x_1(\tau)=\frac{1}{4}C_1q^2A^2(\cos 3\tau-\cos\tau) \tag{37}$$

If we substitute Eqs. (34), (36) and (37) into Eq. (33), we obtain the equation in x_2:

$$\Omega_0^2(x_2''+x_2)+\frac{2C_1q^2A^2(\omega_0^2+\lambda)}{1+2q^2A^2}\cos 3\tau+ \\ +C_1\left\{\left[\frac{C_1q^4A^4(\omega_0^2+\lambda)}{2(1+2q^2A^2)}+2\Omega_0\Omega_1(1+2q^2A^2)+\lambda\right]\cos\tau+\right. \\ +\left[\frac{(\omega_0^2+\lambda)C_1q^2A^2(3q^2a^2+16)}{2(1+2q^2A^2)}+2\Omega_0\Omega_1q^2A^2\right]\cos 3\tau+ \\ \left.+\frac{9C_1q^4A^4(\omega_0^2+\lambda)}{2(1+2q^2A^2)}\cos 5\tau\right\}+ \\ +H_2(\tau,C_j)\left[\frac{2q^2A^2(\omega_0^2+\lambda)}{1+2q^2A^2}\cos 3\tau\right]=0,\ x_2(0)=x_2'(0)=0 \tag{38}$$

No secular term in $x_2(\tau)$ requires that

$$2\Omega_0\Omega_1=-\frac{\lambda}{1+2q^2a^2}-\frac{C_1q^4A^4(\omega_0^2+\lambda)}{2(1+2q^2A^2)^2} \tag{39}$$

From Eqs. (39) and (18), we obtain the frequency in the form:

$$\Omega=\Omega_0-\frac{\lambda}{\Omega_0(1+2q^2A^2)}-\frac{C_1q^4A^4\Omega_0}{4(1+2q^2A^2)} \tag{40}$$

where Ω_0 is given by Eq.(16). The parameter λ can be determined applying the "principle of minimal sensitivity" and thus we obtain

$$\lambda=\frac{C_1\omega_0q^4A^4}{2+4q^2A^2-C_1q^4A^4} \tag{41}$$

This result is substituted into Eq. 3.129 and we have:

$$\Omega=\frac{\omega_0}{1+2q^2A^2}\sqrt{1+2q^2A^2-\frac{1}{2}C_1q^4A^4} \tag{42}$$

Substituting Eqs. (39), (40) and (41) into Eq. (38), we obtain:

$$x_2''+x_2+2C_1q^2A^2\cos 3\tau+ \\ +\frac{C_1^2q^2A^2(5q^4A^4+7q^2A^2+2)}{1+2q^2A^2}\cos 3\tau+ \\ +\frac{9}{2}C_1^2q^4A^4\cos 5\tau+2H_2(\tau,C_j)q^2A^2\cos 3\tau=0, \\ x_2(0)=x_2'(0)=0 \tag{43}$$

There are many possibilities to choose the function $H_2(\tau,C_j)$. The convergence of the solution $x_2(\tau)$ and consequently the convergence of the approximate solution $\bar{x}(\tau)$ depend on the optimal auxiliary function $H_2(\tau,C_j)$. Basically, the shape of $H_2(\tau,C_j)$ must follow the terms appearing in Eq.(3.127), which are $\cos\tau$, $\cos 3\tau$, $\cos 5\tau$ (odd-order harmonics). Therefore we try to choose $H_2(\tau,C_j)$ so that in Eq. 3.127 the product

$$H_2\left[\frac{2q^2A^2(\omega_0^2+\lambda)}{1+2q^2A^2}\cos 3\tau\right]$$

be of the same shape with the other terms (a combination of functions $\cos\tau$, $\cos 3\tau$, $\cos 5\tau$ …).

All three cases presented in this section demonstrate the importance of the function $H_2(\tau,C_j)$ on the accuracy of the solution. In the same time, a larger number of constants in $H_2(\tau,C_j)$ lead to a better accuracy of the results. If the error obtained using a certain $H_2(\tau,C_j)$ is unsatisfactory, one can choose other shapes for this function.

We will consider three cases:

Case 3.1: We consider the function H_2 of the form:

$$H_2(\tau,C_j)=C_2' \tag{44}$$

where C_2' is an unknown parameter. Substituting Eq.(44) into Eq.(43), we obtain the equation in x_2:

$$x_2''+x_2+\left[2(C_1+C_2')q^2A^2+\right. \\ \left.+\frac{C_1^2q^2A^2(5q^4A^4+7q^2A^2+2)}{1+2q^2A^2}\right]\cos 3\tau \\ +\frac{9}{2}C_1^2q^4A^4\cos 5\tau=0\ ,\quad x_2(0)=x_2'(0)=0 \tag{45}$$

The solution of Eq.(45) becomes:

$$x_2(\tau)=\left[\frac{C_1+C_2'}{4}+\frac{C_1^2q^2a^2(5q^4A^4+7q^2A^2+2)}{8(1+2q^2A^2)}\right](\cos 3\tau- \\ -\cos\tau)+\frac{3}{16}C_1^2q^4A^4(\cos 5\tau-\cos\tau) \tag{46}$$

The second-order approximate solution is

$$\bar{x}(\tau)=x_0(\tau)+x_1(\tau)+x_2(\tau)$$

where x_0, x_1 and x_2 are given by Eqs. (34), (37) and (46). Using the transformations (3), the second-order approximate solution of Eq.(1) becomes

$$\bar{u}(t)=M\cos\Omega t+N\cos 3\Omega t+P\cos 5\Omega t \tag{47}$$

where Ω is given by Eq. 3.131 and

$$M=A-\frac{2C_1+C_2'}{4}q^2A^3-\frac{C_1^2q^2A^3(16q^4A^4+17q^2A^2+4)}{16(1+2q^2A^2)} \\ N=\frac{2C_1+C_2'}{4}q^2A^3+\frac{C_1^2q^2A^3(5q^4A^4+7q^2A^2+2)}{8(1+2q^2A^2)} \\ P=\frac{3}{16}C_1^2q^4A^5 \tag{48}$$

Case 3.2: We consider the function $H_2(\tau, C_j)$ if the form

$$H_2(\tau, C_j) = C_2 + C_3\cos 2\tau + C_4\cos 4\tau \tag{49}$$

where C_2, C_3 and C_4 are unknown parameters. Substituting Eq. 3.138 into Eq. 3.132 and avoiding the presence of a secular term, we obtain:

$$C_4 = -C_3 \tag{50}$$

respectively:

$$\begin{aligned} &x_2'' + x_2 + [2(C_1 + C_2)q^2A^2 + \\ &+ \frac{C_1^2 q^2 A^2 (5q^4A^4 + 7q^2A^2 + 2)}{1 + 2q^2A^2}\Big]\cos 3\tau + \\ &+ \Big[\frac{9}{2}C_1^2 q^4 A^4 + C_3 q^2 A^2\Big]\cos 5\tau - \\ &- C_3 q^2 A^2 \cos 7\tau = 0, x_2(0) = x_2'(0) = 0 \end{aligned} \tag{51}$$

With these requirements, the solution of Eq. 3.140 becomes:

$$\begin{aligned} x_2(\tau) = &\Big[\frac{C_1 + C_2}{4} q^2A^2 + \\ &+ \frac{C_1^2 q^2 A^2 (5q^4A^4 + 7q^2A^2 + 2)}{8(1 + 2q^2A^2)}\Big](\cos 3\tau - \cos\tau) + \\ &+ \Big[\frac{3}{16}C_1^2 q^4 A^4 + \frac{1}{24}C_3 q^2 A^2\Big](\cos 5\tau - \cos\tau) - \\ &- \frac{1}{48}C_3 q^2 A^2 (\cos 7\tau - \cos\tau) \end{aligned} \tag{52}$$

The second-order approximate solution in this case is:

$$\bar{u} = \bar{M}\cos\Omega t + \bar{N}\cos 3\Omega t + \bar{P}\cos 5\Omega t + \bar{Q}\cos 7\Omega t \tag{53}$$

where Ω is given by Eq. 3.131 and the coefficients are:

$$\begin{aligned} &\bar{M} = A - \frac{2C_1 + C_2}{4} q^2A^3 - \\ &- \frac{C_1^2 q^2 A^3 (16q^4A^4 + 17q^2A^2 + 4)}{16(1 + 2q^2A^2)} - \frac{1}{48}C_3 q^2 A^3 \\ &\bar{N} = \frac{2C_1 + C_2}{4} q^2A^3 + \frac{C_1^2 q^2 A^3 (5q^4A^4 + 7q^2A^2 + 2)}{8(1 + 2q^2A^2)} \\ &\bar{P} = \frac{3}{16}C_1^2 q^4 A^5 + \frac{1}{24}C_3 q^2 A^3, \bar{Q} = -\frac{1}{48}C_3 q^2 A^3 \end{aligned} \tag{54}$$

Case 3.3: We consider the function $H_2(\tau, C_j)$ of the form:

$$\begin{aligned} H_2(\tau, C_j) = &C_2^* + C_3^*\cos 2\tau + C_4^*\cos 4\tau + \\ &+ C_5^*\cos 6\tau + C_6^*\cos 8\tau + C_7^*\cos 10\tau \end{aligned} \tag{55}$$

where C_2^*, C_3^*, C_4^*, C_5^*, C_6^* and C_7^* are unknown parameters. Substituting Eq.(54) into Eq.(43), we obtain:

$$C_4^* = -C_3^* \tag{56}$$

and then:

$$\begin{aligned} x_2(\tau) = &\Big[\frac{2C_1 + 2C_2^* + C_5^*}{8} q^2A^2 + \\ &+ \frac{C_1^2 q^2 A^2 (5q^4A^4 + 7q^2A^2 + 2)}{8(1 + 2q^2A^2)}\Big](\cos 3\tau - \\ &- \cos\tau) + \Big[\frac{3}{16}C_1^2 q^4 A^5 + \frac{1}{24}(C_3^* + C_6^*)q^2A^2\Big](\cos 5\tau - \\ &- \cos\tau) + \frac{1}{48}(C_3^* - C_7^*)q^2A^2(\cos\tau - \\ &- \cos 7\tau) + \frac{1}{80}C_5^* q^2 A^2 (\cos 9\tau - \cos\tau) + \\ &+ \frac{C_6^*}{120} q^2A^2(\cos 11\tau - \cos\tau) + \frac{C_7^* q^2 A^2}{168}(\cos 13\tau - \cos\tau) \end{aligned} \tag{57}$$

The second-order approximate solution of Eq.(1) becomes:

$$\begin{aligned} \bar{u}(t) = &M^*\cos\Omega t + N^*\cos 3\Omega t + P^*\cos 5\Omega t + \\ &+ Q^*\cos 7\Omega t + R^*\cos 9\Omega t + S^*\cos 11\Omega t + T^*\cos 13\Omega t \end{aligned} \tag{58}$$

where

$$\begin{aligned} &M^* = A - \frac{q^2A^3}{240}(120C_1 + 60C_2^* + 5C_3^* + 3C_4^* + 32C_5^* + \\ &+ 10C_6^* + 45/7C_7^*) - \frac{C_1^2 q^2 A^3 (16q^4A^4 + 17q^2A^2 + 4)}{16(1 + 2q^2A^2)} \\ &N^* = \frac{4C_1 + 2C_2^* + C_5^*}{8} q^2A^3 + \frac{C_1^2 q^2 A^3 (5q^4A^4 + 7q^2A^2 + 2)}{8(1 + 2q^2A^2)} \\ &P^* = \frac{C_3^* + C_6^*}{24} q^2A^3 + \frac{3}{16}C_1^2 q^4 A^5 \\ &Q^* = -\frac{1}{48}(C_3^* - C_7^*)A^3q^2 \\ &R^* = \frac{1}{80}C_4^* q^2A^3, S^* = \frac{1}{120}C_5^* q^2A^3, T^* = \frac{1}{168}C_7^* q^2A^3 \end{aligned} \tag{59}$$

4. NUMERICAL EXAMPLES

We will show through six numerical examples that the error of the solutions decreases when the number of terms in the auxiliary function *H(τ,p)* increases. In Eqs. (1) and (2), we consider $\Lambda = \omega_0 = 1$, $A = 1$ and two cases for q in every of the cases 3.1, 3.2 and 3.3. The optimal values of the optimal convergence-control parameters C_i are obtained using the collocation method.

4.1. For q=1 in the case 3.1, it is obtained:

$$C_1 = -0.401483291\ ,\ C_2' = -0.065781508$$

The second-order approximate solution (47) becomes in this case:

$$\begin{aligned} \bar{u}(t) = &1.092937297\cos\Omega t - 0.123160203\cos 3\Omega t + \\ &+ 0.030222906\cos 5\Omega t \end{aligned} \tag{60}$$

where Ω is obtained from Eq.(42): Ω=0.596353888.

4.2 For q=1 in the case 3.2, it is obtained

$$C_1 = -0.3984315\ ;\ C_2 = -0.0524853\ ;\ C_3 = 0.03417867$$

$$\begin{aligned} \bar{u}(t) = &1.089257032\cos\Omega t - 0.119734278\cos 3\Omega t + \\ &+ 0.031189301\cos 5\Omega t - 0.00712055\cos 7\Omega t \end{aligned} \tag{61}$$

where Ω=0.596211722.

4.3 For q=1 in the case 3.3, we obtain the following results

$C_1 = -0.39573960;\ C_2^* = 0.05812246;\ C_3^* = 0.32324888;$
$C_4^* = 0.15719799;\ C_5^* = -0.0561361\ ;\ C_6^* = -0.4577455;$
$C_7^* = 0.01156349$

$$\begin{aligned}\bar{u}(t) &= 1.080167589\cos\Omega t - 0.099000466\cos 3\Omega t + \\ &+ 0.023760318\cos 5\Omega t - 0.006493445\cos 7\Omega t + \\ &+ 0.001964974\cos 9\Omega t - 0.000467801\cos 11\Omega t + \\ &+ 0.0000688303\cos 13\Omega t\end{aligned} \tag{62}$$

where Ω=0.596086291.

4.4. For q=2 in the case 3.1 we obtain

$C_1 = -0.167434521\ ,\ C_2' = -0.002382096$

$$\begin{aligned}\bar{u}(t) &= 1.081827344\cos\Omega t - 0.165930301\cos 3\Omega t + \\ &+ 0.084102956\cos 5\Omega t\end{aligned} \tag{63}$$

where Ω=0.357278398.

4.5. For q=2 in the case *3.2* it is obtained

$C_1 = -0.1643574\ ;\ C_2 = 0.0174479\ ;\ C_3 = -0.0736105$

$$\begin{aligned}\bar{u}(t) &= 1.071279366\cos\Omega t - 0.146185231\cos 3\Omega t + \\ &+ 0.068771654\cos 5\Omega t + 0.00613421\cos 7\Omega t\end{aligned} \tag{64}$$

where Ω=0.356852829.

4.6 For q=2 in the case 3.3 it is obtained

$C_1 = -0.1612362\ ;\ C_2^* = 0.08982749;\ C_3^* = 0.31938160;$
$C_4^* = 0.21595928;\ C_5^* = -0.13759550;\ C_6^* = -0.4838167;$
$C_7^* = 0.05079732$

$$\begin{aligned}\bar{u}(t) &= 1.106947017\cos\Omega t - 0.142571421\cos 3\Omega t + \\ &+ 0.0505855201\cos 5\Omega t - 0.022382023\cos 7\Omega t + \\ &+ 0.010797964\cos 9\Omega t - 0.004586516\cos 11\Omega t + \\ &+ 0.00120946003\cos 13\Omega t\end{aligned} \tag{65}$$

where Ω=0.356420648.

It is easy to verify the accuracy of the obtained solutions if we graphically compare these analytical solutions with the numerical ones. Figs. 2-7 show the comparison between the present solutions and the numerical integration results obtained by a fourth-order Runge-Kutta method.

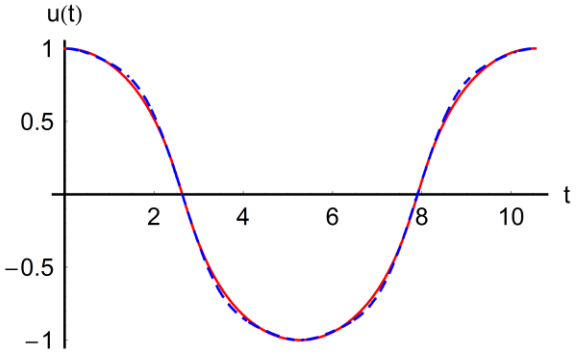

Fig. 2 *Comparison between the approximate and numerical results of Eq.(1) in case 4.1, for $A=\omega_0=a=q=1$: _____ numerical solution, _ _ _ _ approximate solution (60)*

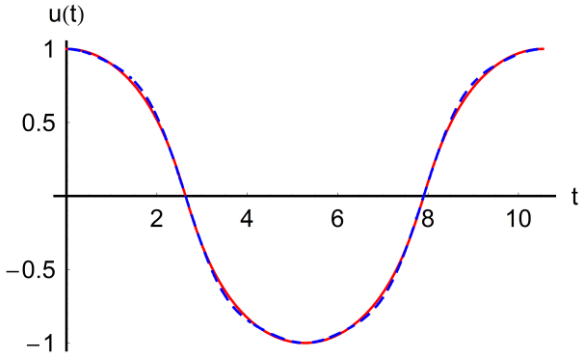

Fig. 3 *Comparison between the approximate and numerical results of Eq.(1) in case 4.2, for $A=\omega_0=a=q=1$: _____ numerical solution, _ _ _ _ approximate solution (61)*

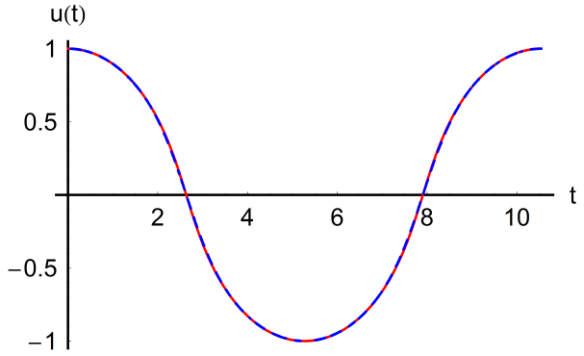

Fig. 4 *Comparison between the approximate and numerical results of Eq.(1) in case 4.3, for $A=\omega_0=a=q=1$: _____ numerical solution, _ _ _ _ approximate solution (62)*

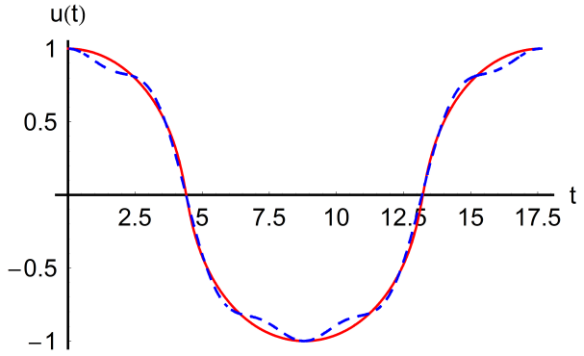

Fig. 5 *Comparison between the approximate and numerical results of Eq.(1) in case 4.4, for $A=\omega_0=a=1, q=2$: _____ numerical solution, _ _ _ _ approximate solution (63)*

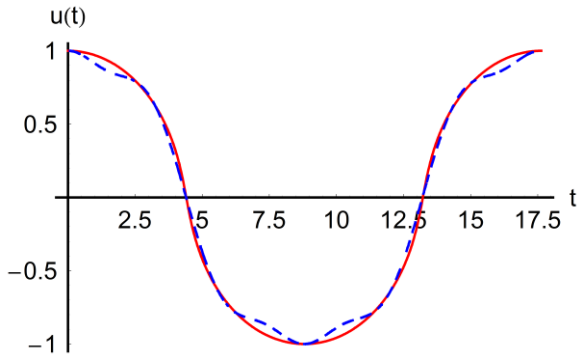

Fig. 6 *Comparison between the approximate and numerical results of Eq.(1) in case 4.5, for $A=\omega_0=a=1, q=2$: _____ numerical solution, _ _ _ _ approximate solution (64)*

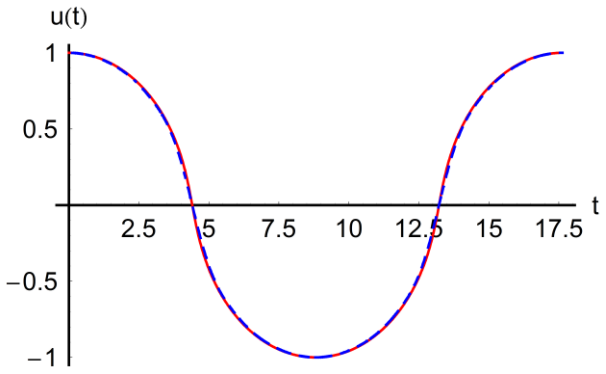

Fig. 7 *Comparison between the approximate and numerical results of Eq.(1) in case 4.6, for* $A=\omega_0=a=1,q=2$*:* _____*numerical solution,* _ _ _ _ *approximate solution (65)*

5. CONCLUSIONS

It can be seen from Figs. 2-7 that the solutions obtained by OHAM are very accurate being nearly identical with the solutions obtained by a fourth-order Runge-Kutta method. Moreover, the analytical solutions obtained by our procedure prove to be more accurate along with an increased number of terms in the optimal auxiliary function $H(\tau,p)$.

REFERENCES

[1] A.H. Nayfeh, D.T. Mook, *Nonlinear Oscillations*, Wiley, New York, 1979

[2] V. Marinca, N. Herisanu, "Determination of periordic solutions for the motion of a particle on a rotating parabola by means of the optimal homotopy asymptotic method", *J of Sound and Vibration* vol.329, pp.1450-1459, 2010

[3] V. Marinca, N. Herisanu, *Nonlinear Dynamical Systems in Engineering. Some Approximate Approaches*, Springer, Berlin Heidelberg, 2011

[4] P. Amore, A. Aranda, "Improved Lindstedt-Poincare method for the solution of nonlinear problems", *J of Sound and Vibration* vol.283, pp.1115-1136, 2009

[5] V. Marinca, N. Herişanu, I. Nemeş, "Optimal homotopy asymptotic method with application to thin film flow", *Cent. Eur. J. Phys*., vol.6, pp.648–653, 2008

[6] N. Herisanu, V. Marinca, "Explicit analytical approximation to large-amplitude non-linear oscillations of a uniform cantilever beam carrying an intermediate lumped mass and rotary inertia", *Meccanica*, vol.45, pp. 847-855, 2010

[7] V. Marinca, N. Herisanu, "An optimal homotopy asymptotic approach to nonlinear MHD Jeffery-Hamel flow", *Mathematical Problems in Engineering*, Article ID 169056, 2011

[8] N. Herisanu, V. Marinca, "Accurate analytical solutions to osciilators with discontinuities and fractional-power restoring force by means of the Optimal Homotopy Aaymptotic Method", *Comput. Math. Appl*., vol.60, pp. 1607-1615, 2010

[9] V. Marinca, N. Herisanu, "The Optimal Homotopy Asymptotic Method for solving Blasius equation", *Appl. Math. Comput*. Vol.231, pp.134-139, 2014

[10] V. Marinca, N. Herisanu, "On the fow of a Walters type B' viscoelastic fluid in a vertical channel with porous wall", *Int. J Heat and Mass Transfer* vol.796, pp.145-165, 2014

University of Nis
Faculty of Occupational Safety
„Politechnica“ University of Timisoara
Faculty of Mechanical Engineering
24th International Conference
NOISE AND VIBRATION
Niš, 29 - 31. 10. 2014.

DYNAMICAL STRUCTURAL RELIABILITY BASED ON THE CASE STUDY ANALYSIS

Miomir Jovanović[1], *Goran Radoičić*[1]

[1] University of Niš, Faculty of Mechanical Engineering, Department for Transport Technique and Logistics
miomir@masfak.ni.ac.rs

Abstract - *An important aspect of the support structures' design is their dynamic behaviour under extreme conditions. Especially actual are the large-range structures. Therefore, the support structure of a mining machine for transport of tailings (stacker) is observed dynamically. The dynamic behaviour of the entire structure in an incidental situation – the failure of a support tie rod for the pylon-platform connection is observed. The aim of this research is to predict the consequences of breaking a structure element for the rest of the support structure. This paper shows the theoretical modelling of structures, numerical solution of differential equations, and vibrations after simulated incident. The paper presents special design – the way of structure testing from the aspect of high structural availability and ability of the structure to compensate overload caused by the incident. To check the model, a real stacker structure was used at the surface mine RBB (The copper mine – Bor, Serbia). The developed numerical model showed the internal stress states of the structure and the law of vibration after the incident. On the basis of more case study analyses, the overall reliability and ability of redundancy of the structure were evaluated.*

Keywords: *case study, frame structures, incident behaviour, modal analysis, reliability, transient analysis.*

1. INTRODUCTION

A good quality of reliable mining machinery is its adjustment to accept all regular and irregular effects that occur during many years of exploitation. On surface mining pits, the significance and price of mining machinery and earth-moving equipment impose tests which are often in the field of rare occurrences. This type of analysis is denoted as the case study analysis on the extreme effects, mainly. Stackers and rotating excavators (dredgers) are particularly sensitive, because despite their big masses they have sensitive structural relationship between under-frame structural stand with caterpillars and rotating platform with *RotheErde* bearing [1]. That relationship between two big masses is a delicate part of the structure which allows many vibrations of the upper mass – rotating platform and boom. The aim of good design is the dynamic stability and high stress utilization of the stacker support structure. The case study analysis is used to calculate structure vibration amplitudes under the forced harmonic effect and structural resistance against incidental events such as impact effect, wind gust, seismic wave and other random effects.

Newer studies [2,3,4,5] analyze the case of failure and consequences caused when certain parts of structure break. Rotating excavators and stackers have very sensitive parts which are very high loaded. These are the support tie rods. So that follow the questions. Will the failure - local fracture of a support tie rod for the connection of the pylon and rotating platform jeopardize the overall structural stability? Will the redundancy enable the stability preservation of the rest of structure? The answer to these questions can be obtained by numerical simulation. The transient dynamic analysis of mechanical structure based on energy balance is suitable to be used in the numerical simulation of fracture incident. This paper researched an incidental situation i.e. the interruption of a responsible element of the stacker for the connection between the pylon and rotating platform (a rear support tie rod). It is not such a frequent failure in practice because it is about the tie rod element with a large moment of inertia of the cross section, but it can occur in exceptional situations such as, for example, a collision of two objects or similar.

2. DYNAMIC STRUCTURE MODELLING

Dynamic modelling of the stacker was performed by forming the discrete system of mass elements of the support structure and installed machine equipment. The masses are coupled mutually by the elastic connections of structural elements. For practical research, the dynamic modelling can be performed by the FEA modeler. For the modelling in this paper, the real structure of the stacker RBB [3,5] was used. The analysis was performed using the finite element method [6] and the MSC software [7]. The stacker's elements, as the rotating platform and boom, are the frame structures, so they were modelled by the beam finite elements. The machine equipment, belt, drums and transported material on the conveyor belt were modelled by the dotted finite elements (concentrated masses). The stacker base (pedestal) without caterpillars is placed rigidly on the ground. By this and earlier investigations [2,3,5], the discrete model for the FEM analysis and numerical solving the differential equations has been developed.

The high fidelity model, shown in Fig. 1, represents the stacker of dimensions L/H/W=55.9/16.88/7.87 m and the total mass of 210680 kg. The model contains 2134 finite elements (masses) and 1016 nodes in total. This large number

of masses makes modelling more realistic and leads to advantages of discrete models.

The aim of structure behaviour analysis is to check the existence of incidental situations that can occur due to failures in structure. The support tie rods are expected to be the first elements in failure because of their high level of stress, variable dynamic loads and big lengths. In the moment of a sudden interruption of element function due to the fracture, the potential energy of the interrupted element is diverted to other elements of the frame structure. This impulse increases the static force redistribution dynamically, so that the question of surrounding elements ability to take over the impact effect could be asked. It is a special aim of design which checks the redundancy of structure in the case of failure, in particular dynamically, according to the character and duration of incident.

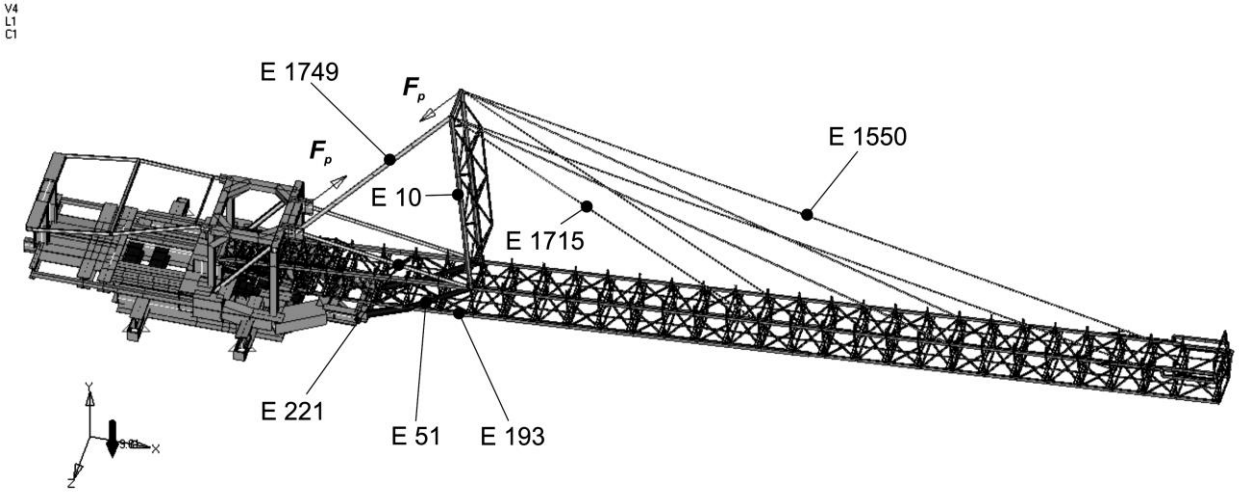

Fig. 1 *Geometric model of the support structure of the stacker (E – selected responsible elements, F_p - axial force)*

3. ANALYSIS OF FREE VIBRATIONS

Before transient analysis, the characteristic frequencies of damped vibration are determined. The equations of free undamped vibrations for a linear mechanical system are expressed in the matrix form, Eq.(1), while the solution of the low of vibration has the harmonic form, Eq.(2) [6,8]. In the normal modes analysis, for solving the free undamped vibrations from Eq.(1), the frequency equation, Eq.(3), is used:

$$\mathbf{M}\ddot{\mathbf{q}} + \mathbf{K}\mathbf{q} = \mathbf{0} \tag{1}$$

$$\mathbf{q} = \mathbf{\Phi}_i \cos \omega_i t \tag{2}$$

$$\left|\mathbf{K} - \omega^2 \mathbf{M}\right| \mathbf{\Phi} = \mathbf{0} \tag{3}$$

In previous equations, **M** is the matrix of masses and inertia coefficients, **K** is the stiffness matrix**,** ω_i is i^{th} natural circular frequency (eigenfrequency) in radians per unit time, **q** and $\ddot{\mathbf{q}}$ are generalized vectors of translation and acceleration respectively, while $\mathbf{\Phi}_i$ is the representative vector of mode shape for i^{th} eigenfrequency. Deformation shapes, specific for each eigenfrequency, are called the mode shapes. The analysis of vibration shapes and eigenfrequencies is called the normal modes analysis.

In this research, the modal analysis was performed using the *Lanczos* method and modified *Givens* method [6]. The modified inverse *Sturm* method was also used to extract the lowest eigenfrequency.

These frequencies are important for the dynamic load of rods. Table 1 indicates the values of the computed eigenfrequencies of stacker boom at lateral and vertical vibration. These vibrations arise after fracture of a rear support tie rod (replaced with the axial force F_p in Fig.1) for the connection between the pylon and rotating platform. The eigenfrequencies from Table 1 are significant for the dynamic load of the support tie rods.

Table 1 *Some characteristic eigenfrequencies of the stacker*

Mode shape	Mode-12 Lateral	Mode-17 Vertical	Mode-20 Vertical	Mode-31 Lateral Torsion	Mode-33 Vertical Torsion	Mode-34 Lateral Torsion
Eigenfrequency Ω [Hz]	0.467861	0.688175	0.766214	1.954615	2.359128	2.521812
Mode shape	Mode-37 Lateral Torsion	Mode-38 Vertical	Mode-46 Lateral Torsion	Mode-50 Vertical Lateral Longitudinal	Mode-66 Vertical Longitudinal	Mode-95 Vertical
Eigenfrequency Ω [Hz]	3.024481	3.181569	4.137398	6.264608	10.79204	12.52006

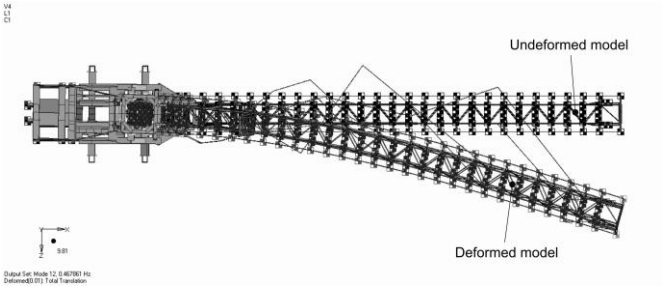

Fig. 2 *Lateral vibration (top view) Mode-12, Ω_{12}=0.467861 Hz*

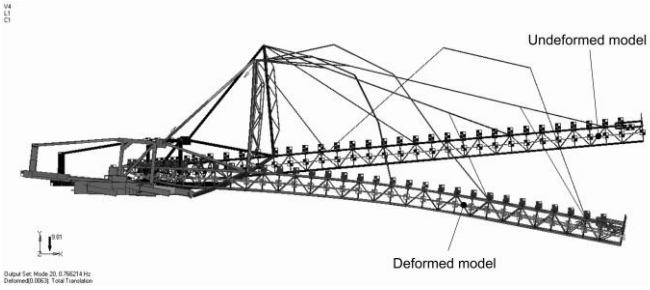

Fig. 3 *Vertical vibration (right view) Mode-20, Ω_{20}=0.766214 Hz*

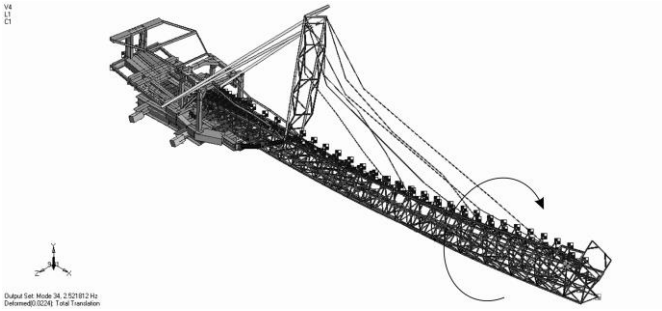

Fig. 4 *Lateral vibration + torsion (isometric view) Mode-34, Ω_{34}=2.521812 Hz*

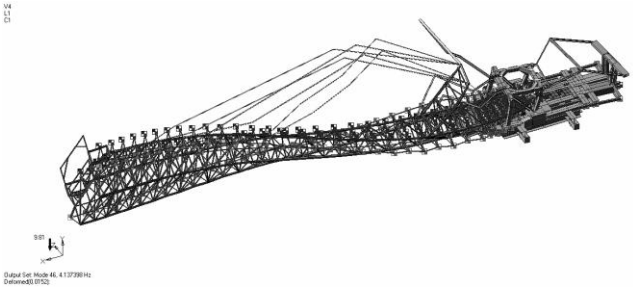

Fig. 5 *Lateral vibration + torsion (a spatial view) Mode-46, Ω_{46}=4.137398 Hz*

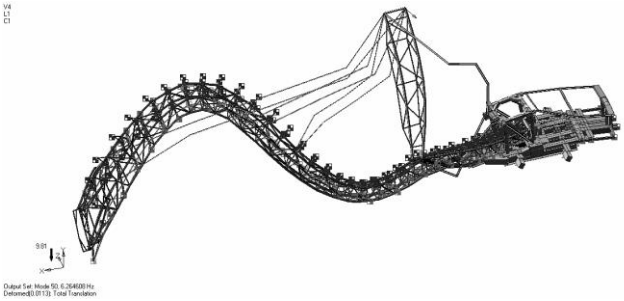

Fig. 6 *Vertical + lateral + longitudinal vibration (a spatial view) Mode-50, Ω_{50}=6.264608 Hz*

The first hundred eigenvalues and eigenvectors (modes) were identified by modal analysis of the developed model. The first hundred eigenfrequencies took place between the values Ω=0.0723452 Hz and 12.75624 Hz. Very low eigenfrequencies are consequences of the massive rotating structure reliance on the moving base over a small *RotheErde* bearing. Various models of the rotating platform reliance were tested in order to determine their influences on eigenvalues. In relation to other structure elements, the reliance usually has the greatest influence on eigenvalues. The first thirty eigenvalues, extracted by modal analysis, are characteristic of support tie rods vibration in the frequency range from 0.0723452 to 1.678639 Hz (Mode-1 to Mode-30). In this range, the lateral - Mode-12 and vertical - Mode-17 and 20 vibration shapes of the boom were exempted. The eigenfrequencies of alternating vertical and lateral bending of the boom, in the presence of a weak torsion, took places in the range from 1.954615 Hz (Mode-31) to 3.196299 Hz (Mode-39). Only the vibrations of the support tie rods occured again in the frequency range from 3.31963 Hz (Mode-40) to 3.692737 Hz (Mode-45). The expressed torsional vibration of the boom occured in the interval from 4.137398 Hz (Mode-46) to 6.775579 Hz (Mode-52), with a small exception. The slightly longitudinal undulation of the boom characterizes the range from 7.327017 to 8.48324 Hz (Mode-53 to Mode-59). The eigenvalues of 8.613748 Hz (Mode-60) and 8.707745 Hz (Mode-61) refer to the boom torsion. The vibrations of the conveyor belt and elements of the belt holder were dominant, starting from the vibration shape Mode-62 (8.756838 Hz) to the last extracted shape Mode-100 (12.75624 Hz). In the final frequency range, a certain vibration of the boom structure occurs, for example such as the vibration shape Mode-95 (12.52006 Hz). Figs. 2 to 6 illustrate the dominant mode shapes of the developed FEM model of the stacker without a tie rod for the connection between the pylon and rotating platform.

For solving the basic task – transient analysis, the two dominant eigenfrequencies, required for energy description (damping velocity), were selected from the modal analysis. Figs. 4 and 5 simply show the mode shapes of these eigenfrequencies. These are the circular frequencies whose eigenvectors indicate a combination of torsion and lateral translation of the structure elements of the stacker (Ω_{34}=2.521812 Hz and Ω_{46}=4.137398 Hz).

4. INCIDENTAL DYNAMIC ANALYSIS

4.1 Theoretic approach

A linear dynamic model which implies significantly less displacements (vibration amplitudes) in relation to dimensions of the modelled structure is adopted in the research. By this assumption the changes in structural configuration become negligible. Consequently, the stiffness matrix **K** is determined by integrating the original structural configuration, and elastic (internal) structural forces are computed by the direct manner (multiplying the stiffness matrix and displacements). The second assumption of this linear model is the application of a linear-elastic material. It allows the use of a constitutive constant matrix of material. The additional assumption includes the immutability of the boundary conditions during the forced effect.

The paper discusses an incidental case of structural behavior limited by geometric linearity. In the case of significant (large) displacements, geometrically nonlinear transient analysis must be conducted. In the case of linear transient analysis, the differential (dynamic) equation of structure motion has form:

$$\mathbf{M}\ddot{\mathbf{q}} + \mathbf{B}\dot{\mathbf{q}} + \mathbf{K}\mathbf{q} = \mathbf{F}(t) \tag{4}$$

Where **M**, **B** and **K** are the mass matrix, damping matrix and stiffness matrix, respectively, **q** is the generalized vector of translation ($\dot{\mathbf{q}}$ – velocity, $\ddot{\mathbf{q}}$ – acceleration), and **F**(*t*) is the external (excitation) generalized force in a vector form.

4.2 Simulation scenario

Shaping of the perturbation force (tie rod axial force) was carried out on the basis of experimental development case study of the real structure under amplified vibrations. An incident – fracture can occur because of the collision of two machines in the immediate proximity or some other random influences.

Fig. 7 shows the critical assumption form of the normalized perturbation force $\Delta F/F$ (for the axial force F_p). In this figure, Δt_{bf} is the time before fracture, Δt_f the fracture time and Δt_{pf} is the post-fracture time. After t=60 s, large deformations of the rear pair of tie rods (for connection between the pylon and rotating platform) and the first sign of fracture occur due to the straining. The total interruption (failure) of a support tie rod occurs in the moment of simulation t=60.5 s. The structure is maximal loaded by the load on the conveyor belt for the whole duration of simulation $T_s = \Delta t_{bf} + \Delta t_f + \Delta t_{pf} = 120$ s.

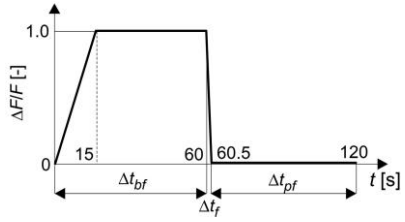

Fig. 7 *Normalized disruptive force*

The overall structural damping coefficient G=0.03 was used in the analysis. Damping is proportional to the velocity of vibration at selected and close frequencies [9] which were determined in previous modal analysis (Chapter 3.0). The integration step was proportionally smaller of highest significant frequency obtained by modal analysis, i.e. 0.01 s. The number of steps amounted to 12000.

4.3 Transient response analysis

The obtained results of the conducted transient analyses are the subject of next analysis evaluation of the structure. The evaluation of system reliability can be performed on the basis of the following five technical categories of dynamic structure behaviour: *a*) the stress level of structural elements in relation to the permissible stress, *b*) the dynamic coefficient of structural elements as the ratio of forces or stresses, *c*) preserved or lost structure stability (the presence of other structural parts fracture), *d*) class – size of some interesting elements displacements (small or large displacements) and *e*) the possibility assessment of event (failure) repetition and calculation of reliability value (stress reserve).

For analysis of transient structural response, the seven responsible elements of the FE assembly were selected. These are: E-1749 - the remaining rear support tie rod for connection between the pylon and rotating platform (Fig.1), E-10 - the main vertical holder of the pylon, E-1550 - the first pair of boom support tie rods – longest boom tie rod, E-1715 - the third pair of tie rods – shortest boom tie rod, E-221 - the slanting rod for fixing the pylon at the root, E-51 - the slanting support carrier and E-193 – the element of the main bottom belt of the boom below the pylon. In these elements, increment of stress and axial force was monitored at the moment of the incident occurrence – fracture of the tie rod element (t=60s).

All obtained static stresses (before fracture) are located in the permissible stress area which corresponds to structural steels of Group I (Yield point of $290 \cdot 10^6$ Nm^{-2}, EuroCode3), for the third load case and the safety coefficient of 1.2 ($\sigma_p = 290 \cdot 10^6 / 1.2 \approx 242 \cdot 10^6$ Nm^{-2}). After the fracture of the tie rod, balancing of internal forces with the help of reserve structural resistance happened again. The structure has suffered the fracture in terms of the first criterion (*a* – above mentioned the stress level). Table 2 provides a preview of initial static stresses before the fracture and maximal dynamic stresses caused by the incident.

Table 2 *Stresses in the selected elements [Nm^{-2}]*

	The first pair of the boom tie rods; element E-1729	The second pair of the boom tie rods; element E-1719	The third pair of the boom tie rods; element E-1550	The boom belt below the pylon; element E-193
Max/min static complex stress*	0.708E+8	0.942E+8	0.890E+8	-0.965E+8
Max/min dynamic complex stress	0.515E+9	0.765E+9	1.745E+9	-1.559E+8

*Static stresses were obtained in the previous static FEM analysis of the structure [3]

Expressed stress changes occur at the tension of the third pair of boom support tie rods (the longest tie rod E-1550) in a longer simulation time (Fig. 8). Tensile stresses have been changed from minimal to extremely high values, above the recommended, in the stepwise time intervals. Thereby, the stress did not exceed the critical value – Yield point. The stresses of pressure were most expressed in the boom belt element (E-193). However, these stresses were significantly lower than the highest stresses of tension, in their absolute values. It is preferred that the stresses, obtained on this way from the dynamic response on incident, are an additional criterion of structural design because one such criterion indicates when structure succeeds to compensate the damage caused by a local incident. The properties of redundancy, obtained on this manner, are special properties which lead to high reliability and low operating costs in exploitation.

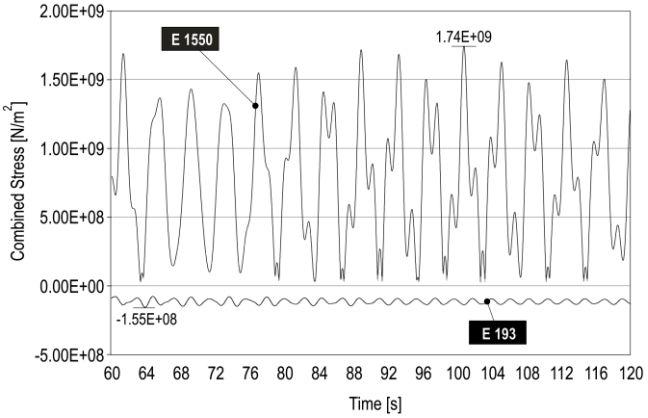

Fig. 8 *Combined stress: maximal E-1550, minimal E-193*

For the evaluation of structure reliability on incidental dynamics the dynamic coefficient K_d is adopted. It is the ratio of the min(pressure)/max(tension) post fracture dynamic force F_{pf} after an incident and the equilibrium force F_{eq} in the same element, Eq.(5), Fig. 9.

$$K_d = \frac{F_{pf}}{F_{eq}}, \quad (K_d > 1) \tag{5}$$

The dynamic response gives the insight into one more dynamic parameter. It is about the coefficient of overall force growth K_F. Actually, this coefficient is the ratio of the min/max post fracture dynamic force F_{pf} and the mean value of the load force before fracture F_{bf} in a selected element, Eq.(6), Fig. 9. The coefficients K_d and K_F indicate the new equilibrium situation of a structure and local reallocation of forces after an incident (redundancy).

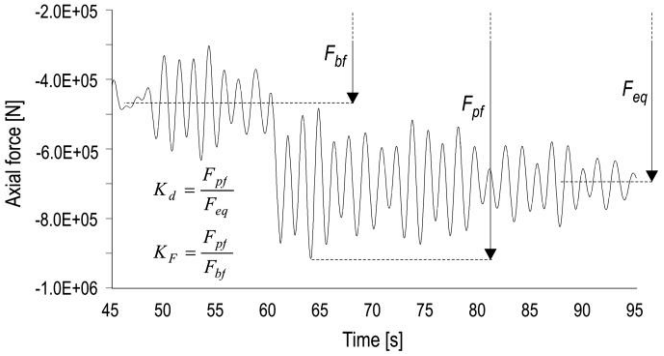

Fig. 9 *An explanation for the dynamic coefficients*

$$K_F = \frac{F_{pf}}{F_{bf}}, \quad (K_F > 1) \tag{6}$$

Table 3 shows the values of axial – internal force of the selected responsible elements of the stacker structure as well as the coefficients K_d and K_F for the same elements. Fig. 10 shows the diagrams of the axial forces. It is about structural elements with a sufficient dynamic reserve since the dynamic coefficients from Table 3 did not exceed the recommended value i.e. $K_d < K_p$=1.5 in the case of fracture of a tie rod.

Table 3 *Dynamic coefficients of the selected structure elements*

Structural element	Before fracture axial force F_{bf} [N]	Post fracture equilibrium force F_{eq} [N]	Min/max post fracture force F_{pf} [N]	Action time* t (s)	Dynamic coefficient K_d [-]	Total force growth coefficient K_F [-]
(1)	(2)	(3)	(4)	(5)	(4)/(3)	(4)/(2)
E-10	-301907	-516267	-673604	62.45	1.30	2.23
E-51	-471173	-697070	-915653	63.95	1.31	1.94
E-221	478677	557306	742057	62.50	1.33	1.55
E-1715	58744	87726	106771	61.00	1.22	1.82
E-1749	279849	489873	642288	62.45	1.31	2.29

*The time in which the max/min force occurs in an element, measured from the beginning of simulation and after a fracture of the tie rod.

The structural elements from Table 3 were selected due to the expected increase in their internal forces. Thus, the biggest value of the axial force of pressure (minimum of force) occurs in the slanting support carrier (E-51) after the incident (fracture) and it is easy to see on the diagram in Fig. 10. On the other hand, the biggest nominal value of the tensile force occurs in the slanting rod for fixing the pylon at the root (E-221) after the interruption of a connection between the pylon and rotating platform, Fig. 10 (maximum of force). The biggest relative jump of force from an equilibrium state was recorded in the remaining rear tie rod (E-1749) which can be seen in Fig. 10 as well as on the basis of the total force growth coefficient K_F=2.29 in Table 3.

From the transient response, one can conclude that the rear tie rod interruption did not jeopardize the total structure stability (criterion *c*) and the local elements damage did not occurr (criterion *a*). However, the tie rod fracture caused the vibration shapes with the dominant lateral translation of the pylon (Δz_{max} in Fig. 11) and the vertical translation of the top of the boom (Δy_{max} in Fig. 12), according to criterion *d*.

Beside the biggest translation in lateral direction Δz_{max}=0.172-(-0.006)=0.178 m, caused by an incidental dynamics, the top of the pylon, introduced by the node N-729, has also longitudinal (Δx_{max}=0.256-0.121=0.135 m) and vertical translation (Δy_{max}=-0.043-(-0.084)= 0.041 m), Fig. 11. On the other hand, the top of the boom, introduced by the node N-387, translates in vertical direction most significantly (Δy_{max}=**-0.484**-(-0.803)=0.319 m) and then in lateral direction (Δz_{max}=0.27 m), Fig. 12. The longitudinal translations of the top of the boom (along *x*-axis) can be regarded as negligible.

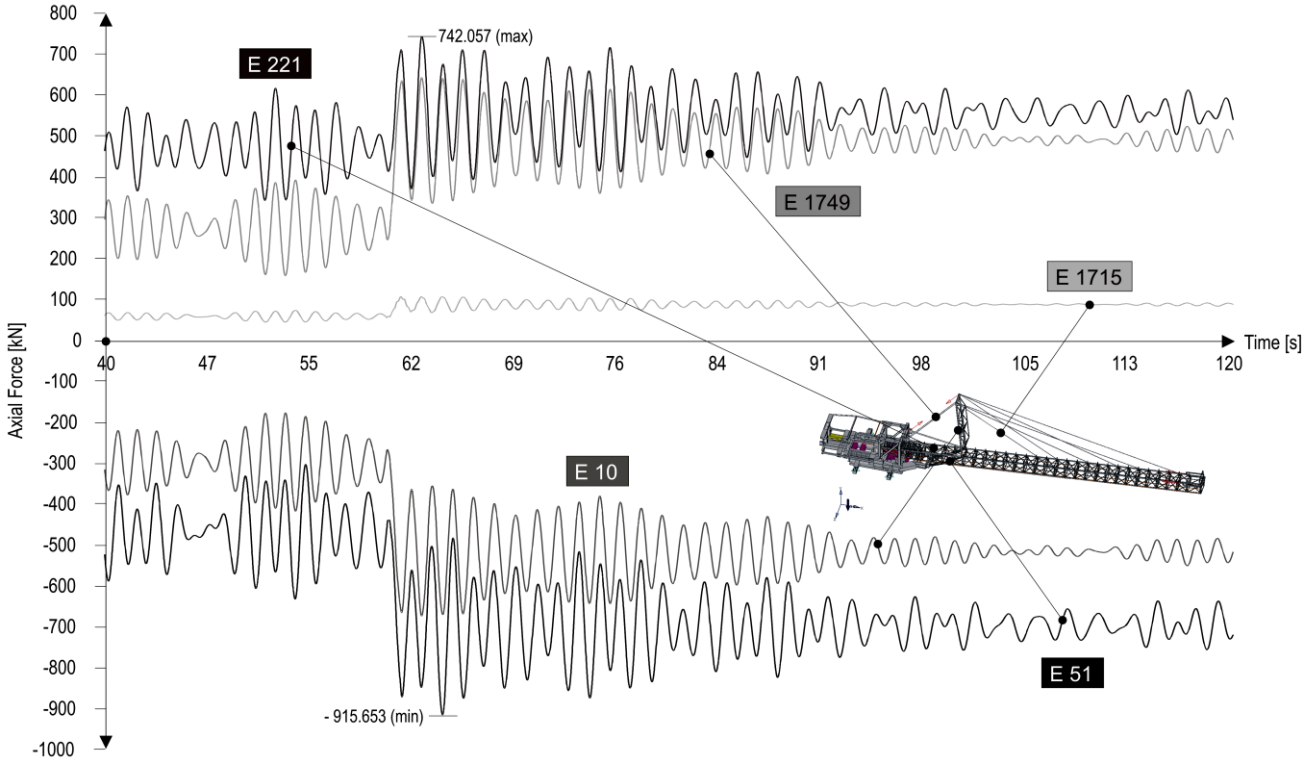

Fig. 10 *Axial forces in the selected responsible elements of the stacker*

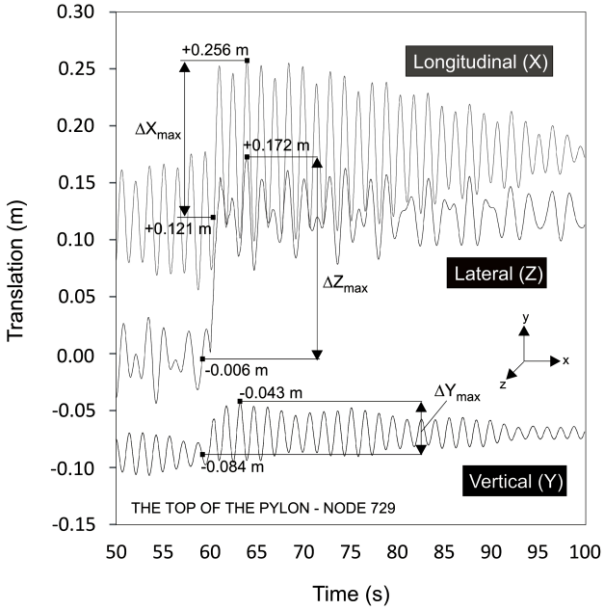

Fig. 11 *Translation of the top of the pylon (Node N-729)*

Reliability of a such frame system is probability that the support structure will perform successfully the function of criteria set, such as the criterion of stability preservation primarily, upon entry into the area of permitted deviations. Stress reserves must be sufficient for preservation of the working functionality of machine in the projected life cycle and conditions of incidental states such as fracture of responsible elements.

Reliability $\mathbf{R}(t)$ can be introduced to the cumulative function without cancellation work in the case of continual state changes [10].

$$\mathbf{R}(t) = 1 - \mathbf{F}(t) = 1 - \int_0^{t_1} \mathbf{f}(t)dt \qquad (7)$$

i.e. in the case of discrete state changes of system

$$\mathbf{R}(t) = \frac{n-N}{n} = \frac{T_{ur} - N \cdot t_{ur}}{T_{ur}} \qquad (8)$$

In Eq.(7) and (8), $\mathbf{F}(t)$ is the cumulative function without cancellation work, $\mathbf{f}(t)$ is the density function of time probability to the failure of frame structure or structural elements, n is the total number of system states, N is the total number of the system states in failure at the moment of observation, $(n\text{-}N)$ is the total number of the system states in operation at the moment of observation, T_{ur} is the total time of system work and t_{ur} is the mean time at work (between discrete failures).

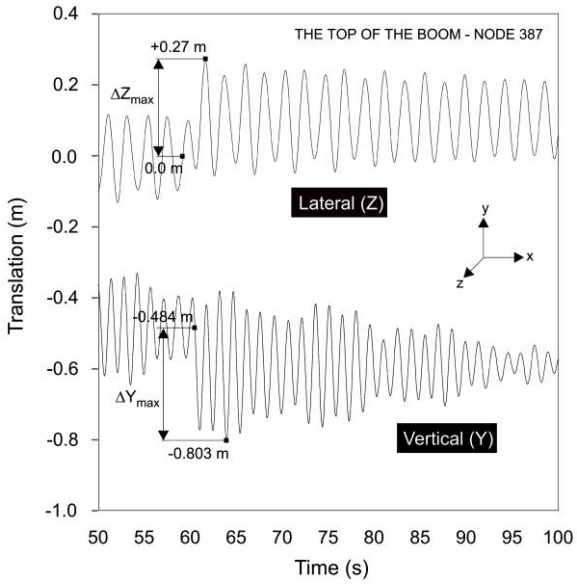

Fig. 12 *Translation of the top of the boom (Node N-387) in two directions (translation in x-direction is negligible)*

The area A_f in Fig. 13 represents a probability that the working stresses in structure will be bigger than the critical. According to this value – probability, the degree of safeness ν, Eq.(9), can be defined and then perform the dimensioning of responsible elements of the stacker structure.

$$\mathbf{f}(\nu) = \frac{\mathbf{f}_c}{\mathbf{f}_w} \tag{9}$$

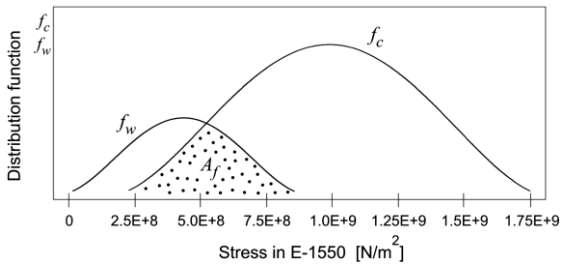

Fig. 13 *Stress distribution functions in the element E-1550: f_w – working stress, f_c – critical stress*

Since stresses are variable at simulation time, the stress distribution function can be used, i.e. $\mathbf{f}_w$ in the case of working stresses and $\mathbf{f}_c$ in the case of critical stresses. Thus, the degree of safeness is not constant but instead changes according to the appropriate distribution $\mathbf{f}(\nu)$ [10].

5. CONCLUSION

On the basis of the conducted dynamic analyses, looking at the exploitation conditions and dynamic properties of the stacker, one can conclude following:

- The quality of proposed FEM model of the stacker lies in a high fidelity of the structure (with very small approximations) introduced for all carrying and constructive elements of the real machine.
- The proposed FEM model has universal usage, making its additional quality. Namely, the model can be easily adjusted in order to check other incidental situations with support tie rods, wind and other additional effects.
- Introduction of the influence of ground is very desirable in dynamic analysis. The ground, on which these machines are placed, usually is unconsolidated because of their origin from the layers of material rejected in mining process (incompact ground).
- The modal analysis and experimental investigation correspond well with each other according to the frequency range in relation to the number of identified frequencies. The investigations indicated a large frequency range of the structure. The amortized vibration frequencies of structural parts were easily extracted in modal analysis according to the direction of eigenvectors propagation.
- The vibratory analyses indicate a stable dynamic behaviour of this frame structure. The local fracture (incident) of a responsible structural element did not jeopardize the total structure stability because the rest of the structure disposes redundancy.
- The stress reserve of the frame stacker structure is large as well as the dynamic coefficient values which indicate a high reliability of the machine even in conditions of repetition events with similar incidental character.
- The model allows the identification of locations to install the sensors for monitoring dynamic properties of the structure in various exploitation situations. It can be a sensor for measurement of acceleration, stress and deformation (translation), so that the transport capacity of material is always held to a maximum.

ACKNOWLEDGEMENTS

The dynamic research have been realized with the help of the Ministry of Education, Science and Technological Development of the Republic of Serbia through Project no. TR-35049. The authors would like to thank the Ministry and participant the Copper Mine – Bor.

REFERENCES

[1] M. Gašić, M. Savković, G. Marković and N. Zdravković, "Analysis of the calculation method of the rings of portal cranes and crawler excavators", *IMK-14 - Research and Development*, vol. 15 (1-2), pp. 37-41, 2009.

[2] D. Ostrić, M. Gašić, M. Simonović and M. Savković, "Dynamic models of portal rotating cranes", in *Proc. XIV ECPD International Conference on Material Handling and Warehousing*, Belgrade, 1996, pp. 4.93-4.98.

[3] M. Jovanović and P. Milić, "Statical tray-boom inspection on transportation system Veliki Krivelj – Bor", Project no. 612-22-70/11, University of Niš, Faculty of Mechanical Engineering, 2011.

[4] T. Maneski, "Vibration measuring on trail supporting structure in mining RBB Bor", Industrial report, IC Faculty of Mechanical engineering, University of Belgrade, December 2010.

[5] M. Jovanović, G. Radoičić and T. Maneski, "Dynamical eigenvalue identification of heavy structures machine", in *Proc.* Heavy Machinery - HM2011, International conference, 2011, pp. B.73-B.78.

[6] *MSC Nastran: Basic Dynamic Analysis - Version 68*, Santa Ana (CA): MSC. Software Corporation, 2004.

[7] MSC NASTRAN, Manuel, Santa Ana (CA): MSC. Software Corporation, 2004, www.mscsoftware.com

[8] S. Makragić, "A contribution to the analysis of dynamic behaviour of the bucket wheel of rotating excavator", *IMK-14 - Research and Development*, vol. 15 (3-4), pp. 99-103, 2009.

[9] G. Radoičić and M. Jovanović, "Experimental identification of overall structural damping of system", *Strojniški vestnik – Journal of Mechanical Engineering*, vol. 59, no. 4, pp. 260-268, 2013.

[10] D. Zelenović and J. Todorović, *Effectiveness of mechanical systems*, Beograd: Naučna knjiga, 1990.

Environmental Noise Monitoring

Noise monitoring is being adopted throughout the world as a means to reduce noise impact from the everyday activities that go on around us. Monitoring produce trend information for planning and compliance purposes as well as process data to highlight noise disturbances for investigation — working with you to reduce noise!

Sound and Vibration - Brüel & Kjær!

Brüel & Kjær is a global company providing local sales, service, and support in more than 55 countries.

Contact your local sales representative:

RMS d.o.o.
Partizanske avijacije 12/3,
11070 Novi Beograd, Srbija,
Tel.: +381(0)11 2280 951
Fax: +381(0)11 2280 751
http://www.rms.rs

Brüel & Kjær Sound & Vibration Measurement A/S / Export Sales
Skodsborgvej 307, DK-2850 Nærum, Denmark
Tel.: +45 7741 2000 — Fax: +45 7741 2015
E-mail: export@bksv.com — Website: http://www.bksv.com

Brüel & Kjær

University of Nis
Faculty of Occupational Safety
„Politechnica“ University of Timisoara
Faculty of Mechanical Engineering
24th International Conference
NOISE AND VIBRATION
Niš, 29 - 31. 10. 2014.

ASPECTS REGARDING THE VIBRATIONS OF A RAILWAY VEHICLE DUE TO WHEEL-RAIL IMPACT FORCES

Eugen Ghita

”Politehnica” University of Timisoara, Romania, Faculty of Mechanical Engineering, eugen.ghita@upt.ro

Abstract *- The vibrations of railway vehicles are caused by the excitations that appear in the wheel-rail contact patch during the rolling process. The running stability of the rail-car is analyzed based on the proposed mechanical model and the general Lagrange`s equation.The pitch of the asperities on the rail head widely influenced the dynamic effect transmitted to the vehicle because of their aleatory distribution. The bouncing and the gallop vibrations of the vehicle are analyzed and their parameters are continuosly recording because of safety reasons.*

1. INTRODUCTION

During the rolling process, some contact forces arise between the vehicle and the railroad. The magnitude of the contact forces depends both by the quality of the vehicle and of the railroad design and influences the safety and the comfort of passengers. There are three possibilities to reduce the wheel-rail impact or contact forces:

- to decrease the mass of the vehicle
- to decrease the acceleration level due to increasing the wheel-rail contact duration
- to eliminate the asperities of the railroad and the external excitation forces as reasons which conduce to a high acceleration level

Anyway, a continuous recording of the wheel-rail contact forces became obviously necessarry because of safety reasons.

2. DYNAMIC WHEEL-RAIL CONTACT ANALYSIS

Let consider a wheel in contact with a pitch of a railroad asperity, [1].

The following notations are considered:

h-the height of the asperity

v-the velocity of the vehicle

S-the distance covered by the wheel

t-the duration to ascend the asperity

D-the rolling diameter of the wheel

According to a simple geometrical theory, $S^2=(D-h)\cdot h$. Because h<<D and $t=\frac{S}{v}$, it results: $S=\sqrt{D\cdot h}$ so $t=\frac{\sqrt{D\cdot h}}{v}$.

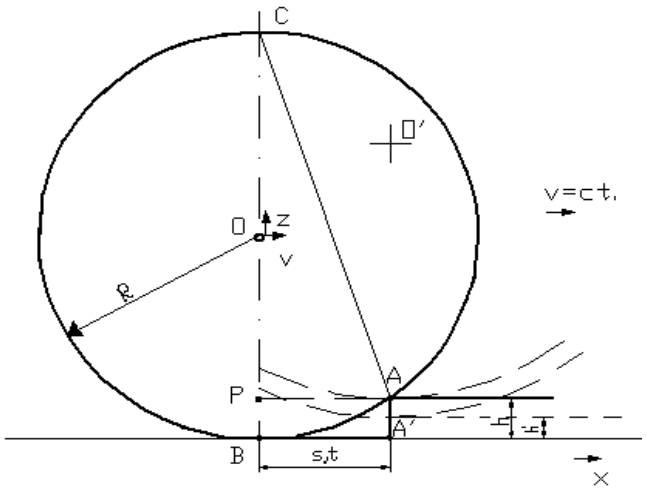

Figure.1. *The geometry of contact*

The system of axys is:

x - the rolling direction

y - the lateral direction

z - the vertical direction

An elastic compression of the pitch takes place when ascending the wheel, so h'< h represents the real height. If „a” represents the ascending acceleration of the wheel , it results:

$$h'=\frac{a\cdot t^2}{2} \qquad (1)$$

so,

$$a=\frac{2v^2}{D}\cdot\frac{h'}{h} \qquad (2)$$

If the vehicle is rigid (without any suspension), the mass of the wheel ($m=\frac{Q_0}{g}$, Q_0 - the static load on the wheel) will raise proportional with the acceleration „a”.

It means that the dynamic inertial wheel-rail contact force will be:

$$Q'_d=m\cdot a=\frac{Q_0}{g}\cdot a=\frac{2\cdot Q_0}{D\cdot g}\cdot\frac{h'}{h}\cdot v^2, \qquad (3)$$

There are presented in table 1 some numerical results for different values of D, v and h'/h.

Table 1. *Numerical results*

$\frac{h'}{h}$	D [m]	1	1	1,25
	V [km/h]	72	90	90
	v [m/s]	20	25	25
	a [m/s^2]	8	12,5	10
0.01	$Q_d' / Q_0 = a/g$	0,8	1,25	10
0.1	$Q_d' / Q_0 = a/g$	8	12,5	1,0
0.5	$Q_d' / Q_0 = a/g$	40	62,5	50
1.0	$Q_d' / Q_0 = a/g$	80	125	100

Right after the force was applied (the initial moment) , only the non-suspended mass (the mass of the wheelset) will translate vertically and will produce a deformation „h`" of the suspension elements.

The elastic force acting both on the wheel and on the rail will be:

$$q_e = k \cdot h', \tag{4}$$

where k-the stiffness of the suspension.

The inertial force produced by the wheel on the rail is:

$$q_i = \frac{q}{g} \cdot a \tag{5}$$

where „q" is the unsuspended weight of the wheel and „g" is the gravity.

The wheel-rail dynamic interaction will be:

$$q_d = q_i + q_e \tag{6}$$

The total dynamic wheel-rail contact force is :

$$Q_d = Q_0 + q_i + q_e = Q_0 + \frac{q}{g} \cdot \frac{2 \cdot v^2}{D} \cdot \frac{h'}{h} + k \cdot h' \tag{7}$$

The same force may be written as:

$$Q_d = (1 + k_d) Q_0 \tag{8}$$

where $k_d = \frac{q_d}{Q_0}$ represents the dynamic coefficient.

Practically, $q_e << q_i$, so $k_d \approx \frac{q_i}{Q_0}$.

A suggestive calculus example for a rail vehicle is presented in table 2 for $k = 2 \cdot 10^6$ [N/m]; $h = 10\,mm$; $\frac{h'}{h} = 0{,}1$; $D = 1{,}25\,m$ and $v = 25\,m/s$. The value q_e/q_i is negligible.

Table 2. *Calculus example*

a/g	q_e [N]	q_i [N]	q_e/q_i
10	2000	200000	0,01

As a partial conclusion, it is necessarry to reduce the rail head evenness deviation, to eliminate the plane areas on the circumference of the wheel and to introduce a high quality suspension, especially for high speed trains.

3. THE ANALYSIS OF THE BOUNCING AND GALLOP VIBRATIONS OF A RAILWAY VEHICLE

The mechanical model of the vehicle is presented in figure 2 :

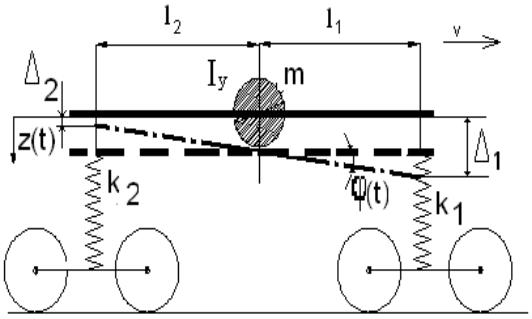

Figure 2. *The mechanical model of the vehicle*

The bouncing motion consists in a translation along "z" axys while the gallop consists in a rotation around "y" axys.

The analysis is performed according to Lagrange`s equation:

$$\frac{d}{dt}\left(\frac{\partial E_c}{\partial \dot{q}}\right) - \frac{\partial E_c}{\partial q} + \frac{\partial E_d}{\partial \dot{q}} + \frac{\partial E_p}{\partial q} = Q(t) \tag{9}$$

where :

q = z – the generalized linear coordinate respectively q = φ – the generalized angular coordinate

Q(t) – the external generalized force (Q=0 for free vibrations).

The kinetical energy of the vibrating masses is:

$$Ec = \frac{1}{2}\, m\, \dot{z}^2 + \frac{1}{2} I_y\, \dot{\varphi}^2 \tag{10}$$

where I_y – the inertial torque

The potential energy stored by the suspension system with the deformations $\Delta_1 = z + l_1 \varphi$ and $\Delta_2 = z - l_2 \varphi$ is :

$$E_p = \frac{1}{2}\sum_{i=1}^{n} k_i \Delta_i^2 = \frac{1}{2} k_1 (z + l_1\varphi)^2 + \frac{1}{2}(z - l_2\varphi)^2 \tag{11}$$

The eliminated energy by the hydraulic dampers

$E_c = \frac{1}{2} \cdot c_z \cdot \dot{z}^2 = 0$, because the proposed model is without any damper.(c_z – the damping coefficient).

According to Lagrange`s equation it results :

$$\begin{cases} \ddot{z} + \frac{k_1 + k_2}{m} z + \frac{k_1 l_1 - k_2 l_2}{m} \varphi = 0 \\ \ddot{\varphi} + \frac{k_1 l_1^2 + k_2 l_2^2}{Iy} \varphi + \frac{k_1 l_1 - k_2 l_2}{I_y} z = 0 \end{cases} \tag{12}$$

The following particular notations will be used for the analysis :

$\omega_z = \sqrt{\frac{k_1 + k_2}{m}}$ — the proper bouncing pulsation;

$\omega_\varphi = \sqrt{\frac{k_1 l_1^2 + k_2 l_2^2}{Iy}}$ — the proper gallop pulsation;

$a_{12} = \frac{k_1 l_1 - k_2 l_2}{m}$ — the influence coefficient of the gallop vibration on the bouncing;

$a_{21} = \frac{k_1 l_1 - k_2 l_2}{Iy}$ — the influence coefficient of the bouncing vibration on the gallop.

If the design of the suspended frame consider a simmetrical solution , $k_1=k_2$ and $l_1=l_2$, it results $a_{12}=a_{21}= 0$, which means that the gallop and bouncing vibrations are completely independent. Than results the equations:

$$\begin{cases} \ddot{z} + \omega_z^2 z + a_{12}\varphi = 0 \\ \ddot{\varphi} + \omega_\varphi^2 \varphi + a_{21} z = 0 \end{cases} \quad (13)$$

The solutions are :

$$z = A\sin(pt + \zeta_1)$$
$$\varphi = B\sin(pt + \zeta_2) \quad (14)$$

where

$$p_{1,2} = \frac{1}{\sqrt{2}}\sqrt{\omega_z^2 + \omega_\varphi^2 \pm \sqrt{(\omega_z^2 + \omega_\varphi^2)^2 - 4(\omega_z^2\omega_\varphi^2 - a_{12}a_{21})}} \quad (15)$$

and $\zeta_{1,2}$- the delays.

The distribution coefficients of the amplitudes are:

$$\mu_1 = \frac{B_1}{A_1}\Big|_{p=p_1} = \frac{p_1^2 - \omega_z^2}{a_{12}} = \frac{a_{21}}{p_1^2 - \omega_\varphi^2} \quad (16)$$

$$\mu_2 = \frac{B_2}{A_2}\Big|_{p=p_2} = \frac{p_2^2 - \omega_z^2}{a_{12}} = \frac{a_{21}}{p_2^2 - \omega^2{}_\varphi}$$

These coefficients represents a measure of the reciprocal influence of the two vibrations.For $k_1l_1 \neq k_2l_2$, which means $a_{12}\neq 0$ it results $\mu_1>0$ and $\mu_1>|\mu_2|$.

The solutions will be:

$$z_1=A_1 \sin(p_1 t + \zeta_1)$$
$$z_2=A \sin(p_2 t + \zeta_2) \quad (17)$$

$$\varphi_1=\mu_1 A_1 \sin(p_1 t + \zeta_1)$$
$$\varphi_2=\mu_2 A_2 \sin(p_2 t + \zeta_2) \quad (18)$$

and the general form is:

$$z = z_1+z_2 \quad (19)$$
$$\varphi = \varphi_1+ \varphi_2$$

The values of amplitude and frequency are very important for comfort estimation.

4. THE COMFORT ESTIMATION

According to the international railway regulations, [2] , there are three coefficients to appreciate the comfort inside a railway vehicle in running conditions.

4.1.The running index W_z

$$W_z = 2{,}7\sqrt[10]{A^3\,\upsilon^5} \quad (20)$$

where :

A-the amplitude of the bouncing oscillation

υ-the frequency of the bouncing oscillation

φ(υ) - correction factor function of frequency

The running index depends both of the vehicle and of the railroad. The quality of the running process is appreciated according to table 3, [2] :

Table 3. *The running quality appreciation*

Quality of running	W_z	Comfort
Very good	1	High sensitivity
Good	2	Medium sensitivity
Almost good	2,5	Very high sensitivity , still bearable
Satisfactory	3	Very high sensitivity
Satisfactory	3,25	Uncomfortable
Still satisfactory	3,5	Extremely uncomfortable
Tolerable,still exploatable	4	Extremely uncomfortable,dangerous in case of long-time exposure
Non-tolerable	4,5	------
Dangerous	5	------

4.2.The fatigue limit for passengers τ[h]

The frequency of 5 Hz is the most disagreeable for the human body. The fatigue limit depends on the running index according to table 4, [1] :

Table 4. *The fatigue limit function of the running index*

W_z	1...2	2,5	3,0	3,5	4,0	4,5	5
τ[h]	24	13	5,5	2,8	1,5	0,9	0,6

4.3.The lateral acceleration a [m/s^2]

The lateral acceleration is the worst one for the human body.Anyway, the lateral forces Y favors the derailment , while the vertical force Q favors the stability. For running conditions , the Nadal`s criterion $\frac{Y}{Q} \leq 1$ must be obeyed because of safety reasons. According U.I.C.`s 518 file, [2], the lateral acceleration a < 0,5 m/s^2 (on "y" direction), for passengers inside a railway vehicle, satisfy the safety condition.

5. THE CONTINUOUS RECORDING OF THE WHEEL-RAIL CONTACT FORCES

The contact forces are recorded using the strain gage measurements method, [3]. The experiments can be performed in-situ or on specialized test benches.It is accepted that "1" is the left wheel and "2" the right wheel of the same wheelset and "φ" the rolling angle.

The measuring wheelsets must obey the following important conditions :

- To record every component of the generalized contact force without any influence from an oscillation to another
- To allow the measurements in the near proximity of the contact area
- To present a high sensitivity
- To obtain a continuous and constant signal function of the rolling angle when a constant loading force is applied in any direction
- Not to be influenced by the following disturbing parameters : velocity, temperature, relative positions of the bodies in contact (wheel and rail) etc.

The measuring system is presented in figure 3 :

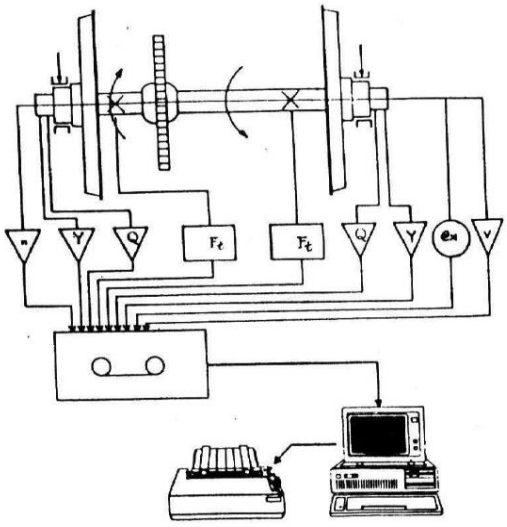

Figure 3. *The measuring system*

An example of a continuous recording is presented in figure 4.

Other notations in figure 3 and 4 are :

F_t – the traction force

e_x – the creep (the difference between sliding and rolling velocity divided by the average between them)

φ – the rolling angle

n – the rotation

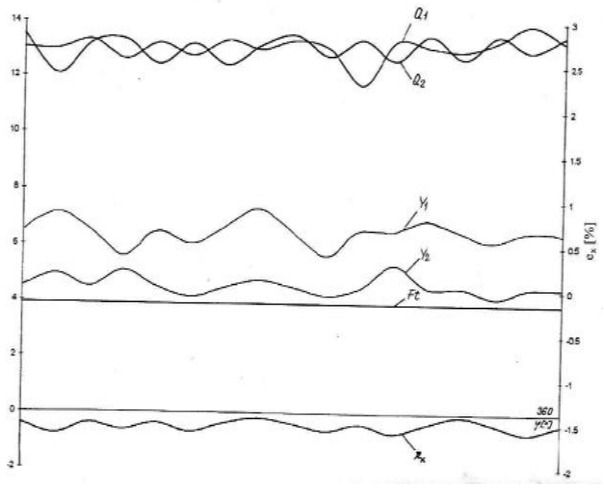

Figure 4. *The continuous recording of the rolling parameters*

So, in every moment the safety may be appreciated in function of the calculation of the derailment criterion.

6. CONCLUSIONS

- The importance of manufacturing a perfect plane railroad is praised , especially for high speed trains , according to results in table 1 and table 2.
- A good quality suspension of the railway vehicle will strongly decrease the contact forces , the amplitude and the frequency of the oscillations but it must be in accordance with the quality of the railroad.
- The theoretical model and the calculation Lagrange`s method is validated by the experimental methods.

REFERENCES

[1] E. Ghita, G. Turos, "*Dynamics of railway vehicle*", Eurostampa Publishing House, Timisoara, 2007

[2] U.I.C.`s International Union of Railways (Carozzi) 518 file

[3] E.Ghita, "*Strength at wheel-rail contact",* Mirton Publishing House, Timisoara, 1999.

University of Nis
Faculty of Occupational Safety
„Politechnica“ University of Timisoara
Faculty of Mechanical Engineering
24th International Conference
NOISE AND VIBRATION
Niš, 29 - 31. 10. 2014.

THEORETICAL AND EXPERIMENTAL STUDIES REGARDING ELECTRODYNAMIC VIBRATORS

Gheorghe Luca[1], *Ramona Nagy*[1], *Karoly Menyhardt*[1]
[1] Politehnica University Timisoara, Faculty of Mechanical Engineering, Romania, ramona.nagy@upt.ro

Abstract - *In the current paper we present an electrodynamic vibrator designed and realized in the framework of the Mechanical and Strength of Material Department, used for testing small sized devices, between 0.5-2.5 kg. Electrodynamic vibrators are the most efficient devices from inertial and signal fidelity point of view. The high cost of such vibrating test devices imposed the in house creation of a shaker that satisfy the requirements with moderate resources. The device was tested to determine its optimal duty cycle. Some theoretical and experimental data regarding an improvement of an electrodynamic oscillator are presented in this paper. Based on the obtained diagrams from different workloads, constructional parameters were chosen for an efficient functioning. Through the experimental results and theoretical studies data was gathered that can be used for a continual improvement of the device for vibration testing of electronic gadgets in automotive, railway and aircraft industries.*

1. INTRODUCTION

The electrodynamic vibrator is a very popular choice used in vibration testing, due to its wide range of forces and frequencies that can be obtained.

Electrodynamic vibrators are equipment that generate oscillating movement having the following advantages:

- large domain of frequency 1-6000 (but can go as high as 20000)Hz;
- can generate harmonic vibrations, shock or random vibrations;
- variable amplitude and frequency control;
- high precision and stability for the working frequency.

They can be used as vibration sources in different technological processes, equipment and material testing or for dynamical study of assembles.

2. THEORETICAL CONSIDERATIONS

The structure of this device resembles to a common loudspeaker, being more robust. At the center of the machine is a coil suspended in a radial magnetic field, acting in the normal plane with respect to the coil axis. This field is produced by building a magnetic permeable circuit to transmit flux from both poles of an axially magnetized permanent magnet or electromagnet [1].

The principle of operation for the electrodynamic vibrator is presented in Fig.1; on the electromagnetic body 3 is mounted a fixed coil 5, connected to a DC source 9. The magnetic field from the fixed coil is closed through an air gap with an mobile coil 4, rigidly fixed to a mobile platter 6 suspended on elastic elements 7 [2,3].

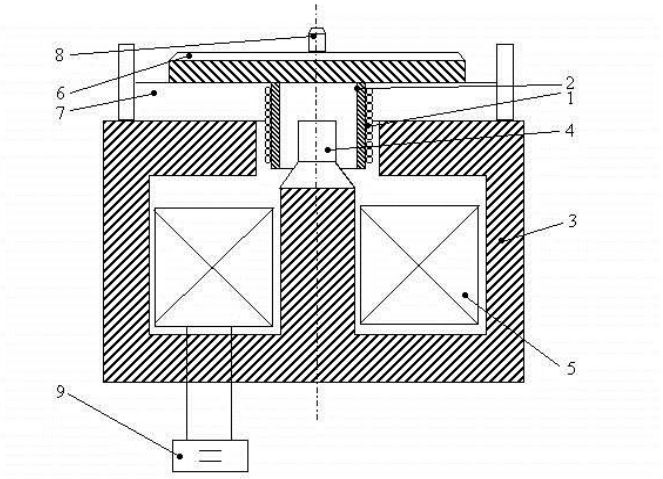

Fig. 1- *Electrodynamic vibrator*

The electrical circuit equivalent for the electrodynamic vibrator is shown in Fig.2, where:

10 – fixed coil inductance;

11 – fixed coil resistance;

12 – power amplifier;

13 – signal generator.

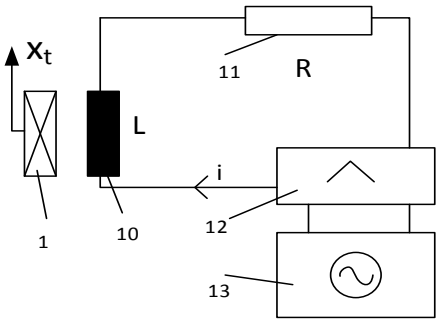

Fig. 2 - *Equivalent electrical circuit*

The electromagnetic vibrator system has 2 degrees of freedom: displacement x of the mobile platter 6 and the electric charge q of the current from the mobile coil 1. The differential equations are:

$$\begin{cases} m\ddot{x} + c\dot{x} - B\ell\dot{q} + kx = 0 \\ L\ddot{q} + B\ell\dot{x} + R\dot{q} = e_0 \sin \omega t \end{cases} \quad (1)$$

where:

- m- the mass of mobile equipment, including the mobile coil, the vibrating object [kg];
- c- damping coefficient of the suspension system [Ns/m];
- k- elastic constant of the suspension system for the mobile coil;
- x(t)- law of motion for the mobile coil from static equilibrium position [m];
- q(t)- electrical charge in the mobile coil circuit [C];
- B- magnetic inductance from the air gap for the mobile coil;
- L- inductance of the mobile coil;
- R- resistance of the mobile coil;
- ℓ- length of the mobile coil conductor;
- $e_0 \sin \omega t$ - supply voltage of the mobile coil circuit.

The general solution for the forced vibrations of the system (1) are:

$$\begin{cases} x = A_1 \sin(\omega t - \varphi_1) \\ q = A_2 \sin(\omega t - \varphi_2) \end{cases} \quad (2)$$

where:

$$A_1 = \frac{B\ell e_0}{\sqrt{\left(Rk - E\omega^2\right)^2 + \omega^2\left(D - mL\omega^2\right)^2}}$$

$$A_2 = \frac{e_0\sqrt{\left(k - m\omega^2\right) + \left(c\omega\right)^2}}{\omega\sqrt{\left(Rk - E\omega^2\right)^2 + \omega^2\left(D - mL\omega^2\right)^2}} \quad (3)$$

$$\operatorname{tg}\varphi_1 = \frac{\omega\left(D - mL\omega^2\right)}{Rk - E\omega^2},\ \operatorname{tg}\varphi = \frac{c\omega}{k - m\omega^2}$$

$$\varphi_2 = \varphi_1 - \varphi$$

$$E = Rm + cL$$

$$D = Lk + B^2\ell^2 + cR$$

3. THEORETICAL STUDY OF THE ELECTRODYNAMIC VIBRATOR OPERATION

For the theoretical study of the electrodynamic vibrator, the following relations can be used:

$$a_{\max} = \omega^2 X = \frac{\omega^2 \ell B e_0}{M} = f_1(f) = \omega^2 A_1$$

The motion amplitude X

$$X = \frac{a_{\max}}{\omega^2} = A_1 = \frac{\ell B e_0}{M} = f_2(f)$$

Maximum electric current from the mobile coil is:

$$I = \omega A_1 = \frac{e_0 N}{M} = f_3(f)$$

The maximum force developed by the electrodynamic vibrator is

$$F_{\max} = B\ell I = \frac{B\ell e_0 N}{M} = f_4(f) \quad (4)$$

where

$$M = \sqrt{m^2\ell^2\omega^6 + C_1\omega^4 + C_2\omega^2 + R^2k^2}$$

$$C_1 = \left(Rm + cL\right)^2 - 2mL\left(Lk + B^2\ell^2 + cR\right)$$

$$C_2 = \left(Lk + B^2\ell^2 + cR\right)^2 - 2kR\left(Rm + cL\right)$$

$$N = \sqrt{m^2\omega^4 + \left(c^2 - 2km\right)\omega^2 + k^2}$$

For theoretical calculus the following parameters were considered:

$$m = (0.54; 1; 1.54; 2; 2.54; 3; 3.54; 4)\,kg$$

$$e_0 = (2; 4; 6; 8; 10)\,V$$

$$d = (0.8; 0.9; 1; 1.1; 1.2; 1.3; 1.4; 1.5)\,mm \quad (5)$$

where *d* is the diameter of the conductor in the mobile coil that lead to the following results:

$$R = (7699; 5407; 3941; 2961; 2281; 1794; 1436; 1167)10^{-4}\,\Omega \quad (6)$$

$$L = (6.3875; 5.047; 4.088; 3.378; 2.838; 2.419; 2.086; 1.817)10^{-4}\,H$$

Different thickness can be used for the elastic membranes, as a result being the modification of the elastic constant:

$$h_1 = 1mm;\ k_1 = 7799\frac{N}{m}$$

$$h_2 = 1.5mm;\ k_2 = 17930\frac{N}{m} \quad (7)$$

$$h_3 = 2mm;\ k_3 = 76750\frac{N}{m}$$

This way, with the help of relations (4), using the given parameters (5,6,7), multiple diagrams can be obtained regarding the operation of electrodynamic vibrators.

In Fig.3 and Fig.4 the variation diagrams are presented for the power and intensity of the maximum current through the mobile coil as a function of frequency for the supply voltage in the mobile coil (5-600 Hz). The representation of the diagrams was done with the aid of a noncommercial software.

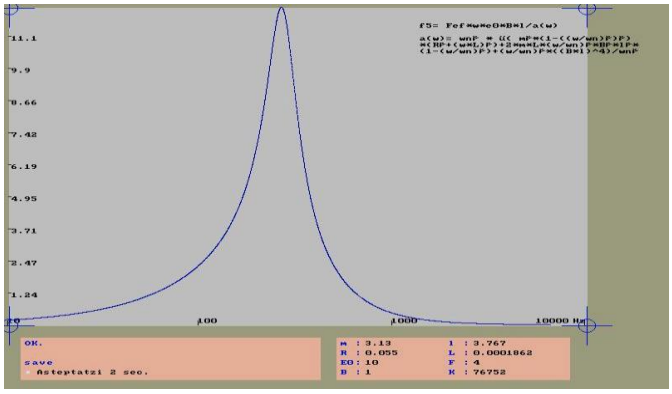

Fig. 3 – Screen capture of *Power curve as a function of frequency, m=3.13 kg, k=9977 N/cm, e_0=10 V*

Analyzing the variation of power of the vibrator as a function of frequency, one can observe that for the same mass and voltage, the peak in power is shifted toward higher frequencies by increasing the elastic constant. Thus for m=0.67kg and e_0=2V the increase of the elastic constant from 9977N/m to 76752.7 N/m leads to displacement of the power peak from 750Hz to 900Hz, practically at the same power. At m=3.13kg and e_0=10V the increase of elastic constant from 9977N/m to 76752.7 N/m leads to a displacement of the power peak from 150Hz to 300Hz, followed by an increase in power by 3.33times. Comparing the power curves at the same elastic constant and voltage e_0, the values are nearly identical, but the increase of mass will produce a displacement of the power peak toward lower frequencies, where the increase from 0.67kg to 3.13kg leads to a drop in frequency from 750Hz to 350Hz.

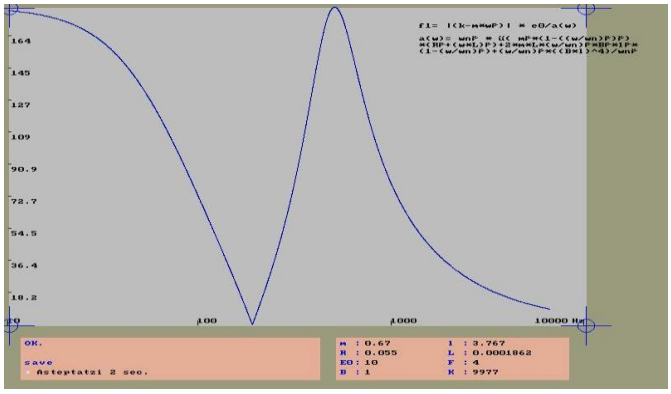

Fig. 4 - Screen capture of *Maximum current as a function of frequency, m=0.67kg, k=9977N/m, e_0=10V*

By analyzing the curves for the variation maximum current (scale x10) of the vibrator as a function of frequency, and choosing different values for the mass, elastic constant and voltage e_0, it is noted a maximum values for the mass m = 3.13 kg and elastic constant k = 76752.7 N/m. Dropping the voltage from 10 V to 2 V, leads to decrease of the maximum current 6 times, maintaining the allure of the curve, maximum current being around 650 Hz. The same observation can be maintained for minimum mass m=0.67 and minimum elastic constant k=9977 N/m, the values for the maximum current dropping with the same ratio, but peak of the current shifting toward 750 Hz. So, by decreasing the mass and elastic constant leads to an increase in frequency.

4. EXPERIMENTAL RESULTS REGARDING THE USE OF ELECTRODYNAMIC VIBRATORS

In the framework of the Mechanics and Strength of Material Department from the Politehnica University Timisoara, there were intense concerns in the field of electromagnetic vibrators. The last designed vibrator has the following characteristics:

- fixed coil with N=1685 windings with a diameter of 1.25 mm;
- air gap induction of B=1 T;
- mobile mass m=0.54 kg;
- mobile coil n=42 windings, d=1.4 mm, l=11.83 m;
- maximum intensity of the current in the mobile coil I=3.8 A.

The block diagram of the utilized equipment for experimental test runs is presented in Fig.5

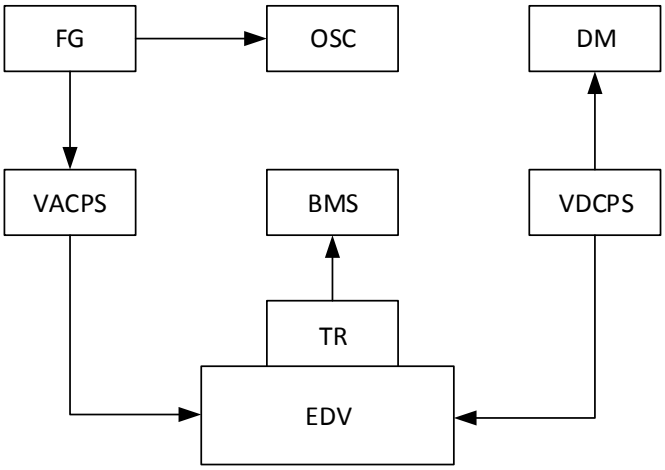

Fig. 5 -*Testing equipment block diagram*

where:

- FG - frequency generator;
- OSC – oscilloscope;
- VACPS - variable alternative current power supply;
- DM – digital multimeter;
- VDCPS – variable direct current power supply;
- EDV – electrodynamic vibrator;
- TR – transducer;
- BMS – bridge measurement system.

For testing purposes, several masses were laid on the mobile platter, with an increase of 0.5 kg per test, up to 4 kg. The voltage of the mobile coil was modified in the sequence of 2-4-6-8-10 V and the frequency between 10-600 Hz.

The curves of variation for the acceleration as a function of frequency were obtained through statistical processing of the experimental data.

The results show that for a mass of 0.67 kg the maximum acceleration and the amplitude of the vibration shifts from 2000 Hz downto 1200 Hz proportionally with the thickness of the elastic membrane (Figs.6,7,8).

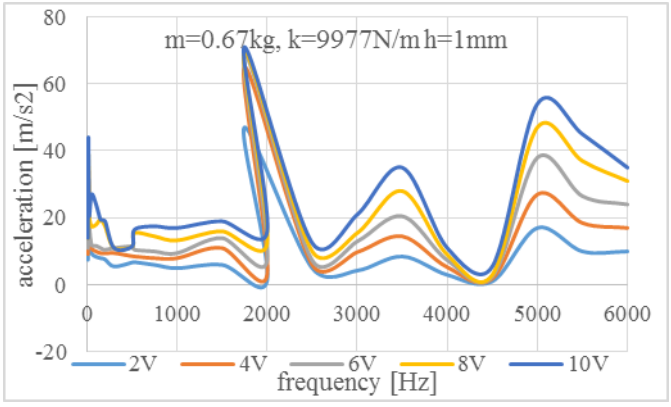

Fig. 6 - *Frequency - acceleration response*

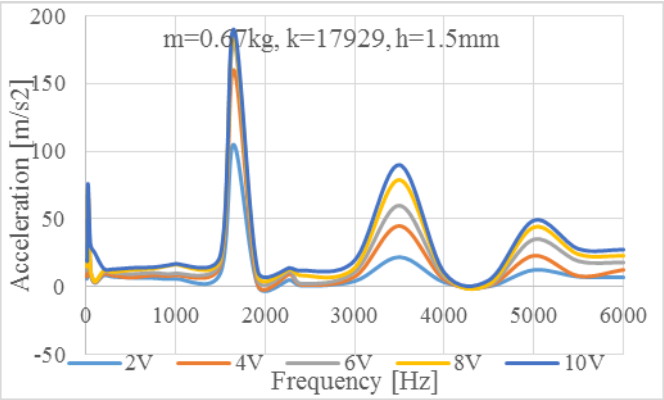

Fig. 7 - *Frequency-acceleration response*

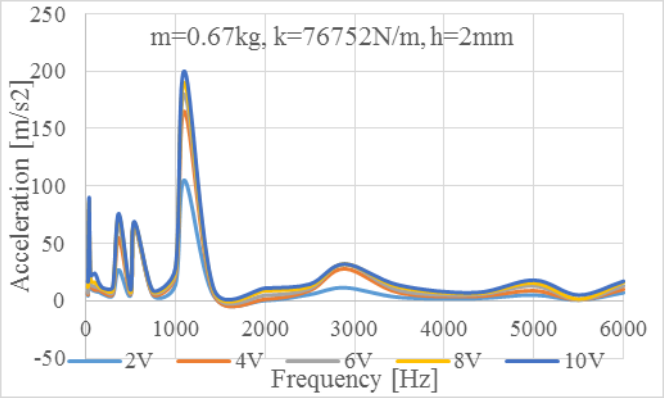

Fig. 8 - *Frequency-acceleration response*

Increasing the mass results in a more rigid response from the vibrator, with the maximum acceleration shifting from 3500Hz down to 1700Hz as one can see in Figs 9,10,11.

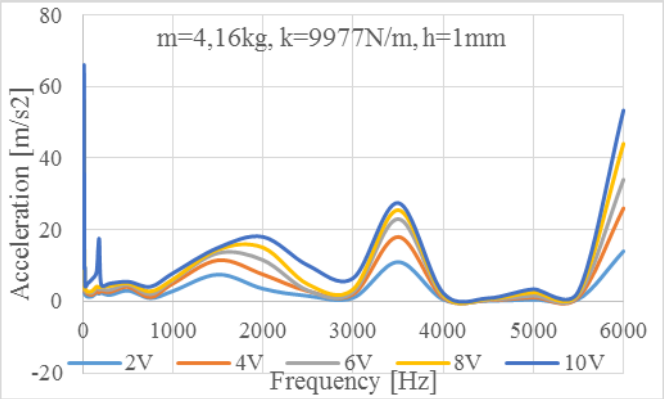

Fig. 9 - *Frequency - acceleration response*

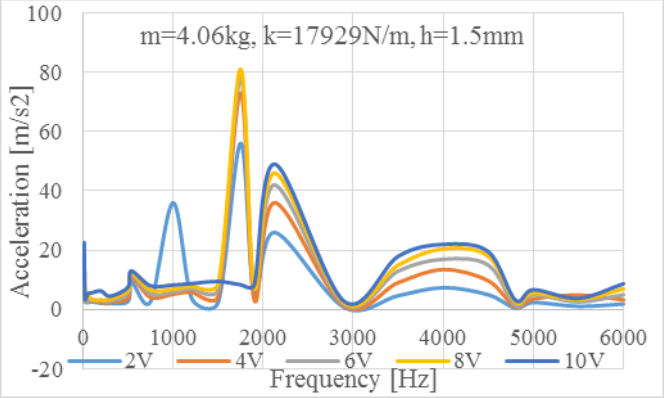

Fig. 10 - *Frequency - acceleration response*

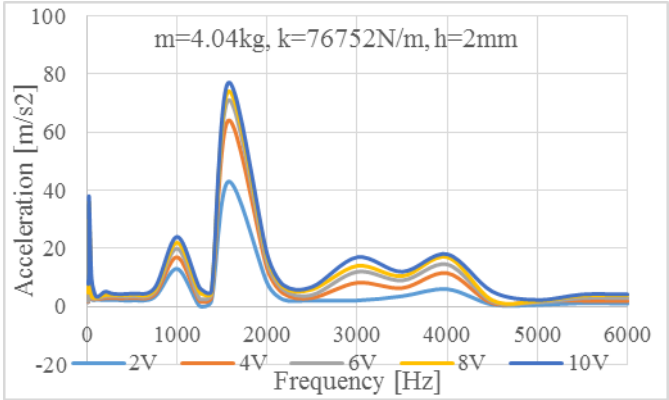

Fig. 11 - *Frequency-acceleration response*

Several tests were also made with masses of 1.165 kg, 1.67 kg, 2.17 kg, 2.64 kg, 3.11 kg and 3.54 kg. In all of them the same trend can be observed for the acceleration-mass-rigidity-frequency relationship.

5. CONCLUSIONS

The current paper presents some of the theoretical and experimental data from the engineering and improvement of electrodynamic oscillators at Mechanics and Strength of Materials Department in Timisoara. During the last 30 years these equipment were purchased or produced in-house according to the needs of the testing objects. The investigated shaker was built for testing relatively small sized electronic devices for the railway industry, between 2-5 kg. From the charts shown (Fig.6-11) and other data gathered it can be concluded that the acceleration response is nonlinear and it increases with the mass of the tested object. The acceleration response based on the controlling frequency can be modified with the variation of supplied voltage. Using a closed loop feedback system it is possible to sustain a required acceleration at even higher frequencies, above 3000Hz, but with steep price in energetic efficiency relative to the tested mass.

Based on the theoretical and experimentally determined frequency characteristics it is possible to select the operating range of electrodynamic vibrators fit to the task. Thus we are able to have a constant acceleration by using the vibrator with frequencies from the flat zone of the chart. To use it in the resonance area it is necessary to use a frequency stabilizer, because a small change can amount to large shifts in amplitude and acceleration.

REFERENCES

[1] K. G. Mcconnell, *Vibration testing: theory and* practice. John Wiley & Sons, NY, 1995.

[2] G. Fox Lang, D. Snyder. Understanding the physics of electrodynamic shaker performance. *Sound &Vibration*, October 2001.

[3] M.V. Nesterenko, V.A. Katrich, Y.M. Penkin, V.M. Dakhov, S.L. Berdnik – Thin Impedance Vibrators – Theory and applications, 2011,XII,233 ISBN:978-1-4419-7849-3

University of Nis
Faculty of Occupational Safety
„Politechnica“ University of Timisoara
Faculty of Mechanical Engineering
24th International Conference
NOISE AND VIBRATION
Niš, 29 - 31. 10. 2014.

ESTIMATION AND PREDICTION OF TRAFFIC-INDUCED VIBRATION ON THE BASIS OF EXPERIMENTAL DATA

Slavko Zdravković[1], Marija Spasojević-Šurdilović[2], Dragan Zlatkov[3], Biljana Mladenović[4], Stefan Conić[5]

[1] University of Niš, Faculty of Civil engineering and architecture, Serbia, slavko.zdravkovic@gaf.ni.ac.rs
[2,3,4,5] University of Niš, Faculty of Civil engineering and architecture, Serbia

Abstract - *The paper deals with estimation and prediction of traffic-induced vibration on the basis of experimental data resulting from the research of structures in Boulevard kralja Aleksandra in Belgrade. The ability of people to anticipate vibration is directly proportional to the velocity and frequency of vibration. Many countries has issued standards concerning the vibration effect on human beings, and German, British and ISO standards are used in this paper. Required quantities for determination of vibration effect on humans are calculated using Fourier integral transform.*

1. INTRODUCTION

The vibrations caused by traffic have proven effect on building, people in them and interfere with the operation of equipment sensitive to vibration, and therefore they present serious problem in big cities. Application of modern construction materials has led to the construction of the high, flexible buildings. This led to serious analysis and measures to reduce exposure of buildings and people to effects of vibration. In addition, more intense traffic is one of the biggest polluters of the environment. Source of vibration, the mechanism of their transfer through the soil, as well as measures for their reduction are the subject of research in many countries. The operating of high-speed trains in European countries causes significant dynamic effects between trains and ground, producing an uncomfortable vibration in nearby buildings. In Serbia, the systematic investigation of the problem of the effects of vibration induced by traffic on buildings and people is only in its infancy. Low-frequency disturbances as a result of movement of heavy vehicles, such as buses, trucks and trams, cause dynamic impact forces that occur at the contact point of wheel with the irregularities of the road surface. These forces generate vibrations in the ground whose predominant frequencies correspond to natural frequencies of oscillation of the soil.

2. VIBRATIONS CAUSED BY TRAFFIC

The traffic caused vibrations are generated due to the effects of dynamic and oscillatory force of the wheel. Oscillatory forces are caused by fluctuations of wheel axles whose frequency depends on the manner of suspension unit, wheelbase, weight and speed of vehicles. The vibrations are transmitted through the soil by body and surface waves, whose amplitudes decrease with distance from the source due to geometrical and material damping. The Rayleigh waves have low frequencies, and potentially less damping, but their amplitudes are greater than amplitudes of body waves and carry the highest energy. Function of amplitude decreasing for Rayleigh waves is given by equation (1) [3]:

$$v = v_0 \left(\frac{r}{r_0} \right)^{-0.5} e^{-\alpha (r - r_0)} \qquad (1)$$

where is:

v – particle velocity at the source,

r_0 – distance from the source of vibration to the reference point,

r – distance from the source to the observed point ,

0.5 – degree of geometrical damping,

α – material damping factor of soil, given in Table 1.

Table 1 *Values of factor* α

Soil type	Coefficient α [m^{-1}]
water logged soil	0.04-0.12
loess	0.10
sand and silt	0.04

The intensity of the vibrations caused by traffic depends on the following factors:

- source of vibration (tram, bus, etc.).
- pavement condition.
- distance of construction objects from the road.
- type of structural system and floor-ceiling.
- geological characteristics of the soil on which the structure is founded, and the type of foundation.

Predominant frequency and amplitude of vibration sources depend on: vehicle weight, suspension unit type and speed of the vehicle. When the road surface is uneven, at a speed of 25 km/h the vibration amplitudes are the same, and at a speed of 50 km/h are twice higher. The natural frequency f of surcharge of thickness H above the base wall, depends on soil stiffness and thickness, and is expressed by the relation (2) [3]:

$$f = \frac{c_s}{4H} \quad [\mathrm{Hz}] \qquad (2)$$

In equation (2) is:

$c_s = \sqrt{\frac{G}{\rho}}$ – particle velocity at the source,

G – shear modulus,

ρ– density.

Generally, the process of measurement and data processing can be divided into four phases [2]:

- data collection and measurement.
- recording the measured values.
- preparation and evaluation of processing data.
- measurements analysis.

Caused vibrations are generated due to the effects of dynamic and oscillatory force of the wheel. Oscillatory forces are caused by fluctuations of wheel axles whose frequency depends on the manner of suspension unit, wheelbase, weight and speed of vehicles.

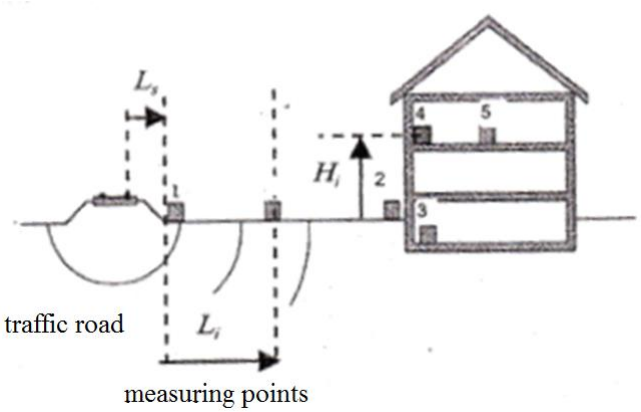

Fig. 1 *Measurement points*

Figure 1 schematically presents the measurement locations in each facility, as well as the dependence of vibration level on the distance from the source. At each measuring point it is necessary to measure the three components of vibration - vertical and two horizontal (in the direction of the road and perpendicular to the road).

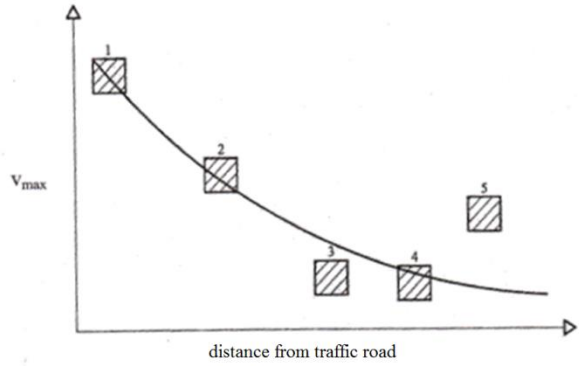

Fig. 2 *Characteristics of traffic induced vibration propagation from source to structure*

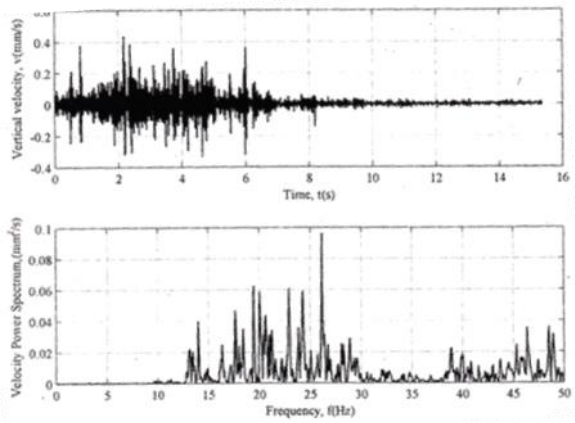

Fig. 3 *The time history and power spectrum of vertical vibrations caused by trams*

Studies have shown that road traffic generates vibrations whose frequencies are between 5 and 25 Hz, velocity amplitudes are in range from 0.05 to 25 mm /s, and the amplitude of acceleration of 0.005-2.0 mm/s^2. Evaluation of vibration effects is evaluation of effects on: people, buildings and sensitive equipment. According the fact that in Serbia there is no standardization, which would define the permissible traffic-induced vibration level, we will analyze the provisions of the German (DIN) and British Standards (BS). In most cases, it is sufficient to measure only vertical vibrations, which have a higher amplitudes and are more efficiently transmitted to the foundation, and then through an construction object, as opposed to the horizontal components of vibration.

2.1 Effect of vibration on buildings

Both British and German standards use, for the assessment of the impact of vibration on buildings, maximum vibration velocity (PPV- peak particle velocity) measured in building foundation. According to both standards, the permitted maximum speed is defined as a function of frequency of oscillation and the construction type. Valuesof the PPV are shown in Tables 2 and 3.

Table 2 *Reference values above which cosmetic damages to buildings as a function of maximum vibration velocity PPV (mm /s) are expected, according to BS 7385: 2*

	PPV[mm/s]			
	frequency / building type	4-15 Hz	15-40 Hz	over 40 Hz
1	Reinforced buildings, industrial and massive commercial buildings	50	50	50
2	Unreinforced buildings, residential or light commercial buildings	15-20	20-50	50

Table 3 *Reference values above which cosmetic damages to buildings as a function of maximum vibration velocity PPV (mm /s) are expected, according to DIN 4150:3*

	PPV[mm/s]			
	frequency / building type	< 10 Hz	10-50 Hz	50-100 Hz
I	Commercial and industrial buildings	50	50	50
II	Residential building, etc.	15-20	20-50	50
III	Other buildings sensitive to vibrations			

Figure 4 shows the time histories of the velocities measured at point 3 (Fig.1).

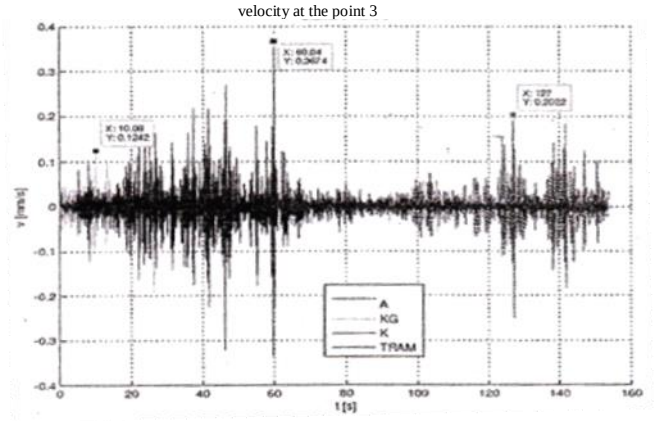

Fig. 4 *Time history of vertical vibration measured at point 3, caused by the action of A-ambient vibrations, KG-truck across the tire, K- truck and T -tram*

Figure 5 shows spectral density (PSD) of vertical vibration in Figure 3.The spectral density gives the frequency distribution of power, i.e. vibration energy of the observed signal. It shows what frequencies correspond to the largest vibrations caused by the movement of vehicles. Based on the assessment of natural frequencies of structures near the road, one can roughly conclude what will be the impact of traffic-caused vibrations on buildings.

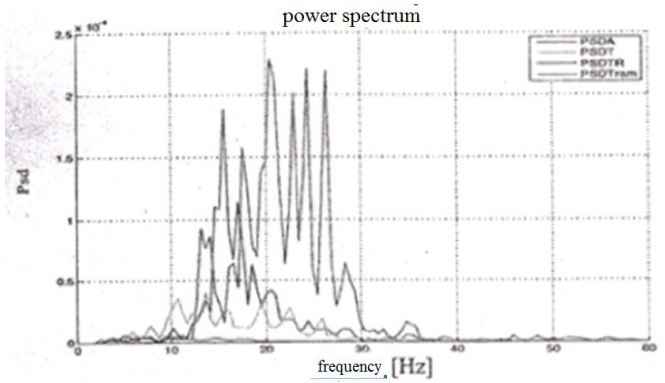

Fig. 5 *Spectral density of vertical vibration measured at point 3, caused by the action of A-ambient vibrations, KG-truck across the tire, K- truck and T -tram*

PSD is determined based on the Fourier transform of the signal $v(t)$. Specifically, using the integral Fourier transform, each signal can be presented as an infinite sum of harmonics with different frequencies:

$$v(\omega) = \int_{-\infty}^{\infty} v(t) e^{i\omega t} dt \qquad (3)$$

Power (density) spectrum is equal to the square of the Fourier transform of vibration velocity:

$$PSD = \left| \int_{-\infty}^{\infty} v(t) e^{i\omega t} dt \right|^2 \qquad (4)$$

Fourier transform of the signal can be determined using the program Matlab and numerical method known as the fast Fourier transform (FFT). Using the direct Fourier transform of N elements, the computation process is a little over N^2 calculations. The algorithm of fast Fourier transform, which is formulated around 1965. is a process of roughly NlnN arithmetical operations. It is easy to determine that the difference between N^2 and NlnN is extremely high for large N.

2.2 Effect of vibration on humans

Vibrations caused by traffic can have disturbing effects on people because of unpleasant physical sensations and noise. People's ability to anticipate vibrations is directly proportional to the speed and frequency of vibration. ISO and BS define the effect of vertical and horiyontal vibration on people in buildings depending on the PPV (Fig.6). As for the buildings, minimum values are permitted in hospitals and buildings with sensitive equipment, and most ones in workshops and factories.

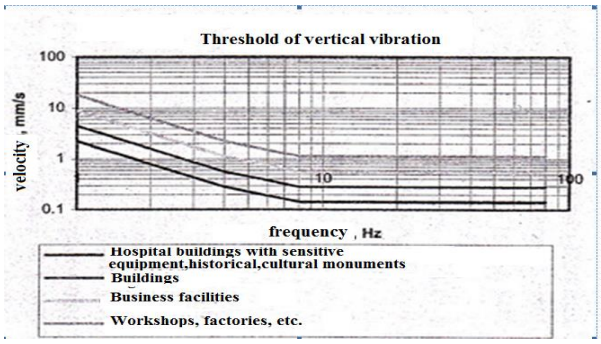

Fig. 6 *Allowable amplitude of vertical vibration, BS 6472*

In Boulevard kralja Aleksandra Street, for measured frequencies higher than 8Hz, tram caused PPV greater than the limit at 16 out of 23 structures, 14 t truck acroos the ramp at 15 of 22, and truck at 8 of 24 structures.

German standard DIN uses the time history of the vibration velocity $v(t)$ for the assessment of effects of vibrations on humans by $KB_F(t)$:

$$KB_F(t) = \sqrt{\frac{1}{\tau} \int_{\xi=0}^{t} e^{-\frac{t-\xi}{\tau}} KB^2(\xi) d\xi} \qquad (5)$$

where is τ=0.125 s, and ξ is time variable.

$KB(t)$ is the signal velocity $v(t)$ normalized and corrected by frequency-dependent factor which is defined by DIN 45669. KB_{Fmax} can be determined using the appropriate procedure in the frequency $KB(f)$ *or the time domain* $KB_F(t)$ and compared with a threshold of vibration given in Table 4.

Table 4 *Threshold for assessing the effects of vibration on comfort people according to DIN 4150-2*

Exposure	Day			Night		
Place	A_u	A_o	A_r	A_u	A_o	A_r
Commercial buildings	0.4	6	0.2	0.3	0.6	0.15
Mostly commercial buildings	0.3	6	0.15	0.2	0.4	0.10
Mixed Zone	0.2	5	0.1	0.15	0.3	0.07
Mostly residential buildings	0.15	3	0.07	0.1	0.2	0.05
Sensitive areas, as hospital	0.1	3	0.05	0.15	0.15	0.05

A method is described for a particular event. However, the vibrations caused by traffic consist of a series of events that are repeated in irregular intervals. This fact must be taken into account. For frequent events, if $A_u \beta KB_{Fmax} \beta A_o$, KB_{FTm} should be calculated according to equation (6) and compared with A_r:

$$KB_{FTr} = KB_{FTm}\sqrt{\frac{T_e}{T_r}}, KB_{FTm} = KB_{FTm}\sqrt{\frac{1}{N}\sum_{i=1}^{N} KB_{FTi}}\,. \qquad (6)$$

In equation (6) T_e is the time of exposure and T_r is the period of measurement prescribed by standard (DIN 45669: 16h during the day, 8h during the night), and $KB_{FTi} = KB_F(t)$ in one stroke *Ti, i = 1, ..., N.* Tact is considered to be a time of 30 s.

3. PREDICTION OF VIBRATION

Prediction of vibration is of great importance in the decision-making process and the design of new roads and railways, as well as in the design of buildings in the vicinity thereof. Experimental models are based on the measurement of vibrations from various sources and defining the transfer function (TRF) between the source of vibration and the vibration in the building. Transfer function can be determined on the basis of:

- maximum measured values, i.e. *v(t)*, ie. PPV.
- rms (*root-mean-square*) values:

$$v_{rms} = \sqrt{\frac{\sum_{i=1}^{N} v_1^2}{N}} \qquad (7)$$

- Fourier spectrum, power spectrum, the octave or third-octave range spectrum.

The simplest transfer function is obtained from the ratio of the maximum amplitude of vibration measured in the two observed points, due to a vibration source:

$$TRF = \frac{PPV_1}{PPV_2} \qquad (8)$$

where the points 1 and 2 are points between which we want to determine the transfer function:

$$TRF = TRF_1 \cdot TRF_2 \cdot TRF_3 \qquad (9)$$

where is

TRF_1 - transfer function for soil from a source to structure,

TRF_2 - transfer function between the point on the ground, next to the building and point in building foundation,

TRF_3 - transfer function between point in the base of building and observed point (e.g. slab on top storey)

One of the most commonly used empirical transfer function from the source to a reference point, which is valid for $_{max}$PPV due to movement of trucks through the bumps in the road, has been defined by Watts [6]:

$$PPV = 0.028a\frac{v}{48}tp\left(\frac{r_0}{6}\right)^x \qquad (10)$$

In equation (10) is:

a - maximum height of the bumps in mm,

v - maximum expected speed of the truck inkm/h,

t - factor which depends on the type of soil [6],

p - coefficient, p = 0.75 if there is a defect just under one point, p=1 if the defect is under both wheels,

r_0 - distance from the reference point to the defect on the road in m,

x - the attenuation factor of the soil, given in reference [6].

Based on the obtained values of the maximum speed at a distance$r_0$from the source, one can determine the PPV in the ground at an arbitrary distance *r*, using the expression (1).

Amplification depends on the type of structure and the observed storey. The relationship between the PPV of point 5, which is located at the center of the slab on the top storey and point 3 in the base of building, for certain types of buildings, are shown in Table 5.

Table 5 *Mean value of the amplification factor*

Mean value of the amplification factor – PPV5/PPV3			
	low buildings	buildings of medium height	high-rise buildings
Tram	6	2.314	2.209
Truck with barricade	3.334	2	1.884
Truck	5.054	2.654	2.1

4. CONCLUSION

The effect of traffic-induced vibration on the buildings, humans and people in the buildings, is of very great importance for human health. The factors that affect the level and frequency of vibration are of interest for the prediction and evaluation of vibration. The vibrations caused by traffic are becoming a serious problem in big cities. They rarely cause damage to buildings, but they have disturbing effect on people. Therefore, there is a need for measurement and assessment of existing vibrations and evaluation of any future vibration caused by the action of the vehicles. The method of

measurement, assessment and prediction of traffic-caused vibration is defined by the standards of many countries (DIN, British Standard, ISO, etc.). The application of these standards is not easy. Because of the stochastic nature of vibrations induced by traffic, measurement and analysis are complex processes that require knowledge of several disciplines, primarily vibration theory and signal processing, which are not very close to structural engineers, and these issues should be dealt by occupational safety engineers, and environmental protection and working environment engineers.

Acknowledgement:

This research is supported by the Ministry of education, science and technological development of the Republic of Serbia for project cycle 2011-2014, within the framework of the project TR36016 „Experimental and theoretical investigation of frames and plates with semi-rigid connections from the view of the second order theory and stability analisys“ of the research organization The faculty of civil engineering and architecture of University of Nis, and inovation project named „Seismo-Safe 2G3-Goseb Building System“ (Project IF ID 476) financed by Innovation Fund of the Republic of Serbia, which is conducted in 2014. in „Projektinzenjering Tim“ d.o.o. in Nis, Serbia.

REFERENCES

[1] D. Cvetković, M.Praščević, *Buka i vibracije*, Univerzitet u Nišu, Fakultet zaštite na radu, Niš, 2005.

[2] M. Bahrekazemi, *Train-Induced Ground Vibration and Its Prediction*, PhD Thesis, Royal Institute of Technology, Stockholm, 2004.

[3] M. Petronijević, M. Nefovska-Danilović, *Vibracije usled saobraćaja: merenje, procena i predviđanje*, Građevinski kalendar, Vol.44, 2011, Savez građevinskih inženjera Srbije, Beograd, UDK 624(059), ISNN 0352-2733, COBISS.SR-ID 43031, UDK:656.1:534.13, str.1-41.

[4] German Institution for Standard, DIN 4150:3 *Efekti vibracija na konstrukcije*, Vibration in Building Construction (1984).

[5] International Standard Organization, ISO 2631-2:2003.

[6] G. R. Watts, *Traffic Induced Vibrations in Buildings*, Research Report 246, Transport Road Research Laboratory, Department of Transport, UK, (1990).

[7] S. Zdravković, P. Petronijević, B. Mladenović, *Modernization of railway line Belgrade-Croation border with the goal of envirement noise reduction*, Geotechnical Society of Bosnia and Hercegovina, Proceedings of GEO-EXPO 2013. May 31- June 2, 2013, Jahorina, ISS 2303-4262, pp.242-249.

KNAUF

zvučna zaštita

Masivna gipsana ploča

Robusna gipsana ploča za masivan karakter sistema suve gradnje
Masa 18,1 kg/m2 za debljinu ploče d=20 mm
Masa 21 kg/m2 za debljinu ploče d=25 mm

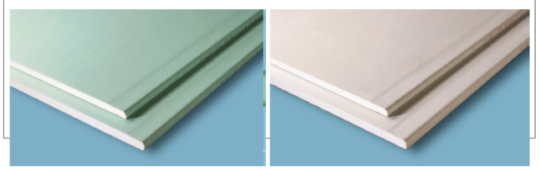

Cleaneo akustik

Perforirane (kružna i kvadratna perforacija) ili šlicovane gipsane ploče sa efektom pročišćavanja vazduha kroz aditiv od dehidriranog zeolita i kaširane akustičnim filcom
Debljina ploče d= 12,5 mm

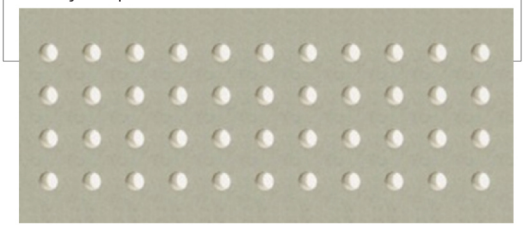

Piano

Gipka gipsana zvučno zaštitna ploča sa optimalnim odnosom osobina zvučne izolacije i mase 10 kg/m2 za debljinu ploče d=12,5 mm

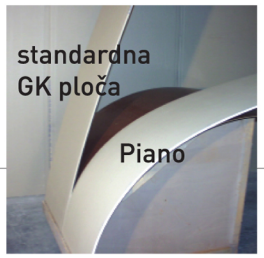

MW profil

Knauf zidni profil za poboljšanu zvučnu izolaciju u „feder-masa" sistemu

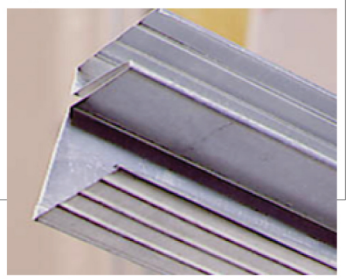

Diamant

Tvrda gipsana ploča
povećane mase = 13,5 kg/m2
za debljinu ploče d=12,5 mm

Silentboard

Gipsana ploča za vrhunsku zvučnu izolaciju Ekstremne mase = 17,5 kg/m2
za debljinu ploče d= 12,5 mm

University of Nis
Faculty of Occupational Safety
„Politechnica“ University of Timisoara
Faculty of Mechanical Engineering
24th International Conference
NOISE AND VIBRATION
Niš, 29 - 31. 10. 2014.

AIRCRAFT NOISE METRICS

Ljubiša Vasov, Branimir Stojiljković, Olja Čokorilo, Petar Mirosavljević, Slobodan Gvozdenović

University of Belgrade, Faculty of Transport and Traffic Engineering, Serbia, lj.vasov@sf.bg.ac.rs

Abstract - *The problem of the aircraft noise is certainly one of the factors that affect not only at the planning of a new airports or expanding of the existing airports, but also at the aviation industry as a whole. In order to mitigate this problem, a series of a different measures are undertaken today, whose effects are finally evaluated by the application of an appropriate indices and the aircraft noise metrics. In this paper, a brief chronological review of the aircraft noise metrics development is shown, as well as their classification according to the different criteria. The analysis of the certain aircraft noise metrics, with the close attention to their interconnections, is accomplished. Additionally for the nowadays frequently used metrics and their advantages and limitations, special attention was given. An overview of the supplemental aircraft noise metrics, which are now proposed and as such can be accepted by the general public, is given.*

1. INTRODUCTION

With the introduction of jet engines in civil aviation, aircraft noise was recognized as environmental issue since from '60s of the 20th century. Today, this problem still persists and may reach unsustainable levels. This is confirmed by the ICAO (International Civil Aviation Organization) predictions, according to which the number of people who are affected by aircraft noise, with the worst scenario, would be increased from today's 25 million to more than 34 million during the next two decades, in other words 36% higher than today [1].

Therefore, the issue of aircraft noise is present in all segments of the air transport and traffic system. There are a number of the aircraft noise abatement measures, with the final goal to reduce or limit noise exposure of people living in vicinity of airports. Comprehensive and economically viable way of the available noise abatement measures application at international airports is contained in the ICAO's "Balanced Approach to Aircraft Noise Management" [1]. One of the principal elements of this approach is a reduction of noise at source, and big improvements are achieved in this field. Due to application of high by-pass turbofan engines and improved airframe design, nowadays new types of transport aircraft generate usually up to 100 times lower sound intensity compared to the same category of the older aircraft.

The effects of these measures are described by appropriate indices and the aircraft noise metrics. Establishing of the proper noise metric system is important in prediction of the impact of noise on people, and loudness and annoyance assessment. But, evaluation of human response to noise is compounded because of complexity of human hearing system and human psychology.

Nevertheless, different influential factors on human reaction to noise are usually combined in one comprehensive indicator or single noise metric. There is number of aircraft noise metric that are more or less in using, and almost all of them are based on the decibel scale. Also, different aviation organization, countries, even airports, use different methods and aircraft noise metrics for assessing noise, and there is no common stand for the most complete and best metric that describe aircraft noise exposure.

2. DEVELOPMENT OF AIRCRAFT NOISE METRICS

One of the first attempts to characterize aircraft noise is dated back to the late 1950s, when Perceived Noise Level (PNL) is developed by Kryter. PNL is primarily used for assessing the annoyance due to jet aircraft flyover noise, because the commonly used A, as well as B and C frequency weighting networks (Figure 1) are unable to emphasize the differences between noisiness of jet aircraft versus propeller aircraft.

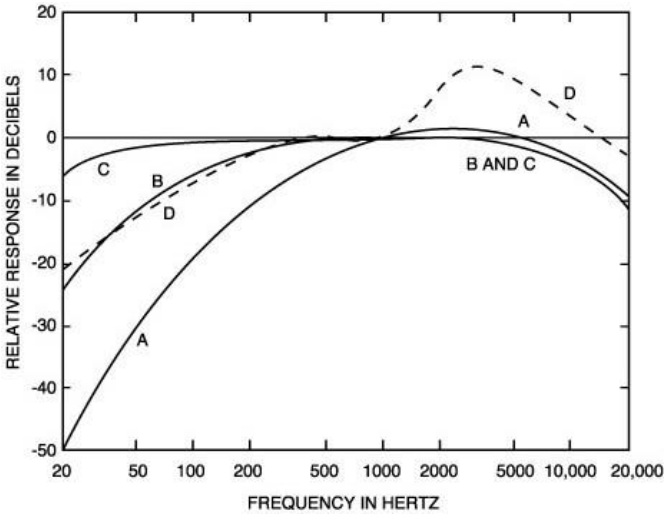

Fig. 1 *Frequency characteristics of the A, B, C and D weighting networks* [2]

PNL as a single event maximum sound level metric basically is calculated from sound pressure levels measured in octave or one-third octave frequency bands. By reason of a quite complex PNL (L_{PN}) calculation method the D weighted sound level (L_D) was introduced later as a simpler approximation of PNL, with the following relation between them [3]:

$$L_{PN} \approx L_D + 7(\pm 1dB) \quad (1)$$

Today, D weighted sound level is rarely used for non-bypass or low-bypass turbojet engines that are fitted only in military aircraft. Also, calculation method of PNL does not involve effects of pure tone "*swish*" that is often present in flyover of turbofan aircraft and duration of a sound. These shortcomings have been overcome later by introducing tone corrected and duration corrected metrics.

During the 1950s the initial assays for estimating community reaction to aircraft noise are led to development of Composite Noise Rating (CNR). An early version of the CNR was designed for any noise source, but the later CNR procedure was shaped for evaluation the aircraft noise exposure and predicting effects of multiple event aircraft operations. The calculation method of CNR (L_{CNR}) is based on data of aircraft operation (i.e. number of daytime and nighttime takeoffs and landing) and PNL (L_{PN}) value for the chosen ground location, and the relation for approximate calculation of CNR is [3]:

$$L_{CNR} \approx L_{\overline{PN}} + 10\log\left(N_d + 16.67N_n\right) - 12 \qquad (2)$$

where: $L_{\overline{PN}}$ is the average maximum of PNL at a ground location of interest, N_d is the number of daytime operations (07:00 to 22:00 hours), N_n is the number of nighttime aircraft operations (22:00 to 07:00 hours), 16.67 is weighting factor for nighttime operations and 12 is an arbitrary constant.

CNR as forerunner to other community noise predictors has few disadvantages that are incorporated through PNL. In the next two decades, from the 1960s to early 1980s, intense and overall researches in the field of psychoacoustic are brought to "*alphabet soup of aircraft noise metric*" [4].

Problem of the noisiness assessment of the sounds with prominent discrete frequencies, that are present in flyover of turbofan aircraft, is solved by introducing of Tone Corrected Perceived Noise Level (PNLT). As a PNL, the PNLT is used in assessing the subjective response to single events, and after reviewing the several different procedures of tone correction, PNLT metric procedure was accepted by Federal Aviation Administration (FAA) in 1969.

Actually, there a few methods of the PNLT calculating, but their essence is examination of the band sound pressure levels in a noise spectrum in order to find if the sound level in any frequency bands exceed its adjoining bands. Then, based on numerical difference between successive band sound pressure levels and the process of elimination if the difference does not exceed certain amount, for each of the 24 one-third octave bands tone correction factor (C) is determined (Table 1).

Table 1 *Tone correction factors* [5]

Frequency f [Hz]	Level difference F [dB]	Tone correction C [dB]
$50 \le f < 500$	$1½ \le F < 3$	$F/3$ - ½
	$3 \le F < 20$	$F/6$
	$20 \le F$	3⅓
$500 \le f < 5000$	$1½ \le F < 3$	$2F/3$ - 1
	$3 \le F < 20$	$F/3$
	$20 \le F$	6⅔
$5000 \le f < 10000$	$1½ \le F < 3$	$F/3$ - ½
	$3 \le F < 20$	$F/6$
	$20 \le F$	3⅓

Because just one tone correction factor may be added to PNL, selection of C_{max} is needed, and PNLT (L_{TPN}) is given by:

$$L_{TPN} = L_{PN} + C_{max} \qquad (3)$$

Certainly, the main disadvantage of PNLT is that it does not account duration of a noise. Influence of noise duration is considered in Sound Exposure Level (SEL), which is actually energy averaged A-weighted sound level over a specified period of time, with the reference of 1 second. Calculation of SEL (L_{AE}) for *temporal sampling is given by relation* [3]:

$$L_{AE} = 10\log\left(\sum_{i=1}^{n} 10^{\frac{L_{A(i)}}{10}}\,\Delta t\right) \qquad (4)$$

where: $L_{A(i)}$ is the instantaneous A-weighted sound level for the i^{th} sample, n is the number of samples taken during the given period and Δt is the time interval between samples. In practice is necessary to take into account sound levels which are within L_{Amax} and (L_{Amax} -10dB) interval, for a noise event such as an aircraft flyover.

Another metric, also A-weighted and energy averaged over specified period of time is Equivalent Continuous Sound Level (L_{Aeq}). This metric as noise descriptor is widespread used for aircraft noise. For continuous time integration L_{Aeq} is:

$$L_{Aeq} = 10\log\left(\frac{1}{t_2 - t_1}\int_{t_1}^{t_2} 10^{\frac{L_A(t)}{10}}\,dt\right) \qquad (5)$$

where: (t_2 - t_1) is the measurement time.

Both, the tone correction and influence of noise duration are included in Effective Perceived Noise Level (EPNL). This is a metric for assesses the noisiness of a single noise event, and EPNL if fundamental metric for aircraft noise certification.

Calculation procedure of EPNL is consisted by few steps with following simplified review [3], [5]:

- measuring of sound pressure levels of the each 24 one-third octave band with sequence of 0.5 second time interval during the aircraft noise event
- calculation of the PNL value ($L_{PN(i)}$) at each (i^{th}) 0.5 second time interval,
- determination of tone correction factor (C_i) at each (i^{th}) 0.5 second time interval,
- computation of PNLT value ($L_{TPN(i)}$) at each (i^{th}) 0.5 second time interval according to:

$$L_{TPN(i)} = L_{PN(i)} + C_i \qquad (6)$$

- identification of the PNLT maximum (L_{TPNmax}), and
- calculation of EPNL (L_{EPN}) according to:

$$L_{EPN} = 10\log\left[\sum_{i=0}^{n} 10^{\frac{L_{TPN(i)}}{10}}\right] - 13 \qquad (7)$$

where: constant –13dB is relating the 0.5 second interval to the 10 seconds reference duration, i.e. 10log(0.5/10) = –13, and n is the number of time samples when PNLT ($L_{TPN(i)}$) is within interval from L_{TPNmax} to (L_{TPNmax} –10dB).

In a number of cases, for EPNL estimation by the SEL can be used according to following approximate relation [3]:

$$L_{EPN} \approx L_{AE} + 4(\pm 3dB) \quad (8)$$

Today, EPNL as a single number evaluator is widely accepted as basic metric for certification of subsonic jet airplanes, propeller-driven airplanes over 8618kg and helicopters over 3175kg. For propeller-driven airplanes below 8618kg noise evaluation measure is maximum A-weighted sound level, and for helicopters below 3175kg noise measure is SEL.

During the 1960s and 1970s have been developed a number of multiple event metrics, based on previously described single event metrics. As improvement of CNR, on the mid of 1960s was introduced Noise Exposure Forecast (NEF). Like the CNR, basic purpose of NEF was estimation of community reaction to the aircraft noise and there is strong correlation [3] between CNR (L_{CNR}) and NEF (L_{NEF}):

$$L_{NEF} \approx L_{CNR} + 70 \quad (9)$$

Calculation of NEF is based on EPNL and data of aircraft operation (i.e. number of daytime and nighttime takeoffs and landing) for different classes of aircraft:

$$L_{NEF(i,j)} = L_{EPN(i,j)} + 10\mathbf{log}\left(N_{d(i,j)} + 16.67N_{n(i,j)}\right) - 88 \quad (10)$$

where: i is the aircraft class, j is flight path, $L_{NEF(i,j)}$ is the NEF for i^{th} aircraft class flying along the j^{th} flight path, $L_{EPN(i,j)}$ is the EPNL at a given ground location generated by i^{th} aircraft class on the j^{th} flight path, $N_{d(i,j)}$ and $N_{n(i,j)}$ number of (d) day (07:00 to 22:00) and (n) night (22:00 to 07:00) operation of the i^{th} aircraft class on the j^{th} flight path, 16.67 is weighting factor for nighttime operations and 88 is an constant.

Then the overall value of the NEF (L_{NEF}) at a given location is the sum of $L_{NEF(i,j)}$ by the aircraft class (i) and flight path (j):

$$L_{NEF} = 10\mathbf{log}\left(\sum_{i=1}^{n}\sum_{j=1}^{m} 10^{\frac{L_{NEF(i,j)}}{10}}\right) \quad (11)$$

Where: n is the number of aircraft class and m is the number of flight paths.

Determined by comprehensive interviews the acceptable NEF values were very helpful as guidelines for proper land use planning and zoning in vicinity to the airports. Numerous of multiple event aircraft noise metrics was developed during the 1907s with basic purpose of land zoning and regulation. For example, one of them is Community Noise Equivalent Level (CNEL) based on A-weighted sound level and developed in the State of California.

CNEL (L^{*}_{den}) is a 24 hour noise rating metric that includes adjustment factors for evening and nighttime periods, and it is introduced as *simplified alternative to the NEF system* [6]:

$$L^{*}_{den} \approx L_{NEF} + 35 \quad (12)$$

The calculation method is based on hourly noise levels [3]:

$$L^{*}_{den} = 10\mathbf{lg}\left[\frac{1}{24}\left(\sum_{i=1}^{12} 10^{\frac{L_{hd(i)}}{10}} + 3\sum_{j=1}^{3} 10^{\frac{L_{he(j)}}{10}} + 10\sum_{k=1}^{9} 10^{\frac{L_{hn(k)}}{10}}\right)\right] \quad (13)$$

where: $L_{hd(i)}$ is hourly noise level for daytime (07:00÷19:00), $L_{he(j)}$ is hourly noise level for evening (19:00÷22:00) and $L_{hn(k)}$ is hourly noise level for nighttime period (22:00÷07:00). Also CNEL can be calculated on yearly basis in order to provide guidelines for compatible land using.

Today, CNR and NEF are rarely used and have been replaced by Day-Night Average Sound Level (DNL). Like CNEL, this DNL (L_{dn}) metric is based on A-weighted sound level over 24 hours, and there is highly correlation between them:

$$L_{dn} \approx L^{*}_{den} \quad (14)$$

DNL as a single number noise descriptor includes both: the sound levels and number of noise events. The characteristics of sound are measured with averaged A-weighted sound level during the given time period, and DNL metric is improved by addition of adjustment factor for the nighttime noise events.

Calculation of DNL can be accomplished by several methods, and one of them is continuous time integration [3]:

$$L_{dn} = 10\mathbf{log}\left[\frac{1}{86400}\left(\int_{07:00}^{22:00} 10^{\frac{L_A(t)}{10}}\,dt + \int_{22:00}^{07:00} 10^{\frac{L_A(t)+10}{10}}\,dt\right)\right] \quad (15)$$

where: L_A is instantaneous A-weighted sound level, 07:00 to 22:00 is the daytime interval, 22:00 to 07:00 is the nighttime interval and 86400 is the number of seconds in 24 hours.

Based on daily calculation of DNL, it can be computed as a Yearly Day-Night Average Sound Level YDNL (L_{dny}):

$$L_{dny} = 10\mathbf{log}\frac{1}{365}\sum_{i=1}^{365} 10^{\frac{L_{dn(i)}}{10}} \quad (16)$$

where: $L_{dn(i)}$ is the daily DNL for the i^{th} day of the year.

By the YDNL, it is possible to estimate the long term aircraft noise impact and determinate the cumulative noise exposure around the airport. DNL is one of the measures for community noise exposure recommended by many agencies, and it is used by FAA as primary measure in describing noise around the airport.

Certainly, with DNL the list of present aircraft noise metric is not completed. That was "*just one spoon of alphabet soup of aircraft noise metrics*" and there is no consensus, which one is most proper and comprehensive.

3. COMMONLY USED AIRCRAFT NOISE METRICS

About two decades ago list of employed aircraft noise metrics was very diverse between countries. Some of them have used somewhat unusual aircraft noise metrics, but in time situation in this area is slightly changing.

There is few examples of European countries [7]: until 1990 in UK was used the Noise and Number Index (NNI) when it is replaced by L_{Aeq}, until February 2003 the Netherlands was used the Kosten Index (Ke) based on L_{Amax}, when it is replaced by L_{den}, in France Psophic Index (IP) based on PNL scale was used the until 2002 when it is replaced by L_{den}, etc.

In European Community, problem of aircraft noise metrics and traffic noise metrics at all, is clarified by Environmental Noise Directive 2002/49/EC of the European Parliament [8].

This Directive harmonizes previous situation, and requires from all Member States to use Day-Evening-Night level (L_{den}) for 24 hour period and night level (L_{night}) metrics, for purpose of environmental noise levels reporting and mapping. The L_{den} is defined by following relation [8]:

$$L_{den} = 10 \lg \frac{1}{24} \left(12 \cdot 10^{\frac{L_{day}}{10}} + 4 \cdot 10^{\frac{L_{evening}+5}{10}} + 8 \cdot 10^{\frac{L_{night}+10}{10}} \right) \quad (17)$$

where: L_{day}, $L_{evening}$, L_{night} are A-weighted long-term average sound level over the day, evening, night period of a year.

Period of 24 hours is divided in three different intervals: 12 hours for day, 4 hours for evening and 8 hours for night. The start of the day may be chosen by the Member States, and a 07:00 hour is default start time of the day.

Day-Evening-Night level (L_{den}) by content is very similar with DNL (L_{dn}) and CNEL (L^{*}_{den}), but there is certain difference between them due to different duration and weighting for the evening and night period.

However, 2002/49/EC requirement does not imply suspension and exclusion of all other aircraft noise metric in any Member State. There are many examples of using additional indicators and list of commonly used aircraft noise metrics in some of worldwide countries is shown in following (Table 2).

Table 2 *Commonly used aircraft noise metrics*

Country	Aircraft Noise Metric
Australia	Australian NEF (ANEF), N_{70}
Austria	L_{den} , L_{night}
Belgium	ago: Psophic Index (IP), now: DNL, SEL
Canada	NEF
Cyprus	L_{den} , L_{night}
Denmark	L_{den} , L_{night}
Estonia	L_{den} , L_{night} , L_{de} , L_{Aeq}
Finland	L_{den} , L_{night} , L_{Aeq}
France	ago: Psophic Index (IP) , now: L_{den} , L_{night}
Germany	ago: Störindex "*Q*" , now: L_{den} , L_{night}
Greece	ago: NEF , now: L_{den} , L_{night}
Hong Kong	NEF
Ireland	L_{den} , L_{night} , L_{Aeq} , L_{Amax}
Italy	L_{VA} equivalent of L_{eq}
Japan	ago: WECPNL[1] , now: L_{eq} based metric
Lithuania	L_{den} , L_{night}
Luxemburg	ago: Störindex "*Q*" , now: L_{den} , L_{night}
Netherlands	ago: Kosten Index, now: L_{den} , L_{night} , L_{Aeq}
New Zealand	DNL
Norway	Equivalent Aircraft Noise (EFN)
Portugal	L_{den} , L_{night}
Romania	L_{den} , L_{night}
Slovakia	L_{den} , L_{night}
Slovenia	L_{den} , L_{night}
Spain	ago: NEF , now: L_{den} , L_{night}
Sweden	ago: FBN , now: L_{den} , L_{night} , L_{day} , $L_{evening}$
Switzerland	hourly L_{eq}
UK	ago: NNI , now: L_{den} , L_{night} , L_{Aeq}
Ukraine	L_{Aeq}
US	DNL, CNEL

[1]Weighted Equivalent Continuous Perceived Noise Level

It is very important to emphasize that Environmental Noise Directive 2002/49/EC foresees using of supplementary noise indicators in some cases, such as [8]:

- noise source operates only small proportion of time,
- the average number of noise events is very low,
- the low frequency content of noise is strong,
- needs for extra protection at the weekend, or specific part of year, or day period, or evening period,
- the noise has an impulsive character, etc.

Previously mentioned issues are subject of discussion how to improve the ability of the aircraft noise impacts prediction and the public understanding of the aircraft noise metrics.

3.1 Aircraft noise metrics classification

Previously mentioned aircraft noise metrics by content can be classified in several groups, based on different criteria. At the aircraft noise metric definition level, there are a several basic factors that determine noise metric character, as:

- the sound level,
- the frequency or pitch of the sound,
- the duration of the sound,
- the number of noise events,
- the time of day (day-evening-night), etc.

Many of previously described aircraft noise metrics aggregate these factors in one single value, and one given metric at the same time can belong on different classes of the aircraft noise metrics. One of commonly used classification separate those according to the criteria of single and multiple events, and the criteria of energy dose and cumulative time metrics (Table 3).

Table 3 *Aircraft noise metrics classification*

Criteria	Aircraft Noise Metrics
Single event maximum sound levels	A-weighted sound level
	D-weighted sound level
	PNL
	PNLT
Single event energy dose metrics	EPNL
	SEL
Cumulative energy average metrics	L_{Aeq}
	DNL
	CNEL
	NEF
	L_{den}
	WECPNL
	NNI
	CNR
Cumulative time metrics	24h Time Above (TA)
	Day-Evening-Night (TA)

In addition to these classes of aircraft noise metric, there is another one with so called supplementary noise metrics, as:

- Statistical Sound Level (L_x),
- Number Above (N_{70}),
- Person Event Index (PEI), etc.

These supplementary noise metrics are noise descriptors with the basic purpose to *improve public understanding of the manner in which aircraft noise is characterized* [4].

4. SUPPLEMENTARY AIRCRAFT NOISE METRICS

Today conventional aircraft noise metric are more often under criticism, because there are some limitations of cumulative energy average metrics, such as commonly used L_{den} or DNL metrics. These limitations are connected with the concept itself of the DNL and L_{den} or any other averaged aircraft noise metric definition. When using DNL to explain noise exposure to the average citizen, a more typical response is "*I don't hear averages, I hear individual airplanes*" [9].

There are a number of reasons of misunderstanding and distrust by the public, and most important are:

- the quantity of noise exposure expressed in 24 hour cumulative time weighted average level is outside of common experience of noise, and *cannot be directly experienced by observation in the same sense as the maximum sound level of a single noise event* [4], and
- by aggregating the different elements of the sound into one single aircraft noise metric, identity of the individual factors is lost, that perturbs understanding of influence of specific elements (maximum levels, frequency, duration, number of noise events, etc.).

In addition to this, logarithmic relations and manipulation in almost all aircraft noise metric are indirect and non-intuitive for wider audiences. For these reasons the certain set of noise indicators have been considered as supplement to the usual conventional noise metrics. Some of the supplemental noise metrics that have been useful to the analysis of aircraft noise exposure are:

- Time Above (TA): time of noise exposure during the observation period at given locations, *above some preselected threshold of A-weighted sound level* [3],
- Statistical Sound Level (L_x): *the A-weighted sound level exceeded for x% of the measurement period* [7] at given location (common used are L_{10}, L_{50} and L_{90}),
- Number of events Above a threshold level (NA): the number of aircraft noise events above the specified noise level for a given location and during a specific period of time, (in Australia is widely used N_{70}, i.e. the number of aircraft noise events above 70dBA),
- Person Event Index (PEI), *the total number of instances where an individual is exposed to an aircraft noise event above a specified noise level over a given period* [7]:

$$PEI(x) = \sum P_N \cdot N \qquad (18)$$

where: x is single event threshold noise level in dBA, P_N is number of persons exposed to N noise events with noise level greater then x (the PEI is summed between N_{min} and N_{max}).

These noise descriptors give answers to simple questions, as: "*how long will it be this noisy during the day*" or "*how many noisy aircraft can be heard throughout the day*". By treating aircraft noise through the noise exposure time or total number in series of the single noise events rather than as calculated cumulative acoustic averages, a more understandable mental picture of noise exposure is enabled.

It is important to emphasize that supplemental aircraft noise metrics are not replacement for energy average metrics. Also, these noise metrics can not increase accuracy of noise impact prediction, but may improve a public understanding of current noise environment and changes of the aircraft noise impact.

5. CONCLUSION

Today, different aircraft noise metrics are in using, and many of these are mutually similar and based on same concept of aggregation of the acoustics and the psychoacoustics factors in to one single noise indicator. There is no common stand for the most complete noise metric that describes aircraft noise exposure. Deficiency of a communication language in relation to aircraft noise with the general public is stumbling block to the effective noise management. Overcoming of this problem can be achieved by using the other supplemental aircraft noise metrics. By using of the supplementary aircraft noise metrics and descriptive discussion of the noise impacts, the confusing and potentially misleading can be avoided.

REFERENCES

[1] Lj. Vasov, S. Gvozdenović, O. Čokorilo, P. Mirosavljević, B. Stojiljković, "Elements of Aircraft Noise Management", 23rd *National Conference &* 4th *International Conference NOISE AND VIBRATION*, Niš, 17-19 October, 2012.

[2] Portland International Jetport Noise Exposure Map, Appendix A: *Noise Metric and Acoustic Terminology*, HMMH Report No. 298410, March, 2004.

[3] R. Benett, K. Pearsons, *Handbook of Aircraft Noise Metrics*, NASA CR-3406, March, 1981.

[4] V. Mestre, P. Schomer, S. Fidell, B. Berry, "Technical Support for Day/Night Average Sound Level (DNL) Replacement Metric Research", DOT/FAA/AEE/2011-2, June, 2011.

[5] ICAO Annex 16, Volume 1, Aircraft Noise, Appendix 2: *Evaluation Method for Noise Certification of Subsonic Jet Airplanes, Propeller Driven Airplanes Over 8618kg, Helicopters*, Sixth Edition, July, 2011.

[6] B. Truax, R. Schafer, *Handbook for Acoustic Ecology*, Cambridge Street Publishing, Second Edition 1999, http://www.sfu.ca/sonic-studio/handbook/index.html

[7] K. Jones, R. Cadoux, *Metrics for Aircraft Noise*, CAA Environmental Research and Consultancy Department, ERCD Report 0904, London, January 2009.

[8] Directive 2002/49/EC of the European Parliament and of the Council, June 2002.

[9] *Improving Aviation Noise Planning, Analysis and Public Communication with Supplemental Metrics*, Department of DNWG, Washington, December 2009.

CENTER OF TECHNICAL DIAGNOSTICS & NOISE AND VIBRATION LABORATORY

UNIVERSITY OF NIŠ
FACULTY OF OCCUPATIONAL SAFETY
Čarnojevića 10a, 18000 Niš
Tel.: 018 529-747; Fax: 018 529-748

Environmental noise & Occupational noise - measurement and analyis

- Rating noise level;
- Frequency analyis;
- Statistical analysis;

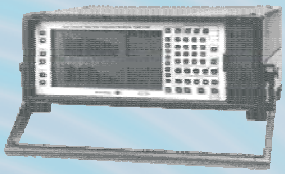

Human vibration

- Hand-arm vibration;
- Whole body vibration;

Sound power of noise sources

- Sound pressure method;
- Sound intensity method;

Predictive/preventive maintenace of machine

- Vibration condition monitoring;
- Vibrodiagnostics;
- Balancing of rotating machine;

Design of noise and vibration control systems

- Design of noise insulation and absorption system;
- Design of vibration insulation and absorption system;
- Design of room acoustics;

Room acoustics

- Time reverberation;
- Airborne sound reduction index
- Impact sound reduction index;

Urban noise

- Noise monitoring;
- Noise zoning;
- Strategic noise maps;

Education

- Workshops;
- Courses;
- Long-term learning;

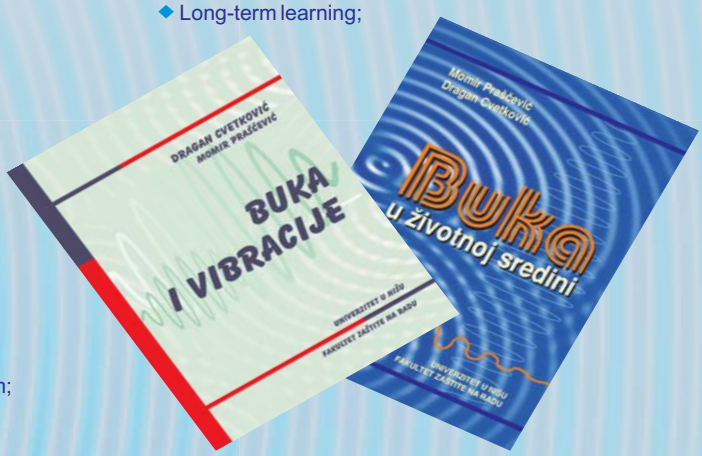

University of Nis
Faculty of Occupational Safety
„Politechnica“ University of Timisoara
Faculty of Mechanical Engineering
24th International Conference
NOISE AND VIBRATION
Niš, 29 - 31. 10. 2014.

ANALYSIS OF NOISE ABATEMENT MEASURES ON EUROPEAN AIRPORTS

Emir Ganić[1], Feđa Netjasov[1], Obrad Babić[1]

[1] University of Belgrade, Faculty of Transport and Traffic Engineering, Division of Airports and Air Traffic Safety, Vojvode Stepe 305, 11000 Belgrade, Serbia, emir.ganic@yahoo.com, f.netjasov@sf.bg.ac.rs, o.babic@sf.bg.ac.rs

Abstract - *Air traffic noise is one of the major constraints of airport development. Many airports recognized noise problem long ago and have introduced a variety of measures to reduce its impact. The number and types of the introduced measures differ between airports. In order to determine the most influential factors for the introduction of noise abatement measures in airport surroundings, the research presented in this paper examined 248 European airports. By analyzing the correlation of specific characteristics related to airports (number of runways and aircraft operations, distance from the city and the population of the city that it serves, gross domestic product (GDP) per capita) and the number of introduced noise abatement measures, five hypothesis were examined: the higher number of aircraft operations causes the introduction of a higher number of noise abatement measures (NAMs); the higher number of runways will affect the introduction of a higher number of NAMs; airports that are closer to the settlement will introduce a higher number of NAMs; the higher population in the vicinity of the airport will affect the introduction of higher number of NAMs; the higher GDP per capita will affect the introduction of a higher number of NAMs. The results of analysis has shown that number of NAMs introduced doesn't have significant functional relationship with observed factors, except in some certain cases.*

1. INTRODUCTION

Aircraft noise is considered as one of the most influencing limiting factors of air traffic development, especially airports. Due to increase of population in cities and their territorial expansion, cities become more closer to airports, which parallel with air traffic growth, results in increase of number of people affected by negative noise effect.

Various organizations at the global level discuss possible solutions to the problem of air traffic noise. In September 2001, within the Resolution A33-7 [1], International Civil Aviation Organization (ICAO) has presented the policies and programs based on the so-called "Balanced approach" of aircraft noise management. In the guidelines for the application of a "Balanced approach", ICAO has recognized the need that the solution for noise problem should be discussed separately at each airport in accordance with the specific characteristics of the observed airport [2]. The guidelines are general and do not require an accurate and uniform application for all airports. However, the same solution can be applied if similar noise problems are identified at airports [2]. The Balanced Approach recommends that noise policy should not target single solutions but use any combination of solutions as the most appropriate option to solve the causes of problems [3] [4].

Many airports recognized noise problem long ago and have introduced a variety of measures to reduce its impact. Since 1999, Boeing maintains a database of airports around the world that implemented measures to reduce noise impacts [5]. The database contains basic information about airports and description of noise abatement measures implemented on specific airport.

Based on data from Boeing's database, Netjasov [3] provides an overview of the measures implemented at airports around the world showing their frequency and diversity. Due to ever-increasing volume of air traffic in the world, it was shown that the number of airports that are facing the problem of noise is increasing and that the number of airports that are introducing some measures to manage noise is increasing [3].

Although there are similarities between airports that are introducing some of the noise abatement measures, the number and type of applied measures are very different among them. In addition to all the previous knowledge of the subject, the question that remains open is [3]: what are the most influential factors for introduction of certain measures? The aim of the research presented in this paper is to analyze and show if the correlation between number of noise abatement measures introduced and specific characteristics related to airports (factors) exist thus to answer this question.

This paper is organized as follows. Section 2 describes types of measures that airports are introduced in order to reduce noise impacts. Particular emphasis was placed on noise abatement measures applied by the airports in Europe. Section 3 explains the research methodology, the main questions that motivated the study, the starting point for research, as well as a database based on which the survey was conducted. By analyzing the correlation of specific characteristics related to airports and the number of introduced noise abatement measures (NAMs), based on data collected for European airports, Section 4 provides the discussion of results obtained. Section 5 contains conclusions and future research directions.

2. NOISE ABATEMENT MEASURES

According to Boeing database, airports around the world have introduced ten different noise abatement measures so far [3] [5]:

1. Noise Abatement Procedures – referring to the procedures, i.e. on the arrival and departure trajectories, as well as recommended flying techniques.

2. Engine Run-Up Restrictions – referring to the restrictions on the engine testing (usually the specific facilities and location at the airports are intended for that) and the use of ‘‘reverse thrust’’ in landing.

3. Preferential Runways – referring to the runways predefined for arrivals and departures in case of airports with multiple runways (if traffic, weather and safety conditions permit).

4. Airport Curfews – referring to the time intervals in which takeoff or landing are not allowed for some or all types of aircraft (usually time intervals during the night or weekend) and they can be changed seasonally (summer, winter).

5. Noise Charges – referring to the additional charge to airlines whose aircraft exceed the allowable values of noise as well as additional charge to companies using older types of aircraft (louder), where the amount of charge can vary with the time of the day (e.g. more expensive during the peak period) and the weight of the aircraft (e.g. more expensive for the heavier aircraft).

6. APU Operating Restrictions – referring to the prohibition of the APU (Auxiliary Power Unit) use while the aircraft is on the ground and recommends the use of fixed or mobile GPU (Ground Power Units).

7. Noise Level Limits – refers to the allowed noise values in certain points of the noise monitoring system (usually per operation), the excess which leads to additional charges (or fines) applied to airlines.

8. ICAO Annex 16 Chapter 3/Chapter 2 Restrictions – refers to the prohibition of flying for the aircraft that are certified in accordance with Chapters 2 and 3 of ICAO Annex 16, Volume 1.

9. Operating Quotas – refers to the limit of the number of commercial operations at the annual or seasonal (summer, winter) level as well as the limited number of actual arrivals and departures during peak hours.

10. Noise Budget Restrictions – refers to the process of giving the time interval for the landing and taking off (slot allocation) in order to meet the defined criteria (e.g. the annual number of operations) and approved overall noise level (noise total volume).

Analyzing Boeing's database it was found that 603 airports applied some of the NAMs in the year 2009. In 2010, the number of airports increased to 630.

In this paper, a special emphasis was given on NAMs that European airports applied. According to Boeing's database, the number of European airports that applied some of the NAMs was 231 in 2009 and 246 in 2010.

Distribution of number of NAMs introduced per airport in Europe for years 2009 and 2010 is shown on **Fig. *1***.

From the **Fig. *1*** it can be seen that in both years, roughly 60% of airports are introducing one to four NAMs and 25% five to six NAMs. Only 1% of the observed airports have implemented all ten analyzed measures.

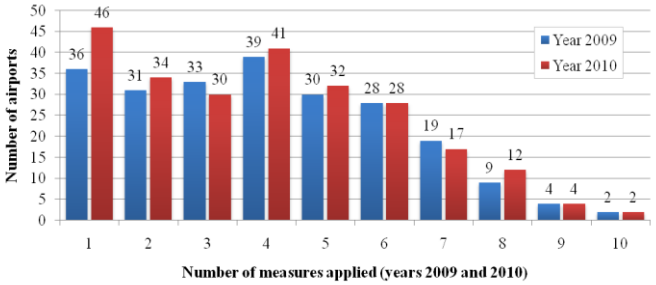

Fig. 1 *Distribution of number of NAMs introduced per airport in Europe for years 2009 and 2010 (based on date from [5])*

Comparison of frequency of NAMs (ten previously mentioned) at European airports in years 2009 and 2010 is given in **Fig. *2***. The most common measures applied are Noise Abatement Procedures followed by Engine Run-Up Restrictions. Only seven airports have applied Noise Budget Restrictions.

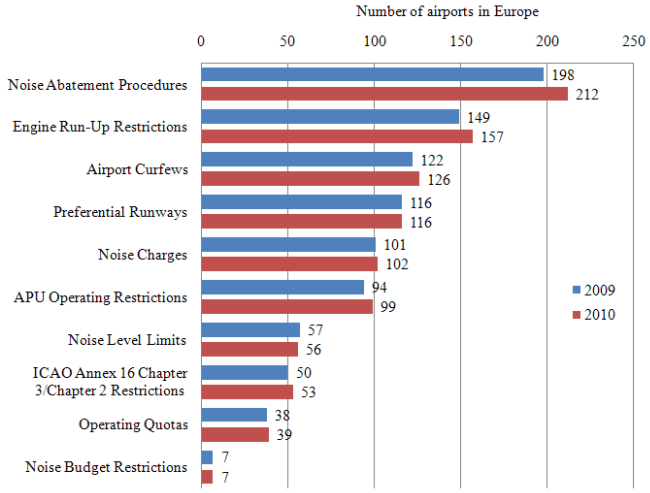

Fig. 2 *Distribution of number of airports in Europe that introduced certain noise reduction measures in years 2009 and 2010 (based on date from [5])*

3. RESEARCH METHODOLOGY

Number of introduced NAMs significantly differs among airports. In order to analyze characteristics of airports or their surroundings that are leading to different resolution of noise problem, first step in this research was to determine potential measurable factors that are presumed to have influence on introduction of NAMs.

3.1. Research Starting Point

Netjasov [3] stated that intuitively it is expected that airports with more aircraft operations (landings and take-offs), higher percentage of heavier aircraft in the fleet mix, closer to the settlements, greater population densities surrounding it, will implement more measures. However, in many cases, it seems that reasons for noise measure introduction are somewhat different [3]. Some of the reasons may be regulations concerning noise, citizen complaints or level of awareness of environmental protection.

To what extent will the airport surroundings be exposed to noise depends on many factors, and the most important are [6]:

- airport characteristics (number of takeoffs and landings, the distribution of traffic throughout the day and night, etc),
- fleet mix (types of aircraft that are using the airport),
- shape and characteristics of departure and arrival procedures, and
- airport location (topography).

Fleet mix, shape and characteristics of departure and arrival procedures, and airport location have a major impact on the creation and propagation of noise. However, in this study, they have not been taken into account because of the unavailability of operational data for a large number of the observed airports and the fact that procedure usage depends on current day meteorological and/or traffic situation.

It is necessary to consider distance from the airport to the city, because settlements closer to the airports are more exposed to noise. Airports with more runways have more options for designing different procedures for takeoff and landing in order to reduce noise and because of that, it is decided to consider the impact of number of runways on introduction of NAMs.

Comprehensive analysis of legislation was not conducted in this paper, but the impact of one EU directive on introduction of NAMs was shown. Number of citizen complaints on noise was not considered in this paper because for most airports data do not exist or are not found in the available databases. GDP per capita is used as a measure of level of awareness of environmental protection. The assumption in this paper is that developed countries, which have a higher GDP per capita, are more concerned about the negative impact of noise than less developed countries.

From all of the assumed factors, for further analysis, the following have been adopted:

- number of aircraft operations (take-offs and landings) on the airport,
- number of airport runways,
- distance from airport to the settlement,
- population in the vicinity of the airport,
- GDP per capita of the country where the airport is located.

Based on the presented research starting points, hypothesis that will be examined in this study are the following:

1. The higher number of airport operations causes the introduction of a higher number of NAMs.
2. The higher number of runways will affect the introduction of a higher number of NAMs;
3. Airports that are closer to the settlement will introduce a higher number of NAMs;
4. The higher population in the vicinity of the airport will affect the introduction of higher number of NAMs;
5. The higher GDP per capita will affect the introduction of a higher number of NAMs.

3.2. Design of Database

To determine functional relationship between proposed factors and number of NAMs, it is primarily necessary to collect data about these factors for each airport that has applied at least one of the NAMs.

The basis for this research was Boeing's database of airports that implemented NAMs [5]. The research was conducted on the data set for years 2009 and 2010.

The data about the number of applied NAMs and number of runways for each observed airport were obtained from Boeing's database [5] (grass runways were excluded). Number of aircraft operations is taken from EUROCONTROL's STATFOR Interactive Dashboard [7]. STATFOR database takes into account only IFR flights. GDP per capita (in dollars) for every country was taken from World Bank website (http://data.worldbank.org/indicator/NY.GDP.PCAP.CD) .

For the purposes of this research, proximity to the settlement was defined as distance from airport to center of a city that airport serves. For most airports, the data about distance to city center and cities that airport serves, was taken from Wikipedia. For some airports, website www.distance.to was used for estimation of distance to the city center. For airports serving several cities, the average distance from the cities was calculated according to the following formula:

$$d_{avg} = \left(\sum_{i=1}^{n} d_i \cdot P_i\right) / \sum_{i=1}^{n} P_i \qquad (1)$$

where: d_{avg} is average distance from the cities, d_i is distance from city i to the airport, P_i is population in city i, n is number of cities.

Since the distance from the noise source limits impact of noise, the following assumption was made: the impact of noise on residents near the airport is only relevant in the radius of 20 km from the airport. However, since this assumption can significantly affect the result of the research, in the first case, all the cities that airports serve are taken into account, while the second case takes into account only cities that are located within a radius of 20 km from the airport. This principal was applied only with airports that serve several cities. For airports that serve only one city, the distance from the city center was taken, regardless of the fact that city is located in the radius of 20 km from the airport. Collecting data about city population was carried out from two sources. For most cities, the data about population was taken from EUROSTAT, and for some of them that were not available, the data was taken from Wikipedia.

4. DISCUSSION OF RESULTS

In order to examine the five above-mentioned hypotheses, the correlation between the proposed factors and the number of NAMs was determined, based on the collected data.

For the same set of data, for the average distance from airport to the city centre and city population, two cases were considered, depending on whether they take into account all or only cities that are located within a radius of 20 km from the airport. The results of statistical analysis for year 2010 are shown in **Table *1***. Statistical indicators that were analyzed are the correlation and determination coefficients, as well as statistical significance.

Table 1 *Results of statistical analysis for year 2010*

			Correlation (Dependent variable - Number of NAMs)		
			Pearson correlation coefficient (r)	Coefficient of determination (r^2)	Sig. (1-tailed)
Independent variable	Number of aircraft operations (in thousands)		0.503	0.253	0.000
	Number of airport runways		0.352	0.124	0.000
	Average distance	All cities	0.173	0.030	0.003
		Within 20 km	0.144	0.021	0.012
	Population (in thousands)	All cities	0.261	0.068	0.000
		Within 20 km	0.238	0.057	0.000
	GDP per capita (in thousands)		0.183	0.034	0.002

Functional relationship between the dependent variable number of NAMs and two independent variables (the number of aircraft operations and the average distance from airport to the city) is given in **Fig. *3***. From the **Fig. *3***, large dispersion can be seen, which is also characteristic for the other independent variables. For the majority of independent variables, positive dependence is found, which is in accordance with all of the hypotheses, except in the case of distance. From the **Fig. *3***, it can be seen that with the increase of the average distance, the number of implemented NAMs also increases, which contradicts the hypothesis regarding distance.

The highest coefficient of determination, but still insignificant, was obtained for the number of aircraft operations (R^2=0.253), while for the number of runways it was 0.124, which can be seen from **Table *1***. For the other independent variable, the coefficient of determination was less than 0.07.

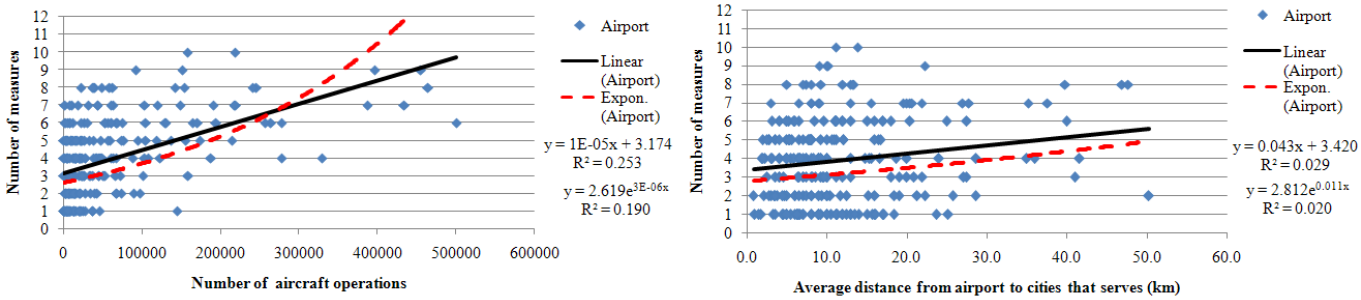

Fig. 3 *Correlation between number of NAMs introduced and specific characteristics related to airports (year 2010)*

4.1. Multiple linear regression

In order to examine correlation between all five proposed factors and the number of introduced NAMs, backwards multiple linear regression was conducted. In the first step, five independent variables entered the model:

- number of aircraft operations (in thousands)
- number of airport runways,
- average distance: all cities (in km),
- city population (in thousands),
- GDP per capita (in thousands).

As a final result of multiple linear regression, only the number of aircraft operations and GDP per capita showed statistical significance. The correlation coefficient with the dependent variable (the number of NAMs) was 0.531, indicating a moderate functional relationship between these variables. The coefficient of determination was 0.282, which means that the number of aircraft operations and the GDP per capita explains 28% of variability of the dependent variable number of NAMs.

4.2. Linear regression based on strategic noise maps data

In 2002, the European Parliament and Council adopted Directive 2002/49/EC relating to the assessment and management of environmental noise, which among other things, requires the development of strategic noise maps and action plans for airports with over 50,000 takeoffs and landings per year, in order to reduce the environmental noise. Strategic noise mapping is defined as the presentation of data on an existing or predicted noise situation in terms of a noise indicator, indicating breaches of any relevant limit value in force, the number of people affected in a certain area, or the number of dwellings exposed to certain values of a noise indicator in a certain area [8].

In this paper, an additional analysis was conducted based on data from available strategic noise maps for 73 European airports. Unlike average distance and city population, which were used in previous analyzes, the number of people exposed to different bands of noise indicators L_{den} and L_{night} was used in this analysis. For noise indicators L_{den}, the number of people outside agglomerations and including agglomerations is shown in the noise bands by 5 dB steps, starting from 55dB. For noise indicators L_{night}, only the number of people outside agglomerations is shown, in the noise bands by 5 dB steps, starting from 50dB.

As in previous analyzes, dependent variable was number of NAMs, and 16 independent variables were analyzed. The correlation between the independent variables and the number of NAMs in year 2009 was determined through linear regression analysis (**Table *2***). Pearson correlation coefficient shown in **Table *2*** take values between -0.11 and 0.28, and indicates that the relationship between the dependent and independent variables is very weak, almost non-existent. For three independent variables, negative correlation was shown. That is because for most airports, the number of people exposed to noise bands over 75 dB for L_{den} and over 70 dB for L_{night} equal to zero (these values correspond to the noise close to the runway) and a few airports that have this value above zero, applied the number of NAMs under the average.

Most of the independent variables did not show statistical significance. The number of people exposed to noise bands over 55 dB, over 65 dB and total number of people for L_{den} including agglomerations, are three independent variables that showed statistical significance. However, correlation coefficient for these three variables is around 0.28, indicating that the correlation between variables is not significant, while the coefficient of determination is little less than 8%.

Table 2 *Results of statistical analysis (regarding strategic noise maps)*

			Correlation Dependent variable (Number of NAMs)		
			Pearson correlation coefficient (r)	Coefficient of determination (r^2)	Sig. (1-tailed)
Independent variable (Population)	Outside agglomerations	55-59 L_{den}	0.152	0.023	0.102
		60-64 L_{den}	0.074	0.005	0.269
		65-69 L_{den}	0.057	0.003	0.317
		70-74 L_{den}	0.055	0.003	0.322
		> 75 L_{den}	-0.091	0.008	0.223
		total L_{den}	0.122	0.015	0.152
		50-54 L_{night}	0.132	0.018	0.135
		55-59 L_{night}	0.128	0.016	0.142
		60-64 L_{night}	0.012	0.000	0.461
		65-69 L_{night}	-0.065	0.004	0.293
		> 70 L_{night}	-0.111	0.012	0.177
		total L_{night}	0.130	0.017	0.137
	Including agglomerations	> 55 L_{den}	0.281	0.079	0.009
		> 65 L_{den}	0.280	0.078	0.009
		> 75 L_{den}	0.141	0.020	0.122
		total L_{den}	0.278	0.077	0.009

4.3. Cluster analysis

For the purpose of grouping and detailed analysis, the observed airports are divided into smaller sets that have similar characteristics.

4.3.1. Number of aircraft operations clusters

Distribution of the number of European airports that are grouped according to the number of aircraft operations in the classes of 50,000 operations is shown on **Fig. *4***.

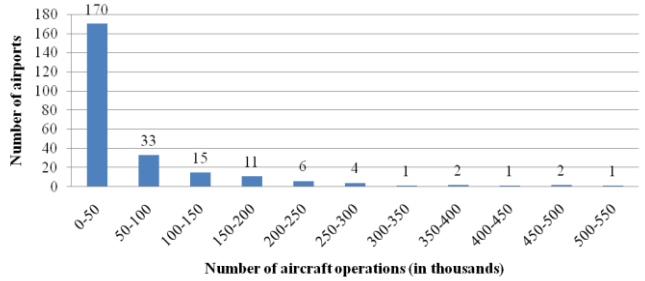

Fig. 4 *Clustering European airports according to the number of aircraft operations (year 2010)*

From the **Fig. *4*** it can be seen that the largest number of airports have up to 50,000 operations, while only seven of the 246 airports have over 300,000 aircraft operations.

The observed airports are divided into three clusters. The first cluster makes 170 airports with up to 50,000 aircraft operations. The second cluster includes 33 airports that have between 50 and 100 thousand operations, while 43 airports with over 100 thousand operations makes the third cluster.

For each cluster, an analysis was conducted in order to determine the correlation between the number of NAMs and the number of aircraft operations for airports in the observed cluster. Scatter chart for the variables number of NAMs and the number of aircraft operations for airports belonging to the first cluster (up to 50,000 aircraft operations) is shown on **Fig. *5***.

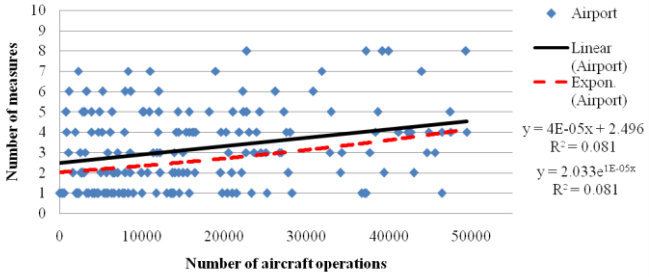

Fig. 5 *Number of implemented NAMs as a function of number of aircraft operations (up to 50000, year 2010)*

From **Fig. *5*** it can be seen that positive dependence is obtained. The coefficient of determination is 0.081, indicating that the correlation between variables is not significant. Similar results were obtained for airports in the second and third cluster.

4.3.2. GDP per capita clusters

The observed sample is divided into clusters based on GDP per capita. Distribution of airports that are grouped according to GDP per capita in the classes of 10 thousand of dollars is shown on **Fig. *6***. It can be seen that the largest number of airports is located in countries that have a GDP per capita between 30 and 50 thousand of dollars.

The observed sample is divided into three clusters. The first cluster makes 62 airports that are located in countries with a GDP per capita up to 30 thousand of dollars. The second cluster includes 161 airport with a GDP per capita between 30 and 50 thousand of dollars, while 23 airports with a GDP per capita over 50 thousand of dollars makes the third cluster.

For each cluster, an analysis was conducted in order to determine the correlation between the number of NAMs and the GDP per capita for airports in the observed cluster. As for clustering according to the number of aircraft operations, similar results were obtained for all GDP per capita clusters. For this reason, only analysis for airports that belong to second cluster will be described here.

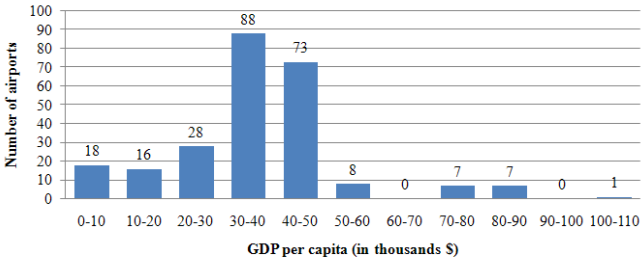

Fig. 6 *Clustering European airports according to GDP per capita (year 2010)*

Scatter chart for the variables number of NAMs and the GDP per capita for airports belonging to the second cluster (between 30 and 50 thousand of dollars) is shown on **Fig. *7***.

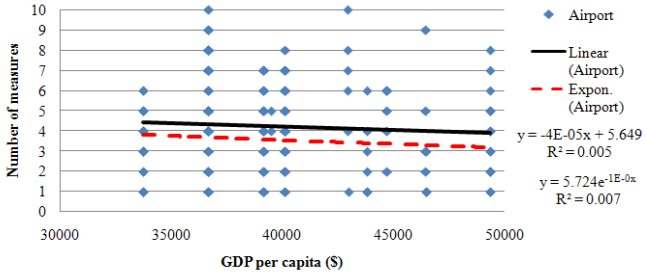

Fig. 7 *Number of implemented NAMs as a function of GDP per capita (30000-50000$, year 2010)*

From **Fig. *7*** it can be seen that negative dependence is obtained, which contradicts the hypothesis that the higher GDP per capita will affect the introduction of a higher number of NAMs. The coefficient of determination is less than 1%, indicating that the correlation between variables is not significant.

4.3.3. Clustering according to number of introduced NAMs

All airports within the sample can be grouped according to the number of applied NAMs in order to conduct detailed analysis and search for their common characteristics. Since the number of aircraft operations and GDP per capita are only two variables that showed any statistical significance in relation to the number of applied NAMs within the multiple linear regression analysis, further work will show the relationship of these two variables for airports with the same number of NAMs. Clustering according to number of introduced NAMs is shown in **Table *3***.

For each group of airports, minimum and maximum values of number of aircraft operations and the GDP per capita are given and the percentage of airports that have applied certain NAMs.

Measures that were mainly applied by airports in each group are marked blue. For example, of all airports that have applied only one measure in 2010, 72% of them have implemented a Noise Abatement Procedures (NAP). In case of airports that have applied eight NAMs, each of them have applied Airport Curfews and Noise Abatement Procedures, while 92% of them applied the Operating Quotas, Engine Run-Up Restrictions and ICAO Annex 16 Chapter 3/Chapter 2 Restrictions. Due to the large overlap of ranges, it cannot be argued with great accuracy how much NAMs the airport should introduced on the basis of the number of aircraft operations at the airport and the GDP per capita of the country in which the airport is located.

Table 3 *The distribution of the number of NAMs on airports in Europe in 2010*

No. of NAMs 2010	No. of airports	No. of operations (minimum)	No. of operations (maximum)	Min GDP	Max GDP	APU	Curfew	NAP	Noise Budget	Noise Charges	Noise Limits	Pref Rwys	Quota	Run-Ups	Stg3-Ch3 Rest
1	46	6	145043	1632	86156	0%	7%	72%	0%	4%	2%	7%	0%	9%	0%
2	34	1624	97678	2974	86156	3%	12%	82%	0%	35%	0%	26%	0%	41%	0%
3	30	1105	159109	5843	86156	40%	43%	70%	0%	30%	0%	37%	3%	77%	0%
4	41	856	329343	6335	56486	46%	56%	98%	0%	32%	20%	59%	7%	78%	5%
5	32	794	214990	7670	70370	59%	81%	88%	0%	56%	31%	66%	19%	78%	22%
6	28	1145	500325	7670	102009	71%	86%	96%	0%	71%	54%	68%	14%	89%	50%
7	17	2271	433836	29863	86156	71%	88%	100%	12%	82%	35%	82%	53%	100%	76%
8	12	22721	464275	21382	56486	83%	100%	100%	17%	67%	83%	75%	92%	92%	92%
9	4	92683	455320	18867	46468	100%	100%	100%	25%	100%	100%	100%	75%	100%	100%
10	2	158162	218776	36703	42960	100%	100%	100%	100%	100%	100%	100%	100%	100%	100%

From the **Table *3*** it can be seen that there are airports that have introduced only one NAMs, but have twice the GDP per capita of the airports that have introduced ten NAMs. Similarly, there are airports that have introduced three NAMs, but have more than 250,000 aircraft operations, while certain airports with less than 25,000 aircraft operations have introduce eight NAMs.

These differences indicate the existence of additional factors that, together with the initial two have influence on the introduction of NAMs. This is confirmed in the results of multiple linear regression analysis, which indicated that the number of aircraft operations and the GDP per capita explains only 25% of variability of the dependent variable number of NAMs.

4.3.4. Clustering by country

In this analysis, observed airports are grouped according to the country where they are located. In order to analyze influence of GDP per capita on number of NAMs per country, the number of implemented measures for each airport is not considered separately, but as the average value on country level.

Impact of GDP per capita on the average number of applied NAMs by European countries in 2010 is shown on **Fig. *8***.

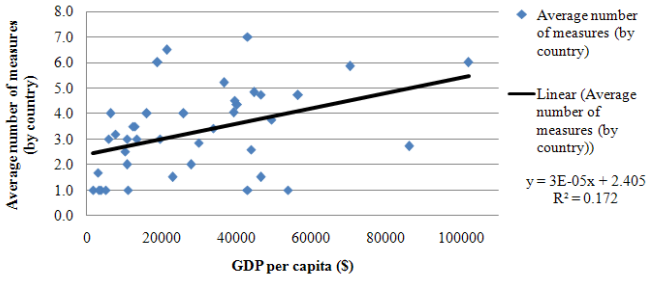

Fig. 8 *Average number of applied measures by country as a function of GDP per capita (year 2010)*

Fig. *8* shows linear dependence between variables. Coefficient of determination was 17%, indicating that the correlation between variables is not significant. Nevertheless, it can be seen that the impact of GDP per capita is much higher when the number of implemented measures is considered as the average value at the state level, in comparison with 3% coefficient of determination when the number of NAMs is considered separately for each airport.

The influences of the number of aircraft operations on the number of implemented measures for airports grouped by countries were also tested in this research. Due to the sample size, only countries with more than ten airports in the sample were analyzed and they are United Kingdom, Germany, France, Italy, Spain and Sweden. The results of analyzes for year 2010 are given in ***Table 4***.

Table 4 *Correlation between number of aircraft operations and number of applied NAMs by country*

Country	No. of measures	No. of airports	Pearson correlation coefficient (r)	Coefficient of determination (r^2)
UK	193	37	0.512	0.262
Germany	126	29	0.607	0.368
France	101	25	0.517	0.267
Italy	82	24	0.453	0.205
Spain	57	20	0.848	0.719
Sweden	64	17	0.559	0.313

From **Table *4*** it can be seen that functional relationship between number of aircraft operations and number of NAMs is the largest for airports in Germany and Spain. Correlation between number of aircraft operations and the number of applied NAMs for airports in Germany for year 2010 is shown on **Fig. *9***. Positive dependence is obtained. The coefficient of determination (R^2_1=0.368) obtained from this cluster analysis is greater than the coefficient of determination obtained on the basis of linear dependence tested on the entire sample (R^2_2=0.253), which was previously presented in the paper.

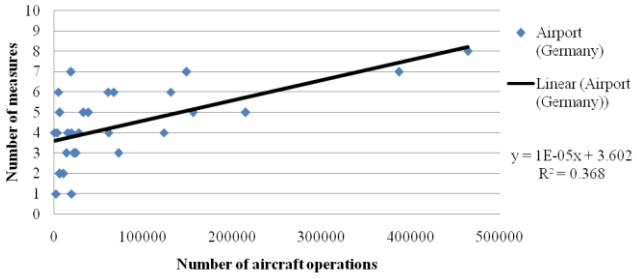

Fig. 9 *Correlation between number of aircraft operations and the number of applied NAMs for airports in Germany*

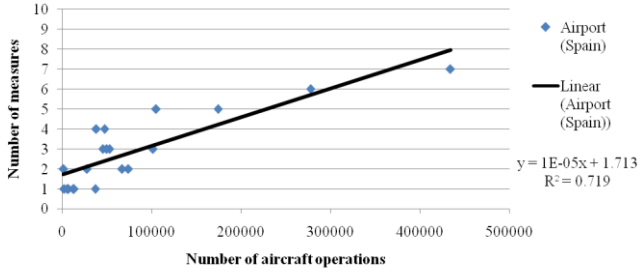

Fig. 10 *Correlation between number of aircraft operations and the number of applied NAMs for airports in Spain*

Much greater difference was observed for airports in Spain (**Fig. *10***). The coefficient of determination was around 72%, indicating a very good correlation between the number of aircraft operations and the number of NAMs implemented at airports in Spain.

4.3.5. Clustering regarding noise monitoring

Another analysis was conducted in this research. The aim was to determine the effect of Directive 2002/49/EC on the implementation of certain NAMs, since this directive also requires that all airports with over 50,000 aircraft operations per year have to introduce a noise monitoring system.

The analysis was based on assumption that most airports that have introduced a noise monitoring system (due to legal obligations or voluntary) will use this system to apply specific NAMs, such as Noise Level Limits or Noise Charges. Both measures include establishment of allowed noise values in certain points of the noise monitoring system (usually per operation) whose exceeding leads to additional charges (or fines) applied to airlines.

The second assumption was that the percentage of non-EU airports with over 50,000 aircraft operations, which applied the two aforementioned NAMs, would be much lower compared to airports located in the European Union, due to the lack of legal requirements for the introduction of noise monitoring system. This could to some extent, prove the impact of regulation on the introduction of NAMs.

The number and percentage of European airports with over 50,000 aircraft operations, which applied specific NAMs in 2010 is shown in **Table *5***. Airports were grouped according to whether they were in the European Union or not.

From **Table *5*** it can be seen that in 2010, 73% of EU airports has implemented Noise Charges, while 45% of them have applied Noise Level Limits. From all of the non-EU airports with more than 50,000 aircraft operations, 30% of them have applied two aforementioned NAMs.

From the results shown, in the case of Noise Charges it can be seen a clear difference between the airports which were located in the European Union and other European airports. The reason for that may be different regulation, but it is necessary to analyze the influence of other factors.

Table 5 *Clustering regarding noise monitoring (based on data from [5])*

Measures in Year 2010	EU (66 airports with more than 50000 aircraft operations)		Non EU (10 airports with more than 50000 aircraft operations)	
APU Operating Restrictions	37	56%	5	50%
Airport Curfews	48	73%	4	40%
Engine Run-Up Restrictions	61	92%	8	80%
Noise Abatement Procedures	63	95%	10	100%
Noise Budget Restrictions	5	8%	0	0%
Noise Level Limits	30	45%	3	30%
Noise Charges	48	73%	3	30%
Operating Quotas	17	26%	1	10%
Preferential Runways	42	64%	6	60%
ICAO Annex 16 Chapter 3/Chapter 2 Restrictions	30	45%	2	20%

5. CONCLUSION

Analysis of noise abatement measures, presented in this paper has shown functional relationship between the observed factors and the number of NAMs introduced at European airports. The research was conducted based on data from Boeing's database for years 2009 and 2010 for 248 European airports. For each airport, data on number of runways and aircraft operations, distance from the city and the population of the city that it serves, GDP per capita of the state in which airport is and the number of introduced NAMs were collected.

Examination of initial hypotheses was performed by testing the correlation between the five proposed factors and the number of introduced NAMs.

Linear regression analysis has shown that all the independent variables are statistically significant, but their association with the dependent variable is weak or almost nonexistent. Only the number of aircraft operations showed a moderate correlation with the number of NAMs, with coefficient of determination of 25%.

Using the backwards multiple linear regression, only the number of aircraft operations and the GDP per capita showed statistical significance, which explains about 28% of the variability of the dependent variable number of NAMs. Based on the obtained results it can be concluded that initial hypotheses were not confirmed.

Based on the information from strategic noise maps for 73 European airports, the correlation between the number of people exposed to different bands of noise indicators L_{den} and L_{night} with a number of NAMs introduced at the airport were analyzed. Also in this case, significant functional relationship between the tested variables was not found.

For the purpose of detailed analysis of introduced NAMs, the observed airports are grouped into specific clusters.

In the case of clustering according to number of aircraft operations, GDP per capita and number of NAMs, correlation coefficients obtained indicated a weaker relationship between variables in the clusters compared to the relationship within the whole sample.

Clustering by country has shown that correlation between average number of applied measures and GDP per capita for each country is not significant, but is much higher in comparison when the number of NAMs is considered separately for each airport. Correlation between number of aircraft operations and number of NAMs for airports in the same country has shown that coefficient of determinations are much higher than those obtained for the whole sample, which shows that at the state level there is a higher correlation between the observed variables. In case of airports in Spain, obtained results indicate that the number of aircraft operations explains 72% of the variability of the dependent variable number of NAMs.

Based on available data, additional analyzes was carried out in order to determine the impact of regulation on the implementation of certain NAMs. The results showed that in 2010, 73% of the airport in the European Union, which has over 50,000 aircraft operations applied Noise Charges on the basis of a noise monitoring system, compared to 30% of the non-EU airport. The reason for this may be the Directive 2002/49/EC, but it is necessary to analyze the influence of other factors.

In addition to analyzes described above, there are several ways to improve the conducted research. As each measure requires the involvement of some resources, analysis of the impact of the necessary resources for introduction of NAMs on the number of introduced NAMs may be the subject of future research. Comprehensive analysis of legislation and its impact on the introduction of NAMs is also planned.

Analysis of the sequence of introduction of NAMs based on Boeing's database for the period 1999-2010 may be useful for better understanding of this subject and may answer the question does airports follow a certain sequence of introduction of NAMs.

Based on this research, it was concluded that it is better to pay particular attention to each measure separately, because of its specificity. This means that future studies should focus on answering the question why airports are introducing certain measure at a certain point rather than to observe measures together.

REFERENCES

[1] ICAO. (2001). Resolutions adopted at the 33rd session of the Assembly. Montreal, Canada: International Civil Aviation Organization.

[2] ICAO. (2008). Guidance on the balanced approach to aircraft noise management, Second edition. Montreal, Canada: International Civil Aviation Organization.

[3] Netjasov, F. (2012). Contemporary measures for noise reduction in airport surroundings. Applied Acoustics , 73 (10), 1076-1085.

[4] Celikel, A., Hustache, J., de Lepinay, I., Martin, K., & Melrose, A. (2005). Environmental tradeoffs assessment around airports. 6th FAA/EUROCONTROL Air Traffic Management R&D Seminar . Baltimore, USA.

[5] Boeing. (2014). Airports with Noise and Emissions Restrictions. Retrieved February 11, 2014, from Boeing: http://www.boeing.com/boeing/commercial/noise/list.page

[6] Mirković, B., Tošić, V., & Babić, O. (2010). Vazduhoplovna pristaništa - praktikum (II dopunjeno izdanje izd.). Beograd: Univerzitet u Beogradu, Saobraćajni fakultet.

[7] EUROCONTROL. (2014, March 1). The STATFOR Interactive Dashboard. Retrieved March 1, 2014, from http://www.eurocontrol.int/statfor

[8] EC. (2002). Directive 2002/49/EC of The European Parliament and of The Council of 25 June 2002 relating to the assessment and management of environmental noise. 12-25. Luxembourg, Luxembourg: European Parliament.

University of Nis
Faculty of Occupational Safety
„Politechnica“ University of Timisoara
Faculty of Mechanical Engineering
24th International Conference
NOISE AND VIBRATION
Niš, 29 - 31. 10. 2014.

RAILWAY NOISE RESOURCES, KEY ENVIRONMENTAL PROBLEM IN THE EUROPEAN UNION

Predrag Petrović[1], Živojin Petrović[2], Stanislav Glumac[1]

[1]Institute „Kirilo Savić“, Vojvode Stepe 51, Belgrade, Serbia
[2]Faculty of Mechanical Engineering – Associate, Kraljice Marije 16, Belgrade, Serbia

Abstract: *Over the wheels of railway assets is realized tractive force, and movement. Trends in railway and other rail vehicles (trams, the buses, trolley, mining wagons, special rail vehicles, cranes, etc.) characterized by movement not deformable point, the not deformable surface, where deformation and point and substrate are negligible.*

In exercise of movement braking, interacting contact point and rail activates the active and passive forces, causing the generation of noise, which extends partially through the structure itself and partly dampens and partly transferred to the atmospheric environment and the negative impact on passengers, operators and, above all, the population of the population.

That made noise adversely affects the health and mood of the people who live and work nearby. The level of noise generated movement of railway funds can not be ignored, no matter what the noise from air and road traffic increased.
This problem, the European Union has joined with utmost responsibility in the areas they pass the railway, but the same applies to road alignment, many solutions attempt to reduce the noise level reasonable and allowable framework. In this sense, they brought many of the Directive relating to noise reduction, then introduce specific construction standards for the construction of this vicinity, mounted acoustic panels mostly disadvantaged sections, incorporates noise and vibration absorbers beneath the rails and wheels, introducing new materials and new technical solutions in the brake system, which initiates lower noise levels, and many other solutions.

This paper gives a brief overview of some of these solutions are applied in the European Union, with the aim of reducing the overall noise level of railway assets.

Keywords: *Noise, Rail, Wheels, UIC, Protection, Environment, Isolation*

1. INTRODUCTION

Noise is defined as unwanted sound, which appears in the space through different aspects: murmur, throbbing, speech, work variety of machinery plant, means of transportation and the like, and interfering with people in their work or on rest.

Criteria adopted by the acoustic noise is one of the physical agents whose involuntary, active or passive, continuous, pulsed or some other effect, contributes to auditory and extra-auditory, psychogenic, psycho-physiological, immune, socioacustic, cardiovascular and other consequences harmful to health humans.

When it comes to road traffic and reducing noise emission generated in this way, the EU is increasingly intensifying transport by rail, which creates a lower noise level.
Both passenger and freight trains reduce the number of cars and trucks on EU roads significantly.

Noise and the CO_2 emissions from the trains themselves are much lower comparing to road traffic.

At a first glance it is one form of benefits, but rail traffic has some disadvantages.

The mere fact that the movement of railway vehicle is realized by rolling on not deformable rail, the not deformable rail-substrate, resulting in creating a fairly high noise emissions in the absence of some acoustic protection, especially in urban areas, the negative impact on the quality of life of the population is very present.

The European Union is particularly in the last decade of this century devoted considerable attention to reducing noise in all areas (road, rail and air traffic, factories, plants, etc..), to reduce the exposure of the population of the surrounding noise. In order to realise this ambition, the EU's "Environmental Noise Directive" (END) came into force in 2002. The directive results in:

- Performs the prediction of sound maps in critical areas and positions in populated areas. For railway noise, these maps will be updated on a regular basis every 5 years (main infrastructures with more than 30.000 trains per year and agglomerations with more than 100.000 inhabitants).
- There are action plans with the introduction of specific noise measurement for the prevention and reduction of background noise and protect environmental quality. These measurements are performed at the source of the noise, set the acoustic barrier, improves maintenance is carried out transport planning, planning field, designing and making tunnels, etc.
- They perform many of the survey population, in order to determine the percentage of citizens who are mentally and physically threatened during the night, depending on the type of traffic, and the results are shown in Fig.1.

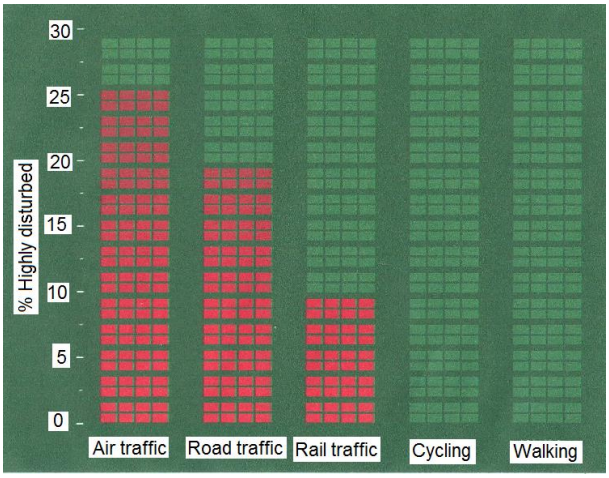

Fig. 1. *Percentage of citizens who are 'highly disturbed' when exposed to night-time noise emissions from transport*

2. MOVING PROCESS AND SOURCE OF NOISE OF RAILWAY VEHICLES

The process of movement of rail vehicles is quite complex, because the movement, there is a different phenomenon of resistance, such as: rolling resistance, resistance in bearings, friction, air, climb, bend, acceleration and etc.).

Determination of resistance depending on the design of railway vehicles is very complex, because the exact process of formation and their mutual dependence has not been fully defined.

In addition to the resistance that have been mentioned specifically expressed conditions that encourage movement of twists and rocking compositions. When moving along a straight track compositions done so-called "swinging", caused by changing the wheels contacts, alternating and without any explanations, sometimes on one, sometimes on the other rail.

These conditions cause the movement of alternating blows on the rail-surface, which initiate noise between wheel and rail with an increase in friction between wheel and rail wreath. The mere fact that the composition crosses the rail structure, with different gaps during different seasons (due to the appearance of joints) and other irregularities, further initiate swinging about a horizontal transverse axis, which leads to the intensification of excitation noise. In the course of time, depending on the intensity of exploitation of rolling stock wheels and rails suffer some uneven wear and the movement comes to increased stochastic shock that initiate increased noise. When there is no such phenomenon, noise level can be lower by up to 10 dB, at the same speeds.

When moving rail vehicles under specific conditions, such as the movement on the slope or in the curves, there is a contact point wreath with rail, creating additional friction caused by lateral sliding and side impact. To eliminate this phenomenon, or reduced, appropriate design solutions using the adjustable cradle to swivel stand, which is due to the weight and centrifugal forces tending in the right direction, which significantly reduces the contact rail and cornice point. The compositions have the option of greasing the wheels and rails, which reduces creaking, and thus the mutual friction force. UIC in this context, has initiated extensive research in order to reduce this problem, but doubts still exist.

UIC is international Union of Railways, with headquarters in Paris, founded in 1922., with the goal of achieving collaboration of European Railways and promotion of rail transport. There are about 200 members (railways, rail operators, infrastructure managers, railway service providers, public transport companies, etc.) and extends to all five continents. [2],[11],[12]

2.1. Kinematics of movement not deformable wheel by not deformable surface

Excitation produced by a rolling wheel, causing the complex modal oscillation that by elastic deformation in the transverse and tangential direction is transmitted to the bogie. Created noise initiated rolling wheels is transmitted through the structure of the supporting elements, than in multiplying and transferred in part to the inside of the wagon, and the other emits into the environment.

Navigating point of rail vehicles is quite simple kinematics case, which is characterized by: the angular and translational speed, load supporting structure of the wheel, the friction between the wheel and brake shoe or pad between the disk and the composite insert the disc brake and rolling friction and sliding friction.

Movement not deformable point by not deformable background, in terms of kinematics and force interaction is the simplest, as compared to other cases and is characteristic of the rolling stock. It is believed that in this case there are some elastic deformation of the contact point with the rail, but they are so small they can be ignored. However, when it comes to the case of movement, it should be borne in mind that the contact area of the tracks is not ideal flat, but wearing a certain micro-layers of metal and other deposits (similar conclusion applies to the wheels), and crossing over such sites leads to increased shock, and therefore the initiation of noise. In Fig. 2, shown is the case of movement, that is, the effect of the force at the point of movement of not deformable wheel on not deformable surface. [9]

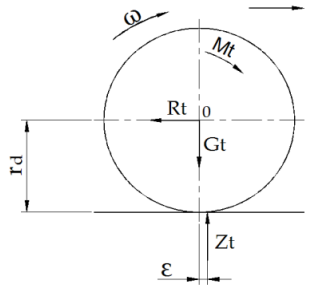

Fig. 2. *Rolling not deformable wheel by not deformable surface (rail)*

2.2. Process braking through initiating noise

When it comes to rail vehicles, in terms of noise generation is particularly important process of braking, no matter what happens, the brake (brake shoes, inserts the disc, or combined electromagnetic rail brakes). Passenger trains with disc brakes all over the tiles are made of cast iron are replaced with composite materials, which have favorable properties of friction and less noise as initiators.

Train cars of freight were typically older structures of travel, and many compositions still use blocks of cast iron brakes, compared to modern passenger trains.

Braking force is equal to the product of the force of pressure on one wheel and the coefficient of sliding friction between the brake pad and the wheel, at the same time leads to the creation of adhesion force, which is equal to the load per wheel and the coefficient of rolling friction between rail and wheel. Almost identical situation and braking traction rolling-stock, and braking of the drive wheels.

The main potential for noise reduction is the replacement of railway brake blocks on 800,000 European freight wagons, cast iron replacement with composite materials (so-called K or LL-blocks). This will cost $ 1 billion to 4 billion euros on European soil, depending on the technical solution for which an agreement is reached. This will bring noise reduction 8-10dB, especially in the night hours when moving the largest percentage of freight trains.

Transport sector, the EU considers that remains one of the key problems of the noise environment for all member states, regardless of the type of transport and for long periods of time, because of their inherent nature of the problem and nothing to do with the increase in transport services. As part of the Directive in terms of measurements of ambient noise, noise mapping is performed on the main roads, railways and airports, for each EU country. Part of the measurement result is shown in Fig. 3, the percentage of the population exposure to noise during the night, depending on the type of transport: air, road and rail. [1]

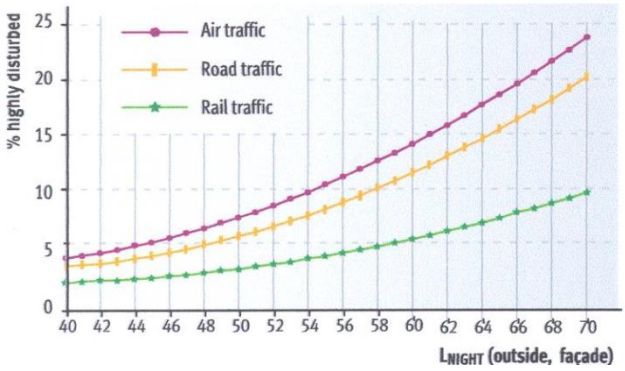

Fig. 3. *Percentage noise exposure for various types of transport: air, road and rail*

Action plans UIC-e show that the traffic that does not require significant financial investment in order to determine the efficiency and balance of infrastructure with the results obtained at the source, taking into account the implementation and characteristics (age) of European wagons and the introduction of local authorities and the population over action plans.

Action plans provide much more detailed analysis to be undertaken on the existing rail assets to generally reduce noise during operation. EU member states (including Norway and Switzerland), carried off the replacement brake pads made of cast iron, with a lining made of composite materials as well as some other changes. All these changes will result in additional material costs, and how they are perceived, is shown in Fig. 4. [2]

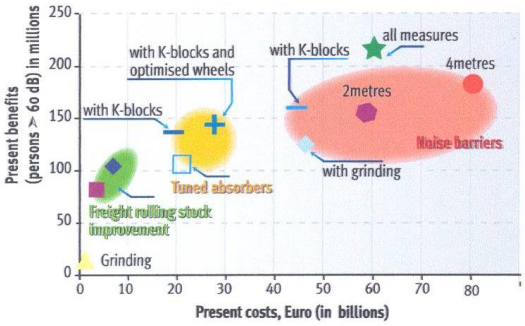

Fig. 4. *Analysis of costs and benefits in reducing noise of railway vehicles*

2.3. Some EU actions to reduce the noise of railway vehicles

The European Union has acceded to the implementation of many actions in order to reduce the noise of rolling stock, all of which are characteristic of the following:

- Examination committed in the EU, show that tuned absorbers, mounted on rails and wheels, can reduce rolling noise and participation to 7 dB, a total rolling noise between 2 and 3 dB, shock absorbing inserts in the wheels.
- The choice of locomotives is very important, but before a decision has to be seen: whether there is a sufficient number of such (quieter) locomotive, is it possible to replace, are adequate in terms of achieving speed and power for the planned sections and others.
- In residential areas are erected sound barriers, as they are higher, the effect is greater, up to 10 dB. However, barriers do not meet the approval of the citizens too, because they can perform the socialization of the population, in terms of investment are quite unprofitable. At the same time they are less effective when it comes to the attenuation of noise generated by the locomotive itself.
- Tunnels and moving through the tunnel are the traditional ways to reduce railway noise, however, they are not a practical option because their noise reduction performance is always different and depend on the terrain.
- Budget choice configuration, in terms of protection of the population is not always possible and depends on many, mostly in the sense of adverse circumstances.

However, the choice of the route is important to rail transport outside urban areas. In Fig. 5 are shown in a selection of the route outside urban areas.

Fig. 5. *Selection of railways outside settlements*

- Planning the use of land for construction of new railway infrastructure in addition to the settlement, and therefore the construction of new houses is very important and a real factor, but it does not open that possibility in every situation.
- Maintaining rails and wheels and remove layers that are created to wear noise reduction of 2-3 dB. Such a process is time consuming and very expensive and requires continuous maintenance which is in many cases impossible.
- Planning of transport, the speed limit is not an option effective action plan, because large reductions can be achieved by a radical reduction in the speed of trains. Such changes are not compatible with commercial work and competitiveness of the railways, the national network where the timetable must be respected, and the trains have to be at a certain location at a certain time in order to meet the requirements of customers of freight and passengers.
- Selection of locomotives in terms of powertrain, such as a diesel engine, although in some cases such a procedure could be counterproductive reducing the number of revolutions or speed, which can cause an increase in noise.
- Diversion Trains is practically impossible or very few feasible because to a large extent depends on the planned traffic and can not be an option effective action plan.

Research shows that the noise level does not depends on small changes in the number of trains, and the measurements are usually incompatible with the work and commercially competitive rail. For passenger trains are required to provide regular services between certain stations, and freight traffic is usually dependent on the commercial operation of the prescribed number of cars, from baseline to end point in a given period of time.

Studies have shown that exposure of the population to noise is much greater than air and road traffic, but the rail, and in general the quality of life of those who live near rail lines is better than those who live near the highway who are exposed to a constant level of noise. [1],[3],[6]

3. INTERNATIONAL STANDARDS FOR MEASUREMENT OF NOISE ROLLING STOCK

Fast growing trend of rail transport in Europe, caused by the growing discontent of the population is affected by noise, during the day and night. To avoid uncontrolled exposure to excessive levels of noise during transport, the European Commission introduced a Directive on ambient noise (2002/49) covering the main roads, railway lines and airports. This is mainly done by defining noise indicators, which continuously monitors the exposure during to a particular period and the required query state members created the conditions for the creation of maps and action plans. Such approach will have each member of the EU to implement within their own country.

International standard ISO 3381 defines the conditions for achieving favorable and comparable measurement results of the general noise level and spectrum of noise in the interior of rail transport equipment.

Based on the defined methodology, obtained results can be used for the following purposes:

1. Categorization of the general noise level in the interior of the rail vehicles.
2. Comparison of results of different types of rail vehicles, in identical conditions defined standards.
3. Determining the dominant noise sources in order to examine the possibility of reduction the overall noise level of rail vehicles.
4. Using standard test, checks the operating noise level which obliges the manufacturer of rail vehicles.
5. Tracking any trends change in the level of noise during operation, and check the conformity of the vehicle.

Within the European Union there are different working groups for railway vehicles, which have an advisory effect in terms of control, of which the most current UIC, CER, UIP. Working groups have the following tasks:

- Developing software for Europe, enabling the identification of control measures noise with an optimal cost of available data on trains and routes,
- Development of methods for identification of noise to the normative sources of noise,
- Providing information flow between working groups.

Serbian Railways for passenger and freight traffic, noise problem treated in terms of satisfying the applicable regulations UIC. This regulation defines: measuring the size, measuring equipment, atmospheric conditions, background conditions, the conditions on the road and the vehicle, the load of vehicles, equipment, speed, conditions, stationary measurements, measuring the position and form of the other procedures.

4. SOME FEATURES ATTENUATION OF THE NOISE SOURCE IN ROLLING STOCK

Due to the very complex process of formation and propagation of noise in rail vehicles, as well as other sound objects, it is important to identify the primary sources of noise, routes of transmission, and the determination of the dominant zone with its acoustic characteristics, in order to adequately and timely manner in the phase designing and developing acted in terms of implementing appropriate acoustic damping material.

For this purpose, in rail transport means used different insulating materials on the basis of good vibroacoustic and thermal and power characteristics, which are usually combined in the form of sandwich materials or independently, as well as the different types of mineral wool, sponge, insulating coatings based resin or bitumen, insulating foam, molded felt and others. Such material is generally applied when it comes to the coach with every side of wagons structure, where possible, and routes of transmission of noise. [7].

When it comes to the trams as a frequent passenger transport means in urban areas, it is very important substrate preparation and setting rails at predicted routes, in order to reduce the noise as much as possible.

Fig. 6a shows one type of performance base of the route of tram tracks, in terms of strength and waterproofing etc., and Fig. 6b and Fig. 6c, the appearance of the outer rubber inserts, provides an overview of installing rails in order to reduce and cut routes of transmission of vibration and noise,

especially on the tram and the substrate. This proper and complete preparation of the surface and the factual setting of rails in absorber of special rubber, which can be placed throughout the length of the rail or in places at certain lengths.

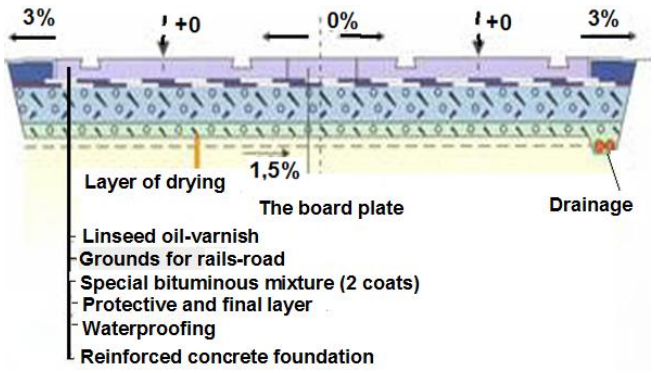

a)

c)

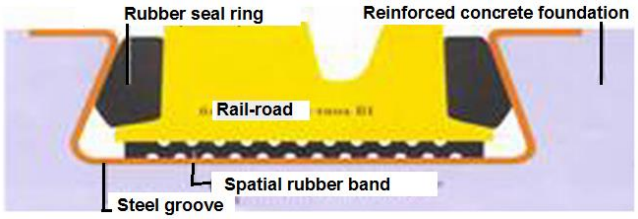

b)

Fig.6. *Installing rubber inserts to reduce noise and improve hydro-insulation*

Particular disadvantage when it comes to the noise of rail vehicles, the braking process, regardless of who creates it (brake shoes, brake insert disc brakes, electromagnetic rail brakes, motor brakes, etc.). Then occurs an intense reactions of braking force, sliding, rolling, etc. which, because of their adhesion characteristics pair of contact elements, causing a very intense noise, which is partly absorbed by the ground, the other through the structure is transferred to the interior of the wagon, and the third part is emitted into the environment. [8]

5. ACOUSTICAL BARRIERS TO NOISE PROTECTION

To solve the problem of the working environment or the effects of direct sound waves, outdoors or indoors, often used so-called sound screens that are placed between the noise source and the object which should reduce the level of direct sound waves. Sound-insulating characteristics result in lower levels of sound pressure behind the screen, which define its acoustic efficiency.

Calculation of reduction of noise by using acoustic screen, usually is on the basis of optical-diffraction image shows the sound field in the area of acoustic shadows behind the screen which takes into account the following assumptions: the sound source was punctuate, screen is infinitely stiff and infinitely wide. The last condition is almost impossible to meet, and therefore the entries most errors in calculation, so it is necessary to take into account the diffraction of sound waves on the sides of the screen of finite size.

In the calculation of the noise reduction using the display of certain dimensions, and its overall effectiveness "$\mathbf{\Delta L_E}$" (dB), it is necessary to scale to show the vertical and horizontal projection of the position: the sound source 1, screen 2, and the observed points on the object 3, as shown on Fig. 7. [5]

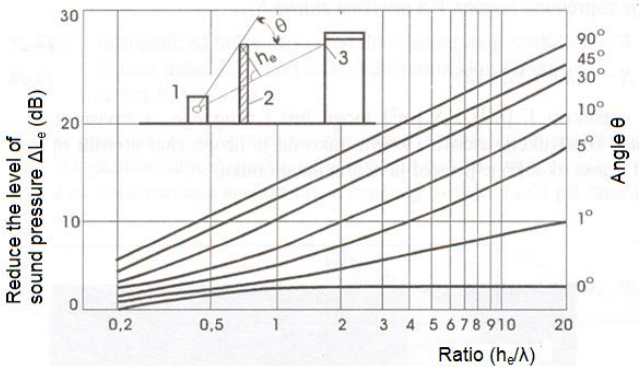

Fig. 7. *Efficiency of acoustic panels*

Then it determines the vertical component of efficiency "$\mathbf{\Delta le_1}$" and two horizontal components "$\mathbf{\Delta le_2}$", "$\mathbf{\Delta le_3}$.". Depending on the height of the screen "H", angle "θ" and the relationship "$\mathbf{he_1}$" and the corresponding wavelength "λ" which is determined from the equation, $\lambda = c \cdot T = c / f$, where: Δ (m) - wave length, T (s) – time period, f (Hz) – frequency:

$$c = \sqrt{\frac{p_s \cdot \gamma}{\rho}} \tag{1}$$

where:

c (m/s) - average speed of sound,

p_s (Pa) - static (atmospheric) pressure,

$\gamma = c_p / c_v$ - ratio of specific heat of gas at constant pressure c_p and at constant volume c_v, for air $\gamma = 1.41$.

Based on the value of the speed of sound in air (c=314 m/s), density ρ=1.20 kg/m^3, for each octave frequency "f_i" determined "$\mathbf{\Delta le_1}$", then the following equation:

$$L = 10 \log \sum_{f=1}^{n} 10^{L(f)/10} \tag{2}$$

where n is the number of spectral components at certain frequencies f (Hz).

Calculated overall sound pressure level "$\mathbf{\Delta le_1}$". For horizontal projection, depending on the screen width and position of points 1 and 3, two values of the efficiency of the screen are determined in the same way using the diagram in Fig. 6, the left side of the screen "$\mathbf{\Delta le_2}$" and the right "$\mathbf{\Delta le_3}$".

Based on certain overall level of noise components, vertical **"Δle_1"** and horizontal **"Δle_2 and Δle_3"**, calculates the overall efficiency of noise reduction behind acoustic screens in the given point of the object.

$$\Delta L_E = 10\log\left[10^{-0,1\Delta Le1} + 10^{-0,1(\Delta Le2+3)} + 10^{-0,1(\Delta Le3+3)}\right]^{-1} \quad (3)$$

Based on the present examples that are commonly encountered in practice, it is possible to calculate the sound pressure level in the outdoors or indoors, if known basic characteristics of sound sources, their distribution, frequency, when it comes to traffic. [5],[3].

6. APPLICATION METHODS OF SOUND INTENSITY IN THE ANALYSIS OF THE EFFICIENCY OF ACOUSTIC DISPLAY

The application of sound intensity in the measurement and analysis of the efficiency of acoustic screens in order to protect settlements along the highway, rail corridors and other roads where noise protection is necessary or desirable, the application can significantly due to its advantages contribute to the efficiency of noise insulation. Measurements of sound intensity have multiple applications, of which the most important are:

- Define the sound power,
- Define the loss of sound energy as it passes through the bulkhead,
- Measurement of the absorption of sound energy,
- Define the contribution of certain parts of the sources of total emissions, sound energy sources,
- Measurement of sound energy into stream of fluid etc.

In order to experimentally determine the level of sound energy from a source, as well as the direction and the direction of its propagation, it is measured: sound pressure p and particle velocity of the fluid $\vec{v}$.

Work that is done in a stationary fluid, the elementary time "dt", "through this area"; that sound energy flux through the "S", represents the scalar product of force which dominates the particle fluids $\vec{F}$ on the left and right sides of the imaginary surface and particle velocity, $\vec{v}$ which "flow" through the area "S" that is:

$$\frac{dW}{dt} = \vec{F}\cdot\vec{v} = \delta S\cdot\vec{v} = \delta S\cdot\vec{v} \quad (4)$$

If the observed flux is reduced to a unit area, then the vector $\vec{v}$, called sound intensity, the tag $\vec{I}$:

$$\vec{I} = p\cdot\vec{v} \quad (5)$$

Thus, the sound intensity is the energy flux through a unit area. It follows that, for the determination of sound power, enough to determine the amount of intensity on the surface bounding the volume in which the source is in a quiet environment, where there is a sound source that produces a plane wave vector sound intensity is defined at each point of the space multiplication current sound pressure and velocity.
Measurement of sound pressure level is not a problem in practice. On the other hand, the definition of the current speed of the particles is not so easy and can resort to the measurement of pressure changes in the gradient of the defined point, because:

$$\frac{\partial v}{\partial t} = -\frac{1}{\rho}\cdot\frac{\partial p}{\partial r}, \quad v = -\int\frac{1}{\rho}\cdot\frac{\partial p}{\partial r}dt \quad (6)$$

In order to define the partial derivative of pressure in the direction of "r", it is necessary to introduce some approximations: density environment is constant in a small distance "r", pressure change is linear in the direction of measurement.

$$v = \frac{1}{\rho}\int\frac{p_B - p_A}{\Delta r}dt, \quad (7)$$

and intensity as:

$$I = -\frac{p_A + p_B}{2\rho\Delta r}\int(p_B - p_A)dt. \quad (8)$$

7. ACOUSTICAL BARRIERS TO THE CORRIDOR RAILROADS

When it comes to noise caused by traffic, setting the acoustic screen besides the noise of vulnerable zones of some roads in some way satisfy both sides. The purpose of the acoustic screen is no longer merely noise protection, but an integral landscape and aesthetic assembly that fits very well in the environment and at the same time different solutions leads to a reduction of monotony, increasing pleasant feeling, with simultaneous primary function, environmental and labor protection.

It is generally used panels of aluminum, which has many advantages, of which the following are the most important: great stability and durability, are suitable for recycling friendly design, not demand any special maintenance, low life-cycle costs, easy installation, cost effectiveness for a wide range of use, a wide range of accessories etc. On Fig. 8, shows the performance of some aspects of acoustic panels in railway traffic.

Fig. 8. *The classic presentation of acoustic panels on roads*

Panels may also have some additional special requirements, such as emergency exit doors in case of unintended consequences, servicing, and a performance wall panel a no graphite staining, from which the graphite can eliminate several times with ordinary washing powder.

New digital printing technique can be directly on the panels reflect the desired image. In some embodiments, the panel can provide the conditions for the growth of vegetation-climbing plants.

Acoustical panels are available as reflecting the one-sided and two-sided highly absorbent, with components that can be combined without any limitations in vertical and horizontal installation.

Since the walls for noise have limited height, the construction dimensioning of the foundations and steel profiles, finishing panels reduce the distance from the sound source and thus increase the acoustic performance. The design opportunities are expanded by transparent panels made of acrylic glass, with regular installing between steel columns and using the grooves that have built-in gaskets that provide the best possible insulation. [11]

8. CONCLUSION

When designing roads and their implementations, depending on the terrain, populated places, roads and other parts of the natural and man-made resources, it is necessary to protect the environment from noise and vibration. It is necessary to consider preventive parameters and the factors that cause the noise of railway assets.

This approach can not be generalized, because the problem is very complex and depends on many parameters that need to be taken into account from the beginning of the design, to the implementation of the project. From the standpoint of the noise and environmental protection should take advantage of the experience of design and implementation of this project, in particular: developing spatial sound map, the prediction of noise during construction, application technology of acoustic panels and other acceptable solutions for the urban environment, as well as the entire process of analysis of the impact of noise on environment.

The European Union is faced with many problems in terms of noise reduction of railway vehicles and environmental protection through numerous action plans and considerable financial investment, makes great efforts to make efficiency plans can be bigger. Perceive many aspects, installation of acoustic barriers to the populated places, the choice of the field if you possible) the rail route, replacing the brake pads (for old cars and mainly freight) of cast iron, with a lining made of composite materials and many other actions.

REFERENCES

[1] "*The Environmental Noise Directive"*, FOCUS, UIC, UIC Noise Network / UIC action program noise reduction freight traffic, Paris, France, 2008

[2] "*Rail Transport and environmental"*, FACTS, FIGURES, UIC, CER, The voice of European Railway, Brussels, Belgium, 2009

[3] Petrovic P.: *"Noise generation diesel engine*", SITS, Monograph, Belgrade, MF, 2009

[4] *"Railways and the environment"*, Building on the Strengths environmental railways, UIC, CER, Brussels, Belgium, 2009

[5] Petrović P., R. Mirović, B Maravić: "*Ecological aspects of noise and vibration in the area of construction of new Belgrade bridge across the Sava river*," XXI conference with international participation "Noise and Vibration", Niš, 2010

[6] Petrović P., Jevtić M., Vukmirović S.: *"The impact of rail transport on global climate change and environmental protection"*, The Conference "Environmental Protection in the energy, mining and supporting industry", Divčibare, Faculty of Environment, University Union, 2010

[7] Ognjanović M.: "*Noise generation in mechanical systems'*, Monograph, Faculty of Mechanical Engineering, Belgrade, 1995.

[8] Petrović P., Šojić-Mirjana Radic: "*Wheels as Generators of Noise of means of transportation, with Particular Reference to Rail Vehicles"*, International Congress Motor Vehicles and Motors, Mechanical engineering faculty Kragujevac, 2006., section D, p.1-7.

[9] Petrović P.: *"Motor vehicle tire noise caused by the interaction with contact surface"*, Journal "Mobility and Vehicle Mechanics", Vol.24, No.2, June 1998., MF Kragujevac.

[10] Šubara N., Stojanović D., Ulniković V.: "*Ecology in rail transport"*, Belgrade, 2003.

[11] Uzunović R.: *"Noise and Vibration"*, Quality of management and the environment, LOLA Institute, Belgrade, 1997.

[12] *"Mega-Trucks versus-Rail Freight"* ,What the admission of Mega-Trucks would Really Mean for Europe, UIC, CER, 2008.

CENTAR ZA TEHNIČKU DIJAGNOSTIKU & LABORATORIJA ZA BUKU I VIBRACIJE

UNIVERZITET U NIŠU
FAKULTET ZAŠTITE NA RADU U NIŠU
Čarnojevića 10a, 18000 Niš
Tel.: 018 529-747; Fax: 018 529-748

Merenje i analiza nivoa buke

- Određivanje ekvivalentnog i merodavnog nivoa buke u zavisnosti od karaktera buke i vremena izloženosti;
- Frekvencijska analiza nivoa buke;
- Statistička analiza nivoa buke;

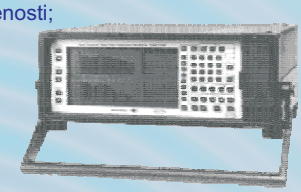

Merenje i analiza nivoa vibracija

- Određivanje merodavnog nivoa vibracija;
- Frekvencijska analiza nivoa vibracija;

Merenje i analiza akustičke aktivnosti mašina

- Određivanje nivoa zvučne snage u realnom ambijentu merenjem intenziteta zvuka;
- Određivanje nivoa zvučnog pritiska merenjem intenziteta zvuka;

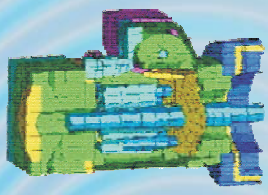

Preventivno održavanje mašinske opreme

- Praćenje stanja mašinske opreme na osnovu nivoa zvuka;
- Praćenje stanja mašinske opreme na osnovu nivoa vibracija;
- Balansiranje rotirajućih elemenata mašinskih sistema;

Projektovanje vibroakustičke zaštite

- Projektovanje sistema za izolaciju i apsorpciju zvuka;
- Projektovanje sistema za vibroizolaciju;
- Projektovanje akustike prostorija;

Merenje i analiza akustičkih karakteristika prostorije

- Vreme reverberacije;
- Izolaciona moć pregradnih zidova i konstrukcija:
- Izoalaciona moć od zvuka udara;
- Koeficijent apsorpcije materijala;

Sistematsko merenje komunalne buke

- Frekvencijska, statistička i procentualna analiza nivoa buke u komunalnoj sredini;
- Zoniranje urbanih prostora u odnosu na nivo buke;
- Izrada strateških karata buke;
- Ispitivanje uticaja akustičke aktivnosti instalirane opreme u javnim objektima na životnu sredinu;

Obrazovanje

- Instruktivni seminari;
- Studije za inovaciju znanja;
- Specijalističke studije;

University of Nis
Faculty of Occupational Safety
„Politechnica“ University of Timisoara
Faculty of Mechanical Engineering
24th International Conference
NOISE AND VIBRATION
Niš, 29 - 31. 10. 2014.

CONTRIBUTION TO RESEARCH OF THE AUTOMOTIVE ENGINE NOISE

Dragoljub Radonjić[1], *Rajko Radonjić*[2]

[1] University of Kragujevac, Faculty of Engineering, Serbia, e-mail:drago@kg.ac.rs
[2] University of Kragujevac, Faculty of Engineering, Serbia

Abstract – *Cosidered on the total level, both internal and external noise of the motor vehicle contained a significant proportion of the noise power train - IC engines. Bearing in mind always current demands of living and working environment, in this paper, attention is paid to the analysis of sources of engine noise, identifying the level and structure of the transmission. Exposed his own approach to research due to combustion noise and mechanical noise of the engine. Formed as appropriate models for simulation and parameter identification of noise. Shown are typical results of the research.*

1. INTRODUCTION

Allowable noise levels of motor vehicles and their components prescribe legislator [1], [2],[3] and requirements of customers and markets are often more stringent. Sources of IC engine noise, account for a significant share in the overall level of noise due to the choice, installation and adjustment of the IC engine given special attention. These problems can be, according to its importance, in the same category with the problems related to the reduction of exhaust gases emissions, reducing fuel consumption and the like. At the same requirements are to some extent contradictory, and to explore and implement a compromise solution.

2. METHODOLOGY

The total noise of IC engine is the result of summing up the partial noise levels originating from different sources and are transferred to a different channel power structures and environments. As shown in Fig. 1, depending on the place of originating and modes of transmission, the total noise power is decomposed into two components: a / directly produced, b / indirectly produced. The first component originates from the excitation of pulsating gas flow in the intake and exhaust pipes as well as the cooling system, especially the fan. Sources of other components of the noise excitation system during combustion in the engine and mechanical excitation of the impact forces, inertial forces, ancillary supplies and equipment.

Sound produced due to the pulsating flow, without further transformation of the energy is emitted primarily from the corresponding holes in the inlet and outlet of the fan motor and the environment. These components are developed efficient methods of identification, separation and damping. So, they are still relatively easy to manage. Are much more complex research methods and measures of damping other components - the noise that is generated in an indirect manner.

Excited by the noise due to combustion is reduced to the pressure oscillations in the combustion space of the closed valves. As for the burning time there is no direct coupling workspace with the atmosphere to the oscillations of pressure transmitted to the parts that border and forming the combustion chamber.

From there it passed through various channels to the outer surface (transmission of sound through solids), and with them emit and still transmit sound through the air space. From other indirect sources of noise, as has been said, mechanical excitation system, the sound is transmitted through a motor structure to the external surface and from them transmitted to the surrounding area and is defined as the mechanical noise.

Depending on the engine type, constructive - exploitation parameters and modes differ in the mutual relations of indirect noise components and their share in the total amount of engine noise, ie, noise from vehicles. From this point of interest are the methods for their individual identification, and measures for reducing their level.

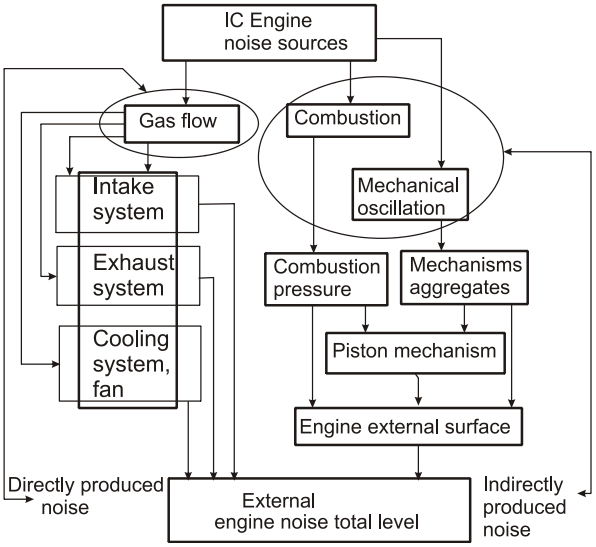

Fig. 1 *Sources and transmission channels of IC engine noise*

3. POSSIBILITY OF IC ENGINE NOISE COMPONENTS MEASURING

When using the traditional methods of measuring and processing of data, there was a view that the components of direct engine noise can be relatively easily measured and interpreted, with the previous effective preparation of the experiment and the isolation of individual noise sources [4]. On the other hand, the noise due to combustion in the engine, can not be directly measured due to the presence of noise, mechanical stake. In this regard, some approaches have been used to burn the portion of the noise is obtained as a difference between the total noise power of the fully loaded and noise of other engine driven motor, for example an electric motor. However, a large number of engines, especially diesel engines, this difference may be of the order of error of measurement, and thus the results obtained on the basis of comparisons only exit system is not reliable. Therefore, here raises a legitimate question: If combustion noise can not be measured directly can you be reliably determined on the basis of previously identified the structure of the engine and transmission of measured inputs, ie, the parameters of the dominant noise source? Some of the methods used so far give a partial answer to this question. The experiments in [5] were conducted in an acoustically isolated room. In parallel with the measurement of combustion pressure was measured sound pressure level at 1m removal from power. The share of mechanical engine noise was known in advance of the conducted experiments on a motorcycle driven by an electric motor. Of the total noise power is turned off, the share of mechanical noise and amplitude differences obtained, as a share of combustion noise are brought into connection with the amplitudes of pressure combustion, excitation (source), and thus the parameters of the corresponding transmission channels in the frequency domain. In doing so, according to the view in Fig. 2, it can analyze the impact of dominant parameters, the first two blocks 1, 2, the noise levels due to cobmustion, block 3.

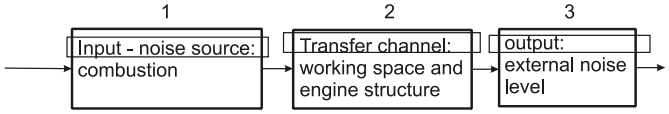

Fig. 2 *Generating phase noise of the IC engine.*

Certain observations can be made regarding the application of the above procedure are shown with "on-line" identification engine and transmission structure "of-line" eliminating mechanical noise. In this regard, we proposed a more efficient method for solving the above mentioned problems. A brief overview of the methods and some test results are given in the following sections.

4. DETERMINATION OF THE IC ENGINE NOISE

The algorithm of the proposed method for identifying the parameters of the transmission channel, and noise is shown in Fig. 3 a, b. According to the Fig. 3a, the registered signal sound pressure p_z (t), as the equivalent noise is produced indirectly in relation to the noise source due to combustion, the registered signal combustion pressure p_s (t), and a source of mechanical noise, immeasurable signal p_m (t). On the basis of these specifications has been formed is equivalent to the block diagram in Fig. 3b. Specifically, an invaluable source of noise $p_m(t)$, is reduced to the output of the system and added to the "remnant", $N(f) + P_m(f)$, [6],[7]. Based on the results of pressure recording in the area of combustion engines, $p_s(t)$ and sound pressure near the engine, $p_z(t)$, identifies the transmission characteristics of the channel output, Z, input S:

$$H_{zs}(f) = S_{zs}(f) / S_{ss}(f) \qquad (1)$$

$$\gamma_{zs}^2(f) = \left|S_{zs}(f)\right|^2 / S_{ss}(f) S_{zz}(f) \qquad (2)$$

$$P_m(f) + N(f) = P_z(f) - P_{zc}(f) \qquad (3)$$

where, $H_{zs}(f)$, transfer function of sound pressure as output – combustion pressure as input; $S_{zs}(f)$ cross-spectrum of output – input, $S_{ss}(f)$ auto-spectrum of input, $\gamma_{zs}^2(f)$ – coherence function, $P_{zc}(f)$ – output part coherent with input, $P_m(f) + N(f)$ – output "remnant".

The identified characteristics $H_{zs}(f)$, and the measured pressure combustion p_s (t) presented in the frequency domain as, $P_s(f)$, determine the coherent part of noise due to combustion, $P_{zc}(f)$. The part of mechanical noise contained in "the remnant" of the system output, through the spectrum of "the remnant". As a result of the identification of the transmission channel noise of pressure combustion get the parameters of amplitude-frequency, phase-frequency characteristics, as well as of coherence function, suitable for the interpretation of measurement data [6],[7],[8],[9].

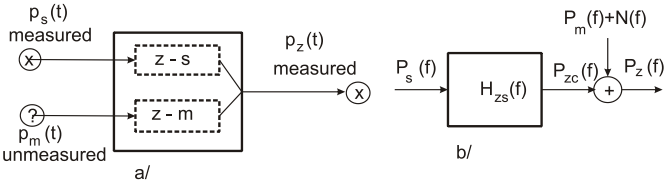

Fig. 3 *The procedure of inentifying the noise of combustion a) time domain, system with two input, single output: $p_s(t)$- combustion pressure, is measured, $p_m(t)$ – source of mechanical oscillation, unmeasured, $p_z(t)$ – total noise level, measured; b) frequency domain, above system reduced to system with single input- single output*

5. EXPERIMENTAL AND SIMULATION SYSTEMS AND RESULTS

The results presented here are based on the theoretical - experimental analysis. Formed the simulation models for the study of work processes in IC engines and analyze the impact of the dominant factors. The structure and parameters of the model were verified through experimental research. In the second phase of the experimental studies were identified transmission channels relevant to the generation of noise due to combustion and spending share of mechanical noise in the third stage used the results of simulation and identification obtained in the first two phases, the analytical determination of the components of the noise level of the engine for different combinations of parameters.

As the object of simulation and testing was used classic diesel engine for trucks, four-cylinder, water-cooled, maximum power 60 kW at 4000 rpm, maximum torque 150 Nm at 2400 rpm. The total mass of the vehicle in which the engine is installed is up to 3500 kg. For the experimental study using

piezoelectric quartz sensors to record the pressure in the workplace engine products company, "Kistler" and condenser measurement microphones to capture sound pressure surrounding the engine, the products of "Bruel and Kjaer." In addition, an experimental system includes a contactless encoder speed of the crankshaft the engine, magnetic and optical products company "Hottinger Baldwin Messtechnik". Records the number of revolutions of the encoder used as a control in testing the stationary regime of the engine as measuring, involved in data acquisition, processing and interpretation of the data, the testing of non-stationary mode of operation.

Fig. 4 a, b, shows the illustrative examples of segments of time history signal of pressure in the workplace cylinder engines, which include the combustion process, the stationary mode, engine speed of the crankshaft, 2000 min^{-1}. Under these test conditions (n = const) results in a simple conversion between the time base signal, t, and workflow engines relevant variables, α, the angle of rotation of the crankshaft the engine:

$$\alpha = 6 * n * t \qquad (4)$$

where n - the number of revolutions per minute of the crankshaft , t – time.

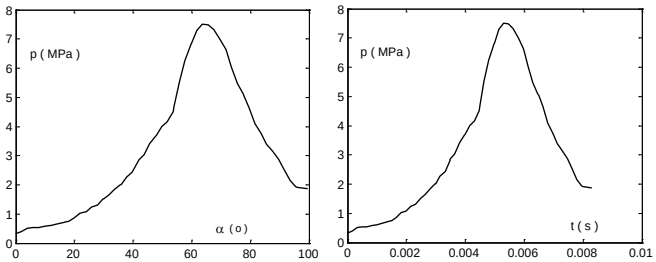

Fig. 4 *a) the time history of the combustion pressure in the engine cylinder, b) the relation of combustion pressure and turning angle of the engine crankshaft.*

With Fig. 4.a, is evident, that the observed signal combustion pressure as a source of combustion noise, short duration and complex pulse shape, which is reflected in its frequency content and hence its share in total generation of noise. The relationship of the signals, p, and α, in Fig. 5, closer to defining the parameters of the field sound sources and their changes depending on the operating mode. However, at the non-stationary engine speeds this relationship presented in the frequency domain is a efficient means to research of the connection between the internal, state variables and external, output variables of the engine in form of transfer function. In this paper, the relation in Fig. 4, were used for defining and determining the frequency content of the sound source, as shown in Fig. 5.

According to the example in Fig. 5 frequency content of the noise source of combustion is related not only to pressure levels, but also with the space in which these levels are realized. Components of the frequency characteristics point to a sharp decline of the frequency content at higher frequencies and some phase lead. Thus, the fixed parameters and engine speeds, the field of noise sources can be modeled by choosing characteristic noise generator and the characteristics of the filter.

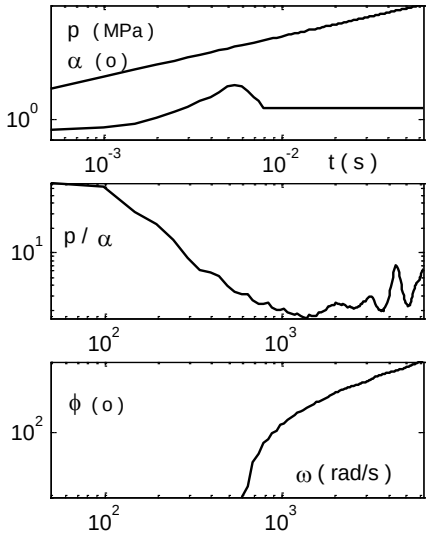

Fig. 5 *Frequency characteristics of the noise source of combustion in the engine cylinder presented in form of transfer function*.

In accordance with a mathematical model (1) and the algorithm, as shown in Fig. 2 and 3, the available experimental records, is identified the transfer function of the channel: a source of combustion noise - noise proportion of combustion, and the relevant segment is shown in Fig. 6 In the double logarithmic display these characteristics with satisfactory accuracy shows approximate true slope 75 dB/decade. The typical frequency characteristics of the noise source in Fig. 5 and the characteristics of the transmission channel, Fig. 6, enable an effective analysis of components of engine noise in accordance with the instructions specified at the beginning of this chapter.

For verified simulation model of engine working processes and idetified characteristics according to Fig. 6, the task is reduced to database forming of parameters of field sources noise, based on the simulation analysis of the dominant factors. In this regard, with formed database, can be illustrate different impacts on the generating combustion noise, for example the number of revolutions of the crankshaft, load torque and so on.

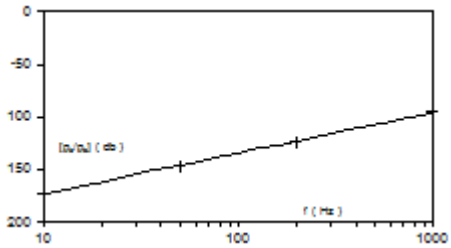

Fig. 6 *Amplitude-frequency characteristic in trasfer channel: external noise – combustion pressure*

CONCLUSIONS

The total noise power is a result of superposition of partial noise levels, which originate from different sources and are transferred to a different channel power structures and environments.

Noise due to combustion in the engine cylinders can not be measured directly because of the superimposition of the mechanical noise. Cross-spectral analysis allows reliable

identification of the transmission power structure and the separation of influential components of noise.

The relationship between flow-pressure combustion and turning angle of the crankshaft the engine provides an opportunity for a more realistic assessment of the frequency content of the noise source and the parameters of combustion.

Combining simulation methods for analyzing workflows combustion engines and methods of identifying its transmission structure creates a realistic basis for calculating the components of the noise, understanding of influential factors, with the displacement of the experimental research on the simulation, computational methods.

REFERENCES

[1] ISO R362

[2] Law on the grounds of road safety official list, 18th edition. Belgrade, 2000 certified

[3] E/ECE/324/TRANS/505, Regulation No. 51, „Uniform provision concerning the approval of motor vehicles having at least four wheels with regard to their noise emissions“, 1995

[4] T. Priede, "Engine design parameters and noise", ISVR Proc., Southampton, 1985

[5] H. Gross, "Einfluss Verbrennung der auf das Motorgerausch", VDI - Meetings, Cologne, 1976

[6] R. K. Otnes, L. Enochson, "Applied time series analysis", John Wiley &Sons, 1978

[7] J. Bendat, A. Piersol, "Engineering applications of correlation and spectral analysis", John Wiley & Sons, 1993

[8] L. Lamula et al, "Cylinder pressure generated noise of medium speed diesel engine", Acoustics Meeting, Rejkjavik, Iceland, 2008

[9] D. J. Challen, D. M. Crocker, "A review of recent progress in diesel engine noise reduction", SAE 820515

University of Nis
Faculty of Occupational Safety
„Politechnica“ University of Timisoara
Faculty of Mechanical Engineering
24th International Conference
NOISE AND VIBRATION
Niš, 29 - 31. 10. 2014.

NOISE EXPOSURE OF PASSENGERS IN URBAN PUBLIC TRANSPORT ROAD VEHICLES (BUSES)

Jovan Miočinović[1]

[1]TEHPRO DOO, Beograd-Železnik, Serbia, jovan.miocinovic@tehpro.rs

Abstract - *While regulations demand noise control measures in the workplace and in environment as well, people are exposed to noise on the way to work and while returning home after work. This paper presents the results of noise measurements made in situ on a sample of public transport road vehicles (buses). Evaluation is made according to the Regulations on noise exposure at workplace, Directive 2003/10/EC, environmental noise regulation and ISO 1996 (parts 1 and 2) for four descriptor quantities (equivalent continuous A-weighted sound pressure level as two of them, the maximum sound pressure level and C-weighted peak sound pressure level) and for the octave-band analysis results. Assessment is made by comparing to limit values given by Regulations on noise exposure at workplace, Directive 2003/10/EC and the environmental noise regulation regarding possible health hazard and annoyance. For one type of vehicle equivalent level of 92 dB(A) is measured and that presents a health risk when spending longer than 30 minutes in everyday ride. The average equivalent level of 80 dB(A) in buses results in need for reducing the limit values for the noise exposure at workplace by 1dB or 2 dB for the persons spending times in bus transport of durations of 50 to 160 minutes daily, depending on the limits considered.*

1. INTRODUCTION

Urban population usually uses public transportation regulary in their everyday life when going to their work and returning homes. Therefore people are exposed to a veriety of environmental conditions including noise. Experimental evaluation of the noise exposure during transportation in public transport road vehicles (buses) was made in order to establish probable noise exposure levels in everyday transport. Experimental measurements were made on the sample of buses on the same public line in Belgrade on the same route considered representative for Belgrade roads. Evaluation is made according to Regulations on noise exposure at workplace [1], [2], Directive 2003/10/EC [3], environmental noise regulation [4], ISO 1996-1 [5] and ISO 1996-2 [6].

2. INSTRUMENTATION, SAMPLE AND MEASUREMENT LOCATION AND CONDITIONS

2.1. Instrumentation

For measurements was used SVAN 958 four channels sound (Type 1 IEC 61672-1:2002) and vibration (Type 1 ISO 8041:2005) level meter and analyser (Fig. 1).

Fig. 1 *SVAN 958 four channels sound and vibration level meter and analyser*

2.2. Sample and measurement location and conditions

Measurements were made in situ in real conditions in vehicles, on the total sample of 11 buses of 3 types. In total 18 measurements were made. Number of vehicles in the sample and number of measurements taken and number of measurements taken per vehicle type and per individual vehicle are given in Tables 1 and 2.

Table 1 *Number of vehicles in the sample*

Vehicle type	Number of vehicles	Number of measurements taken
IKARBUS	2	2
MAN SG 313	6	12
MAZ 203	3	4

As for subsamples of vehicles in the sample, subsample of vehicles of type MAZ and subsample of vehicles of type MAN seem to be homogenous regarding age and condition. As for subsample of two vehicles of type IKARBUS it seem

to be inhomogeneous, vehicles are of different ages and conditions.

Table 2 *Number of measurements per vehicle type and per individual vehicle*

Vehicle type	vehicle serial no.	Number of measurements taken
IKARBUS	1276	1
IKARBUS	1296	1
MAN SG 313	1304	5
MAN SG 313	1321	1
MAN SG 313	1328	1
MAN SG 313	1336	2
MAN SG 313	1337	2
MAN SG 313	1342	1
MAZ 203	2151	1
MAZ 203	2156	1
MAZ 203	2267	2

Measurements were taken on the same position in vehicles - on the right passenger seat on the left side of vehicle opposite to middle door (Fig. 2).

Measurements were taken according to Regulation [1], ISO 9612 [7], ISO 1996-1 and ISO 1996-2, with a microphone position in the level of the ear of person seated according to ISO 9612.

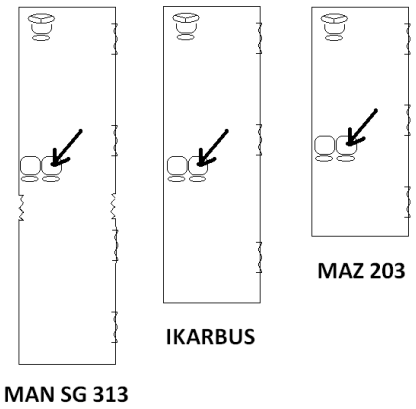

Fig. 2 *Measurement positions in vehicles for different types of vehicles in the sample. Positions are marked with an arrow pointing to the measurement position*

Measurements were made in controlled real environment. In addition to controlling parameters already mentioned - dividing the sample in subsamples by type and performing repeated measurements on the same vehicle, the third controlled parameter is the route. All the measurements were taken on is the same route on the public transportation line, line 511 in Belgrade. All measurements that are included are taken from bus station Palata pravde to the exit from the Obrenovački drum (road to Obrenovac) to Železnik. Measurement interval was devided in two segments, one from station Palata pravde to entering point to Obrenovački drum, and this one is considered representative to urban transportation conditions (regarding the road condition and stopping points on stations and traffic lights). The other segment is the one from entering Obrenovački drum to exiting to Železnik. This is the straight road with no damage and vehicle drive is uniform with no stopping. Measurements on this part of the route are used for comparing the results with the measurements on the first segment. Measurements were made in the same time of the day - between 7:30 and 9 in the morning on working days, from January to March this year in the same weather conditions (dry road). Measurement duration was 7 - 10 min. for the first segment, and 7 - 10 min. for the second segment, i.e. duration of vehicle drive on the segments of the road.

3. MEASUREMENT RESULTS

3.1. Noise descriptors

As the descriptors, four quantities are taken. First two are equivalent continuous A-weighted sound pressure level, L_{AeqT} according to ISO 1996-1, ISO 1996-2, ISO 1999 [8] or equivalent level, L_{eq} according to Regulation [1], taken on the second and on the first segment of the road, as described in 2.2, L_{AeqT1} and $L_{AeqT2.}$ The third one is maximum time-weighted and frequency-weighted sound pressure level, L_{AFmax} according to ISO 1996-1, ISO 1996-2 on the first segment of the road, hereafter referred to as the maximum sound pressure level. The fourth is C-weighted peak sound pressure level, $L_{p,Cpeak}$ as defined by ISO 9612 and in accordance with ISO 1996-1, ISO 1996-2. In the addition, the octave-band analysis is made. The octave-band analysis is one of the the main analysis factor according to ISO 1996-1 for the noise with the strong low-frequency content and also demanded by the Regulation [1] which gives the limit values.

The first two quantities are the descriptors of equivalent noise exposure and are good indicators for comparing with the limits regarding possible noise-induced hearing loss as well the fourth one and the third one is an indicator of noise annoyance. The frequency content is relevant as for the possible noise-induced hearing loss as well as for the noise annoyance.

For the measured L_{AeqT} values adjustments are made regarding impulsiveness, according to ISO 1996-1 and Regulation [1]. According to ISO 1996-1 and Regulation [1], sound exposure levels should be adjusted for type of the sound. Regulation [2] and Directive [3] require particular attention to the type of noise including any exposure to impulsive noise. Former version of ISO 9612 [9] in Annex C.3 gave a criterion for the prominence of the impulsiveness and impulse adjustment. According to this, impulse adjustment is the difference between A-weighted impulse sound pressure level, $L_{AIeq,T}$ and equivalent continuous A-weighted sound pressure level, $L_{Aeq,T}$:

$$K_I = L_{AIeq,T} - L_{Aeq,T} \quad (1)$$

And the criterion is that for the noise with $K_I \leq 2$ dB the impulse adjustment can be neglected. Regulation [1] in case of impulsive noise requires for comparing to limit values A-weighted impulse sound pressure level to be taken, i.e. Equation (1). Values are corrected according to [1] when the difference between A-weighted impulse sound pressure level and equivalent continuous A-weighted sound pressure level is greater then 3 dB.

3.2. Main results

As the main result is taken the average value of measured levels.

Average value is calculated as a mean value of the mean values of measurements on subsamples. The idea is that all the subsamples should be represented equally in the average value, that is, the probability for the passenger when catching the bus is equal for all the types of buses.

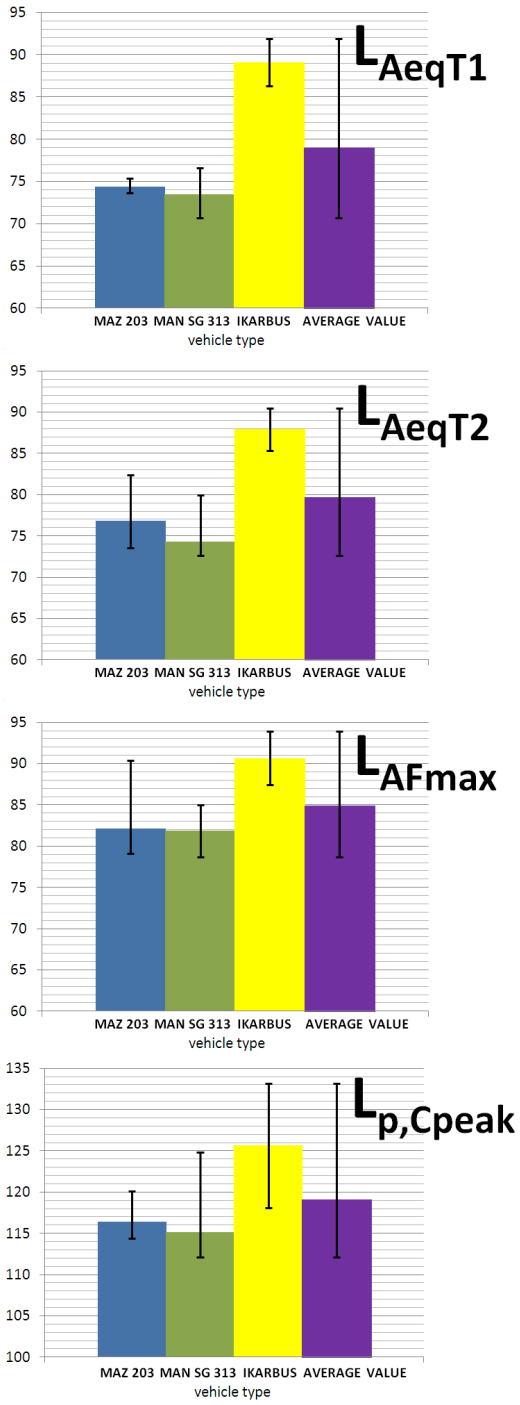

Fig. 3 *Equivalent continuous A-weighted sound pressure level on the flat road (L_{AeqT1}), in real riding conditions (L_{AeqT2}), maximum time-weighted and frequency-weighted sound pressure level (L_{AFmax}) and C-weighted peak sound pressure level ($L_{p,Cpeak}$), for different vehicle types and average value. On each column corresponding span from minimal to maximal values measured is presented.*

The results for subsamples and the average values with span from minimal to maximal values measured are presented in Fig. 3. Vehicle type (MAZ 203, MAN SG 313 and IKARBUS) and the average value are presented with a column in the chart each from left to right. Column represents the mean value with the corresponding span from actual minimal to maximal values.

The results for first and second segment of the road are practically the same. That is, the measurements made on the flat road are good indicators of the values obtained in the real environment. The difference on the sample of buses of type MAZ 203 (3 dB) is mainly due to impulsiveness adjustment made for the ride in city conditions unlike the steady noise measured on the flat road ride.

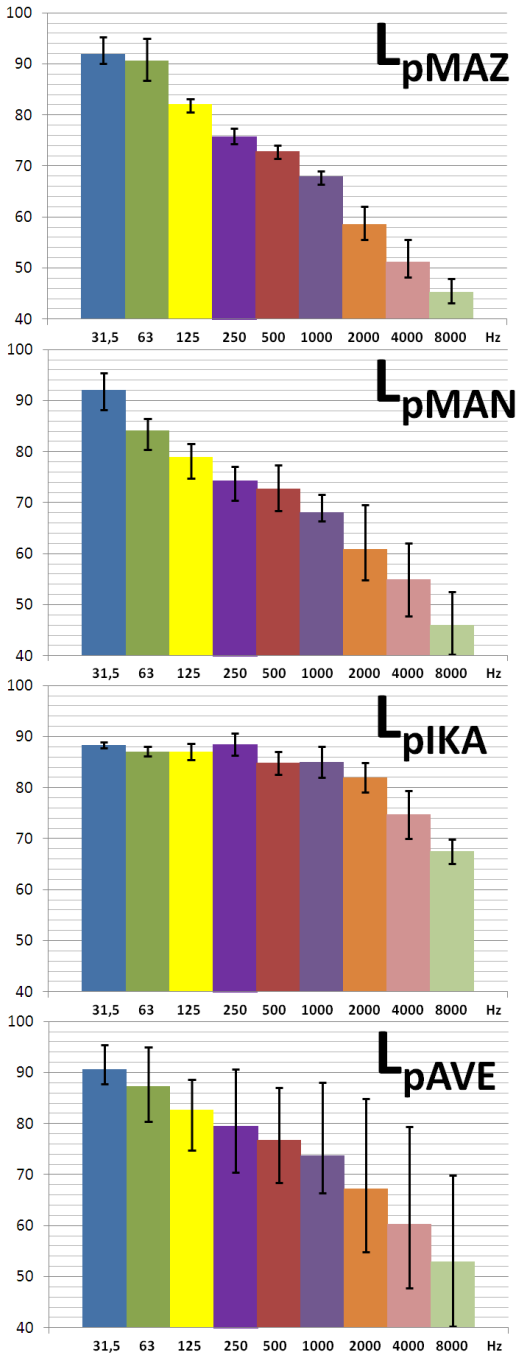

Fig. 4 *Octave-band analysis results for different vehicle types and average value. On each column corresponding span from minimal to maximal values measured is presented.*

Maximum sound pressure level as an indicator of noise annoyance is better represented by maximal value rather then mean value. Therefore for the results for maximum sound pressure level more relevant indicators are the maximal values measured then their mean values.

As well as for the maximum sound pressure level, the maximal values measured are more relevant indicators for the results for the C-weighted peak sound pressure level.

The octave-band analysis results are presented in Fig. 4. The results for subsamples and the average values with span from minimal to maximal values measured are presented. The analysis results for vehicle type (MAZ 203, MAN SG 313 and IKARBUS) and the average value are presented in a chart each from top to bottom. Each column on the chart represents the mean value of measured sound pressure in corresponding mid-band frequency with the span from minimal to maximal values measured.

From the figure it can be seen that for one type of vehicle (IKARBUS) frequency content is strongly in low and middle frequencies and for the other two types it is strongly in low frequencies.

4. EVALUATION

4.1 Comparing to limit values regarding possible health hazard

As for assessment of noise with respect to health, there are limit values regarding the occupational noise exposure. While the noise treated in this paper is not strictly the occupational noise, people are exposed to this noise in their everyday going to work and returning home after, and the effect of this noise adds to their regular daily noise exposure at work.

When comparing to the limits there are limit values given by Regulations [1], [2] and Directive 2003/10/EC. Regulations [1], [2] give limit value of 85 dB(A) as noise exposure level normalized to a nominal 8 h working day $L_{EX,8h}$ according to ISO 1999 and ISO 9162 for the prevention of hearing impairment. This is the upper exposure action value according to Directive 2003/10/EC. Regulation [2] gives action value of 80 dB(A) as $L_{EX,8h}$ and this is the lower exposure action value according to Directive 2003/10/EC.

Corresponding times for the passenger spent in vehicle needed to achieve the limit values, being exposed to L_{AeqT1} and L_{AeqT2} (see Fig. 3) are given in the Table 3. The results are given for all the measurements (average value in Fig. 3) and for each vehicle type separately. Considered are the mean values and maximum values of L_{AeqT1} or L_{AeqT2}, for which one is greater. The values for the comparing with limits are normalized to a nominal 8 h working day for the average values of noise exposure at workplace of 50 and 70 dB(A) respectively.

According to ISO 9162, the noise contribution from task *m* to the daily A-weighted noise exposure level, $L_{EX,8h,m}$, can be calculated from:

$$L_{EX,8h,m} = L_{p,A,eqT,m} + 10\lg\left(\frac{\overline{T}_m}{T_0}\right)dB \qquad (2)$$

Equation (3) allows the calculation of the A-weighted noise exposure level from the noise contribution of each of the tasks:

$$L_{EX,8h} = 10\lg\left(\sum_{m=1}^{M} 10^{0,1\times L_{EX,8h,m}}\right)dB \qquad (3)$$

Taken m=1 for noise exposure at workplace and m=2 for noise exposure in vehicle, Equation (3) gives:

$$L_{EX,8h} = 10\lg\left(10^{0,1\times L_W} + \frac{T_V}{T_0} * 10^{0,1\times L_{AeqT}}\right)dB \qquad (4)$$

where L_W is average noise exposure at workplace, T_0=8h and T_V time spent in vehicle. The values in the Table 3 are obtained as corresponding times T_V needed to achieve limit values for $L_{EX,8h}$.

In the table 3 times that seem probable to be spent in public transportation vehicles are shaded. One can see that the limit is probably reached with no necessery additional noise exposure at work for one type of vehicle, in 25 to 90 minutes of daily ride. As for other tested types of vehicles and for the average estimated noise exposure in public transportation, for noise exposures at workplace less then 70 dB(A) limits are not likely to be achieved.

Table 3 *Corresponding times spent in vehicle needed to achieve the limit values for measured equivalent continuous A-weighted sound pressure, for all the measurements and for each vehicle type separately. The times that seem probable to be spent in public transportation vehicles are shaded.*

Descriptor evaluated	Time to achieve limit values (in minutes)			
	Regulation [2] action value and Directive [3] lower exposure action value		Regulation [1], [2] limit value and Directive [3] upper exposure action value	
	For noise exposure at workplace of 50 dB(A)	For noise exposure at workplace of 70 dB(A)	For noise exposure at workplace of 50 dB(A)	For noise exposure at workplace of 70 dB(A)
ALL VEHICLES ($L_{AeqT1(max)}$=91,9 dB(A), $L_{AeqT2\ (mean)}$ =79,7 dB(A))				
$L_{AeqT2\ (mean)}$	-	-	-	-
$L_{AeqT1(max)}$	28	25	88	85
MAZ 203 ($L_{AeqT2(max)}$=82,4 dB(A), $L_{AeqT2\ (mean)}$ =76,8 dB(A))				
$L_{AeqT2\ (mean)}$	-	-	-	-
$L_{AeqT2\ (max)}$	246	228	-	-
MAN SG 313 ($L_{AeqT2(max)}$=82,4 dB(A), $L_{AeqT2\ (mean)}$ =74,3 dB(A))				
$L_{AeqT2\ (mean)}$	-	-	-	-
$L_{AeqT2\ (max)}$	-	-	-	-
IKARBUS ($L_{AeqT1(max)}$= 91,9dB(A), $L_{AeqT1\ (mean)}$ =89,1 dB(A))				
$L_{AeqT1\ (mean)}$	53	43	167	163
$L_{AeqT1(max)}$	28	25	88	85

Further we can use Eq. (4) if we want to compare the daily A-weighted noise exposure level that includes the time spent in bus transport to limit values, assuming an exposure in bus to the average value of 79,7 dB(A).

Doing so, the daily exposure to an average value of noise in bus transport for 158 minutes would result in limiting the 8-hour noise exposure level at workplace to 84 dB(A), if we want to keep the daily A-weighted noise exposure level in limit of 85 dB(A) (i.e. Regulation [1], [2] limit value). Also, applying this to Regulation [2] action value of 80 dB(A), we

see that the daily exposure to an average value of noise in bus transport for 50 minutes would result in limiting the 8 hour noise exposure level at the workplace to 79 dB(A) and the exposure in bus for 134 minutes would result in limiting the noise exposure level at the workplace to 78 dB(A). That is, spending times in bus transport of duration of 158 minutes daily would require reducing the limit value by 1dB and spending times in bus transport of durations of 50 and 134 minutes daily would require reducing the action value by 1 and 2 dB for the 8-hour noise exposure level at workplace.

When comparing C-weighted peak sound pressure level ($L_{p,Cpeak}$) to the limits it can be seen that maximum value measured (133,2 dB(C)) doesn't exceed limit value of 135 dB(C) (i.e., action value according to Regulation [2] and lower exposure action value according to Directive 2003/10EC).

When comparing octave-band analysis results to the limits regarding hearing impairment hazard, according to Regulation [1] for 120 min of exposure daily, it can be seen that the limits are not exceeded (Table 4).

Table 4 *Average values and maximum values measured of sound pressure level in octave-bands and limit values for preventing hearing imparement hazard according to Regulation [1]*

octave-band	31,5	63	125	250	500	1x 10^3	2x 10^3	4x 10^3	8x 10^3
average value	90,7	87,3	82,7	79,5	76,8	73,7	67,2	60,3	52,9
maximum value	95,4	95	88,6	90,6	87,1	88	84,9	79,4	69,8
limit values *	-	-	120	109	101	94,5	90	88	96
* for 120 minutes of exposure daily									

4.2 Comparing to limit values regarding annoyance

As for assessment of noise with respect to annoyance, there are limit values regarding environmental noise exposure. While the noise treated in this paper is not strictly environmental noise as treated in the environmental noise regulation [4], people are exposed to this noise as much as any other environmental noise in their everyday life. When comparing to the limits one could compare the measured L_{AFmax} to maximum limits given in [4], i.e., 65 dB(A) as a value given for the open space and 40 dB(A) as a value given for indoor space. From the Fig. 3 one can see (mean values are 83 to 91 dB(A)) that theese values are greatly exceeded.

Table 5 *Average values and maximum values measured of sound pressure level in octave-bands and limit values for disturbing noise according to Regulation [1]. The values that exceeded the limit values are shaded.*

octave-band	31,5	63	125	250	500	1x 10^3	2x 10^3	4x 10^3	8x 10^3
average value	90,7	87,3	82,7	79,5	76,8	73,7	67,2	60,3	52,9
maximum value	95,4	95	88,6	90,6	87,1	88	84,9	79,4	69,8
IKARBUS	88,3	87,1	87,0	88,5	84,8	85,0	82,0	74,7	67,5
limit values *	106,5	94,7	87,2	81,7	77,9	75	72,6	70,8	69,2
* in the situation that there is no need for any observation of environment									

When comparing octave-band analysis results to the limits regarding annoyance, comparing to the limits given by Regulation [1] for disturbing noise in the situation that there is no need for any observation of environment (Table 5), it can be seen that for one type of vehicle (IKARBUS) limits are exceeded in middle and high frequencies (250 - 4000 Hz), and for the maximum values measured limits are exceeded partly in low and in middle and high frequencies (125 – 8 000 Hz).

However, as seen from the Figure 4, frequency content is strongly in low frequencies. That type of noise is very annoying as there is a much more rapid increase in loudness and annoyance with increasing sound pressure levels at low frequencies than at mid or high frequencies (ISO 1996-1, Annex C).

5. CONCLUSION

Assuming that average exposure of passenger would be as in this paper calculated average value of equivalent continuous A-weighted sound pressure, 80 dB(A), discussed limits regarding the health, i.e., $L_{EX,8h}$ of 80 and 85 dB(A) are not likely to be exceeded for noise exposures at workplace less then 70 dB(A). In addition, including this everyday exposure in transport would result in need for reducing the limit values: spending 158 minutes in bus daily would require reducing the limit value by 1dB and spending times in bus transport of durations of 50 and 134 minutes daily would require reducing the action value by 1 and 2 dB. However, riding longer than 30 minutes in one type of tested types of vehicles everyday would be a health risk without additional noise exposure at workplace at all, and riding in some of tested vehicles of the other type tested (measured levels greater then 80 dB(A)) would be a significant contribution to the daily noise exposure. As for the annoyance and discussed limit values for descriptors, the limit values are greatly exceeded by all measured levels.

Octave-band analysis shows that discussed limit values are exceeded for one type of vehicle in middle and high frequencies. In addition, frequency content is strongly in low frequencies and that type of noise is perceived more loud and annoying then noise of the same equivalent sound pressure level that is stronger in middle and high frequencies.

REFERENCES

[1] Regulation on occupational safety measures and norms for noise protection at workplace. Off. J. SFRJ. 1992, 21, pp. 310-316

[2] Regulation on preventive measures for health and safety at work regarding noise exposure. Off. J. RS. 2011, 96, pp. 10-12

[3] Directive 2003/10/EC of the European Parliament and of the Council of of 6 February 2003 on the minimum health and safety requirements regarding the exposure of workers to the risks arising from physical agents (noise). Off. J. Eur. Commun. L 42, 15.2.2003, p. 38

[4] Decree on noise indicators, limit values, evaluation methods for noise indicators, annoyance and nocive effects of environmental noise. Off. J. RS. 2010, 75, pp. 10-13

[5] ISO 1996-1:2003 Acoustics - Description, measurement and assessment of environmental noise - Part 1: Basic quantities and assessment procedures

[6] ISO 1996-2:2007 Acoustics - Description, measurement and assessment of environmental noise - Part 2: Determination of environmental noise levels

[7] ISO 9612:2009 Acoustics - Determination of occupational noise exposure - Engineering method

[8] ISO 1999:2013 Acoustics - Estimation of noise-induced hearing loss

[9] ISO 9612:1997 Acoustics - Guidelines for the measurement and assessment of exposure to noise in a working environment

University of Nis
Faculty of Occupational Safety
„Politechnica“ University of Timisoara
Faculty of Mechanical Engineering
24th International Conference
NOISE AND VIBRATION
Niš, 29 - 31. 10. 2014.

ONE REALIZATION OF THE SYSTEM FOR MEASURING AIRFLOW RESISTANCE

Milan Kolarević[1], Branko Radičević[1], Vladan Grković[1], Zvonko Petrović[1]

[1] University of Kragujevac, Faculty of Mechanical and Civil Engineering Kraljevo, Serbia, kolarevic.m@mfkv.kg.ac.rs

Abstract - *Airflow resistance is one of the main non-acoustic parameters, which shows the behaviour of porous materials used in sound-absorbing systems. The standard SRPS ISO 9053 specifies two methods for measuring airflow resistance: a steady-state airflow method and an alternating airflow method. The paper presents the possibility of realization of the measurement system for measuring airflow resistance by using the existing laboratory equipment. The constant airflow is provided by a vacuum pump. The advantage of using this measurement system is a considerably lower price in comparison with commercial solutions, and the procession of measurement results which is not complete automated is seen as the weakness.*

Keywords: *determination of airflow resistance, porous acoustic materials, absorption coefficient*

1. INTRODUCTION

Airflow resistance is a standard value defined as the ratio between the pressure drop and the volumetric airflow rate through a test sample. The standard ISO 9053 specifies the procedure and the principle sketch of the steady-state method. The calibrated differential pressure gauge and the volumetric airflow rate metre are the most important measuring instruments in the system for measuring airflow resistance. The airflow source must create a sufficiently small air velocity so that the measured airflow resistance could not depend on air velocity. In the steady-state method, airflow resistance is determined for the airflow velocity of 0.5 mm/s in the measuring cell. The equipment used for measuring differential pressure must allow measurement of low pressures of 0.1 Pa.

Standard methods require special instruments which are available only in specialised laboratories. Taking this circumstance into account, the authors describe a solution of the measurement system for measuring airflow resistance of porous materials. Its application requires the measuring instruments and equipment available in most laboratories for fluid technique and acoustics. Only the measuring cell was specially made for the needs of measuring airflow resistance of porous materials.

The final aim of these measurements is determination of the sound absorption coefficient in porous materials. By measuring airflow resistance for porous materials, the sound absorption coefficient can be determined depending on the frequency for different densities and thicknesses of porous materials. For manufacturers of sound absorbing materials and designers of noise protection systems, it is important that they have the possibility to estimate sound absorption on the basis of their knowledge of structural and mechanical properties of those materials.

2. METHODS FOR DETERMINATION OF AIRFLOW RESISTANCE

Measurement systems for determination of airflow resistance allow testing samples for the purpose of research and development of porous absorbing materials as well as quality control of these materials in the production process. The standard SRPS ISO 9053 foresees two methods for measuring airflow resistance, as it is shown in Figure 1.

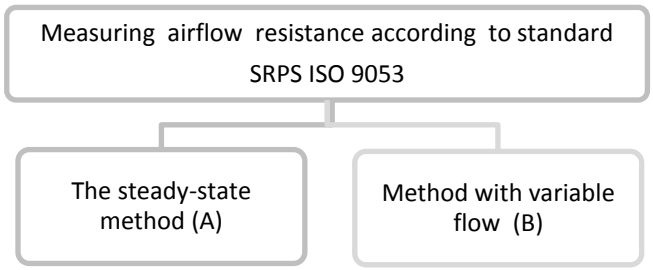

Fig. 1 *Methods for measuring airflow resistance*

The air which has a definite velocity and volumetric flow rate laminarly flows through the surface of the sample made of porous material. The difference in pressure is measured on the front and rear sides of the sample. The schematic presentation of the measuring process is shown in Figure 2.

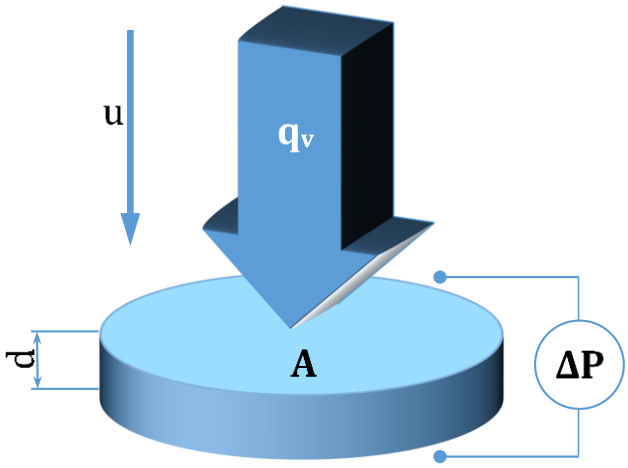

Fig. 2 *Schematic presentation of measuring airflow resistance*

The airflow resistance represents the ratio between the difference in pressure and the volumetric flow rate.

$$R = \frac{\Delta p}{q_v}\left[\frac{Pa \cdot s}{m^3}\right] \quad (1)$$

where:

Δp – the difference in air pressure in front and behind the test sample in relation to the atmosphere, in Pascal

q_v - the (volumetric) airflow rate through the test sample, in cubic metres per second

In acoustics, the specific airflow resistance (Rs) is used more frequently, and it actually represents the acoustic impedance. The specific airflow resistance (Rs) is particularly useful for comparing acoustic materials because it does not depend on the area. Variations in material thickness and pore size will change the value of specific airflow resistance.

The specific airflow resistance is calculated according to the expression:

$$R_s = R \cdot A\left[\frac{Pa \cdot s}{m}\right] \quad (2)$$

where:

R_s – the airflow resistance of the test sample, in Pascal seconds per metre

A – the area of the cross section of the test sample normal to the direction of flow, in square metres

The airflow resistivity is the value which is suitable for selection of thickness of the absorbing material. It is particularly important for open-cell foam materials because they can be manufactured in a lot of different thicknesses. The airflow resistivity is determined according to the expression:

$$r = \frac{R_s}{d}\left[\frac{Pa \cdot s}{m^2}\right] \quad (3)$$

where:

R_s – the specific airflow resistance of the test sample, in Pascal seconds per metre

d – the thickness of the test sample in the direction of flow, in metres

2.1 Method of calculation of the sound absorption coefficient

The standard EN 12354-6: 2003 recommends the calculation of the diffuse sound absorption coefficient of porous materials. For a diffuse acoustic field, the absorption coefficient α_s can be determined as:

$$\alpha_s = \int_0^{\pi/2} \alpha_\varphi \sin 2\varphi d\varphi \quad (4)$$

$$\alpha_\varphi = 1 - \left|\frac{Z'\cos\varphi - 1}{Z'\cos\varphi - 1}\right|^2 \quad (5)$$

$$Z' = Z_c' \coth \gamma d \quad (6)$$

where:

φ - the angle of incidence, in radians

α_φ - the absorption coefficient for a plane sound wave, incident at an angle φ

Z'- $\rho_0 c_0$ – the normalized surface impedance of the layer

Z_c' - $\rho_0 c_0$ – the normalized characteristic impedance of the absorbing material

γ - the propagation coefficient in the absorbing material, in radians/m

d – the thickness of the layer, m

The normalized characteristic impedance Z_c' and the propagation coefficient γ can be determined if the specific flow resistance of porous materials r is known using theoretical models:

Table 1 *Models for calculation of the absorption coefficients of fibrous and open-cell foam materials*

A. Delaney & Bazley's relationships (for fibrous material)		B. Duun & Davern's relationships (for open-cell foams)	
$Z_c' = \left(1 + 0.0571 \cdot C^{0.754}\right) - i\left(0.087 \cdot C^{0.732}\right)$	(7)	$Z_c' = \left(1 + 0.114 \cdot C^{0.369}\right) - i\left(0.0095 \cdot C^{0.758}\right)$	(9)
$\gamma = k_0\left(0.189 \cdot C^{0.595}\right) + ik_0\left(1 + 0.0978 \cdot C^{0.7}\right)$	(8)	$\gamma = k_0\left(0.168 \cdot C^{0.715}\right) + ik_0\left(1 + 0.136 \cdot C^{0.494}\right)$	(10)

where:

$$C = \frac{r}{\rho_0 f} \quad (11)$$

r – the airflow resistivity, [Pa·s/m^2]

f – the frequency [Hz]

ρ_0 - the density of air, [kg/m^3] (≈ 1.2 kg/m^3)

3. THE STEADY-STATE METHOD

The method is based on the passage of one-way airflow through the test sample in the form of a circular cylinder or a rectangular parallelepiped and measuring of the resulting pressure drop between two free surfaces of the sample.

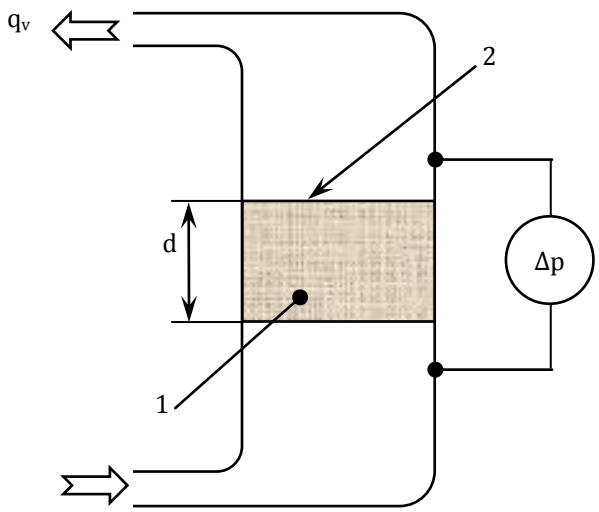

1. Porous material – sample
2. Cross section (area – A)

q_v – Volumetric airflow rate

d – Sample thickness

Δp – Change in pressure

Fig. 3 *Steady-state method (method – A) – Basic principle*

Depending on the way of airflow supply, the steady-state method can be realized in several ways. Airflow can be created by: a vacuum pump, compressed air, a water tank and an injector (Fig. 5).

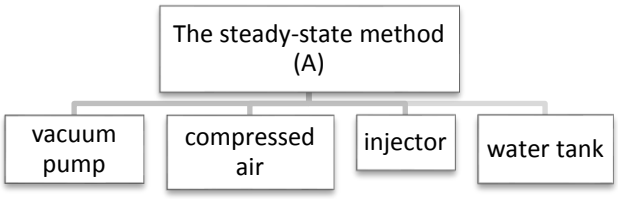

Fig. 4 *Ways of airflow supply in the steady-state method*

3.1 Test samples

The shape of the sample can be circular or rectangular. In our case, the measuring cell is of a circular cross section, which results in the shape of the sample. When soft, compressible materials, such as fibrous and open-cell foam materials are tested, in preparation of samples the possibility of air leakage along their edges must be reduced as much as possible. This problem is solved by preparing samples whose sides are a little longer than the measuring cell. Samples made of rigid material must have the same dimensions as the measuring cell.

As for the thickness of samples, the holder of samples must be equipped with a micrometre or another indicator which measures the thickness of samples with the accuracy of ±2.5% of the specified value. The thickness of the test sample is chosen in such a way to obtain a measurable pressure drop. If test samples are of insufficient thickness to create a measurable pressure drop, the test samples can be piled up, five samples at the most. The piled samples must be selected in the same manner.

The number of test samples must be taken from at least three products and from each of them three trial samples for testing must be cut out.

3.2 Test procedure

1. The test sample is placed in the measuring cell
2. It should be checked whether the edges are well sealed. For fibrous and open-cell foam absorbing materials, most frequently no additional sealing is necessary. For sealing rigid samples, sealing which can be performed by applying different sealing materials can be provided. The standard recommends bitumen-based masses. As for the selection of the sealing mass, easy removal of the mass after sealing should be allowed in order not to prevent further measurements by its presence on the walls of the measuring cell. Besides, attention should be paid to the time necessary for hardening of the mass and what can be used to remove it from the walls of the measuring cell. Scratching of the hardened sealing mass can damage the wall of the measuring cell. The use of additional chemical agents for removal of the sealing mass slows down the measuring process and leads to unnecessary costs. Therefore, depending on the material of the sample, it is important to determine the sealing material which can easily be deposited and removed.
3. If the thickness of the test sample is not known, the measuring device which is an integral part of the measuring cell measures the thickness in the so-called free state of the sample where the sample is just lightly touched by means of a piston with the grid.
4. The thickness of the samples is recorded and this measurement is used for determination of the volume in free state.
5. The measuring cell is designed in such a way to allow measuring airflow resistance in the samples made of fibrous and open-cell foam materials, whose thickness can be changed. The change of thickness is performed by the pressure exerted by the piston with the grid and by fixing the piston, which makes the sample remain in a compressed state.
6. The thickness of the sample is recorded and this measurement is used for determination of the volume in compressed state.
7. As specific airflow resistance in a lot of absorbing materials increases with the increase in air velocity in a certain range of velocities, it must be measured at the lowest air velocity. For the lower limit, the recommended air velocity is $0.5 \cdot 10^{-3}$ m/s. This value of particle velocity corresponds to the sound pressure of 0.2 Pa.

4. AN EXAMPLE OF REALIZATION OF THE SYSTEM FOR MEASURING AIRFLOW RESISTANCE

The steady-state method, in which airflow is provided by means of a vacuum pump, was selected for measuring airflow resistance. This method is based on the passage of one-way airflow through the test sample in the form of a circular cylinder or a rectangular parallelepiped and measuring the resulting pressure drop between two free surfaces of the sample (Fig. 5).

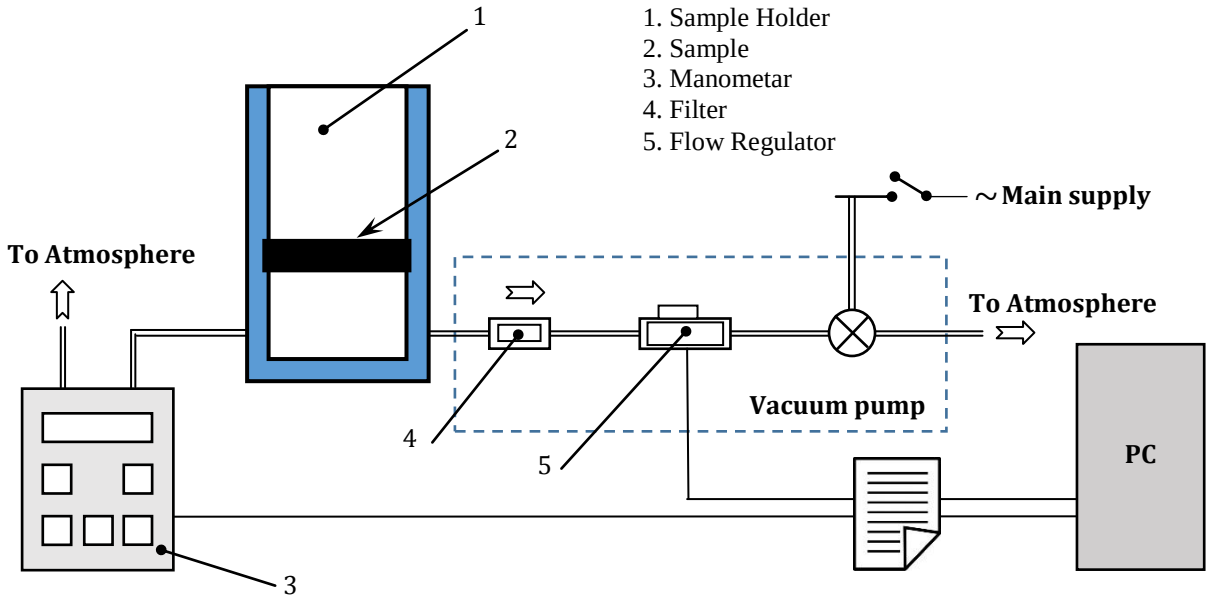

Fig. 5 *Block diagram of the steady-state airflow system*

The structure of the measurement system which uses the steady-state method, which is provided by means of a vacuum pump, is presented in the block diagram in Figure 5.

The vacuum pump make ZAMBELLI, type ZB1, is used as the device for creation of airflow. The pump is of a small weight (7 kg) and therefore it is suitable both for laboratory and field measurements. The pump is of a membrane type and can realize the maximum free flow of 30 l/min. The underpressure produced by the pump is higher than 0.773 bar (580 mmHg). The pump has two airflow metres, which operates on the principle of the ball rotametre. Smaller airflows in the range of 0.2÷6 l/min are measured by means of the smaller rotametre, and higher flows in the range of 5÷30 l/min are measured by means of the bigger rotametre. The maximum flow measurement error is ± 2%. The pump allows the fine control of flow and the stability of flow in the part of the measuring cell which is behind the sample. By its characteristics, the pump provides a sufficiently small air velocity so that the measured airflow resistance could not depend on air velocity. The pump enables airflow velocity of $0.4 \cdot 10^{-3}$ m/s in the measuring cell, which completely corresponds to the recommendations from the standard SRPS ISO 9053 ($0.5 \cdot 10^{-3}$ m/s).

In the measuring cell, the atmospheric pressure is on one side of the sample, and the underpressure produced by the vacuum pump is on the other side of the sample. In order to provide conditions for maintaining underpressure, the measuring cell must be well sealed on one side. The differential pressure gauge TESTO 512 is used for measuring the difference in pressures on both sides of the sample. This gauge has a measuring range of 0 to 200 Pa with the resolution of 0.1 Pa. The equipment used allows measurement of differential pressure up to the accuracy of ±5% of the specified value.

The measuring cell has the form of a circular cylinder, and it is made of plexiglass so that placing of the sample could be visually monitored. The inner diameter of the measuring cell is 100 mm, which satisfies the requirement of the standard SRPS ISO 9053 that the inner diameter must be longer than 95 mm.

Fig. 6 *Look of the realized measurement system for determination of airflow resistance*

The height of the cell is 300 mm so that the airflow which gets in and out from the test sample could be laminar. The height of the measuring cell should be by at least 100 mm bigger than the thickness of the sample. The test sample must be placed in the measuring cell, above and at a sufficient distance from the cell base to achieve the above mentioned requirements. The sample support should have uniformly distributed openings across at least 50% of its surface. The minimum diameter of the opening is also prescribed (3 mm).

The minimum percent of opening is prescribed in order not to limit airflow through the sample. The airflow resistance in such elements (measured with the air velocity higher than the highest velocity used for testing samples) must be smaller than 1% of the airflow resistance measured while testing the samples.

The measuring cell is placed at the flange which can be fastened to the holder of the measuring cell either horizontally or vertically. The measuring cell can also be used without its fastening to the holder, so that it is suitable both for field work and directly in the production process and inspection of acoustic materials.

4.1 Test conditions

In case of the procedure which uses constant airflow, the pressure drop Δp can be measured either directly at the velocity of 0.5 mm/s or gradually by its reducing to the lowest limit of air velocity. At a gradual reduction of air velocity, a graphical presentation of specific airflow resistance as a function of air velocity is given for each sample. Specific airflow resistance at the flow velocity of $0.5 \cdot 10^{-3}$ m/s is determined from the diagram, by averaging or, if necessary, by extrapolation.

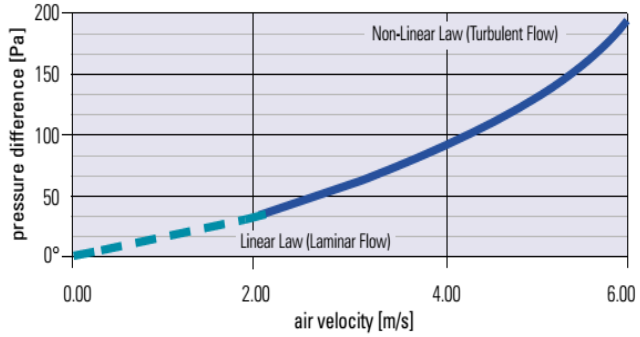

Fig. 7 *Airflow resistance – test conditions: linear and non-linear* [6]

In order to perform accurate measurement of airflow resistance, airflow must be linear and cannot be provided by typical equipment which does not have the possibility of adjusting very small flows.

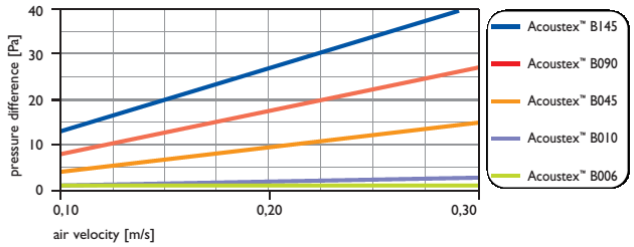

Fig. 8 *Dependence of the pressure drop for different types of materials* [6]

Certain renowned world manufacturers of acoustic materials (such as SaatiTech) perform measurement of specific airflow resistance at low pressures (tolerance up to 0.1 Pa) and air velocities of 0.3 m/s (Figure 8).

4.2 Measurement results and their procession

Measurement results are written in the database on a paper or can be directly entered in an Excel sheet. The sheet contains input and output data. The input data can be divided into two groups. The first group is made of the data whose value is constant because they relate to design parameters of elements of the measurement equipment or the sample. An example of data belonging to this group is: sample diameter, diameter of the hose for the vacuum pump air and diameter of the measuring cell. The second group consists of data whose values are variable. This group includes data about the selected volumetric flow rate and the measured pressure drop. The output data represent the calculated values of airflow resistance, specific airflow resistance and airflow resistivity.

In order to determine specific airflow resistance, it is necessary to select 10 values of volumetric flow rate and for them measure the pressure drop through the sample. It is necessary to reduce the laminar airflow velocity to the value of 0.5 mm/s, if it is allowed by the pump flow. Namely, at the lowest airflow, the pressure drop must be measurable. If it is not possible to measure the pressure drop at the limit vale of airflow velocity of 0.5 mm/s, the value of specific airflow resistance is determined by extrapolation.

Table 2 *Input and output data at the concrete sample in the procedure of measuring airflow resistance*

q_v	Δp	u	R	R_s	r
[lit/min]	[Pa]	[mm/s]	[Pa·s/m^3]	[Pa·s/m]	[Pa·s/m^2]
20	3.3	42.4	9900	77.8	3887.7
17	2.4	36.1	8470.6	66.5	3326.4
15	2	31.8	8000	62.8	3141.6
12	1.5	25.5	7500	58.9	2945.2
11	1.2	23.3	6545.5	51.4	2570.4
10	1	21.2	6000	47.1	2356.2
9	0.9	19.1	6000	47.1	2356.2
8	0.8	17	6000	47.1	2356.2
7	0.7	14.9	6000	47.1	2356.2
6	0.5	12.7	5000	39.3	1963.2

For the sponge sample made of polyurethane foam, density 25 kg/m^3, specific airflow resistance was determined to be 26.2 [Pa s/m]. Determination of this value is presented in the diagram (Figure 9). The linear regression line was obtained on the basis of 10 values of airflow within the range of 20÷6 [l/min]. After determination of the linear regression equation, the value of airflow resistance for the velocity of 0.5 mm/s was determined by extrapolation. Based on the value of the Pearson correlation coefficient (R=0.978), it can be seen that the correlation between specific airflow resistance and flow velocity is very high.

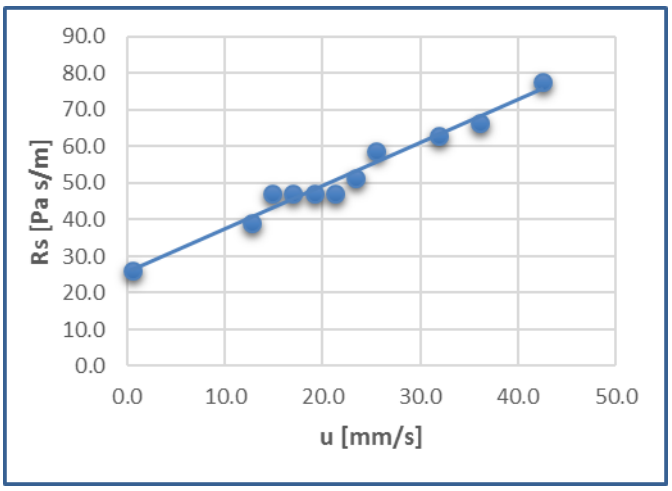

Fig. 9 *Dependence of the specific airflow resistance on the flow velocity*

The final aim of such measurements is to obtain the dependence of the absorption coefficient on the frequency. For the mentioned sponge sample, according to the Duun & Davern's model (9; 10), for open-cell foam materials, the sound absorption coefficient was determined and presented in the form of diagram in Figure 10.

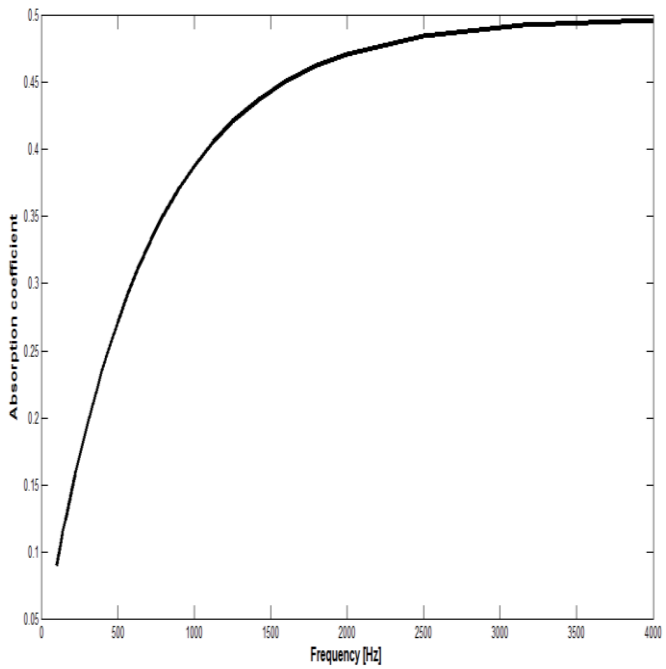

Fig. 10 *Sound absorption coefficient depending on the frequency*

The aim of the paper was to present an engineering solution of a measurement system for determination of airflow resistance. Therefore, the discussion related to the obtained measurement results is in the second plan.

5. CONCLUSION

The method of determination of airflow resistance allows fast estimation of the values of the sound absorption coefficient in porous materials. This method is defined by the standard SRPS ISO 9053:1994, which makes practical realization of the measurement system easier. Commercial solutions are rather expensive, so that the measurement system was designed by using the existing laboratory equipment. After a successful engineering realization of the measurement system for determination of the airflow resistance, it can be concluded that other measurement methods may also be realized by using the existing laboratory equipment, which results in huge financial saving. One of the obstacles toward that goal is the lack of information about the existing measurement equipment both in scientific-research institutions and at the state level. The realized engineering solution of the measurement system can be used both for measurements for scientific-research purposes and for quality control of acoustic materials in the production process. The next step in the research is validation of the measurement results obtained by this method by comparing the measuring values with the measurement results obtained by other methods.

Acknowledgement: The paper is a part of the research done within the project TR37020. The authors would like to thank to the Ministry of Education and Science of the Republic of Serbia for supporting this research.

REFERENCES

[1] Delany, M.E. & E.N. Bazley, Acoustical properties of fibrous absorbent materials, Applied Acoustics 3 (1970), 105.

[2] Dunn, I.P. & W.A. Davern, Calculation of acoustic impedance of multi-layer absorbers, Applied Acoustics 19(1986), 321.

[3] SRPS ISO 9053, Acoustics - Materials for acoustical applications - Determination of airflow resistance (ISO 9053:1991)

[4] EN 12354-6, Building Acoustics - Estimation of acoustic performance of buildings from the performance of elements - Part 6: Sound absorption in enclosed spaces

[5] M. Mirowska, K. Czyżevski, Estimation of sound absorption coefficients of porous materials, ICSV14, Cairns, Australia, 2007

[6] http://www.satiamericas.com

[7] http://www.redwing.org.uk

[8] http://www.instrumant.com

University of Nis
Faculty of Occupational Safety
„Politechnica“ University of Timisoara
Faculty of Mechanical Engineering
24th International Conference
NOISE AND VIBRATION
Niš, 29 - 31. 10. 2014.

INFLUENCE OF DESIGN PARAMETERS ON MODAL BEHAVIOUR OF SANDWICH PANELS

Aleksandar Vranić[1], Nenad Todić[1], Snežana Ćirić Kostić[1]

[1] The Faculty of Mechanical and Civil Engineering in Kraljevo, University of Kragujevac, Serbia, vranic.a@ mfkv.kg.ac.rs

Abstract - *This paper discusses the influences of various core configurations and other design parameters on vibrations of sandwich panels. The presented analysis contributes to efforts to resolve the contradiction between the requests for increased stiffness and reduced mass of mechanical structures by additive manufacturing technologies. The technologies enable manufacturing of complex lattice structures and design of optimal sandwich structures that satisfy both requests. Structural characteristics of a sandwich panel (core shape, wall thickness of plates and core, width of core) can be selected independently of the other parameters, thus changing modal behavior of the panel. Influence of the structural characteristics was studied by numerical calculation of natural frequencies and mode shapes of sandwich structures designed for production by additive manufacturing. Analyses of the obtained results allow insight into processes in elastic structure of the studied systems.*

1. INTRODUCTION

Modal behavior, as characteristic structure property, is determined by material and geometric properties (mass, stiffness and damping) and boundary conditions of the structure. Change of any of those characteristics leads to changes of modal behavior [1]. High stiffness of a structure is very important for its good resistance to natural vibrations. On the other hand, lightweight design (mass reduction) is requirement that is met by modern designers with increased occurrence. These two requirements, important from the aspect of the modal behavior of the structure, are contradictory to each other.

The idea of the paper is to consider use of AM technologies for manufacturing of complex lattice and cellular structures that would simultaneously meet two requests: reduction of mass and reduction of vibrations (and consequently noise emission) of housing panels. Sandwich panels, comprising thin plates enclosing a core, are increasingly common structural elements in variety of applications, including vehicle and aircraft panels, aircraft fuselages, lightweight housings and bulkheads. More than 700 honeycomb core structures for sandwich components were produced in the past 50 years just by one manufacturer [3, 4, 5]. However, sandwich panels with arbitrary core structure are almost impossible to be manufactured by means of traditional manufacturing technologies.

The paper presents initial results of research of modal behavior of sandwich panels with various shapes and density of lattice structures, with the ultimate goal to determine the optimal sub-structure of a panel from the aspect of reduction of vibrations and sound emission. For example, it has been shown [2] that it is possible to reduce noise emission of gearboxes by increasing the structural stiffness and reduction the vibration of panels with large and positive acoustic contribution coefficients.

Sandwich panels consist of two parallel thin plates and a core between them. The parallel plates withstand normal forces, which arise from bending, tension or pressure, and the core withstands shear forces, like in the case of I-beam geometry. The stiffness of the sandwich structure can be increased by appropriate selection of the core structure. In addition, increasing the distance between the parallel plates by the lightweight core increases the second moment of area (and hence the bending stiffness) of the material cross-section with only a small increase in weight. Likewise, changing of wall thicknesses of plates and/or core can significantly change stiffness, masses and modal frequencies of sandwich plates.

For the purpose of analysis of influence of shapes and dimensions of sub-structures (core structure) on vibration behavior of sandwich panels are used results of modal analysis by FEM.

2. AM TECHNOLOGIES

Unlike traditional methods of manufacturing, where product is made by removing or forming of material, additive manufacturing technologies make product by joining successive layers of a material. There are various types of additive manufacturing technologies, using different materials. The AM technology that enables manufacturing of products with mechanical properties comparable to those made by traditional technologies is called “selective laser sintering” (SLS). SLS offers freedom to build quickly complex and freeform parts that are more durable and provide better functionality than other AM technologies. SLS technology uses laser beam directed by optical system to melt plastic or metal powder. The melted powder is cooling and sintering after the illumination, thus forming a horizontal cross-section of a 3D object. After sintering, the layer is lowered and a new layer of powder is applied on top of it. The new layer is then melted, thus forming the next section, which is simultaneously joining with the previous layer during the cooling phase. Therefore, during the cooling phase the melted powder is joining in both horizontal and vertical direction. The process is repeated until the 3D object is made. This new technology enables manufacturing of complex structures with cellular structure that have low mass, high

stiffness good stress resistance (Fig. 1a). SLS opens many possibilities for lightweight design. EOS, German SLS machine manufacturer, demonstrated ability to produce metal sandwich structures using this technology (Fig. 1b). It means also that it is possible to manufacture various types of sandwich structures of housing panels by SLS technology [6, 7]. EADS has been testing wind brackets (Fig. 1c) and hinges for engine covers to evaluate technical and commercial feasibility of parts produced by SLS [8, 9]. Considerable savings and weight reduction is gained without endangering bracket functionality.

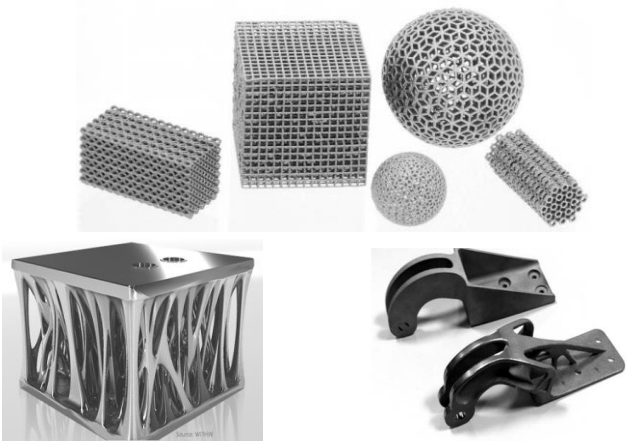

Fig. 1: *Lightweight structures manufactured by SLS* [10]:
a) Cellular structures
b) Sandwich structure with low core density;
c) Titanium bracket with optimized topology

However, SLS technology has also its limitations. The main limitations are connected to limited minimal wall thickness of the parts (0.4 mm), limited dimensions of the manufactured objects (250x250x330 mm) and limited selection of materials that may be processed by the technology. Available materials are 15-5 Stainless Steel, Maraging Steel, Cobalt Chrome, Titanium Ti64, Nickel Alloy N62 and Aluminum alloys. Parts are being manufactured on building platform, which has role to remove heat and prevent motion and deformation of objects that may occur due to the residual stresses caused by thermal dilatation. The manufactured parts are thus connected to the platform by supports that are manufactured simultaneously with the object. The supports sometimes present an additional limitation in design for additive technologies.

3. MODELS DEVELOPMENT

Modeling and analysis of the results are conducted in two stages.

In the first stage were developed twenty-three geometric models of sandwich panels with variable core structure for the purpose of analysis of the influence of substructure shape on natural vibrations of sandwich panels. Widths of the sandwich cores were h_c =13 mm, thicknesses of parallel cover plates were t_p = 1 mm and thicknesses of core walls were t_c = 1 mm (Fig. 2). The models were subjected to analysis of modal behavior by numeric methods, which led to calculation of natural frequencies of the modelled sandwich structures.

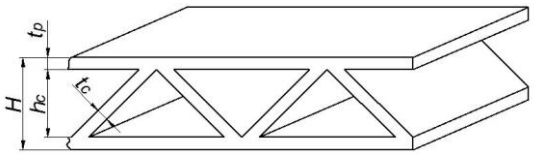

Fig.2: *Sandwich panel structure*

Models were made using Solid Works software package. Three different methods were used for modeling of 3D models of substructures. The first method was extrusion of a 2D sketch to 3D solid model (Fig. 3a). The second method was application of Boolean operations to obtain the model by adding or subtracting primitives (Fig. 3b). The third method was multiplication of 3D solid blocks obtained by extrusion of a 2D sketch (Fig. 3c).

All of the panels had the same length and heights 300x200 mm. The solid block with the same dimensions would have density of 7850 kg/m^3 and its mass would be 7.065 kg. Densities of the sandwich panels varied from 1823.33 kg/m^3 to 4338.88 kg/m^3, and the masses varied from 1.641 kg to 3.905 kg.

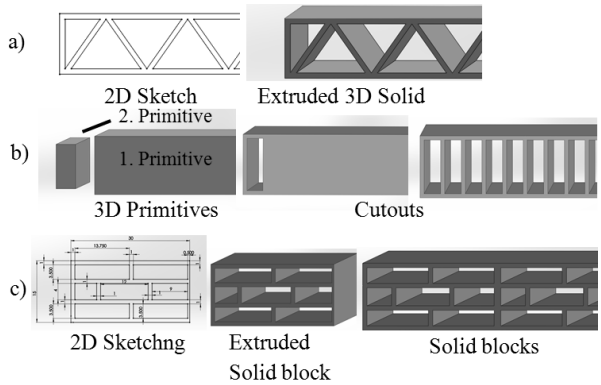

Fig. 3: *Illustration of different methods for modelling of sandwich panels*

The developed models of sandwich panels are presented in Table 1.

In the second stage was studied modal behavior of sandwich structure that has the highest values of natural frequencies. The study consisted in variation of plate thickness, core wall thickness and core width and calculation of natural frequencies for each variation of the sandwich panel. The plate thickness was varied from 1 mm to 4 mm and the core wall thickness was varied from 1 mm to 3 mm, all with 1 mm steps. The core widths were selected to provide sandwich panel widths of 15 mm, 20 mm and 25 mm.

4. MODAL ANALYSIS

Modal analysis represents the first step in research of vibrations of mechanical systems. Natural frequencies and modal shapes of the studied types of sandwich panels were determined using software package ANSYS.

Modal analysis was performed by applying the finite elements method with the linear 3D-brick finite elements with 8 nodes. Each of the elements had 24 degrees of freedom (three translations per each node). Total number of the finite elements varied from minimal 33500 for the solid panel to maximal 157986 for model V21, depending on complexity of the core geometry.

Table 1: *Sandwich structures with various sub-structures' shapes*

Ver.	Sandwich structure design	Mass kg	Density kg/m^3	No of modal shapes	Ver.	Sandwich structure design	Mass kg	Density kg/m^3	No of modal shapes
V1		1.88	2088.9	8	V14		3.91	4333.3	7
V2		2.16	2400.0	7	V15		3,16	3511.1	7
V3		1.74	1944.4	9	V16		2.38	2644.4	9
V4		2.19	2433.3	10	V18		2.38	2644.4	11
V5		2.16	2400.0	11	V19		2.84	3155.5	7
V6		2.48	2755.5	12	V20		3.51	3888.8	7
V8		2.65	2944.4	9	V21		3.59	3988.8	7
V9		2.78	3088.8	10	V22		1.64	1822.2	9
V10		2.10	2333.3	11	V23		2.19	2433.3	10
V11		2.35	2611.1	9	V2.1		2.72	3022.2	7
V12		1.68	2866.6	7	V2.2		2.72	3022.2	7
V13		1.77	1966.6	10	Solid model		7.06	7850	6

The discretized model of a sandwich panel is shown in Fig. 4. Boundary conditions are defined by fixing nodes at the bottom side of panels (Fig. 4).

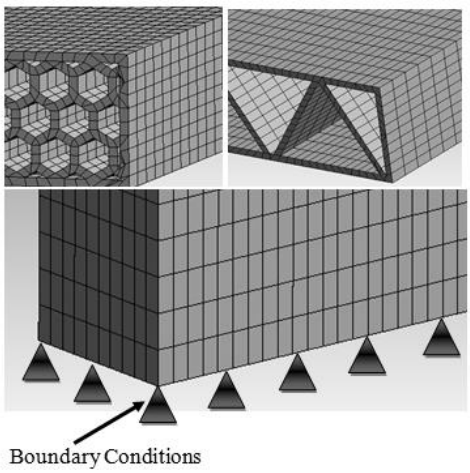

Fig. 4: *The discretized model of a sandwich panel*

Frequency range for modal analysis was from 0 Hz to 3000 Hz. The assumed material of the models in the presented modal analysis was steel.

5. RESULTS AND DISCUSION

For solid model of panel were determined six natural frequencies and modal shapes of vibrations within the studied frequency range. The number of determined vibration modes of sandwich panels developed in the first stage was between 7 and 12 in the studied frequency range (Table 1). Modal shapes for the model V12 are presented in Fig 5.

Minimal number of seven vibration modes was determined for the following nine sandwich panels: V2, V12, V14, V15, V19, V20, V21, V2.1, V2.2. Natural frequencies of these models of sandwich panels are presented in Fig.6. A brief analysis of the results obtained during the first stage shows that the solid model has the highest density and the lowest natural frequencies (Fig. 6) of all studied models.

It means that the sandwich structures have substantially lower weights and wider operational bandwidths than solid panels, which justifies the effort to replace solid panels by sandwich panels. The Fig. 6 also shows that the highest modal frequencies are obtained for the model V12. On the other hand, the corresponding amplitudes of natural vibrations of solid panel are the smallest, as expected (Fig.7). That means that all aspects of vibration behavior of sandwich structures need careful consideration before a selection is made for a specific application.

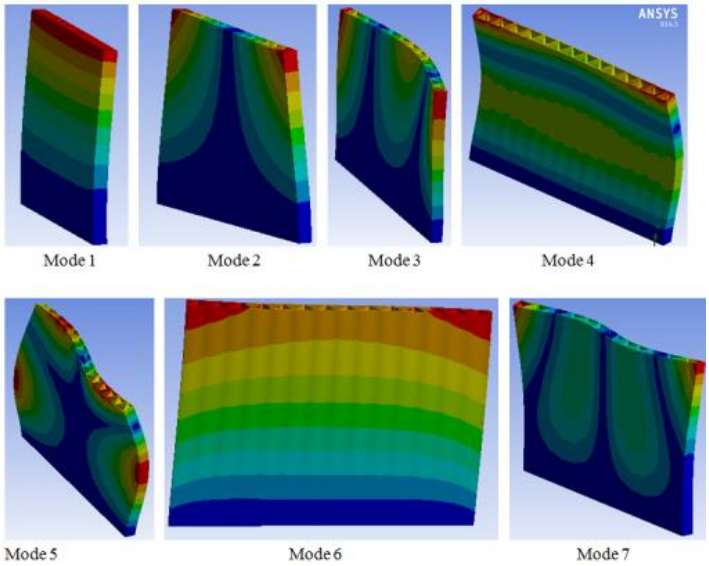

Fig.5: *Modal shapes of a sandwich panel - model V12*

Since the model V12 had the lowest mass, and also belongs to the group of models with the smallest number of natural vibration modes with frequencies in the considered range, it was selected to be the object of the analyses in the second stage of the research.

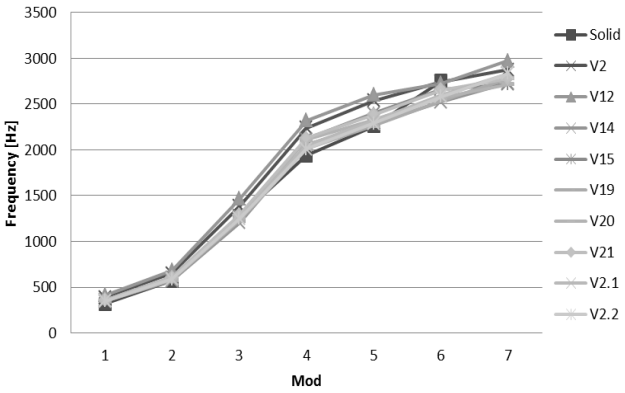

Fig. 6: *Diagram of the natural frequencies*

According to the previously described plan of research were developed models of V12 sandwich panels with variable plate thickness, core wall thickness and core width. Natural frequencies of all the models were calculated using the ANSYS software package and the results are presented in Fig. 8-Fig. 10.

In the Fig. 8 is shown dependency of the natural frequencies on:

- core wall thickness, where plate thickness was kept constant (shown in the diagram on the left);
- plate thickness, where core wall thickness was kept constant (shown in the diagram in the middle);
- thicknesses of both core wall and plate, which were kept equal (shown in the diagram on the right);

In all the considered cases panel width was kept constant at $H = 15$ mm.

The presented diagrams show that:

- the increase of the core wall thickness leads to decrease of natural frequencies of the structure;
- natural frequencies of the structure are the highest when the plates are twice thicker than the core walls;
- natural frequencies decrease if both the core wall thickness and the plate thickness are equally increased;

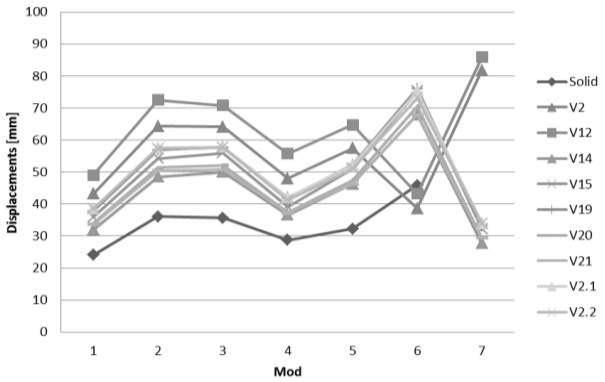

Fig. 7: *Diagram of the maximal displacements*

The observed existence of maximum in dependence of natural frequencies on the ratio between plate thickness and core wall thickness was further studied by analyzing the effects of variation of the panel width. The results of the analyses are shown in the Fig. 9, which shows that the increase of the panel width leads to decrease of number of natural vibration modes in the considered frequency range. The number of natural vibration modes is six or even (depending on the plate thickness and core width,) for the models with panel width $H = 15$ mm, five for the models with panel width $H = 20$ mm, and only four for the models with panel width $H = 25$ mm. However, natural frequencies of all the natural vibration modes had the highest value when the plates were twice thicker than the core wall.

The influence of core width to the frequencies of natural vibrations was also studied and the results are presented in the Fig. 10, which shows that the frequencies of natural vibration modes increase with increase of the core width.

The changes of all geometric parameters of a sandwich structure influence its mass and density, and thus also to amplitudes of its natural vibrations. In general, the corresponding amplitudes decrease with increase of density, which is presented in the Fig. 11, where these two quantities are shown in a log-log diagram.

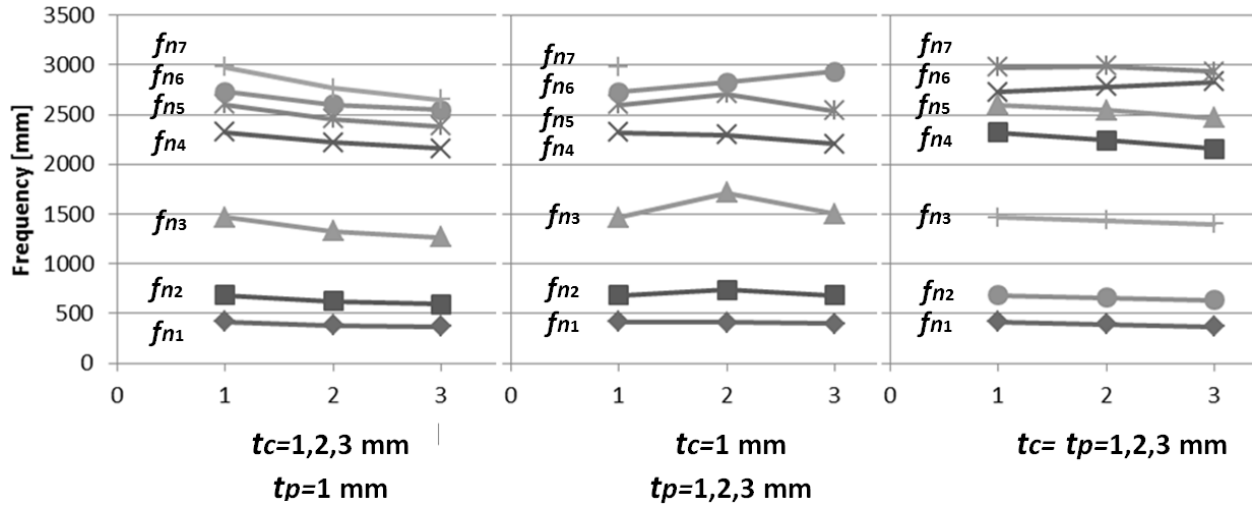

Fig. 8: *Dependence of natural frequencies on core wall thickness (t_c) and plate thickness (t_p) for sandwich panels with width H=15 mm*

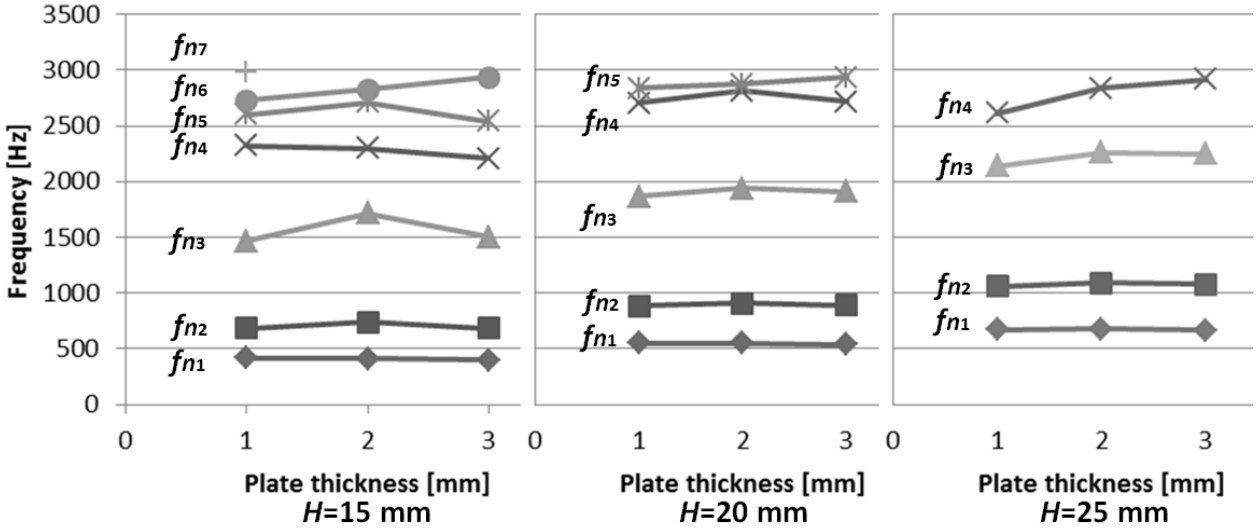

Fig. 9: *Dependence of natural frequencies on plate thickness (t_p=1,2,3 mm) and panel width (H) for constant value of core wall thickness t_c=1mm*

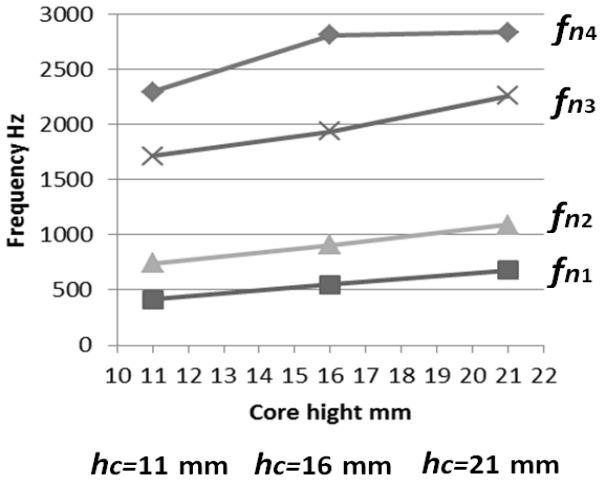

Fig.10: *Dependence of natural frequencies on core width (h_c) for core wall thickness t_c=1 mm and plate thickness t_p=2 mm*

The solid lines have slope equal to -1/2, which corresponds to proportionality of the amplitudes to inverse square root of the density, as it is the case with solid panels. The figure shows that low-frequency modes obey the inverse-square-root dependence for all samples. On the other hand, high-frequency modes show significant deviations from the inverse-square-root dependence. It means that the shape of the substructure of the core influences the amplitudes of natural vibrations at high frequencies.

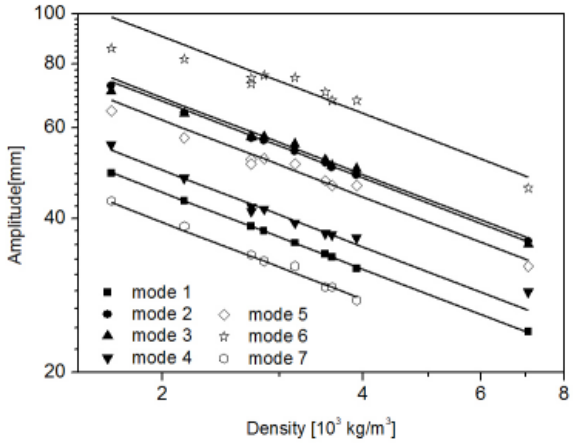

Fig. 11: *Dependence of the corresponding amplitudes on the density of the sandwich panels*

Such behavior may be explained by ratio between the wavelengths of vibrations and characteristic dimensions of the substructures. When the wavelengths of vibrations are large in comparison with characteristic dimensions of the substructure, then the whole volume of the substructure cells is subjected to approximately constant stress, as it is the case with solid panels. Therefore, the differences between shapes of the substructures have no influence on the amplitudes of low-frequency vibrations. On the other hand, when the wavelengths of vibrations are small, then various parts of the substructure cells are subjected to various stresses, and the shape of the substructure influences the amplitudes of the vibrations.

6. CONCLUSON

The presented research considered influence of geometric parameters on modal behavior of sandwich panels. Modal behavior of twenty-three types of sandwich panels was studied by numerical methods. One specific type, with the lowest mass density and comparatively small number of natural vibrations in the frequency range 0-3000 Hz was selected for further studies. The further studies consisted in analyses of influence of plate thickness, core wall thickness and panel width to frequencies of natural vibration modes of the sandwich panel.

The results have shown that the natural frequencies of the sandwich panel of the selected type have the highest natural frequencies when the plates are twice thicker than core walls. The dependency is more pronounced with thin sandwich panels and panels with thin core walls.

Increase of core wall thickness leads to decrease, and increase of the core width leads to increase of the natural frequencies of sandwich panels of the selected type.

The results also confirmed previous results [11] that the amplitudes of the natural vibrations depend on the shape of substructure when the wavelength of the vibrations is comparable to characteristic dimensions of the substructure.

ACKNOWLEDGEMENT

The authors wish to express their gratitude to Ministry for education, science and technology of Republic of Serbia for support through research grants TR35006.

REFERENCES

[1] Ćirić-Kostić, S., Ognjanović, M.: "The Noise Structure of Gear Transmission Units and the Role of Gearbox Panels." *FME Transactions* 35 (2), pp. 105-112, 2007.

[2] Zhou, J., Sun, W., Tao, Q.: "Gearbox Low-Noise Design Method Based on Panel Acoustic Contribution", *Mathematical Problems in Engineering*, vol. 2014, Article ID 850549, 10 pages, 2014.

[3] Kopp, G., Kuppinger, J., Friedrich, H.E., Henenning, F.: "Innovative Sandwich Structures for Functionally Integrated Lightweight Design", *ATZ worldwide*, Volume 111, Issue 4, pp. 44-49, 2009.

[4] Nilsson, E., Nilsson, A.C.: "Prediction and measurement of Some Dynamic properties of Sandwich Structures with Honeycomb and Foam Cores", *Journal of Sound and Vibration*, 251(3), pp. 409-430, 2002.

[5] Harish, R., Sharma, R.S.: "Vibration Response Analysis of Honeycomb Sandwich Panel with Varying Core Height", *International Journal of Emerging Technologies in Computational and Applied Sciences (IJETCAS)*, 13-433, pp. 582-586, 2013.

[6] McCarthy, D.L., Williams, C.B.: " Creating Complex Hollow Metal Geometries Using Additive Manufacturing and Electroforming ", *International Solid Freeform Fabrication Symposium*, pp. 108-120, 2012.

[7] Suman, D. et al. "Direct Laser |Freeform Fabrication of High Performance Metal Components." *Rapid Prototyping Journal* 4.3, pp.112-117, 1998.

[8] Tomlin, M., Meyer, J.: "Topology Optimization of an Additive Layer Manufactured (ALM) Aerospace Part." *The 7th Altair CAE Technology Conference*, pp.1-9, 2011.

[9] Additive manufacturing - Strategic Research Agenda 2014, AM Platform, 2014.

[10] www.eos.info

[11] Vranić, A., Ćirić-Kostić, S., Tatić, B.: "Influence of Sub-Structures' Shape on Vibration Behaviour of Sandwich Walls", Proceedings of the VIII International Conference Heavy Machinery – HM 2014, pp. E17-22, Kraljevo, Serbia, 2014.

University of Nis
Faculty of Occupational Safety
„Politechnica“ University of Timisoara
Faculty of Mechanical Engineering
24th International Conference
NOISE AND VIBRATION
Niš, 29 - 31. 10. 2014.

SOUND INSULATION OF A MECHANICAL WORKSHOP

Zoran Petrović[1], Branko Radičević[1], Milan Kolarević[1], Vladan Grković[1]

[1] University of Kragujevac, Faculty of Mechanical and Civil Engineering Kraljevo, Serbia, petrovic.z@mfkv.kg.ac.rs

Abstract - *The paper presents a design process related to sound insulation of a small mechanical workshop for storing eccentric presses, which is located in a densely populated housing estate. Starting from the theoretical model of acoustic insulation power of a single solid partition, a complex partition and a multi-layer partition, the acoustic insulation power of the walls and the ceiling in the workshop was determined. The results of calculation of workshop isolation coincide to a great extent with the experimental results of measuring noise levels.*

Keywords: *noise, mechanical workshop, sound insulation*

1. INTRODUCTION

Small production workshops are often located in business-residential zones. Analysis of their impact on the environment implies that they must fulfil certain noise requirements. Noise sources must not generate noise levels whose rating level exceeds limit values of noise indicators in the environment.

The paper is based on the request for designing acoustic protection of a workshop for storing two eccentric presses. The future workshop should be part of a business facility in a densely populated housing estate, where the façade of the next door neighbour is only 5 m away. The tendency was to organise the entire production process at one location because the production of parts on the eccentric presses had been dislocated due to the problem with noise. Such a manner of production had led to increased costs of production. Based on the preliminary design of sound insulation of the new workshop, the owner decided to invest some funds in sound insulation and consolidate the production process.

The acoustic quality of a building defined by a project task or only by corresponding standards is obligatorily controlled during its technical acceptance after the completion of construction. The basic standard in the field of acoustics in civil engineering, SRPS U.J6.201, defines the obligation of checking acoustic quality of buildings during their technical acceptance.

2. NOISE SOURCES

The eccentric press is a machine for deforming, in which the operating stroke of the eccentric press is accomplished through the eccentre which converts the circular motion of the drive shaft into the rectilinear motion of the tool. In the workshop, there are two eccentric presses driven by an electromotor. The torque is transmitted from the electromotor to the flywheel which serves to reduce impact loads. The flywheel is placed on the eccentric shaft and they rotate together. A joint which drives the eccentric press and converts the circular motion of the driving motor into the rectilinear motion of the tool is fixed to the eccentre of the shaft.

Small serial and medium serial production is most frequently realized in the workshop. The dominant operations are cutting and punching performed by using tools on the eccentric presses. Two eccentric presses whose nominal deformation forces are 800 KN and 500 KN are to be installed in the workshop.

The equivalent noise level measured at the distance of 0.7 m from the press is 95.8 dB(A).

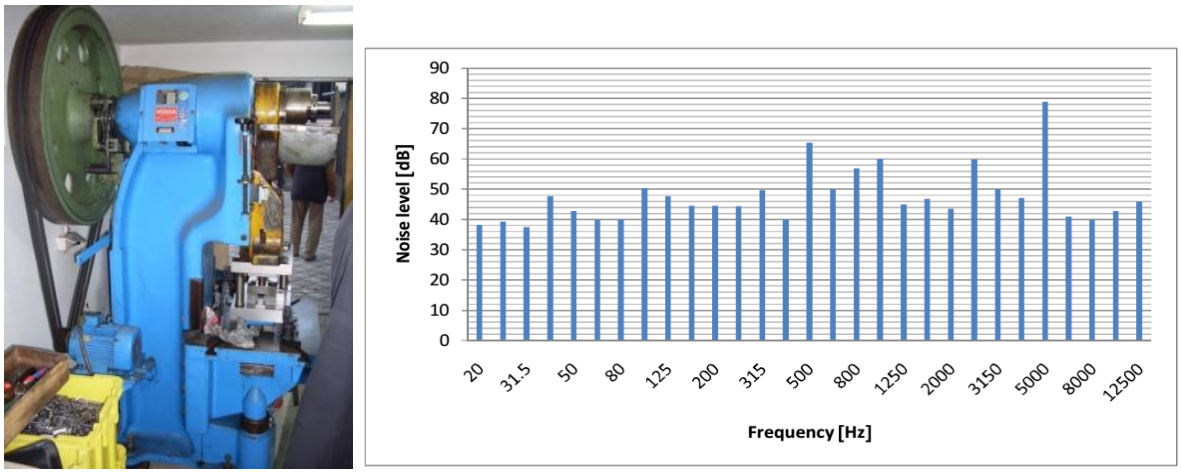

Fig. 1 *Eccentric press WÖGTLE (500 KN) and its frequency characteristic at individual operation*

3. METHODOLOGY OF ESTABLISHING SOUND INSULATION

The main procedure in reducing the isolation of any two rooms to a given value means establishing all paths of the passage of sound energy between them. Adequate interventions to a necessary exent can be allowed only by complete consideration of possible paths of sound passage. A lot of mistakes in solving sound protection have been the consequence of wrongly considered significance of certain paths of energy.

The minimum values of sound insulation R_w and maximum values of the level of impact sound L_w are given in the standard SRPS U.J6.201 for individual functions of partitions as a function of purpose of the building. The acoustic insulation power, R, is a value expressed in decibels and defined as the logarithm of the reciprocal value of the transmission coefficient τ (ratio of the sound energy transmitted through the partition to the total sound energy incident on it).

$$R = 10\log\frac{1}{\tau}\left[dB\right] \quad (1)$$

The acoustic insulation power of a solid partition at low frequencies can be approximately expressed by the following relation:

$$R = 20\log\left(f \cdot m_s\right) - 47\left[dB\right] \quad (2)$$

where:

f - the frequency

m_s – the surface mass of the partition.

It can be seen that the acoustic insulation power increases with the increase in the frequency and the partition mass. Due to the increase in the acoustic insulation power with the increase in the partition mass, the previous expression is often called ”the law of mass”. The acoustic insulation power of partitions is given in dB depending on the frequency.

3.1 Acoustic insulation power of a complex partition

Complex partitions are those partitions which include different elements or materials, e.g. a wall with an inserted window. The acoustic insulation power of a complex partition is determined by the acoustic insulation power of its weakest part, which means that there is no sense in making a partition of high acoustic insulation power if it will have inserted openings (doors and windows) whose acoustic insulation power is low.

The acoustic insulation power of a complex partition is determined by the expression:

$$R = 10\log\left[\frac{1}{\left(\frac{S_z / S_u}{10^{R_z/10}}\right) + \sum_{i=1}^{n}\left(\frac{S_{oi} / S_u}{10^{R_{oi}/10}}\right)}\right]\left[dB\right] \quad (3)$$

$$S_z = S_u - \sum_{i=1}^{n} S_{oi} \quad (4)$$

where:

S_u – the total area of the partition, m^2

S_o – the area of the opening, m^2

S_z – the pure area of the wall, m^2

R_z – the acoustic insulation power of the wall, dB

R_o – the acoustic insulation power of the opening, dB

3.2 Acoustic insulation power of a multi-layer partition

Multi-layer partitions consist of a certain number of solid partitions (walls) with an air gap. This gap is relatively narrow and the whole structure made of walls with the gap must be observed as a unit. These partitions are, for practical and economical reasons, most often made as double partitions. Double partitions, due to the air gap, have the resonant frequency. In the neighbourhood of resonance, the acoustic insulation power of these partitions is reduced, whereas above the resonant frequency it increases with the speed of 18 dB/ octave.

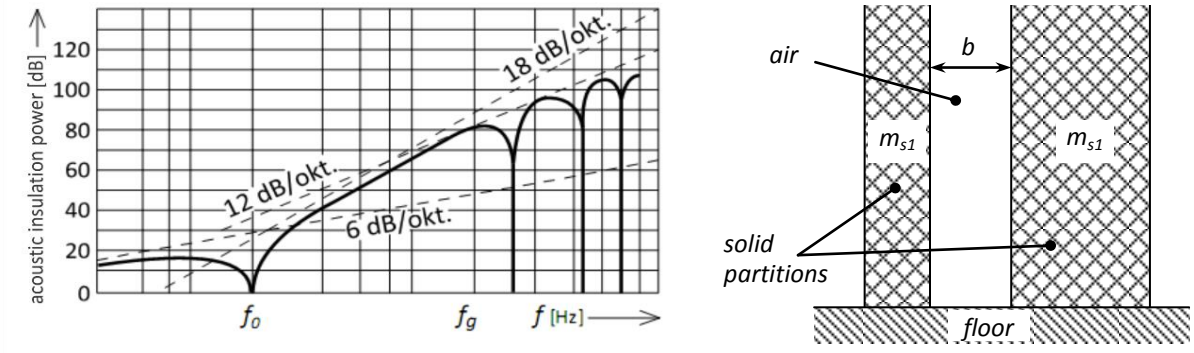

Fig. 2 *Diagram of the acoustic insulation power of a double partition as a function of frequency*

The double partition has the resonant frequency given by the expression:

$$f_0 = \frac{1}{2\pi}\sqrt{\frac{1{,}8 \cdot \rho \cdot c^2}{b}}\left(\frac{1}{m_{s1}} + \frac{1}{m_{s2}}\right) = 80{,}23\sqrt{\frac{m_{s1} + m_{s2}}{b \cdot m_{s1} \cdot m_{s2}}}\left[Hz\right] \quad (5)$$

where:

m_{s1} and m_{s2} - the surface masses of the partitions, kg/m^2

$$m_s = d \cdot m_t\left[kg/m^2\right] \quad (6)$$

where: d – the thickness of the partition in cm

m_t – the surface mass of the material $\left[kg/m^2, cm\right]$ (table value)

b - the distance between the partitions, m.

Below the resonant frequency, the acoustic insulation power is identical to the one of a solid homogeneous partition whose surface mass is equal to the sum of surface masses of individual partitions, i.e.

$$R \approx 20\log\left[f \cdot \left(m_{s1} + m_{s2}\right)\right] - 47 \ \left[dB\right] \qquad (7)$$

The acoustic insulation power below this frequency increases with the speed of 6 dB per octave.

It can be taken that the improvement of the acoustic insulation power due to the existence of a double partition structure approximately begins only at the frequency which is by an octave higher than the resonant frequency f_0 given by the expression (5).

With a further increase in frequency, the acoustic insulation power increases by 18 dB/oct. In this zone, the acoustic insulation power is proportional to the product of surface masses of individual partitions and distances between them, i.e.:

$$f_g = \frac{c}{2 \cdot \pi \cdot b} \approx \frac{55}{b} \left[Hz\right] \qquad (8)$$

At the frequency f_g, the acoustic insulation power is found from the relation:

$$R_{(f_g)} \approx R_1 + R_2 + 20\log\left(f \cdot b\right) - 29\left[dB\right] \qquad (9)$$

$$R_1 \approx 20\log\left(f \cdot m_{s1}\right) - 47\left[dB\right] \qquad (10)$$

$$R_2 \approx 20\log\left(f \cdot m_{s2}\right) - 47\left[dB\right] \qquad (11)$$

3.3 Isolation

The isolation between two rooms depends on the the acoustic insulation power of the partition, the area of the common wall and the total area of the reception room. The isolation can be determined by the expression:

$$D = R - 10\log\frac{S_{12}}{A_2}\left[dB\right] \qquad (12)$$

where:

D – the isolation

R – the acoustic insulation power of the partition

S_{12} – the area of the common wall

A_2 – the total absorption area of the other room

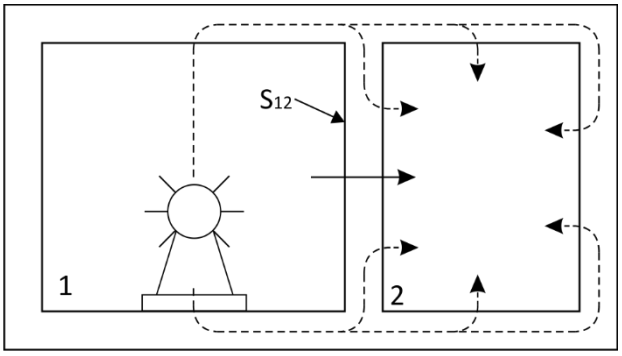

Fig. 3 *Paths of transmission of sound energy between two rooms*

The noise level in the reception room is calculated according to the expression:

$$L_2 = L_1 - D\left[dB\right] \qquad (13)$$

where:

L_1 – the noise level in the room where the source is placed

L_2 – the noise level in the reception room

4. CALCULATION OF THE SOUND INSULATION OF THE MECHANICAL WORKSHOP

Workshop – 1 is located in the business facility shown in Figure 4.

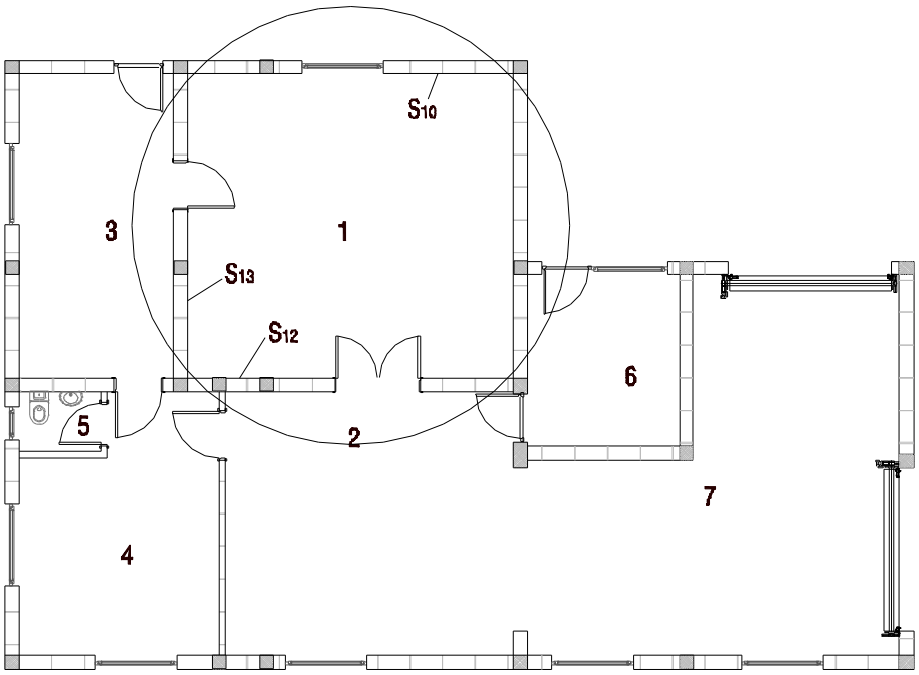

Fig. 4 *Base of the ground floor where the mechanical workshop is located*

The necessary isolation of walls of the mechanical workshop is determined for each wall depending on the purpose of the neighbouring rooms.

In the mechanical workshop, the critical wall is S_{1o} because it represents a complex partition with an inserted window. That wall borders its residential surroundings and represents a potential danger from the aspect of noise. The problem is enhanced by the fact that the facade of the closest residential unit is only 5 m away from the workshop window.

Table 1 *Rooms of the business facility*

Ord. no.	Name of the room	Floor treatment	Floor area [m^2]
1.	Mechanical workshop	reinforced concrete	33,57
2.	Workshop - 2	reinforced concrete	25.73
3.	Storeroom for wood	reinforced concrete	15.94
4.	Storeroom for coal	reinforced concrete	15.87
5.	Sanitary block	ceramic tiles	1.65
6.	Office	ceramic tiles	8.79
7.	Garage	reinforced concrete	38.35

4.1 Selection of materials for the walls

YTONG blocks were selected from the wall building materials that can be found in the market. The selection was done on the basis of price and acoustic insulation power. One wall of the workshop does not have any acoustic openings. The other three walls have a window, a single-wing door and double-wing door, as it is shown in Figure 3. The appearance of the selected block for walls is seen in Figure 5., and the main technical characteristics are presented in Table 2.

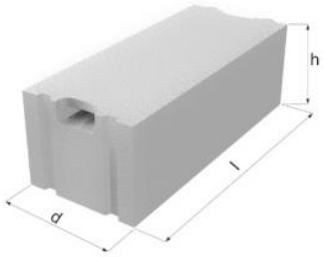

Fig. 5 *Appearance of YTONG block ZBZ 25** [8]*

Table 2 *Catalogue data for YTONG block ZBZ 25** [8]*

Type of materials	Label	Dimensions			Sound insulation [dB]
		l	d	h	
P-5,0/0,65	ZBZ 25**	625	250	200	52

The acoustic insulation power of the block is presented in Figure 6. It is a figure from the manufacturer's catalogue and it also presents the values of acoustic insulation power for other types of building blocks.

The blocks are manufactured in two variants of density. Blocks with higher density (marked by** in the manufacturer's catalogue) are used for the walls which reqiure higher acoustic insulation power. The block with the acoustic insulation power of 52 dB was selected (Figure 6.) for the walls of the mechanical workshop.

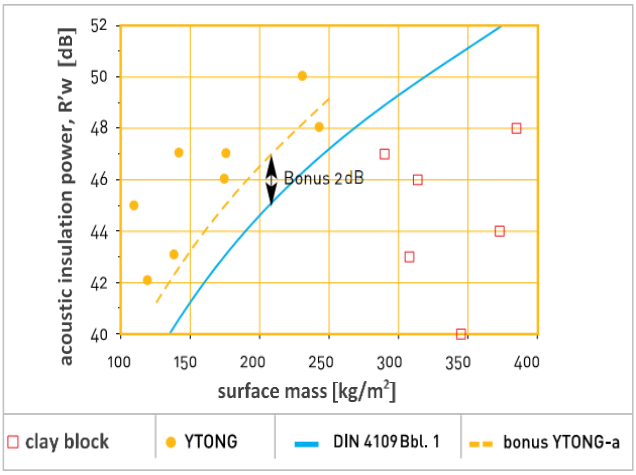

Fig. 6 *Values of the sound insulation RW for YTONG block ZBZ 25** [8]*

4.2 Acoustic insulation power of windows and doors

The calculation of acoustic insulation power of windows can be determined according to the expression:

$$R = 20\log d + 12\log(2.5 + b) + 25[dB] \qquad (14)$$

where:

d – the total thickness of the pane, cm

b – the distance between the panes

The window on the wall has three panes. The thickness of the pane is 4 mm, and the distance between the panes is 9 mm. The acoustic insulation power R of such a window is 36 dB.

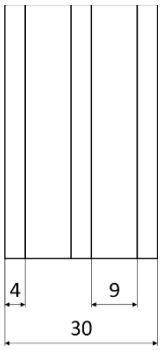

Fig. 7 *Three-chamber window (measures given in mm)*

Table 3 *Classification of windows and doors into classes of acoustic quality (according to the standard SRPS U.J6.201)*

WINDOWS		DOORS	
class	**acoustic insulation power [dB]**	**class**	**acoustic insulation power [dB]**
special class	> 40	special class	> 35
Class I	35 - 39	Class I	30 - 34
Class II	30 - 34	Class II	25 - 29
Class III	25 - 29	Class III	20 - 24
Class IV	20 - 24	/	/

According to Table 3, it can be concluded that the window belongs to Class I of acoustic quality.

4.3 Calculation of acoustic insulation power of the walls which represent complex partitions

In the mechanical workshop, three walls are realized as complex acoustic partitions. These walls have openings which are, in principle, always weak acoustic points. Openings reduce the value of acoustic insulation power, but they cannot be avoided because of the purpose of the room.

Table 4. presents the results of calculation of acoustic insulation power of complex partitions of the mechanical workshop. The values are determined according to the expressions (3) and (4).

Table 4 *Acoustic insulation power of the workshop walls which represent complex partitions*

Ord. no.	Opening	Designation of the wall	S_u [m^2]	S_z [m^2]	S_o [m^2]	R_z [dB]	R_o [dB]	R [dB]
1.	Window	S_{10}	18	16.77	1.28	52	36	46 (46.2)
2.	Single-wing door	S_{13}	16.8	14.91	1.89	52	30	39 (39.3)
3.	Double-wing door	S_{12}	18	9.52	8.48	52	30	33 (33.2)

Figure 8. presents the wall with an iserted window. The sizes of the wall and the window are given as well as the position of the window on the wall.

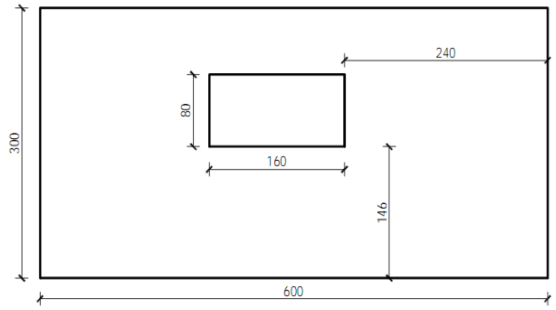

Fig. 8 *Wall with an inserted window*

4.4 Calulation of the acoustic insulation power of the ceiling

The ceiling is realized as a double partition which consists of brick with the thickness of 200 mm and the concrete screed with the thickness of 30 mm. The plates are completely mechanically and acoustically isolated from each other and the gap between them is filled with styropor with the thickness of 50 mm (Figure 9.). The surface mass of the blocks m_{s1} is 21 kg/m^2, and the surface mass of concrete is 23 kg/m^2.

Based on Figure 2 and the expressions (5) through (11), the necessary values which influence the acoustic insulation power of the multi-layer partition, in this case the ceiling, can be determined. The results of calculation are presented in Table 5.

Table 5 *Acoustic insulation power of the ceiling*

m_{s1}	m_{s2}	f_o	R	f_g	R_1	R_2	R_{fg}
[kg/m^2]	[kg/m^2]	[Hz]	[dB]	[Hz]	[dB]	[dB]	[dB]
420	69	46,6	37	1100	66,3	50,6	123

The acoustic insulation power R is calculated for the frequency of 31.5 Hz.

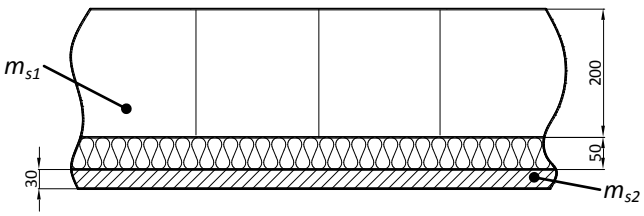

Fig. 8 *Ceiling in the mechanical workshop*

4.5. Isolation of the mechanical workshop

The isolation (D) from the neighbouring rooms of the mechanical workshop was calculated based on the calculated acoustic insulation power of the partitions (Rw), the area of the common walls (S_{1i}) and the total absorption area of the reception rooms.

Table 6 *Isolation of the mechanical workshop*

Connection between the rooms		R_w [dB]	S_{1i} [m^2]	A_2 [m^2]	D [dB]
workshop - 1	workshop - 2	33	15,9	112,5	41,2
workshop - 1	room - 3	39	16,8	82,6	45,9
workshop - 1	external environment	46	18	18	46

In the middle of the mechanical workshop in which two eccentric presses operate simultaneously, the noise level is 94 dB(A).

In the case of the mechanical workshop, it is most important to determine the noise level toward the external environment. The noise level in the reception room can be calculated based on the calculated isolation (Table 7.) and the measured noise level in the workshop. Since in this case there is no room, but an external environment, the noise level was measured directly on the window.

Table 7 *Isolation of the outer wall of the workshop*

Measuring point	Workshop	Window (theoretically)	Window (experimentally)
Noise level	[dBA]	[dB]	[dBA]
	94	48	47

As the workshop is located in the business-residential area (acoustic zone IV with the allowed values of noise indicators for daily conditions of 60 dBA, and 50 dBA for night conditions), its isolation is sufficient to provide the noise level in the environment within the allowed limits.

For experimental determination of the acoustic insulation power of each partition, it is necessary to perform measurement according to the standards SRPS ISO 717-1 and SRPS ISO 717-2.

5. CONCLUSION

The calculated values of acoustic insulation power of the walls of the mechanical workshop determined by theoretical models and the experimental results obtained by measurement of noise levels, after the completion of the mechanical workshop, coincide to a great extent. Based on this, it can be concluded that the theoretical model is adequate. The designed sound isolation of the workshop for storing eccentric presses provides such values of noise levels in the workshop environment that will not result in exceeding the limit values of noise indicators in the environment. Such a solution of sound protection can be applied in other similar cases of workshops which store machines that generate high noise levels.

Acknowledgement: The paper is a part of the research done within the project TR37020. The authors would like to thank to the Ministry of Education and Science of the Republic of Serbia for supporting this research.

REFERENCES

[1] Radičević B., Petrović Z., Todosijević S., Petrović Zv., „Design of noise protection of industrial plants – case study of a plywood factory “, 23rd National Conference & 4th International Conference “Noise and vibration”, Niš, 2012, pages 71-75

[2] Petrović, Z., Radičević, B.,Šoškić Z., Bjelić, M. - Zaštita od buke industrijski postrojenja - Buka i vibracije, XXI konferencija sa međunarodnim učešćem, Tara 2008

[3] Petrović Z., Radičević B., Bjelić M., „Designing main fan noise protection system in mine “Jarando“ – Baljevac“, Podzemni radovi, br.15, (133-138), Rudarsko geološki fakultet, Beograd, 2006

[4] Drinčić D., Pravica P., ”*Akustika – zbirka rešenih zadataka”*, Visoka škola elektrotehnike i računarstva strukovnih studija, Beograd, 2011

[5] Standard: SRPS ISO 1996-1: 2010, Opisivanje, merenje i ocenjivanje buke u životnoj sredini - Deo 1: Osnovne veličine i procedure ocenjivanja

[6] Standard: SRPS ISO 1996-2: 2010, Opisivanje, merenje i ocenjivanje buke u životnoj sredini - Deo 2: Određivanje nivoa buke u životnoj sredini

[7] Standard: SRPS U.J6.201: 1990, Akustika u građevinarstvu – Tehnički uslovi za projektovanje i građenje zgrada

[8] http://www.ytong.rs

[9] http://www.index-spa.com

University of Nis
Faculty of Occupational Safety
„Politechnica“ University of Timisoara
Faculty of Mechanical Engineering
24th International Conference
NOISE AND VIBRATION
Niš, 29 - 31. 10. 2014.

VIBRATION FEATURE EXTRACTION METHODS FOR GEAR FAULTS DIAGNOSIS -A REVIEW

Ninoslav Zuber[1], Rusmir Bajrić[2], Dragan Cvetković[3]

[1] Faculty of Technical Sciences, University of Novi Sad, Trg Dositeja Obradovića 6, Serbia
[2] Public enterprise Elektroprivreda BiH, Coal Mines Kreka, Mije Keroševica 1, Tuzla, BiH
[3] Faculty of Occupational Safety, University of Niš, Čarnojevića 10a, 18000 Niš, Serbia

Abstract - *The key point of condition monitoring and fault diagnosis of gearboxes is a fault feature extraction. The study of fault feature detection in rotating machinery from vibration analysis and diagnosis has attracted sustained attention during past decades. In most cases determination of the condition of a gearbox requires study of more than one feature or a combination of several techniques. This paper attempts to survey and summarize the recent research and development of feature extraction methods for gear fault diagnosis, providing references for researchers concerning with this topic and helping them identify further research topics. First, the feature extraction methods for gear faults diagnosis are briefly introduced, the usefulness of the method is illustrated and the problems and the corresponding solutions are listed. Then, recent applications of feature extraction methods for gear faults diagnosis are summarized, in terms of industrial gearboxes. Finally, the open problems of feature extraction methods for gear fault diagnosis are discussed and potential future research directions are identified. It is expected that this review will serve as an introduction summary of vibration feature extraction methods for gear faults diagnosis for those new to the concepts of its applications to gear fault diagnosis based on vibration.*

1. INTRODUCTION

Vibration diagnosis is the most commonly used technique to monitor the condition of gearboxes. Gearbox is one of the core component in rotating machinery and has been widely employed in various industrial equipments. Faults occurring in gearbox such as gears and bearings defects must be detected as early as possible to avoid fatal breakdowns of machines and prevent loss of production and human casualties. Vibration signal collected from these equipments during operation contains valuable information about the condition of machine condition. The vibration signal is often a compex signal which contains stationary, non-stationary and noisy components. Therefore, the information for maintenance decisions is not readily available from these vibration data unless the appropriate signal processing techniques are chosen [1]. Different fault diagnosis methods have been developed and used to detect and diagnose gear faults. One of the principal tools for diagnosing gear faults is the vibration-based analysis because of the ease of vibration measurements [2, 3]. By employing appropriate data analysis algorithms, it is feasible to detect changes in vibration signals caused by fault components, and to make decisions about the gearboxes health status [4] and gear fault evaluation. Feature extraction is a mapping process from the measured signal space to the feature space. Representative features associated with the conditions of machinery components should be extracted by using appropriate signal processing and calculating approaches [4]. Over the past few years, various techniques including Fourier transform (FT), envelope analysis (EA), wavelet transform (WT) and some other time frequency distributions were employed to processing the vibration signals [5, 6]. Based on these processing techniques, statistic calculation methods, autoregressive model (AR), singular value decomposition (SVD), principal component analysis (PCA) and independent component analysis (ICA) have been adopted to extracting representative features for machinery fault diagnosis [7]. Even though several techniques have been proposed in the literature for feature extraction, it still challenge in implementing a diagnostic tool for real-world monitoring applications because of the complexity of machinery structures and operating conditions. This paper attempts to summarize and review the recent research and development of feature extraction methods in fault diagnosis of gear faults. It aims to synthesize and place the individual pieces of information on this topic in context and provide references for researchers, helping them develop advanced research in this area.

2. FEATURE EXTRACTION

2.1.Time-domain feature extraction

The time-domain signal collected from a gearbox usually changes when damage occurs in a gear. Both, amplitude and content may be different from those of the time domain signal of a normal gear. Root mean square reflects the vibration amplitude and energy in time domain. Standard deviation, kurtosis, crest factor and shape factor may be used to represent the time series distribution of the signal in the time domain. First, five time-domain features, namely, standard deviation, root mean square, kurtosis, crest factor and shape factor, are calculated. They are defined as follows [8]:

(1) Standard deviation (STD)

$$\mathrm{STD} = \sqrt{\frac{1}{(n-1)}\sum_{i=1}^{n}(x_i - \bar{x})^2}$$

where x_i (i=1,…,n) is ith sampling point of the signal x; n is the number of points in the signal, and $\bar{x}$ is the average of the signal.

(2) Root mean square (RMS)

$$\mathrm{RMS} = \sqrt{\frac{1}{n}\sum_{i=1}^{n}(x_i)^2}$$

(3) Kurtosis (KR)

$$\mathrm{KR} = \frac{n\sum_{i=1}^{n}(x_i - \bar{x})^4}{\left(\sum_{i=1}^{n}(x_i - \bar{x})^2\right)^2}$$

(4) Crest factor (CF)

$$\mathrm{CF} = \frac{\max|x_i|}{\sqrt{\frac{1}{n}\sum_{i=1}^{n}(x_i)^2}}$$

(5) Shape factor (SF)

$$\mathrm{SF} = \frac{\sqrt{\frac{1}{n}\sum_{i=1}^{n}(x_i)^2}}{\frac{1}{n}\sum_{i=1}^{n}|x_i|}$$

Despite od traditional time domain signal analysis, advanced methods of gearbox vibration analysis deal with 5 different forms of vibration time waveforms: raw signal, time synchornized and averaged signal, residual signal, differential signal, bandpass filtered timewave – filtered around gearmesh frequency (Figure 1).

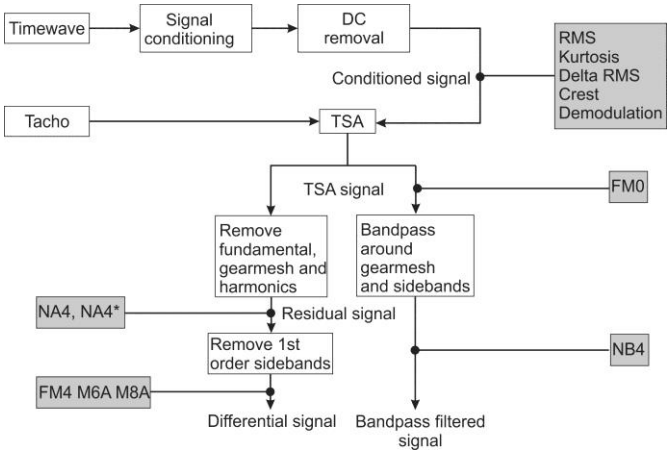

Figure 1. *Alghorithm for calculating different time domain features for gearbox failures detection*

Time Synchronous Averaging (TSA) is a fundamentally different process than the usual spectrum averaging that is generally used in FT analysis. While the concept is similar, TSA results in a time domain signal with lower noise than would result with a single sample. An FT can then be computed from the averaged time signal. The signal is sampled using a trigger that is synchronized with the signal. The averaging process gradually eliminates random noise because the random noise is not synchronous with the trigger signal. Only the signal that is synchronous and coherent with the trigger will persist in the averaged calculation. With TSA the result is a time domain signal with very low noise because the averaging is performed in the time domain, not the frequency domain. In addition it is posible to compute an FT of the averaged time signal resulting in a spectrum with low noise. When time domain averaging is computed on a vibration signal from a real machine, the averaged time record gradually accumulates the components of the signal that are synchronized with the trigger. Other components of the signal, such as noise and components from rotating parts of the machine are effectively averaged out. This is the only type of averaging that actually does reduce noise in the time domain. Another important application of time synchronous averaging is in the waveform analysis of machine vibration, especially in the case of gear drives. In this case, the trigger is derived from the tachometer that provides one pulse per revolution of a gear in the machine. This way, the time samples are synchronized in that they all begin at the same exact point related to the angular position of the gear. After performing a sufficient number of averages, spectrum peaks that are harmonics of the gear rotating speed will remain while non-synchronous peaks will be averaged out from the spectrum. As a typical features of the time synchnized signal the above mentioned parameters are used as well as another one, FM0 parameter. FM0 is defined as

(6) FM0

$$\mathrm{FM0} = \frac{PP_x}{\sum_{h=0}^{H} P_h}$$

where PP_x is the maximum peak-to-peak value of signal x, Ph is the amplitude of the hth harmonic of the meshing frequency, and H is the total number of harmonics considered.

After processing (Figure 1) other features are defined also.

(7) FM4

$$\mathrm{FM4} = \frac{n\sum_{i=1}^{n}(d_i - \bar{d})^4}{\left(\sum_{i=1}^{n}(d_i - \bar{d})^2\right)^2}$$

where d_i is the ith measurement of the difference signal of the signal x and $\bar{d}$ is the average of the difference signal. The shaft frequencies and their harmonics, the meshing frequencies and their harmonics, and all first-order sidebands are defined to be the regular meshing components. By removing the regular meshing components from signal x, the so called difference signal is generated. FM4 is actually the kurtosis of the difference signal. It is designed to complement FM0 by detecting damage isolated to only a limited number of teeth and supposed to work well for detection of initial faults.

(8) NA4

$$\mathrm{NA4} = \frac{\frac{1}{n}\sum_{i=1}^{n}(r_i - \bar{r})^4}{\left(\frac{1}{N}\sum_{j=1}^{N}\left(\frac{1}{n}\sum_{k=1}^{n}(r_{jk} - \bar{r}_j)^2\right)\right)^2}$$

where r_i is the ith measurement of the residual signal of time record x_i and $\bar{r}$ is the average of r_i, r_{jk} is the kth measurement in the jth time record residual signal r_j, $\bar{r}_j$ is the average of r_j, and N is the number of time records in a run ensemble. The complete data series collected is called a run ensemble. It is further divided into N time records each including n data points. The residual signal is generated by removing the regular meshing elements which include the shaft frequencies and their harmonics, and the meshing frequencies and their

harmonics. NA4 is created to overcome the shortcoming of FM4 that becomes less sensitive to the progression of fault in both number and severity. For this reason, it is supposed to be able to not only detect the onset of fault, as FM4 does, but also continue to react to the damage as it spreads and increases in magnitude.

(9) NB4

$$\mathrm{NB4} = \frac{\frac{1}{n}\sum_{i=1}^{n}(s_i - \bar{s})^4}{\left(\frac{1}{N}\sum_{j=1}^{N}\left(\frac{1}{n}\sum_{k=1}^{n}(s_{jk} - \bar{s_j})^2\right)\right)^2}$$

where s_{jk} is the kth measurement in the jth time record envelope s_j; s_j is the average of s_j, and N is the number of time records in a run ensemble. The theory behind NB4 is that the damage on gear teeth will cause transient load fluctuation that is different from that caused by normal teeth, and that this can be seen in the envelope of the signal.

(10) Energy ratio (ER)

$$\mathrm{ER} = \sqrt{\frac{\frac{1}{n}\sum_{i=1}^{n}(d_i)^2}{\frac{1}{n}\sum_{i=1}^{n}(d_i')^2}}$$

where d_i is the ith measurement of the difference signal, and d_i' is the ith measurement of the regular meshing components, which include the shaft frequencies and their harmonics, the meshing frequencies and their harmonics, and all first-order sidebands. ER is defined as the ratio of the root mean squares between the difference signal and the signal containing only regular meshing components.

(11) Energy operator (EOP)

$$\mathrm{EOP} = \frac{n\sum_{i=1}^{n}(re_i - \bar{re})^4}{\left(\sum_{i=1}^{n}(re_i - \bar{re})^2\right)^2}$$

where r_{ei} is the ith measurement of the resulting signal re, and $\overline{re}$ is the average of the resulting signal. The energy operator is then computed by taking the kurtosis of the resulting signal.

2.2. Frequency-domain feature extraction

Four frequency-domain feature parameters are extracted from the frequency spectrum of a gear vibration signal in this work. These frequency-domain parameters may contain information that is not present in the time-domain feature parameters. They are defined as follows[9]:

(1) Mean frequency (MF)

$$\mathrm{MF} = \frac{1}{K}\sum_{k=1}^{K} X_k$$

where X_k s the kth measurement of the frequency spectrum of signal x and K is the total number of spectrum lines.

(2) Frequency center (FC)

$$\mathrm{FC} = \frac{\sum_{k=1}^{K} f_k X_k}{\sum_{k=1}^{K} X_k}$$

where f_k is the frequency value of the kth spectrum line and X_k is the kth measurement of the frequency spectrum.

(3) Root mean square frequency (RMSF)

$$\mathrm{RMSF} = \sqrt{\frac{\sum_{k=1}^{K} f_k^2 X_k}{\sum_{k=1}^{K} X_k}}$$

(4) Standard deviation frequency (STDF)

$$\mathrm{STDF} = \sqrt{\frac{\sum_{k=1}^{K}(f_k - FC)^2 X_k}{\sum_{k=1}^{K} X_k}}$$

MF indicates the vibration energy in the frequency domain. FC and RMSF show the position changes of the main frequencies. STDF describes the convergence degree of the spectrum power.

2.3. Time–frequency-domain feature extraction

In Sections 2.1 and 2.2, the time and frequency-domain features are extracted from the vibration signals, respectively. In order to acquire additional characteristic information of gear damage, advanced signal processing techniques are used. Gearboxes often operate under some small fluctuation around nominal load/speed conditions during their normal service. These fluctuations result in a variation of both the modulations and their carrier frequencies (gear mesh harmonics) that blurs the sideband components in the spectra of the vibration measurement, often making it difficult to be recognized [10]. Such smearing effect can be abated by the order tracking technique or the time synchronous averaging (TSA) that acquires the measurements synchronized at identical angle increment instead of the identical sampling period. Although TSA is a well-established technique for analyzing gearbox vibration signals its commercial implementation is limited because of the requirement for additional shaft mounted encoders to provide a measure of shaft angular position and sophisticated interpolation algorithms to resample the vibration data. Since such equipment and resources lead to increased cost to applications, they are usually absent in most industrial applications. In such cases, the conventional method is to extract the measurement over a shorter time duration using a sliding window during which the gearbox is presumed to operate under stationary condition. However, these shorter length vibration signals are usually analyzed using Fourier transforms that has limitations such as the limited frequency resolution and spectral leakage, while the small operational speed oscillations continue to exist [11]. To avoid the extra cost incurred in implementation of TSA and shortcomings of the Fourier transform based analysis, a time domain methods wavelet transform (WT) was recently employed.

WT is a relatively new and powerful tool in the field of signal processing, which overcomes problems that other techniques face, especially in the processing of non-stationary signals. WT is not a self-adaptive signal decomposition method essentially [12]. Combet and Gelman have proposed optimal denoising, using Wiener filter based on the spectral kurtosis

(SK) methodology, to enhance the small transients in gear vibration signals, in order to, detect local tooth faults such as pitting at early stage [13]. The problem of local fault detection in gears can be related to the more general problem of transient detection in a signal. In that purpose, a SK detection technique has been proposed [14]. The SK is a tool sensitive to non-stationary patterns in a signal and that can indicate at which frequencies those patterns occur. Furthermore, the SK can be used to design detection filters that adaptively extract the fault signal from the noisy background [13]. From the SK-based filtered residual signal, called the SK-residual, it is possible to define the local power as the smoothed squared envelope, which can be interpreted as the sum of the time-frequency energy distribution weighted by the values of the SK at each frequency, and so by the degree of non-stationary of the transients [13]. Wang [15] proposed to apply the resonance demodulation technique which was based on envelope analysis of the residual signal after band-pass filtering within an excited resonance. Multiwavelet denoising techniques suffer from such main drawbacks as the fixed basis functions independent of the input dynamic response signals and the universal threshold denoising [16]. This may lead to the loss of some critical but relatively weak information in the fault feature detection [16]. In order to overcome the above limitations for effective gear fault detection, a novel method incorporating the customized multiwavelet lifting schemes with sliding window denoising is proposed by the same authors. Proposed method outperforms various wavelet methods as well as SK [16].

Higher order cumulant (HOC) analysis is a new technology, which has been developed rapidly in recent years, that could be an important tool for the processing of non-Gaussian signals, nonlinear signals and the blind signal. Using [17] the HOC method, this paper analyzes signal features of a gear system with a single fault and complex fault. As the spectrum characteristics of the various faults are different they can be identified from them. The results show that the method has a notable advantage in detecting the secondary phase and higher order phase coupling characteristics of the vibration signal, and is an effective method of fault diagnosis for gear system. The effectiveness of the method under low running conditions is good, however it decreases in the high speed state, due to each order multi-frequency generated by the meshing frequency relating to the rotating speed that participate in the secondary and higher order phase coupling vibration. In the low speed state, the peaks are mainly concentrated in the low-frequency zone and the fault type is easily identified. As the speed increases the fault feature become less obvious and the distinguishing degree of various faults is reduced.

Based on the versatility and flexibility of Overcomplete rational dilation discrete wavelet transform (ORDWT), a fault feature extraction technique is proposed. The proposed technique [18] is applied in a range of engineering applications to extract fault features of various characteristics, including periodical impulses, AM/FM contents and transient vibration contents masked by overwhelming noise. In the diagnostic process, ORDWT is used as a pre-processing signal decomposition tool, and other auxiliary signal processing approaches are employed to post-process the reconstructed wavelet sub bands of the vibration signals according to specific analysis demands.

3. CONCLUSION

This paper provides a review of the literature, progress and changes over the years on feature extraction for fault detection of gears using vibration signal processing techniques. Time feature extraction methods try to offer more direct approach; however all of them do some sort of averaging on the signal, which might suffer loss of time information. This is a disadvantage when operating with signals that have very short duration or suddenly occurring component, like a signal generated from faulty gears. Time-frequency technique are more advanced in localization of nonstationary gear fault feature from one point but from another point they are more complicate to implement in practice. To date, various types of feature extraction methods have been proposed. However, the question of how to choose a suitable one among them to match the signal structure remains an open issue.

REFERENCES

[1] H. Hong, M. Liang, Separation of fault features from a single-channel mechanical signal mixture using wavelet decomposition, Mechanical Systems and Signal Processing, 21 (2007) 2025-2040.

[2] E.B. Halim, M.A.A. Shoukat Choudhury, S.L. Shah, M.J. Zuo, Time domain averaging across all scales: A novel method for detection of gearbox faults, Mechanical Systems and Signal Processing, 22 (2008) 261-278.

[3] M.A. Jafarizadeh, R. Hassannejad, M.M. Ettefagh, S. Chitsaz, Asynchronous input gear damage diagnosis using time averaging and wavelet filtering, Mechanical Systems and Signal Processing, 22 (2008) 172-201.

[4] B. Li, P.-l. Zhang, H. Tian, S.-s. Mi, D.-s. Liu, G.-q. Ren, A new feature extraction and selection scheme for hybrid fault diagnosis of gearbox, Expert Systems with Applications, 38 (2011) 10000-10009.

[5] J. Lin, L. Qu, FEATURE EXTRACTION BASED ON MORLET WAVELET AND ITS APPLICATION FOR MECHANICAL FAULT DIAGNOSIS, Journal of Sound and Vibration, 234 (2000) 135-148.

[6] R.B. Randall, J. Antoni, S. Chobsaard, THE RELATIONSHIP BETWEEN SPECTRAL CORRELATION AND ENVELOPE ANALYSIS IN THE DIAGNOSTICS OF BEARING FAULTS AND OTHER CYCLOSTATIONARY MACHINE SIGNALS, Mechanical Systems and Signal Processing, 15 (2001) 945-962.

[7] W. Li, T. Shi, G. Liao, S. Yang, Feature extraction and classification of gear faults using principal component analysis, Journal of Quality in Maintenance Engineering, 9 (2003) 132-143.

[8] Y. Lei, M.J. Zuo, Z. He, Y. Zi, A multidimensional hybrid intelligent method for gear fault diagnosis, Expert Systems with Applications, 37 (2010) 1419-1430.

[9] Y. Lei, Z. He, Y. Zi, Q. Hu, Fault diagnosis of rotating machinery based on multiple ANFIS combination with GAs, Mechanical Systems and Signal Processing, 21 (2007) 2280-2294.

[10] C. Li, M. Liang, Time–frequency signal analysis for gearbox fault diagnosis using a generalized synchrosqueezing transform, Mechanical Systems and Signal Processing, 26 (2012) 205-217.

[11] L. Hong, J.S. Dhupia, A time domain approach to diagnose gearbox fault based on measured vibration signals, Journal of Sound and Vibration, 333 (2014) 2164-2180.

[12] J. Cheng, D. Yu, J. Tang, Y. Yang, Application of frequency family separation method based upon EMD and local Hilbert energy

spectrum method to gear fault diagnosis, Mechanism and Machine Theory, 43 (2008) 712-723.

[13] F. Combet, L. Gelman, Optimal filtering of gear signals for early damage detection based on the spectral kurtosis, Mechanical Systems and Signal Processing, 23 (2009) 652-668.

[14] J. Antoni, The spectral kurtosis: a useful tool for characterising non-stationary signals, Mechanical Systems and Signal Processing, 20 (2006) 282-307.

[15] W. Wang, EARLY DETECTION OF GEAR TOOTH CRACKING USING THE RESONANCE DEMODULATION TECHNIQUE, Mechanical Systems and Signal Processing, 15 (2001) 887-903.

[16] J. Yuan, Z. He, Y. Zi, Gear fault detection using customized multiwavelet lifting schemes, Mechanical Systems and Signal Processing, 24 (2010) 1509-1528.

[17] R. Shao, W. Hu, X. Huan, L. Chen, Multi-damage feature extraction and diagnosis of a gear system based on higher order cumulant and empirical mode decomposition, Journal of Vibration and Control, (2013).

[18] B. Chen, Z. Zhang, C. Sun, B. Li, Y. Zi, Z. He, Fault feature extraction of gearbox by using overcomplete rational dilation discrete wavelet transform on signals measured from vibration sensors, Mechanical Systems and Signal Processing, 33 (2012) 275-298.

Tehničko Razvojni Centar, TRCpro
Preradovićeva 31, 21131 Petrovaradin
tel/fax: 021/6433-774, 021/6433-824
email: ninoslav.zuber@trcpro.rs
web: www.trcpro.rs
Kontakt: Dr Ninoslav Zuber +381 64 6404323

TRCpro BUKA I VIBRACIJE

TRCpro partneri u oblasti buke i vibracija:

01dB acoustics & vibration METRAVIB technologies
Akustika i vibracije
www.01db-metravib.com

Damalini Measurement And Alignment Technology
Lasersko centriranje
www.damalini.com

METRIX INSTRUMENT CO.
Senzori i transmiteri
www.metrix1.com

mobius
Obuka vibrodijagnostičara
www.ilearninteractive.com

Senzori

Davači ubrzanja, brzine i pomeranja
-jednoosni -piezoelektrični
-troosni -piezorezistivni
-proximity probe (klizni ležajevi)
Oprema
-udarni čekići za modalnu analizu
-kalibratori davača ubrzanja i kalibratori zvuka
Mikrofoni

On-line monitoring vibracija

Jednostavni low cost vibro-switcheri za zaštitu mašina
-mehanički -elektronski -1 ili 2 - kanalni

Online višekanalni sistemi za zaštitu mašina
- funkcija zaštite, nadzora i dijagnostike stanja na bazi merenja vibracije, temperature i stanja ulja

MVX 16/24/32
Višekanalni sistem za praćenje vibracija i zaštitu mašina.Sinhrono praćenje svih kanala u realnom vremenu. Strategijska akvizicija uz defincju više kombinacija radnih uslova i nivoa alarma.

Offline periodični monitoring vibracija

MVP - 200
Izuzetan prenosivi sistem za prikupljanje podataka (rutiranje), analizu, balansiranje i analizu redova. Pored dva kanala za merenje vibracija, sadrži integrisan senzor za beskontaktno merenje temperature i broja obrtaja, kao i mogućnost identifikacije mernog mesta. Komande i na srpskom jeziku!!!

XPR - 300
Softver za prediktivno održavanje na bazi merenja i analize vibracija, stanja ulja, termovizije i procesnih parametara (OPC). Podržava online i offline sisteme. Verzije: desktop, client/server, web server aplikacija.

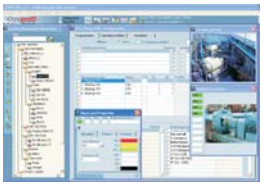

Lasersko centriranje i geometr. merenja

Sistem karakteriše robusnost i lakoća korišćenja. Tačnost metode je 1μm! Program obuhvata:centriranje vratila, geometrijska merenja (pravosti, ravnosti, normalnosti, paralelnosti), poravnanje remenica i lančanica.

Višekanalni PC akvizicioni sistemi

Orchestra

NetdB

Vrhunski višekanalni sistemi za najnaprednija merenja i analize (modalna analiza, ODS) podržani dbFA32 i MeScope softverom. Simultana akvizicija na svim mernim kanalima. Broj kanala neograničen. Merni pretvarači: akcelerometri, termoparovi, mikrofoni, merne trake... Veza sa PC-em: LAN, FireWire.

Prenosivi merači nivoa buke (SLM)

SOLO
Uređaj visokih performansi za sve oblasti akustike. Karakterišu ga veliki ekran, mogućnost praćenja više različitih parametara, velika memorija i dug vek baterije. Primena:
-zaštita okoline (praćenje buke u gradovima, usled drumskog, železničkog ili aero saobraćaja...)
-zdravlje i bezbednost (praćenje buke u pogonima i radnim mestima)
-akustika građevinskih objekata
-industrija (razvoj proizvoda, kontrola kvaliteta...)

Prenosivi analizatori humanih vibracija

MAESTRO
Aplikacije:
- analiza uticaja vibracija na celo telo (3 kanala)
- analiza uticaja vibracija na šaku (3 kanala)
- analiza nivoa buke (1 kanal)
- analiza opštih vibracija (1 kanal)

Mapiranje buke

Usluge

TRCpro, kao specijalizovana kuća za poslove merenja, analize, upravljanja i softvera na složenim tehničkim sistemima, sa bogatim iskustvom, Vam nudi svoje usluge u oblasti kako pojedinačnih, specijalnih merenja, tako i u oblasti permanentnog nadzora svih vitalnih postrojenja u sklopu Vaših pogona, izveštavanje o stanju postrojenja u radu, kao i sve dodatne aktivnosti balansiranja u sopstvenim ležajevima, lasersko poravnavanje i centriranje i slično.

I JOŠ MNOGO TOGA... KONTAKTIRAJTE NAS ZA DETALJE!

University of Nis
Faculty of Occupational Safety
„Politechnica“ University of Timisoara
Faculty of Mechanical Engineering
24th International Conference
NOISE AND VIBRATION
Niš, 29 - 31. 10. 2014.

PSEUDORANDOM VIBRATION TEST MACHINE

Ramona Nagy[1], Karoly Menyhardt[1], Remus Stefan Maruta[1]

[1] Politehnica University Timisoara, Faculty of Mechanical Engineering, Romania, ramona.nagy@upt.ro

Abstract - *The aim of this paper is to present the conversion of an oscillating equipment into a fatigue testing machine with pseudorandom vibrations. A kinematic study is given in detail. Fatigue testing is an expensive and long term test, not being the most accurate one, due to the fact that the functioning of any machine is not repetitive nor reproducible regarding vibrations. Random vibration tests are an efficient and rapid alternative, using only a fraction of the time needed for classical fatigue tests.*

There are a variety of finite element method software that simulate rather than analyze random vibrations. The results of the simulation, based on mathematical apparatus that is limited by the generation of values more or less random, cannot be compared with data gathered from a real physical test.

Thus, it was considered necessary the engineering of an adequate testing equipment, with a high fidelity response and a low inertia. Electro-magnetic shakers are very sensitive but, can only be used for low masses. For high masses, hydraulic, pneumatic or mechanical machines with increased power are needed.

For various motives, we opted for the conversion of a mechanical vibroimpact machine, which through a variable speed controller can (re)produce vibrations with velocity, acceleration and jerk similar to those from real life. In this case, the modified parameter is the frequency, generated by a computer programmed for constant, random or imposed workflow. The stages for the creation of this machine together with some of the results are presented in this article.

1. INTRODUCTION

Fatigue failures can occur quite suddenly with catastrophic effects, regardless of the material (metal, ceramic, polymer) structure, complexity or destination. The process occurs with the initiation and propagation of cracks, mostly when the fracture surface is nearly perpendicular to the direction of maximum tensile stress.

Vibration fatigue describes a material fatigue caused by forced vibration of random nature. Randomness implies a non-order in a sequence of numbers and the association of a function to a curve should be impossible. The excited structure responds proportionally to its natural-dynamics modes, which results in a dynamic stress load in the material [1]. Thus the process is governed by the shape of the excitation profile and the response it produces. For a random process, the amplitude cannot be described as a function of time, because of its probabilistic nature.

Random vibration tests are usually performed with the aid of a finite element method software. Commercial or noncommercial finite element method software include limited capabilities to perform probabilistic structural static or dynamic analyses with little post-processing [2]. A physical test is the closest thing to reality that can imitate and evaluate the functioning of a module. There are three types of possible fluctuating stress-time modes possible: completely reversed constant amplitude, repeated constant amplitude and random stress level amplitude and frequency.

As vibration testing evolved, methods that better represent real world data were researched, random vibration testing providing statistical confidence with random time data that has an average targeted frequency content and amplitude. By controlling frequency and amplitude, test data can be correlated to real world data sets [3][4].

Initially employed for the aerospace industry, random vibration data can be used for automotive applications.

Applications range from production stress screening of electronic components to prototype testing. Because of globalization, a critical factor is the transportation and handling of the various parts, sensible to vibrations induced by the irregularities in the road track (Fig.1), even before the test object is put in service. This is an offline possible cause of failure that also must be taken in consideration and tested for [5].

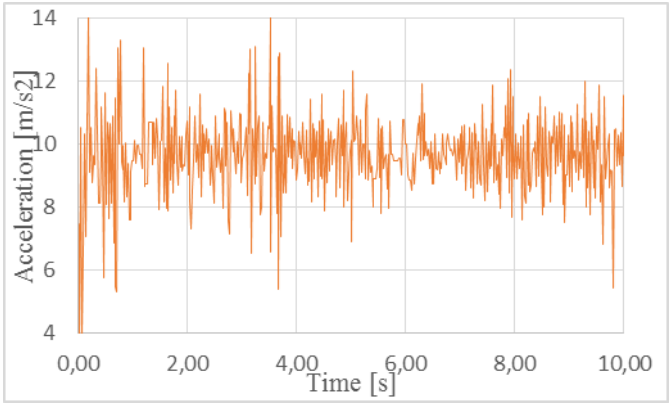

Fig. 1 - *True random vibration due to road irregularities*

2. CONSTRUCTIVE SOLUTIONS

The earliest testing machines, Fig.2, used a crank mechanism. The main disadvantage was the lack in control of variable amplitude *x* and frequency *f*.

The amplitude can be modified offline by varying the length of the OA crank (Fig.3).

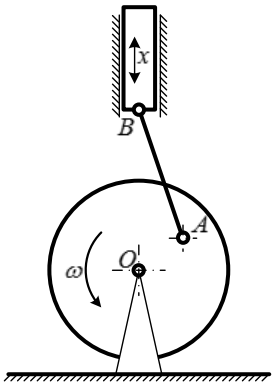

Fig. 2 - *Classical sinusoidal test machine*

This was primarily used to determine the resonance frequency by varying the angular velocity ω.

Fig. 3 - *Mechanical oscillator*

An electric alternative to this approach is the electrodynamical vibrator – shaker. This has the dissadvantage of relatively low amplitude and high energy consumption for increased tested weights. It could be combined to result a solution as seen in Fig.2.

The amplitude x_e is controlled by the magnetic flux passing through the coil and influence the amplitude *x* of the tested object.

A computer generated random signal is fed into the electrodynamical shaker and the amplitude x_e overlapped with the phase of the *OA* crank would result in an amplitude *x* acting on the target object close to a random vibration.

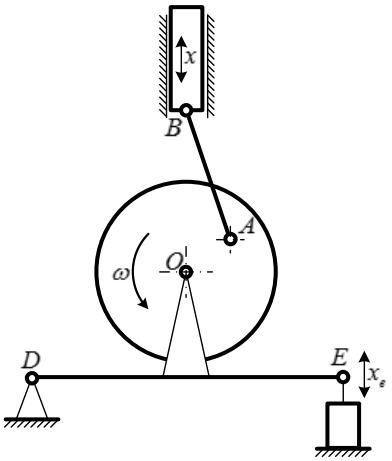

Fig. 4 - *Hybrid vibrator*

This model has the dissadvantage that the electrodynamic vibrator cannot displace a large weigth, consisting from the rotor, crank mechanism and the tested equipment.

The third model, Fig.4, is similar to the previous one but, the crank mechanism is sustained by air cushions. In this case, the resulting vibration is influenced by the velocity of the rotor, the electrodynamic vibrator and the air pressure inside the air cushions. Thus, the result is not so predictable because the pressure inside the air cushions is difficult to quantify. This is why we considered for this model a supplementary spring and damper.

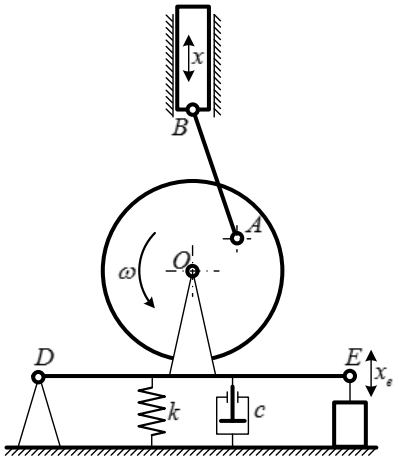

Fig. 5 - *Hybrid air cushion vibrator*

3. KINEMATIC STUDY OF THE TEST MACHINE

For the model from Fig.2 the law of motion of the tested object is subject to:

$$x = \ell \sin \omega t \qquad (1)$$

where $\ell = OA$ is constructively variable $\ell \in [0;200]mm$, being the length of the crank and ω is the constant angular velocity of the rotary motor at any given time t. This model is used for the study of vibrations with large and very large amplitudes, high accelerations $a_{\max} = \omega^2 \ell$, due to the mass

of the piston (5 kg), resulting for a revolution of 300 rpm, frequency of 5Hz a force of 2kN.

The horizontal component is considered to be negligeable.

$$x = \ell\cos(\omega t + \varphi) + A\cos(\omega_e t + \varphi_e) \qquad (2)$$

Where A is the amplitude of the dynamic vibrator and $\omega_e = 2\pi f_e$, f_e its frequency, φ, φ_e are the phase shifts for the rotary motor and the electrodynamic oscillator.

This law of motion can be written as:

$$x = a\cos(\omega_f t + \varphi_f) \qquad (3)$$

where

$$a = \ell^2 + A^2 + 2\ell A\cos\left[(\omega_e - \omega)t\right]$$

$$\operatorname{tg}\varphi_f = \frac{\ell\sin\left(\varphi - \frac{(\omega_e-\omega)t}{2}\right) + A\sin\left(\varphi_2 + \frac{(\omega_e-\omega)t}{2}\right)}{\ell\cos\left(\varphi - \frac{(\omega_e-\omega)t}{2}\right) + A\cos\left(\varphi_2 + \frac{(\omega_e-\omega)t}{2}\right)}$$

$$\omega_f = \frac{\omega + \omega_e}{2}$$

Depending on the ratio between the size of the crank and displacement of the electrodynamic vibrator there are three scenarios:

a) the amplitude of the crank is larger than the amplitude of the shaker, in which case the overall harmonic envelope remains, as seen in Figs.6-8

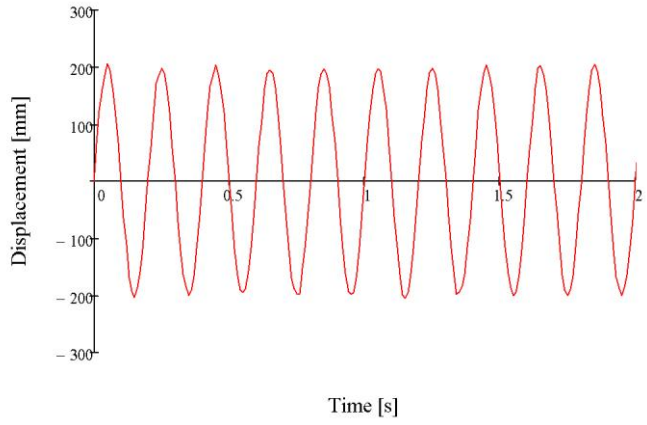

Fig. 6 – *Near harmonic displacent of the plater*

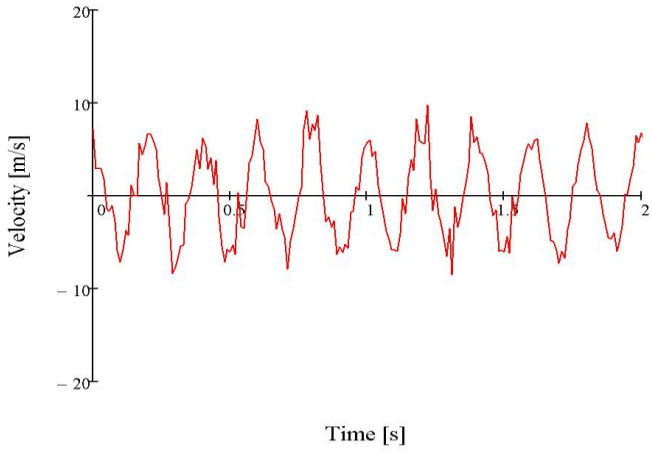

Fig. 7 - *Near harmonic velocityof the plater*

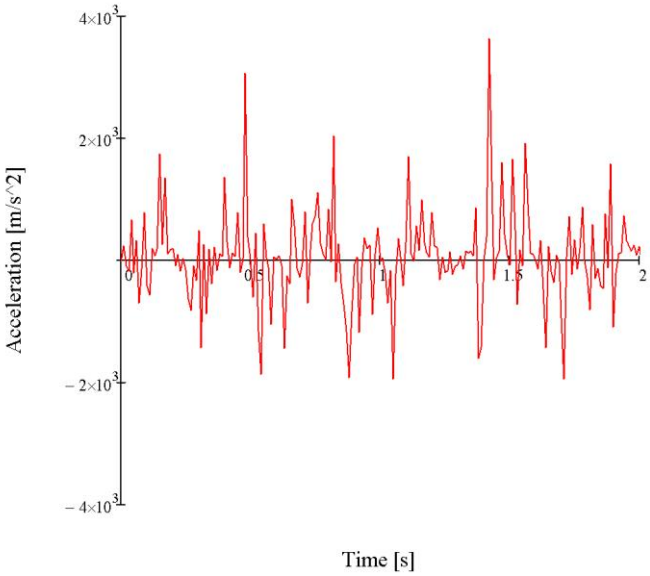

Fig. 8 - *Acceleration of the plater*

b) the amplitude of the crank is about the same as the amplitude of the shaker, in which case the overall harmonic envelope still remains, as seen in Figs.9-11.

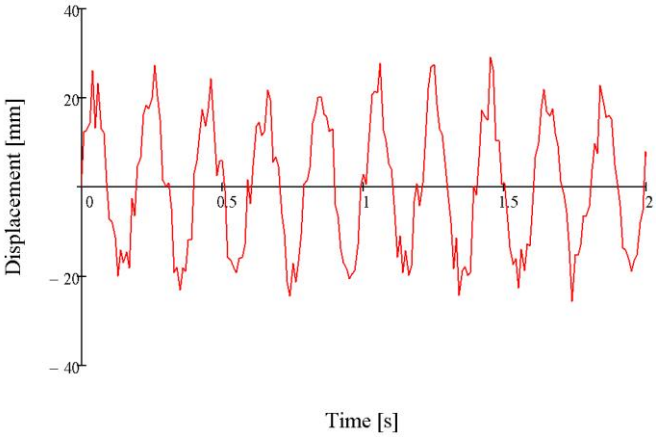

Fig. 9 – *Disturbed displacement of the plater*

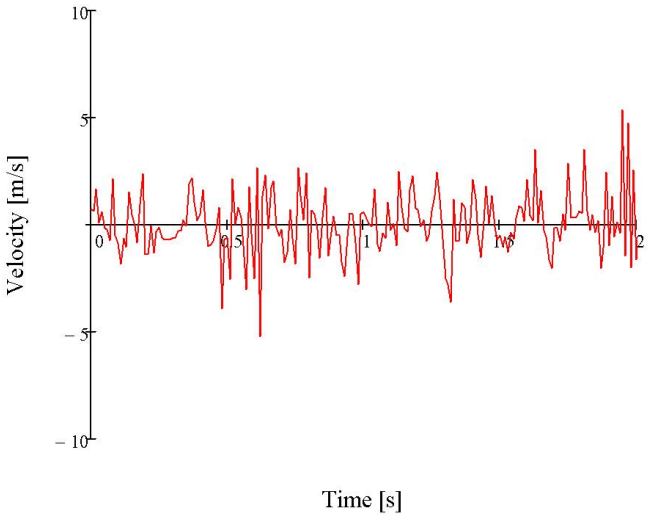

Fig. 10 – *Disturbed velocity of the plater*

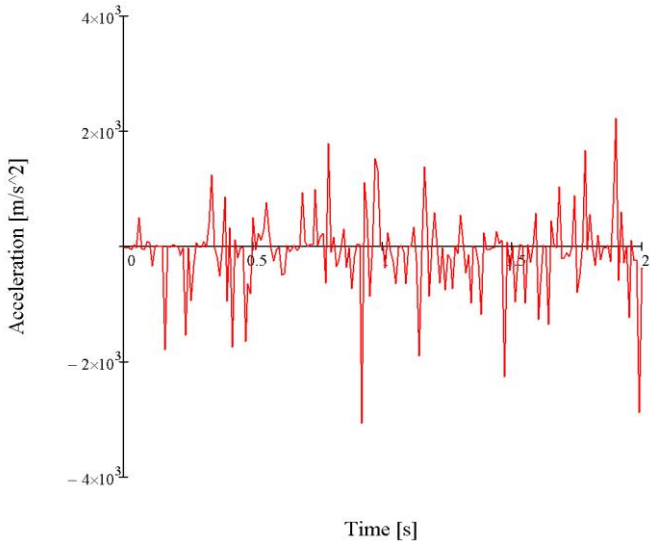

Fig. 11 – *Disturbed acceleration of the plater*

c) the amplitude of the crank is smaller than the amplitude of the shaker, in which case the pseudorandom factor starts to appear, depending on the input signal of the electrodynamic vibrator, as seen in Figs.12-14.

This comes with a price: the force as a function of acceleration depends on the displacent of the tested object.

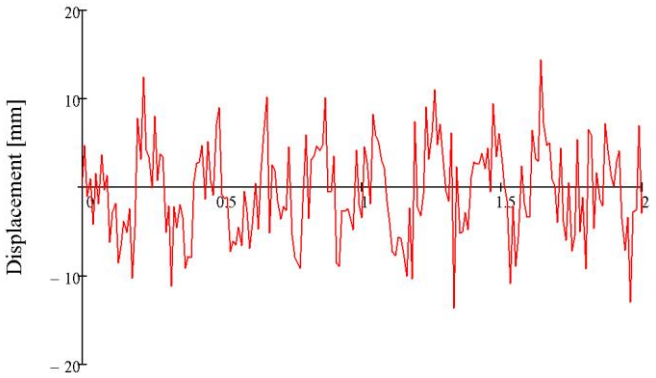

Fig. 12 – *Random displacement of the plater*

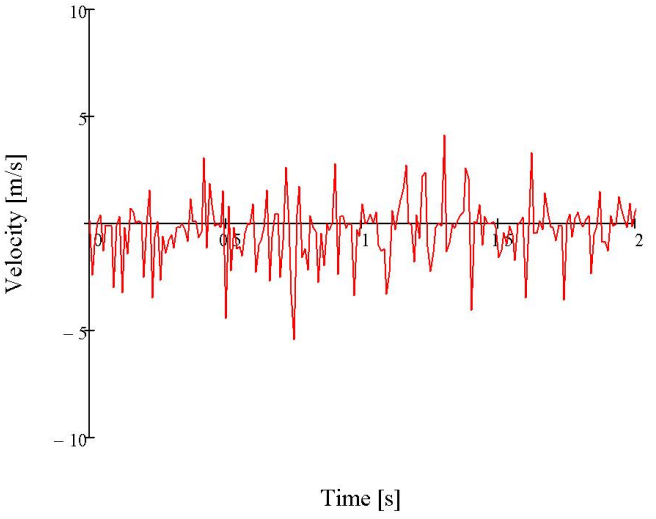

Fig. 13 – *Random velocity of the plater*

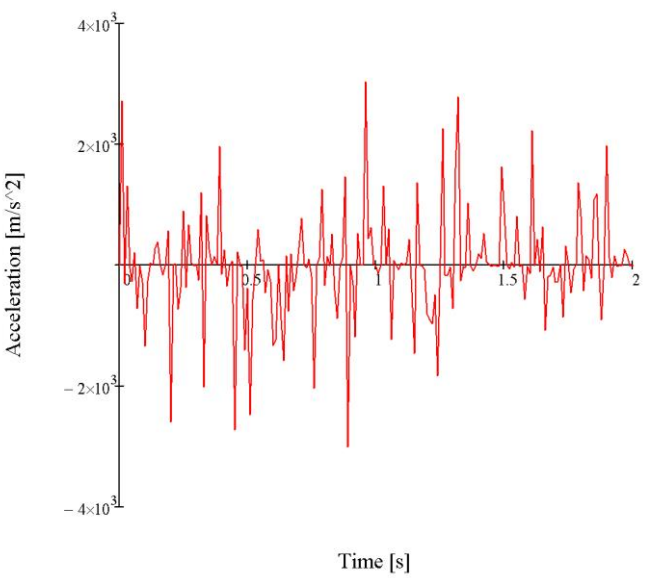

Fig. 14 – *Random acceleration of the plater*

4. CONCLUSIONS

To generate random vibrations the crank length must be as small as possible and not be greater than the amplitude of the shaker.

Experimentally can be shown that the maximum acceleration can be increased with a higher angular velocity for the mechanical oscillator or a higher frequency in the electrodynamic vibrator. Due to safety reasons, limiters must be placed to avoid destruction of the electrodynamic vibrator because there is the possibility for the oscillations to be in antiphase.

Because of high acceleration and jerk, it is necessary to develop high quality fixtures and guides to attach the test specimen, in order to avoid detachments.

Although engineering is an exact science, because of the large number of input variables, random vibration tests are very tricky to perform, requiring extensive engineering knowledges, experience and intuition.

REFERENCES

[1] Nuno Manuel Mendes, Maia. Theoretical and experimental modal analysis. Baldock: Research Studies Press, 1997, ISBN 0863802087.

[2] T. L. Paez, Random vibration- a brief history, Sound & vibrations, The noise and vibration control magazine, January 2012

[3] Dave S. Steinberg, Vibration Analysis for Electronic Equipment, Second Edition, Wiley-Interscience, New York, 2000, ISBN 978-0471376859

[4] Loren D. Lutes, Shahram Sarkani, Random Vibrations: Analysis of Structural and Mechanical Systems, 2003, ISBN 978-0750677653

[5] ISO 13355:2001 – Packaging – Complete, Field transport packages and unit loads – Vertical random vibration

University of Nis
Faculty of Occupational Safety
„Politechnica“ University of Timisoara
Faculty of Mechanical Engineering
24th International Conference
NOISE AND VIBRATION
Niš, 29 - 31. 10. 2014.

VIBRATIONS OF FLOOR SLAB STRUCTURES EXCITED BY HUMAN ACTIVTIES

D. Zlatkov[1], *S. Zdravković*[2], *D.Stojić*[3], *Ž. Cuckić*[4], *D. Turnić*[5]

[1] University of Nis, Faculty of Civil Engineering and Architecture, Serbia, dragan.zlatkov@gaf.ni.ac.rs
[2] University of Nis, Faculty of Civil Engineering and Architecture, Serbia, slavko.zdravkovic@gaf.ni.ac.rs
[3] University of Nis, Faculty of Civil Engineering and Architecture, Serbia, dragoslav.stojic@gaf.ni.ac.rs
[4] Dadge International L.L.C, dadgeserbia@yahoo.com
[5]University of Nis, Faculty of Civil Engineering and Architecture, Serbia, dragana.turnic@gaf.ni.ac.rs

Abstract - *The paper deals with the sensitivity of humans to vibrations and criteria which should be met by the floor slab structures. The potential problems for vibrations are lightweight and long-span floor slabs. The sources of vibrations, apart from the human activities such as walking, running, jumping, feet thumping etc. are also the operation of machinery, of elevators, cranes, presses or construction works in buildings. The paper analyzes the influences created by the human motion. The criteria of serviceability states are based on the criteria of human sensibility to vibrations according to the corresponding standards.*

Key words - *vibrations, international structures, human activities, serviceability.*

1. INTRODUCTION

Contemporary floor slab structures are becoming increasingly lightweight and flexible, which makes them more susceptible to vibrations in service. They must meet the conditions for the unimpeded work and stay of the people, and for the operation of sensitive instruments and equipment and other reasons. Regarding that complaints concerning the vibrations come from the people who live and stay in housing/special structures, will constrain ourselves to consideration of the serviceability state of floor structures due to human activities. Vibrations may represent a potential problem, because the floor structures are lightweight and they have increasing spans, practically over 5m (6-8m and more). Those are mostly lightweight and semi-lightweigth floor structures for which there is a problem of meeting of serviceability conditions considering vibrations. It is very often necessary to compose the structures from simple or laminate timber beams, as well from steel sheet metal and reinforced concrete slabs. Prefabricated prestressed slabs are often hollow, which along with the small static height – low rigidity results in relatively small weight, so there is no potential for the considerable level of response during dynamic influences. In general, in classic reinforced concrete floor slabs, there is seldom the serviceability problem in respect to the vibration in housing and business buildings, and it occurs only in the rooms with sensitive equipment, which is not discussed in this paper.

2. SENSIBILITY OF PEOPLE TO VIBRATIONS AND SERVICEABILITY CRITERIA

The vibration magnitudes should not exceed the irritation threshold and disturb comfort of people both during activities in housing buildings and while using instruments that cause vibrations etc.

Sensitivity to vibrations is an extremely individual category, depending on the age, sex and other factors. The phenomenon of physical and mental fatigue in humans as a consequence of vibrations are nowadays particularly studied for the purpose of mitigating them.

The first research of human sensibility to vibrations were conducted by Reisher and Meister [1], whereby the impact of continuous harmonic vibrations on the entire body was treated, under the impact of frequencies and displacement levels in vibrations. The vibrations are classified as imperceptible, hardly perceptible, clearly perceptible, fatiguing, annoying and painful, based on the Lenzen [2] research, who included damping, so the so called modified Reisher-Meister scale was formed (see Fig.1)

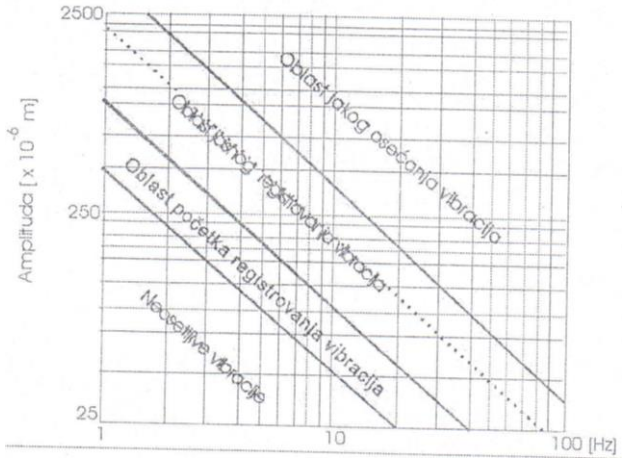

Fig.1 *Modified Reisher-Meister vibration sensitivity scale*

Regarding the obvious complexity of the problem of the sensitivity of human beings to vibrations, in Fig.2 is presented the qualitative description of human reactions.

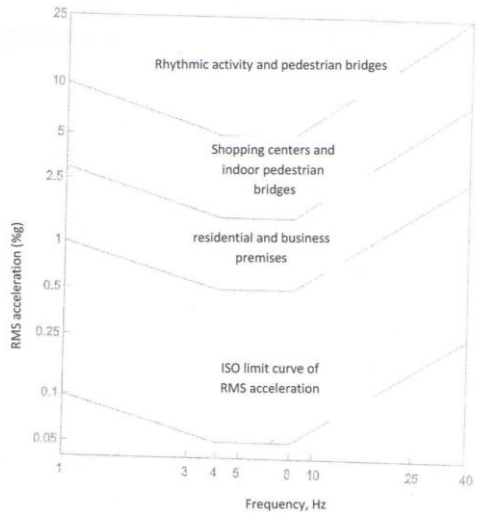

Fig.2 *Qualitative description of human reactions to systematic steady reaction*

The degree of sensitivity also depends on the character of vibrations, which comprises:

- Vibration frequency f_0
- Duration of exposure, and
- Amplitudes of displacement, velocity and acceleration u_0, v_0 and a_0.

Standard ISO is based on the position of the human body, as the most important factor when it is exposed to vibrations and it defines appropriate referential axes in respect to the standing, sitting and prone position, Fig.3:

- x-axis defined from the back to the chest,
- y-axis defined from left to right and
- z-axis defined from the feet to the head.

In the frequency terms, the humans are most sensitive to vibrations in the rang 4-8Hz (periodes T=0,25-0,50 seconds) in z direction, and the range 0-2Hz is critical for human exposure to vibrations in the directions x and y with Fig.3.

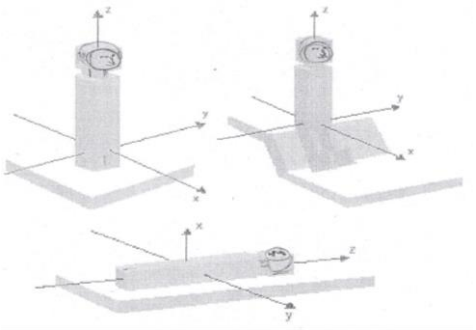

Fig.3 *Referential axes through the human body in standing, sitting and prone position for the analysis of exposure and sensibility in respect to vibrations*

The different intervals are the consequence of the fact that within these limits there are eigenfrequencies of internal human organs, so the capacity for damping within the mentioned limits is the lowest. The resonance is occurs when the frequency of acting vibrations coincides with the frequency of tissue of a certain organ. In those cases even the vibrations with relatively low amplitude can bring large displacements in internal organs. One of the most important "elements" of this system in respect to the vibrations and impacts is marked as "chest-abdomen" with the vibration in the range 3-6 Hz, depending on whether the person stands or sits (see table 1).

The problem with vibrations occurs when they become considerable and fatiguing, and this occurs in the case of serviceability of the topical floor slabs in the structures where people live and work.

Table1 *Characteristic resonant frequencies of generalized "subsystems"*

A part of the human body	**f_0 [Hz]**
head-axial	25
eyeball, intraocular structures	30-80
shoulder belt	4-5
the lower part of the arm	16-30
spinal cord-axial	10-12
hand grip	50-200
person in standing position	
thorax	60 Hz
hand-arm	
abdominal mass	4-8
person in a sitting position	
legs with knees bent	2
feet when standing	>20

3. DYNAMIC CHARACTERISTICS OF FLOOR SLAB STRUCTURES AND IMPACTS CAUSED BY HUMAN MOTION

For the behaviour of the floor slab, their dynamic characteristics are relevant as proof of serviceability state, i.e. frequency of the primary tone of eigenfrequency, damping coefficient and modal mass of the first tone.

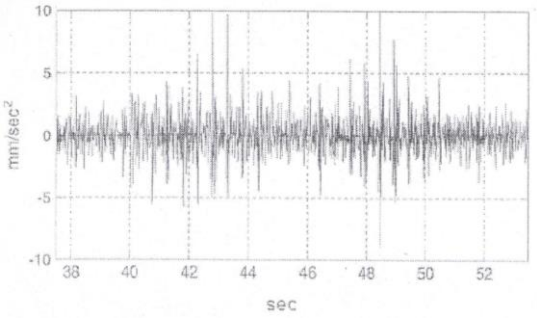

Fig.4 *Typical response (time history of acceleration) of high frequency floor slab due to the excitation by human walking*

Fig.4 presents the response of high frequency floor slab caused by human walking. The border between high frequency and low frequency eighenfrequency is in range 9-12 Hz. An extremely important parameter is the assessment of critical damping coefficient of the adequate type of floor structures. The viscous damping coefficient ranges between 0,8 and 5,0 % from the critical one.

Dynamic effects, forces, are different, both in terms of intensity and time dependence, and the way they are transferred on the structure are presented in Fig. 5.

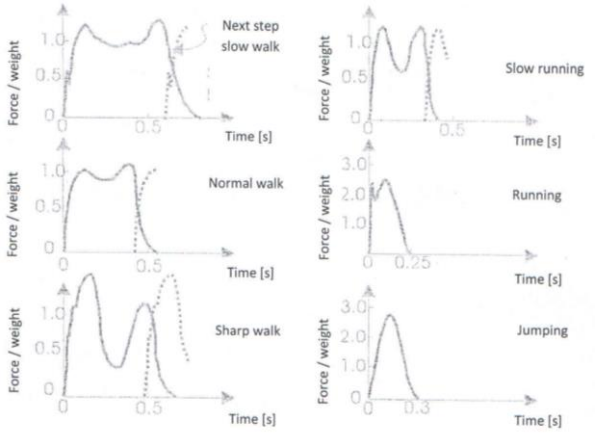

Fig.5 *Typical forms of force function during walking and running*

When walking, people may have both feet on the floor at some moment, but during running, there is a time when no feet is on the ground. The forms of contact force function are presented in Fig. 5. In table 2 are presented the approximate values of velocity, gait length and frequency during various forms of human motion which represent the possible excitation of floor structures.

Table 2 *Approximate values of velocity, gait length and frequency of various forms of human motion.*

Type of activity	Speed [m/sec]	Stride length [m]	Frequency [Hz]
Slow walking	1,10	0,60	1,70
Normal walking	1,50	0,75	2,00
Faster walking	2,20	1,00	2,30
Slow running	3,30	1,30	2,50
Fast running	5,50	1,50	3,20

The values in table 2 represent basic entry data when the control (design) of floor structure is performed regarding the vibrations. The functional dependence of force on time is determined by the Fourier analysis, and according to ISO 10137, the design model includes the first three harmonics of the force, equation (1)

$$F_p(t) = G\left[1 + \sum_{1}^{3} \alpha_i \sin(2i\pi f_s t + \varphi_i)\right] \tag{1}$$

In the expression for the force, equation (1), G is the weight of the person that moves, α_i are appropriate Fourier amplitudes of harmonics, φ_i phase angles, while f_s is the walking velocity expressed in Hz. In the calculations is mostly adopted the weight of the person within the interval 700-800N, and the frequency of walk within the interval 1,6-2,4 Hz. Regarding that the harmonics are not in sinphase, in the analysis is included a certain phase shift given through the phase angles φ_i, which have different values for different types of human activities.

The contemporary methods of calculation of floor structures at various forms of human motion are conducted using software packages for structural design on the basis of final elements method (FEM).

4. CRITERIA OF ASSESSMENT OF SERVIEABILITY STATE

The criteria for assessment of serviceability state of floor structures are based on the criteria of human sensitivity to vibrations which are presented in part 2. The criteria which are based on modified Reishner-Meister scale, that is, ISO 2631 vibration sensitivity/registering scale are given further in the text.

One of the most frequently applied criteria is the so called Murray criterion expressed by the relation (2).

$$\xi \geq 35 A_0 f_0 + 2{,}5 \tag{2}$$

By Zeman and Boswell the expression given by the relation (3) is given

$$\xi \geq 209 A_0 f_0 - 1 \tag{3}$$

By the criteria (2) and (3) is determined the minimum value of damping, ξ%, which must be possessed by the floor structure. This value depends on the maximum amplitude, $A_0(in)$, and the frequency of the first tone of own vibrations of the structure, f_0(Hz). The values A_0 f_0 (Hz·in) can be determined through the appropriate straight lines as presented in Fig. 6.

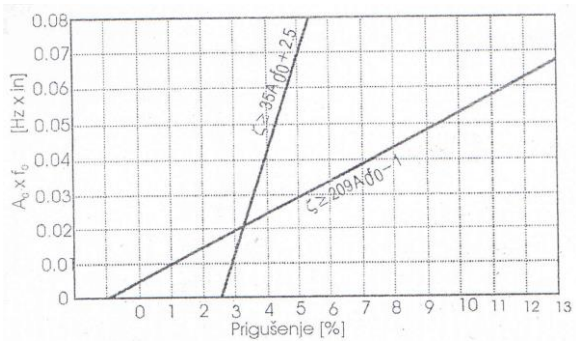

Fig.6 *The graphic presentation of the criteria given by the relations (2) and (3) with the areas of acceptable parameter values below the appropriate straight lines.*

The parameter for the assessment of serviceability state according to ISO 2631 standard, utilizes the so called root-mean-square acceleration, a_{RMS}(ms^{-2}) and it is defined by the equation (4). The other parameter which is given by the relation (5) is the value of (Vibration Doze Value - *VDV*).

$$a_{RMS} = \left[\frac{\int_{t_1}^{t_2} a_w^2(t)dt}{t_2 - t_1}\right]^{1/2} \tag{4}$$

$$VDV = \left[\int_{t_1}^{t_2} a_w^4(t)dt\right]^{0.25} \tag{5}$$

The calculation of the parameters given by the relations (4) and (5), a_{RMS} and *VDV*, is done on the basis of weighted acceleration, a_W. It is a weighted acceleration value by frequencies, which takes into consideration the different human sensitivity to different frequency vibrations.

5. CONCLUSION

The presented basic elements relevant for the serviceability analysis of floor structures in respect to vibrations unambiguously indicate the complexity of the problem, as well as the inexistence of the single approach to solving it. Practically, the innovation of the procedures of serviceability state is incessantly innovated, which is primarily contributed by the perfection of experimental methods for response determination. It should be considered that the floor slab lies under several rooms, that is, behaves as a continuous slab rested on the number of walls, so it represents an elastically restrained slab. In this sense, both globally and nationally, research in this field is very topical and attractive for researchers.

Acknowlegment: This research is supported by the Ministry of education, science and technological development of the Republic of Serbia for project cycle 2011-2014, within the framework of the project TR36016 "Experimental and theoretical investigation of frames and plates with semi-rigid connections from the view of second order theory and stability analysis" of the research organization The Faculty of civil engineering and architecture of University of Nis.

REFERENCES

[1] D. Cvetković, M. Praščević: Buka i Vibracije - 4. Vibracije i ljudsko telo, Univerzitet u Nišu, Fakultet zaštite na radu, 2005.

[2] Z. Mišković: Stanje upotrebljivosti međuspratnih konstrukcija s obzirom na vibracije, Građevinski kalendar, Vol.41, 2009., Savez građevinskih inženjera Srbije, Beograd, str. 171-200, ISSN 0352-2733

[3] K. H. Lenzen, Vibration of steel joist-concrete slab floors, Engineering Journal, AISC., Vol 18(3), pp. 133-136, 1966.

[4] S. Zdravković, Ž. Mitić, V. Dimitrov: Uticaj krutosti veza na statički i dinamički proračun armirano-betonskih tavanica, IV Naučni skup INDIS'94, FTN Novi Sad, Institut industrijske gradnje, str.27-34, 1994.

[5] T. M. Murray, Acceptability Criterion for Occupant-Induced Floor Vibration, AISC Sngineering Journal, Vol 18 (2), pp 62-70, 1981.

University of Nis
Faculty of Occupational Safety
„Politechnica“ University of Timisoara
Faculty of Mechanical Engineering
24th International Conference
NOISE AND VIBRATION
Niš, 29 - 31. 10. 2014.

“TENT” TURBINE-GENERATOR SETS VIBRATION MEASUREMENT USING VIRTUAL INSTRUMENT VIBROMETAR-VM1

Miroljub Kovačević[1], Dragoslav Đorović[2]

[1] Powerplants Nikola Tesla, Obrenovac Serbia
[2] AN LAB CO d.o.o., Beograd, Serbia, Trgovačka 79

Abstract - *In recent years, we have developed and built our own instrument Vibrometar-VM1 aimed for vibration measurement and vibration analysis of rotating machinery. The device is designed as a virtual instrument that gives many advantages compared to conventional instruments. It is based on computer aided measurement and computer aided data acquisition technology and replaces several traditional instruments. VM1 has 16 channels and simultaneously performs measurements and vibration analysis on all channels. It can perform complete measurement of all necessary vibrational parameters, on all channels, in only one second. Using a suitable and simple user interface, changes in the vibrational parameters, with time or with variable speed, can be obtained in the form of a chart. Vibrometar-VM1 has been successfully used for over two years, in measurement and analysis of vibrations of large steam turbine-generator sets (up to 670MW) in “Powerplants Nikola Tesla” Obrenovac Serbia. Despite the existence of instruments from renowned companies such as “Schenck” and “Bentley Nevada”, Vibrometar-VM1, with its quality, imposed itself as the main instrument for the measurement and analysis of vibrations in large steam turbine generator sets at “TENT”. Application of the instrument VM1 in the Powerplants “TENT” in the past two years is a great reference.*

1. INTRODUCTION

Between 2011–2013, our own instrument VM1 was conceived, developed, implemented and tested. VM1 is aimed for vibration measurement and vibration analysis of rotating machinery. The device is incorporated with a PC and designed as a Virtual Instrument (VI), which gives certain advantages compared to conventional instruments. We have named this instrument Vibrometar-VM1. Vibrometar-VM1 has already been used successfully for the measurement and analysis of vibration of steam turbine-generator sets (power of 32MW to 670MW) for over two years, at all four powerplants at „TENT“ – Obrenovac Serbia.

It should also be noted that the Vibrometer-VM1, in „TENT“ (in addition to existing instruments from renowned companies such as Schenck and Bently Nevada), established itself as the main instrument for the measurement and analysis of vibrations of steam turbine-generator sets. This was result of its functionality, simplicity and convenient user interface.

Fig. 1 *Virtual Instrument Vibrometar-VM1*

Conception, development, software writing and testing was done by Mr Miroljub Kovačević (Mechanical Engeneer). Development and implementation of hardware with galvanic isolation was done by Mr Dragoslav Đorović (Electrical Engeneer).

2. VIRTUAL INSTRUMENT VIBROMETAR-VM1 DESCRIPTION

2.1. Instrument VM1 basic characteristics

VM1 device has the following characteristics:

- 16 analog inputs (one input for the reference signal and 15 inputs for vibration signals);
- AD conversion resolution: 16-bit;
- Sampling method: simultaneously (on all channels at the same time);
- The maximum input voltage: ± 35V;
- Types of vibration sensors that can be used: sensors whose output is proportional to the vibration velocity or displacement or vibrational acceleration;
- At every 1.03 sec, measurement is completed and all vibrational parameters for all 15 vibrational sensors simultaneously are displayed, (direct measurements using data acquisition device);
- When processing digitized signal from the file - processing is executed 3 to 6 times faster comparing to direct measurement using data acquisition device.

2.2. Instrument VM1 components

Virtual instrument (VI) VM1 is composed of the following components:

- The software part - VM1.EXE application that runs on a personal computer;
- Data acquisition device - the hardware part;
- Personal computer with two monitors and color laser printer.

Fig. 2 *Vibrometar-VM1 Acquisition device*

2.2.1. Software component

Software component is a 32-bit Windows application VM1.EXE developed in Delphi IDE - Version 7 using Pascal. Application runs on 64-bit operating system MS Windows 8.

2.2.2. Hardware component

Hardware contains:

- Units for a galvanic isolation and signal conditioning, and
- 16 channel general purpose multifunction data acquisition device USB-1616FS manufactured by Measurement Computing. This device has 16 analog-to-digital converters, one per channel that allows simultaneously sampling (digitizing) on all channels. This is important characteristic in the applications for vibration testing of the mechanical systems.

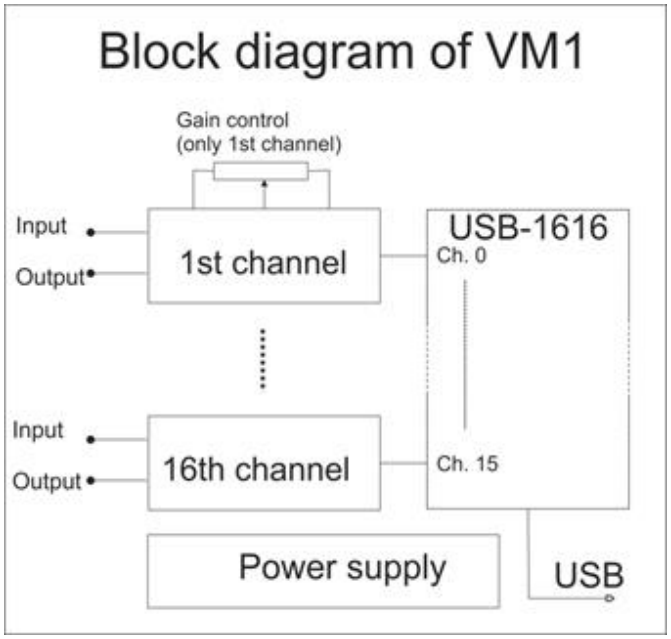

Fig. 3 *Block diagram of Vibrometar-VM1*

Hardware serves to transfer signals from vibration sensors to the computer for digital signal processing. The signal from sensor is electrical values (voltage) continuously changed in time we call it analog signal. Signal changes are carrying information about vibration state of the machine but only after its processing. Computer and software cannot process any raw signals that are coming from sensors. It is necessary to represent signals in digital form (digitally represented data) by analog-to-digital conversions. Analog-to-digital conversion transforms analog values in digital values which are suitable for processing in the computer. Digital data is easy transmitted to the computer by a serial port e.g. RS232 or USB. Fig. 3 is presenting a block diagram of VM1 that contains device for analog-to-digital conversions. USB data acquisition module USB-1616FS manufactured by Measurement Computing from US is chosen for analog-to-digital conversions.

USB data acquisition (DAQ) module has very good performance for this application. It can transmit vibration signal to computer entirely without significant loss of information. DAQ module has high resolution and high conversion speed that allows to measure low signals, like vibration signals, on several sensors. The smallest signals that can be measured by this DAQ module is 15 μV, for illustration AA battery has 100 000 times higher voltage. Herewith, the low level signals can be acquired easily. The speed of data acquisition is very important characteristic. High speed means more data and more information after data processing. USB-1616FS acquires 200000 data (samples of analog signals) per second. If all 16 channels is used then acquisition speed is around 9500 samples per second. According to Nyquist–Shannon sampling theorem the frequency of signals which can be observed is up to 4,75 kHz. The standards (ISO 10816, ISO 7919, etc.) are prescribing frequency band up to 1 kHz because all relevant information are in this range. USB-1616FS module is fully applicable for signal acquisition during vibration testing on machines.

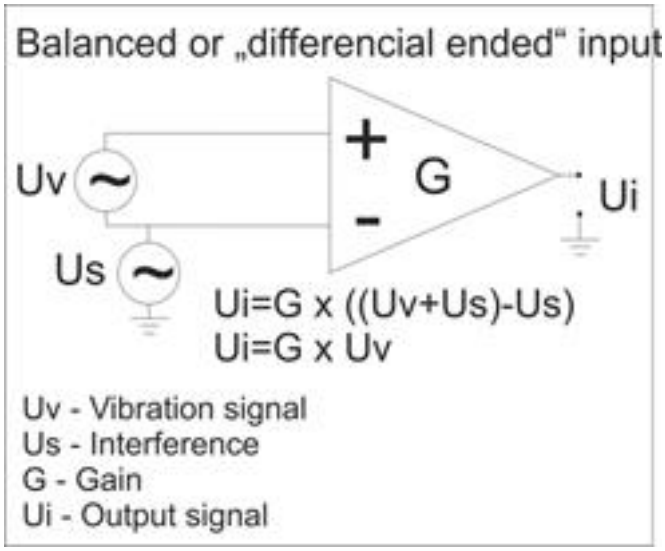

Fig. 4 *Differential input of Vibrometar-VM1*

Analog signals, which are acquired from sensors, contain (beside information about vibration in useful range up to 1 kHz) unwanted signals above 1kHz even above 4,75 kHz, which is limit for proper analog-to-digital conversion. In order to eliminate unnecessary signals which interfere

analog-to-digital conversion we filter analog signals. Useful signals are extracted by filtering and these signals are frequency limited. Lower cut-off frequency in AC mode is 1 Hz (-3dB, first order high-pass filter) can be switched-on on the front side of VM1. Also, user can choose DC mode without high-pass filtering. In this way universality can be reached and VM1 can be used for vibration measurement of shaft where DC component of signal is useful. High frequency cut-off is fixed on 2 kHz (-3dB, 4 order low-pass filter) in order to fulfil Nyquist–Shannon sampling theorem and eliminate occurring of aliasing. Aliasing is unwanted effect if signal frequency is higher than half of sampling speed.

Vibration measurements are typically performed in an industrial environment where there are very large sources of interference. These disturbances may originate from other devices nearby and from the facility at which the measurements are made. The most common cause of interference is the electromagnetic field. Electromagnetic field inducts interference in the cables that connect the sensors to the measuring system. It is not possible to eliminate interference completely, but it is possible to significantly reduce it by using the appropriate input circuit of the measuring device. Vibrometar-VM1 allows two ways to connect the sensor to the input: Symmetrical (Differential ended) and unbalanced (single ended) input. Selecting a differential input in most cases will eliminate interference caused by electromagnetic fields. In the Fig. 4 and Fig. 5 is shown an action of the differential inputs to a reduction of the interference. The simplified model of an ideal differential amplifier is presented for illustration only. It can be seen that the differential amplifier suppresses common interferences at the entrance in the output signal, ideal noise suppression is infinite but in practice it is more than 80dB. In unbalanced inputs are equally amplified useful signal and signal interference.

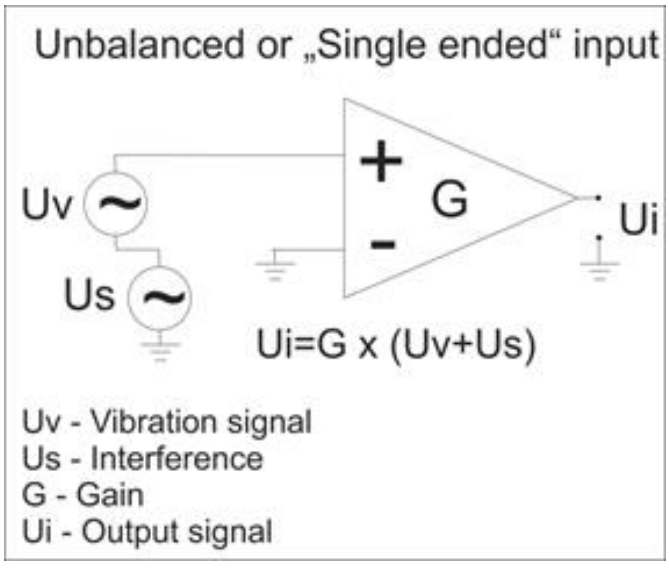

Fig. 5. *"Single ended" input of Vibrometar-VM1*

In practice, it may happen that the metal parts of sensors, connectors or cables are touching other metal surfaces that may be at the voltage level higher than the level of the ground. In this case, when the measuring device is grounded, its potential is close to the ground potential there is a flow of current, which can destroy the measuring device. This and electrostatic discharge are the most common causes of failure of measurement system. The voltage difference can be several hundred volts, which is more than measuring systems can handle. To prevent the dangerous flow current between the sensor circuit and the rest of measuring system, there is set galvanic isolation. It is a break in the wire, which allows the passage of signals only. This interruption can be realized by transformer, capacitive or optical connection. In the Vibrometar-VM1 the galvanic isolation is achieved by capacitive connection and allows to segregates voltages up to 1000V.

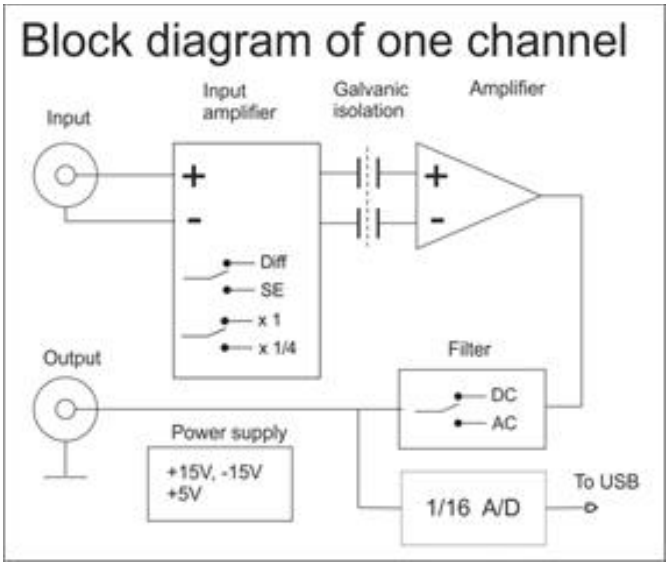

Fig. 6 *Block diagram of one channel of Vibrometar-VM1*

Electrostatic voltage can occur on all parts isolated from ground. The most common source of ESD is the man. When man is wearing shoes made of insulating material, or when he walks on the floor made from electricaly insulated materials then it can charge the human body with a few thousand volts. If the measuring device is not immune to a large discharging it can be destroyed by touch. Vibrometar-VM1 has adequate protection from electrostatic discharge.

Vibrometar-VM1 allows acquisition of signals from the sensor of vibration velocity and relative displacement and accelerometer at 16 channels simultaneously. The first channel could be used for the connection of the sensor of the reference signal and is equipped with a potentiometer for adjusting the amplitude of the output signal, and then the remaining 15 channels can be used to collect the signals from the vibrational sensors.

Entire hardware, except USB-1616FS, is designed and manufactured in Serbia.

2.2.3. Personal computer and printer

Vibrometar-VM1 devices, which are used in TENT, work reliably with PCs based on Intel Core I3 3,3GHz processor with 4GB of RAM and a hard drive of 1TB. That is PC configuration of Dell Optiplex 390 computer (Fig. 1). In such a configuration, application VM1 is running (on 64-bit Windows-8) with ease and uses only a portion of the processor's power, even while recording the digitized signal to the computer's hard disk. We use graphics card with two monitor ports and two 22-inch monitors. Monitors and color laser printers do not require high end models. It is desirable that the hard drive has large enough capacity, because files with recorded digitized signals can grow up to several tens of

GB, depending on how long the recording was done and depending on recording conditions settings (Fig. 16).

Fig. 7 *Vibrometar-VM1 measuring vibrations at turbine-generator set B1-TENT-B (670MW) 12-10-2012.*

3. PURPOSE OF VI VIBROMETAR-VM1

Virtual Instrument VM1 can be used for the measurement and analysis of vibration, as well as for balancing rotors of rotating machines in general. It is particularly suitable for machines (up to 15 channels) with a greater number of bearings. In „TENT“ VM1 is mainly used on high power steam turbine-generator sets, but it can be successfully used on the following machines (whether large or small power):

- electric motors;
- pumps;
- fans;
- mills;
- turbocompressors;
- hydro turbines with higher speeds;
- gas turbines, etc..

Fig. 8 *Vibrometar-VM1 measuring vibrations at turbine-generator set A6-TENT-A (348MW) 13-05-2013.*

Using VI VM1 measurements we can do the following tasks successfully:

- vibrational state evaluation of rotating machinery (control and trend monitoring) in accordance with the relevant standards ([1] and [2] for steam turbine-generator sets);
- vibrodiagnostics in cases of increased or changed vibrations of rotating machines;
- correction or repair of faults, which cause increased vibrations of rotating machinery (eg rotor balancing in the field).

4. CLASSICAL INSTRUMENTS REPLACED BY VIRTUAL INSTRUMENT VM1

Virtual instrument Vibrometar-VM1 (in accordance with its functional capabilities) replaces the following classical instruments, because VM1 is doing all of their functions used in daily operations related to the vibrations of rotating machines:

- classic instrument for vibrations measurement (and mechanical multichannel switch);
- spectrum analyzer (frequency analysis);
- multichannel tape recorder;
- oscilloscope;
- XY printer;
- signal generator.

5. RUNNING MODES OF VM1 SOFTWARE

Vibrometer-VM1 can operate in any of the following modes:

- Direct measurement from vibrational sensors via a data acquisition device. Acquisition is performed first eg. digitizing a portion (1 second long) of the analog signals (all 16). This produces 1 block of the digitized signals 1second long. After that, mathematical processing (digital signal processing) is going on. Finally, results are displayed on the screen.
- Direct measurement from vibrational sensors via a data acquisition device, wherein the mathematical processing and displaying on the screen is done in parallel (simultaneously) with the acquisition (digitization) of the next block of signals. Acquisition is performing in the background. Mathematical processing and presentation is performing in the foreground. Thanks to the simultaneous execution of both jobs, a complete cycle is shorter and takes about 1030 ms for a block. This mode is usually used.
- Direct measurement (either of the previous two) with simultaneous recording of digitized signals to a file on computer’s hard drive.
- Subsequent processing based on reading the digitized signals from the file. In this case, the data acquisition device is not used. The results of the measurements are 100% identical to the results of direct measurements at which the recording was made in the file. This is a very useful feature, because subsequent detailed processing and analysis can be performed, using permanently stored signals. The digitized signals are obtained and stored with sampling frequency of 8192 Hz.
- Processing using generated signals (reference signal and vibrational signal). Signals are generated by software in the application VM1.EXE itself and

simulate real signals. This is useful for training and understanding, as well as for the purpose of performing various tests.

6. THE ORDER OF PROCESSING IN DIRECT MEASUREMENT MODE – VM1

Instrument VM1 measuring process can be started in two ways.

- The first one is to press the "**1 Obrada**" button (in the main application's window) which initiates and performs only one measurement cycle.
- Another way is to press the "**START**" button which initiates a process of continuous measurement that takes place continuously.

Below will be roughly described the sequence of actions, that are carried out, in one complete measurement cycle (which takes about 1030 ms) when VM1 runs in direct measurement mode (acquisition - in the background) while in continuous measurement:

- The acquisition is initiated (in the background) to get one block of signals from all 16 channels (the next block - for the next measurement cycle). This acquisition lasts 1000 ms approximately. During of the acquisition it is constantly checked whether the acquisition of the current block is completed; if so - immediately starts acquisition of the next block.
- Simultaneously with the initiation of the acquisition, (in the foreground) the mathematical processing also starts and results are displayed on the screen. Mathematical processing treats the previous block (which is digitized in previous measurement cycle).

Procedure of *mathematical processing and results displaying* is doing following steps:

1) Digitized time-signals from the previous block are converted to voltage values and to vibrational parameters.
2) Existence of a valid reference signal is checked.
3) If so, several math treatments of the reference signal is done.
4) Sets a zero point of reference signal.
5) Determines the frequency of the first harmonic and rotor speed, using reference signal.
6) Performs the FFT signal processing on all channels.
7) Determines all the necessary vibrational parameters for all channels (vibration velocity, displacement).
8) Records a block of digitized signals to a file if it is included.
9) Performs on screen displaying of all measurement results in digital form. Performs displaying of graphs and orbits if included.

Complete procedure of mathematical processing and results displaying for one block, is 100ms to 400ms long, depending on what is required.

7. ADVANTAGES OF VIRTUAL INSTRUMENT VM1 COMPARED TO CONVENTIONAL INSTRUMENTS

Virtual instrument VM1 has more indisputable and obvious advantages over classical instruments, that have been used in TENT before 2013. Some of these advantages are:

1) Most conventional instruments have only 1 channel. They can measure only 1 signal, from one sensor and only one specific vibration parameter (eg. only summary vibration velocity, or only the first harmonic of vibration velocity, or only the first harmonic of the displacement, etc..). VI-VM1 can simultaneously measure signals from 15 sensors and it is doing calculation and displaying (for all 15 channels) all necessary vibrational parameters such as summary value, first harmonic, second harmonic, etc (displacement and vibration velocity). The consequence of this, is that the technicians who measure the vibrations on all bearings of 300MW-turbine-generator set, will spend minimum, 12 to 15 minutes to perform a **complete measurement task** (manually typing it into the appropriate forms) using instrument such as eg. Schenck-Vibroport-41. In contrast, the VI-VM1 allows the same job to be done in only 1 second (exactly 1030ms) and complete measurement - all 15 channels and all the listed vibrational parameters. This means that the engineer has a complete picture of the current vibrational state of the entire rotating machine in every second (continuous measurement). This makes it possible to get valid complete measurement every second, even when turbine speed is changing, which is particularly important, and it is impossible to do this using a conventional single-channel instrument. Complete measurement can easily be printed at any time with one click of the mouse.
2) In addition to displaying the current values in digital form (Fig. 10), VM1 provides a graphical representation of the change with time or change with the machine rotational speed, of all the necessary vibrational parameters (Fig. 12 and Fig. 13). Changing the amplitude and phase angle of the first harmonic can be displayed in a polar coordinate system (Fig. 14). All these charts can be zoomed in many times in order to get the finest details, and can also be easily printed on a color laser printer.
3) Recording to a file of digitized signals can be done, by allowing subsequent detailed processing and analysis based on recorded signals from a file. Starting of the recording is very simple and is carried out using four types of triggers.
4) VM1 allows detailed and accurate representations of vibrational signals in time domain and in frequency domain.
5) The measurement results and high precision graphs can be displayed on large computer's screens, instead of small displays of conventional instrument.
6) The user interface of VM1 is designed to be very intuitive and easy to use. Technitians using and working with VM1 need only minimal training. All

measurements and graphs can be obtained and printed quickly and easily.

7) Allows the measurement of absolute shaft vibrations.

8) Allows you to measure and display the Orbit (Fig. 15) of: relative shaft vibration; absolute bearing vibration; absolute shaft vibration.

9) VM1 has the ability to be customised according to user's preferences and requirements.

10) During the development of VM1, we found a startling finding where during comparative measurements, the renowned instrument made by German company Schenck - Vibroport-41 made a significant error in measuring the phase difference of the first harmonic (the error is particularly large at lower speeds). Older Schenck's models, like Vibroport-30, make the same error. Thus, for example, at 777 rpm error of Schenck-Vobroport-41 is 107 degrees! It is absolutely unacceptable. All of this is clearly confirmed by comparative measurements (performed 06-09-2012.) using three instruments: Vibroport-41; Vibrometar-VM1; Bentley Nevada ADRE-208. The last instrument was owned by company TURBOMEHANIKA from Kutina-Croatia. Representatives of Turbomehanika Ivan Majstrović and Zoran Majstrović participated in this comparative measurement. These shortcomings of Schenck's instruments, subsequently were confirmed by comparative measurements using Bentley Nevada ADRE-408 instrument.

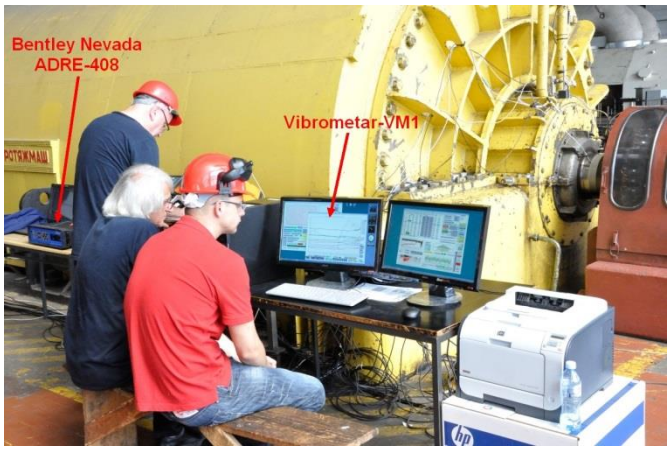

Fig. 9 *Vibrometar-VM1 measuring vibrations at turbine-generator set A2-TENT-A (210MW) 05-07-2013.*

All of VM1's advantages are generally referred to (in relation to the single-channel or two-channel) conventional vibration measurement instruments. However, the photo (Fig. 9), very eloquently speaks more about the qualities of VI-VM1. The photo was taken 05-07-2013 during the usual vibration measurements on turbine-generator set - unit A2-TENT-A during startup after repair. In addition to Vibrometar-VM1, the top-level multi-channel *Bently Nevada ADRE-408* instrument is also installed and doing measurements (see left side of the photo). It is obvious that engineers ignore the ADRE-408 and prefer using the Vibrometar-VM1!!

8. AVAILABLE MEASUREMENTS AND ANALYSIS TYPES - VIBRODIAGNOSTICS TOOLS

Following measurement types and analysis types can be performed using the Vibrometar-VM1:

1) Summary effective vibration velocity, the first, second and higher harmonics of the velocity (first harmonic: amplitude and angle of the vibrations vector) [mm/s] in digital form for all channels (Fig. 10).

2) Vibrational displacement - summary, the first harmonic (amplitude and angle), the second harmonic and higher harmonics as needed [μm] in digital form for all channels (Fig. 10).

3) Machine's rotor speed [rpm] and frequency of the first harmonic (Fig. 10).

4) The frequency spectrum of vibrational signal (vibration displacement and velocity) (Fig. 11).

5) Harmonics analysis ie. plot of changes of the first harmonic (amplitude and angle - Bode – Fig. 13) and higher harmonics and summary vibrations value (Fig. 12) when changing machine's rotor speed [rpm] (in a rectangular coordinate system).

6) Change of the first harmonic when changing machine's rotor speed [rpm] – displayed in a polar coordinate system (Fig. 14).

7) Plot of changes of the vibrational parameters (summary effective vibrational velocity (Fig. 18); harmonics of vibrational velocity; summary vibrational displacement) with time.

8) Orbit (Fig. 15) plot of: absolute bearing vibration; relative vibration of the rotor; absolute vibration of the rotor. Orbits can be displayed for: summary signal; in a given frequency range (Fig. 15); for a selected harmonic; for a group of selected harmonics.

9) Vibrations vector (amplitude and angle) (in vertical and horizontal direction) of absolute shaft vibration – Fig. 15 (in addition to the vibration vector of relative shaft vibrations and the vibration vector of absolute bearing vibration).

10) Plot of digitized vibrational time signals - summary or harmonics and plot of digitized reference time signal (Fig. 17).

Measuring windows of Vibrometar -VM1, listed above, can be seen in the following figures.

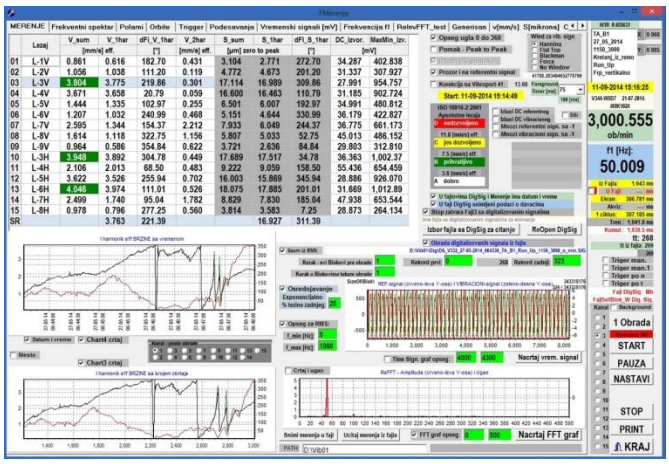

Fig. 10 *Vibrometar-VM1 - window "Merenje" - B1-TENT-B (670MW) 27-05-2014.*

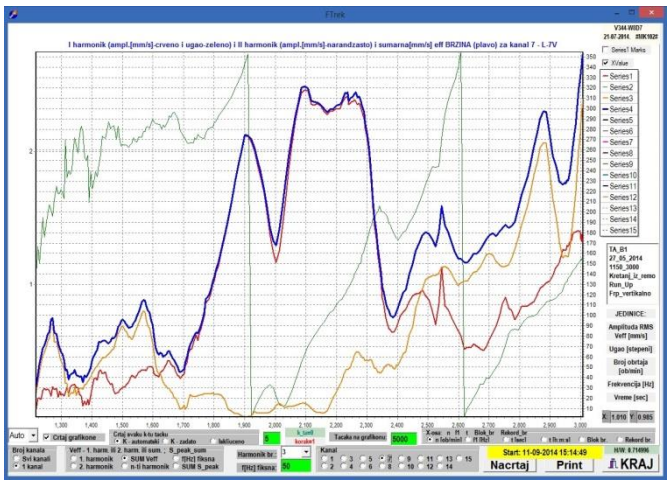

Fig. 13 *VI-VM1- window "FTrek" – first and second harmonic - one channel - B1-TENT-B (670MW) 27-05-2014.*

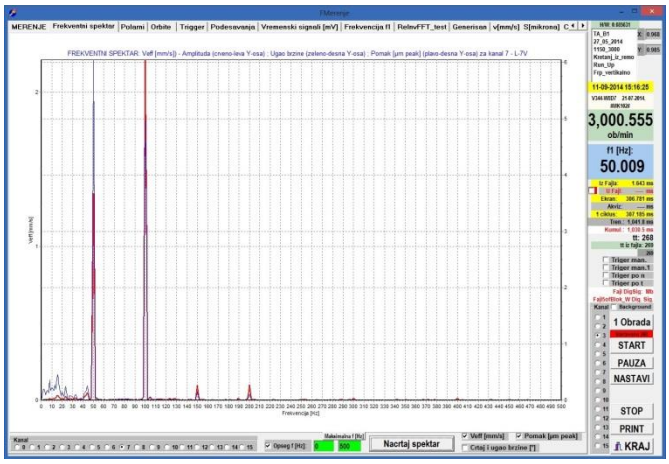

Fig. 11 *Vibrometar-VM1- window "Frekventni spektar" - bearing 7V - B1-TENT-B (670MW) 27-05-2014.*

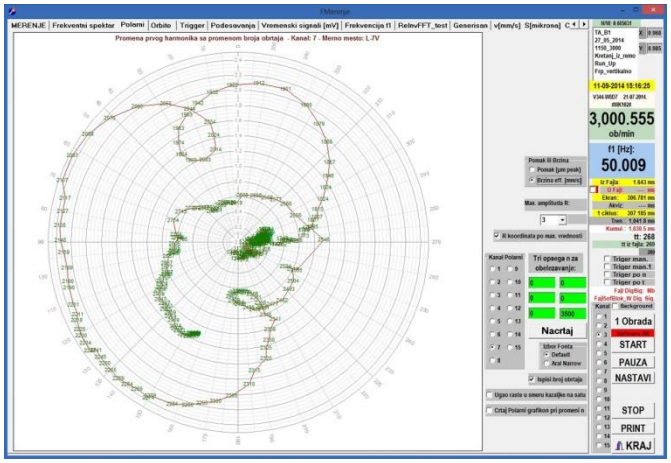

Fig. 14 *Vibrometar-VM1- window "Polarni" - bearing 7V - B1-TENT-B (670MW) 27-05-2014.*

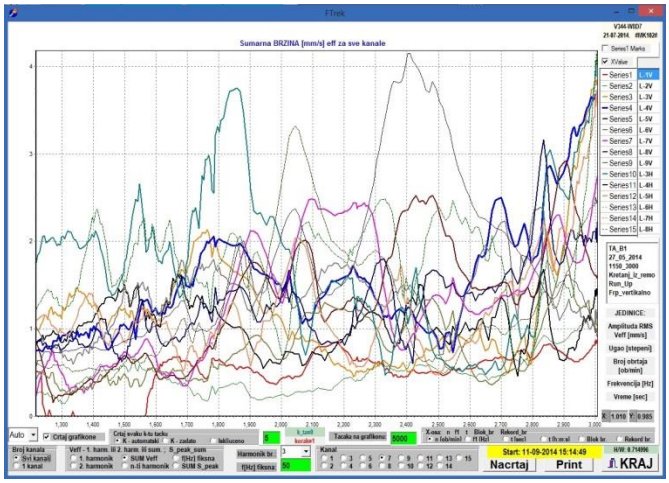

Fig. 12 *Vibrometar-VM1- window "FTrek" – summary - all channels - B1-TENT-B (670MW) 27-05-2014.*

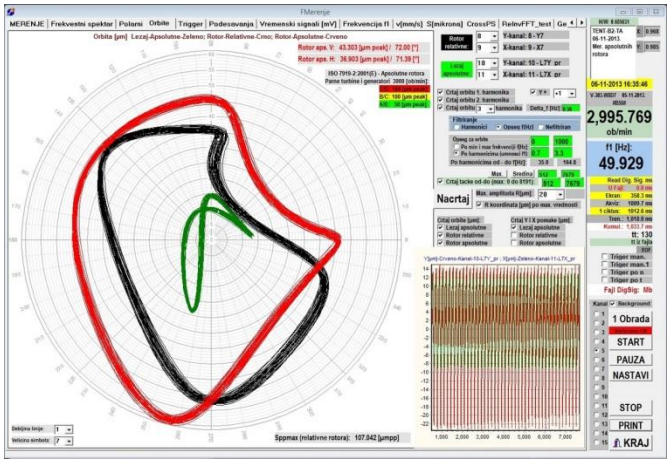

Fig. 15 *Vibrometar-VM1- window "Orbite" - near bearing 7 – B2-TENT-B (620MW) 06-11-2013.*

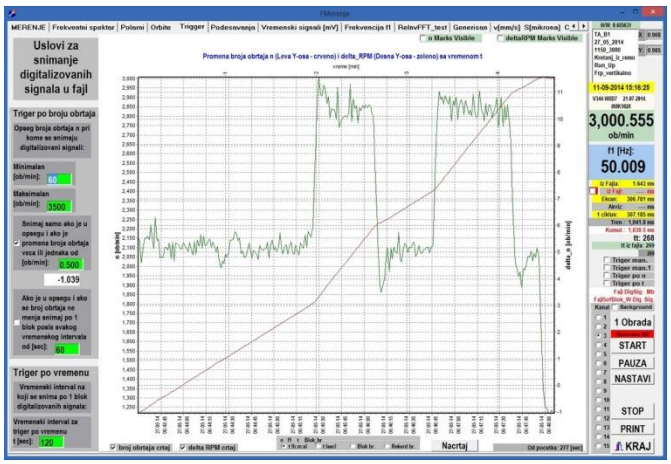

Fig. 16 *Vibrometar-VM1 - window "Trigger" - B1-TENT-B (670MW) 27-05-2014.*

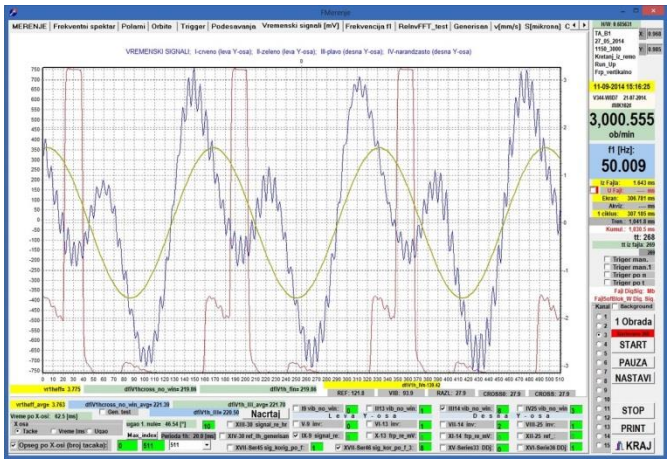

Fig. 17 *Vibrometar-VM1- window "Vremenski signali" - bearing 8V - B1-TENT-B (670MW) 27-05-2014.*

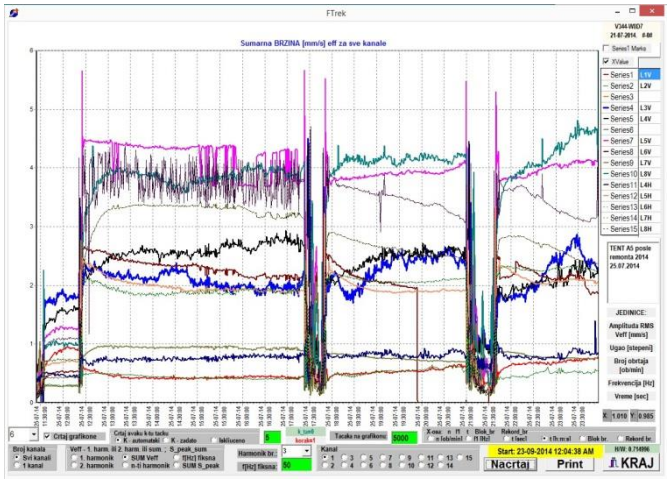

Fig. 18 *Vibrometar-VM1- window "FTrek" – summary - all channels – with time – A5-TENT-A (308MW) 25-07-2014.*

Fig. 19 *Vibrometar-VM1 – measuring Orbit at test machine – 30-04-2014.*

9. CONCLUSION

Virtual instrument vibrometer-VM1 has more indisputable and obvious advantages over conventional instruments, as discussed in Section 7.

In addition, Vibrometar-VM1 is produced in Serbia and serviceed in Serbia. Therefore, there is much shorter service and repair time, which is also a significant advantage. This provides for much greater availability of our product, while in contrast, the instruments of renowned companies such as Schenck, LDS Dactron and Bentley Nevada, are doing services and repairs abroad (Germany, USA) for 3 to 6 months.

REFERENCE

[1] ISO 10816-2:2001 Mechanical vibration — Evaluation of machine vibration by measurements on non-rotating parts Part 2:
Land-based steam turbines and generators in excess of 50 MW with normal operating speeds of 1 500 r/min, 1 800 r/min, 3 000 r/min and 3 600 r/min

[2] ISO 7919-2:2001(E) Mechanical vibration — Evaluation of machine vibration by measurements on rotating shafts Part 2:
Land-based steam turbines and generators in excess of 50 MW with normal operating speeds of 1 500 r/min, 1 800 r/min, 3 000 r/min and 3 600 r/min

University of Nis
Faculty of Occupational Safety
„Politechnica“ University of Timisoara
Faculty of Mechanical Engineering
24th International Conference
NOISE AND VIBRATION
Niš, 29 - 31. 10. 2014.

THE EXPERIENCE OF DRIVERS AND THE PERFORMANCE OF DRIVING AS IMPACT FACTORS OF VIBRATION LEVELS IN AGRICULTURAL TRACTORS

Boban Cvetanović[1] Dragan Cvetković[2], Miljan Cvetković[1]

[1] *College of applied technical sciences Niš, Republic of Serbia,* boban.cvetanovic@vtsnis.edu.rs
[2] *Faculty of occupational safety, University of Niš, Republic of Serbia*

Abstract - *During everyday operations with tractors, drivers are exposed to harmful effects of various factors. One of the negative factors are vibrations deriving from driving aggregates and implements combined with the rough soil. These oscillatory loads are transferred to the cab, and through the floor and the seat to the body of the driver. In case of high level vibrations and during a long period of exposure to them, many health problems occur. Harmful effect of the vibrations is especially obvious in older models of tractors which don't have proper suspension, but are equipped with simple mechanical seats.. During measuring of vibrations at the seat of the driver, high intensities of vibrations were found, above permitted limits. A quality seat and suspension as well as good tires affect both the intensities of vibrations and their reduction. Organizational measures such as shorter working shifts and a change of drivers can only reduce the level of daily exposure, but can't affect neither the intensity of vibrations nor their reduction. On the other hand, the drivers' awareness of vibrations' harmful effect, detailed trainings and drivers' experience can affect the vibration level significantly. This work presents an attempt to show the effect of drivers' experience on the intensities of vibrations. A skillful driver, i.e. the performance of his driving, can have considerable influence on vibration level, with the effect more obvious in older tractor models than in new ones. The measurement results, with three different drivers (in the same working conditions: the same tractor model, type of soil and working operation), show how influential for the vibration level the driver's skills i.e. well-performed driving are. A skillful driver, in almost same working conditions, can reduce vibration levels even 20 times in comparison to an inexperienced one.*

Key words: *agriculture tractor, vibration, plowing, driver's experience, the performance of driving*

1. INTRODUCTION

Without a doubt, agricultural tractors have contributed enormously to the efficiency of agricultural operations making them easy and, in some cases, eliminating human labor completely. On the other hand, during their everyday activities, tractor drivers are exposed to many harmful influences which have complex negative effect to the health and hinder drivers' performances. These influences come both from the tractor system (noise, inadequately designed controls) and from the working conditions (precipitation, high relative humidity, dust, agriculture chemicals, high or low temperatures etc.). One of the important negative factors are vibrations [1]. Namely, during the operations, the entire tractor construction is subject to complex oscillatory processes induced by the combined influences of rough soil and a tractor aggregate and its implements. These high levels of vibrations that arise in such a complex system like the tractor are transferred from the cab floor to the seat and on to the whole body of the driver.

Vibrations can have high values and unfavourable frequencies imposing great risk to the driver's health. Because of combined influences of vibrations and other occupational health risks, it is not always possible to establish the correlation between the effect of vibrations and the illness of drivers. However, numerous scientific studies, bio-dynamic models and present knowledge of human body show that prolonged exposure to high-level vibrations can lead to low-back injuries, digestive system illnesses and cardio-vascular problems [2-6].

The harmful impact of vibrations is especially evident in older models of tractors which are not equipped with appropriate suspension system for shock and vibration absorption. The case of modern models, from that aspect, is better because they are equipped with improved suspension systems and seats. However, in comparison to improvements in the categories of power, fuel consumption, velocity or electronic controls, there is still room for additional improvements in protection of drivers from vibrations.

In Serbia there are 410 894 tractors, most of which (about 350 000) were manufactured by a Serbian manufacturer IMT - Industrija motora i traktora Beograd and all of them are more than 20 years old [7]. During the development of the tractors, from the aspect of oscillations, little attention was paid to comfort in driving in different working conditions, i.e. to tractors' capacity to reduce the negative influence of the oscillation of individual components on the driver to the least possible extent. In these tractors, shock absorption is done by tires and mostly simple mechanical seats, without additional suspension systems. Even today, this manufacturer considers optimizing of the elastic suspension system as a significant cost in production. The measurements of vibration levels at IMT tractor seats and their evaluations showed that the daily levels of exposure to vibrations were high [8].

A quality seat, suspension system and good tires affect both vibration levels and their reduction, but they are too expensive for farmers. Organizational measures such as shorter working shifts and a change of drivers can only reduce the level of daily exposure, but can't affect neither the intensity of vibrations nor their reduction. On the other hand, the drivers' awareness of vibrations' harmful effect, detailed trainings and drivers' experience can affect the vibration level significantly.

This paper is an attempt to learn how much a well-performed driving, i.e. the experience of a driver affect the level of vibrations. A skillful driver, i.e. the performance of his driving, can have considerable influence on vibration level, with the effect more obvious in older tractor models than in new ones

2. THE METHOD OF MEASUREMENTS

For the purpose of vibration level measurements (RMS accelerations), IMT 533 and 539 tractor models were used. The models have almost the same characteristics and they are said to be the most numerous models in Serbia. All of the tractors are equipped with simple mechanical seats and have the same engine - IMR M33/T, with the power of 35 to 39 HP. The difference was in the date of manufacturing, and the measuring was performed during plowing (the depth of 25 cm), during which high vibration levels occur. The average velocity of the tractors was 5km/h. The plowing was performed with two-furrow plows, on a similar types of soil.

Fig 1. *Tractor No 1 IMT 539*

Tractor No. 1., IMT 539, was manufactured in 1990, with about 1300 hours at the moment of measurement (fig. 1). The driver weighted 90 kg and was 187 cm tall and had 10-year experience in operating with the tractor whose number of hours was small.

The tractor No 2. was also IMT 539, manufactured in 1987, and had, at the moment of measuring, 5500 hours (fig 2). The driver weighted 75 kg, and was 173 cm tall, with 30 years of experience in working with tractors.

Fig 2. *Tractor No 2 IMT 539*

Tractor No 3 was IMT 533, manufactured in 1978., with over 10 000 hours at the moment of measuring. (two overhauls). The driver weighted 81 kg and was 175 cm tall with the longest experience of all three drivers in driving tractors

Fig 3. *Tractor No 3 - IMT 533*

Table 1. *Relevant data*

Driver	Tractor model	Manufactured in	Driver's experience (years)	Driver's age
1	IMT 539	1990.	10	45
2	IMT 539	1987.	30	63
3	IMT 533	1978.	35	60

For the measuring of vibration level a human vibration measuring device was used. The model was Brüel & Kjær Type 4447, with an accelerometer enclosed in a rubber pad, placed on the driver's seat (fig. 4)

Each measuring lasted at least 20 min, when the device displayed (except RMS acceleration values along all three axes) the level of daily exposure of drivers to vibrations A(8) for the reference time of 8 working hours. Obtained values were compared to the highest permitted values specified in EU Directive 2002/44/EC [9] and in Serbia specified in Serbian Rulebook of Safety precautions during exposure to vibrations [10].

Fig. 4. *Human Vibration Analyzer Type 4447*

In case of daily exposure to whole body vibrations, two values were suggested: an exposure limit value (ELV) which in professional working conditions must not be exceeded and is 1,15m/s^2 and exposure action value (EAV), above which employers must control health risks deriving from vibrations and which is 0,5m/s^2.

3. RESULTS

During the measurements, RMS values for all three axes were obtained. The highest values in all three cases were along X-axis, i.e. along the direction of tractors' motions (Table 2).

Table 2. *Intensities of RMS accelerations*

Driver	Tractor model	max RMS acceleration [m/s^2]
1	IMT 539	8.942
2	IMT 539	4.494
3	IMT 533	0.824

In order to compare to legally permitted values (Table 3), with these obtained values the daily level of exposure can be calculated for 8-hour reference time A(8) which is usual working shift. Obtained values show what the daily value of exposure of the driver would have been, if he had spent 8 hours of his shift operating with the tractor, without any interruptions, with the values of acceleration measured. The instrument itself calculates daily level of exposure for 1 hour- A(1), 4 hours – A(4) and 8 hours of continuous work - A(8), which makes possible to analyze values in case the driver had spent half the shift (or 1 hour only) driving, and the rest of the time performing some other activities not related to driving or having breaks during the shift.

In order to calculate daily values of exposure for different periods of exposure, an appropriate free software for calculating daily values of exposure A(8) for given periods is available.

Table 3. *Daily levels of exposure*

Driver	Tractor model	Daily level of exposure A(8) m/s²	Time to EAV [h:min]	Time to ELV [h:min]
1	IMT 539	12.519	00:00	00:04
2	IMT 539	6.292	00:03	00:16
3	IMT 533	1.153	01:30	07:56

4. DISCUSSION

The technical features of tractors, during measuring, were almost identical, with IMT 539 a bit more better than IMT 533 in terms of power and date of production. The daily levels of exposure of the drivers to vibrations were above the highest permitted values in all three cases. Mostly, that was because of the life of the tractors and the fact that the design and construction of the tractors dated 40 years ago, when ergonomic requests were not observed. Outdated suspension and seats cannot absorb vibrations, generated during the work of old diesel engines that are parts these tractors, combined with the rough soil. However, the expectations of new models to reduce the vibration levels haven't been fulfilled, which indicates that some other factors, such as the quality of driving, may affect the vibration level at the driver's seat significantly.

The measuring of vibrations at the seat of the first tractor lasted 25 min, and the calculation for 8-hour reference time gave extremely high daily level of exposure A(8)=12,519m/s^2, which is almost 10 times higher than legally permitted value (Fig. 5). A driver mustn't operate this tractor more than 4 min. This tractor was the best in terms of technical conditions, with the least number of hours.

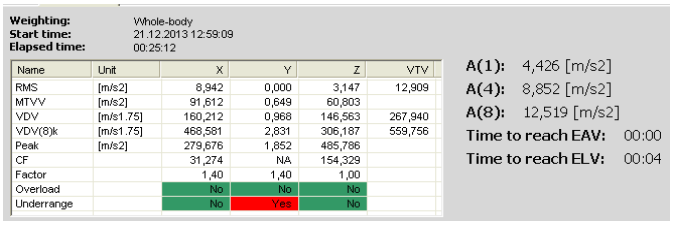

Fig 5. *Values of acceleration and levels of daily exposure for tractor No 1. IMT 539*

The measuring of vibrations at the seat of the second tractor IMT 539 lasted 48 min, and obtained daily level of exposure A(8)=6,292 m/s^2 was more than 5 times higher than legally permitted value. A driver could operate this tractor for only 16 min., when the permitted value of exposure would be reached (Fig.6).

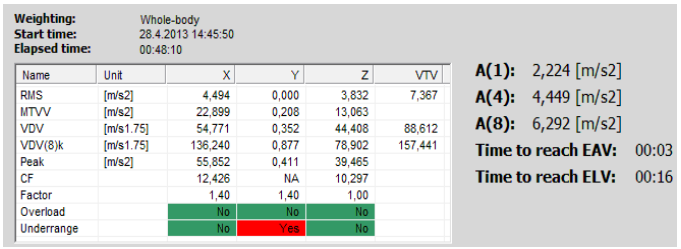

Fig 6. *Values of acceleration and levels of daily exposure for tractor No 2. IMT 539*

The model of IMT 533 was, in terms of technical conditions, the worst in comparison to other two tractors, but the level of daily exposure was nearly at the limit value. A driver could operate this tractor almost full 8-hour working shift. It seems that this driver performed the plowing better and faster, although this tractor moved at the same velocity like two other tractors.

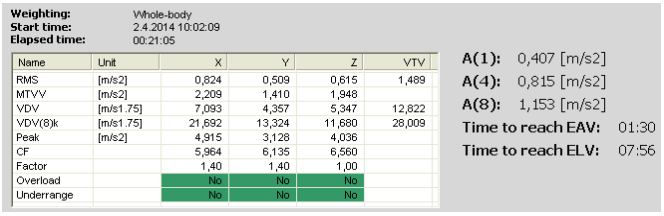

Name	Unit	X	Y	Z	VTV
RMS	[m/s2]	0,824	0,509	0,615	1,489
MTVV	[m/s2]	2,209	1,410	1,948	
VDV	[m/s1.75]	7,093	4,357	5,347	12,822
VDV(8)k	[m/s1.75]	21,692	13,324	11,680	28,009
Peak	[m/s2]	4,915	3,128	4,036	
CF		5,964	6,135	6,560	
Factor		1,40	1,40	1,00	
Overload		No	No	No	
Underrange		No	No	No	

Fig 7. *Values of acceleration and levels of daily exposure for tractor No 3. IMT 533*

5. CONCLUSION

The measurements of vibration levels in three IMT tractors (models 533 i 539) showed that when plowing with these tractors, drivers face health risks from vibrations. Although the working conditions and working modes were similar, the lowest levels of vibrations were in the oldest tractor, IMT 533, which was operated by the most experienced driver. On the other hand, the first tractor IMT 539 was manufactured 10 years after the third one, but was operated by a relatively inexperienced driver, so the values of daily exposure reached unacceptable figures, ten times more than legally permitted ones. It indicates the importance of experience in driving tractors, not only in terms of vibration levels, but also in terms of drivers' safety.

Without a doubt, technical measures affect the level of vibrations and their reduction. However, one should always keep in mind that the vibration levels, and especially their spreading, is also affected by a driver himself. A skilled and experienced driver, who is familiar with his vehicle and aware of harm from vibrations as well, will be able to affect the vibration levels efficiently. The experience of drivers is especially obvious in driving tractors without proper shock and vibration absorption system.

6. REFERENCES

[1] M.Bovenzi et al., An epidemiological study of low back pain in professional drivers, *Journal of Sound and Vibration* 298 (3) (2006) 514-539.

[2] H.C.Boshuizen et al., Self-Reported Back Pain in Tractor Drivers Exposed to Whole-Body Vibration, *International Archives of Occupational and Environmental Health.* 62 (1990) 109-115.

[3] O.O. Okunribido, M. Magnusson, M.H. Pope, Low back pain in drivers: The relative role of whole-body vibration, posture and manual materials handling, *Journal of Sound and Vibration* 298 (3) (2006) 540-555.

[4] M.Bovenzi, C.T.Hulshof, An Updated Review of Epidemiologic Studies on the Relationship Between Exposure to Whole-Body Vibration and Low Back Pain, *Journal of Sound and Vibration* 215(1998) 595-611.

[5] M.Futatsuka et al**.,** Whole-Body Vibration and Health Effects in the Agricultural Machinery Drivers, *Industrial Health.* 36(1998) 127-132.

[6] B.Cvetanović, J.Jovanović, A review of harmful effects to the health of tractor drivers from the impact of whole body vibration, *Tractors and power machines* 18 (3) (2013) 58-65.

[7] A.J.Scarlett, J.S.Price, R.M.Stayner, Whole – body vibration: Evaluation of emission and exposure levels arising from agricultural tractors, *Journal of terramechanics* 44 (2007), 65-73.

[8] B.Cvetanović, D.Zlatković, Evaluation of whole-body vibration risk in agricultural tractor drivers. *Bulg. J. Agric. Sci.* 19 (2013) 1161-1166.

[9] I.Hostens, K.Deprez, H.Ramon, An improved design of air suspension for seats of mobile agricultural machines, *Journal of Sound and Vibration*, 276(1–2) (2004) 141-156.

[10] Agricultural list 2012 - Agriculture in the Republic of Serbia, Institute of Statistics, 2012.

[11] European Parliament and the Council of the European Union: Directive 2002/44/EC on the minimum health and safety requirements regarding the exposure of workers to the risks arising from physical agents (vibration), 2002., Official Journal of the European Communities, OJ l 177,13

[12] The Official Gazette of Republic of Serbia, No. 101/05, Rulebook of Safety precautions during exposure to vibrations, 2005.

University of Nis
Faculty of Occupational Safety
„Politechnica“ University of Timisoara
Faculty of Mechanical Engineering
24th International Conference
NOISE AND VIBRATION
Niš, 29 - 31. 10. 2014.

HEALTH RISK EVALUATION OF WBV BY ISO 2631-1 FOR PASSENGERS IN URBAN PUBLIC TRANSPORT ROAD VEHICLES (BUSES)

Jovan Miočinović[1]

[1]TEHPRO DOO, Beograd-Železnik, Serbia, jovan.miocinovic@tehpro.rs

Abstract - *This paper presents experimental evaluation of the vibration exposure for the health risk prediction during vehicle transportation. The vibration measurements were carried out on a sample of public transport road vehicles (buses). The vibration levels were measured in situ for different types and vehicle speed conditions in controlled real environment. Basic evaluation method and additional evaluation is applied. Based on the analysis of the results for some types of buses weighted r.m.s. acceleration according to ISO2631-1, a_w exceeded 1,1 m/s^2. For the passengers that spent more than 1 h daily in public transport, e.g. going to their work and returning homes this puts them well into the health guidance caution zone according to the Eq B.2 of ISO2631-1, and for those who ride longer into the zone according to the Eq B.1. Average value of 0,65 m/s^2 for all included types of vehicles, would contribute to adverse health effects by daily exposure duration longer than 130 min. However, this indicates that these effects should be taken in addition to the exposure to whole-body vibration during regular working hours.*

1. INTRODUCTION

Urban population usually uses public transportation regulary in their everyday life when going to their work and returning homes. Therefore people are exposed to a variety of environmental conditions including whole-body vibration. Experimental evaluation of the vibration exposure during transportation in public transport road vehicles (buses) was made in order to establish probable vibration exposure levels in everyday transport and estimate the possible resulting health risk. Experimental measurements were made on the sample of buses on the same public line in Belgrade on the same route considered representative for Belgrade roads. Evaluation is made according to ISO 2631-1 [1]. Basic evaluation metod is applied and the additional for the measurements that required it. Measurement results were compared to health guidance caution zones according to ISO 2631-1 and daily exposure action and limit values according to Directive 2002/44/EC [2].

2. INSTRUMENTATION, SAMPLE AND MEASUREMENT LOCATION AND CONDITIONS

2.1. Instrumentation

For measurements was used SVAN 958 four channels sound (Type 1 IEC 61672-1:2002) and vibration (Type 1 ISO 8041:2005) level meter and analyser with seat accelerometer for whole-body measurements with DYTRAN 3143M1 - IEPE type triaxial accelerometer (Fig. 1).

Fig. 1 *SVAN 958 four channels sound and vibration level meter and analyser*

2.2. Sample and measurement location and conditions

Measurements were made in situ in real conditions in vehicles, on the total sample of 15 buses of 3 types. In total 30 measurements were made. Number of vehicles in the sample and number of measurements taken and number of measurements taken per vehicle type and per individual vehicle are given in tables 1 and 2.

Table 1 *Number of vehicles in the sample*

Vehicle type	Number of vehicles	Number of measurements taken
IKARBUS	5	5
MAN SG 313	7	16
MAZ 203	3	9

As for subsamples of vehicles in the sample, subsample of vehicles of type MAZ and subsample of vehicles of type MAN seem to be homogenous regarding age and condition. As for subsample of vehicles of type IKARBUS it seem to be inhomogeneous, vehicles are of different ages and conditions, including internal environment e.g. seat material - wooden, plastic and cushioned seats, that might make a difference in measured vibration exposure.

Table 2 *Number of measurements per vehicle type and per individual vehicle*

Vehicle type	vehicle serial no.	Number of measurements taken
IKARBUS	1267	1
IKARBUS	1276	1
IKARBUS	1292	1
IKARBUS	1296	1
IKARBUS	1303	1
MAN SG 313	1304	6
MAN SG 313	1321	2
MAN SG 313	1328	1
MAN SG 313	1336	2
MAN SG 313	1337	3
MAN SG 313	1342	1
MAN SG 313	1344	1
MAZ 203	2151	2
MAZ 203	2156	4
MAZ 203	2267	3

Measurements were taken on the same position in vehicles - on the right passenger seat on the left side of vehicle opposite to middle door (Fig.2).

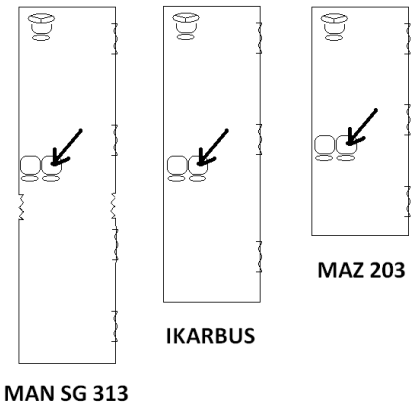

Fig. 2 *Measurement positions in vehicles for different types of vehicles in the sample. Positions are marked with an arrow pointing to the measurement position*

Measurements were taken according to ISO 2631-1 in seated position, with a person seated on the seat accelerometer according to a coordinate system in Fig. 3.

Measurements were made in controlled real environment. In addition to controlling parameters already mentioned - dividing the sample in subsamples by type and performing repeated measurements on the same vehicle, the third controlled parameter is the route. All the measurements were taken on is the same route on the public transportation line, line 511 in Belgrade. All measurements that are included are taken from bus station Palata pravde to the exit from the Obrenovački drum (road to Obrenovac) to Železnik. Measurement interval was devided in two segments, one from station Palata pravde to entering point to Obrenovački drum, and this one is considered representative to urban transportation conditions (regarding the road condition and stopping points on stations and traffic lights). The other segment is the one from entering Obrenovački drum to exiting to Železnik. This is the straight road with no damage and vehicle drive is uniform with no stopping. Measurements on this part of the route are used for considering the influence of speed of vehicle on measured weighted r.m.s. acceleration. Measurements were made in the same time of the day - between 7:30 and 9 in the morning on working days from January to March this year in the same weather conditions (dry road). Measurement duration was 7 - 10 min. for the first segment, and 7 - 10 min. for the second segment, i.e. duration of vehicle drive on the segments of the road.

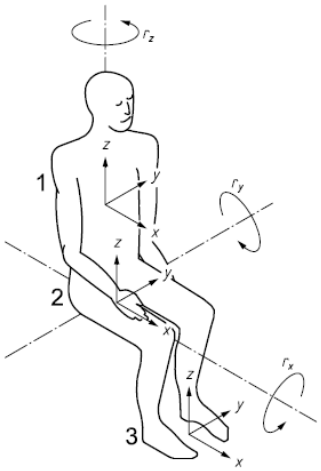

Fig. 3 *Basicentric axes of the human body for seated position according to ISO 2631-1*

3. MEASUREMENT RESULTS

3.1. Weighted r.m.s. accelerations

Measurements were taken in x-, y- and z-axis oriented as in Fig. 3. As the main result is taken the average value of measured weighted r.m.s. acceleration in x, y and z directions.

Average value is calculated as a mean value of the weighted mean values of measurements on subsamples. As the weigting factors for the calculation of the mean values of measurements made on subsamples square of the reciprocal value of measurement error is taken. As a measurement error for those measurements repeated on the same vehicle standard deviation corrected for the Student's t-distribution (for the level of confidence of 68%, i.e., 90%) is taken. For the measurements made only once on the same vehicle the error is estimated as uncertainty according to the adopted model [3], i.e. 0,16*ā for the measurements along x- and y-axes and 0,20*ā for the measurements along z-axis. The average value is calculated as an arithmetic mean value of values of subsamples. As for the expanded uncertainties estimation, the same errors are taken into account as for the level of confidence of 68% (i.e., standard deviations corrected for the Student's t-distribution or uncertainties as specified above) multiplied with 1,65. The idea is that real values would better be represented with repeated measurements, single measured rides would be well-described

with the uncertainty based on the mentioned model and that all the subsamples should be represented equally in the average value, that is, the probability for the passenger when catching the bus is equal for all the types of buses.

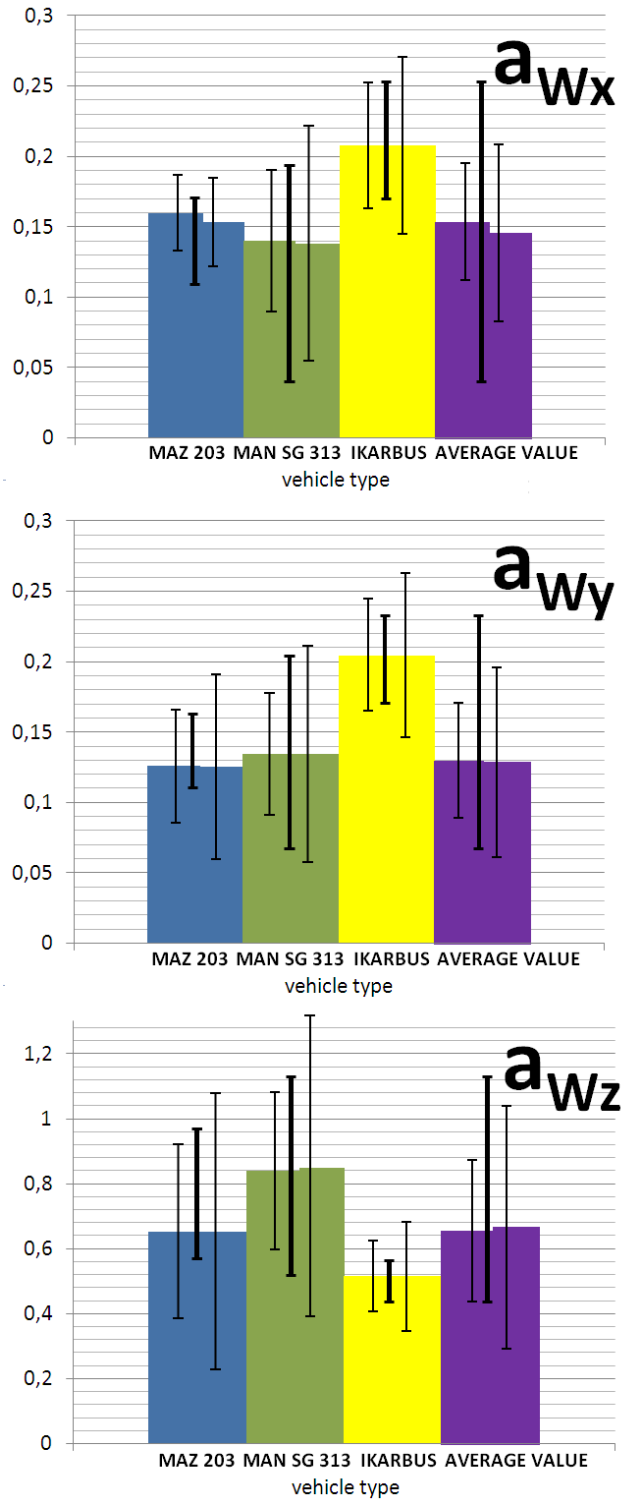

Fig. 4 *Weighted r.m.s. acceleration in x, y and z direction for different vehicle types and average value. On the left of the each column standard error (level of confidence of 68%) is presented, on the right side expanded uncertainty (level of confidence of 90%) and corresponding span from minimal to maximal values measured in the middle.*

The results for subsamples and the average values with standard errors, expanded uncertainties and span from minimal to maximal values measured are presented in Fig. 4. Vehicle type (MAZ 203, MAN SG 313 and IKARBUS) and the average value are presented with a column in the chart each from left to right. Left side of column represents mean value of weighted r.m.s. acceleration with standard error (level of confidence of 68% assuming Student's t-distribution for the measurements repeated on the same vehicle), right side mean value with expanded uncertainty (level of confidence of 90%) and the middle the mean value with the corresponding span from actual minimal to maximal values.

The results for x- and y-axis are practically the same. Small differencies of 15% could be due to vehicle braking and starting. Measured values made on subsample of IKARBUS are 50% greater then those made on the other two subsamples. As for the results for z-axis, values measured on that subsample are lower than measurements made on the others and only for that subsample comparable to the results for x- and y-axes, namely vibration components in x and y direction make 40% of the z direction component and therefore for that subsample might be convinient to include them in evaluation, according to [1]. Doing so, according to ([1], eq. (10))

$$a_v = (k_x^2 a_{Wx}^2 + k_y^2 a_{Wy}^2 + k_z^2 a_{Wz}^2)^{1/2} \qquad (1)$$

where k_x=k_y=1,4 and k_z=1 would result in multiplication of weighted r.m.s.acceleration values for the subsample by 1,3.

3.2. Influence of speed of vehicle on measured weighted r.m.s. acceleration

For considering influence of vehicle speed on weighted r.m.s. acceleration measured the measurement results taken on straight road are used, as discussed in 2.2.

In Fig. 5 correlations between vehicle speed and weighted r.m.s. acceleration measurements are presented. In the first line the relation between vehicle speed and measured weighted r.m.s. acceleration is presented for all vehicles and in second, third and fourth corresponding relation for subsamples, i.e. for different types of vehicles. On the left charts measured values for all 3 axes are presented and on the right ones values for x- and y-axes so that the relation on the larger scale could better be seen.

In the first chart the results for all vehicles are presented. Considering results for a_{Wz} it seems that the results are not related. Even when removing 5 measurments as outliners correlation coefficient becomes 0,75, but the results still remain scattered. On the left on the larger scale one can see better that the measurements in x and y directions are scattered. When considering the measurements on the subsamples same pattern can bee seen, all except the measurements made on MAZ 323 in z direction (chart in second line on the left). Here one can clearly see the linear dependance, with correlation coefficient 0,89.

So in the range of vehicle speeds (44 - 52 km/h) the measurements were done, there is no evident influence of difference in speed on measurement results, except for subsample of measurements made on buses type MAZ 323, where increase of weighted r.m.s. acceleration in z direction with increase of speed can be found.

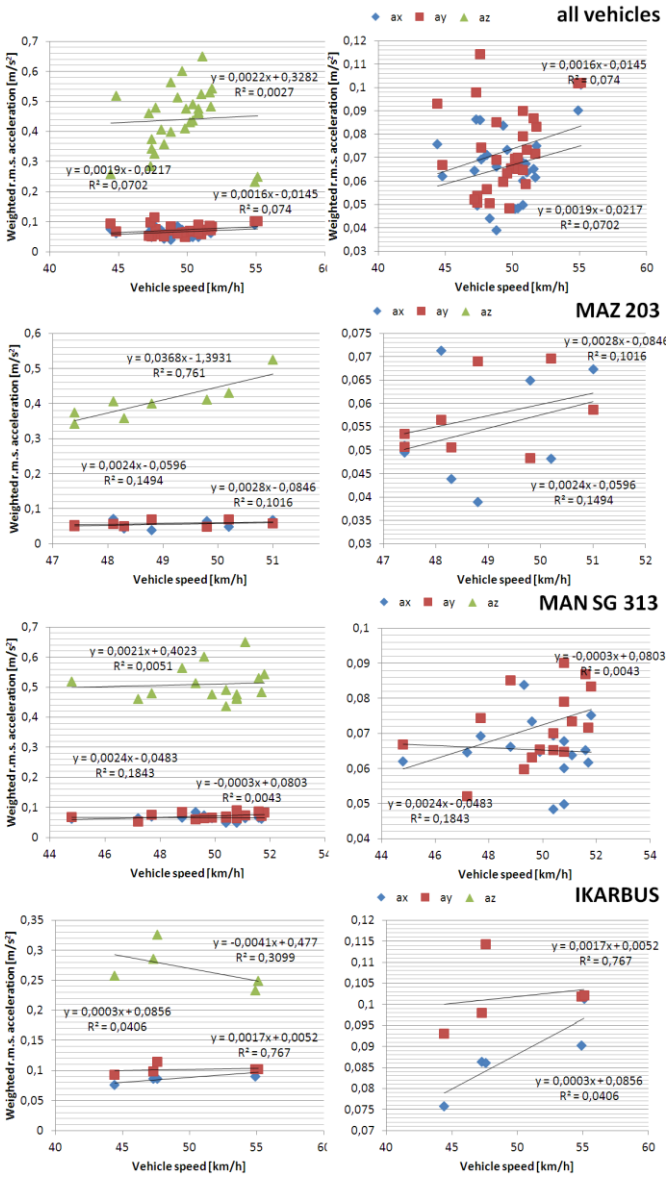

Fig. 5 *Correlation between vehicle speed and weigted r.m.s. acceleration for all vehicles and for different types of vehicles separately*

4. EVALUATION

4.1 Basic evaluation method

As for assessment of whole-body vibration with respect to health, there are several limit values for comparing with daily vibration exposures.

For basic evaluation method in ISO 2631-1 there are health guidance caution zones (Fig. 6), given in Figure B.1 in Annex B of the standard. Zones are defined with equations ([1], eq. (B.1) and (B.2)) :

$$a_{W1} * T_1^{1/2} = a_{W2} * T_2^{1/2} \quad (2)$$

$$a_{W1} * T_1^{1/4} = a_{W2} * T_2^{1/4} \quad (3)$$

where a_{W1} and a_{W2} are the weighted r.m.s acceleration values for the first and second exposures and T_1 and T_2 are the corresponding durations. First equation determines zone indicated by dashed lines in figure, and second equation the one indicated by solid lines.

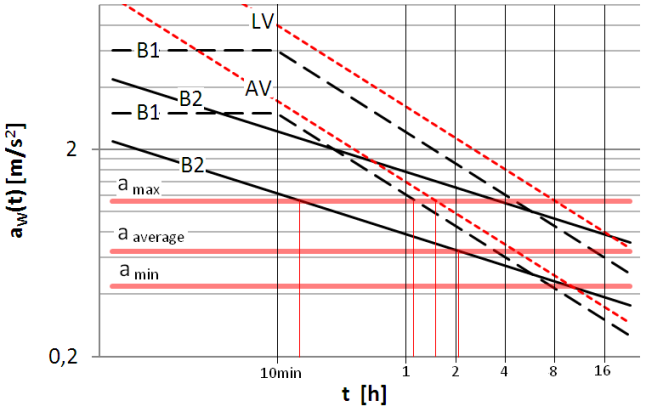

Fig. 6 *Health guidance caution zones. With solid lines is indicated the zone that corresponds the equation B.2 of ISO2631-1, with dashed lines the zone that corresponds the equation B.1. of the same standard and with dotted red lines the zone that is defined with action value and limit value of Directive 2002/44/EC. Horizontal red lines represent the experimental measured weighted r.m.s. acceleration values in z direction, maximal, average and minimal. Vertical red lines indicate the time when the corresponding caution zone is reached.*

Directive 2002/44/EC for basic evaluation method gives daily exposure action value of 0,5 m/s^2 standardised to an eight-hour reference period and daily exposure limit value of 1,15 m/s^2 standardised to an eight-hour reference period, and those values determine zone indicated by red dashed lines in Fig. 6.

When comparing measured values in z direction with zone limits according to B.1, B.2 and Directive (cross section of horizontal red lines and zone borders in the figure) one can see that in average, $a_{Waverage}$=0,65 m/s^2, health caution zone is achieved when spending 130 min in public transportation, according to eq. B.2. In fact, for urban population that isn't unlikely at all to spent all that time in transportation daily. As for the maximum acceleration value measured, a_{Wmax}=1,13 m/s^2, health caution zone is achieved after 14 minutes spent in the vehicle (first limit of zone B2), spending 70 minutes will bring the passenger in zone B1 and after 94 minutes the exposure exceeds daily exposure action value.

These values, corresponding times spent in vehicle needed to achieve the limit values for all measurements, i.e. average, minimum and maximum weighted r.m.s. acceleration values in z direction (see Fig. 4), together with corresponding ones for each vehicle type separately are given in the table 3.

In the table 3 times that seem probable to be spent in public transportation vehicles are shaded. In addition to the consideration taking into account all vehicles together and concerning values represented by red horizontal lines in Fig. 6, one can see that health guidance caution zones for basic evaluation method is possible or likely to achieve for two types of vehicles, MAZ 203 and MAN SG 313. For IKARBUS vehicle it is needed to spent nearly 5 hours riding minimum to enter the zone, that seems very unlikely. However, if the vibration components along x- and y-axis are included in evaluation, according to (1) as dicussed in 3.1, corresponding times in table 3 should be devided by 2,6 and

that would enable reaching the health guidance zone in a 110 minutes ride.

Table 3 *Corresponding times spent in vehicle needed to achieve the limit values for measurements made in z direction, for all the measurements and for each vehicle type separately. The times that seem probable to be spent in public transportation vehicles are shaded.*

Value evaluated	Time to achieve limit values (in minutes)					
	B.1. first limit	B.1. second limit	B.2. first limit	B.2. second limit	Directive action value	Directive limit value
ALL VEHICLES						
a_{Wz}	216,2	864,8	130,7	2091,2	288,3	1525,0
a_{Wmax}	70,6	282,3	13,9	222,9	94,1	497,9
a_{Wmin}	468,5	1874,0	613,7	9818,5	624,7	3304,4
MAZ 203						
a_{Wz}	211,0	844,0	124,5	1991,7	281,3	1488,3
a_{Wmax}	95,7	382,7	25,6	409,4	127,6	674,8
a_{Wmin}	277,2	1108,9	214,9	3438,0	369,6	1955,3
MAN SG 313						
a_{Wz}	124,0	495,9	43,0	687,4	165,3	874,4
a_{Wmax}	70,6	282,3	13,9	222,9	94,1	497,9
a_{Wmin}	333,2	1332,6	310,3	4965,0	444,2	2349,8
IKARBUS						
a_{Wz}	339,5	1358,2	322,3	5157,3	452,7	2394,9
a_{Wmax}	283,7	1135,0	225,19	3601,7	378,3	2001,4
a_{Wmin}	468,5	1874,0	613,7	9818,5	624,7	3304,4

4.2 Additional evaluation method

As for the additional evaluation of vibration when the basic evaluation method is not sufficient, the fourth power vibration dose method was used. Additional evaluation method is used in cases where the basic evaluation method may underestimate the effects of vibration (high crest factors, occasional shocks, transient vibration). ISO 2631-1 gives two alternative evaluatiom methods - the running r.ms. and the fourth power vibration dose, and there is also the evaluation method described in ISO 2631-5[4] as a third alternative. The indicators for using the additional method according to ISO 2631-1 are: crest factor greater then 9 and VDV/(a_W*$T^{1/4}$) greater then 1,75.

Table 4 *Number of measurements that needed the additional evaluation per vehicle type*

Vehicle type	Cases when additional method needed	evaluation in x or y direction needed	evaluation in z direction needed	total sample of measure-ments taken
IKARBUS	3	1	2	5
MAN SG 313	3	1	3	16
MAZ 203	3	1	2	8

As it happened the additional evaluation was needed for 9 measured values. In total,the indicators were exceeded in 3 measured values in x or y direction and 7 measured values in z direction. For different types of vehicle in the sample, the nubers are given in the table 4.

From the table it seems that cases when additional evaluation method was needed are equaly distributed in the total measurement sample, when taking into account separatly for z direction and for x and y direction together (horizontal directions), that is 0,2 - 0,4 in sample, only in the sample of measurements taken on MAN SG 313 need for additional evaluation is slightly less frequent (0,06 in sample).

Measured VDV values for all the cases that needed the additional method are given in the table 5. All values are normed for 1 hour exposure period.

Table 5 *Measured VDV values for the cases that needed the additional evaluation method. Values are normed for 1 hour exposure period.*

vehicle serial no.	vehicle type	VDVx [m/s^{1,75}]	VDVy [m/s^{1,75}]	VDVz [m/s^{1,75}]
2151	MAZ 203	2,16	-	-
2151	MAZ 203	-	-	18,79
2267	MAZ 203	-	-	11,05
1304	MAN SG 313	-	-	15,21
1337	MAN SG 313	2,06	2,10	17,36
1342	MAN SG 313	-	-	19,62
1267	IKARBUS	-	-	9,84
1292	IKARBUS	-	-	9,41

When comparing basic evaluation method values with the additional evaluation method values for cases that required additional evaluation it can be seen that values are strongly correlated (Fig. 7).

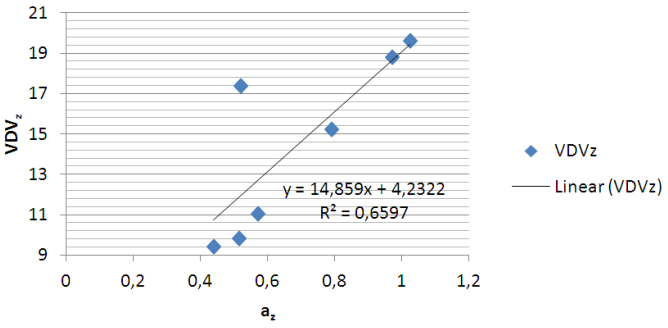

Fig. 7 *Correlation between VDV and weighted r.m.s. acceleration values in z direction*

When supstracting the outliner from the group the correlation factor is 0,997, that is, the relation is linear. That means that for only the one measurement the additional method gives something new. That is, for almost all the measurements that require the adittional evaluation VDV could be estimated well knowing weighted r.m.s. accelerations and this relation.

When comparing measured values with limit values, there are limits defined by B.2 [1] in health guidance caution zones figure (Fig. 6), when taking for estimated vibration dose value, eVDV=1,4*a_W*$T^{1/4}$, values 8,5 m/s^{1,75} and 17 m/s^{1,75} for the lower and upper bonds of the zone B.2.

Directive 2002/44/EC gives for exposure action value vibration dose value of 9,1 m/s^{1,75} and for exposure limit value vibration dose value of 21 m/s^{1,75}.

Corresponding times spent in vehicle needed to achieve the limit values (for the measurements made in z direction) are given in the table 6.

Table 6 *Corresponding times spent in vehicle needed to achieve the limit values for measurements made in z direction that required the additional evaluation method.The times that seem probable to be spent in public transportation vehicles are shaded.*

vehicle serial no.	**vehicle type**	**VDVz** (normed for 1h duration period) in $m/s^{1,75}$	**Time to achieve limit values (in minutes)**			
			B.2. first limit (8,5 $m/s^{1,75}$)	**B.2. second limit** (17 $m/s^{1,75}$)	**Directive action value** (9,1 $m/s^{1,75}$)	**Directive limit value** (21 $m/s^{1,75}$)
2151	MAZ 203	18,79	2,5	40,2	3,3	93,5
2267	MAZ 203	11,05	21,0	336,6	27,6	783,8
1304	MAN SG 313	15,21	5,8	93,5	7,7	217,8
1337	MAN SG 313	17,36	3,4	55,1	4,5	128,4
1342	MAN SG 313	19,62	2,1	33,9	2,8	78,8
1267	IKARBUS	9,841	33,4	534,4	43,9	1244,4
1292	IKARBUS	9,410	39,9	639,0	52,5	1488

In the table the times that are probable to be spent in public transportation vehicles are shaded. One can see that all the measurements that needed the addition evaluation method achieve the health caution zone in 2 to 40 minutes and Directive action value in 3 to 50 minutes, and that time spent in vehicle is very probable. As for longer rides, the second limit of B.2. zone is likely to achieve when spending 40 to 90 minutes and even Directive limit value is possible to achieve when spending 80 to 130 minutes in such vehicles.

5. CONCLUSION

Assuming that average exposure of passenger would be as in this paper calculated average value of weighted r.m.s. acceleration, $0,65 m/s^2$, first limit of health caution zone (according to eq. B.2 of [1]) is achieved when spending daily 130 min in public transportation. Focusing on transportation vehicle type, when riding in 2 of 3 experimentaly tested types is likely to achieve the first limit of health caution zone in 45 to 125 minutes. Regarding individual vehicles, riding in some tested ones would bring the passenger into first zone in 14 minutes, second limit would be reached in 70 minutes and in 94 minutes the exposure would even exceed the daily exposure action value. As for the additional evaluation method, where needed, limits of zone B.2 may be reached in 2 minutes, action value in 3 minutes, zone B.2 second limit in 30 minutes and limit value in 80 minutes. While according to weighted r.m.s. acceleration method for one vehicle type of three tested is most unlikely to achieve limit of health caution zone (when including the z axis only), situations that need the additional method are likely to occure by all the vehicle types and in such cases by all the vehicle types is possible to achieve the limit. All this indicates that under these conditions of everyday long ride in city bus transport urban population is exposed to a potential health risk. Due to additive and cumulative effect of vibration on health, this potential risk would be advisable to pay attention to as an additional factor when considering working urban population in those jobs the workers are normaly exposed to whole-body vibration.

REFERENCES

[1] ISO 2631-1:1997+A1:2010 Mechanical vibration and shock - Evaluation of human exposure to whole-body vibration - Part 1: General requirements.

[2] Directive 2002/44/EC of the European Parliament and of the Council of 25 June 2002 on the minimum health and safety requirements regarding the exposure of workers to the risks arising from physical agents (vibration). Off. J. Eur. Commun. 2002, L177, pp. 13-19

[3] Miočinović, J. "Measurement uncertainty estimation in evaluation of human exposure to WBv for passengers in urban buses", *24th International Conference "Noise and Vibration"*, Niš, 2014

[4] ISO 2631-5:2004 Mechanical vibration and shock - Evaluation of human exposure to whole-body vibration - Part 5: Method for evaluation of vibration containing multiple shocks

University of Nis
Faculty of Occupational Safety
„Politechnica“ University of Timisoara
Faculty of Mechanical Engineering
24th International Conference
NOISE AND VIBRATION
Niš, 29 - 31. 10. 2014.

MEASUREMENT UNCERTAINTY ESTIMATION IN EVALUATION OF HUMAN EXPOSURE TO WBV FOR PASSENGERS IN URBAN BUSES

Jovan Miočinović[1]

[1]TEHPRO DOO, Beograd-Železnik, Serbia, jovan.miocinovic@tehpro.rs

Abstract - *ISO 17025 requires that testing laboratories apply procedures for estimating uncertainty of measurement. General guide to the expression of uncertainty is given in ISO GUM 1995. While relevant standards for determination of noise exposure (ISO 9612, ISO 1996-2) have normative procedures for the evaluation of measurement uncertainties, vibration standards for evaluation of human exposure have, if any, list of possible sources of errors of measurement (e. g. EN 1032, ISO 20643). In this paper the uncertainty model for the measurement uncertainty in measurement of human exposure to whole-body vibration for passengers in buses is suggested and experimentally evaluated from the sample of in situ measurements made in public transport road vehicles (buses) according to ISO 2631-1.*

1. INTRODUCTION

ISO 17025 [1] requires that testing laboratories apply procedures for estimating uncertainty of measurement. Knowing the uncertainty associated with measurement results is essential for the correct interpretation of the results, e.g. for comparison with limit values.

There are two different approaches in determing measurement uncertainty. One is based on GUM model [2] and the other on ISO 5725 Parts 1 to 6 [3]. First one predicts the uncertainty in the form of a variance on the basis of variances associated with inputs to a mathematical model, so called “bottom-up” approach. The other uses the fact that, if those same influences vary representatively during the course of a reproducibility study, the observed variance is a direct estimate of the same uncertainty, so called “top-down” approach.

2. TWO APPROACHES IN THE UNCERTAINTY DETERMINATION

2.1 The GUM approach

The Guide to the expression of uncertainty in measurement (GUM) provides a methodology for evaluating the measurement uncertainty associated with a result *y* from a model of the measurement process.

According to GUM contributions to uncertainty may be evaluated either by the statistical analysis of a series of observations (“Type A evaluation”) or by any other means (“Type B evaluation”), for example using data such as published reference material or measurement standard uncertainties or, where necessary, professional judgement.

Separate contributions are expressed in the form of of standard deviations and combined as such.

If we represent the measured value as $y=f(x_1, x_2,\ldots, x_N)$, that is, as a function that relates the measurement result y to input quantities x_i, combined standard uncertainty is:

$$u_C^2(y)=\sum_{i=1}^{N}\left(\frac{\partial f}{\partial x_i}\right)^2 u^2(x_i)+ +2\sum_{i=1}^{N-1}\sum_{j=i+1}^{N}\frac{\partial f}{\partial x_i}\frac{\partial f}{\partial x_j}u(x_i,x_j) \quad (1)$$

Here $c_i = \partial f/\partial x_i$ are the sensitivity coefficients, $u(x_i)$ are standard uncertainties, i.e. measurement uncertainties expressed in the form of standard deviations and $u(x_i, x_j)=u(x_i)*u(x_j)= r_{ij}$ is the covariance between x_i and x_j, where r_{ij} is correlation coefficient.
If the input quantities are not significantly correlated this may be written as:

$$u_C^2(y)=\sum_{i=1}^{N}c_i^{\,2}u^2(x_i) \quad (2)$$

After calculating the combined standard uncertainty expanded uncertainty is calculated by multiplying it with a coverage factor *k*.

$$U = ku_C \quad (3)$$

Usually *k=1,65* or *k=2* is used, that means level of confidence of 90% or 95% respectively.

2.2 The collaborative study approach

Second approach is collaborative study approach. The simplest model underlying the statistical treatment of collaborative study data is given in equation be written as:

$$y = m + B + e \quad (4)$$

here *m* is the expectation for *y*, *B* the laboratory component of bias under repeatability conditions, assumed to be normally distributed with standard deviation σ_L and *e* is the random error under repeatability conditions, assumed to be normally distributed with standard deviation σ_W. *B* and *e* are assumed to be uncorrelated.

When applied to this model eq. (2) gives:

$$u^2(y) = u^2(B) + u^2(e) \quad (5)$$

σ_L^2 and σ_W^2 are the variances associated with B and e respectively and that these are estimated by the between-laboratory variance s_L^2 and the repeatability variance s_r^2 obtained in an inter-laboratory study, so that $u(B) = s_L$ and $u(e) = s_r$, (5) gives:

$$u^2(y) = s_L^2 + s_r^2 \quad (6)$$

or, according to ISO 5725-2, estimated reproducibility standard deviation, s_R.

3. MEASUREMENT UNCERTAINTY IN EVALUATION OF HUMAN EXPOSURE TO VIBRATION

In relevant standards for determination of noise exposure (ISO 9612 [4], ISO 1996-2 [5]) normative procedures for the evaluation of measurement uncertainties are given. That is, if standardized measurement procedure is followed all uncertainty components and the corresponding sensitivity coefficients for equations (1), (2) are given (so called uncertainty budget). Unlike this in standards concerning evaluation of human exposure to vibration (e.g. ISO 2631-1 [6], ISO 5349-1 [7]) there is no word relating to uncertainty estimation.

3.1 Sources of errors in vibration measurement

Concerning hand-arm vibration Clauses 6.2. and 7. of ISO 5349-2 [8] and Annex B of ISO 20643 [89], and concerning whole-body vibration Clauses 6.3. and 7. of EN 14253 [10] and Annex C of EN 1032 [11] consider sources of errors in vibration measurement as factors that should be considered in uncertainty evaluation.

Sources of uncertainty in vibration measurement according to ISO 5349-2, for measurement of hand-arm vibration and according to EN 14253, for measurement of whole-body vibration are presented in Table 1.

ISO 20643 and EN 1032 also give the list of possible sources of errors during vibration measurements as a guide to avoid the main errors in measurement, that adds to ones already listed in table 1 measurement duration, factors concerning measurement equipment adjustment, operational conditions and operators' experience (Table 2).

As for short measurement duration as a source of error, recommended minimal integration times according to ISO 5349-2, EN 1032 and EN 14253 are presented in table 3. Measurements of very short duration (e.g. less than 8 s) are unlikely to be reliable, particularly in their evaluation of low-frequency components, and should be avoided where possible.

Table 1 *Sources of uncertainty in vibration measurement according to ISO 5349-2 and EN 14253.*

ISO 5349-2 (concerning HAV)	EN 14253 (concerning WBV)
Sources of uncertainty in vibration measurement	
cable connector problems	
electromagnetic interference	
triboelectric effect	
	loss of contact between subject and seat
Factors related to individual measurements	
instrumentation accuracy	
calibration	
electrical interference	
mounting of accelerometers	
mass of accelerometers	
location of accelerometers	
	orientation of accelerometers
changes from the normal operation brought about by the measurement process (e.g. presence of accelerometers and associated cables) of:	
the power tool	the machine
and changes to:	
hand posture	body posture
changes in the operator's method of working as a result of being the subject of measurement.	
changes which occur in the course of any working day	
changes in the condition of:	
power tool and inserted tool (e.g. changing the wheel of a grinder may change the vibration transmitted to the operator dramatically)/	machine and equipment (e.g. changes in tyre pressure with temperature)
changes in posture and applied forces	
changes in the characteristics of:	
the materials being processed	the travelling surface
Factors related to the estimation of exposure duration	
measurements of the durations:	
of exposure	of operations or work cycles;
estimates of the number:	
of work cycles per day	of operations or work cycles per day
exposure time estimates supplied by the operators	
	variability of the working task from one day to another.

Table 2 *Possible sources of errors during vibration measurements according to ISO 20643 and EN1032.*

ISO 20643 (concerning HAV)	**EN 1032** (concerning HAV and WBV)
unsuitable mounting or fastening of accelerometers	
inadequate fastening of cables	
lack or misadjustment of band-pass filter	
not nulling output of amplifiers after mounting of transducers	
misalignment of directions of transducers, or inappropriate or varying position of the transducers	
inappropriate signal conditioning (band-pass, signal-to-noise ratio, overload, etc.)	
too short duration of measurement	
lack of calibration before and after measurement	
inappropriate definition of operational conditions	
unexperienced operators using inappropriate grip forces	
unstable operating conditions, such as fluctuating feed forces and varying motor speed	

Table 3 *The recommended minimal integration times to avoid errors in vibration measurement*

	ISO 5349-2	**EN 1032**	**EN 14253**
Measurement of HAV	8s	12s	N/A
Measurement of WBV	N/A	180 s	180 s

3.2 Uncertainty estimation in machinery test methods

In standards concerning test methods of machinery in order to determine the vibration emission value (EN 12096 [12] for vibrating machinery, EN 1032 for mobile machinery, EN 13059 [13] for industrial trucks, ISO 28927 Parts 1 to 11 [14] for hend-held portable power tools) as well as for assessment of exposure to vibration using information provided by manufacturers (CEN/TR 15350 [15]) uncertainty is estimated in accordance with EN 12096.

The uncertainty of the declared vibration emission value from the manufacturer is given as a *K* value.

For a single machine, if *a* is the measured vibration emission value for the machine,

$$K = 1{,}65 * \sigma_R \tag{7}$$

σ_R is the standard deviation of reproducibility as specified by the vibration test code (e.g. EN 1032 for whole-body vibration, ISO 20643 and ISO 28927 Parts 1 to 11 for hand-arm vibration). If there is no test code, or if it does not specify σ_R an estimation is used:

$$\sigma_R = \sqrt{\sigma_{op}^{\ 2} + \sigma_{rec}^{\ 2}} \tag{8}$$

where σ_{op} and σ_{rec} are the standard deviations of the recorded values from the different operators and from the same operator respectively.

Standard deviation of reproducibility is the standard deviation of measured values obtained under reproducibility conditions, i.e. the repeated measurement on the same machinery at different times and under different conditions (different laboratory, different operators, different apparatus). Therefore it includes the standard deviation of repeatability, σ_r, that is the standard deviation of measurements obtained under repeatability conditions - the repeated measurement on the same machine within a short interval of time under same conditions (same laboratory, same operators, same apparatus). It is estimated by

$$s_R = \sqrt{\frac{1}{n-1}\sum_{i=1}^{n}(a_i - \bar{a})^2} \tag{9}$$

where a_i are the results achieved at n different laboratories and $\bar{a}$ is their mean value.

For a batch of machinery,

$$K = 1{,}5 * \sigma_t \tag{10}$$

σ_t is the total standard deviation. (10) is based on ISO 7574-4 [16] and results in a 5% risk of rejection for the sample of three machines.

The total standard deviation is composed of the standard deviation of reproducibility and the standard deviation of production:

$$\sigma_t = \sqrt{\sigma_R^{\ 2} + \sigma_p^{\ 2}} \tag{11}$$

The standard deviation of reproducibility is given by the relevant vibration test code. The determination of the standard deviation of production is done by the manufacturer, based on his experience of the production variation.

σ_t can be estimated as:

$$s_t = \sqrt{s_R^{\ 2} + s_p^{\ 2}} \tag{12}$$

s_p is an estimation of standard deviation of production for sample of three or more:

$$s_p = \sqrt{\frac{1}{n-1}\sum_{i=1}^{n}(a_i - \bar{a})^2} \tag{13}$$

where a_i is the measured vibration emission value of each machine in the sample and $\bar{a}$ is the mean value of the sample. If reasonably large sample is not available, s_p may be estimated from experience.

If data required for the determination of *K* are unavailable, uncertainty may be estimated according to values given in Table 4.

Table 4 *Uncertainty **K** for different measured values **a** according to EN 12096*

Measured value a		**Uncertainty K**
Hand-arm vibration	Whole-body vibration	
2,5 m/s^2 < a ≤ 5 m/s^2	0,5 m/s^2 < a ≤ 1 m/s^2	0,5a
a > 5 m/s^2	a > 1 m/s^2	0,4a

Standards for test methods for evaluating vibration emission (EN 13059 and ISO 28927 Parts 1 to 11) give similar values for uncertainty *K* as in Table 4. Values for *K* used in standard machinery vibration test methods are given in Table 5.

Table 5 *Uncertainty **K** for different measured values **a** according to EN 13059 and ISO 28927 Parts 1 to 11*

Standard test method	Type of vibration tested	K, tests on single machines	K, tests on batches of machines
EN 13059	WBV	0,3ā	0,3ā
ISO 28927-Parts 1 and 4	HAV	0,33ā	1,5σ_t,according to (12) where s_r=0,2ā
ISO 28927-Parts 2, 3, and 5 to 11	HAV	0,1ā + 0,5*	s_r=0,06ā + 0,3*
* or according to (12), whichever is the greater			

Values in table are valid when coefficient of variation C_V of measurements obtained according to the standard measurement procedure is less then 0,15.

$$C_V = \frac{s_{n-1}}{\bar{a}} \tag{14}$$

Values for *K* are based on empirical estimations of σ_R (eq. 9).

3.3 Uncertainty budget in evaluation of human exposure to vibration

Detailed consideration of possible sources of errors in vibration measurement and experimental evaluation of the respective uncertainties are given by Schenk [17] based on measurements made on a variety of hand held machinery. In Table 6 are given the values of measurement uncertainties relating sources of influence.

Table 6 *Measurement uncertainties (level of confidence 90%) for sources of errors in measurement of vibration emission from hand held vibrating machinery according to Shenk*

measurement technology including calibration	10%
mounting of accelerometers	5%
transducer position	30%
with operator	8%
on test bench	4%
from the different operators	15%
for a batch of machinery	8%

All this combined for one machine (without including the uncertainty for a batch of machinery) would give 36%, that is in accordance with the values given in Table 4.

One can see from Table 6 that the highest contribution to uncertainty is from the accelerometer position, and this is specific to HAV measurements. One should expect much less influence from differencies in seat accelerometer position in measuring WBV.

As for the instrumentation as a source of uncertainty in vibration measurement, one could use the data used for uncertainty estimation in acoustics. In Table 7 uncertainty budget is given according to ISO 9612.

Table 7 *Sources of uncertainty considered in determining the expanded uncertainty of A-weighted equivalent continuous sound pressure levels or noise exposure levels normalized to an 8 h working day for job-based measurement, according to ISO 9612*

Source of uncertainty	Application	Subscript
Sampling of job noise levels	Job-based measurement	1
Instrumentation	All strategies	2
Microphone location	All strategies	3

Uncertainty according to Table 7 is:

$$u^2(L_{EX,8h}) = \sum_{i=1}^{3} c_i^{\,2} * u_i^{\,2} \tag{15}$$

Sensitivity coefficients for the uncertainty due to the instrumentation and measurement position, c_2 and c_3 are:

$$c_1 = c_2 = 1 \tag{16}$$

Standard uncertainty, u_2 for the instrumentation used is given in Table 8.

Table 8 *Standard uncertainty, $\boldsymbol{u_2}$ for the instrumentation used, according to ISO 9612*

Type of instrumentation	Standard uncertainty, u_2 [dB]
Sound level meter as specified in IEC 61672-1:2002, class 1	0,7
Sound level meter as specified in IEC 61672-1:2002, class 2	1,5

Standard uncertainty, u_3, due to measurement position is 1,0 dB.

While the instrumentation used in vibration and acoustical measurement is the same, one could adopt the values given in table 8.

Converting the values into percentage would give 0,08 for class 1 instrument and 0,17 for class 2 instrument. When comparing to the value of 10% from table 6, one should multiply the values by 1,65, that would give 13,2 % and 28%. That is, the value of uncertainty for measurements made with class 1 instrument adopted from the Table 8 would give the similar contribution as according to Shenk.

While adopting the uncertainty for instrumentation from acoustical model seems reasonable, as for the contribution due to measurement position, value of 1 dB is based on empirical data for acoustical measurements. It comprises influences from the screening and the reflections from the workers body when microphone position is close to body or differences from the true workers position when measured in workers absence, and that does not seem to be applicable in vibration measurements.

4. EXPERIMENTAL EVALUATION OF UNCERTAINTY MODEL IN MEASUREMENT OF HUMAN EXPOSURE TO WBV FOR PASSENGERS IN URBAN BUSES

Experimental measurements were made on the sample of buses on the same public line in Belgrade on the same route

considered representative for Belgrade roads. Evaluation is made according to ISO 2631-1.

4.1 Instrumentation, sample and measurement location and conditions

4.1.1 *Instrumentation*

For measurements was used SVAN 958 four channels sound (Type 1 IEC 61672-1:2002) and vibration (Type 1 ISO 8041:2005) level meter and analyser with seat accelerometer for whole-body measurements with DYTRAN 3143M1 - IEPE type triaxial accelerometer.

4.1.2. *Sample and measurement location and conditions*

Measurements were made in situ in real conditions in vehicles, on the total sample of 15 buses of 3 types. In total 30 measurements were made. Number of vehicles in the sample and number of measurements taken and number of measurements taken per vehicle type and per individual vehicle are given in tables 9 and 10.

Table 9 *Number of vehicles in the sample*

Vehicle type	Number of vehicles	Number of measurements taken
IKARBUS	5	5
MAN SG 313	7	16
MAZ 203	3	9

As for subsamples of vehicles in the sample, subsample of vehicles of type MAZ and subsample of vehicles of type MAN seem to be homogenous regarding age and condition. As for subsample of vehicles of type IKARBUS it seem to be inhomogeneous, vehicles are of different ages and conditions, including internal environment e.g. seat material - wooden, plastic and cushioned seats, that might make a difference in measured vibration exposure.

Table 10 *Number of measurements per vehicle type and per individual vehicle*

Vehicle type	vehicle serial no.	Number of measurements taken
IKARBUS	1267	1
IKARBUS	1276	1
IKARBUS	1292	1
IKARBUS	1296	1
IKARBUS	1303	1
MAN SG 313	1304	6
MAN SG 313	1321	2
MAN SG 313	1328	1
MAN SG 313	1336	2
MAN SG 313	1337	3
MAN SG 313	1342	1
MAN SG 313	1344	1
MAZ 203	2151	2
MAZ 203	2156	4
MAZ 203	2267	3

Measurements were taken on the same position in vehicles - on the right passenger seat on the left side of vehicle opposite to middle door (Fig.1).

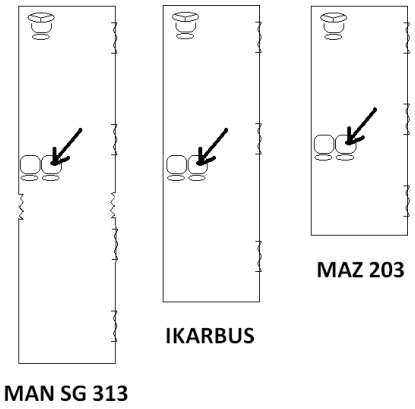

Fig. 1 *Measurement positions in vehicles for different types of vehicles in the sample. Positions are marked with an arrow pointing to the measurement position*

Measurements were taken according to ISO 2631-1 in seated position, with a person seated on the seat accelerometer according to a coordinate system in Fig. 2.

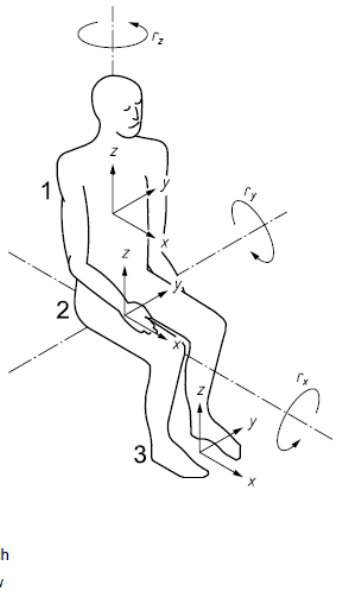

Fig. 2 *Basicentric axes of the human body for seated position according to ISO 2631-1*

Measurements were made in controlled real environment. The route all the measurements were taken on is the same route on the public transportation line, line 511 in Belgrade. All measurements that are included are taken from bus station Palata pravde to the exit from the Obrenovački drum (road to Obrenovac) to Železnik. Measurement interval was devided in two segments, one from station Palata pravde to entering point to Obrenovački drum, and this one is considered representative to urban transportation conditions (regarding the road condition and stopping points on stations and traffic lights). The other segment is the one from entering Obrenovački drum to exiting to Železnik. This is the straight road with no damage and vehicle drive is uniform with no stopping. Measurements on this part of the route are used for

considering the uncertainty attributions. Measurements were made in the same time of the day - between 7:30 and 9 in the morning on working days, from January to March this year in the same weather conditions (dry road). Measurement duration was 7 - 10 min. for the first segment, and 7 - 10 min. for the second segment, i.e. duration of vehicle drive on the segments of the road.

4.2. Uncertainty model and the measurement results

Basing on the model for uncertainty given in section 3.3 in this paper, Table 7 and eq. 15, uncertainty budget is presented in Table 11.

The additional factor, uncertainty due to the road is added suggesting that vehicle ride in the real environment would give an additional uncertainty due to vehicle ride characteristics on the road (accelerating, breaking, stopping) and road characteristics (small damages, bumps, etc.) comparing to driving uniformly on the straight road, that is already presented with factors representing influence of the accelerometer position and instrumentation. Keeping this in mind, the dispersion of measurements on the flat road could be attributed to the accelerometer position and instrumentation, and the dispersion of measurements on the road considered as representative for urban bus ride could be attributed to all three factors.

Table 11 *Sources of uncertainty in evaluation of human exposure to WBV in buses*

Source of uncertainty	Application	Subscript
Sampling	evaluation of human exposure to WBV in buses	1
Instrumentation	evaluation of human exposure to WBV in buses	2
Accelerometer position	evaluation of human exposure to WBV in buses	3
Road	evaluation of human exposure to WBV in buses	4

The calculations for this model are based on measurements made on the same vehicles, when three or more measurements are made, i.e. in repeatability conditions as discussed in section 3.3. That is, in absence of reproducibility, results are based on repeatability conditions. This has been done for 4 vehicles, two of each type of MAZ 203 and MAN SG 313. The standard deviations of measurement results are given in Table 12. The results are given for x, y and z axis separately.

Table 12 *Standard deviations of measurements of weighted r.m.s. acceleration on flat road and in real environment*

Vehicle serial number	Number of measurements made	Weighted r.m.s. acceleration		Standard deviation	
		flat road	real environment	flat road	real environment
z-axes					
2156	3	0,405633	0,652417	0,005793	0,015384
2267	3	0,35845	0,69547	0,015777	0,171814
1304	6	0,488655	0,865087	0,057127	0,088775
1337	3	0,521233	0,835213	0,041969	0,305282
x-axes					
2156	3	0,05836	0,1288	0,017165	0,001887
2267	3	0,048143	0,128323	0,003735	0,00879
1304	6	0,062142	0,129752	0,008174	0,012836
1337	3	0,0658	0,106873	0,003642	0,057809
y-axes					
2156	3	0,05794	0,131827	0,010433	0,014293
2267	3	0,05164	0,120053	0,001647	0,009116
1304	6	0,066117	0,141185	0,008979	0,015043
1337	3	0,07545	0,147827	0,009199	0,071927

Uncertainties are calculated as the mean values of respective coefficients of variation C_V (eq. 14) and uncertainty due to the road as:

$$u_4 = \sqrt{C_{Vr}{}^2 - C_{Vf}{}^2} * \bar{a} \qquad (17)$$

In table 13 values for coefficients of variation C_V and calculated uncertainty due to the road are given.

Table 13 *Values for coefficients of variation C_V and estimated uncertainty due to the road u_4*

Measure-ment direction	coefficients of variation, C_V		$u_4/\bar{a} = \sqrt{(C_{Vr}{}^2 - C_{Vf}{}^2)}$
	flat road, C_{Vf}	real environment, C_{Vr}	
z-axes	0,105686	0,199442	0,169139
x-axes	0,120579	0,157534	0,1013755
y-axes	0,13204	0,167576	0,103184

Values for uncertainty due to the accelerometer position and instrumentation are likely to be the same for the measurement in all three directions, and from the Table 13 may be evaluated as:

$$\overline{C}_{Vf}{}^2 * \bar{a}^2 = u_2{}^2 + u_3{}^2 = 0{,}12^2 * \bar{a}^2 \qquad (18)$$

If we compare this value to the uncertainty estimated according to EN 13059 (Table 5):

$$u = \frac{K}{1{,}65} = 0{,}18 * \bar{a} \qquad (19)$$

We see that the component due to instrumentation and accelerometer position in this model is 1/3 less then the one considered in EN 13059. Uncertainty estimation in this standard is more likely to present all three components from this model.

As for the road components, it seems from the model that the components might differ along z-axis and along x and y-axes:

$$u_4{}^{z} = 0{,}17 * \bar{a}$$
$$u_4{}^{x,y} = 0{,}1 * \bar{a} \quad (20)$$

The resolution of the components 2 and 3 could be made according to estimations from acoustics (Table 8) or according to Shenk (Table 6). Values for the component are given in Table 14.

Table 14 *Values for uncertainty due to instrumentation for IEC 61672-1:2002, class 1 instrument estimated according to ISO 9612 and according to Shenk*

	Uncertainty due to instrumentation, u_2
Estimation based on ISO 9612	0,08*ā
Estimation based on [17]	0,06*ā

If the average value is taken, the resulting component u_3 from eq. 18 is:

$$u_3 = 0{,}1 * \bar{a} \quad (21)$$

The combined standard uncertainty, excluding the uncertainty due to sampling, according to this model is:

$$u^2 = u_2{}^2 + u_3{}^2 + u_4{}^{z\,2} \quad (22)$$

that is,

$$u = 0{,}21 * \bar{a} \quad (23)$$

for the measurements made along z-axis and:

$$u^2 = u_2{}^2 + u_3{}^2 + u_4{}^{x,y\,2} \quad (24)$$

that is,

$$u = 0{,}16 * \bar{a} \quad (25)$$

for the measurements made along x-and y-axes.

The expanded uncertainty is U=1,65*u, that is:

$$U = 0{,}35 * \bar{a} \quad (26)$$

for the measurements made along z-axis and:

$$U = 0{,}26 * \bar{a} \quad (27)$$

for the measurements made along x- and y-axes.

5. CONCLUSION

According to a model adopted in this paper, based on measurements in repeatability conditions on a sample of 4 buses and total of 30 measurements in x-, y- and z-direction each, for measurement uncertainty in measurement of human exposure to WBV for passengers in urban buses is found to be composed of 3 main components, non including the one due to sampling. It seems that one of the components, named the road component, differs depending on measurement axis. Comparing to the uncertainty given in EN 13059 this new component is separated from the instrumentation component and the accelerometer position component. It is expected that this model would work in the other situations of measurement of human exposure to WBV (e.g. not in vehicles) where this road component wouldn't appear.

REFERENCES

[1] ISO/IEC 17025:2005+Cor 1:2006 General requirements for the competence of testing and calibration laboratories

[2] ISO/IEC Guide 98-3:2008 Uncertainty of measurement - Part 3: Guide to the expression of uncertainty in measurement (GUM:1995)

[3] ISO 5725 Parts 1 to 4 Accuracy (trueness and precision) of measurement methods and results

[4] ISO 9612:2009 Acoustics - Determination of occupational noise exposure - Engineering method

[5] ISO 1996-2:2007 Acoustics - Description, measurement and assessment of environmental noise - Part 2: Determination of environmental noise levels

[6] ISO 2631-1:1997+A1:2010 Mechanical vibration and shock — Evaluation of human exposure to whole-body vibration — Part 1: General requirements

[7] ISO 5349-1:2001 Mechanical vibration - Measurement and evaluation of human exposure to hand-transmitted vibration - Part 1: General requirements

[8] ISO 5349-2:2001 Mechanical vibration - Measurement and evaluation of human exposure to hand-transmitted vibration - Part 2: Practical guidance for measurement at the workplace

[9] ISO 20643:2005+A1:2012 Mechanical vibration - Hand-held and hand-guided machinery - Principles for evaluation of vibration emission

[10] EN 14253:2003+A1:2007 Mechanical vibration. Measurement and calculation of occupational exposure to whole-body vibration with reference to health. Practical guidance

[11] EN 1032:2003+A1:2008 Mechanical vibration. Testing of mobile machinery in order to determine the vibration emission value

[12] EN 12096:1997 Mechanical vibration. Declaration and verification of vibration emission values

[13] EN 13059:2002+A1:2008 Safety of industrial trucks. Test methods for measuring vibration

[14] ISO 28927 Parts 1 to 11 Hand-held portable power tools - Test methods for evaluation of vibration emission

[15]CEN/TR 15350:2013 Mechanical vibration - Guideline for the assessment of exposure to hand-transmitted vibration using available information including that provided by manufacturers of machinery

[16]ISO 7574-4:1985 Acoustics - Statistical methods for determining and verifying stated noise emission values of machinery and equipment. Methods for determining and verifying stated values for batches of machines

[17]Schenk, Th. "Vermeidung von Messfehlern bei der Ermittlung der Schwingungsemission vibrierenden Handmaschinen", *Arbeitswissenshaftliche Erkenntnisse Nr. 119*, Bundesanstalt für Arbeitsscutz und Arbeitsmedizin, Dortmund, 2000

University of Nis
Faculty of Occupational Safety
„Politechnica“ University of Timisoara
Faculty of Mechanical Engineering
24th International Conference
NOISE AND VIBRATION
Niš, 29 - 31. 10. 2014.

EQUIPMENT MAINTANANCE – FACTOR OF PROFESSIONAL NOISE EXPOSURE REDUCTION

Simion Sorin[1], Artur G. Găman[1], Pupăzan Daniel[1], Angelica Călămar[1]

[1] INCD INSEMEX Petroşani, România, e-mail: sorin.simion@insemex.ro

Abstract - *Noise is a technological metabolism by-product, representing one of the most important discomfort factors for personnel that work in energetic coal extracting and preparation processes.*

Being aware of the general risks specific to energetic coal extracting and preparation activities, generated by exposure to noise, helps quantifying the effects upon workers, such as: blanking, auditory fatigue, sonorous trauma, partial loss of hearing, professional deafness.

Prolonged exposure to high intensity noise may lead, in time, to professional deafness. Unlike auditory fatigue, which is a transitory and reversible phenomenon, noise caused deafness is characterized by definitive and irreversible loss of hearing.

The number of people exposed to noise is continuously rising because of the equipment's increasing work speed and power and increased mechanization.

The current paper analyzes the evolution of the main sources of noise specific to energetic coal extracting and preparation processes, depending on maintenance and refurbishment.

Keywords: noise, ear protection, occupational diseases.

1. INTRODUCTION

Industrial development has led to increased power and work speed of equipment used in the production processes, leading to a diversified and increased number of noise sources and hence increased number of people exposed.

Noise is one of the most important industrial emissions that generate occupational hazards by becoming a harmful factor, occurring from equipment damage and / or malfunction. [1;3]

Noise has a noxious influence on human body, this influence being firstly felt by the hearing organ. Systematic prolonged action of intense noise may represent a cause for decreases in the auditive capacity and, in severe cases, cause of total hearing loss.

In the mining and coal preparation activity developed in the Jiu Valley, the presence of risks generated by noise can not be ignored, because it affects the health and safety of workers.

Strategically, the issue of exposure to noise is unitarily approached at European level, according to European practices, by progressive implementation of regulations and techniques used by EU member states regarding the monitoring of noise emission levels in workplaces. [2]

To improve working conditions, specific guidelines for physical noxae (noise, vibration, electromagnetic radiation, etc.) were developed, providing minimum requirements that guarantee an optimal level of protection for workers. The purpose of these Directives is to reduce the number of occupational disease occurrence. Occupational deafness and hyperacusis influence all the activities of affected people by creating discomfort both in private life and workplace. Occupational deafness and hyperacusis affect more and more workers, leading to increasing costs for the healthcare system because these diseases are irreversible.

2 THE PURPOSE OF NOISE DETERMINATIONS

The technological processes of energetic coal extraction and preparation use noise generating machinery and equipment.

Main noise sources may be found in the following processes:

- horizontally and vertically mining mass transportation,
- water discharge
- compressed air production,
- crushing mining mass,
- preparation and separation of coal from the rock mass,
- tailings transportation to dumps, etc.

In order to improve occupational health and safety conditions and achieve the objective of reducing noise exposure, some general principles should be considered, regarding:

- occupational risks prevention;
- protecting the health and safety of workers,
- elimination of accidents and professional diseases hazards [3, 4]

3. THE PARTICULARITIES OF NOISE DETERMINATIONS IN THE MINING INDUSTRY

The noises emitted during technological processes of energetic coal extraction and preparation are continuous (present when generating pneumatic energy, discharging groundwater, during mining mass preparation) or intermittent (when drilling, blasting, transporting minerals and tailings).

The particularities of extraction and preparation activities are:

- Impairing the ability of exposed workers to perceive noises made by underground mining pressure, eruptions of gases and fines particles etc.
- Masking warning acoustic signals (e.g. the conveyor's on / off signal, funicular start/ stop signal, etc.)

Noise levels produced by the equipment and facilities used in extraction and preparation of energetic coal comprise all types of noise including impulse noise that also produce effects on humans.

Noises in the process of extraction and preparation of energetic coal are among the ones with most numerous effects on the human body. Depending on the level of noise intensity and exposure time, there are several types of harmful effects on workers, namely:

- The masking effect,
- Hearing tiredness;
- Acoustic trauma;
- Acute hyperacusis;
- Occupational deafness.

In processes of energetic coal extraction and preparation, most appropriate methods for noise control at existing sources consist of active and passive protection measures.

The purpose of noise reduction is to achieve optimum acoustic comfort without affecting the production capacity at an affordable price.

4. THE EQUIPMENT USED

For noise noxae determinations, we used Bruel & Kjaer type 2250 integrated sound meter, Bruel & Kjaer type 4231 calibrators and the BZ 5503 determinations software. For ensuring the quality of results, sound meters and calibrators are inspected in accordance with the effective legislation.

In order to determine the A-weighted sound exposure and /or the level of equivalent continuous A-weighted sound pressure, the measurement of sound pressure was performed with the microphone placed in the position (s) usually occupied by the worker's head.

If during the measurement the necessity for the worker to be present or to move nearby came up, then the microphone was positioned at about 0.10 m ± 0.01 m from the entrance to the ear canal, where it receives the highest level of A- weighted sound exposure and /or highest level of equivalent continuous A-weighted sound pressure [2;5]

An estimate of the measurement's overall uncertainty was included when reporting the results, taking into account the influence of factors such as:

- Measuring equipment;
- Microphone's location;
- Number of measurements;
- Noise source time and space variation.

5. RESULTS

Table 1 shows the average results of measurements performed on noise generating equipment used in energetic coal mining and preparation activities carried out in Jiu Valley and their evolution in time, over a period of seven years. [2;3]

The evolution of noise depending on time, and also the tear, wear and changes occurring after maintenance and overhaul operations may be noticed.

Lack of major investments in new technologies is noticeable by the increased level of noise emitted by equipment in the monitoring period.

TABLE 1 *Experiment results*

Job / equipment name	P90 Pneumatic Drill	CA14 jackhammer	Scraper Conveyor TR 3	TMB belt conveyor	Funicular mining unit	Crusher	Picking belt	Vibrating screen	Funicular preparation unit	Tailings Belt conveyor
Year	*Noise level dB(A)*									
2007	101,6	109,1	93,9	88,4	88,1	91,5	92,2	97,3	87,9	89,5
2008	102,3	108,3	94,2	88,5	89,2	91,2	93,2	97,1	88,1	89,9
2009	102,5	107,2	94,1	88,9	89,8	96,9	96,3	98,1	88,2	91,8
2010	101,2	108,5	95,2	91,1	96,1	92,0	96,3	99,2	100,4	92,6
2011	104,3	108,4	95,6	91,6	88,5	90,3	98,2	99,1	90,9	100,5
2012	102,4	107,1	96,2	96,1	91,3	92,0	95,5	98,2	92,2	89,2
2013	103,6	108,5	95,2	95,2	92,5	93,2	100,3	101,7	95,1	89,4

Diagram no.1 shows the evolution in time of equipment that has been subjected to a regular maintenance program.

Due to the relatively low costs and low complexity, periodic maintenance of equipment like pneumatic drills, jackhammers, scraper conveyors, belt conveyors, crushers, can be performed by own mechanical workshops, which does not require an additional financial effort from the economic operators. Performing maintenance influences the levels of noise emissions; we noticed a relatively small variation in noise up to 4 dB(A) per analyzed period.

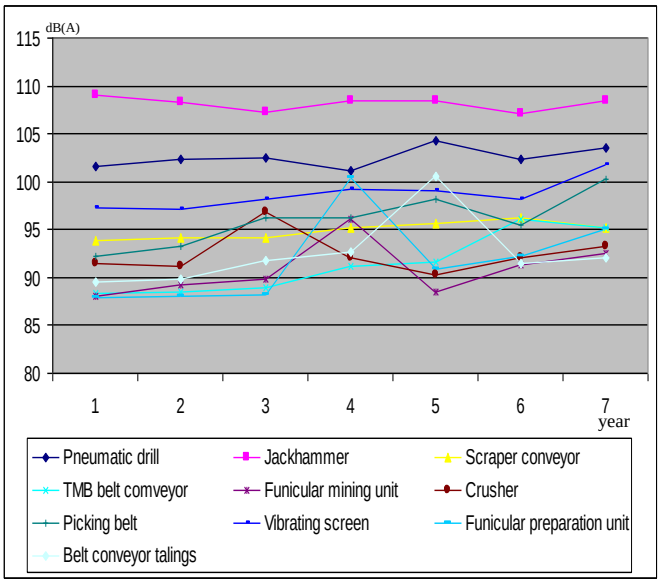

Fig. 1 *Evolution of equipment that has been subjected to a regular maintenance program*

Diagram no.2 shows the time evolution of two machines, whose maintenance calls for allocation of large funds. Maintenance of these two devices takes a long cut-off time from the activity and granting of significant funds for economic operators.

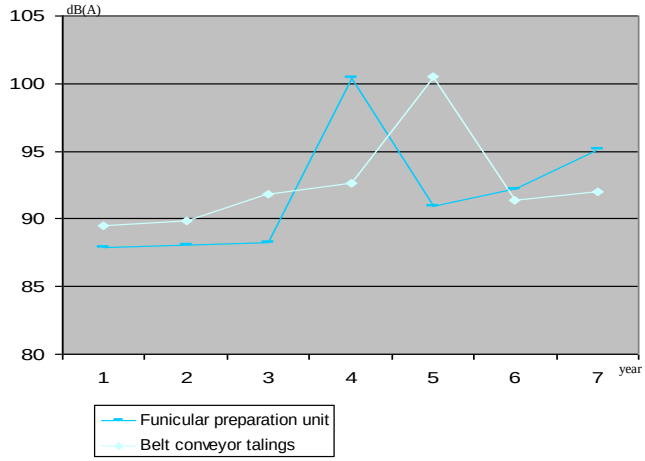

Fig. 2 *Time evolution of two machines whose maintenance requires large repair funds*

The repair works were not made with the same rigor because of the high cost of maintenance for the two devices, of the decreased production capacity, lack of funds for investment, restructuring of the mining filed; this led to higher levels of noise emissions generated by the wear of cable transportation system components.

One can notice that the funicular noise increases with wear within the period 2007-2010 when no repairs were made, and in 2011, after conducting major overhaul and maintenance operations (replacement of the traction cable, main actuator replacement, replacement of rollers, cups etc.) we notice a decreasing in noise emission by about 10 dB(A) approximately returning to 2007 parameters.

The major overhaul of tailings belt conveyor (rollers replacement, belt, actuation stations) carried out in 2011 has reduced noise by approx. 11 dB(A).

Regarding energetic coal extraction and preparation processes, the effectiveness of a maintenance programs may be monitored by knowing the noise level evolution in time depending on equipment wear out. The effectiveness of maintenance programs should not be viewed only through the prism of economic efficiency, cost / productivity, but also in terms of safety and health at work. A well established and kept maintenance program reduces noise levels and /or maintains them within the parameters specified by the manufacturer.

Increased knowledge also allows retrofitting old equipment and lowering noise emissions that are affecting the health and safety of workers.

The analysis of specific noise sources in the processes of extraction and preparation of energetic coal showed that the optimal noise reduction solutions are:

- Upgrading / replacement of equipment with silenced new one;
- Carrying out maintenance processes in accordance with the manufacturer specifications for equipment;
- Installation of acoustic screens in the vicinity of noise source and replacement of control elements;
- Use of individual hearing protection;
- Limitation of exposure time.

6 CONCLUSIONS

From the above we subtracted the following conclusions:

- Maintenance activities have a major influence on noise levels, being able to can contribute to the improvement of work conditions.
- The relatively low request for energetic coal leads to reduced allocation of funds for upgrading / buying quieter new equipment. Lack of funds for investment in the processes of extraction and preparation of energetic coal, high degree of physical and moral wear of equipment used, lead to increased number of people exposed to hazardous noise levels that may affect safety and health.
- Contrary to financial difficulties in purchasing appropriate equipment and facilities that generate acceptable levels of noise emissions, we notice a positive trend on the use of protective equipment to noise, due to informing and raising awareness between workers.
- The lack of markings regarding noise emissions makes it difficult to assess the effectiveness of maintenance work in terms of workers exposure to noise. The effectiveness of these works can be determined only by measuring noise during a relatively long period of time or by comparison with similar equipment.
- Applying markings for acoustic power on equipment and informing the workers led to creating a safer working environment by reducing exposure to this noxae.

In order to verify the effectiveness of noise reducing methods, regardless of their nature (technical, organizational) we propose periodic audiograms of workers because hearing loss is an irreversible disease that affects the quality of both personal and professional life. [2].

REFERENCES

[1] A. Darabont, "Prevention and control of noise in mining". Bucharest 1973.

[2] Simon Sorin "Research on noise and vibration in the basin of Jiu Valley mines 2012".

[3]Sorin Simion, C. Vreme, M. Kovacs, L. Toth "Exposure of Workers to Noise in Mining Industry" International Symposium AVMS-Timişoara, May 26, 2013

[4] ***Law 319/2006. Law on occupational safety and health

[5] ***Directive 2003/10/EC of 6 February 2003 on the minimum health and safety requirements regarding the exposure of workers to the risks arising from physical agents (noise) [Seventeenth individual Directive within the meaning of Art. 16 para. (1) of Directive 89/391/EEC].

[6] ***SR ISO 1999:1996. Acoustics. Determination of occupational noise exposure and estimation of noise - induced hearing impairment.

University of Nis
Faculty of Occupational Safety
„Politechnica“ University of Timisoara
Faculty of Mechanical Engineering
24th International Conference
NOISE AND VIBRATION
Niš, 29 - 31. 10. 2014.

SUFFIXATION AS A WORD FORMATION PROCESS

Jelica Tošić[1]

[1] University of Nis, Faculty of Occupational Safety, Serbia, jelica.tosic@znrfak.ni.ac.rs

Abstract *- This paper has focused on the process of suffixation as one of the very frequent morphological processes to be used in word formation. It specifically deals with the -ed, -ing, and -scape suffixes that proved to be quite productive in noise protection discourse. The book that was used for this analysis was „Noise Mapping in the EU - Models and Procedures“ edited by Gaetano Licitra.*

1. INTRODUCTION

The book that was used as a basis for this analysis is *Noise Mapping in the EU – Models and Procedures* (2013) edited by Gaetano Licitra. Its eighteen chapters served as a starting point for undertaking the lexical analysis of the titles and subtitles appearing throughout the book. This corpus was analysed without taking account of the titles and subtitles of a general type like *Introduction*, *Conclusion*, *Contents*, *References*, *Comments*, *Summary*, *Note*, *General Remarks*, *Glossary*, *Acknowledgement*. Therefore, apart from the book title and the eighteen chapter titles, the book comprises five section titles and 263 subtitles – altogether 287 subjects for our analysis.

The lexical analysis undertaken in this study deals with the specific noise protection discourse. Rather, it is concerned with suffixation as one of the morphological processes of word formation. In some science or scientific field, just as in ordinary language, new words are constantly introduced, some words get modified, some disappear. This all depends on the pace of development of the field or science. Language users in these fields are simply led by practical reasons to manipulate words but the result is the changed lexicon which subsequently enters the specialised language dictionaries first, and then, if the words become widely accepted, the general dictionaries of the language.

2. THE *-ED* AND *-ING* SUFFIXES FOR ADJECTIVE FORMATION

A suffix is a letter or letters, sound or sounds, or syllable or syllables that are added to the end of a word to make another word. The result, therefore, is a new word or the addition of some grammatical function, which is not of any interest in this paper. The basic word is called the root because it cannot further be decomposed without losing its identity and meaningfulness. In other words, if we reverse the definition, it is that part of the word that is left when all the affixes, either preceding or following it, are removed. From the semantic point of view, the root carries the main or the basic meaning in the word. The process of adding some ending(s) to a word is called suffixation. Derivational suffixes denote or change the type to which the word belongs. Suffixes are quite telling about whether some word is a noun, an adjective, adverb etc. Thus, recognition of the suffix is helpful because it enables you to understand the meaning of the word without necessarily looking it up.

Although they can also serve as inflectional suffixes, the *-ed* and *-ing* suffixes are also morphologically significant as a way of adjective formation. They are both added to verbs changing this class into the adjective. Following the general rule, the *-ed* suffix[1] denotes the quality that has arisen out of some process that has been finished or done, and the *-ing* suffix denotes the quality that is the outcome of some evolving process. The following *-ed* and *-ing* adjectives have been found in the book:

Table 1. *The* ***-ed*** *and* ***-ing*** *suffixes forming the adjectives*

-ed	***-ing***
integrated database[2]	*rolling* stock
triangulated network	*rolling* noise
(highly) *annoyed* people	*surrounding* area
calculated noise levels	*rolling* noise component
measured noise levels	*existing* noise methods
soundscape-based action plans	
perception-oriented action plans	

3. COMPOND-FORMING SUFFIXES

Some other suffixes can also be thought of as having acquired a more autonomous status than the previous ones. This means that, although they can be treated as suffixes and as such can be found in the affixes lists in the dictionaries, they can also be treated as full-meaning words. *Proof*, for example, is both a suffix or combining form in the dictionaries, but it is also an adjective in its own right. The earliest dictionary (1974) used

[1] *Although generally applicable to irregular verbs as well as a mark of the past participle and thus as an adjective, this suffix was restricted in our analysis to regular verbs only.*

[2] *The single word* database *was probably first written as a compound made from two words:* data base *and* data-base *(analogous to the example in Potter 1976: 86). The* Webster's New World Dictionary *gives the hyphenated variation with the addition of a two-word variation.*

for this analysis does not even have *-proof* in its *Affixes* list – it is just treated as a separate entry, marked as an adjective. Anyway, when this suffix, combining form or word is added to some noun, the resulting form is an adjective. Likewise, the other suffix analysed here *-scape* is also added to nouns, but the resulting form is a noun. Although this suffix cannot be found in modern dictionaries as a separate entry, one cannot help mentioning its etymological significance – 'the Old English *-ship* is related to *shape* and *scape* in *landscape*.' (Potter 1976: 87). To illustrate how linguistic processes work in word formation, it might be useful to list and compare the words derived by means of these two suffixes with the integrated meanings:

Table 2. *-proof* and *-scape* suffixes

-proof	***-scape***
1. resistant to, unaffected by *2. protected from or against*	*1. a specified kind of view or scene* *2. a drawing, painting, etc. of such a view or scene*
waterproof	landscape
rustproof	seascape
bullet-proof	moonscape
splinter-proof	cityscape
fireproof	cloud-scape
soundproof (soundproof room/walls)	soundscape
foolproof (a foolproof machine)	
inflation-proof pension	
to proof (make something proof)	to scape*
to soundproof a room	to soundscape a square

Some of the words in this table are written as one unit i.e. one word. Some other words are written with a hyphen. These variations are present because of the lexicographers' stance as to the degree to which the constituents have grown compact.

It goes without saying that these suffixes or combining forms can be avoided because there are some other ways of saying the same thing, but these combinations 'are useful ways of condensing information and they add variation to the way we refer to concepts in discourse' (Hatch-Brown 1995: 191). The same authoresses add that the use of the field-specific words or the jargon of the field 'also establishes membership. If you don't know the words, you don't belong.' (ibid.: 312).

4. SOUNDSCAPE

To go back to the book that was the subject of our analysis, the word *soundscape* has become its focus. The term *soundscape* is a brave innovation devised by a Canadian composer Murray Schafer, who called his project the *World Soundscape Project* (WSP). The composer, or the artist, could not but think creatively about the sounds in an environment. His and his followers' goal was to achieve the overall effect of *tranquillity* (p. 376) experienced in the environment or to approach the desired concept of non-annoying or pleasing sounds for the environment's occupants. But, his explanations give a dual definition of the term: on the one hand, it simply denotes an acoustical environment; on the other hand, it means the environment that is artificially created by sound. The following table illustrates the way this word is used in the book *Noise Mapping in the EU – Models and Procedures*:

Table 3. *The negative vs. positive meanings of „soundscape"*

Soundscape	
an existing acoustical environment ***noise pollution*** ***diagnostics***	***an environment artificially created by sound*** ***creativity***
to induce artificial variations in the soundscape	superimposing an artificial soundscape to the existing, polluted one
artificially induced variations in a soundscape	action plans based on the effect of positive soundscapes
actions that...directly affect the soundscape in an area	not just noise reduction but positive soundscape management
noise polluted soundscape	the Soundscape Concept in action plans
add to the existing soundscape some gentle suggestions	soundscape design
soundscape-specific indicators	soundscape-specific tools
direct or indirect modifications of the soundscape	
preassessment of the soundscape, intervention, postassessment	the re-soundscaped[3] square
soundscape research	
soundscape-specific indicators	
noise maps, which will describe soundscapes	
assessment of soundscape quality outdoors	
NEGATIVE	***POSITIVE***
no control	***control established***

[3] *This is how the caption under a picture of a square in Florence, Italy (2010) (p.386) begins. Prefix* -re *emphasises going back or returning to a previous state, but here it is returning to the same square which has been modified somehow in terms of noise perception i.e. it has been soundscaped.*

Therefore, the two meanings of the word *soundscape* can be formulated like this: 1. all the sounds and noises characteristic of a specific environment. The excess of sounds and noises usually has an unpleasant effect on the people living or staying in this environment and it is therefore termed *noise pollution*. The term is burdened with a very negative connotation because the word *pollution* is immediately suggestive of something negative. If the term is accepted, then the only thing that people can do in such an environment is defend themselves. Murray Schafer suggested a more active approach: 2. you are the one who can create your acoustical environment – this is the second meaning of his definition of *soundscape*. In this sense, soundscapes are the new subjects of mapping and, consequently, of action plans. This is something that you can add to your acoustic environment i.e. these are the sounds which are artificially created so as to qualitatively change the negatively coloured sounds of your environment. It is, therefore, possible to say that in this sense soundscape is a possibility, something that you as an individual, group, or community can do to make the existing acoustical environment better to the extent that it is completely changed by the sounds you yourself introduced because they are what you want to hear. It all seems to be a matter of choice: you are the creator and not the one who is passive and does nothing about the things you don't like.

5. CONCLUSION

This paper has tried to shed light on some of the morphological processes operative in noise protection discourse. Apart from more ordinary *-ed* and *-ing* suffixes used for adjective formation, the suffix *-scape* seems quite productive in inventing the new nouns. Its initial use as a noun-forming suffix opened the way to the process of conversion as a linguistic process of word formation whereby it is possible 'to create additional lexical items out of those that already exist' (Hatch-Brown 1995: 179) e.g. to use a noun as a new, so-far non-existent verb. Converting the lexemes of a language is not only a sign of language change, it is also a sign of individual creativity. Soundscaping (a verbal noun) therefore involves creativity both in terms of noise protection and in terms of linguistics. Even though no dictionary I consulted gives the exact entry of the word, either as a noun or a verb, the inherent possibilities allow the noun compounds and verb formation – if *landscape*, *seascape*, etc. are possible, why shouldn't there be a *soundscape*? And, by analogy, if *landscaping* is possible, why shouldn't there be *soundscaping*? If you can plan or change the natural scenery of a place for a desired purpose or effect, then why is it not possible to soundscape (plan and change the acoustics of) the same place? Noise experts have proved that it is possible. Lexicography is a bit slower, it lags behind the developing reality. New words may sound strange for a time, but then people get used to the new use of the word. The word *soundscape* is an example of the fact that language changes all the time. 'There is no standstill in language', and the changes are most conspicuous in lexical or vocabulary items, which 'tend to be added, replaced, or changed in meaning more rapidly than any other aspect of language' (Aitchinson 2001: 16-17).

REFERENCES

[1] Aitchison, Jean. 2001. *Language change: progress or decay?*. Cambridge: Cambridge University Press.

[2] Hatch, Evelyn and C. Brown. 1995. *Vocabulary, Semantics, and Language Education*. Cambridge: Cambridge University Press.

[3] Klajn, Ivan i M. Šipka. 2010. *Veliki rečnik stranih reči i izraza*. Novi Sad: Prometej.

[4] Kristal, Dejvid. 1998. *Enciklopedijski rečnik moderne lingvistike*. Beograd: Nolit.

[5] Licitra, Gaetano. 2013. *Noise Mapping in the EU – Models and Procedures*. Boca Raton: CRC Press.

[6] *Longman Dictionary of English Language and Culture*. 1998. Harlow: Addison Wesley Longman.

[7] *Oxford Advanced Learner's Dictionary of Current English*. 1974. London: Oxford University Press.

[8] Potter, Simeon. 1976. *Our Language*. Harmondsworth: Penguin Books Ltd.

[9] *Webster's New World Dictionary*. 1988. Cleveland: Simon and Schuster, Inc.

Акредитационо тело Србије 00035
Accreditation Board of Serbia

Београд
Belgrade

додељује
awards

СЕРТИФИКАТ О АКРЕДИТАЦИЈИ
Accreditation Certificate

којим се потврђује да организација
confirming that

Универзитет у Нишу
Факултет заштите на раду у Нишу
Центар за техничка испитивања
Ниш

акредитациони број
accreditation number
01-393

задовољава захтеве стандарда
fulfils the requirements

SRPS ISO/IEC 17025:2006
те је компетентна за обављање послова испитивања
and is competent to perform testing

који су специфицирани у обиму акредитације
as specified in the scope of accreditation

Важеће издање обима акредитације доступно је на интернет адреси: www.ats.rs

Сертификат додељен
Date of issue
21.05.2013.

Акредитација важи до
Date of expiry
20.05.2017.

ATC

В. Д. Директор
Acting Director

М.П.

Акредитационо тело Србије је потписник Мултилатералног споразума о признавању еквивалентности система акредитације Европске организације за акредитацију (EA MLA) и ILAC MRA споразума у овој области. / Accreditation Body of Serbia is a signatory of the European co-operation for Accreditation (EA) Multilateral Agreement for accreditation and ILAC MRA in this field.

University of Nis
Faculty of Occupational Safety
„Politechnica“ University of Timisoara
Faculty of Mechanical Engineering
24th International Conference
NOISE AND VIBRATION
Niš, 29 - 31. 10. 2014.

NOISE IN THE TOURIST RESORT - AN ENVIRONMENTAL PROBLEM OR LUXURY THAT FOLLOWS EVERYDAY LIFE

Nikolić Aleksandar[1], *Mladenka Vujošević*[2]

[1]Faculty of Business Studies of the Mediterranean Tivat, Montenegro, tipotek@t-com.me
[2]Institute of Public Health, Podgorica, Montenegro

Abstract: *In developed countries citizens clearly recognize problem with exessive noise as factor that negatively affects population health. Unfortunately, this is not the case in our country where this problem is especially pronounced in the coastal region during summer seasons. In order to verify these claims in practice, recordings of environmental noise levels were carried out in the tourist settlement Donja Lastva within the Tivat municipality. The measurement results indicate the presence of environmental noise in the tourist settlement Donja Lastva. Deviations observed in both summer and winter period, classify enviromental noise in a group of pollutants that significantly affect the lives and health of people. Exceeding of the allowed values also indicate the presence of problems that could endanger future generations.*

1. INTRODUCTION

Compared with other environmental factors, there is little understanding regarding the control of communal noise, and it is not considered as one of the priorities to be addressed in order to protect the environment and health. Insufficient knowledge about effects of noise on human life, health and the environment can be specified as a reason, particularly when exposure to noise lasts for an extensive period of time. This is particularly evident in developing countries where institutions responsible for dealing with noise problems considered communal noise as "luxury" that follows everyday life. In developed countries, citizens clearly recognize the problem and point to the noise as the main factor that negatively affects entire population. Unfortunately, this is not the case in Montenegro where noise problem is prominent in the coastal region, especially during the peak of tourist season. In order to verify these claims in practice, recordings of environmental noise levels were carried out in the tourist resort Donja Lastva within the Tivat municipality. Following noise sources have been identified: road traffic noise taking place along the Adriatic highway and local traffic routes close to the coast, air traffic noise connected with Tivat airport, noise caused by loud music from tourist and hospitality facilities, from floating facilities, noise created by air conditioners and noise due to the presence of large number of people.

2. METHODOLOGY

Tourist settlement Donja Lastva extends close to the shore. In the area from the the church "St. Roch" to playground "Zog" series of stone houses, waterfront, several "small moles" and small beaches are located. Four positions characterized with different noise sources were selected to perform the experiment (Figure 1).

Figure 1 *Satellite image of settlement with measurement points (marked with stars)*

First selected position (position 1) is located close to the local road and in front of the church "St. Roch". Nearby is located riva which brings together a large number of bathers and which also serves as a dock. Noise sources originate from motor vehicles, motorcycles, boats, ships and bathers.

Second measurement position (position 2) is also next to the the road in front of a local cafe bar "Mar-Mar". This position was selected in order to determine impact of noise generated by the guests, the music program emitted in cafe, as well as traffic taking place on local roads.

The third position (position 3) is right in front of a residential building, which is located along the street equipped with

airconditioning system. This position was selected in order to determine noise emitted by vehicles and air conditioning system.

The fourth measurement position (position 4) is located right next to road in front of the former cafe "Donja Lastva" and a small beach. Presence of a large number of people during the summer months is typical for this position, as well as the presence of "urban canyon" (two buildings separated by streets, which ensures the propagation of sound without significant reduction of of energy that is otherwise characteristic when range-distance increases in relation to the noise source).

Data on noise generated by the people, the traffic, and the effect of increasing the level of noise due to the "urban canyon" were collected at this position. Sound levels were measured using precise modular analyser (Brüel and Kjær, type 2250, meets IEC 6160804). In accordance with the ISO 1996 standard, the measuring instrument is set to be on the minimum distance of 1.5m from any reflective surface and the height of 1.2m from the ground. Selecting of measurement interval is observed by Article 6 in Rulebook of measurement methods and instruments to be met by the organization to measure the noise[1]. According to this Rulebook, changeable noise levels are measured in three intervals during the day (06h-22h) and two intervals during the night (22h-06h). Minimum duration of the measurement interval is 15 minutes.

The first measurement interval was from 07:00 h to 07:15 h.

The second measurement interval was from 11:00 h to 11:15 h.

The third measurement interval was from 18:00 h to 18:15 h.

The fourth measurement interval was from 23:00 h to 23:15 h.

The fifth measurement interval was from 01:00 h to 01:15 h.

Values of environment noise level are normatively regulated (2), so that noise levels in residential areas must not exceed the permissible value for a particular residential zone. In this case, residential area is classified in zone V, where the equivalent noise level limit shall not exceed a value of 60 dB for daytime and evening period, while during night time, equivalent noise level must not exceed 50dB. Characteristics of climatic conditions during the measurement process are clear and quiet weather (air speed ≤ 5 m/s), temperature varied in the range 13-320C, air pressure was in the range 880-1020mbar, and humidity of 59-93 %.

3. RESULTS

Analysis of the obtained results will determine whether equivalent noise levels on the selected measurement points exceed the allowable limits for exposure to environmental noise, as well as causes of excessive noise. Measuring instrument performs a statistical analysis of noise levels. Measured noise levels are grouped in classes width 0.2 db. Based on the data for equivalent noise levels, percentile levels, the distribution of noise and the cumulative distribution are determined (Figure 2). At the same time, the instrument performs a parallel real-time analysis of the defined bandwidth. Measurement parameters were determined from a sample of variable noise in all frequency bands with a defined bandwidth and center frequency (Figure 3).

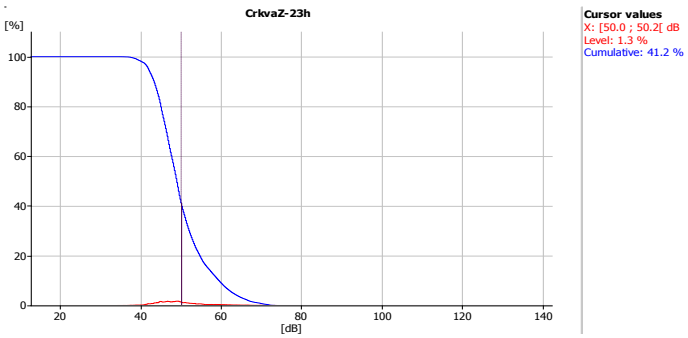

Figure 2-*Cumulative distribution of noise levels*

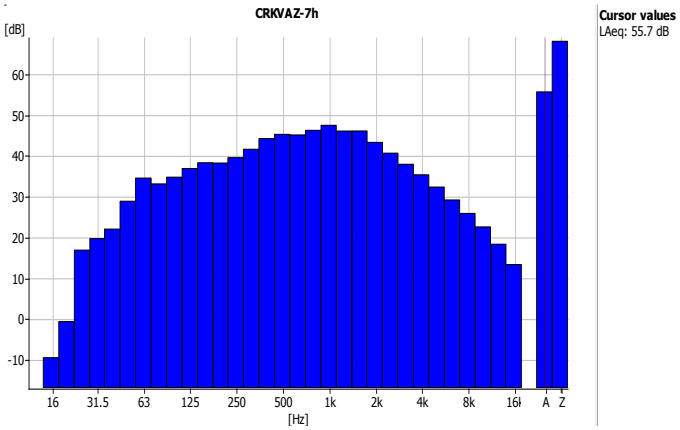

Figure 3 *Frequency analysis diagram of noise levels*

3.1. Analysis of results of measurements performed in winter season

During January 2014 the measurement of noise levels were conducted on four selected measurement ositions in five different measurement terms lasting 15 minutes. Measurement results for all measurement positions show a table (Table 1).

Table 1 *Measurement results of noise levels in winter season for all four positions in five terms*

TERM	Poz. 1 $L_{Aeq[dB]}$	Poz. 2 $L_{Aeq[dB]}$	Poz. 3 $L_{Aeq[dB]}$	Poz. 4 $L_{Aeq[dB]}$	Allowed $L_{Aeq[dB]}$
TERM 1	56	48	59	51	60
TERM 2	55	44	55	52	60
TERM 3	51	55	57	72	60
TERM 4	57	59	52	62	50
TERM 5	50	51	49	51	50

Table 1 shows that exceedences in relation to he allowable value of equivalent noise levels for day and evening hours were not recorded at three selected positions. The exception is the result for the position 4 in the term 3, where equivalent noise level was Leq = 72dB. Deviation from the allowed value is 12 dB, and there is a need for more detailed analysis. From the diagram (Figure 4), it is evident the presence of a sound event in which level of equivalent noise amounts to Leq = 85.1dB.

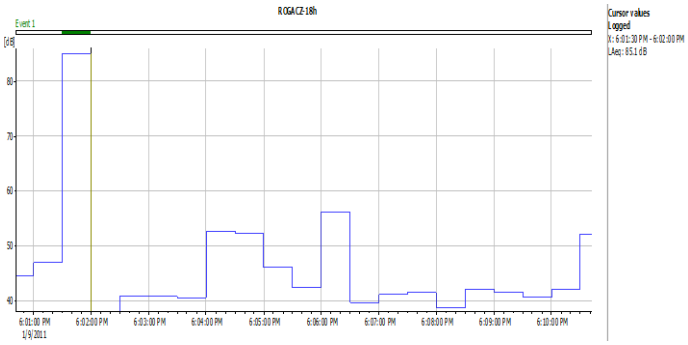

Figure 4 *Leq change for the position 4 in the term 3*

Diagram (Figure 4) shows that over time of recording level of the noise was in the range from 40-60 dB, ie. within the allowed limits. Therefore single event has caused the equivalent noise level for the whole period of recording to raise and cross the permitted value of 12 dB. To determine the characteristics of this event, a diagram of frequency analysis was analyzed (Figure 5).

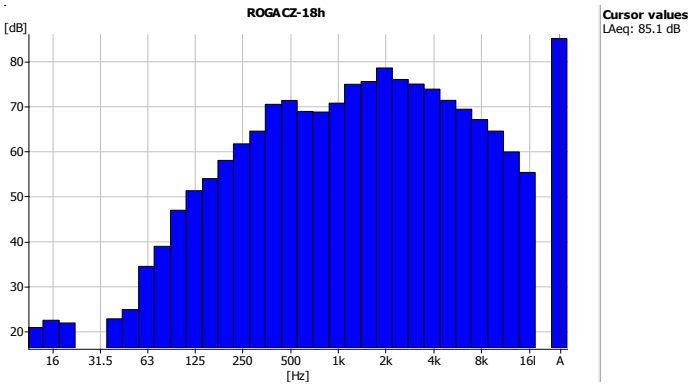

Figure 5 *Frequency analysis diagram of sound events with Leq = 85dB*

The diagram shows that the highest values recorded Leq that varies between 1.5kHz to 3KHz, ie. at higher frequencies. Given the duration of the event, it can not be characterized as an impulse event. Therefore, this event for its duration, frequency characteristics and of equivalent level of generated noise, refers to traffic noise, ie. noise from motorcycles. [3] Therefore is considered that passing of the motorcycle on road that is located right next to measuring point, caused more noise pollution. Given the level of the recorded noise of 85,1 dB, it was probably a motorcycle that passed at a speed greater than 50km/h or had been damaged / with revised exhaust system [4].

Differences that were recorded in night hours were in the range from 2 dB to 12 dB. As the main sources of noise there have been identified vehicles running local road and two external air conditioning units that were activated during recording.

3.2. Analysis of results of measurements performed in summer season

Noise levels measurements during the summer season were made in the period from 15-18.7.2014. for all four measurement positions. In period 31.7-1.08.2011 measurement were at Position 1 and Position 4 in all terms, in order to check the noise level in the peak of tourist season on places where large number of bathers is gathered. Measurements for all positions are presented (Table 2).

Table 2 *Measurement results of noise levels in summer season for all four positions in five positions*

TERM	Poz. 1 $L_{Aeq[dB]}$	Poz. 2 $L_{Aeq[dB]}$	Poz. 3 $L_{Aeq[dB]}$	Poz. 4 $L_{Aeq[dB]}$	Allowed $L_{Aeq[dB]}$
TERM 1	58	50	51	51	60
TERM 2	81	64	63	78	60
TERM 3	71	65	65	73	60
TERM 4	64	54	57	61	50
TERM 5	66	52	52	55	50

Table 2 showed that in daily terms (Term 1, Term 2, Term 3) recorded values exceeding the allowable values at all four elected positions. Exceedings are somewhere in range between 3 dB to 21 dB. In order to determine the causes of these exceedings, diagrams of the equivalent noise level changes during the measurement period were analyzed. As an example, we can present considering the value of a position for Term 3, designated as the place where it gathers a large number of swimmers and boats dock. The diagram (Figure 2) shows noticeable presence of five events that describe the noise of about 80 dB, resulting from the passage of vehicles or motorcycles. The noise level is mainly ranged from 60 dB to
75 dB as a result of the presence of a large number of people and music that comes from the coffee bar nearby.

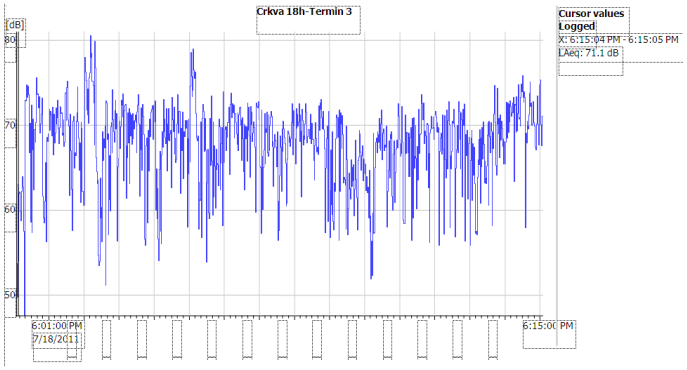

Figure 5 *Change of the equivalent noise level in time for position 1 in the period from the 18h CET*

From Table 2, for night periods (Term 3 and Term 4), we can see clear deviations in the range from 2 dB to 16 dB. A detailed analysis showed that the main causes of noise exceeding are motorcycles, which presence is expressed in the summer. Also, noise that coming from the restaurants and the noise made by tourists during the summer season, gathering people in groups and parties that lasted till early morning hours.

4. CONCLUSION

Measurement results indicate presence of increased environment noise level in the tourist settlement Donja Lastva in Tivat. Significant exceeding are especially pronounced in the peak of tourist season. Exceeding noise level which is up to 21 dB indicates the presence of a problem which is certainly a disturbing factor. Range and magnitude of negative impacts on the life of local population, tourists and the environment from identified noise sources (cars, motorcycles, air conditioners, music from the restaurants, meeting more people), is an issue which should be carefully considered by competent authorities and the entire community.

REFERECES

[1] Rules on the methods and instruments of measurement noise and the conditions to be met by the organization to measure noise, Federal Republic Yugoslavia Official Gazette, nr.37/03.

[2] Regulations on limited values of environmental noise, Republic of Montenegro Official Gazette, nr.75/06 from 8.12.2006.

[3] David B. Torrey and Jeffrey R. Mc Culley," Limiting Motorcycle Exhaust Noise", Temple Journal of Sci. Tech. & Envt. Law, vol. XXV, 49-57 (2005).

[4] P. Frisman, Motorcycle Noise Standards, ORL, Research report, 2003.

[5] R. Vladušić, The impact of aircraft noise on the environment, Faculty of Mathematical Science, Split, 2005.

[6] Law on Environmental Noise (OG M 28/11)

[7] A. Kostadinović, M. Vuković, Environmental Management, College of Professional Studies for the management of traffic, Niš, (2009).

[8] M. Praščević, and D. Cvetković, Enviromental noise, Faculty of occupational safety, Niš, (2005).

[9] J. R. Hassall, K. Zaveri and M. Phil, Acustic Noise measurements, Bruel&Kjaer, (1979).

University of Nis
Faculty of Occupational Safety
„Politechnica“ University of Timisoara
Faculty of Mechanical Engineering
24th International Conference
NOISE AND VIBRATION
Niš, 29 - 31. 10. 2014.

NONLINEAR BEHAVIOUR OF THE OSCILLATOR WITH LINEAR AND CUBIC ELASTIC RESTORING FORCE AND QUADRATIC DAMPING

Nicolae Herisanu[1], *Vasile Marinca*[2]

[1] ”Politehnica” University of Timisoara, Faculty of Mechanical Engineering, Romania, nicolae.herisanu@upt.ro
[2] ”Politehnica” University of Timisoara, Faculty of Mechanical Engineering, Romania, vasile.marinca@upt.ro

Abstract - *This paper investigates the oscillator with linear and cubic elastic restoring force and quadratic damping which approximately describes some real systems for which the damping is produced by a turbulent liquid flow inside the damper. A typical example of an oscillator with quadratic damping is the suspension of a vehicle equipped with hydraulic shock absorbers. Analytical developments are performed by means of a nonlinear analytical technique, namely the Optimal Homotopy Asymptotic Method, which is proved to be very effective for this class of oscillators. Numerical simulations showed an excellent agreement between numerical and analytical results.*

1. INTRODUCTION

The oscillator with linear and cubic elastic restoring force and quadratic damping used in this paper approximately describes those real systems for which the damping of the oscillations is produced by a turbulent liquid flow inside the damper. A typical example of an oscillator with quadratic damping is the suspension of a vehicle equipped with hydraulic shock absorbers. By neglecting the elasticity of the tires and the coupling between the vibrations of the front and rear axles, the vibrations of the vehicle that are symmetrical with respect to the longitudinal axis may be studied on the single-degree-of-freedom. Suspensions with nonlinear elastic and damping characteristics are frequently utilized, because nonlinearity limits displacements and velocities, reduces the extreme values of the acceleration, and leads to a more uniform dynamic loading of the suspension. The damping nonlinearity is usually achieved by using hysteretic or hydro-pneumatic shock absorbers [1], [2].

We consider an oscillator with linear and cubic elastic restoring force and quadratic damping of the form

$$\ddot{u} + u + \alpha \dot{u}^2 + \beta u^3 = 0, \quad u(0) = A, \quad u'(0) = 0 \tag{1}$$

where dot denotes derivative with respect to time, and α, β, A are known constants, A>0.

Making the transformations

$$\tau = \Omega t, \quad u(t) = Ax(\tau) \tag{2}$$

where Ω is the frequency of the system, Eq.(1) can be written as

$$x'' + \Omega^{-2} x + \alpha A x'^2 + \beta A^2 \Omega^{-2} x^3 = 0 \tag{3}$$

with the initial conditions

$$x(0) = 1, \quad x'(0) = 0 \tag{4}$$

where prime denotes derivative with respect to the new variable τ.

2. METHODOLOGY

The purpose of this section is to use a version of the Optimal Homotopy Asymptotic Method (OHAM) in order to obtain an approximate solution for the nonlinear differential equation [3-8]

$$L[u(x)] + N[u(x)] = 0, \tag{5}$$

subject to the initial conditions

$$B\left[u(x), \frac{du(x)}{dx}\right] = 0 \tag{6}$$

after only one iteration, solving a simple linear differential equation. If $\phi(x, p; C_i)$ is a unknown function such as

$$\phi(x, p; C_i) = u_0(x) + p u_1(x, C_i) \tag{7}$$

where it is known that $p \in [0,1]$, and $u_0(x)$ is an initial approximation of $u(x)$ which has the properties

$$L[u_0 x)] = 0, \quad B\left[u_0(x), \frac{du_0(x)}{dx}\right] = 0 \tag{8}$$

The first-order approximate solution of Eq.(5) is given by

$$\bar{u}(x, C_i) = \phi(x, 1, C_i) = u_0(x) + u_1(x, C_i) \tag{9}$$

where C_i are unknown parameters at this moment, and the first approximation $u_1(x, C_i)$ will be determined as described below.

By means of the linear operator L and nonlinear operator N from Eq.(5), we can construct a family of equations

$$\begin{aligned} &\mathbf{H}[L(\phi(x, p, C_i)), H(x, C_i), N(\phi(x, p, C_i))] = \\ &= L[u_0(x)] + p[L(u_1(x, C_i)) - H(x, C_i) N(u_0(x))] \end{aligned} \tag{10}$$

which satisfies the properties:

$$\begin{aligned} &\mathbf{H}[L(\phi(x, 0, C_i)), H(x, C_i), N(\phi(x, 0, C_i))] = \\ &= L[u_0(x)] = 0 \end{aligned} \tag{11}$$

$$\mathbf{H}[L(\phi(x,1,C_i)), H(x,C_i), N(\phi(x,1,C_i)] = \\ = H(x,C_i)(L(\bar{u}(x,C_i)) - N(\bar{u}(x,C_i))] = 0 \tag{12}$$

with $H(x,C_i)$ an arbitrary optimal auxiliary function.

Identifying the coefficients of p^i, i=0,1 into Eq.(10) we can obtain the governing equation of $u_0(x)$ from Eq.(8) and the governing equation of $u_1(x,C_i)$:

$$L(u_1(x,C_i)) = H(x,C_i)N(u_0(x))] \tag{13}$$

with the initial/boundary conditions

$$B\left[u_1(x,C_i), \frac{du_1(x,C_i)}{dx}\right] = 0 \tag{14}$$

The unknown optimal auxiliary function $H(x,C_i)$ is chosen so that the product $H(x,C_i)N(u_0(x))$ and $N(u_0(x))$ be of the same shape. The parameters C_1, C_2,… which appear in the first-order approximate solution can be determined in many ways, such as the least square method, the collocation method, the Ritz method and so on. It is clear that in this way, the approximate solution (9) is well-determined.

We will illustrate our procedure for the nonlinear oscillator with linear and cubic elastic restoring force and quadratic damping.

3. ANALYTICAL SOLUTION

In accordance with Eq.(3), the linear and nonlinear operators are given by

$$L[x(\tau)] = x'' + x \tag{15}$$

$$N[x(\tau)] = (\Omega^{-2} - 1)x + \alpha A x'^2 + \beta A^2 \Omega^{-2} x^3 \tag{16}$$

The initial approximation x_0 will be determined from the equation

$$x_0'' + x_0 = 0, \quad x_0(0) = 1, \quad x_0'(0) = 0 \tag{17}$$

whose solution is

$$x_0(\tau) = \cos\tau \tag{18}$$

The nonlinear operator (16) for the initial approximation given by Eq.(18) can be expressed as

$$N[x_0(\tau)] = \left(\frac{3\beta A^2 + 4}{4\Omega^2} - 1\right)\cos\tau - \\ - \frac{1}{2}\alpha A\cos 2\tau + \frac{\beta A^2}{4\Omega^2}\cos 3\tau + \frac{1}{2}\alpha A \tag{19}$$

If we choose the auxiliary function as

$$H(\tau, C_i) = C_1 + 2C_2\cos\tau + 2C_3\cos 2\tau + \\ + 2C_4\cos 3\tau + 2C_5\cos 4\tau \tag{20}$$

the equation (13) becomes

$$x_1'' + x_1 = \left[\left(\frac{3\beta A^2 + 4}{4\Omega^2} - 1\right)C_1 + \frac{1}{2}\alpha A C_2 + \left(\frac{\beta A^2 + 1}{4\Omega^2} - 1\right)C_3 - \right. \\ \left. - \frac{1}{2}\alpha A C_4 + \frac{\beta A^2}{4\Omega^2}C_5\right]\cos\tau + B_0 - 3B_1\cos 2\tau - 8B_2\cos 3\tau - \\ - 15B_3\cos 4\tau - 24B_4\cos 5\tau - 35B_5\cos 6\tau - 48B_6\cos 7\tau, \\ x_1(0) = x_1'(0) = 0 \tag{21}$$

where

$$B_0 = \frac{1}{2}\alpha A C_1 + \left(\frac{3\beta A^2 + 4}{4\Omega^2} - 1\right)C_2 - \frac{1}{2}\alpha A C_3 + \frac{\beta A^2}{4\Omega^2}C_4$$

$$B_1 = \frac{1}{6}\alpha A C_1 + \left(\frac{1}{3} - \frac{\beta A^2 + 1}{3\Omega^2}\right)C_2 - \frac{1}{3}\alpha A C_3 + \\ + \left(\frac{1}{3} - \frac{3\beta A^2 + 4}{12\Omega^2}\right)C_4 + \frac{1}{6}\alpha A C_5$$

$$B_2 = -\frac{\beta A^2}{32\Omega^2}C_1 + \frac{1}{16}\alpha A C_2 + \left(\frac{1}{8} - \frac{3\beta A^2 + 4}{32\Omega^2}\right)C_3 - \\ - \frac{1}{8}\alpha A C_4 + \left(\frac{1}{8} - \frac{3\beta A^2 + 4}{32\Omega^2}\right)C_5$$

$$B_3 = -\frac{\beta A^2}{60\Omega^2}C_2 + \frac{1}{30}\alpha A C_3 + \\ + \left(\frac{1}{15} - \frac{3\beta A^2 + 4}{60\Omega^2}\right)C_4 - \frac{1}{15}\alpha A C_5$$

$$B_4 = -\frac{\beta A^2}{96\Omega^2}C_3 + \frac{1}{48}\alpha A C_4 + \left(\frac{1}{24} - \frac{3\beta A^2 + 4}{96\Omega^2}\right)C_5$$

$$B_5 = -\frac{\beta A^2}{140\Omega^2}C_4 + \frac{1}{70}\alpha A C_5; \; B_6 = -\frac{\beta A^2}{192\Omega^2}C_5 \tag{22}$$

The condition required to eliminate the secular term in Eq.(21) is

$$\Omega^2 = \frac{(3\beta A^2 + 4)C_1 + 4(\beta A^2 + 1)C_3 + \beta A^2 C_5}{2(2C_1 - \alpha A C_2 + 2C_3 + \alpha A C_4)} \tag{23}$$

The first-order approximate solution of Eq.(1) can be obtained solving Eq.(21) and by means of Eq.(18) and (9):

$$\bar{u}(t) = AB_0 + A(1 - B_0 - B_1 - B_2 - B_3 - B_4 - B_5 - \\ - B_6)\cos\Omega t + AB_1\cos 2\Omega t + AB_2\cos 3\Omega t + \\ + AB_3\cos 4\Omega t + AB_4\cos 5\Omega t + \\ + AB_5\cos 6\Omega t + AB_6\cos 7\Omega t \tag{24}$$

4. NUMERICAL EXAMPLES

In order to show the validity and accuracy of the Optimal Homotopy Asymptotic Method, we consider the following cases:

4.1. If α=1/3, β=1, A=1, the convergence-control parameters and the frequency Ω are determined by a collocation approach as:

C_1= -1.11297600564616; C_2= -2.331751818465062;

C_3= 1.708450419812395; C_4= 0.04529558689726963;

C_5= 2.281140631488463; Ω = 1.4341036

The first-order approximate solution given by the Eq.(24) will be

$$\bar{u}(t) = -0.117061 + 1.22195\cos\Omega t - 0.144089\cos 2\Omega t + \\ + 0.0408032\cos 3\Omega t - 0.012363\cos 4\Omega t + \\ + 0.00583336\cos 5\Omega t + 0.0107053\cos 6\Omega t - \\ - 0.00577683\cos 7\Omega t \tag{25}$$

The approximate solution (25 and the numerical solution of Eq.(1) are presented in fig.1.

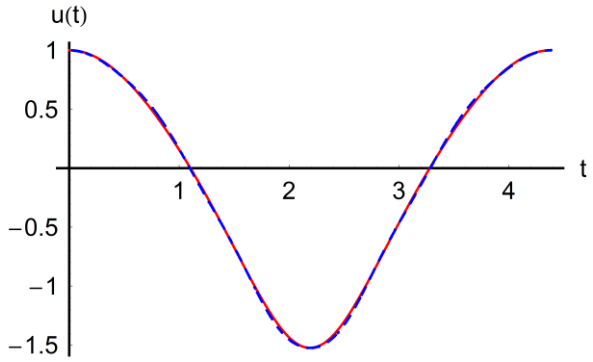

Fig. 1 *Comparison between the approximate solution (25) and numerical solution of Eqs.(1) and (2) for α=1/3, β=1, A=1: numerical - solid line, approximate - dashed line*

4.2. In this case α=1/4, β=1 and A=1 and we have

C_1=1.3830976579366836; C_2=-1.4348624216700008;

C_3=1.56785715145014; C_4=-1.6885127635352009;

C_5=0.710985521468802; Ω = 1.4014862

The first-order approximate solution becomes

$$\bar{u}(t)=-0.081559+1.14417\cos\Omega t-0.0960442\cos 2\Omega t+ \\ +0.0394004\cos 3\Omega t+0.00111721\cos 4\Omega t- \\ -0.0138791\cos 5\Omega t+0.00867966\cos 6\Omega t- \\ -0.00188531\cos 7\Omega t \qquad (26)$$

In Fig.2 we present this approximate solution in comparison with corresponding numerical solution.

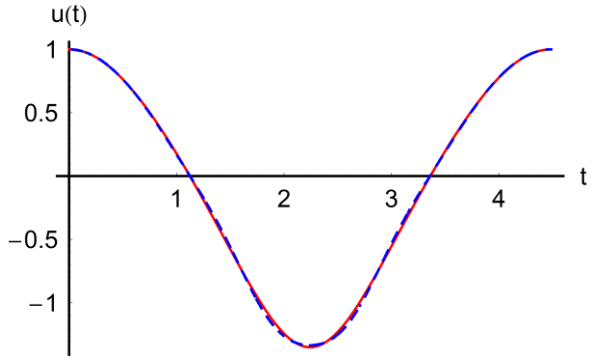

Fig. 2 *Comparison between the approximate solution (26) and numerical solution of Eqs.(1) and (2) for α=1/4, β=1, A=1: numerical - solid line, approximate - dashed line*

4.3. If α=1/4, β=1 and A=2 we obtain

C_1=0.3376263819490409; C_2=-1.1378967342745472;

C_3=1.1278896877749445; C_4=-1.4228624298867956;

C_5=0.8638879365788908; Ω = 2.373378

The first-order approximate solution becomes

$$\bar{u}(t)=-0.240599+2.59356\cos\Omega t-0.53593\cos 2\Omega t+ \\ +0.236103\cos 3\Omega t-0.0480581\cos 4\Omega t- \\ -0.0254596\cos 5\Omega t+0.0267754\cos 6\Omega t- \\ -0.00639017\cos 7\Omega t \qquad (27)$$

In Fig.3 we present the approximate solution given by Eq.(27) and the numerical solution.

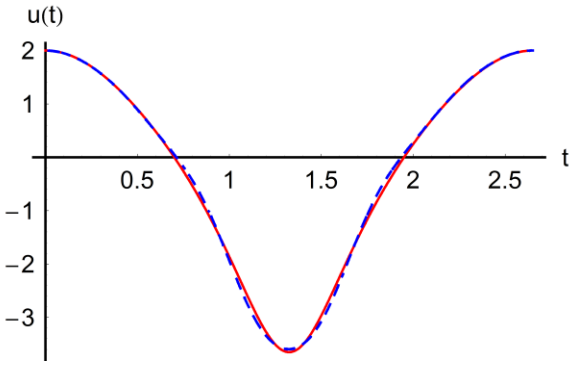

Fig. 3 *Comparison between the approximate solution (27) and numerical solution of Eqs.(1) and (2) for α=1/4, β=1, A=2: numerical - solid line, approximate - dashed line*

4.4. In the last case, we consider α=1/5, β=1 and A=2, such that

C_1=-0.031354847858872485; C_2=-1.4172470375817974;

C_3=1.935582555818684; C_4=-0.17494255572266407;

C_5=1.6944002658680275; Ω = 2.2857339

$$\bar{u}(t)=-0.189372+2.39188\cos\Omega t-0.362366\cos 2\Omega t+ \\ +0.160839\cos 3\Omega t-0.00805104\cos 4\Omega t- \\ -0.000693107\cos 5\Omega t+ \\ +0.021278\cos 6\Omega t-0.0135131\cos 7\Omega t \qquad (28)$$

In fig.4 are shown the approximate solution and corresponding numerical one.

It is clear that the approximate results match very well with the numerical ones.

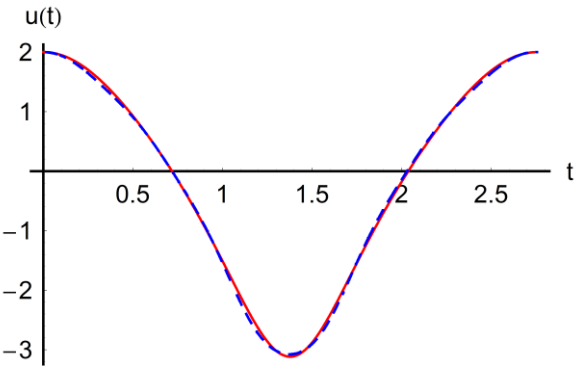

Fig. 4 *Comparison between the approximate solution (28) and numerical solution of Eqs.(1) and (2) for α=1/5, β=1, A=2: numerical - solid line*

5. CONCLUSIONS

Very accurate solutions are achieved through the Optimal Homotopy Asymptotic Method which ensure a very rapid convergence of the solutions after only one iteration. The cornerstone of the validity and flexibility of our method is the choice of the linear operator L and auxiliary function H. The convergence of the solutions strongly depends on the auxiliary function. OHAM does not need employment of restrictive conditions and the initial approximations are rigorously determined from Eq. (8). We must underline that the proposed method is straightforward, concise and can be applied to other nonlinear problems.

REFERENCES

[1] F. Dincă, C. Teodosiu, *Nonlinear and Random Vibrations*, Academic Press, NY, London, 1973

[2] F. Dincă et al., "Vibration of mechanical systems with applications to road vehicle suspension. Optimization of restoring force and damping in road vehicle suspension", *CMS Rep*. Bucharest, 1970

[3] V. Marinca, N. Herisanu, *Nonlinear Dynamical Systems in Engineering. Some Approximate Approaches*, Springer, Berlin Heidelberg, 2011

[4] N. Herisanu, V. Marinca, "Explicit analytical approximation to large-amplitude non-linear oscillations of a uniform cantilever beam carrying an intermediate lumped mass and rotary inertia", *Meccanica*, 45 (2010) 847-855

[5] N. Herisanu, V. Marinca, "Accurate analytical solutions to osciilators with discontinuities and fractional-power restoring force by means of the Optimal Homotopy Aaymptotic Method", *Comput. Math. Appl*., vol.60, pp. 1607-1615, 2010

[6] N. Herisanu, V. Marinca, "An optimal approach to study the nonlinear behavior of a rotating electrical machine", *Journal of Applied Mathematics*., vol.2012, ID 465023, 2012

[7] N. Herisanu, V. Marinca, "OHAM approach to self-excited vibrations", *Appl. Mechanics and Materials*, vol. 430, pp.27-31, 2013

[8] V. Marinca, N. Herisanu, "Optimal homotopy asymptotic approach to nonlinear oscillators with discontinuities", *Scentific Research Essays*, 8 (2013) 161-167

University of Nis
Faculty of Occupational Safety
„Politechnica“ University of Timisoara
Faculty of Mechanical Engineering
24th International Conference
NOISE AND VIBRATION
Niš, 29 - 31. 10. 2014.

DYNAMIC CHARACTERISTICS OF A DAMAGED STEEL BRIDGE - CASE STUDY

Slobodan Ranković[1], Todor Vacev[2], Srđan Živković[3]

[1] University of Nis, Faculty of Civil Engineering and Architecture, Serbia, slobodan.rankovic@gaf.ni.ac.rs
[2] University of Nis, Faculty of Civil Engineering and Architecture, Serbia, todor.vacev@gaf.ni.ac.rs
[3] University of Nis, Faculty of Civil Engineering and Architecture, Serbia, srdjan.zivkovic@gaf.ni.ac.rs

Abstract - *In the paper are presented results of experimental investigations of the dynamical characteristics of the road steel truss bridge in Vranjska Banja, Serbia, after the damage caused by impact of a mobile crane into the upper chord stiffening bracing. Eigenvalue frequency of the bridge oscilation, damping factor, and dynamical coefficient were examined through measured values of the dynamical deflection of the bridge, and through the dilatations in the members of the main truss girder. Analysis of the signal was carried out using CATMAN software and FFT analysis.*

1. INTRODUCTION

Incidental impact of a mobile crane at the entry portal and upper stiffening bracing caused damage of the structure of the road steel bridge across Južna Morava river near Vranjska Banja. For the reasons of checking of the bearing capacity and servicebility of the bridge, an examination of the static and dynamic parameters under test load was done *in situ*. Besides the damage from incidental, impact load, the bridge is damaged by corrosive action during a long period due to atmospheric and other influences, which aditionally affects the total bearing capacity. The exact year of the completeing of the bridge is not known, but it is supposed that it was in the sixties of the last century, with one reconstruction in the eighties. The design documentation was not available (besides only two drawings), so geometric characteristics are defined on the spot. The examination was performed acording to the current standards for bridge testing, SRPS U. M1. 046. [1]. Because of the limited space, and in concordance with the Conference topic, in this paper will be presented only part of the examination under test load for dynamic influences and analysis of the obtained results. The detailed expertise of the bridge is given in [2].

2. SHORT DESCRIPTION OF THE BRIDGE STRUCTURE

The bearing structure of the bridge is steel truss with the static system of a simply supported beam with span of 61.20 m, divided to 12 bays with axial distance of 5.10 m. Axial distance of the main girders is 5.4 m. Axial distance between the chord members is variable, ranging from 5.0 to 7.6 m. Truss members are made of hot rolled profiles with different dimensions, and connected by gusset plates using rivets. During the bridge reconstruction the bridge deck was replaced, and now it has 4 longitudinal secondary girders I525 and corrugated sheet metal with transversal ribs 300 mm high. Bridge deck width is 4.60 m, with one pedestrian footpath on the downstream face with width of 0.80 m. Bridge deck pavement is made of asphalt, 5 cm thick. At both the down and the upper chord are stiffening bracings. The damaged elements are the entry portal and the uper bracing in two bays, pointing from the direction of Vranje. The detais are given in graphic presentations.

Fig. 1 *Longitudinal and cross section of the bridge*

3. DAMAGES OF THE BRIDGE FROM VEHICLE IMPACT

Impact of the mobile crane damaged (teared and deformed) the entry portal from Vranje direcrion and the upper stiffening bracing (four diagonal and two horizontal members) in two fields, with length of 5.1 m. (Fig. 2). As an effect of the tearing of those members, deformation (ovalization) of the rivet holes on top chord members of the main girder ocurred. There is a suspect that the impact also caused partial deformations of the diagonal in the fourth bay. Other visible damages from the impact were not observed.

Fig. 2 *Damages of the bridge*

4. INSTRUMENTATION OF THE BRIDGE

For examination of the bridge structure under test load electronical and optical measuring instruments were used.

For the measurements that define the deflection curve of the girder in longitudinal direction, that is, for determination of the deformations (deflections) an inductive displacement transducer (LVDT) W50 (Fig. 4), and a geodetic instrument were used. Elektronic displacement transducer were used besides for the static deflections, even for the dynamic deflections. Elektronic acceleration gauge B20, was set in the midspan on the main girder (bottom chord member), and it was also used defining of the dynamic characteristics of the bridge. Tracking of the support displacements (support deflections) was done geodetically.

Determination of dilatations, and indirectly the stresses in the truss members was done using electro-resistant tensometers (strain gauges) Hottinger with a 6 mm base and reference $t=1\times10^{-6}$ with automatic elimination of temperature effects (Fig. 5, 6).

For signal recording of the static and dynamic response of the bridge structure a multichannel acquisition system SPIDER 8 produced by HBM (Hottinger Baldwin Mestechnik) was used, connected with a PC (Fig. 8).

Setting of the measuring instruments was conditioned by the static systemom and by type of the structure, as well as by real conditions at the site, and it was realized according to the principle of the circumscribing of the cross section by measuring instruments. Equipment for tracking of deformations and stresses in the characteristic cross section wher macimal influeneces were expected (in the midspan). Instrumentation was done at the section across three members of the main truss girder and vertical member in the midspan, as well as the diagonal member at the support. Acceleration encoder was installed on the bottom chord member in the bridge midspan. Displacement gauge (LVDT) W50 was set on a free tubular scaffold at the most distant accesible spot towards the midspan, that is, on the transversal girder at 20.40 m from the movable support. It was used to track static deformations and to record dynamic deflection. Over the supports, in the fourths and in the halves of the span the deflections were determined using geodetic instrument at 10 measuring spots in total (5 on both sides of the bridge deck. Strain gauges were set on chord members, on the diagonal, and on the vertical member of the main truss girder. Those encoders were used for determination of the dilatations at static and dynamic load.

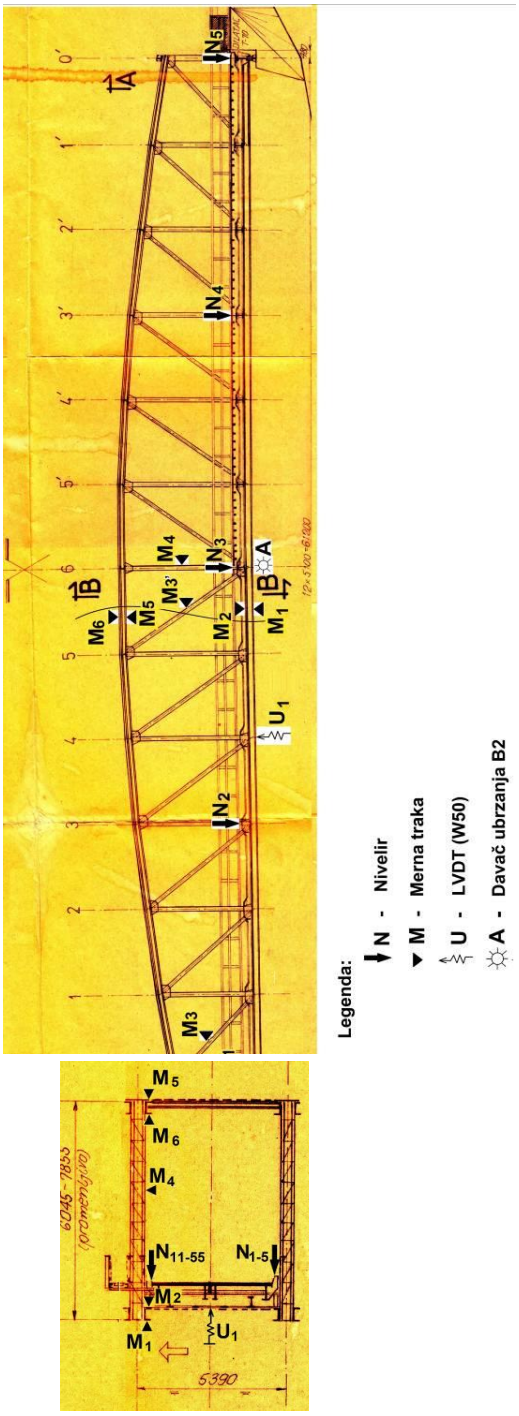

Fig. 3 *Setting of the measuring instruments*

5. MEASURING OF THE DYNAMIC INFLUENCES

The test load consisted of two trucks with four axles each, with total mass of approx. 25 t each, which passed axle wighing.

For determination of the dynamic parameters of the bridge, four constellations of dynamic load were used. Passing of a truck at valocity of: V=5 km/h, V=20 km/h, and V=40 km/h, as well as passing across an obstacle (plank with a height of h=5 cm) at velocity of V=20 km/h.

5.1. Passing of a truck at velocity of V=5 km/h

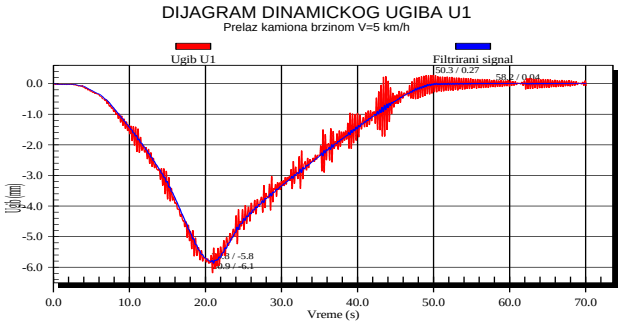

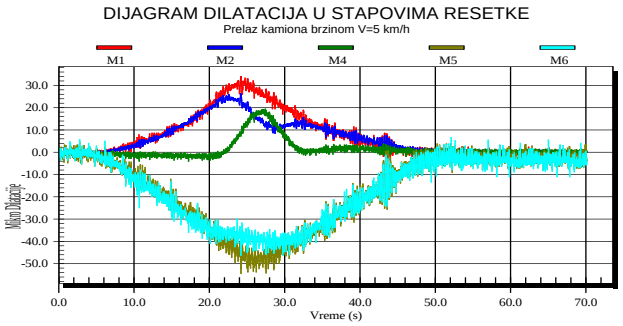

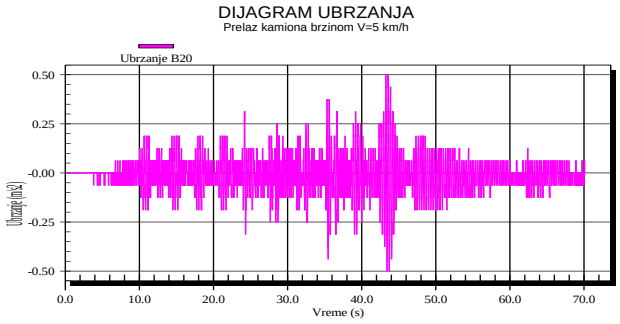

5.2. Passing of a truck at velocity of V=20 km/h

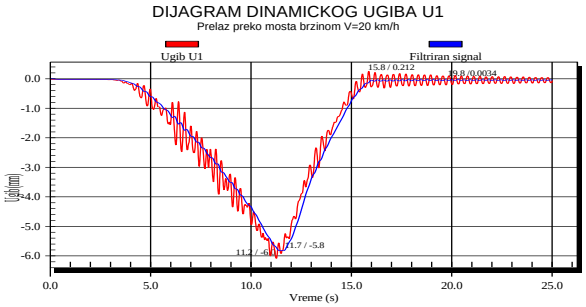

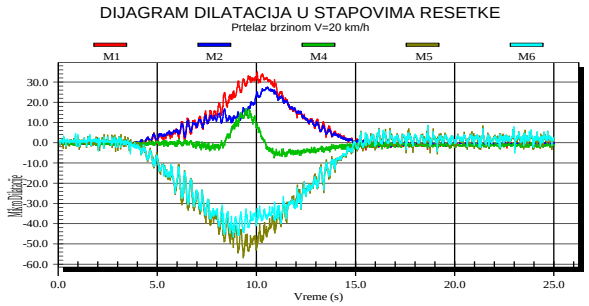

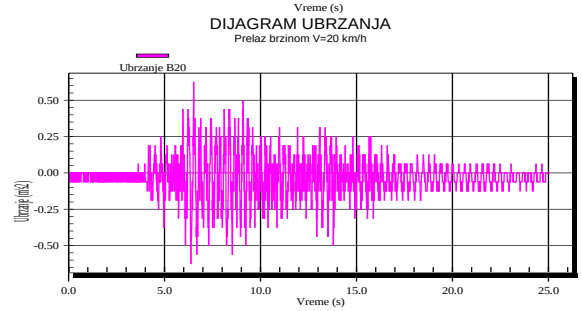

5.3. Passing of a truck at velocity of V=40 km/h

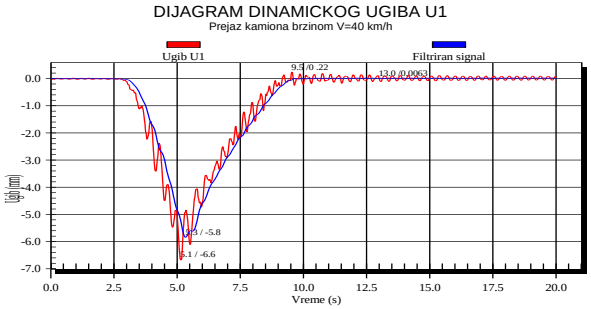

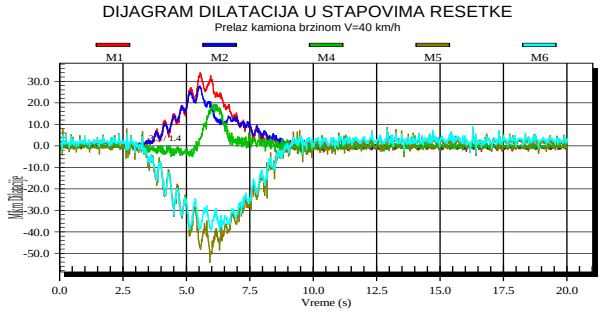

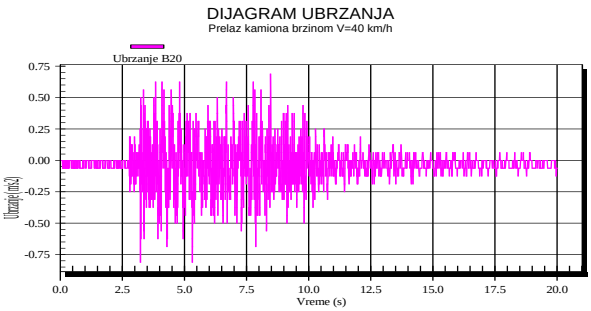

5.4. Passing of a truck of across an obstacle at velocity of V=20 km/h

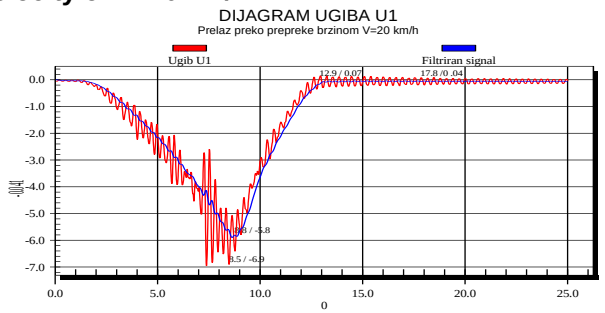

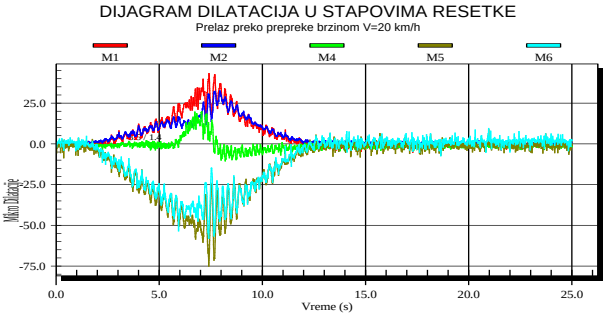

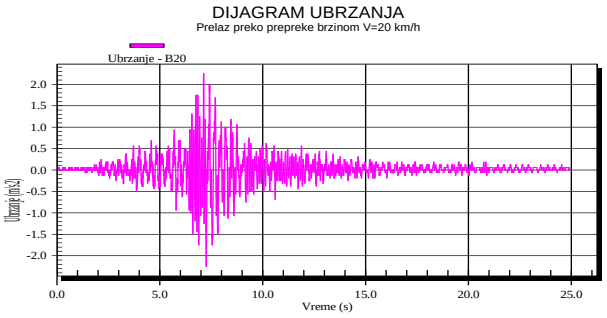

6. ANALYSIS OF THE SIGNAL (RESPONSE) OF THE STRUCTURE

Response of the free vibrations of the structure (oscillation frequency) was analyzed by FFT (Fast Fourier Transformation) and using Hottinger software package CATMAN. Analysis was carried out via dynamic deflection U1.

6.1. Free oscillation frequency

- Truck passing at velocity of V=5 km/h

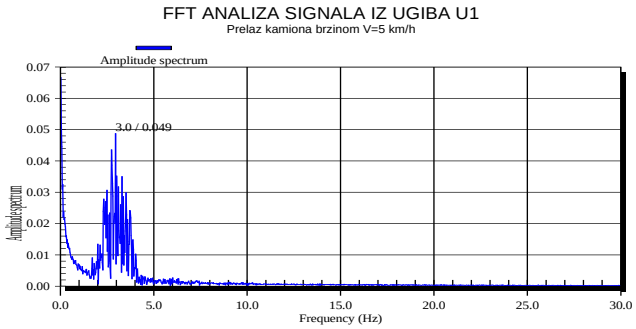

- Truck passing at velocity of V=20 km/h

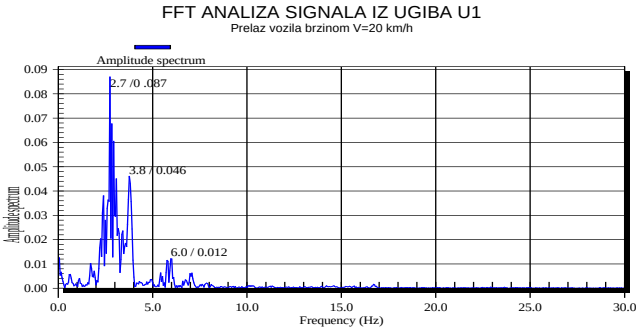

- Truck passing at velocity of V=40 km/h

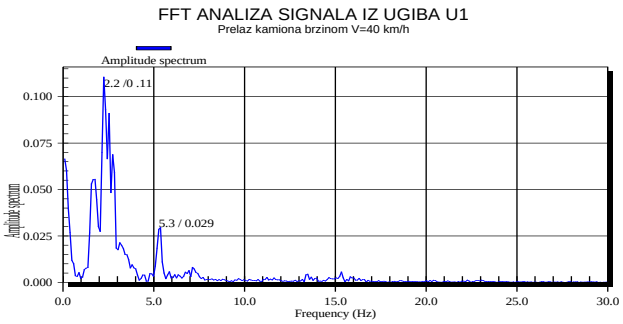

- Truck passing across an obstacle at velocity V=20 km/h

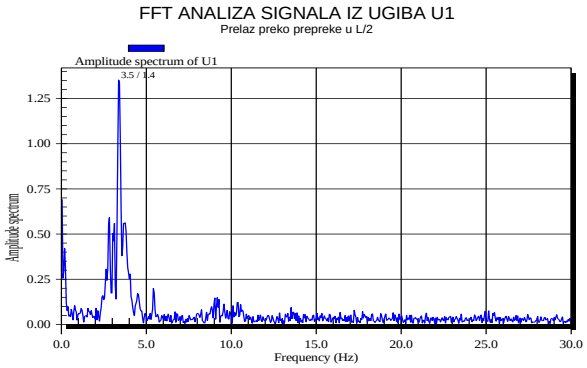

6.2. Dynamic coefficient

Value of the dynamic coefficient was determined from the relation of the maximal deflections at dynamic excitation and the quasi-dynamic diagram obtained by digital filtration of the signal, which represented the static component of the deflection. Values of the dynamic coefficient were determined for different dynamic excitation of the structure.

- For a vehicle passing at velocity of V=5 km/h

$$\varphi = \frac{U_{din}}{U_{stat}} = \frac{6,1}{5,8} = 1,05$$

- For a vehicle passing at velocity of V=20 km/h

$$\varphi = \frac{U_{din}}{U_{stat}} = \frac{6,3}{5,8} = 1,086$$

- For a vehicle passing at maximal velocity V=40 km/h

$$\varphi = \frac{U_{din}}{U_{stat}} = \frac{6,6}{5,8} = 1,138$$

- For a vehicle passing across an obstacle with 5 cm height (plank) in the midspan at V=20 km/h

$$\varphi = \frac{U_{din}}{U_{stat}} = \frac{6,9}{5,8} = 1,189$$

6.3. Damping (logarithmic decrement)

For passing at velocity of V=5 km/h from deflection U-1:

$$\delta = \frac{1}{n} \cdot \ln \frac{A_0}{A_n} = \frac{1}{22} \cdot \ln \frac{0,27}{0,04} = 0,087$$

For passing at velocity of V=20 km/h from deflection U-1:

$$\delta = \frac{1}{n} \cdot \ln \frac{A_0}{A_n} = \frac{1}{14} \cdot \ln \frac{0,212}{0,034} = 0,130$$

For passing at velocity of V=40 km/h from deflection U-1:

$$\delta = \frac{1}{n} \cdot \ln \frac{A_0}{A_n} = \frac{1}{11} \cdot \ln \frac{0,220}{0,063} = 0,114$$

For passing across an obstacle at velocity of V=20 km/h from deflection U-1:

$$\delta = \frac{1}{n} \cdot \ln \frac{A_0}{A_n} = \frac{1}{15} \cdot \ln \frac{0,07}{0,04} = 0,037$$

7. ASSESSMENT OF THE EXAMINATION RESULTS

7.1. Free oscillation frequency

The measured frequency of free oscillations of the bridge structure resulting FFT (Fast Fourier Transformation) analysis, with the help of the original HBM Catman software package is f = 3,0÷2,2 Hz, slightly higher than usual for this type of structures, but it is within the theoretical values (f = 100 / L).

7.2. Dynamic coefficient

Dynamic coefficient obtained by passing of vehicle across the bridge at different velocities has values ranging from φ=1.05 to 1.14 and shows tendency of growing with the velocity increase, but stays in allowed limits.

Dynamic coefficient obtained by passing of vehicle across an obstacle (plank) with thickness of 5 cm, amounting φ=1.19 shows that with emerging of impact action (impact pits on the bridge deck) dynamic coefficient may have significant unfavourable effects on the bridge structure. In such cases it is necessary for the investor, i.e., for the user of the bridge not to allow any significant damages of the deck pavement (impact pits), i.e., that in such case commits sanation so that the bridge lifetime remains undisturbed.

7.3. Logarithm decrement

Values of this dynamic parameter point to the flexibility of the structure and on relatively low damping of the generated oscillations. Oscillation amplitudes are relatively small, so there are no discomforts in dynamic sense, that is, ocurring of flutter or resonance.

8. CONCLUSION

Based on performed investigations by examination of the bridge structure under test (dynamic) load, one may conclude that global bearing capacity and stability of the structure is preserved even after incidental (impact) load caused by the impacto of the mobile crane. Damage (rupture) of the members for top chord stiffening did not significantly decreased bearing capacity of the bridge, regarding the traffic load acception. Dynamic parameters are in the limits of the theoretical and design values. After sanation of the damage caused by vehicle impact, additional examinations under test load and their analysis are proposed, wherewith would be defined the bearing condition for scheduled traffic load and for the design load scheme by a standard vehicle V300, which is in accordancewith current standard for bridge loads. Other damages of the bridge (corrosion and lack of maintanance) were not subject of this paper.

9. PHOTO DOCUMENTATION

Fig. 4 *View of the bridge during the phase of examination under test load*

Fig. 5 *Displacement transducer LVDT (W50) set on the transverse girder*

Fig. 6 *Passing of vehicle during measuring of dynamic parameters of the bridge*

Fig. 7 *Strain gauge M2 set on the bottom chord member in the midspan*

Fig. 8 *Measuring device (SPIDER8 connected to a PC)*

REFERENCES

[1] SRPS U.M1.046, 1987: *Ispitivanje mostova probnim opterećenjem*.

[2] "Ekspertiza stanja čeličnog druskog mosta preko reke Južne Morave na regionalnom putu Vranje – Vranjska Banja". Institut za građevinarstvo i arhitekturu Građevinsko-arhitektonskog fakulteta Niš, Niš, April 2014.

[3] Radojković M.: *Ispitivanje konstrukcija*, Građevinski fakultet, Beograd, 1979.

[4] Bruel&Kjaer: *Piezoelectric accelerometer and vibration preamplifier handbook*, Naerum, Denmark,1987.

[5] Dally J.W. and Rily W.F.: *Experimental Stress Analysis*, Mc Graw Hill international editions, 1991.

University of Nis
Faculty of Occupational Safety
„Politechnica“ University of Timisoara
Faculty of Mechanical Engineering
24th International Conference
NOISE AND VIBRATION
Niš, 29 - 31. 10. 2014.

INFLUENCE OF VEHICLE CHARACTERISTICS ON RIDE COMFORT

Rajko Radonjić[1], Branislav Aleksandrović[2], Dragoljub Radonjić[3], Aleksandra Janković[4], Momir Praščević[5]

[1]University of Kragujevac, Faculty of Engineering, Serbia, rradonjic@kg.ac.rs
[2]Technical College of Applied Studies Kragujevac, Serbia, banealeksandrovic@gmail.com
[3]University of Kragujevac, Faculty of Engineering, Serbia, drago@kg.ac.rs
[4]University of Kragujevac, Faculty of Engineering, Serbia, alex@kg.ac.rs
[5]University of Nis, Faculty of Occupational Safety, Serbia, momir.prascevic@znrfak.ni.ac.rs

Abstract - *Some actual problems related to examination of vehicle's oscillatory processes in terms of dynamic loads and ride comfort are discussed in this paper. A method for research of influence of the relevant vehicle's characteristics and interactions with the excitations from the environment are presented. An adequate simulation model and experimental system were developed as the base for results verification. The influence of the excitation type from road onto intensity of generated vibration during different weight conditions of the vehicle was analysed. The method for optimization of driver's seat vibratory parameters is proposed. The method is based on the vibrational comfort evaluation criteria.*

1. INTRODUCTION

The oscillatory processes arising from the movement of motor vehicles on the unevenness roadway generate dynamic forces that affect to life of the elements and components of vehicles but also lead to fatigue of the driver and passengers, which is reflected in their ability to work and health [1,2,3,4]. In this regard, a certain constructive measures are undertaken that lead to reduction of the level of dynamic forces, and aimed for optimisation of the characteristics of tires, the characteristics of primary system of elastic suspension, the elastic suspension of the trucks cabins and the commercial vehicles, as well as the characteristics of the seat [5,6,7,8]. The considerable efforts to improve of the oscillatory characteristics of the elastic suspension with passive components were made in the previous period [6,7,9]. However, the results achieved in this field almost reached the limit with respect to the actual requirements and standards relating to the life and the comfort of the vehicle. [5,7]. Further improvements are possible using of new types of suspension systems and elements, components with active and semi-active control, software support and integration of vital vehicle functions [7,9,10] etc.

Some specific features and limitations of passive systems of elastic suspension as well as some phenomena of vehicle's excitation from the environment that must be taken into account during selecting and developing appropriate solutions are discussed in this paper, bearing in mind the above presented problems. This approach is based on the aspect of isolation of human body from the harmful effects of oscillations and the possibilities gained by usage of new types of suspension systems with respect to the development of the trends in this area.

2. METHODOLOGY

This chapter will summarize the subject of work and used methodology based on the conducted analysis and conclusions given in the introduction. The first section deals with the problems of forming appropriate models for simulation-based investigation. In this sense, an oscillatory model of two-axle vehicle whose structure and parameters are shown in Fig.1. was chosen.

The marks in the figures have the following meaning: l - wheelbase, a, b, h - the coordinates of the mass center, c_1, k_1,, c_2, k_2 - elastic - damping parameters of elastic suspension of front and rear axle, respectively, c_{1p}, k_{1p}, c_{2p}, k_{2p} - elastic - damping parameters of front and rear tires, respectively, $h(x)$ - the original function of uneven length profile of the soil, $z_o(x)$ - the equivalent function of longitudinal unevenness of the soil profile obtained by filtering the original function through H_1 and H_2 modules, which include the effects of the interaction of subsystems, rubber - ground. Apart from these, the marks of vehicle sprung mass, m, corresponding moment of inertia about the transverse axis of the vehicle, I, unsprung masses, m_1, m_2, the coordinates of the characteristic points, l_s and l_c, the direction and the orientation of velocity, v, are presented in Fig. 1.

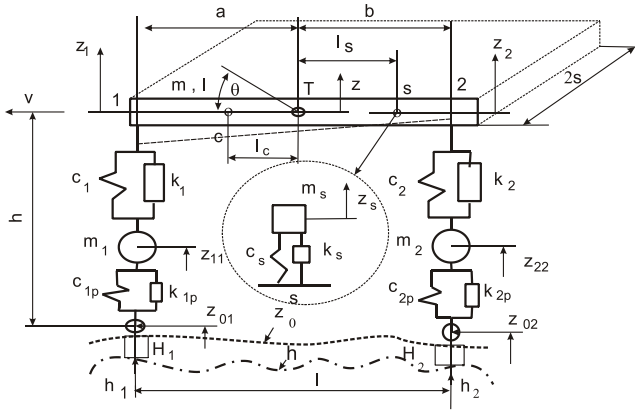

Fig. 1 *Oscillatory model of two-axle vehicle*

In general, the model has five degrees of freedom, two degrees of freedom of elastically sprung mass, m, marks of alternative, $z \rightarrow \theta$, vertical and angular displacement of sprung mass, or $z_1 \rightarrow z_2$, vertical movement of the front and rear side of the sprung mass, respectively. Then one degree of freedom of movement unsprung masses, m_1, m_2, therefore, their vertical displacements, z_1, z_2, respectively, and one degree of freedom of the basic, longitudinal movement of the tractor in the direction of coordinate, x, by velocity, v.

Differential equations in the summary form are written for presented model,

$$m\ddot{z} + F_{ck1} + F_{ck2} = 0 \quad (1)$$

$$-I\ddot{\theta} - F_{ck1}a + F_{ck2}b = 0'' \quad (2)$$

$$m_1\ddot{z}_{11} - F_{ck1} + F_{pck1} = 0 \quad (3)$$

$$m_2\ddot{z}_{22} - F_{ck2} + F_{pck2} = 0 \quad (4)$$

$$F_{pck1} = F_{zo1}, \qquad F_{pck2} = F_{zo2} \quad (5)$$

$$F_0 = R_f + R_v + R_j + R_\alpha + R_P \quad (6)$$

In addition to the marks given in Fig. 1, the following marks are also used in the above expressions: F_{cki}, i=1,2, the resultants of elastic and damping forces of elastic suspension of the front axle, i=1, and the rear axle, i=2; F_{cki}, i=1,2, the resultants of elastic and damping forces at the front tires, i=1, and the rear tires, i=2; F_{zoi}, i=1, 2, excitation forces in the tire and road contact of the front wheels, i=1, and rear wheels i=2; F_0 – vehicle's tractive force; R_f, R_v, R_α, R_j, R_p, the rolling resistance of air, slope, inertia and towed vehicles, respectively.

A detail of oscillatory sub-model of the seat mounted at a distance l_s from the center of mass, T, with marked parameters: m_s - the total mass of the seat and the driver, c_s, k_s - characteristics of stiffness and damping seat, respectively, S - binding site of the seat on the vehicle's chassis and the appearance of vertical oscillations is also shown in Fig. 1.

Levels of oscillations in some points of the vehicle's chassis depend on their position in relation to the reference points or axes, for example the center of mass, the axis of front, i.e., rear wheels, center of oscillation. Therefore, when the location of the seats, l_s, is being choosing, these levels should be taken into account, but the impact will also express also some other factors: structural constraints, the position of the controls, the requirements of specific working and transport operations. The adopted vehicle model structure with the sub-model of seat suspension passive system (Fig. 1) provides further simplification of simulation models and reduces the time needed. In fact, considering that the mass of the seat with the driver is significantly less than the total mass of the vehicle, then this mass exerts a negligible effect on overall levels of oscillation of systems. This allows the system shown in Fig, 1, to spread into two oscillatory models; the first is two-dimensional model of the vehicle with mass, m, and one sub-model of the seats with concentrated mass, m_s, on a mobile platform. In this way, the vehicle model can be analysed separately from the model of the seats, and thus it is possible to describe its relevant oscillatory processes depending on influential parameters, then the same could be imported into a database and used in all cases of seat's selection or replacement. On the other hand, the partial sub-model shown in Fig. 1, excited by oscillations of the moving platform, i.e., vehicle's chassis, which can be quickly generated or used from database, is used for the analysis of oscillatory processes of the seats, in terms of its filtering properties.

Fig. 2 *Self-driven measuring platform with equipment.*

The platform of a truck with its own drive and measuring equipment, shown in Fig. 2, was used in simulation studies. This is universal purpose platform, for stationary, quasi-stationary and dynamic testing of road, off-road, commercial vehicles, their aggregates, sub-assemblies and components. For the purposes of this study, i.e., for the proposed methodology, this platform can be used for testing and identifying of sub-models of elements and components of the elastic suspension of the road vehicles and other working machines. With regard to the concept of open supporting structure and the lateral position of the wheels, the wheels with tires of different types and sizes can be set up and examined on the platform. The part of measuring equipment is shown in Fig. 2, including measuring dynamometer of traction force and speed sensor Leitz-Correvit LG 2, and three-axial acceleration sensor, drive encoder HBM, eight channel measuring system and data measuring acquisition system, HBM Spider 8 and notebook.

3. RESEARCHING RESULTS

Simulation studies shown in this paper were carried out on the basis of vehicle oscillatory model, shown in Fig.1, which is reduced from spatial to planar model assuming the longitudinal symmetry and the corresponding mathematical model described by differential equations from (1) to (6). Thus, two weight conditions of the vehicle and four characteristic impacts from uneven road were observed. The required input data for simulation studies, elastic-damping characteristics of the tires and the primary elastic suspension of the vehicle were obtained using the measuring platform presented in Fig. 2. Some typical results for the above-mentioned cases are shown in Fig. 3 to Fig. 10.

Fig. 3 shows the time history of the vertical displacement of center of gravity, z and angular swing of sprung mass of the vehicle around the transverse axis, θ at impulse excitation of the front axle by individual impulse of the road, with the height of 0.1m and duration 1 second.

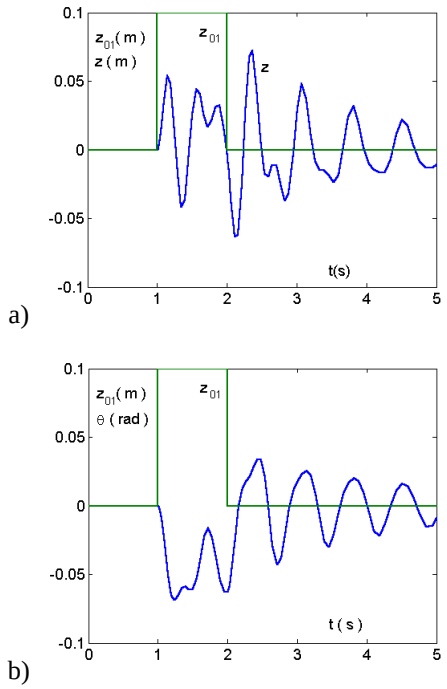

Fig. 3 *The change of vehicle sprung mass coordinates, a) vertical displacement, z (m), b) angular swing θ (rad), during impulse excitation of front wheels by road at the given parameters, z_{01} / t=0.1m/1s.*

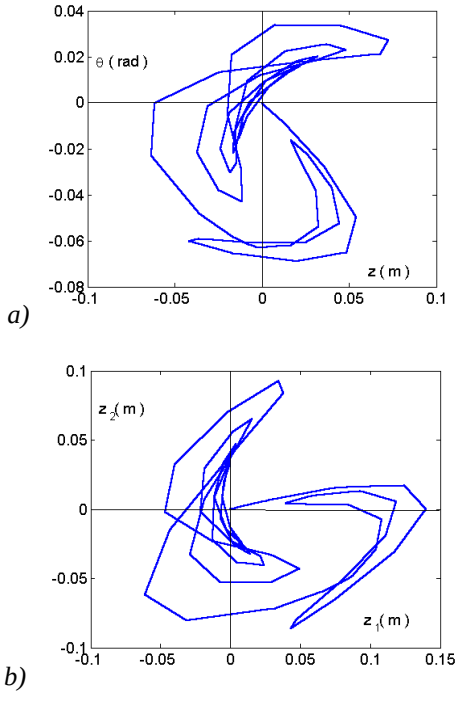

Fig. 4 *Lissajous plot of coordinates, a) $\theta \rightarrow z$, b) $z_2 \rightarrow z_1$ Impulsive excitation through the front wheels z_{01}/t=0.1m/1s*

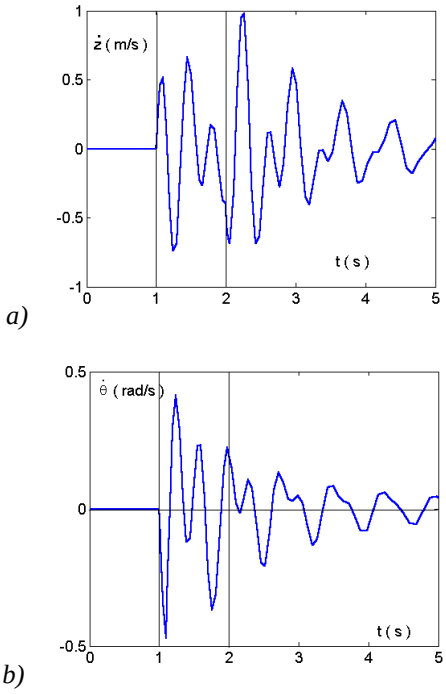

Fig.5 *a) Vertical, B) Angular speed of vehicle sprung mass. Impulsive excitation same as in Fig. 4.*

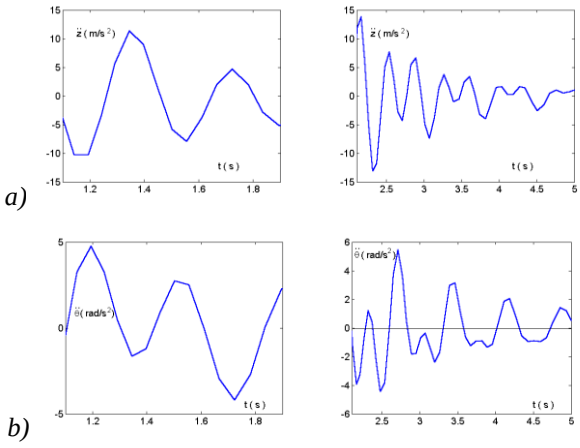

Fig. 6 *a) Vertical, b) Angular acceleration of vehicle sprung mass. Impulsive excitation same as in Fig. 4.*

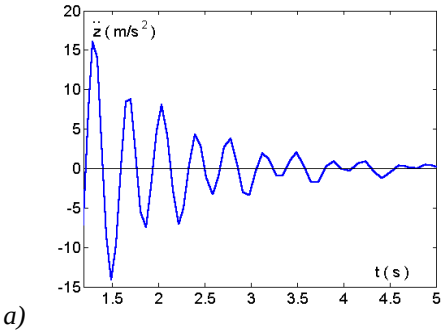

a)

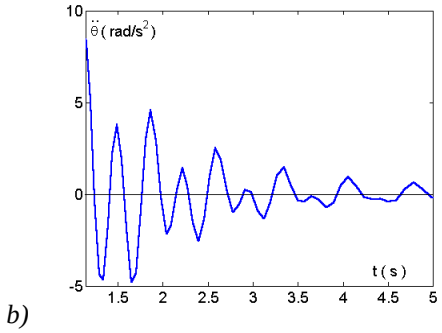

b)

Fig. 7 *a) Vertical, b) Angular acceleration of vehicle sprung mass. Impulsive excitation of the front wheels from uneven road at the given the parameters, z_{01} / t =0.1m/0.1s*

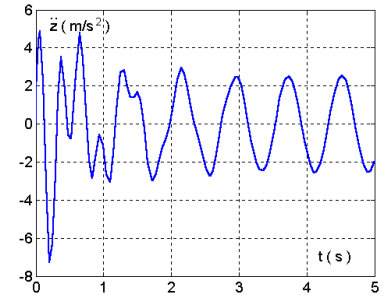

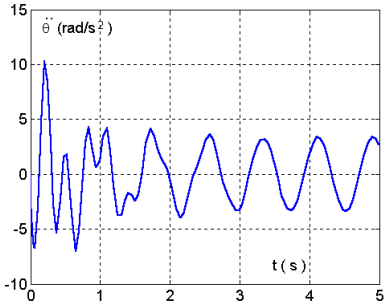

Fig. 8 *a) Vertical, b) Angular acceleration of vehicle sprung mass at the sinuous excitation of the front wheels from uneven road at the given the parameters, $z_{0\,1}$ / λ =0.1m / 0.5m*

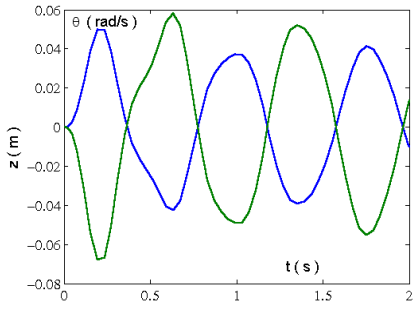

a)

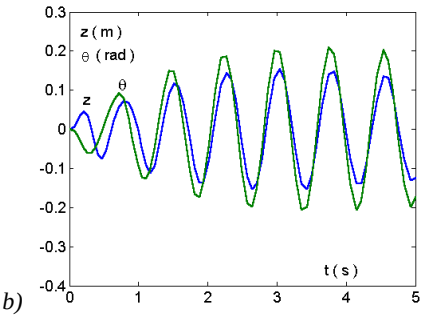

b)

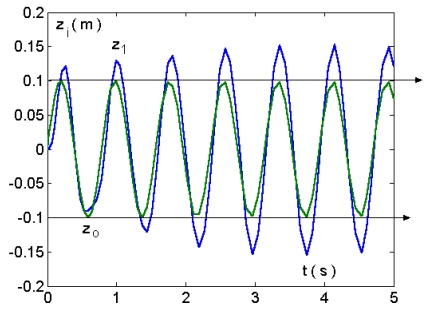

c)

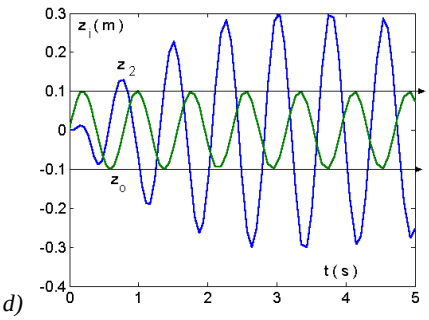

d)

Fig. 9 *Oscillation of sprung mass of the vehicle at the sinuous excitation front wheels from uneven road at the given the parameters, z_{01} / λ / v = 0.1m/0.5m. a) unladen vehicle, coordinate $\theta \rightarrow z$,;b) laden vehicle, coordinate $\theta \rightarrow z$; c) and d) laden vehicle coordinates, z_1 ,z_2 in relation to the excitation of the front wheels, z_{01}, respectively.*

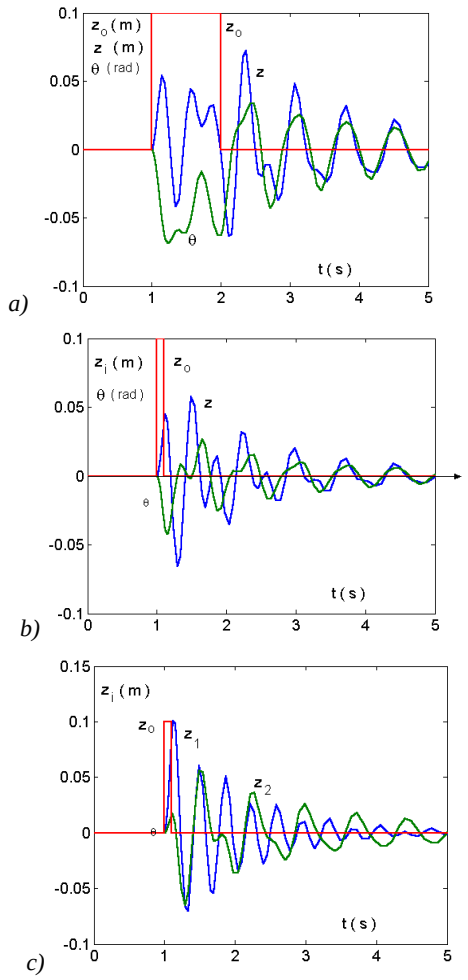

Fig.10. *Transient processes of vehicle sprung mass movement, a) at impulse excitation type 1, time histories of the coordinates z, θ, and excitation, z_0, b) at impulse excitation type 2, time histories of the coordinates, z, θ and excitation z_0, c) at impulse excitation type 2, time histories of the coordinates, z_1, z_2 and excitation z_0.*

Fig. 10a provides a comparative overview of time histories from which it is obvious that the observed transient processes are phase-asynchronized during the interval of impulsive excitation of the front wheels. Thereby, the vertical displacement of center of gravity, *z*, is changing sign, while the swing angle θ retains a negative sign for the same time. After the excitation is off, the processes are oscillatory damped and phase-synchronized.

Lissajous loops (Fig. 4) show the mutual dependence of the observed coordinates of the vehicle sprung mass, $\theta \rightarrow z$, $z_2 \rightarrow z_1$, respectively, as an alternative position coordinates of sprung mass. The shape and position of these diagrams indicate two characteristic phases of the observed processes that are presented also in Fig. 10a.

The time histories of the translational and angular velocity during these transitional processes are shown in Fig. 5 a, b, respectively, and the corresponding accelerations in Fig. 6 a, b, respectively. Thus, acceleration time history shown in Fig. 6 a, b, have breakpoints in the time-points of 1 second and 2 seconds, respectively, i.e., at the occurrence of pulses and the disappearance of pulses, respectively, with extremely high values of the shock acceleration. In addition; the high values of vibratory accelerations are marked during the impulse excitation interval and at the beginning of an damping process interval (for the considered case shown in Fig. 6 - vertical acceleration range from -10m/s^2 to 10m/s^2 and -14m/s^2 do 14m/s^2, respectively and angular acceleration range from 4.8 rad/s^2 to -4.2 rad/s^2 and from -4.2 rad/s^2 to 4.8 rad/s^2, respectively).

Higher levels of the vertical and angular accelerations are achieved in the case of impulse excitation type 2, i.e., the same height, the same impulse intensity, but the shorter duration, shown by a transition process in Fig. 10 b, c, and levels of the acceleration in Fig. 7 a, b. It can be observed from Fig. 6 and 7 that the angular acceleration is in a greater degree asymmetric in relation to horizontal axis than vertical acceleration.

A simulation of the process for the case of sinusoidal excitation was carried for the purpose of comparative analysis of road excitation impact on vehicle oscillatory processes and determination of impact on the levels of vertical and angular accelerations relevant for the evaluation of ride comfort of the vehicle [10,11,12]. Thereby, the model of front wheels excitation was used, described in the spatial domain by expression, $z(x) = A\sin\Omega x = A\sin(2\pi/\lambda)x$, and in the time domain by expression, $z(t) = A\sin\omega t = A\sin(2\pi/T)t$. Using dependence of spatial and time coordinates, the mathematical model of periodic excitation of front wheels from the road is obtained in the form: $z(t) = A\sin(2\pi/\lambda)vt$, which establishes a relationship between the height of road roughness *A*, their wavelength, λ and speed *v*. Simulation results presented in Fig. 8 and 9 were obtained for the following values: A=0.1m, λ=0.5m, which approximates the roughness parameters of lower quality road.

The researching results presented in Fig. 8 a, b, show the vertical acceleration time history of vehicle sprung mass and its angular acceleration during rotation over the transverse axis, respectively. The transitional process of the acceleration takes about 2 seconds, and then it is establish a process of forced oscillation with frequency that coincides with frequency of sinusoidal excitation. Maximum accelerations are achieved at the beginning of the transitional period: maximum vertical acceleration of - 7.3m/s^2 and the maximum angular acceleration of - 10.2 rad/s^2. It is obvious from above presented pictures that vibratory acceleration levels at steady, forced oscillation process are significantly lower compared to the above extreme values. In addition, this type of excitation does not generate shock acceleration, which occurs in previously presented impulsive excitation.

The time history of coordinates, $z \rightarrow \theta$ of sprung mass of the unladed vehicle with the basic parameters of the corresponding variant of vehicle with decoupled oscillation of the front and rear axles are given in Fig. 9a. The results presented in Fig. 9 b, c, d show time history of position coordinates, $z \rightarrow \theta$, the coordinates of the front part of the sprung mass and excitation $z_1 \rightarrow z_0$, the coordinates of the rear part of the sprung mass and excitation $z_2 \rightarrow z_0$, for loaded vehicle. Whereby, load growth has led to the coupling oscillation of the front and rear axles, i.e., the oscillation of the rear side of the vehicle at excitation of the front wheels only. That was not the case in the previous example of unloaded vehicle.

From point of view of the vehicle's ride comfort, all three variables of state of oscillatory process, above presented, are important: displacement, velocity and acceleration observed in the time and frequency domain [5,10]. However, the previous works in the domain of vehicle oscillations and development of criteria for their evaluation in terms of comfort, usually were based on correlation between acceleration levels and frequency, subjective assessments, identification of vibration exposure criteria curves (with equal observations of human factor) [1,2,3,4]. An example of these curves proposed in the ISO for the vibration frequency range 0.63 to 100 Hz is presented in Fig. 11 [13,14].

The vibration levels of the curves shown in Fig. 11 are given as RMS acceleration levels that produce equal fatigue – decreased job proficiency.

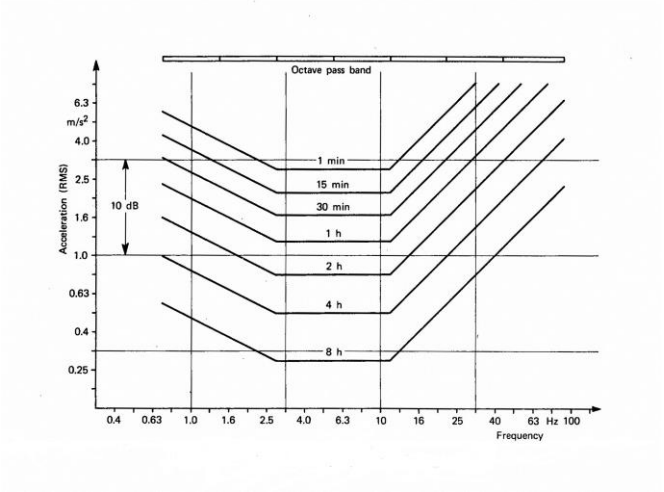

Fig. 11 *Vibration exposure criteria curves.*

The curve shapes in Fig. 11. indicate human sensitivity to vibration magnitude and frequency. The range of the RMS levels is 20 dB, in the middle frequency domain for exposure time from 1 min to 8 h. The RMS acceleration levels, obtained in this paper, for observed road disturbance, crossover the levels exposure curves by corresponding frequency. The vehicle seat must reduce acceleration overshoot. An approach to optimal design of the vehicle seat request the inverted exposure curves in Fig. 11, then identified oscillatory processes of sprung mass by means above presented method and with these data can estimation of the transfer function of seat with respect of vehicle ride comfort.

4. CONCLUSIONS

Oscillation processes generated by vehicle movements and unevenness of road produce dynamic forces that impact to the driver and passengers, which is reflected in their ability to work and health in general. The base features of the uneven road, movement state, the characteristics of the vehicle - especially a the weight condition, then primarily elastic support of the vehicle, seats, cab affect on the intensity of these processes. Change of the weight conditions of the vehicle, i.e. its useful payload, reflects to increased total weight, weight distribution, the position of the center of mass, the oscillation coupling degree of the front and rear axles. The baseline characteristics exert significant influence, i.e. potential excitation properties of road as a deterministic functions, impulse, step, ramp, sinuous as stochastic excitations of the real profile of the road. The results of this research have shown that negative effects especially manifest impulse excitation of individual obstacles of the road. They generate shock acceleration in characteristic transient spots of impulse generation. Generated acceleration depends on the level of the impulse, its duration, and the regime of movement and structural characteristics of the vehicle. The performance of the intensity of the impact processes can be obtained by the comparison with those processes obtained with sinusoidal excitations of the road, in terms of the extreme values of acceleration and transient, damped and forced oscillation phases. The obtained results are the basis for qualification of influential system parameters on comfort during the ride for a specific vehicle and its current situation, and for the optimal choice of the seats for the platform on the bases of inverted iso-comfort curves and identified vibration processes of the vehicle chassis, as a platform on which the seat will be placed.

REFERENCES

[1] N. Mansfield, "Human response to vibration". 2005 .

[2] ISO 2631, „Evaluation of human exposure to whole-body vibration. General requirrements".

[3] ISO 5007, „Agricultural wheeled tractors and field machinery – Measurement of whole – body vibration of the operator".

[4] D. Simić, "Beitrag zur Optimirung der Schwingungs-eigenschaften des Fahrzeugs – Physiologische Grudlagen des Schwingugskomfort". Dissertation, TU Berlin D83, 1970.

[5] H.Appel, T.Meissner, "Grundlagender Kraftfahrzeug technik II". TU, Berlin, 1998.

[6] J.Wong." Theory of ground vehicle". Third edition, John Wiley & Sons, 2001.

[7] H – P. Willumeit,"Fahrzeugdynamik". TU Berlin, Institut fur Kraftfahrzeuen, Berlin, 1998.

[8] M. Mitschke, ''Dynamik der Kraftfahrzeuge." Springer – Verlag, 1972.

[9] A. Janković, "Dinamika automobila", Mašinski fakultet Kragujevac, 2008.

[10] R. Radonjić, "Identifikacija dinamičkih karakteristika motornih vozila", Monografija, Mašinski fakultet, Kragujevac, 1995.

[11] R. Robichand, M. Molnan, "Measuring soil roughness changes with an ultrasonic profiler", Trans. ASAE 33, 6, 1851 – 1858, 1990.

[12] B. Volfson, ''Comparison of two simulation models of tire – surface interaction'', Proc. 13th Intl. Conf. of ISIVS, p. 311 – 318, 1999.

[13] J. T. Broch, "Mechanical vibration and shock measurement", The Application of the Bruel & Kjaer Measuring Systems, 1976.

[14] V. de Buen., A. Martinez., J. Botey., J. Plans, "Les vibrations mecaniques des vehicules et leur effet sur le corps human". VDI – Berichte, Nr. 369, 1980.

University of Nis
Faculty of Occupational Safety
„Politechnica“ University of Timisoara
Faculty of Mechanical Engineering
24th International Conference
NOISE AND VIBRATION
Niš, 29 - 31. 10. 2014.

PERSONALITY DETERMINATION USING VIBRATING MOVEMENT PARAMETERS

Mihaela Picu

Engineering Faculty Braila, Galati University, 47 Domneasca Str., Galati, Romania

Abstract *- The human body responds to stimuli by organizing a response depending on purpose. How each person responds to external stress is determined by psychophysical reactions to these factors. But one key aspect that has not been studied enough so far, is the individual personality. This depends on a huge number of external factors (educational, cultural, social background characteristics, etc.), and also internal (genetic, anatomical, etc.). Practically every man has his personality and therefore it is impossible to classify in this respect. To study this issue, we used Likert scale, which quantifies the degree of discomfort due to external stress. Depending upon how the subject chooses a certain level of the 5 of the Likert scale, we determined the personality of the subject. Several individuals underwent the same type of vibrations. To measure the whole-body vibrations transmitted by the vibrating platform, we used the multiple acquisition vibrations system NetdB. We fixed PCB Piezotronics 356A16 triaxial accelerometers on the subjects. We processed the data with the dBFA Suite-Software acquisition control and post-processing data; we have maintained constant parameters to study how different subjects perceive the same external stimulus. We evaluated the perception's magnitude with the Likert degree of discomfort scale: with values ranging from 1 (very little discomfort) to 5 (extreme discomfort) and we calculated, based on Rasch's model, the θ coefficient, which indicates the type of personality for the studied subject.*

Keywords: *vibrations, degree of discomfort, model for personality determination, Likert scale*

1. INTRODUCTION

The human body responds to stimuli by organizing a response depending on our purpose [(1), (4)]. How each person responds to external stress is determined by psychophysical reactions to these factors.

But one key aspect that has not been studied enough so far, is the individual personality. This depends on a huge number of external factors (educational, cultural, social background characteristics, etc.), and internal (genetic, anatomical, etc.). Practically every man has his own personality and therefore it is impossible to classify in this respect [5].

In this paper we studied how workers perceive the transmission of vibration from vibrating platforms through the whole body (WBV) [(3), (6), (8)].

Quantifying the perception of external stress is best represented by Likert Scale [2]. This is a psychometric scale based on Rasch's Model [7]. It is widely used in questionnaires, in survey research, so the term is often used interchangeably with the scale of assessment, even though the two are not synonymous (Table 1). When responding to a Likert item, the subjects state their agreement on questions of the questionnaire and/or conducting an experiment.

All calculations that are made to determine the degree of discomfort due to vibrations, should take into consideration the subject's size. For this, we calculated the Body Mass Index (BMI=m/h^2) (Table 2) and Body Volume Index for each case (BVI refers to the relationship between mass and its distribution throughout the body, taking into account the chest circumference and chest/waist ratio). In all experiments, the subjects were in the normal range of BMI and BVI.

Depending on how the subject chooses a particular level from the 5 above, one can determine personality of the subject.

Table 1 *Degree of discomfort scale*

Degree of discomfort	Likert Scale
Not at all	0-1
A little	1-2
Moderate	2-3
Strong	3-4
Very strong	4-5

Table 2 *Body Mass Index*

Category	BMI [kg/m^2]
Very severely underweight	< 15
Severely underweight	15.0 - 16.0
Underweight	16.0 - 18.5
Normal (healthy weight)	18.5 - 25
Overweight	25 - 30
Obese Class I (Moderately obese)	30 - 35
Obese Class II (Severely obese)	35 - 40
Obese Class III (Very severely obese)	> 40

2. PROCEDURE

Several people were subject to the same type of vibrations. To measure the whole-body vibrations transmitted by the vibrating platform (Fig. 1) the vibrations multiple acquisition system, NetdB, was used. The PCB Piezotronics 356A16 triaxial accelerometers were fixed on the subjects. The data were processed with the dBFA Suite-Software of data acquisition control and post-processing; the parameters were kept constant, to study how different subjects perceive the same external stimulus. The θ coefficient, which indicates the type of personality the studied subject has, was calculated based on Rasch's model.

Rasch's model is used for analyzing data from assessments, such as skills, attitudes and personality traits; is increasingly used in other areas, of which the most important is occupational health. Mathematical theory underlying Rasch models is based on the theory of item response. For example, in the logistic model of the three parameters, the probability of correctly answer for the i item is: $P_i=c_i+\frac{1-c_i}{1+e^{-a_i(\theta-b_i)}}$, where θ is the person's parameter (ability), and a_i, b_i, and c_i are the item's parameters.

Fig. 1 *Subject on a vibrating platform*

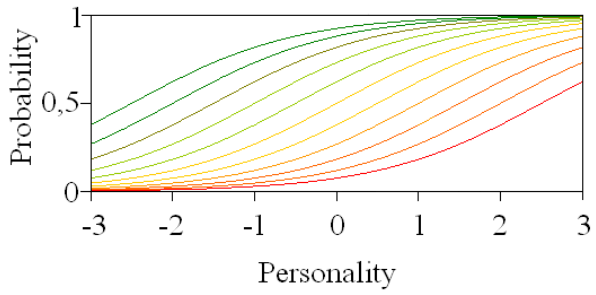

Fig. 2 *Probability curves for a number of items*

Table 3 *Personality Scale*

θ	Personality Type
0-0.5	Very Weak Personality
0.5-1	Weak Personality
1-1.5	Weak to Average Personality
1.5-2	Average to Strong Personality
2-2.5	Strong Personality
2.5-3	Very Strong Personality

Probability curves (Fig. 2) are colored to highlight the changes in probability of a correct answer depending on the location of personality (Table 3). The person is likely to respond correctly to the questions (left) and is unlikely to answer the questions correctly (right).

In this paper will be presented the results obtained from determinations made on 58 subjects, with ages between 19 and 54 years with a majority normal BMI. Among these, 41 subjects are smokers and 6 subjects drink more than 2 glasses of wine per day. Also, 27 subjects are students, 26 are workers and the rest have university degree (desk jobs).

The subjects agreed with taking part at the experiments. First, they answered multiple specialised questionnaires in order to determine each one's personality [9], [10], [11].

3. RESULTS AND DISCUSSIONS

Following the answers given by the subjects, 3 types of personalities were established:

- class A: a weak to average personality
- class B: a very weak personality
- class C: a strong to very strong personality

Hereinafter are presented the mediate results for each class.

Class A

Vibration time was 1min, the measured r.m.s accelerations are: 0.85; 0.87; 0.91; 0.93 and 0.95m/s^2, at the frequencies: 4, 6, 8, 11 and 16Hz. Measure of Perception (MP) is presented in Fig. 3 and Fig. 4.

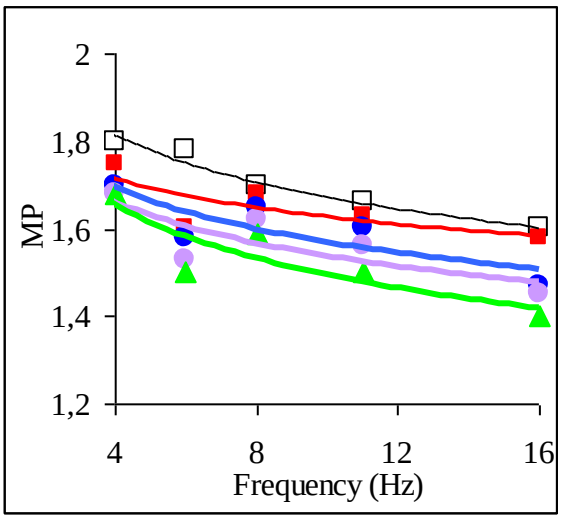

Fig. 3 *Measure of Perception for vertical vibrations versus frequency (□) – 0.85m/s^2; (■) – 0.87m/s^2; (●) – 0.91m/s^2; (●) – 0.93m/s^2; (▲) – 0.95m/s^2*

Curves equations from Fig. 3 are (Eq. 1):

$$\text{For } a=0.85\text{m/s}^2 \Rightarrow MP=2.0569v^{-0.0896} \ (R^2=0.9618)$$
$$\text{For } a=0.87\text{m/s}^2 \Rightarrow MP=1.8566v^{-0.0575} \ (R^2=0.8609)$$
$$\text{For } a=0.91\text{m/s}^2 \Rightarrow MP=1.9073v^{-0.0848} \ (R^2=0.8889) \quad (1)$$
$$\text{For } a=0.93\text{m/s}^2 \Rightarrow MP=1.8673v^{-0.0844} \ (R^2=0.8484)$$
$$\text{For } a=0.95\text{m/s}^2 \Rightarrow MP=1{,}9297v^{-0{,}1109} \ (R^2=0.9457)$$

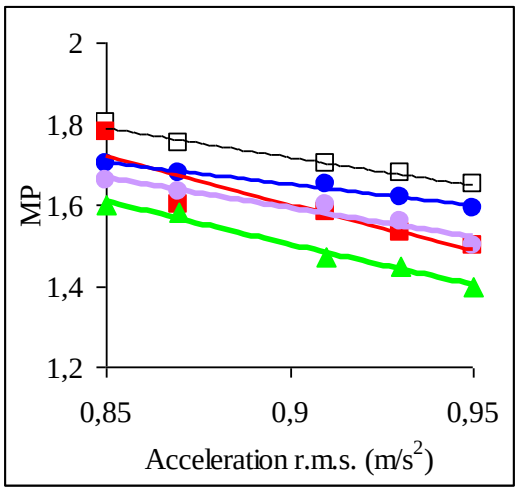

Fig. 4 *Measure of Perception for vertical vibrations versus acceleration (□) - 4Hz; (■) - 6Hz; (●) - 8Hz; (●) - 11Hz; (▲) - 16Hz*

Curves equations from Fig. 4 are (Eq. 2):

For ν=4Hz $\Rightarrow$ $MP=3.6043e^{-0.8233a}$ (R^2=0.8795)
For ν=6Hz $\Rightarrow$ $MP=5.914e^{-1.4527a}$ (R^2=0.9025)
For ν=8Hz $\Rightarrow$ $MP=2.9413e^{-036425a}$ (R^2=0.9212) (2)
For ν=11Hz $\Rightarrow$ $MP=3.6368e^{-0.918a}$ (R^2=0.9504)
For ν=16Hz $\Rightarrow$ $MP=5.1652e^{-1.3723a}$ (R^2=0.9718)

We consider that the two estimates of the measure of perception (depending on the frequency and on acceleration) must be identical, and then we can obtain a relation between acceleration and frequency for each case. From Eq. (1) and Eq. (2) we get Eq. (3) for acceleration as a function of frequency, for each case (Fig. 5).

$a_{4Hz} = 0.6818+0.1088\cdot\ln\nu$
$a_{6Hz} = 0.7974+0.0395\cdot\ln\nu$
$a_{8Hz} = 0.6740+0.1319\cdot\ln\nu$ (3)
$a_{11Hz} = 0.7261+0.0919\cdot\ln\nu$
$a_{16Hz} = 0.7174+0.0808\cdot\ln\nu$

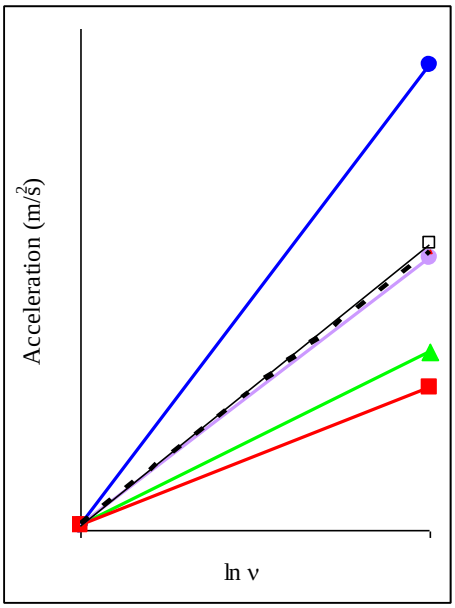

Fig. 5 *Acceleration versus frequency (Subject A) (□) - a_{4Hz}; (■) - a_{6Hz}; (●) - a_{8Hz}; (●) - a_{11Hz}; (▲) - a_{16Hz}; (- - - - -) - $a_{the\ most\ probable}$*

In Fig. 5, inside the area between the five lines is the line which represents the most probable relation between acceleration and frequency, for the studied cases; by extrapolation the dotted line was found, whose equation is given by:

$a=0.72103+0.08858\cdot\ln\nu$ (R^2=0.9921) (4)

Next we calculate θ, which represents the subjects' personality quantification, using Rasch's theory, where items were noted:

- $a_i=\nu_i$ (Frequency)
- $b_i=MP_i$ (Measure of Perception)
- $c_i=a_i$ (Acceleration)

This estimation is needed to see if the subjects' personality is strong enough that the evaluation he did, with Likert Scale, is correct or not.

We consider, for each case that the probability of giving a correct answer equals the deviation ($P_i = R_i^2$). From Rasch's equation:

$$P_i=c_i+\frac{1-c_i}{1+e^{-a_i(\theta-b_i)}}$$, by replacing the items we obtain:

$$R_i^2= a_i+\frac{1-a_i}{1+e^{-\nu_i(\theta-MP_i)}}$$

Replacing the values from Fig. 3 and 4 and from Eq. (2), results:

- Case 1: ν_1=4Hz; MP_1=1.8; a_1=0.85m/s²; R_1^2=0.8795 $\Rightarrow$ θ_1=1.448185
- Case 2: ν_2=6Hz; MP_2=1.6; a_1=0.87m/s²; R_2^2=0.9025 $\Rightarrow$ θ_2=1.416897
- Case 3: ν_3=8Hz; MP_3=1.65; a_3=0.91m/s²; R_3^2=0.9212 $\Rightarrow$ θ_3=1.406125
- Case 4: ν_4=11Hz; MP_4=1.65; a_4=0.93m/s²; R_4^2=0.9504 $\Rightarrow$ θ_4=1.569231
- Case 5: ν_5=16Hz; MP_5=1.4; a_5=0.95m/s²; R_5^2=0.9718 $\Rightarrow$ θ_5=1.434877

After excluding θ_4=1.569231 (which is outside the field), we obtain the average θ_a=1.426521 (Fig. 6).

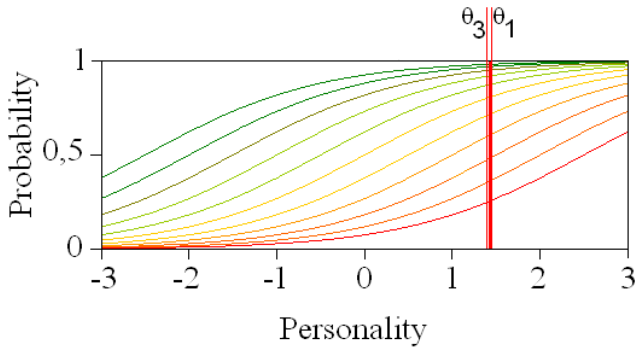

Fig. 6 *The A subjects have a weak to average personality: $\theta\in(1.40\text{-}1.44)$*

Class B

The experimental data are the same as were for Class A. Measure of Perception is presented in Fig. 7 and Fig. 8.

For the same reasons as Class A, we can obtain relations between acceleration and frequency for each case. From Eq. (5) and Eq. (6) we get Eq. (7) for acceleration as a function of frequency, for each case (Fig. 9).

Curves equations from Fig. 7 are (Eq. 5):

$$\begin{aligned}
&\text{For } a=0.85\text{m/s}^2 \Rightarrow MP=0.8099\nu^{-0.3499} \ (R^2=0.9913)\\
&\text{For } a=0.87\text{m/s}^2 \Rightarrow MP=0.5396\nu^{-0.2708} \ (R^2=0.8238)\\
&\text{For } a=0.91\text{m/s}^2 \Rightarrow MP=0.5762\nu^{-0.3807} \ (R^2=0.7613)\\
&\text{For } a=0.93\text{m/s}^2 \Rightarrow MP=0.6569\nu^{-0.5178} \ (R^2=0.9767)\\
&\text{For } a=0.95\text{m/s}^2 \Rightarrow MP=0.5975\nu^{-0.5912} \ (R^2=0.8369)
\end{aligned} \quad (5)$$

Curves equations from Fig. 8 are (Eq. 6):

$$\begin{aligned}
&\text{For } \nu=4\text{Hz} \Rightarrow MP=77.363e^{-5.9888a} \ (R^2=0.8526)\\
&\text{For } \nu=6\text{Hz} \Rightarrow MP=108.96e^{-6.5904a} \ (R^2=0.8718)\\
&\text{For } \nu=8\text{Hz} \Rightarrow MP=98.405e^{-6.5378a} \ (R^2=0.9102)\\
&\text{For } \nu=11\text{Hz} \Rightarrow MP=91.09e^{-6.5821a} \ (R^2=0.9504)\\
&\text{For } \nu=16\text{Hz} \Rightarrow MP=105.1e^{-10.599a} \ (R^2=0.9503)
\end{aligned} \quad (6)$$

From Eq. (5) and Eq. (6) we get Eq. (7) for acceleration as a function of frequency, for each case (Fig. 9).

$$\begin{aligned}
a_{4Hz}&=0.7624+0.0584\cdot\ln\nu\\
a_{6Hz}&=0.8055+0.0411\cdot\ln\nu\\
a_{8Hz}&=0.7861+0.0582\cdot\ln\nu\\
a_{11Hz}&=0.7493+0.0786\cdot\ln\nu\\
a_{16Hz}&=0.7925+0.0557\cdot\ln\nu
\end{aligned} \quad (7)$$

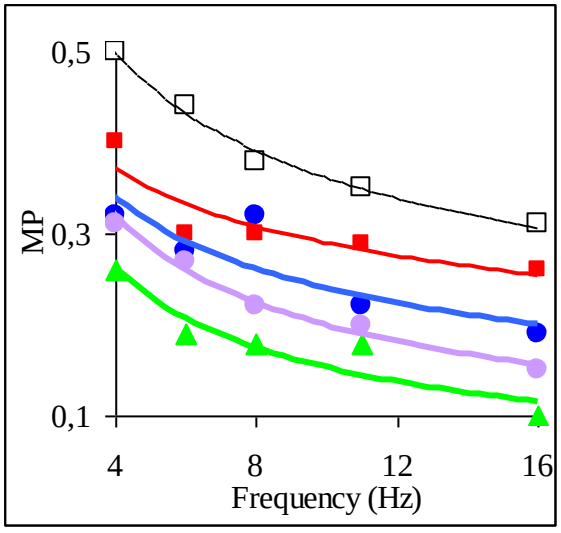

Fig. 7 *Measure of Perception for vertical vibrations versus frequency (□) – 0.85m/s²; (■) – 0.87m/s²; (●) – 0.91m/s²; (●) – 0.93m/s²; (▲) – 0.95m/s²*

In Fig. 9, inside the area between the five lines is the line which represents the most probable relation between acceleration and frequency, for the studied cases; by extrapolation the dotted line was found, whose equation is given by:

$$a=0.852+0.941\cdot\ln\nu \quad (R^2=0.9874) \quad (8)$$

Next we calculate θ, which represents subjects' B personality quantification. Replacing with the values from Fig. 7 and Fig. 8 and from Eq. (6), we obtain:

- Case 1: ν_1=4Hz; MP_1=0.5; a_1=0.85m/s²; R_1^2=0.8526 ⇒ θ_1=-0.509409
- Case 2: ν_2=6Hz; MP_2=0.3; a_1=0.87m/s²; R_1^2=0.8718 ⇒ θ_2=-0.410967
- Case 3: ν_3=8Hz; MP_3=0.25; a_3=0.91m/s²; R_3^2=0.9102 ⇒ θ_3=-0.513377
- Case 4: ν_4=11Hz; MP_4=0.2; a_4=0.93m/s²; R_4^2=0.9504 ⇒ θ_4=-0.269005
- Case ν_5=16Hz; MP_5=0.1; a_5=0.95m/s²; R_5^2=0.9503 ⇒ θ_5=-0.219373

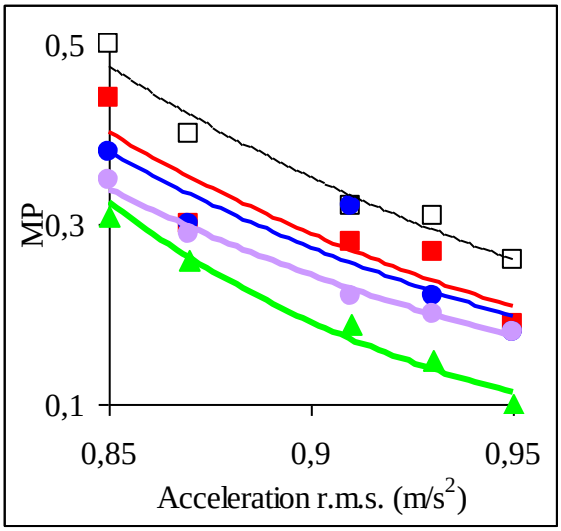

Fig. 8 *Measure of Perception for vertical vibrations versus acceleration (□) - 4Hz; (■) - 6Hz; (●) - 8Hz; (●) - 11Hz; (▲) - 16Hz*

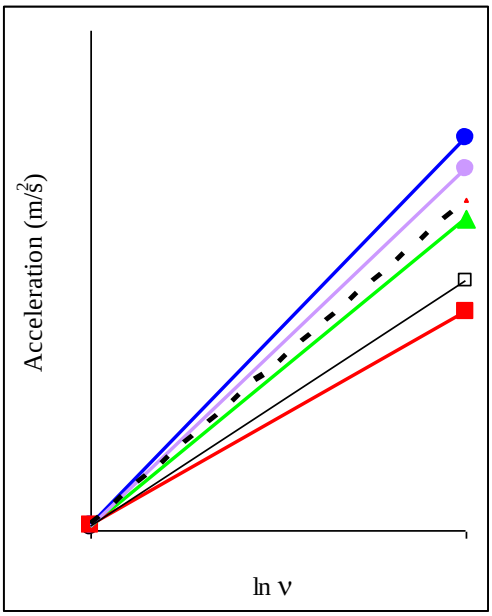

Fig. 9 *Acceleration versus frequency (Subject B) (□) - a_{4Hz}; (■) - a_{6Hz}; (●) - a_{8Hz}; (●) - a_{11Hz}; (▲) - a_{16Hz}; (- - - -) - $a_{the\ most\ probable}$*

Subjects always said that they do not feel anything; insisting to quantify the magnitude of perception on the Likert Scale, the notes given by them are increasingly lower for MP. They displayed negativity, even rebellion: refuse to cooperate.

Of the averaging results: θ_a=-0.384426, or if we give up the last two values, which do not fall in the previous values range, is obtained: θ_a=-0.477917 which fits best the θ coefficients range (Fig. 10).

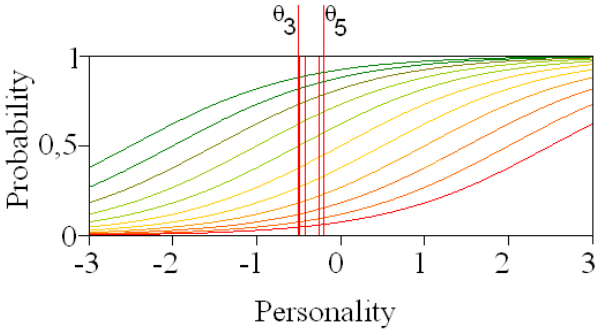

Fig. 10 *The B subjects have a very weak personality:*

$$\theta \in (-0.219 \div -0.513)$$

Class C

The experimental data are the same as were for Class A. Measure of Perception is presented in Fig. 11 and Fig. 12.

Curves equations from Fig. 11 are (Eq. 9):

$$\begin{aligned}
&\text{For } a=0.85\text{m/s}^2 \Rightarrow MP=1.514\cdot\nu^{0.1205} \ (R^2=0.9692)\\
&\text{For } a=0.87\text{m/s}^2 \Rightarrow MP=1.4719\cdot\nu^{0.1893} \ (R^2=0.9645)\\
&\text{For } a=0.91\text{m/s}^2 \Rightarrow MP=1.7461\cdot\nu^{0.0858} \ (R^2=0.9760) \qquad (9)\\
&\text{For } a=0.93\text{m/s}^2 \Rightarrow MP=2.6118\cdot\nu^{0.0598} \ (R^2=0.9794)\\
&\text{For } a=0.95\text{m/s}^2 \Rightarrow MP=2.5584\cdot\nu^{0.1557} \ (R^2=0.9485)
\end{aligned}$$

Curves equations from Fig. 12 are (Eq. 10):

$$\begin{aligned}
&\text{For } \nu=4\text{Hz} \Rightarrow MP=0.5259\cdot e^{1.4397a} \ (R^2=0.9872)\\
&\text{For } \nu=6\text{Hz} \Rightarrow MP=0.7425\cdot e^{1.1195a} \ (R^2=0.9931)\\
&\text{For } \nu=8\text{Hz} \Rightarrow MP=0.4692\cdot e^{1.654a} \ (R^2=0.9935) \qquad (10)\\
&\text{For } \nu=11\text{Hz} \Rightarrow MP=0.2442\cdot e^{2.6831a} \ (R^2=0.9910)\\
&\text{For } \nu=16\text{Hz} \Rightarrow MP=0.153\cdot e^{3.4161a} \ (R^2=0.9507)
\end{aligned}$$

For the same reasons as Class A, we can obtain relations between acceleration and frequency for each case. From Eq. (9) and Eq. (10) we get Eq. (11) for acceleration as a function of frequency, for each case (Fig. 13).

$$\begin{aligned}
&a_{4Hz}=0.7344+0.0836\cdot\ln\nu\\
&a_{6Hz}=0.6112+0.1690\cdot\ln\nu\\
&a_{8Hz}=0.7945+0.0518\cdot\ln\nu \qquad (11)\\
&a_{11Hz}=1.4327+0.0222\cdot\ln\nu\\
&a_{16Hz}=0.8245+0.0455\cdot\ln\nu
\end{aligned}$$

In Fig. 13, inside the area between the five lines is the line which represents the most probable relation between acceleration and frequency, for the studied cases; by extrapolation the dotted line was found, whose equation is given by:

$$a=0.8814+0.07511\cdot\ln\nu \quad (R^2=0.9902) \qquad (12)$$

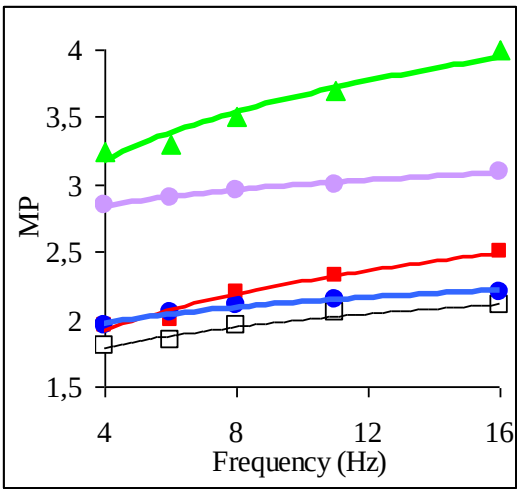

Fig. 11 *Measure of Perception for vertical vibrations versus frequency (□) – 0.85m/s²; (■) – 0.87m/s²; (●) – 0.91m/s²; (●) – 0.93m/s²; (▲) – 0.95m/s²*

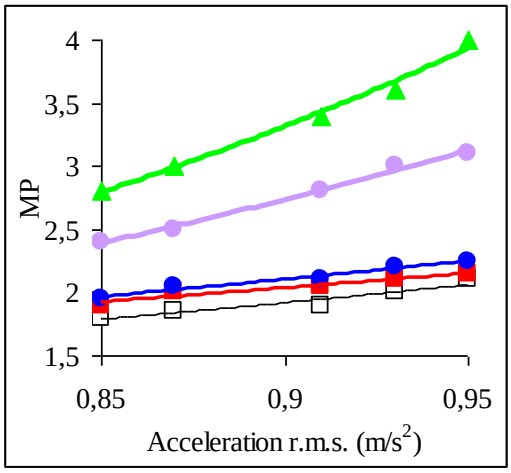

Fig. 12 *Measure of Perception for vertical vibrations versus acceleration (□) - 4Hz; (■) - 6Hz; (●) - 8Hz; (●) - 11Hz; (▲) - 16Hz*

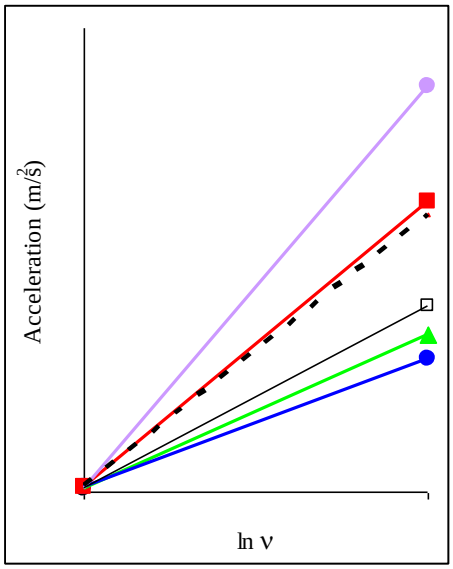

Fig. 13 *Acceleration versus frequency (Subject A) (□) - a_{4Hz}; (■) - a_{6Hz}; (●) - a_{8Hz}; (●) - a_{11Hz}; (▲) - a_{16Hz}; (- - - - -) - $a_{the\ most\ probable}$*

Next we calculate θ, which represents subjects' C personality quantification. Replacing with the values from Fig. 11 and Fig. 12 and from Eq. (10), we obtain:

- Case 1: ν_1=4Hz; MP_1=1.8; a_1=0.85m/s^2; R_1^2=0.9872 ⇒ θ_1=2.393856
- Case 2: ν_2=6Hz; MP_2=2; a_2=0.87m/s^2; R_2^2=0.9931 ⇒ θ_2=2.480245
- Case 3: ν_3=8Hz; MP_3=2.1; a_3=0.91m/s^2; R_3^2=0.9935 ⇒ θ_3=2.419130
- Case 4: ν_4=11Hz; MP_4=2.3; a_4=0.93m/s^2; R_4^2=0.9910 ⇒ θ_4=2.473968
- Case 5: ν_5=16Hz; MP_5=2.4; a_5=0.95m/s^2; R_5^2=0.9507 ⇒ θ_5=2.665912

Of the averaging results: θ_a=2.486622, or if we give up θ_1 and θ_5, which do not fall in the previous values range, is obtained: θ_a=2.457781 which fits best the θ coefficients range (Fig. 14).

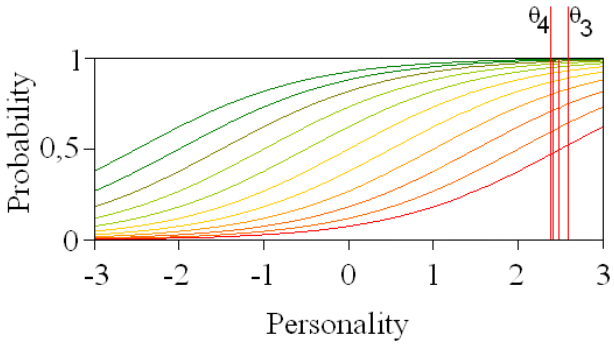

Fig. 14 *The C subjects have a strong to very strong personality: θ∈(2.39-2.66)*

4. CONCLUSIONS

For the A subjects, from the five values of θ, only one θ_4=1.57 is outside the very narrow range where the others are, θ∈(1.40-1.44); they have a weak to average personality and they are able to respond correctly to the most simple questions. This type of person might have been influenced by the fact that he had to participate in an experiment, by the presence of equipment, by the fact that he was subject to vibrations, etc., so there is a possibility that the evaluation he made with the Likert Scale is not fully correct.

For the B subjects, from the five values of θ, the last two were far from the average. This was the moment when the subjects lost interest and stop concentrating. We do not know if this is something that usually happens to them or if it is just hostility towards something new. The subjects totally refused to participate to the 2nd part of the experiment. They have a very weak personality and they try to hide it with bravery; they do not agree to even a single direction and they are not influenced by the presence of a professor. They are able to answer correct but there is a very high possibility that their assessment with the Likert Scale is not correct.

For the C subjects, from the five values of θ, two are outside the very narrow range where thee other are, θ∈(2.41-2.48); they have a strong to very strong personality. Also it can be said that they can answer correct to questions. This type of person will never be influenced by the fact he has to take part to an experiment, by the presence of equipment or by the fact that he was subject to vibrations. For sure, his assessment with the Likert Scale was correct almost entirety.

The cumulated results are presented in Table 4 and Fig. 15.

Table 4 *Number of subjects – relative to the BMI and to the type of personality*

BMI [kg/m^2]	Number of subjects	Class A	Class B	Class C
< 15	-	-	-	-
15.0 – 16.0	-	-	-	-
16.0 – 18.5	2	1	1	
18.5 – 25	37	31	1	5
25 – 30	16	11	5	-
30 – 35	2	1	-	1
35 – 40	1	-	1	-
> 40	-	-	-	-
Total	58	44	8	6

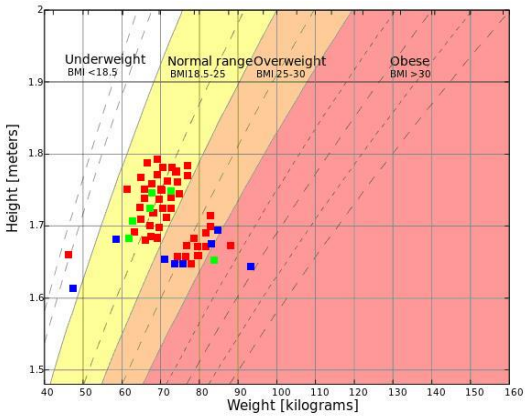

Fig. 15 *Subjects' distribution – relative to the BMI and to the type of personality (■) – class A; (■) – class B; (■) – class C*

It was observed that in all the cases, the results obtained from the answers given at the questionnaires concur with the results obtained from the vibrations experimental measurements.

In conclusion, from the measurements of the vibrations perception magnitude one can determine someone's type of personality. This determination is as least as precise as the classic questionnaires method, because it represents a result of practical experimental measurements.

REFERENCES

[1] Ashton, M. C. and Lee, K., A short measure of the major dimensions of personality, Journal of Personality Assessment, 91, 340-345, 2009.

[2] Herzog, T.N., Scheuren, F.J. and Winkler, W.E., Data quality and record linkage techniques, Pszchometrika, Vol. 73, Springer New York, 2008.

[3] Kim, Y.G., et all, Correlation of ride comfort evaluation methods for railway vehicles, Proceedings of the Institution of Mechanical Engineers Part F - Journal of Rail and Rapid Transit, 217(2), 73-88, 2003.

[4] Lee, K., Ashton, M. C., Pozzebon, J. A., Visser, B. A. and Ogunfowora, B., Similarity and assumed similarity of personality reports of well-acquainted persons, Journal of Personality and Social Psychology, 96, 460-472, 2009.

[5] Marcus, B., Lee, K., and Ashton, M. C., Personality dimensions explaining relationships between integrity tests and counterproductive behavior, Personnel Psychology, 60, 1-34, 2007.

[6] Paddan, G.S. and Griffin, M.J., Evaluation of whole-body vibration in vehicles, Journal of Sound and Vibration, 253(1), 195-213, 2002.

[7] Rasch, G., Probabilistic models for some intelligence and attainment tests, The University of Chicago Press., 1960.

[8] South, T., Managing Noise and Vibration at Work. A practical guide to assessment, measurement and control, Elsevier Butterworth-Heinemann, Linacre House, Jordan Hill, Oxford, 2004.

[9] http://www.humanmetrics.com/cgi-win/jtypes2.asp

[10] http://www.personalitypathways.com/type_inventory.html

[11] https://answers.yahoo.com/question/index?qid=20090530212359AA651RN

UNIVERSITY OF NIŠ

FACULTY OF OCCUPATIONAL SAFETY

Basic Academic Studies at two study programmes

- OCCUPATIONAL SAFETY
- ENVIRONMENTAL PROTECTION

The study programme structure complies with the Accreditation Standards for the First and Second Level of Higher Education. The study programme lasts 4 years (8 semesters), comprising 240 ECTS credits.

Master Academic Studies at five study programmes:

- ENVIRONMENTAL ENGINEERING
- OCCUPATIONAL SAFETY ENGINEERING
- FIRE PROTECTION
- EMERGENCY MANAGEMENT
- COMMUNAL SYSTEM MANAGEMENT

The study programme structure complies with the Accreditation Standards for the Second Level of Higher Education. The study programme lasts one year (2 semesters), comprising 60 ECTS credits.

Doctoral Academic Studies at two study programmes:

- OCCUPATIONAL SAFETY ENGINEERING
- ENVIRONMENTAL ENGINEERING

The study programme structure complies with the Accreditation Standards for the Third Level of Higher Education. The study programme lasts 3 years (6 semesters), comprising 180 ECTS credits.

REPUBLIC OF SERBIA, Čarnojevića 10A, 18000 Niš
Phone: 381 18 529701, 381 18 529755, Fax: 381 18 249962
www.znrfak.ni.ac.rs

University of Nis
Faculty of Occupational Safety
„Politechnica“ University of Timisoara
Faculty of Mechanical Engineering
24th International Conference
NOISE AND VIBRATION
Niš, 29 - 31. 10. 2014.

VIBRATION ANALYSIS HYDRAULIC EXCAVATORS

Vesna Jovanović[1], Dragoslav Janošević[1], Jovan Pavlović[1], Nikola Petrović[1]

[1]University of Niš, Faculty of Mechanical Engineering, Serbia, e-mail: vesna.nikolic@masfak.ni.ac.rs

Abstract - *The work will include the presentation of research results vibrations hydraulic excavator certain based on the measured values in the state of excavator operating conditions. The survey results will show influence of elastic-damping behavior of hydraulic actuators (hydraulic motor and hydraulic cylinder) driving mechanisms of excavator the vibrations that occur when operating the machine. The paper presents a dynamical mathematical model based on the hydraulic excavator that was subject to vibration analysis of machine.*

Key words: *hydraulic excavators, vibratory analysis*

1. INTRODUCTION

Among the mobile (construction, mining, transportation, agricultural, communal) machines hydraulic excavators have the world's largest production (Caterpillar, Liebherr, Komatsu) with models of different sizes, which are characterized by high performance engineering, industrial and ergonomic design defines certain standards and quality. Certain standards relating to, among the other things, the permissible level of noise in the cabin and work environment of hydraulic excavators [1] [2].

This paper gives the part of results of the investigation the causes of vibrations excitation that occur during operation of hydraulic excavators.

2. MATHEMATICAL MODEL

For the analysis of vibration excitation and determination of the acceleration place of command operator hydraulic excavators developed a mathematical model based on the measured size of the state of the excavator when working machine in real-operating conditions. Mathematical model is developed which comprised five-member configuration of the excavator kinematic chain comprising: thrust-motional mechanism L_1 Fig. 1, rotating platform L_2, and a three-member planar manipulator with: boom L_3, stick L_4 and bucket L_5. Actuators drive thrust-motional mechanism and rotating platform are hydraulics motor, while actuators of manipulator are hydrocylinders: boom C_3, stick C_4 and bucket C_5.

Thrust-motional mechanism of excavator with a plane of the substrate builds unmanaged zero joint third class of possible movements in the plane of the substrate. The centre of the joint O_2 kinematics pair, thrust segment-rotating segment, is point of normal irruption joint vertical axis through the horizontal plane in which lies the centres of axial bearing rolling elements which are linked thrust-motional and rotating segment of chain. The centres of manipulator joints (O_i, i =3,4,5) are points of joints horizontal axis irruption through symmetry plane of the kinematic chain manipulator excavator. Irruption of cutting edge bucket through the plane of the manipulator is the centre of the bucket cutting edge O_w.

The assumptions of a mathematical model of kinematic chain excavator are:

•The substrate reliance and segments of excavatorkinematic chain are modeled with rigid bodies,

•kinematic chain excavator is an open configurationwith the fact that during the digging operation, whenhas a closed configuration, is viewed as an open chainconfiguration, on which the last segment-bucket actingtechnological resistance to digging W

•During manipulative task on kinematic chain excavatoroperating gravitational, inertial and external(technological) force - resistance to digging.

Space of excavator model is determined by absolutely coordinate system $OXYZ$ (Fig.1).

Segment of the kinematic chain L_i model is defined in its local coordinate system $O_i\, x_i\, y_i\, z_i$ with values set: [3]:

$$L_i = \left\{ \hat{\boldsymbol{e}}_i, \hat{\boldsymbol{s}}_i, \hat{\boldsymbol{t}}_i, m_i, J_i \right\} \tag{1}$$

where: $\hat{\boldsymbol{e}}_i$ - joint axis unit vector O_i by which are segment L_i linked for previous segment L_{i-1} Fig.1, $\hat{\boldsymbol{s}}_i$ - the position vector of the joint center O_{i+1} by which are segment L_i linked for to the following segment L_{i-1} (the vector intensity $\boldsymbol{s}_i$ represent kinematic length of segment), $\hat{t}_i$ - the position vector of centre of mass segment L_i, m_i - segment mass, $\hat{J}_i$ -tensor of moment inertia of members. Vectors marked caps apply to local coordinate system and no cap on the absolute coordinate system.

Allocated measured values state of excavator at work in the real exploitation conditions under which the developed a mathematical model are given in Table 1.

Based on the measured size c_i, double differencing, determine the speed $\dot{c}_i$ and acceleration $\ddot{c}_i$ of actuator drive mechanism of excavator:

$$\dot{c}_i = \frac{c_{i(t+\Delta t)} - c_{i(t-\Delta t)}}{2\Delta t} \tag{2}$$

$$\ddot{c}_i = \frac{c_{i(t+2\Delta t)} - 2c_{i(t)} + c_{i(t-2\Delta t)}}{4\Delta t^2} \tag{3}$$

where: $c_{i(t+\Delta t)}$ the measured size of the time t, $c_{i(t+\Delta t)}$, $c_{i(t-\Delta t)}$ - the measured size of the time which is the time interval Δt is greater than or less than the t, Δt - the interval of time between two successive measured values.

Based on the size of the state of the actuator $(c_i, \dot{c}_i, \ddot{c}_i)$ i defined transfer functions driving mechanisms excavators, determined: generalized coordinates θ_i, velocity $\dot{\theta}_i$ and acceleration $\ddot{\theta}_i$, vectors of the center of the joint $\boldsymbol{r_i}$ and the center of mass $\boldsymbol{r_{ti}}$ members of the kinematic chain of excavator trajectory center of the cutting edge of bucket $\boldsymbol{r_w}$ [4]. Internal (generalized) coordinates θ_i represent angles of rotation around the axis of the joints, and determine the relative position of members L_i compared to the previous article L_{i-1}.

Kinematic variables of member the chain L_i are linear v_i and angular ω_i velocity, and linear w_i and angular acceleration ε_i, where is taken that the movement of previous member L_{i-1} portable, and movement observed member L_i of the joint O_i relative.

To determine the size of the kinematic chain member L_i with respect to the absolute coordinate system, using the recursive equation [4][5]:

$$\boldsymbol{\omega}_i = \boldsymbol{\omega}_{i-1} + \dot{\theta}_i \, \boldsymbol{e}_i \tag{4}$$

$$\boldsymbol{v}_i = \boldsymbol{v}_{i-1} + \left(\boldsymbol{\omega}_{i-1} \times \left(\boldsymbol{s}_{i-1} - \boldsymbol{t}_{i-1}\right)\right) + \left(\boldsymbol{\omega}_i \times \boldsymbol{t}_i\right) \tag{6}$$

$$\begin{aligned}\boldsymbol{w}_i = \boldsymbol{w}_{i-1} &+ \left(\boldsymbol{\varepsilon}_{i-1} \times \left(\boldsymbol{s}_{i-1} - \boldsymbol{t}_{i-1}\right)\right) + \boldsymbol{\omega}_{i-1} \times \left(\boldsymbol{\omega}_{i-1} \times \left(\boldsymbol{s}_{i-1} - \boldsymbol{t}_{i-1}\right)\right) \\ &+ \left(\boldsymbol{\varepsilon}_i \times \boldsymbol{t}_i\right) + \boldsymbol{\omega}_i \times \left(\boldsymbol{\omega}_i \times \boldsymbol{t}_i\right)\end{aligned} \tag{7}$$

where: $\dot{\theta}_i, \ddot{\theta}_i$ - angular velocity, and acceleration velocity members L_i in the joint O_i.

Based on the previous recursive equations, among other things, determine the acceleration vector at the place M (Fig. 1) operator in the cab of excavator:

$$\begin{aligned}\boldsymbol{w}_M = \boldsymbol{w}_1 &+ \left(\boldsymbol{\varepsilon}_1 \times \left(\boldsymbol{s}_1 - \boldsymbol{t}_1\right)\right) + \boldsymbol{\omega}_1 \times \left(\boldsymbol{\omega}_1 \times \left(\boldsymbol{s}_1 - \boldsymbol{t}_1\right)\right) \\ &+ \left(\boldsymbol{\varepsilon}_2 \times \boldsymbol{t}_m\right) + \boldsymbol{\omega}_2 \times \left(\boldsymbol{\omega}_2 \times \boldsymbol{t}_m\right)\end{aligned} \tag{8}$$

where: $\boldsymbol{t_m}$ position vector operator M in the excavator cab.

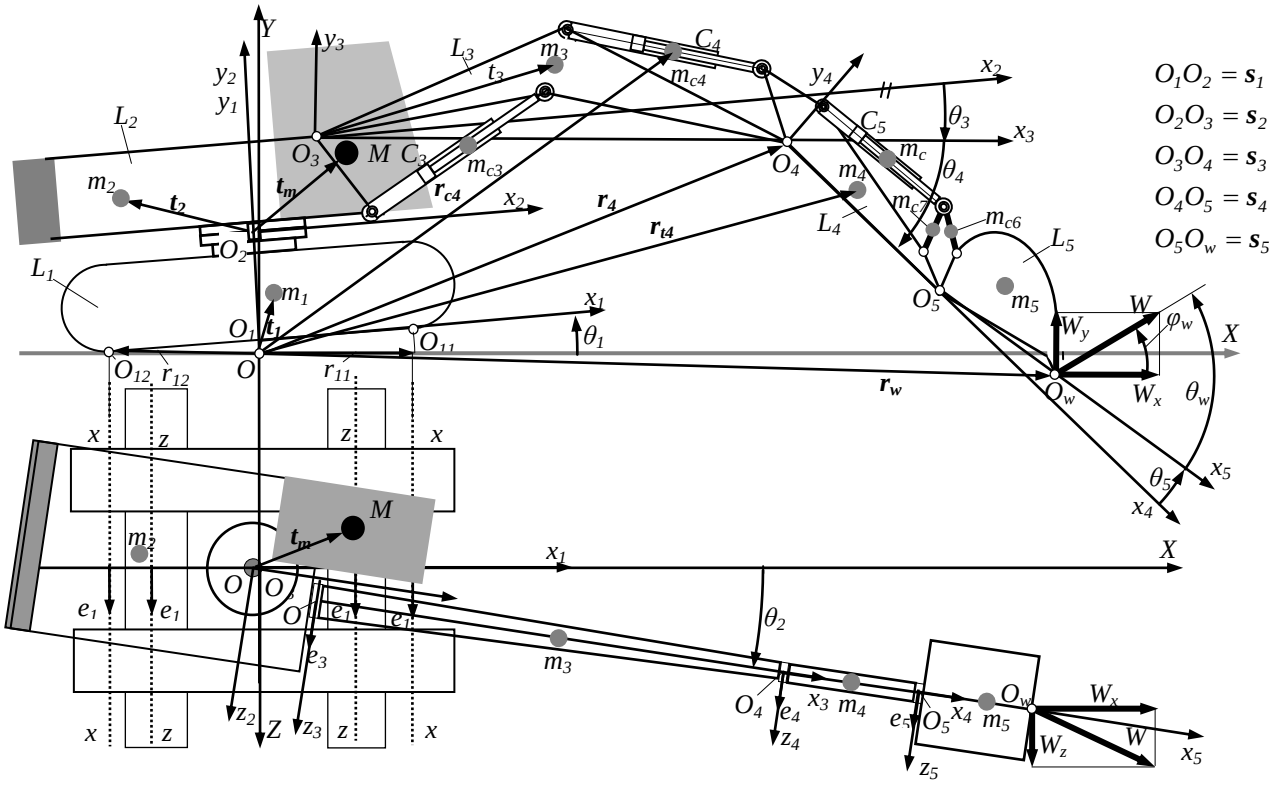

Fig.1 *The mathematical model of the hydraulic excavator with shovel manipulator*

Table 1 The measured size

Measurement place	Name of measured values	Mark	Dimensio
M1	Moving thrust-motional mechanism	c_1	*m*
M2	The angle of rotation of the platform	c_2	*o*
M3	Stroke hydraulic cylinder of boom	c_3	*m*
M4	Stroke hydraulic cylinder of stick	c_4	*m*
M5	Stroke hydraulic cylinder of bucket	c_5	*m*

Determination and analysis of the vibrational characteristics of excavators were carried out on the basis of test results crawler excavators BGH 600C, production IMK 14. Octobar - Kruševac, mass *16000 kg* and the power *70 kW* equipped with shovel manipulator with a bucket capacity *0,6* m^3. The study was conducted on the polygon of Development laboratory of the Institute IMK "14.Oktobar" in Krusevac. [7]. Sampling of the measured values was done in the time interval $\Delta t=0,032s$. ime during the test: Sunny, quiet, temperature at 21ºC. Measurements by penrtometar found that during the study was carried out excavation III and IV categories of soil.

During the tests have been conducted measuring forty-two full cycles, operation of digging through the transfer and unloading of land to restore operations at a new start digging with a different manipulative tasks in a whole working range excavator. Analysis was performed using a program developed by a defined mathematical model and measured quantities states excavators at work in the operating conditions Table 1.

Using the measured values c_i as input data, program must first determine, as a function of time during operation cycle, geometric and kinematic size: generalized coordinates, coordinates of the center of the joints, angular velocity and angular acceleration of the members of the kinematic chain excavators. Of the total number of measurements in this study were selected and analyzed measurement cycle at digging canals, which is the same width as a bucket, from the graund surface, and depth around 3,2 *m*.

From the results obtained are given diagrams Fig.2 changes the components of the vector acceleration (w_{Mx},w_{My},w_{Mz}) position of the operator *M* in the cabin of excavator, in the absolute coordinate system, and changes in movement stroke hydraulic cylinder of boom and angle of inclination thrust-motional mechanisms of excavator bagera depending on the duration of the operation cycle.

The diagrams show that the hydraulic excavator, in work, appear as parametrically sensitive oscillatory systems. Expressed the elastic elements of excavator occur hydrostatic actuators (motors and hydraulic cylinders) drive mechanisms that act as a "hydraulic spring" caused by the compressibility

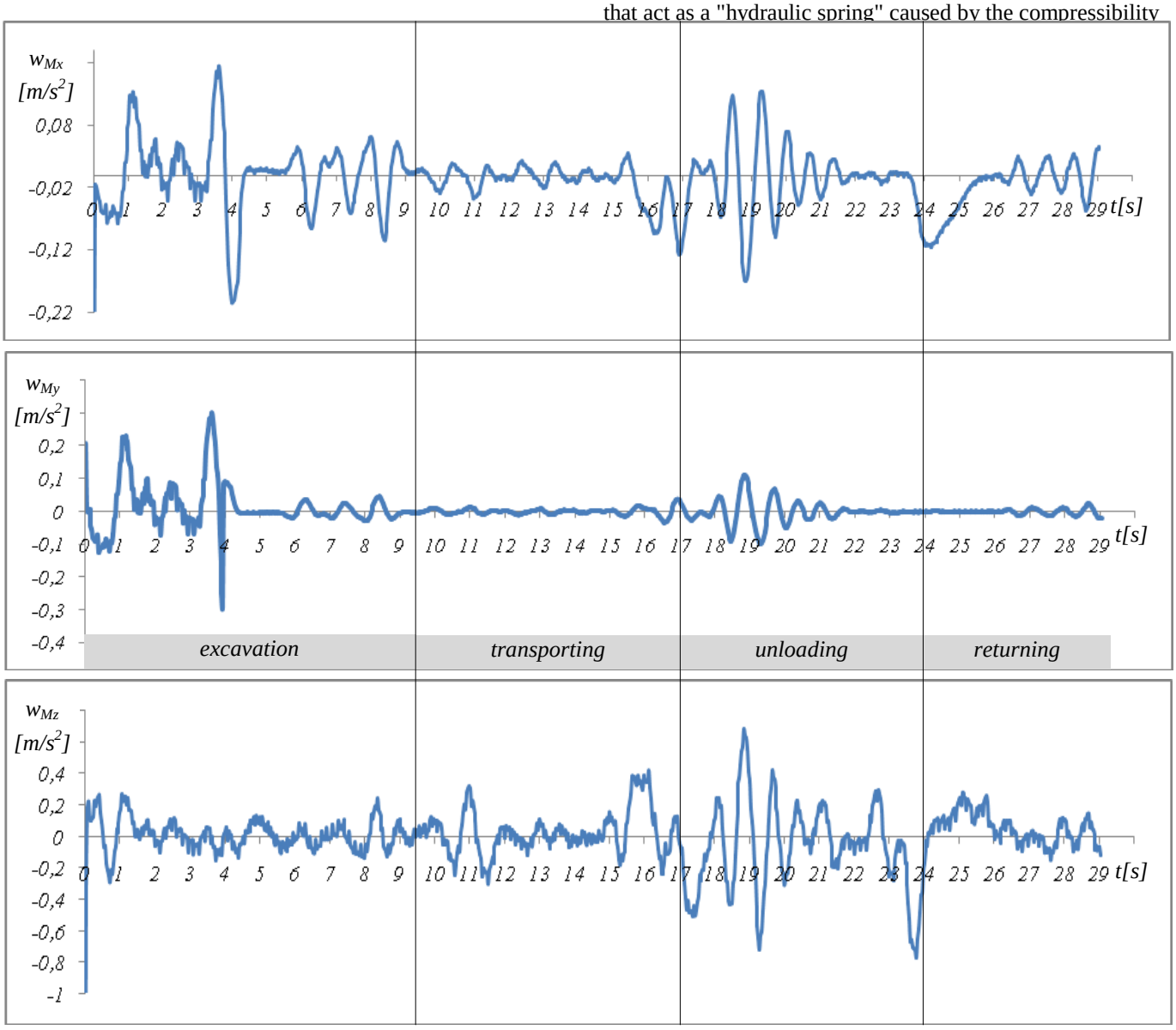

Fig. 2 *Change of components acceleration vector position operator M in the cabin of excavator, depending on the duration of the operation cycle*

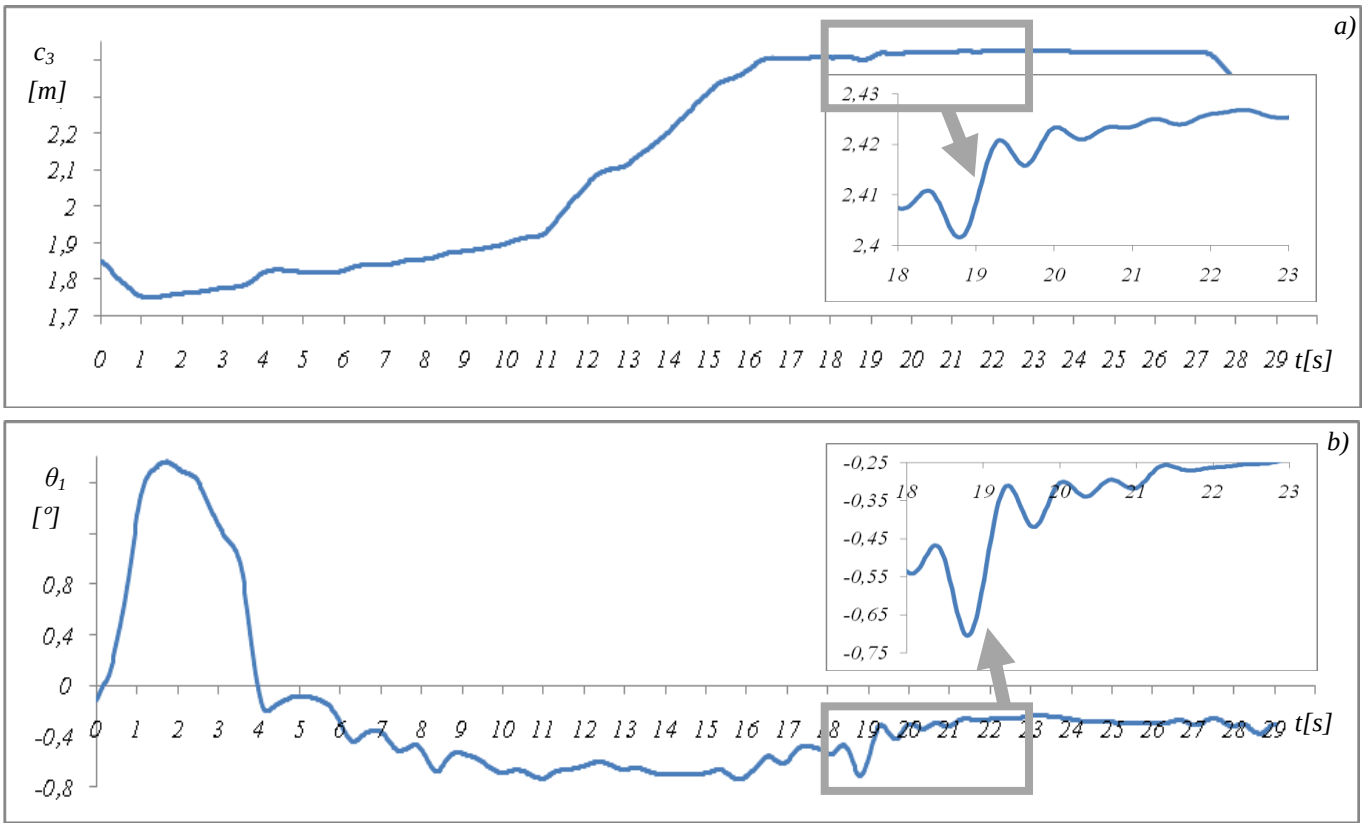

Fig. 3 *Displacements: a) stroke hydraulic cylinder of boom and b) the angle of inclination thrust- motional mechanisms of excavator depending on the duration of the operation cycle*

of the hydraulic oil. This is indicated by the diagram Fig3. changes in stroke hydraulic cylinder of manipulator. Oscillatory excitation occur at the beginning and at the exit from the bucket digging when resistance of digging is growing rapidly, or decreases, and occurs as an impulse force acting on the elastic damping system of the excavator. Then, at the beginning of the rapid transporting of materials by running the boom, or when emptying buckets when rapidly changing dynamic system parameters: mass and moment of inertia of the affected material. To sudden changes in the amplitude of acceleration occurs during starting and stopping the revolving platform from digging plane in the unloading plane of excavator and vice versa, wherein the operating lines of hydraulic motor for rotation platforms act as a "hydraulic spring." By vibratory excitation leads to sudden movements of thrust- motional mechanism θ_1 Fig.3b ie. revolving platform and cabin that feels and excavator operator.

CONCLUSION

The research results presented in this paper show that hydraulic excavators in performing manipulation tasks behave as highly sensitive dynamic oscillatory systems. As a highly-elastic damping elements appear hydrostatic actuators (hydraulic motor and hydraulic cylinder) driving mechanisms of kinematic chain excavators in the form of "hydraulic spring" caused by the compressibility of the hydraulic oil. Obtained results indicate the sources of excitation that cause vibration in the operator's cabine of excavator. Sources excitations occur due the frequent and sudden changes in movement members of kinematic chain in each operation work then the stochastic changes in external digging resistance and changes in mass and moment of inertia of the affected material.

ACKNOWLEDGEMENT

This paper is result of technological project No. TR35049, supported by Ministry of Education, Science and Technological Development of the Republic of Serbia

REFERENCES

[1] SAE J1384 Vibration Performance Evaluation of Operator, 2007.

[2] ISO 5007 Agricultural wheeled tractors - Operator's seat - *Laboratory measurement of transmitted vibration*, 2003.

[3] V. Jovanović, D. Janosević, J. Pavlović, "Experimental determination of resistance digging of hydraulic excavator ", *IMK-14 Research & Developement in Heavy Machinery* Vol. 19, No.3, EN83-88, 2013.

[4] Janošević D.: "Optimal Synthesis of Drive Mechanisms in Hydraulic Excavators", doctoral dissertation, *Faculty of Mechanical Engineering, University of Niš*, 1997.

[5] M. Vukobratović, D. Stokić, N. Kirćanski, M. Kirćanski, D. Hristić, B. Karan, D. Vujić, M. Djurović, " Uvod u robotiku", *Institut Mihajlo Pupin, Beograd, 1986.*

[6] Guofu D., Zhongyan Q., Shuangxia P.,"Active Vibration Control of Excavator Working Equipment with ADAMS", *International ADAMS User Conference,* 2000.

University of Nis
Faculty of Occupational Safety
„Politechnica“ University of Timisoara
Faculty of Mechanical Engineering
24th International Conference
NOISE AND VIBRATION
Niš, 29 - 31. 10. 2014.

STRESSING ISSUE OF A PIEZOCERAMIC CANTILEVER WITH ELECTRODE COATINGS AND TRANSVERSAL POLARIZATION

Igor Jovanović[1], *Ljubiša Perić*[2], *Uglješa Jovanović*[1], *Dragan Mančić*[1]

[1] University of Niš, Faculty of Electronic Engineering, Serbia, igor.jovanovic@elfak.ni.ac.rs
[2] Regional Chamber of Economy Niš, Serbia

Abstract - *This paper presents a general case of stressing a rectangular piezoceramic cantilever with transversal polarization which is loaded at the free end by a concentrated force. Two mutually opposite surfaces of the rectangular cantilever are with electrode coatings on which an excitation electric voltage is applied to. By applying the reverse method for solving the problems of electroelasticity theory, componential displacements, electric potential, specific strains, electric fields and piezoelectric displacements are determined for the rectangular piezoceramic cantilever made from PZT4 piezoceramic material.*

1. INTRODUCTION

In application of mathematical theory of electroelasticity, are met versatile tasks and problems, where the subjects of studying are different piezoelectric bodies of concrete dimensions [1, 2]. In general, depending on what is known all tasks of the linear theory of electroelasticity may be ranked into three groups: body loading (mechanical, electric, or combined), conditions on boundary surfaces of the observed body, or displacements of points on the surface of the electroelastic piezoelectric body [3].

Regarding the choice of unknown variables, there are three mathematical methods to solve the problems of the theory of electroelasticity: direct method, reverse method and semi-reverse method. Besides analytical and numerical methods, significant place also take experimental examinations of stress and strain state of stressed electroelastic body.

Piezoelectric cantilever beams have received considerable attention for vibration-to-electric energy conversion [4,5,6,7]. The use of a piezoelectric unimorph cantilever allows both electrical actuation and electrical sensing. Cantilever piezoelectric power generators are being used because of their high strain and high power output even under lower acceleration amplitudes. This paper considers a general case of stressing rectangular prismatic piezoceramic cantilever with transversal polarization and electrode coatings on the two mutually opposite surfaces $z=\pm h/2$, loaded on the left free end by a concentrated force, vector of external loading $\vec{F}$ which is aimed in direction of the axis Oz (Fig. 1). It is assumed that electric potential difference $2U_0$ is applied on electrodes. Furthermore, it is also assumed that effect of the electromechanical characteristics of the electrode coatings may be neglected. Coordinate system $Oxyz$ is set at the free end of the cantilever. Axes Oy and Oz are main central axes of inertia of the cross section, while axis Ox is geometric axis. Axis Oz is directed downwards.

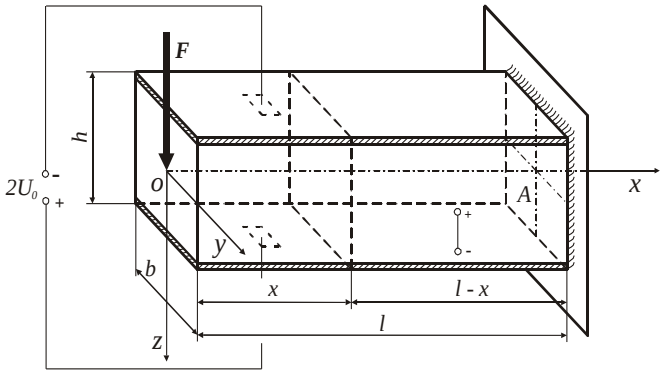

Fig. 1 *Stressing of the piezoceramic cantilever with transversal polarization and electrodes*

2. FUNDAMENTAL EQUATIONS

According to the hypothesis of Журавский, for a cantilever loaded at the free end by a concentrated force $\vec{F}$, there are only normal stress σ_x in axial direction and tangential stress τ_{xz} in plane of the cross section, aimed in direction of the force $\vec{F}$ [8]. Volume forces are neglected, so the stresses are given by stress tensor matrix:

$$\mathbb{N} = \begin{bmatrix} \sigma_x & \tau_{xz} & 0 \\ \tau_{xz} & 0 & 0 \\ 0 & 0 & 0 \end{bmatrix} \tag{1}$$

Since the dimensions of the cross section of the rectangular cantilever are small in regard to the length l ($(b/h)<<1$, $(b/l)<<1$), this stress state can be considered as planar, in plane Oxz. From strength of materials it is known that componential stresses for this case of stressing are [8]:

$$\sigma_x = -\frac{F}{I_y} xz, \qquad \tau_{xz} = -\frac{F}{8I_y}\left(h^2 - 4z^2\right) \tag{2}$$

while componential mechanical stresses on the sides $y=\pm b/2$ have values:

$$\sigma_y\Big|_{y=\pm\frac{b}{2}} = 0, \quad \tau_{yx}\Big|_{y=\pm\frac{b}{2}} = 0, \quad \tau_{yz}\Big|_{y=\pm\frac{b}{2}} = 0 \tag{3}$$

In agreement with the hypothesis of Журавский, componential mechanical stresses are equal to zero in the internal points of the piezoceramic rectangular cantilever. Also, according to this hypothesis, an assumption is introduced that componential displacements of the body points u and w are independent from coordinate y, i.e.:

$$u = u(x, z), \quad v = v(x, z) \tag{4}$$

For a piezoceramic cantilever with transversal or longitudinal polarization an additional assumption is introduced that the component of the piezoelectric displacement vector in direction of axis Oy is equal to zero:

$$D_y = 0 \tag{5}$$

therefore, the function of electrostatic potential ψ is independent from coordinate y:

$$\psi = \psi(x, z) \tag{6}$$

Boundary conditions on the sides $z=\pm h/2$ are expressed in the following way:

$$\sigma_z\Big|_{z=\pm h/2} = 0, \ \tau_{zx}\Big|_{z=\pm h/2} = 0, \ \psi\Big|_{z=\pm h/2} = \pm U_0 \tag{7}$$

On the surface $x=0$, stand following integral conditions:

$$\sigma_x\Big|_{x=0} = 0, \qquad -2b\int_{-h/2}^{h/2} \tau_{xz}\Big|_{x=0} dz = F \tag{8}$$

Conditions for the fixed end of the cantilever for the frontal surface $x=l$ are:

$$u(l, 0) = 0, \quad w(l, 0) = 0, \quad \frac{\partial w}{\partial z}\Big|_{\substack{x=l \\ z=0}} = 0 \tag{9}$$

The proposed task is solved by application of reverse method, such that components u and w of the displacement vector $\vec{s}$ and electric potential ψ are assumed in a polynomial form:

$$\begin{aligned} u &= a_0 + a_1 x + a_2 z + a_3 z^3 + a_4 x^2 z \\ w &= b_0 + b_1 z + b_2 x + b_3 x^3 + b_4 z^2 x \\ \psi &= c_1 z + c_2 x + c_3 x z^2 \end{aligned} \tag{10}$$

Equations of electrostatics in absence of free electric charges, i.e. simplified Maxwell's partial differential equations are [3]:

$$\begin{aligned} div\vec{D} &= \frac{\partial D_x}{\partial x} + \frac{\partial D_y}{\partial y} + \frac{\partial D_z}{\partial z} = 0 \\ \vec{E} &= -grad\,\psi = -\left(\frac{\partial \psi}{\partial x}\vec{i} + \frac{\partial \psi}{\partial y}\vec{j} + \frac{\partial \psi}{\partial z}\vec{k}\right) \end{aligned} \tag{11}$$

Cauchy's kinematic equations are:

$$\begin{aligned} \varepsilon_x &= \frac{\partial u}{\partial x}, \ \varepsilon_y = \frac{\partial v}{\partial y}, \ \varepsilon_z = \frac{\partial w}{\partial z} \\ \gamma_{xy} &= \frac{\partial u}{\partial y} + \frac{\partial v}{\partial x}, \ \gamma_{xz} = \frac{\partial u}{\partial z} + \frac{\partial w}{\partial x}, \\ \gamma_{yz} &= \frac{\partial v}{\partial z} + \frac{\partial w}{\partial y} \end{aligned} \tag{12}$$

By substituting the assumed solutions (10) into expressions (11) and (12), respectively, following expressions are obtained:

$$\begin{aligned} E_x &= -c_2 - c_3 z^2, \ E_y = 0, \\ E_z &= -c_1 - 2c_3 xz, \ \varepsilon_x = a_1 + 2a_4 xz, \\ \varepsilon_y &= 0, \ \varepsilon_z = b_1 + 2b_4 xz, \\ \gamma_{xz} &= a_2 + b_2 + (a_4 + 3b_3)x^2 + (b_4 + 3a_3)z^2, \\ \gamma_{xy} &= 0, \ \gamma_{yz} = 0 \end{aligned} \tag{13}$$

Expressions for specific strains (dilatations and slides) and components of the piezoelectric displacement vector are [1]:

$$\begin{aligned} \varepsilon_x &= \varepsilon_{11}^E \sigma_x + \varepsilon_{12}^E \sigma_y + \varepsilon_{13}^E \sigma_z + b_{31} E_z, \\ \varepsilon_y &= \varepsilon_{12}^E \sigma_x + \varepsilon_{11}^E \sigma_y + \varepsilon_{13}^E \sigma_z + b_{31} E_z, \\ \varepsilon_z &= \varepsilon_{13}^E (\sigma_x + \sigma_y) + \varepsilon_{33}^E \sigma_z + b_{33} E_z, \\ \gamma_{xy} &= \varepsilon_{66}^E \tau_{xy} = 2(\varepsilon_{11}^E - \varepsilon_{12}^E)\tau_{xy}, \\ \gamma_{xz} &= \varepsilon_{44}^E \tau_{xz} + b_{15} E_x, \quad \gamma_{yz} = \varepsilon_{44}^E \tau_{yz} + b_{15} E_y, \\ D_x &= d_{11}^\sigma E_x + b_{15} \tau_{xz}, \\ D_y &= d_{11}^\sigma E_y + b_{15} \tau_{yz}, \\ D_z &= d_{33}^\sigma E_z + b_{31}(\sigma_x + \sigma_y) + b_{33}\sigma_z \end{aligned} \tag{14}$$

where: D_x, D_y, D_z are components of the piezoelectric displacement vector in C/m^2; ε_{11}^E, ε_{12}^E, ε_{13}^E, ε_{33}^E, ε_{44}^E are coefficients of elastic power at given electric field in m^2/N; b_{31}, b_{15}, b_{33} are coordinates of piezomodulus tensor in C/N; d_{11}^σ, d_{33}^σ are dielectric constant (dielectric permeability) at given mechanical stress in F/m.

Thirteen unknown coefficients: a_0, a_1, a_2, a_3, a_4, b_0, b_1, b_2, b_3, b_4, c_1, c_2, c_3, which enter into expressions (10) and (13), have to be determined in order to fulfill the system of equations of electroelasticity (14) and boundary conditions (7), (8) and (9):

$$\begin{aligned} a_1 + 2a_4 xz &= -\varepsilon_{11}^E \frac{F}{I_y} xz - c_1 b_{31} - 2c_3 b_{31} xz, \ \Big|_{\varepsilon_x} \\ b_1 + 2b_4 xz &= -\varepsilon_{13}^E \frac{F}{I_y} xz - c_1 b_{33} - 2c_3 b_{33} xz, \ \Big|_{\varepsilon_z} \\ a_2 + b_2 + (a_4 + 3b_3)x^2 + (b_4 + 3a_3)z^2 &= \\ = -\varepsilon_{44}^E \frac{F}{8I_y} h^2 + \varepsilon_{44}^E \frac{F}{2I_y} z^2 - b_{15} c_2 - c_3 b_{15} z^2, \ &\Big|_{\gamma_{xz}} \\ D_x = -\left(\frac{F b_{15}}{8I_y} h^2 + c_2 d_{11}^\sigma\right) + \left(\frac{F b_{15}}{2I_y} - c_3 d_{11}^\sigma\right) z^2, \\ D_z = -c_1 d_{33}^\sigma - \left(\frac{F b_{31}}{I_y} + 2c_3 d_{33}^\sigma\right) xz, \\ U_0 = c_1 \frac{h}{2} + c_2 x + c_3 x \frac{h^2}{4}, \ &\Big|_{z=\frac{h}{2}} \end{aligned} \tag{15}$$

$$-U_0 = -c_1\frac{h}{2} + c_2 x + c_3 x\frac{h^2}{4}\ ,\ \Big|_{z=-\frac{h}{2}}$$

$$u\Big|_{\substack{x=l\\z=0}} = a_0 + a_1 l = 0,$$

$$w\Big|_{\substack{z=0\\x=l}} = b_0 + b_2 l + b_3 l^3 = 0, \qquad (16)$$

$$\frac{\partial w}{\partial x}\Big|_{\substack{z=0\\x=l}} = b_2 + 3b_3 l^2 = 0,$$

$$-2c_3 d_{33}^{\sigma} - b_{31}\frac{F}{I_y} = 0,\ \Big|_{div\vec{D}=0}$$

that is:

$$a_1 = -b_{31}c_1,\ \ 2a_4 = -\varepsilon_{11}^E\frac{F}{I_y} - 2b_{31}c_3,$$

$$b_1 = -b_{33}c_1,\ \ 2b_4 = -\varepsilon_{13}^E\frac{F}{I_y} - 2b_{33}c_3,$$

$$a_2 + b_2 = -\varepsilon_{44}^E\frac{F}{8I_y}h^2 - b_{15}c_2, \qquad (17)$$

$$b_4 + 3a_3 = \varepsilon_{44}^E\frac{F}{2I_y} - b_{15}c_3,$$

$$a_4 = -3b_3,\ \ c_2 = -c_3\frac{h^2}{4}$$

From the system of equations (15), (16) and (17) unknown coefficients are determined as:

$$a_0 = \frac{2U_0}{h}b_{31}l,\ \ a_1 = -\frac{2U_0}{h}b_{31},$$

$$a_2 = \frac{F\varepsilon_{11}^E}{2I_y}\left(1-k_{31}^2\right)l^2 - \frac{F\varepsilon_{44}^E}{8I_y}h^2\left(1-k_\tau^2\right),$$

$$a_3 = \frac{F\varepsilon_{13}^E}{6I_y}\left(1-k_S^2\right) + \frac{F\varepsilon_{44}^E}{6I_y}\left(1-k_\tau^2\right),$$

$$a_4 = -\frac{F\varepsilon_{11}^E}{2I_y}\left(1-k_{31}^2\right),\ \ b_0 = \frac{2}{3}\frac{F\varepsilon_{11}^E}{2I_y}\left(1-k_{31}^2\right)l^3,$$

$$b_1 = -\frac{2U_0}{h}b_{33},\ \ b_2 = -\frac{F\varepsilon_{11}^E}{2I_y}\left(1-k_{31}^2\right)l^2, \qquad (18)$$

$$b_3 = \frac{1}{3}\frac{F\varepsilon_{11}^E}{2I_y}\left(1-k_{31}^2\right),\ \ b_4 = -\frac{F\varepsilon_{13}^E}{2I_y}\left(1-k_S^2\right),$$

$$c_1 = \frac{2U_0}{h},\ \ c_2 = \frac{F}{2I_y}\frac{b_{31}}{d_{33}^{\sigma}}\frac{h^2}{4},$$

$$c_3 = -\frac{F}{2I_y}\frac{b_{31}}{d_{33}^{\sigma}},\ \ k_{31}^2 = \frac{b_{31}^2}{\varepsilon_{11}^E d_{33}^{\sigma}},$$

$$k_S^2 = \frac{b_{31}b_{33}}{\varepsilon_{13}^E d_{33}^{\sigma}},\ \ k_\tau^2 = -\frac{b_{15}b_{31}}{\varepsilon_{44}^E d_{33}^{\sigma}}$$

Coefficients k_{31}^2, k_S^2 and k_τ^2 are called coefficients of electromechanical static relations.

By introducing the obtained values for coefficients (18) into expressions (10) and (13), one gets solutions for: componential displacements of the displacement vector $\vec{s}$, electric potential ψ, specific strains (dilatations ε_x and ε_z, and slide y_{xz}), electric fields E_x and E_z, and piezoelectric displacements D_x and D_z, for the rectangular prismatic cantilever with transversal polarization and electrode coatings on the sides $z=\pm h/2$, in form of:

$$u = \frac{2U_0}{h}b_{31}(l-x) +$$

$$+\frac{F}{2I_y}\left\{\left[\varepsilon_{11}^E\left(1-k_{31}^2\right)l^2 - \varepsilon_{44}^E\frac{h^2}{4}\left(1-k_\tau^2\right)\right]z + \right.$$

$$\left. +\frac{1}{3}\left[\varepsilon_{13}^E\left(1-k_S^2\right) + \varepsilon_{44}^E\left(1-k_\tau^2\right)\right]z^3 - \varepsilon_{11}^E\left(1-k_{31}^2\right)x^2 z\right\},$$

$$w = -\frac{2U_0}{h}b_{33}z +$$

$$+\frac{F}{2I_y}\left\{\varepsilon_{11}^E\left(1-k_{31}^2\right)\left[\frac{2}{3}l^3 - l^2 x + \frac{1}{3}x^3\right] - \varepsilon_{13}^E\left(1-k_S^2\right)z^2 x\right\},$$

$$\psi = \frac{2U_0}{h} + \frac{F}{2I_y}\frac{b_{31}}{d_{33}^{\sigma}}\left(\frac{h^2}{4} - z^2\right)x,$$

$$\varepsilon_x = -\frac{2U_0}{h}b_{31} - \frac{F\varepsilon_{11}^E}{I_y}\left(1-k_{31}^2\right)xz, \qquad (19)$$

$$\varepsilon_z = -\frac{2U_0}{h}b_{33} - \frac{F\varepsilon_{13}^E}{I_y}\left(1-k_S^2\right)xz,$$

$$\gamma_{xz} = -\frac{F\varepsilon_{44}^E}{8I_y}\left(1-k_\tau^2\right)\left(h^2 - 4z^2\right),$$

$$E_x = -\frac{F}{8I_y}\frac{b_{31}}{d_{33}^{\sigma}}\left(h^2 - 4z^2\right),$$

$$E_z = -\frac{2U_0}{h} + \frac{F}{I_y}\frac{b_{31}}{d_{33}^{\sigma}}xz,$$

$$D_x = \frac{F}{2I_y}\left(b_{15} + \frac{b_{31}}{d_{33}^{\sigma}}d_{11}^{\sigma}\right)\left(z^2 - \frac{h^2}{4}\right),$$

$$D_z = -\frac{2U_0}{h}d_{33}^{\sigma}$$

3. NUMERICAL ANALYSIS AND DISCUSSION

Subject of observation in this paper is stressing of rectangular PZT4 piezoceramic cantilever [9], with the following dimensions: b = 4.1 mm, h = 20.1 mm and l = 30.1 mm, density ρ = 7500 kg/m^3, loaded by the concentrated force (Fig. 1). This material belongs to the hexagonal crystal system of crystal class 6 mm (C_{6v}), and its material tensors are: matrix of elastic power constants tensor, matrix of piezomodulus tensor, and matrix of dielectric constants tensor, presented respectively as follows:

$$\left[\varepsilon_{ij}^{E}\right]=\begin{bmatrix}\varepsilon_{11}^{E} & \varepsilon_{12}^{E} & \varepsilon_{13}^{E} & 0 & 0 & 0\\ \varepsilon_{12}^{E} & \varepsilon_{11}^{E} & \varepsilon_{13}^{E} & 0 & 0 & 0\\ \varepsilon_{13}^{E} & \varepsilon_{13}^{E} & \varepsilon_{33}^{E} & 0 & 0 & 0\\ 0 & 0 & 0 & \varepsilon_{44}^{E} & 0 & 0\\ 0 & 0 & 0 & 0 & \varepsilon_{44}^{E} & 0\\ 0 & 0 & 0 & 0 & 0 & 2(\varepsilon_{11}^{E}-\varepsilon_{12}^{E})\end{bmatrix}=$$

$$\begin{bmatrix}12{,}3 & -4{,}05 & -5{,}31 & 0 & 0 & 0\\ -4{,}05 & 12{,}3 & -5{,}31 & 0 & 0 & 0\\ -5{,}31 & -5{,}31 & 15{,}5 & 0 & 0 & 0\\ 0 & 0 & 0 & 39 & 0 & 0\\ 0 & 0 & 0 & 0 & 39 & 0\\ 0 & 0 & 0 & 0 & 0 & 32{,}7\end{bmatrix}10^{-12}\left[\frac{m^2}{N}\right] \quad (20)$$

$$\left[b_{ij}\right]=\begin{bmatrix}0 & 0 & 0 & 0 & b_{15} & 0\\ 0 & 0 & 0 & b_{15} & 0 & 0\\ b_{31} & b_{31} & b_{33} & 0 & 0 & 0\end{bmatrix}=$$

$$\begin{bmatrix}0 & 0 & 0 & 0 & 496 & 0\\ 0 & 0 & 0 & 496 & 0 & 0\\ -123 & -123 & 289 & 0 & 0 & 0\end{bmatrix}\cdot 10^{-12}\left[\frac{C}{N}\right] \quad (21)$$

$$\left[d_{ij}^{\sigma}\right]=\begin{bmatrix}d_{11}^{\sigma} & 0 & 0\\ 0 & d_{11}^{\sigma} & 0\\ 0 & 0 & d_{33}^{\sigma}\end{bmatrix}=$$

$$=\begin{bmatrix}13{,}05 & 0 & 0\\ 0 & 13{,}05 & 0\\ 0 & 0 & 11{,}5\end{bmatrix}\cdot 10^{-9}\left[\frac{F}{m}\right] \quad (22)$$

Based on the obtained solutions (19), numerical analysis was performed using Matlab software package, and biparametric surfaces of spatial state were obtained for componential displacement $u(x,z,F,U)$, componential displacement $w(x,z,F,U)$, electric potential $\psi(x,z,F,U)$, specific strain – dilatation $\varepsilon_x(x,z,F,U)$, specific strain – dilatation $\varepsilon_z(x,z,F,U)$, specific strain – slide $y_{xz}(z,F)$, electric field $E_x(z,F)$, electric field $E_z(x,z,F,U)$, and piezoelectric displacement $D_x(z,F)$. Due to the limited space, only few of the obtained results are presented in the following text.

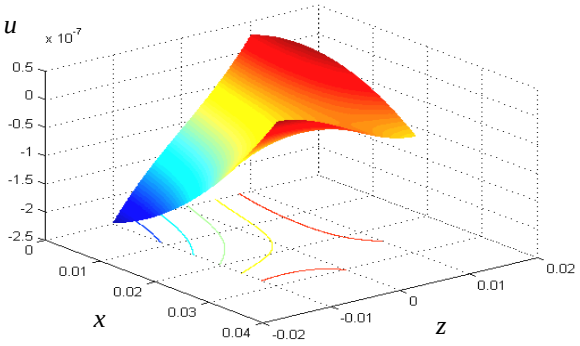

Fig. 2 *Componential displacement u=u(z, x)*

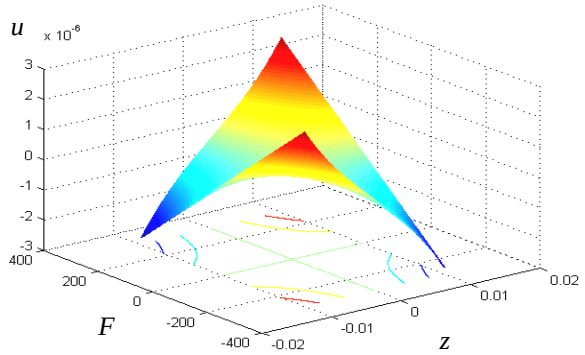

Fig. 3 *Componential displacement u=u(z, F)*

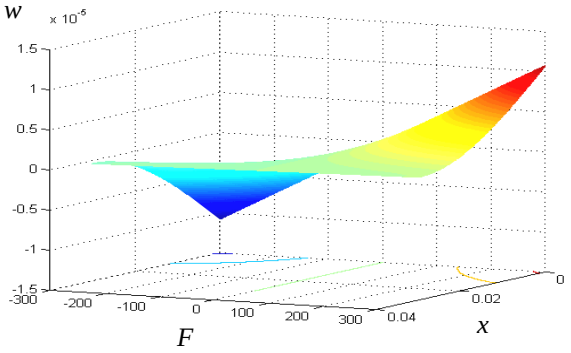

Fig. 4 *Componential displacement w=w(x, F)*

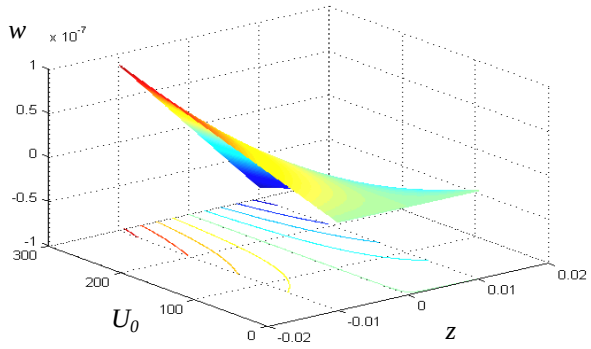

Fig. 5 *Componential displacement w=w(z, U_0)*

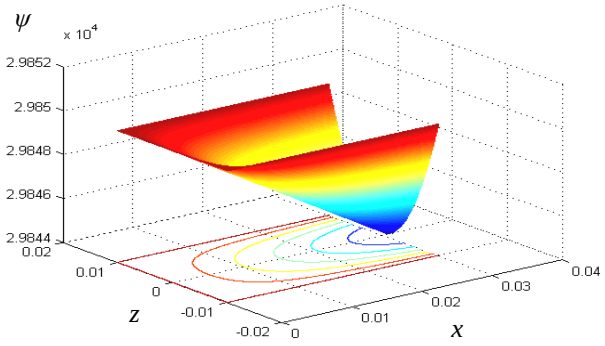

Fig. 6 *Electric potential ψ=ψ(x, z)*

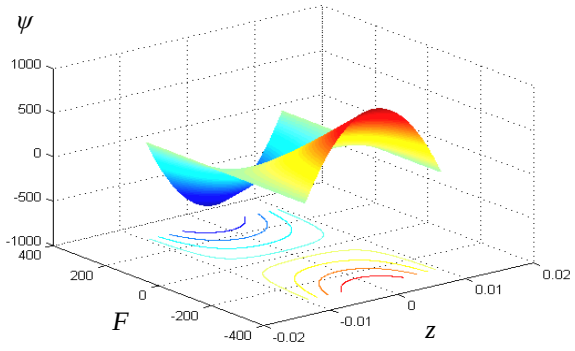

Fig. 7 *Electric potential $\psi=\psi(z, F)$*

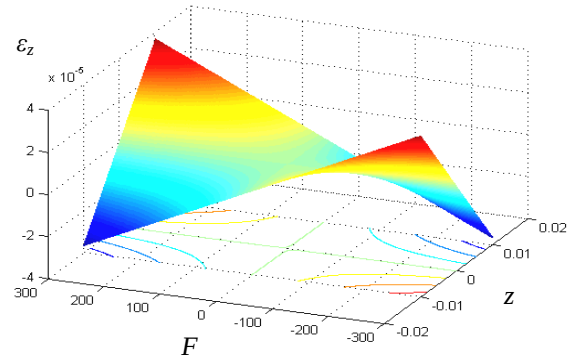

Fig. 11 *Specific strain $\varepsilon_z=\varepsilon_z(z, F)$*

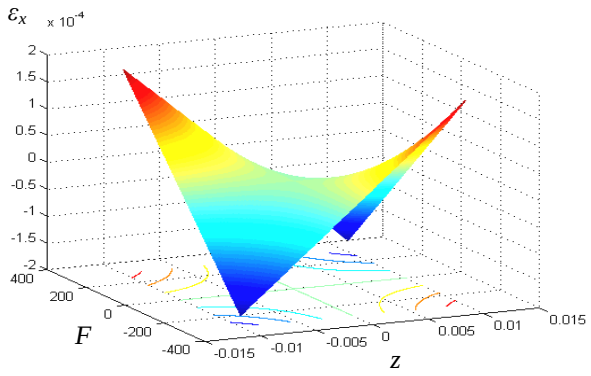

Fig. 8 *Specific strain $\varepsilon_x=\varepsilon_x(z, F)$*

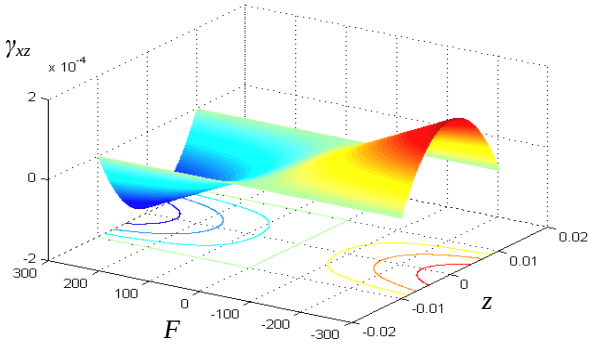

Fig. 12 *Specific strain $\gamma_{xz}=\gamma_{xz}(z, F)$*

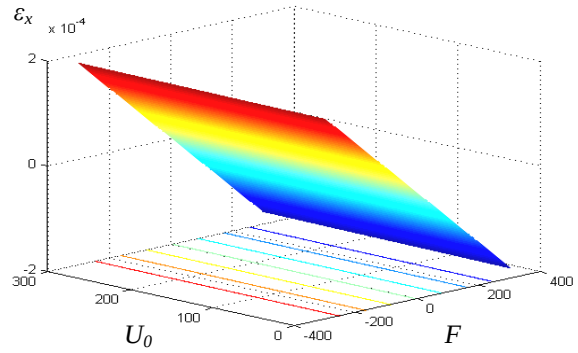

Fig. 9 *Specific strain $\varepsilon_x=\varepsilon_x(F, U_0)$*

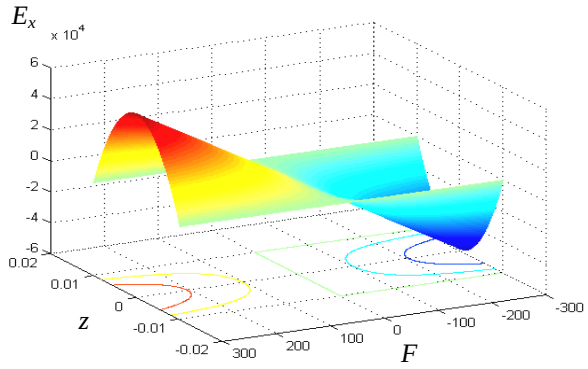

Fig. 13 *Electric field $E_x=E_x(F, z)$*

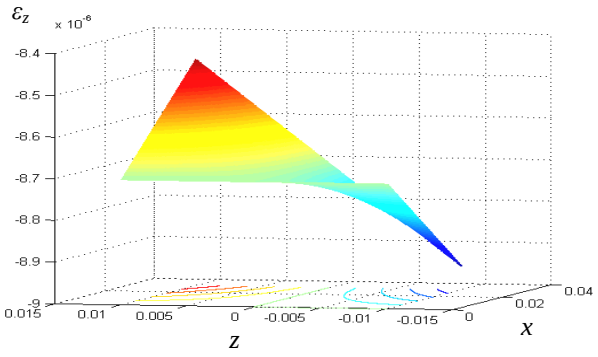

Fig. 10 *Specific strain $\varepsilon_z=\varepsilon_z(x, z)$*

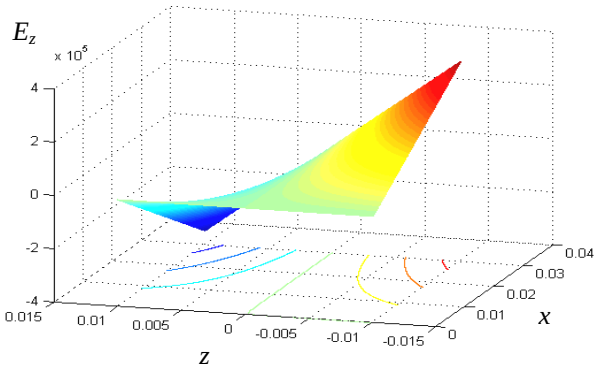

Fig. 14 *Electric field $E_z=E_z(x, z)$*

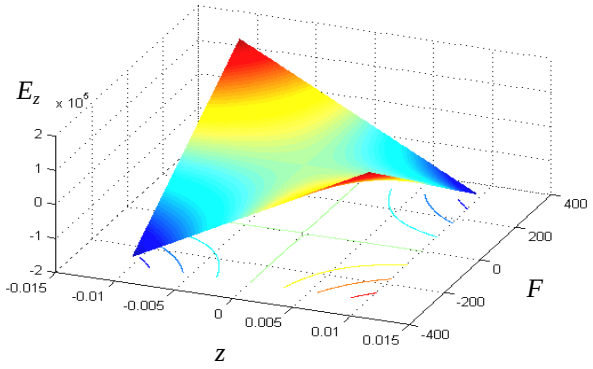

Fig. 15 *Electric field $E_z=E_z(F, z)$*

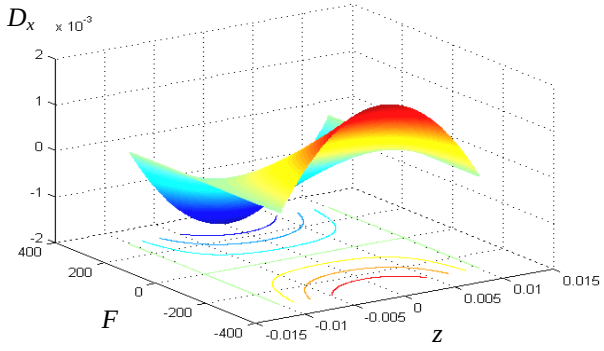

Fig. 16 *Piezoelectric displacement $D_x=D_x(z, F)$*

Fig. 2 shows biparametric surface of the componential displacement $u=u(z,x)$ in function of coordinate z and coordinate x, at dominant electric voltage U_0. Componential displacement has extreme values in points of the surface for $z=\pm h/2$ and in points of the frontal surface for $x=0$, while in the points of the fixed end cross section, for $x=l$, its value is equal to zero.

Biparametric surface of the componential displacement $u=u(z,F)$, in function of coordinate z and external concentrated force F, is presented on Fig. 3. Componential displacement has characteristic spatial surface in shape of a saddle. Extreme values of the componential displacement are achieved in surface points for $z=\pm h/2$, at maximum values of the concentrated force $\pm F$.

On Fig. 4 biparametric surface of the componential displacement $w=w(x,F)$ in function of coordinate x and external concentrated force F is presented. Componential displacement has extreme values for maximum intensity of the concentrated force $\pm F$ and in points of the frontal surface for $x=0$, while in the points of the fixed end cross section, for $x=l$, its value is equal to zero.

Biparametric surface of the componential displacement $w=w(z,U_0)$, in function of coordinate z and electric voltage U_0, is shown on Fig. 5.

Fig. 6 shows biparametric surface of the electric potential $\psi=\psi(x,z)$ in function of coordinate x and coordinate z. Electric potential has minimum value in point of frontal surface for $x=l$ when $z=0$.

On Fig. 7 biparametric surface of the electric potential $\psi=\psi(z,F)$, in function of coordinate z and external concentrated force F is shown. Extreme values of the electric potential are obtained in the sectional plane for $z=0$ and at maximum intensity of the force $\pm F$.

Fig. 8 illustrates biparametric surface of the specific saddle shaped strain, $\varepsilon_x=\varepsilon_x(z,F)$ in function of coordinate z and external concentrated force F.

Biparametric planar surface of the specific strain $\varepsilon_x=\varepsilon_x(F,U_0)$, in function of concentrated force F, and electric voltage U_0, is shown on Fig. 9.

On Fig. 10 biparametric surface of the specific strain $\varepsilon_z=\varepsilon_z(x,z)$ in function of coordinate x and coordinate z is presented.

Biparametric surface of the specific strain $\varepsilon_z=\varepsilon_z(z,F)$, in function of coordinate z and external concentrated force F, is illustrated on Fig. 11.

Fig. 12 illustrates biparametric surface of the specific strain $y_{xz}=y_{xz}(z,F)$ in function of coordinate z and external concentrated force F.

Fig. 13 shows biparametric surface of the electric field $E_x=E_x(F,z)$, in function of external concentrated force F and coordinate z.

On Fig. 14 is shown biparametric surface of the electric field $E_z=E_z(x,z)$ in function of coordinate x and coordinate z.

Biparametric saddle shaped surface of the electric field $E_z=E_z(F,z)$, in function of external concentrated force F and coordinate z, is presented on Fig. 15.

Biparametric surface of the piezoelectric displacement $D_x=D_x(z,F)$ in function of coordinate z and external concentrated force F is shown on Fig. 16. Extreme values of the piezoelectric displacement are obtained in the sectional points for $z=0$ and at maximum values of the concentrated force $\pm F$.

4. CONCLUSION

In solving problems of the theory of electroelasticity, for a general case of stressing three-dimensional electroelastic deformable bodies, one encounters on great mathematical difficulties. In this paper, the entire qualitative picture of stressed state of the loaded rectangular prismatic piezoceramic cantilever with transversal polarization and electrode coatings is observed. For the particular piezoceramic cantilever different state diagrams, numerically processed with a PC, were determined and presented. This kind of analysis enables to predict the characteristics of piezoceramic cantilevers with analyzed configuration before their construction. It is expected that the obtained solutions for this kind of task from the theory of oscillations can directly be applied in engineering practice.

ACKNOWLEDGEMENT

The research presented in this paper is financed by the Ministry of Education, Science and Technological Development of the Republic of Serbia under the project TR33035.

REFERENCES

[1] Lj. Perić, *Coupled Tensors of Piezoelectric Materials State and Applications*, Le Locle, Switzerland, 2005.

[2] K. Hedrih, Lj. Perić, D. Mančić, M. Radmanović: "Problem naprezanja pravougaone piezokeramičke ploče sa poprečnom polarizacijom bez elektroda" (in serbian), *Zbornik XLV konferencije za ETRAN*, II sv., pp. 314-317, Bukovička Banja, jun 2001.

[3] D. Rašković, *Teorija elastičnosti* (in serbian), Beograd: Naučna knjiga, 1985.

[4] N.N. More, "Finite Element Analysis of Piezoelectric Cantilever", *International Journal of Innovations in Engineering and Technology (IJIET)*, Vol. 2, Issue 3, pp. 100-105, June 2013.

[5] J. Ajitsaria, S.Y. Choe, D. Shen, D.J. Kim, "Modeling and analysis of a bimorph piezoelectric cantilever beam for voltage generation", *Smart Materials and Structures*, Vol. 16, pp. 447-454, 2007.

[6] D.L. DeVoe, A.P. Pisano, "Modeling and Optimal Design of Piezoelectric Cantilever Microactuators", *Journal of Microelectromechanical Systems*, Vol. 6, No. 3, pp. 266-270, September 1997.

[7] A. Erturk, D.J. Innam, "On mechanical modeling of cantilevered piezoelectric vibration energy harvesters", *J. Intell. Mater. Syst. Struct.*, Vol. 19, pp. 1311–1325, 2008.

[8] D. Rašković, *Otpornost materijala* (in serbian), Beograd: Naučna knjiga, 1980.

[9] *Five piezoelectric ceramics*, Bulletin 66011/F, Vernitron Ltd., 1976.

УНИВЕРЗИТЕТ У НИШУ

ФАКУЛТЕТ ЗАШТИТЕ НА РАДУ У НИШУ

Студијски програми основних академских студија

- ЗАШТИТА НА РАДУ
- ЗАШТИТА ЖИВОТНЕ СРЕДИНЕ

Структура студијског програма усклађена је са Стандардима за акредитацију студијских програма првог нивоа високог образовања. Студијски програм траје 4 године (8 семестара) и обима је 240 ЕСПБ бодова.

Студијски програми мастер академских студија

- ИНЖЕЊЕРСТВО ЗАШТИТЕ ЖИВОТНЕ СРЕДИНЕ
- ИНЖЕЊЕРСТВО ЗАШТИТЕ НА РАДУ
- ИНЖИЊЕРСТВО ЗАШТИТЕ ОД ПОЖАРА
- УПРАВЉАЊЕ ВАНРЕДНИМ СУТУАЦИЈАМА
- УПРАВЉАЊЕ КОМУНАЛНИМ СИСТЕМОМ

Структура студијског програма усклађена је са Стандардима за акредитацију студијских програма другог нивоа високог образовања. Студијски програм траје 1 годину (2 семестара) и обима је 60 ЕСПБ бодова.

Студијски програми докторских академских студија

- ИНЖЕЊЕРСТВО ЗАШТИТЕ ЖИВОТНЕ СРЕДИНЕ
- ИНЖЕЊЕРСТВО ЗАШТИТЕ НА РАДУ

Структура студијског програма усклађена је са Стандардима за акредитацију студијских програма трећег нивоа високог образовања. Студијски програм траје 3 године (6 семестара) и обима је 180 ЕСПБ бодова.

РЕПУБЛИКА СРБИЈА, ЧАРНОЈЕВИЋА 10 А, 18000 НИШ
Телефон: 018 529701, 018 529755, Телефакс 018 249962
www.znrfak.ni.ac.rs

University of Nis
Faculty of Occupational Safety
„Politechnica“ University of Timisoara
Faculty of Mechanical Engineering
24th International Conference
NOISE AND VIBRATION
Niš, 29 - 31. 10. 2014.

ANALISYS OF LONGITUDINAL OSCILLATIONS OF FREE PRISMATIC PIEZOCERAMIC BEAMS

Uglješa Jovanović[1], Ljubiša Perić[2], Igor Jovanović[1], Dragan Mančić[1]

[1] University of Niš, Faculty of Electronic Engineering, Serbia, ugljesa.jovanovic@elfak.ni.ac.rs
[2] Regional Chamber of Economy Niš, Serbia

Abstract - *This paper presents analysis of longitudinal (extensional) oscillations of a free prismatic piezoceramic beams with longitudinal polarization and electrode coatings on frontal sides. It is assumed that beam is supplied by an AC electric voltage applied on frontal electrodes, and that external mechanical loads are not applied on the beam. Finally, for the particular piezoceramic beam made from PZT4 material biparametric surfaces of state and electromechanic values, are presented which are numerically obtained by using Matlab software package.*

1. INTRODUCTION

When disturbance of the equilibrium state of electroelastic body, which is not under action of external forces, is performed, motion, i.e., vibration of body particles will occur [1]. Motion of the particles is transferred through the whole body, so a wave process arises. Wave process is characterized with feature that in every point of the electroelastic body occurs the same disturbance state, just with phase delay.

Vibration of particles may be performed in two ways:

- when disturbance is performed in stressed state of the body, and
- when disturbance is performed in non-stressed state of the body.

Wires and membranes are not resistant to bending, so they can vibrate only when disturbance is performed in stressed state. However, bars, rods, and plates resist to bending, so they can vibrate in both ways [2, 3, 4, 5].

In this paper the case of longitudinal oscillations of the prismatic piezoceramic beam with longitudinal polarization and electrode coatings on frontal sides is considered. It is assumed that the beam is supplied by an AC electric voltage applied on frontal electrodes (z=0, z=l), and without applied external mechanical loads. It is also assumed that cross section of the beam of length l remains plane during these oscillations, and that all sectional points exert motion only in direction of axis Oz, so only displacements w=w(z, t) exist. Due to the great wavelength of these oscillations comparing with cross section height, influence of the cross section contraction may be neglected. Coordinate origin of adopted Descartes' coordinate system is located on the left end of the beam (Fig. 1).

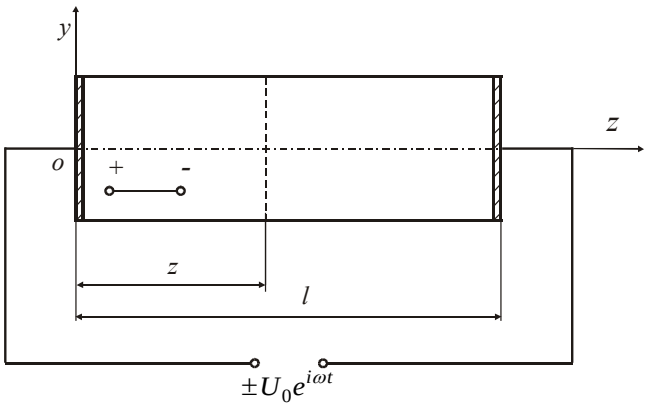

Fig. 1 *Prismatic piezoceramic beam supplied by an AC electric voltage applied on frontal electrodes*

2. FUNDAMENTAL EQUATIONS

Electric boundary conditions for frontal surfaces may be expressed as [1]:

$$\psi(z,t)\Big|_{\substack{z=0\\z=l}} = \pm U_0 e^{i\omega t} \tag{1}$$

Fundamental equations of piezoelectric effect state, for adopted type of polarization, may be written in form of:

$$\begin{aligned} \varepsilon_z &= \varepsilon_{33}^E \sigma_z + b_{33} E_z \\ D_z &= d_{33}^\sigma E_z + b_{33} \sigma_z \end{aligned} \tag{2}$$

Navier's equations of motion for deformable electroelastic body have form of:

$$\frac{\partial \sigma_z}{\partial z} = \rho \frac{\partial^2 w}{\partial t^2} \tag{3}$$

Equations of quasi-statics are:

$$\frac{\partial D_z}{\partial z} = 0, \quad E_z = -\frac{\partial \psi}{\partial z} \tag{4}$$

and Cauchy's kinematic equation is:

$$\varepsilon_z = \frac{\partial w}{\partial z} \tag{5}$$

Longitudinal displacements and electric potential are functions of axis coordinate z and time t:

$$w = w(z, t), \quad \psi = \psi(z, t) \tag{6}$$

From the first equation of the system (2) componential mechanical stress can be determined:

$$\sigma_z = \frac{1}{\varepsilon_{33}^E}\varepsilon_z - \frac{b_{33}}{\varepsilon_{33}^E}E_z \tag{7}$$

By substituting expression (7) into Navier's equation of motion (3), following expression is obtained:

$$\frac{1}{\varepsilon_{33}^E}\frac{\partial \varepsilon_z}{\partial z} - \frac{b_{33}}{\varepsilon_{33}^E}\frac{\partial E_z}{\partial z} = \rho\frac{\partial^2 w}{\partial t^2} \tag{8}$$

By substituting expression for ε_z (5) and E_z (4) into the last equation (8), it is finally obtained:

$$\frac{\partial^2 w}{\partial z^2} + b_{33}\frac{\partial^2 \psi}{\partial z^2} = \rho\varepsilon_{33}^E\frac{\partial^2 w}{\partial t^2} \tag{9}$$

Now the derivative of the second equation from the system (2) on coordinate z has to be found, and then equated with zero, by accordance with the first equation of quasi-electrostatics (4):

$$d_{33}^{\sigma}\frac{\partial E_z}{\partial z} + b_{33}\frac{\partial \sigma_z}{\partial z} = 0 \tag{10}$$

By substituting expressions for electric field E_z (4) and for componential mechanical stress σ_z (7) into the last equation (10), and after certain algebraic operations, final expression is:

$$\frac{b_{33}}{\varepsilon_{33}^E}\frac{\partial^2 w}{\partial z^2} - d_{33}^{\sigma}\left(1-k_{33}^2\right)\frac{\partial^2 \psi}{\partial z^2} = 0 \tag{11}$$

where $k_{33}^2 = b_{33}^2 / \varepsilon_{33}^E d_{33}^{\sigma}$ is coefficient of electromechanical static relation in longitudinal direction.

If the electric potential is excluded from the equation (9), using equation (11) one gets general system of two wave equations for longitudinal oscillations of the prismatic piezoceramic beam:

$$\begin{aligned} \frac{\partial^2 w}{\partial z^2} &= \frac{1}{c^2}\frac{\partial^2 w}{\partial t^2} \\ \frac{\partial^2 \psi}{\partial z^2} &= \frac{1}{b_{33}}\frac{k_{33}^2}{1-k_{33}^2}\frac{\partial^2 w}{\partial z^2} \end{aligned} \tag{12}$$

where $c = 1/\sqrt{\rho\varepsilon_{33}^E\left(1-k_{33}^2\right)}$ is velocity of longitudinal waves propagation in piezoceramic electroelastic rod, which is for elastic rod calculated by expression $c = \sqrt{E/\rho}$.

Particular solution of dynamic wave equation from system (12) may be obtained by method of particular integrals of Bernoulli Daniel [1]. This solution is calculated by multiplying two functions:

$$w(z,\ t) = W(z)\cdot T(t) \tag{13}$$

each of them depends on a single variable (coordinate z and time t). Solutions for $w(z, t)$ are such that fulfill boundary conditions, i.e., for a free beam following condition is fulfilled:

$$W'(0)\cdot T(t) = W'(l)\cdot T(t) = 0 \tag{14}$$

By substituting correspondent derivatives of the solutions (13), into the first partial differential equation of second order (12), it gets reduced to ordinary differential equation of second order:

$$W''\,T\ - c^{-2}T''\,W = 0 \tag{15}$$

Equation (15) is satisfied if simultaneously are satisfied two differential equations of second order in form of:

$$\begin{aligned} W'' + CW &= 0 \\ T'' + c^2 CT &= 0 \end{aligned} \tag{16}$$

where C is an arbitrary constant. In this way, the problem of integration of the first partial differential equation (12) is reduced to two homogenous differential equations of second order with constant coefficients. If $C>0$ then integrals of both equations (16) are expressed by trigonometric functions.

If it is $C=\lambda^2$ and $\omega=c\lambda$ solutions of equations (16) gain form:

$$\begin{aligned} W(z) &= A_1\cos(\lambda z) + A_2\sin(\lambda z) \\ T(t) &= A_3 e^{i\omega t} \end{aligned} \tag{17}$$

The typical case of oscillations of piezoceramic prismatic beams is a case of a free beam that oscillates in longitudinal direction with electrode coatings located on the frontal sides, supplied by AC electric voltage $\pm U_0 e^{j\omega t}$ (Fig. 1).

Mechanical boundary conditions and orthogonal functions may be written as:

$$\begin{aligned} z = 0,\ \ \sigma_z(0, t) = 0,\ \ W'(0) = 0, \\ z = l,\ \ \sigma_z(l, t) = 0,\ \ W'(l) = 0 \end{aligned} \tag{18}$$

Using the first boundary condition (18), for surface z=0, it is obtained:

$$\begin{aligned} W'(z) &= -\lambda A_1\sin(\lambda z) + \lambda A_2\cos(\lambda z) \\ W'(z)\Big|_{z=0} &= -A_1\sin(0) + A_2\cos(0) = 0 \ \Rightarrow \\ A_1 \neq 0,\ \ A_2 = 0 \ &\Rightarrow\ W(z) = A_1\cos(\lambda z) \end{aligned} \tag{19}$$

Using the second boundary condition (18), for surface $z=l$, it follows:

$$\begin{aligned} W'(z)\Big|_{z=l} &= A_1\lambda\sin(\lambda l) = 0 \ \Rightarrow \\ \sin(\lambda l) = 0,\quad \lambda_n &= \frac{n\pi}{l} = \frac{\omega_n}{c}, \\ \omega_n = \lambda_n c = \frac{n\pi}{l}\ &\frac{1}{\sqrt{\rho\varepsilon_{33}^E(1-k_{33}^2)}} = 2\pi f \ \Rightarrow \\ \lambda_n &= \frac{2\pi}{c} f, \quad n = 1, 2, 3, \ldots \end{aligned} \tag{20}$$

where λ_n is eigenvalue (for piezoelectric ceramic PZT4 it may be adopted that $\lambda_n \approx 1.53\cdot 10^{-3}\cdot f$) given in [$m^{-1}$], f is frequency given in [Hz], ω_n is circular frequency of oscillation given in [s^{-1}] and c is velocity of wave propagation in piezoceramic body (phase velocity) given in [m/s].

Solutions of the system of partial differential equations (12) may now be written in form of:

$$w_n(z,\ t) = \sum_{n=1}^{\infty} \hat{w}_n(z)\ e^{i\omega_n t}$$
$$\psi_n(z,\ t) = \sum_{n=1}^{\infty} \hat{\psi}_n(z)\ e^{i\omega_n t} \tag{21}$$

Functions $\hat{w}_n(z)$ and $\hat{\psi}_n(z)$ are amplitude eigenfunctions of the coupled fields, which fulfill conditions of orthogonality.

Amplitude eigenfunction $\hat{\psi}_n(z)$ is obtained by integration of the second partial differential equation (12), so that amplitude eigenfunctions $\hat{w}_n(z)$ and $\hat{\psi}_n(z)$, gain form:

$$\hat{w}_n(z) = A_n \cos(\lambda_n z)$$
$$\hat{\psi}_n(z) = B_n\ z + C_n + \frac{1}{b_{33}} \frac{k_{33}^2}{1-k_{33}^2}\ \hat{w}_n(z) \tag{22}$$

With the help of amplitude eigenfunctions for componential displacement and electric potential (22), which fulfill boundary conditions and conform to the *n*-th mode of oscillation, it is easy to determine amplitude eigenfunctions of remaining parameters of coupled field state: mechanical strain, electric field, mechanical stress, piezoelectric displacement and electric current strength, in form of:

$$\hat{\varepsilon}_{(n)z}(z) = -\lambda_n A_n \sin(\lambda_n z)$$
$$\hat{E}_{(n)z}(z) = -B_n - \frac{1}{b_{33}} \frac{k_{33}^2}{1-k_{33}^2}\ \hat{\varepsilon}_{(n)z}(z)$$
$$\hat{\sigma}_{(n)z}(z) = \frac{1}{\varepsilon_{33}^E\left(1-k_{33}^2\right)} \hat{\varepsilon}_{(n)z}(z) + \frac{b_{33}}{\varepsilon_{33}^E} B_n \tag{23}$$
$$\hat{D}_{(n)z} = -d_{33}^{\sigma}(1-k_{33}^2)B_n$$
$$\hat{I}_n = -i\omega_n S\hat{D}_{(n)z},\quad n = 1,\ 2,\ 3,\ \ldots$$

Constants in obtained expressions (22) and (23) are determined from the conditions for satisfying the boundary conditions for electric potential, electric boundary conditions (1), and for mechanical stress, mechanical boundary conditions (18), so that it is obtained:

$$A_n = \frac{2b_{33}\left(1-k_{33}^2\right)}{\lambda_n l \sin(\lambda_n l) - k_{33}^2\left(1-\cos(\lambda_n l)\right)} U_0$$
$$B_n = \frac{2\lambda_n \sin(\lambda_n l)}{\lambda_n l \sin(\lambda_n l) - k_{33}^2\left(1-\cos(\lambda_n l)\right)} U_0 \tag{24}$$
$$C_n = -\frac{\lambda_n l \sin(\lambda_n l) + k_{33}^2\left(1+\cos(\lambda_n l)\right)}{\lambda_n l \sin(\lambda_n l) - k_{33}^2\left(1-\cos(\lambda_n l)\right)} U_0$$

Finally, following solutions are obtained: componential displacement, electric potential, mechanical strain (dilatation), electric field, mechanical stress, piezoelectric displacement and electric current intensity of coupled electromechanical fields. Summary of the obtained solutions is:

$$w(z,\ t,\ f,\ U_0) = \sum_{n=1}^{\infty} \hat{w}_n(z,\ f, U_0)\, e^{i\omega_n t} =$$
$$= \sum_{n=1}^{\infty} \frac{2b_{33}\left(1-k_{33}^2\right)\cos(\lambda_n z)}{\lambda_n l \sin(\lambda_n l) - k_{33}^2\left(1-\cos(\lambda_n l)\right)} U_0\, e^{i\omega_n t} \tag{25}$$

$$\psi(z,\ t,\ f, U_0) = \sum_{n=1}^{\infty} \hat{\psi}_n(z,\ f, U_0)\, e^{i\omega_n t} =$$
$$= \sum_{n=1}^{\infty} \frac{(2z-l)\lambda_n \sin(\lambda_n l) - k_{33}^2\left(1+\cos(\lambda_n l) - 2\cos(\lambda_n z)\right)}{\lambda_n l \sin(\lambda_n l) - k_{33}^2\left(1-\cos(\lambda_n l)\right)} \cdot U_0\, e^{i\omega_n t} \tag{26}$$

$$\varepsilon_z(z,\ t,\ f, U_0) = \sum_{n=1}^{\infty} \hat{\varepsilon}_{(n)_z}(z,\ f, U_0)\, e^{i\omega_n t} =$$
$$= -\sum_{n=1}^{\infty} \frac{2b_{33}\left(1-k_{33}^2\right)\lambda_n \sin(\lambda_n z)}{\lambda_n l \sin(\lambda_n l) - k_{33}^2\left(1-\cos(\lambda_n l)\right)} U_0\, e^{i\omega_n t} \tag{27}$$

$$E_z(z,\ t,\ f, U_0) = \sum_{n=1}^{\infty} \hat{E}_{(n)z}(z,\ f, U_0)\, e^{i\omega_n t} =$$
$$= \sum_{n=1}^{\infty} \frac{2\lambda_n\left(k_{33}^2 \sin(\lambda_n z) - \sin(\lambda_n l)\right)}{\lambda_n l \sin(\lambda_n l) - k_{33}^2\left(1-\cos(\lambda_n l)\right)} U_0\, e^{i\omega_n t} \tag{28}$$

$$\sigma_z(z,\ t,\ f, U_0) = \sum_{n=1}^{\infty} \hat{\sigma}_{(n)z}(z,\ f, U_0)\, e^{i\omega_n t} =$$
$$= \sum_{n=1}^{\infty} \frac{2b_{33}\lambda_n\left(\sin(\lambda_n l) - \sin(\lambda_n z)\right)}{\varepsilon_{33}^E\left[\lambda_n l \sin(\lambda_n l) - k_{33}^2\left(1-\cos(\lambda_n l)\right)\right]} U_0\, e^{i\omega_n t} \tag{29}$$

$$D_z(t,\ f, U_0) = \sum_{n=1}^{\infty} \hat{D}_z(f, U_0)\, e^{i\omega_n t} =$$
$$= -\sum_{n=1}^{\infty} \frac{2d_{33}^{\sigma}(1-k_{33}^2)\lambda_n \sin(\lambda_n l)}{\lambda_n l \sin(\lambda_n l) - k_{33}^2\left(1-\cos(\lambda_n l)\right)} U_0\, e^{i\omega_n t} a \tag{30}$$

$$I(t,\ f, U_0, S) = -\sum_{n=1}^{\infty} \hat{I}(f, U_0, S)\, e^{i\omega_n t} =$$
$$= i \sum_{n=1}^{\infty} \frac{4\pi\, d_{33}^{\sigma}(1-k_{33}^2)\lambda_n f\, S \sin(\lambda_n l)}{\lambda_n l \sin(\lambda_n l) - k_{33}^2\left(1-\cos(\lambda_n l)\right)} U_0\, e^{i\omega_n t} \tag{31}$$

3. NUMERICAL ANALYSIS AND DISCUSSION

Subject of observation in this paper is stressing of the prismatic PZT4 piezoceramic free beam, with the following dimensions: $b \times h$ (or d) and l=0.5 m, density ρ=7500 kg/m^3 (Fig. 1). Tensors of material coefficients are [6]:

- Matrix of elastic power constants tensor:

$$\left[\varepsilon_{ij}^E\right] = \begin{bmatrix} \varepsilon_{11}^E & \varepsilon_{12}^E & \varepsilon_{13}^E & 0 & 0 & 0 \\ \varepsilon_{12}^E & \varepsilon_{11}^E & \varepsilon_{13}^E & 0 & 0 & 0 \\ \varepsilon_{13}^E & \varepsilon_{13}^E & \varepsilon_{33}^E & 0 & 0 & 0 \\ 0 & 0 & 0 & \varepsilon_{44}^E & 0 & 0 \\ 0 & 0 & 0 & 0 & \varepsilon_{44}^E & 0 \\ 0 & 0 & 0 & 0 & 0 & 2(\varepsilon_{11}^E - \varepsilon_{12}^E) \end{bmatrix} =$$
$$\begin{bmatrix} 12{,}3 & -4{,}05 & -5{,}31 & 0 & 0 & 0 \\ -4{,}05 & 12{,}3 & -5{,}31 & 0 & 0 & 0 \\ -5{,}31 & -5{,}31 & 15{,}5 & 0 & 0 & 0 \\ 0 & 0 & 0 & 39 & 0 & 0 \\ 0 & 0 & 0 & 0 & 39 & 0 \\ 0 & 0 & 0 & 0 & 0 & 32{,}7 \end{bmatrix} 10^{-12}\left[\frac{m^2}{N}\right] \tag{32}$$

- Matrix of piezomodulus tensor:

$$[b_{ij}]=\begin{bmatrix} 0 & 0 & 0 & 0 & b_{15} & 0 \\ 0 & 0 & 0 & b_{15} & 0 & 0 \\ b_{31} & b_{31} & b_{33} & 0 & 0 & 0 \end{bmatrix}= \\ =\begin{bmatrix} 0 & 0 & 0 & 0 & 496 & 0 \\ 0 & 0 & 0 & 496 & 0 & 0 \\ -123 & -123 & 289 & 0 & 0 & 0 \end{bmatrix}\cdot 10^{-12}\left[\frac{C}{N}\right] \tag{33}$$

- Matrix of dielectric constants tensor:

$$[d_{ij}^{\sigma}]=\begin{bmatrix} d_{11}^{\sigma} & 0 & 0 \\ 0 & d_{11}^{\sigma} & 0 \\ 0 & 0 & d_{33}^{\sigma} \end{bmatrix}= \\ =\begin{bmatrix} 13{,}05 & 0 & 0 \\ 0 & 13{,}05 & 0 \\ 0 & 0 & 11{,}5 \end{bmatrix}\cdot 10^{-9}\left[\frac{F}{m}\right] \tag{34}$$

Based on the derived solutions (equations (25)÷(31)) numerical analysis is performed using Matlab software package, and biparametric surfaces of state of amplitude eigenfunctions of mutually coupled fields are obtained, for the piezoceramic free beam with longitudinal polarization and electrode coatings on frontal sides (Fig. 1). Using Matlab biparametric surfaces of amplitude eigenfunctions are obtained for:

- componential displacement $\hat{w}=\hat{w}(z,f)$ presented in Fig. 2;
- componential displacement $\hat{w}=\hat{w}(z,U_0)$ illustrated in Fig. 3;
- componential displacement $\hat{w}=\hat{w}(f,U_0)$ shown in Fig. 4;
- electric potential $\hat{\varphi}=\hat{\varphi}(z,f)$ displayed in Fig. 5;
- electric potential $\hat{\varphi}=\hat{\varphi}(z,U_0)$ as can be seen in Fig. 6;
- electric potential $\hat{\varphi}=\hat{\varphi}(f,U_0)$, illustrated in Fig. 7;
- specific strain $\hat{\varepsilon}_z=\hat{\varepsilon}_z(z,f)$ shown in Fig. 8;
- specific strain $\hat{\varepsilon}_z=\hat{\varepsilon}_z(z,U_0)$ presented in Fig. 9;
- specific strain $\hat{\varepsilon}_z=\hat{\varepsilon}_z(f,U_0)$ displayed in Fig. 10;
- electric field $\hat{E}_z=\hat{E}_z(z,f)$ presented in Fig. 11;
- electric field $\hat{E}_z=\hat{E}_z(z,U_0)$ displayed in Fig. 12;
- electric field $\hat{E}_z=\hat{E}_z(f,U_0)$ shown in Fig. 13;
- mechanical stress $\hat{\sigma}_z=\hat{\sigma}_z(z,f)$ illustrated in Fig. 14;
- mechanical stress $\hat{\sigma}_z=\hat{\sigma}_z(z,U_0)$ as can be seen in Fig. 15;
- mechanical stress $\hat{\sigma}_z=\hat{\sigma}_z(f,U_0)$ shown in Fig. 16;
- piezoelectric displacement $\hat{D}_z=\hat{D}_z(f,U_0)$ shown in Fig. 17;
- electric current strength $\hat{I}=\hat{I}(f,U_0)$ as can be seen in Fig. 18;
- electric current strength $\hat{I}=\hat{I}(f,S)$ presented in Fig. 19, where S is cross-section of the specific beam and the electric current intensity is dependent on the size of cross-section S;
- electric current strength $\hat{I}=\hat{I}(U_0,S)$ displayed in Fig. 20;
- electric current strength $\hat{I}=\hat{I}(f,l)$ illustrated in Fig. 21;
- electric impedance Z[dB]=$Z(f,S)$ displayed in Fig. 22;
- electric impedance Z[dB]=$Z(f,S)$ presented in Fig. 23;
- electric impedance Z[dB]=$Z(f,l)$ illustrated in Fig. 24;
- electric impedance Z[dB]=$Z(f,l)$ shown in Fig. 25.

Due to the large range of electric impedance change $Z=U_0/I$ its representation is performed as $20\log|(Z/50)+1|$ [dB] in function of frequency f (Figs. 22, 23, 24, 25).

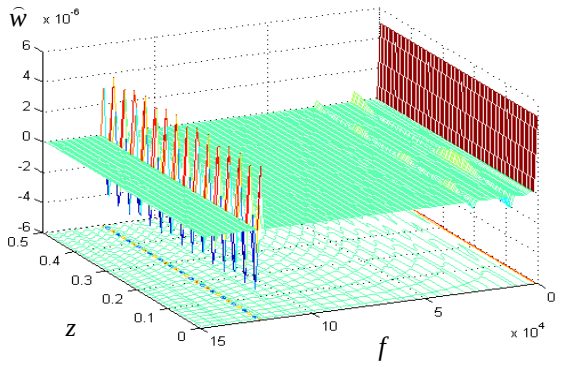

Fig. 2 *Componential displacement* $\hat{w}=\hat{w}(z,f)$

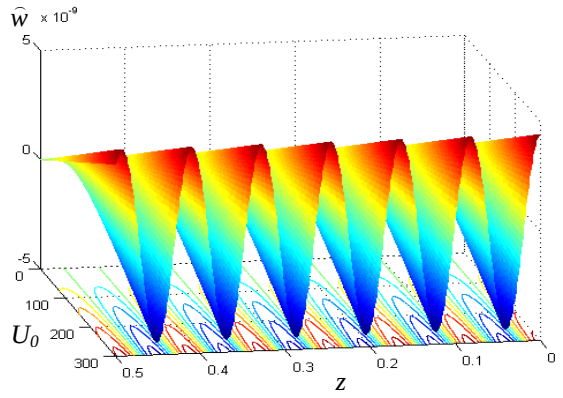

Fig. 3 *Componential displacement* $\hat{w}=\hat{w}(z,U_0)$

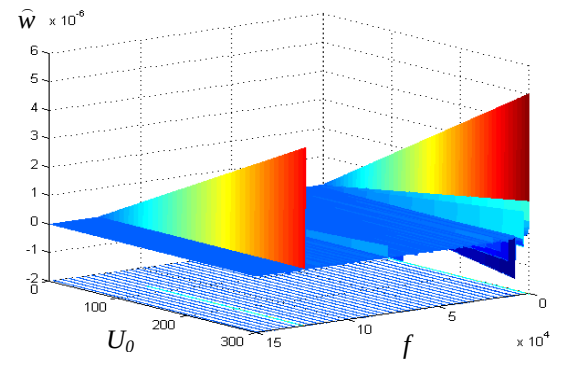

Fig. 4 *Componential displacement* $\hat{w}=\hat{w}(f,U_0)$

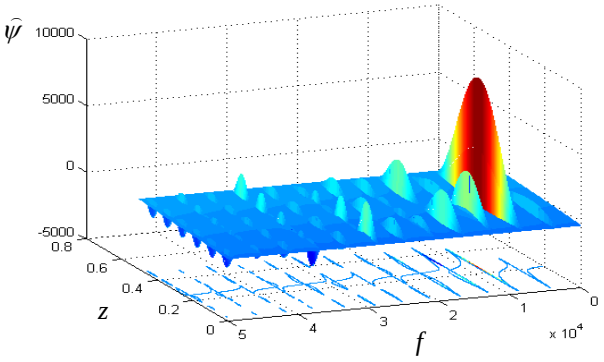

Fig. 5 *Electric potential* $\bar{\psi} = \bar{\psi}(z, f)$

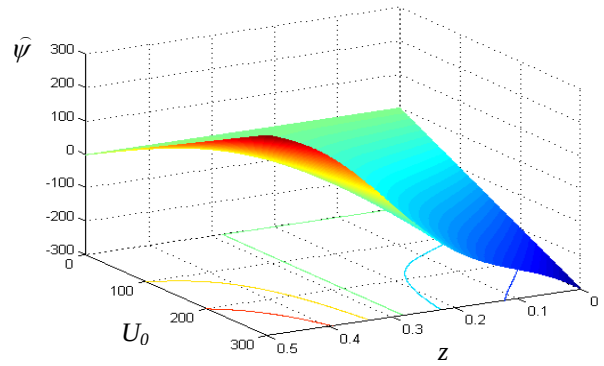

Fig. 6 *Electric potential* $\bar{\psi} = \bar{\psi}(z, U_0)$

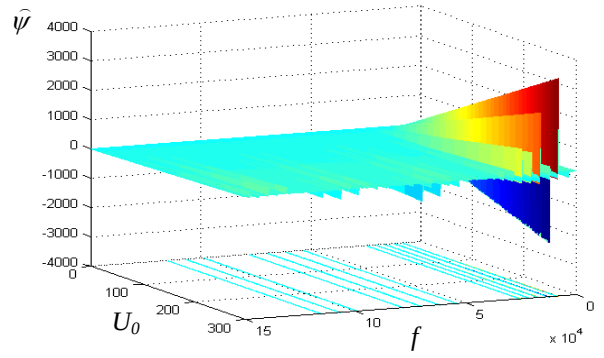

Fig. 7 *Electric potential* $\bar{\psi} = \bar{\psi}(f, U_0)$

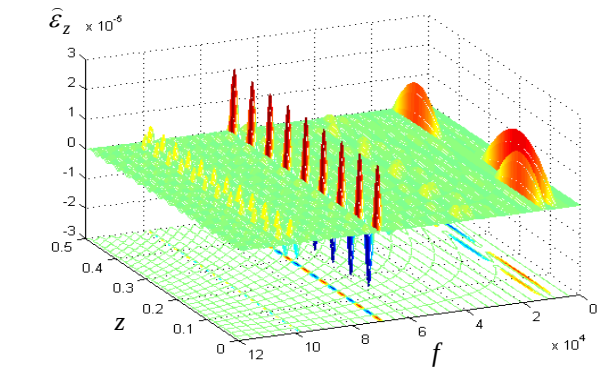

Fig. 8 *Specific strain* $\bar{\varepsilon}_z = \bar{\varepsilon}_z(z, f)$

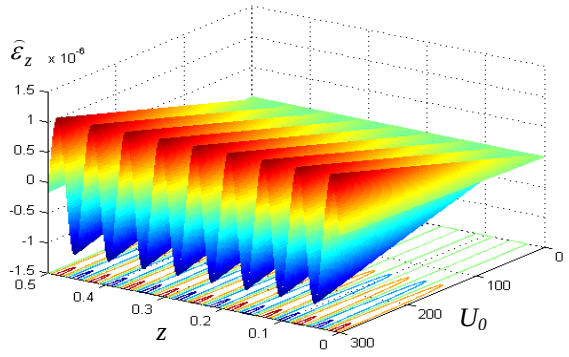

Fig. 9 *Specific strain* $\bar{\varepsilon}_z = \bar{\varepsilon}_z(z, U_0)$

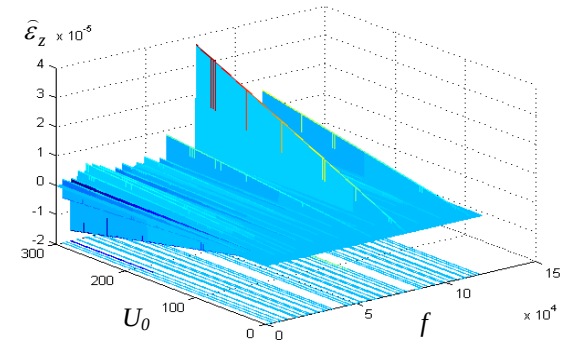

Fig. 10 *Specific strain* $\bar{\varepsilon}_z = \bar{\varepsilon}_z(f, U_0)$

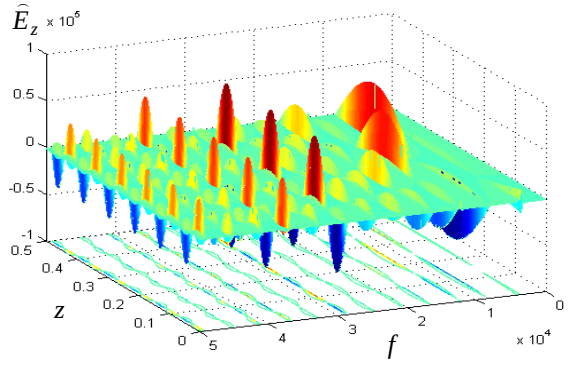

Fig. 11 *Electric field* $\bar{E}_z = \bar{E}_z(z, f)$

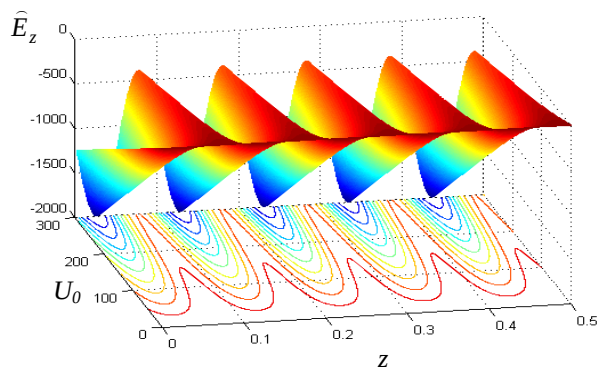

Fig. 12 *Electric field* $\bar{E}_z = \bar{E}_z(z, U_0)$

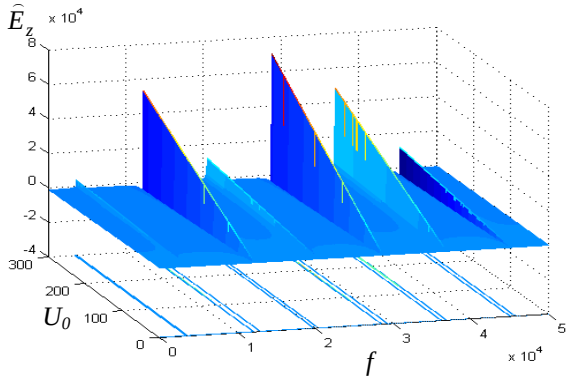

Fig. 13 *Electric field* $\widehat{E}_z = \widehat{E}_z(f, U_0)$

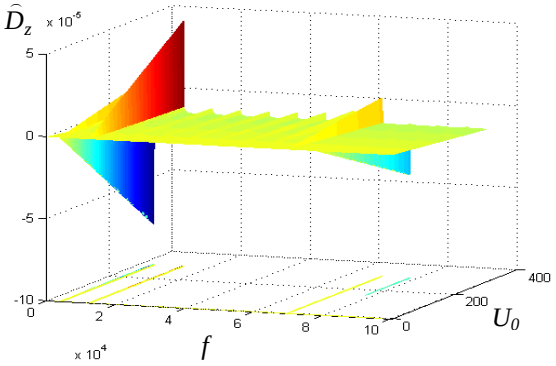

Fig. 17 *Piezoelectric displacement* $\widehat{D}_z = \widehat{D}_z(f, U_0)$

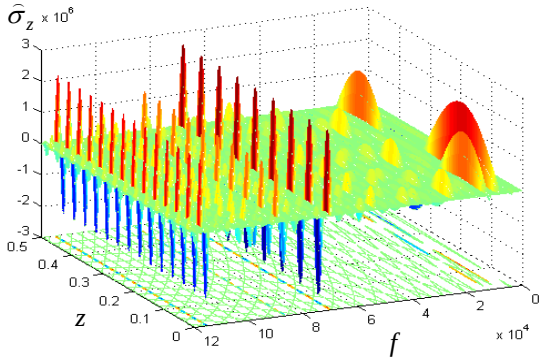

Fig. 14 *Mechanical stress* $\widehat{\sigma}_z = \widehat{\sigma}_z(z, f)$

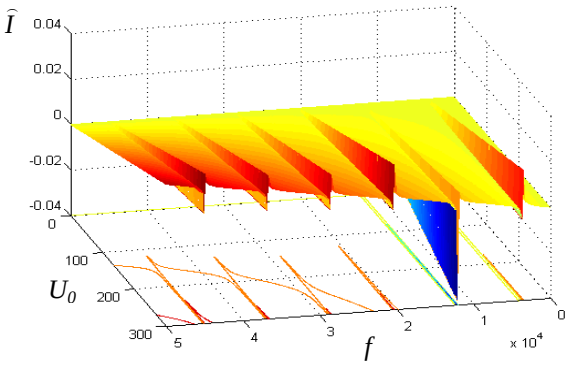

Fig. 18 *Electric current strength* $\widehat{I} = \widehat{I}(f, U_0)$

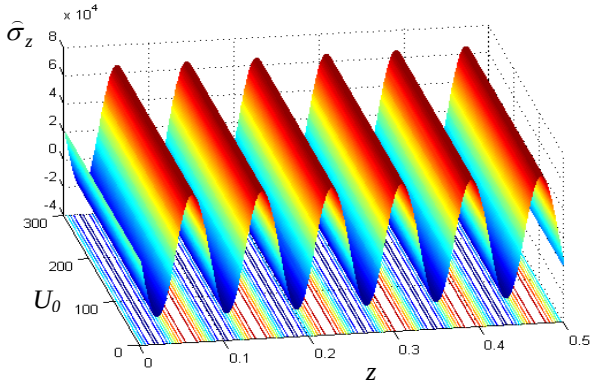

Fig. 15 *Mechanical stress* $\widehat{\sigma}_z = \widehat{\sigma}_z(z, U_0)$

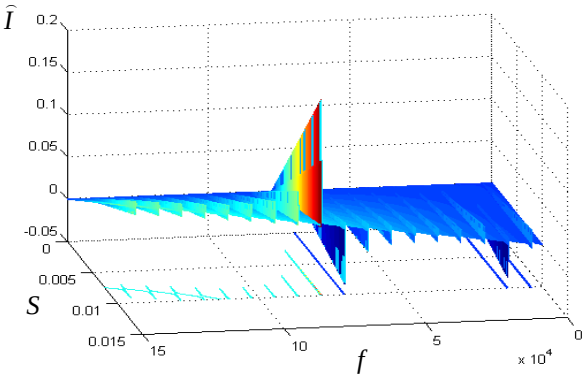

Fig. 19 *Electric current strength* $\widehat{I} = \widehat{I}(f, S)$

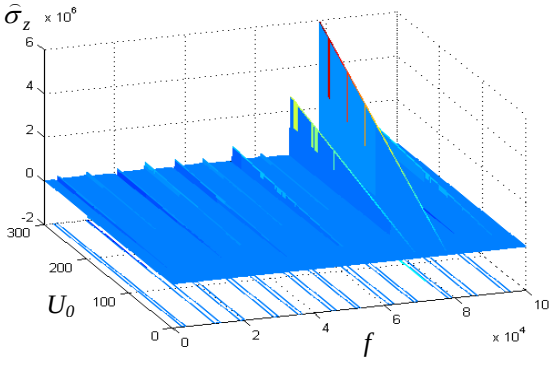

Fig. 16 *Mechanical stress* $\widehat{\sigma}_z = \widehat{\sigma}_z(f, U_0)$

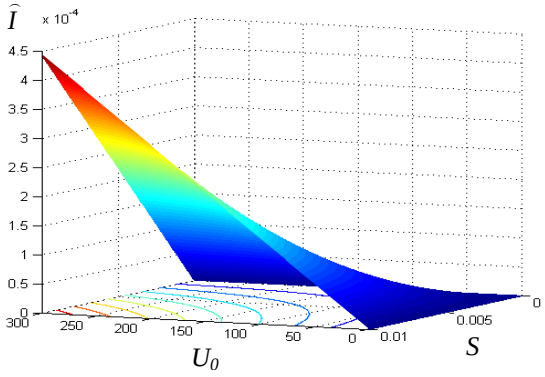

Fig. 20 *Electric current strength* $\widehat{I} = \widehat{I}(U_0, S)$

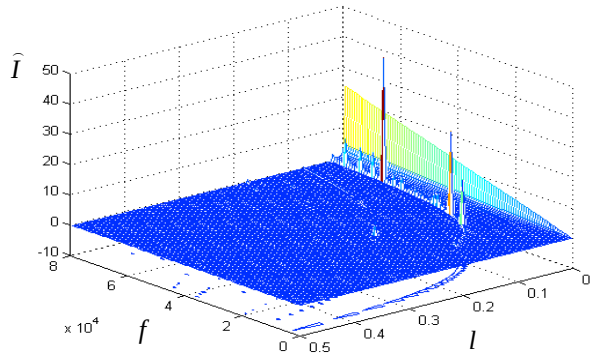

Fig. 21 *Electric current strength* $\hat{I} = \hat{I}(f, l)$

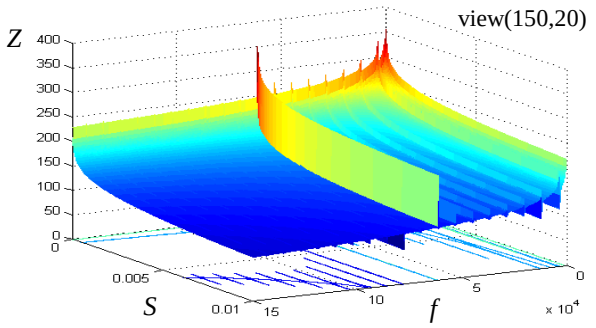

Fig. 22 *Impedance* $Z[dB] = Z(f, S)$

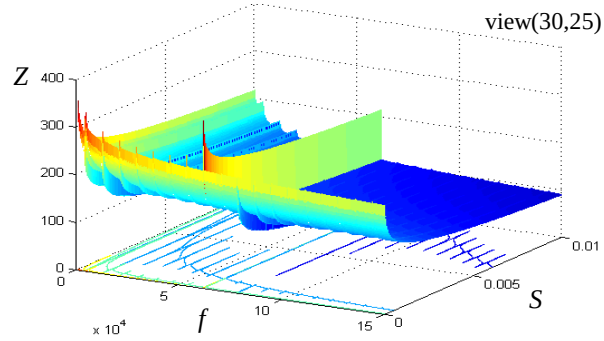

Fig. 23 *Impedance* $Z[dB] = Z(f, S)$

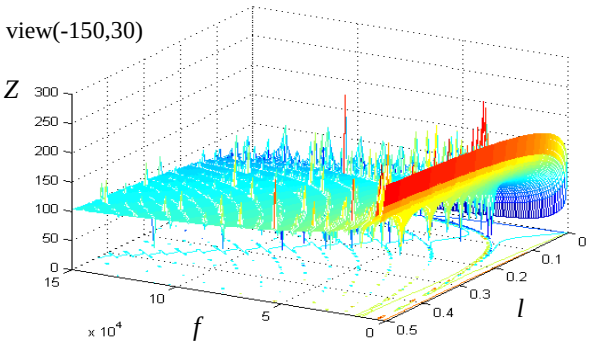

Fig. 24 *Impedance* $Z[dB] = Z(f, l)$

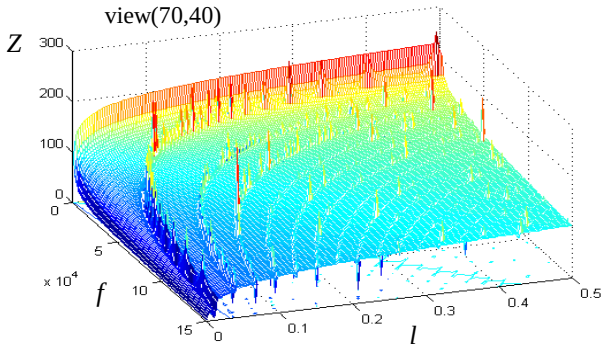

Fig. 25 *Impedance* $Z[dB] = Z(f, l)$

4. CONCLUSION

This paper presents analytical method for modelling of electromechanical values, dynamic and kinetic parameters of free prismatic piezoceramic beems with arbitary dimensions oscillating in longitudinal direction.

For the particular PZT4 piezoceramic beem are presented obtained biparametric surfaces of state electromechanic values, numerically processed using Matlab software package. For a case of oscillation of the free piezoceramic beam with electrode coatings on frontal sides are presented: componential displacement, electric potential, mechanical strain (dilatation), electric field, mechanical stress, piezoelectric displacement, electric current intensity and input electric impedance.

ACKNOWLEDGEMENT

The research presented in this paper is financed by the Ministry of Education, Science and Technological Development of the Republic of Serbia under the project III43014.

REFERENCES

[1] Lj. Perić, *Coupled Tensors of Piezoelectric Materials State and Applications*, Le Locle, Switzerland, 2005.

[2] R. Gausmann, S. Koenig, W. Seemann, "Nonlinear model of the longitudinal oscillations of a piezoelectric rod", *Proc. SPIE 4693, Smart Structures and Materials 2002: Modeling, Signal Processing and Control*, 191, doi:10.1117/12.475215, July 2002.

[3] Z. Lin-Nan, S. Zhi-Fei, "Analytical solution of a simply supported piezoelectric beam subjected to a uniformly distributed loading", *Applied Mathematics and Mechanics*, Vol. 24, No.10, pp.1215-1224, 2003.

[4] J. Wauer, "Vibrations of Piezoceramic Rods", *Proc. Appl. Math. Mech.*, 4, pp. 121–122, Weinheim, 2004.

[5] D. Mažeika, R. Bansevičius, "Study of resonant vibrations shapes of the beam type piezoelectric actuator with preloaded mass", *Mechanika*, Vol. 76, No. 2, pp. 33-37, 2009.

[6] *Five piezoelectric ceramics*, Bulletin 66011/F, Vernitron Ltd., 1976.

Development of methodologies and means for noise protection of urban areas

UrbaNoise

Goals

Provide technical support to implementation of national strategy for protection from environmental noise by:

- Developing certified facility for characterization of noise sources
- Developing software support for local noise mapping and modeling
- Design of modular noise protection means

Project concept

WP-5 Management
WP-4 Promotion

WP-1	WP-2	WP-3
Development of methods for estimation of exposition to noise	Development of materials and means for reduction of noise emission	Design of means for noise protection

Objectives

- Study on dominant noise sources in urban areas
- Design of the database for description of urban noise sources
- Construction of reverberation chamber and semi-anechoic chamber
- Development of software modules for noise modeling
- Study on state–of–the–art of noise protection means
- Design of modular barriers for noise protection

Financial resources

220,000 EUR

- Personnel costs 140,000 EUR
- Equipment 60,000 EUR
- Other 20,000 EUR
- Ministry of Education and Science
- City of Niš
- City of Kraljevo

Supported by

Government of the Republic of Serbia
Ministry of Education, Science and Technological Development

Implemented by

Faculty of Mechanical and Civil Engineering
University of Kragujevac

Faculty of Occupational Safety
University of Niš

Faculty of Traffic Engineering
University of Belgrade

University of Nis
Faculty of Occupational Safety
„Politechnica“ University of Timisoara
Faculty of Mechanical Engineering
24th International Conference
NOISE AND VIBRATION
Niš, 29 - 31. 10. 2014.

BELT CONVEYOR DRIVE GEARBOX PROBLEM CAUSED BY UNPAIRED GEARS: A CASE STUDY

Milena Jovanović[1], Dragan Jovanović[2], Nenad Živković[1], Ljiljana Živković[1], Miomir Raos [1]

[1] University of Nis, Faculty of Occupational Safety, Serbia, milena.jovanovic@znrfak.ni.ac.rs
[2] University of Niš, Faculty of Mechanical Engineering, Serbia

Abstract - *Belt conveyors for all kinds of materials are very important piece of equipment in mining and excavation industries. This paper is presenting a case study of belt conveyor driving unit vibration analysis. The analyzed belt conveyor is operating in cooper production plant and it is conveying cooper ore from mining site to process plant. In order to detect the possible defects on belt conveyor drive units, vibration measurements are conducted on all four drive units. Measurement points are set on bearing housings of electric motor and gearbox as defined by ISO 10816-1.*

1. INTRODUCTION

Belt conveyors for all kinds of materials are very important piece of equipment in mining and excavation industries. Continuous operation process in this industries demands continuous operation of belt conveyors in order to ensure planed capacities. Possible defects than can cause belt conveyor malfunction and shut down are:

- Driving unit defect;
- Conveyor belt defect;
- Rollers defect;
- Drums defect.

This paper is presenting a case study of belt conveyor driving unit vibration analysis. The analyzed belt conveyor is operating in cooper production plant and it is conveying cooper ore from mining site to process plant.

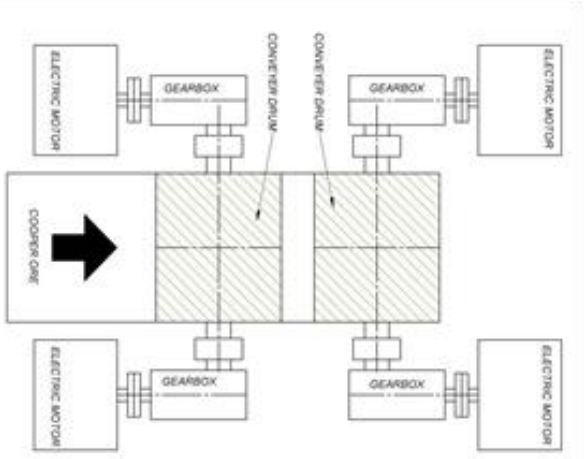

Fig. 1 *Schematic display of the belt conveyor and the driving units*

Belt conveyor specifications:

- Length of conveyor: 1000[m];
- Width of conveyor belt: 2000[mm];
- Capacity: 1200[t/h].

Belt conveyor has two drums each powered by two 250[kW] electric motors with gearboxes – figure 1. Three motors are always active and the fourth serves as a back up.

2. BELT CONVEYOR DRIVE UNIT DESIGN AND SPECIFICATIONS

Belt conveyer consists of following parts and sub-assemblies:

- Electric motor: Pem=250[kW], 6 poles, Nem= 980[rpm];
- Coupling: Hydrodynamic coupling type NKBS 500;
- Gearbox: type RKHA2 500SS, i=22,4 ; Nin=980[rpm]; Nout=43,7 [rpm].

Gearbox is two stage gearbox with transmission ratio of i=22,4. First stage are the pair of bevel gears; bevel gear pinion z=10; driven bevel gear z=41.Second stage are the pair of cylindrical gears with sloping teeth; pinion z=15; driven gear z=82 – figure 2.

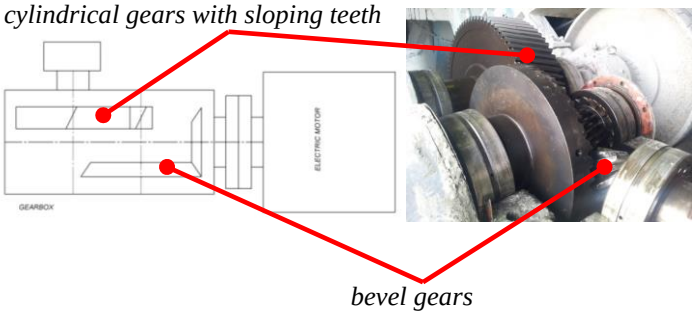

Fig. 2 *Schematic display of driving unit and picture of two stage gearbox*

In order to detect the possible defects on belt conveyor drive units, vibration measurements are conducted on all four drive units. Measurement points are set on bearing housings of electric motor and gearbox as defined by ISO 10816-1 standard – figure 3.

- L1 and L2 bearings (measurement points) on electric motor;
- L3 and L4 bearings (measurement points) on gearbox input shaft;
- L5 and L6 bearings (measurement points) on gearbox middle shaft;
- L7 and L8 bearings (measurement points) on gearbox output shaft.

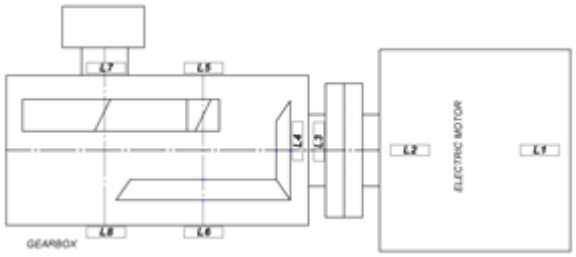

Fig. 3 *Driving unit measurement points*

Vibrations were measured at all points in all three directions – figure 4.

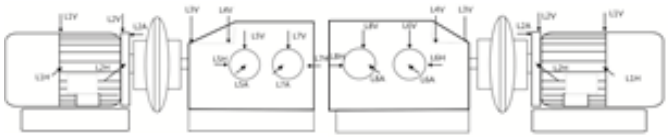

Fig. 4 *Directions of vibration measurements*

3. POTENTIAL DEFECTS AND DEFECT FREQUENCIES

Each sub-assembly of driving unit carries potential defect and distinguishing defect frequencies. This means that defects can be divided in three groups:

I. Electric motor defects

When analyzing vibrations of electric motor, the attention should be focused on two defects: bearing defect and electric problems. Bearing problems are indicated by high amplitudes at characteristic frequencies for each bearing: BPFI, BPFO, FTF, BSF – figure 5.

Table 1 *Bearing types in electric motor*

Measurement point	Bearing type
L1	6322
L2	NU322

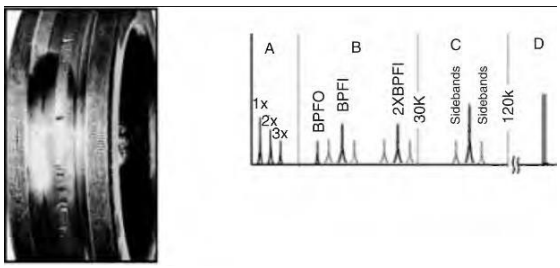

Fig. 5 *Characteristic of frequency spectrum of bearing defect*

Electric problems can be:

- *Rotor defects;*
- *Stator defects;*
- *Phasing problem.*

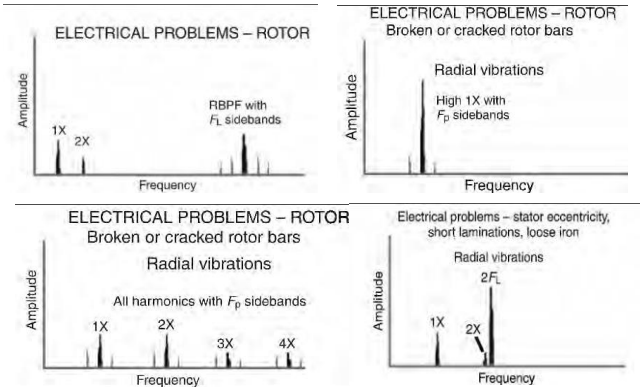

Fig. 6 *Characteristic frequency spectrums of electrical problems [1]*

Electrical problems are indicated by high amplitudes at characteristic frequencies, as shown in table 2.

Table 2 *Characteristic electric problems frequencies*

Defect frequencies	
1x	16.4 Hz
F_L - line frequencies	50 Hz
Fs - slip frequencies	0.267 Hz
Fp – pole pass frequencies	1.6 Hz
P – No. of poles	6

II. Coupling defects

Two types of shaft misalignment can be diagnosed: parallel misalignment and angular misalignment. In many cases, both types of misalignment can be diagnosed on the same machine. Both parallel and angular misalignment are indicated by high amplitudes at 1x, 2x and 3x running speed – figure 7.

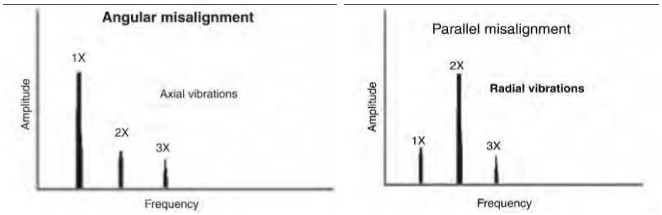

Fig. 7 *Characteristic frequency spectrums of misalignment [1]*

III. Gearbox defects

As for electric motor defects, the attention should be focused on two defects: bearing defect and gearing defects. Bearing problems are indicated by high amplitudes at characteristic frequencies for each bearing: BPFI, BPFO, FTF,BSF.

Table 3 *Bearing types in gearbox*

Measurement point	Bearing type
L3	***32324***
L4	***22328***
L5	***22332***
L6	***22332***
L7	***23052***
L8	***23052***

Gearing defects can be:

- *Gear tooth wear;*
- *Gear tooth load;*
- *Gear eccentricity and backlash;*
- *Gear misalignment;*
- *Cracked or broken tooth.*

Gearing defects are indicated by high amplitudes at characteristic frequencies:

Table 4 *Characteristic gearbox frequencies*

Defect frequencies	Hz
1x – input shaft	16.09 Hz
2x - input shaft	32.18Hz
1x – middle shaft	3.92Hz
1x – output shaft	0.728 Hz
GMF 1/ ZP1 first stage gears	161.7 Hz
GMF 2/ ZP2 second stage gears	58,88 Hz

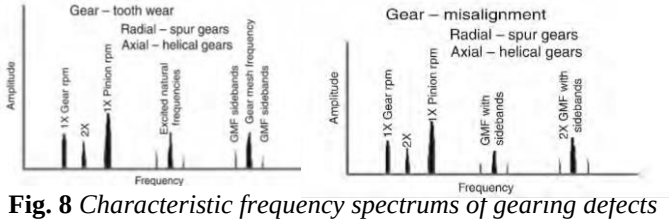

Fig. 8 *Characteristic frequency spectrums of gearing defects [1]*

4. VIBRATION ANALYSIS AND RESULTS

Driving units 1 and 4 have the highest vibrations and most visible defects.

Driving unit 1 - When analyzing the frequency spectrum measured on electric motor it is clear that both parallel and angular misalignment is present - figures 9, 10, 11 and 12.

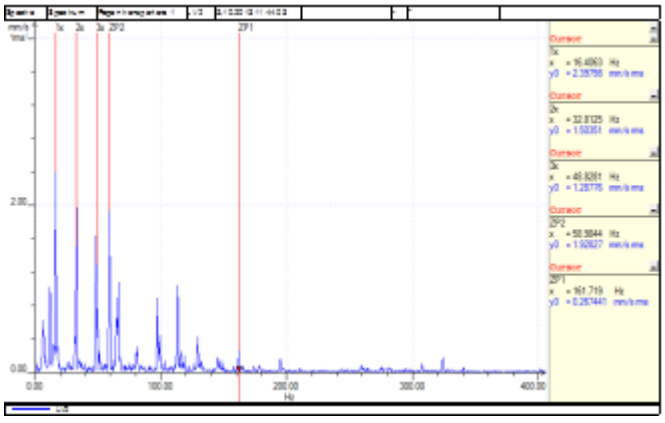

Fig. 9 *Drive unit 1 - LV1 frequency spectrums – parallel misalignment*

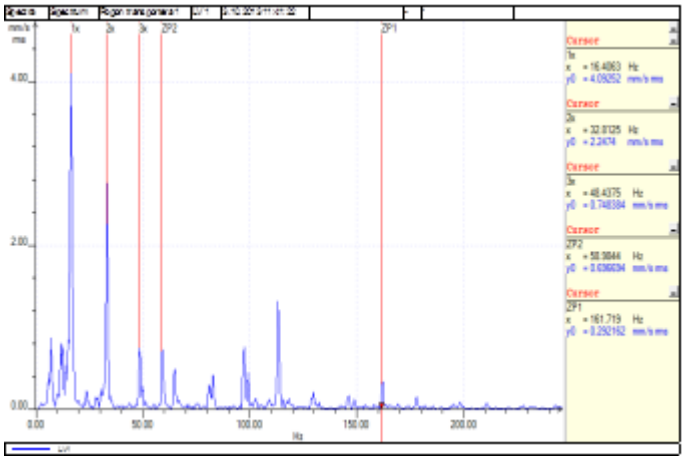

Fig. 10 *Drive unit 1 - LV2 frequency spectrums – parallel misalignment*

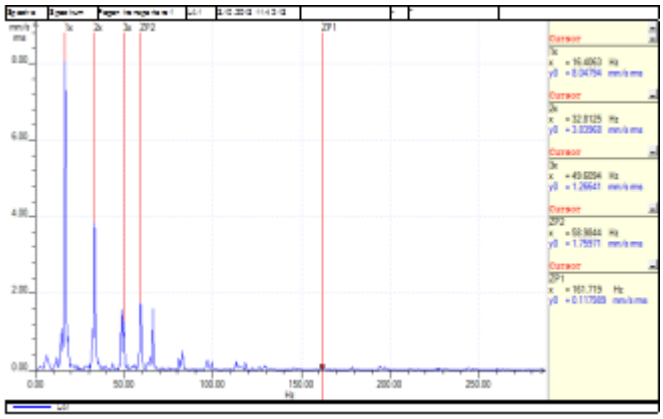

Fig. 11 *Drive unit 1 - LA1 frequency spectrums – angular*

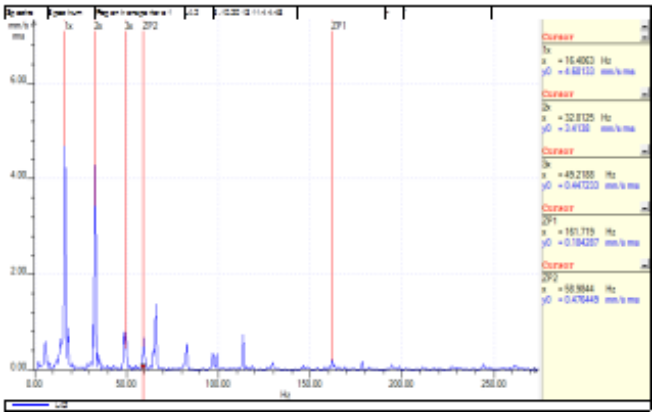

Fig. 12 *Drive unit 1 - LA2 frequency spectrums – angular*

Table 5 *Measured values of parameters LV1, LV2, LV3*

	LV1 [mm/s]	***LV2[mm/s]***	***LV3[mm/s]***
1x - 16.4Hz	4.1	2.4	5.9
2x - 32.8Hz	2.2	1.5	2.2
3x - 49.2Hz	0.75	1.3	0.53

Table 6 *Measured values of parameters LA1, LA2*

	LA1 [mm/s]	***LA2[mm/s]***
1x - 16.4Hz	8,0	4,7
2x - 32.8Hz	3,8	3,4
3x - 49.2Hz	1,3	0,44

Frequency spectrums measured on gearbox indicate that higher vibration levels are caused by first stage gears misalignment. This is determined by high amplitudes of first stage gear mesh frequencies harmonics – GMF1, GMF2 and GMF3.

Table 7 *Measured values of parameters LH3, LV3, LH4*

	LH3 [mm/s]	***LV3 [mm/s]***	***LH4 [mm/s]***
1xGMF1 - 161.7Hz	*1.15*	*3.26*	*0,75*
2xGMF1 - 323.8Hz	*1.1*	*2,84*	*2,44*
3xGMF1 - 485.5Hz	*2.8*	*1,15*	*2,35*
1xGMF2– 58.88Hz	*0.2*	*0.4*	*0.3*

Table 8 *Measured values of parameters LH5, LH6, LH7*

	LH5 [mm/s]	***LH6 [mm/s]***	***LH7 [mm/s]***
1xGMF1 - 161.7Hz	0.7	0.8	0.8
2xGMF1 - 323.8Hz	1.2	0.4	0.6
3xGMF1 - 485.5Hz	1.0	1.1	0.4
1xGMF2– 58.88Hz	0.2	0.4	0.3

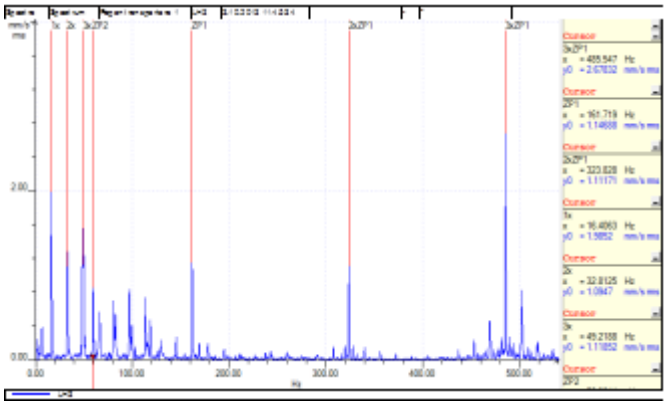

Fig. 13 *Drive unit 1-LH3 gearbox input shaft-frequency spectrums first stage gears misalignment*

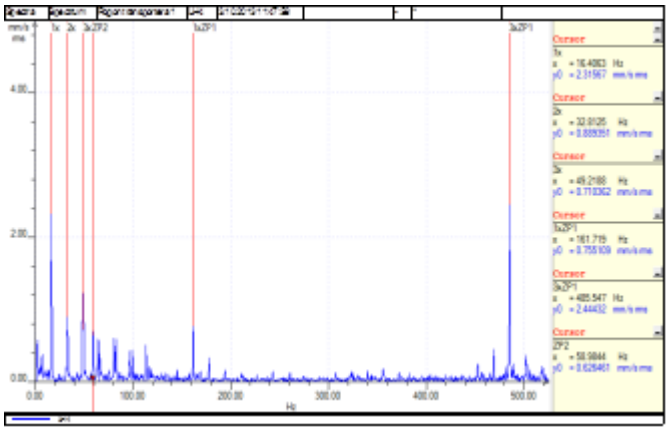

Fig. 14 *Drive unit 1- LH4 gearbox input shaft-frequency spectrums first stage gears misalignment*

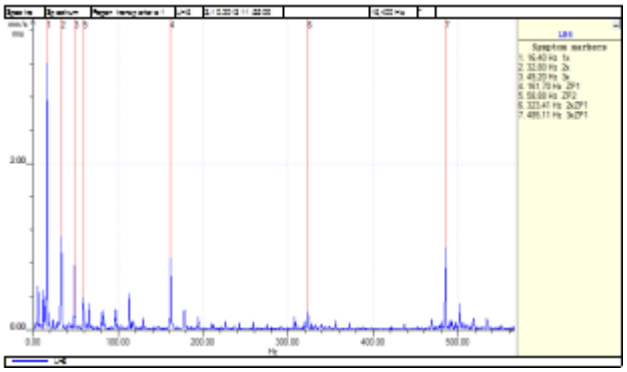

Fig. 15 *Drive unit 1 – LH6 gearbox middle and output shaft - frequency spectrums first stage gears misalignment*

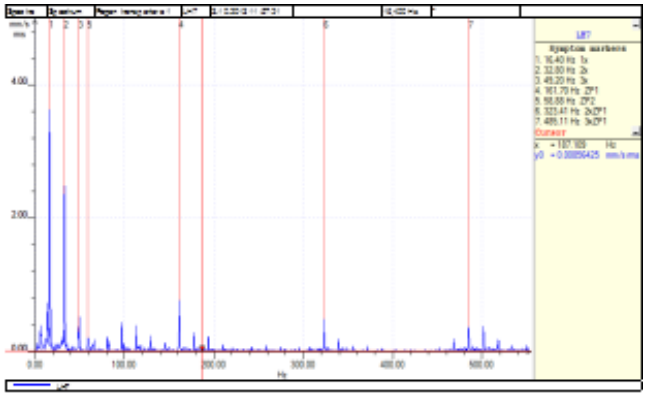

Fig. 16 *Drive unit 1 –LH7 gearbox middle and output shaft - frequency spectrums first stage gears misalignment*

Second stage gears are working properly which is indicated by low amplitudes of GMF2.

Driving unit 4 - When analyzing the frequency spectrum measured on electric motor it is clear that both parallel and angular misalignment is present like with the drive unit 1 – figures 17, 18, 19 and 20.

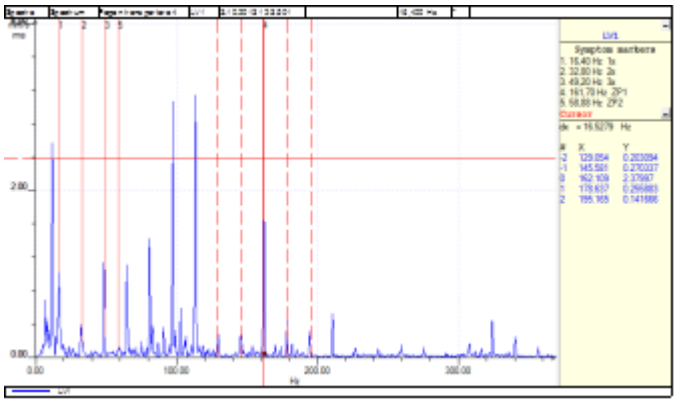

Fig. 17 *Drive unit 4 - LV1 frequency spectrums – parallel misalignment*

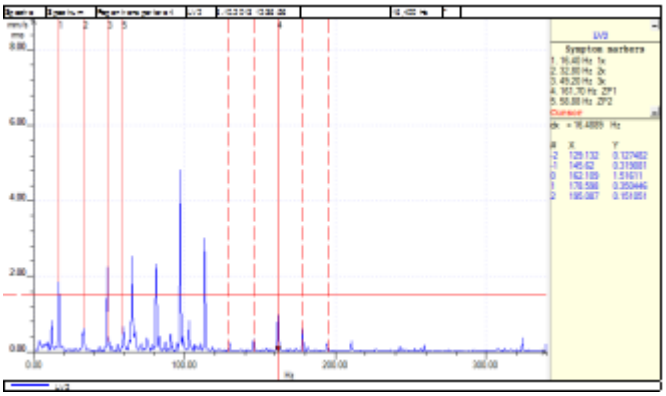

Fig. 18 *Drive unit 4 - LV2 frequency spectrums – parallel misalignment*

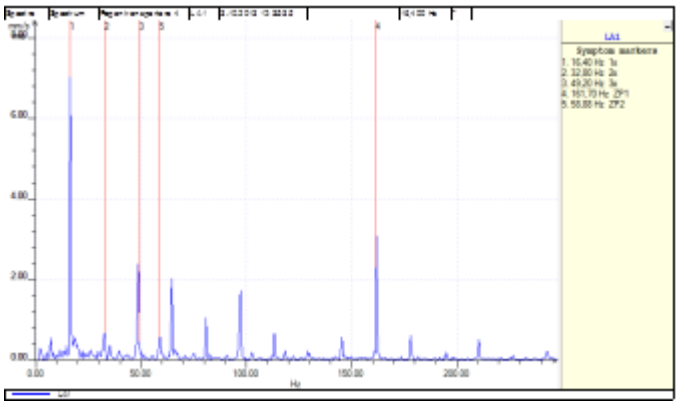

Fig. 19 *Drive unit 4 - LA1 frequency spectrums - angular misalignment*

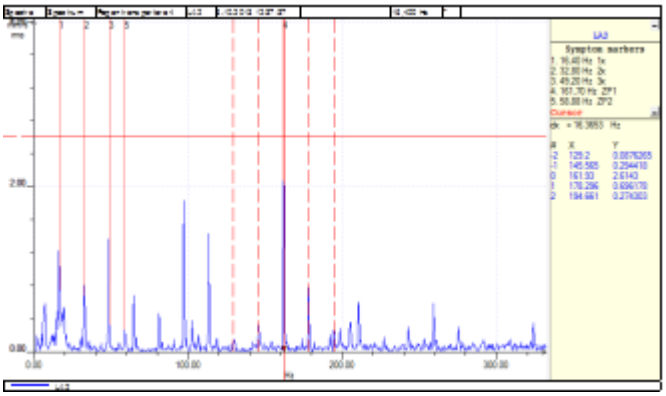

Fig. 20 *Drive unit 4 - LA2 frequency spectrums - angular misalignment*

Table 9 *Measured valuesof parametersLV1, LV2, LV3*

	LV1 [mm/s]	***LV2[mm/s]***	***LV3[mm/s]***
1x - 16.4Hz	1.1	1.9	4.3
2x - 32.8Hz	0.2	0.5	0.4
3x - 49.2Hz	1.2	2.4	1.8

Table 10 *Measured valuesof parameters LA1 and LA2*

	LA1 [mm/s]	***LA2[mm/s]***
1x - 16.4Hz	6,8	1,2
2x - 32.8Hz	0,8	0,8
3x - 49.2Hz	2,3	1,6

Frequency spectrums measured on gearbox indicate that higher vibration levels are caused by first stage gears tooth wear. This is determined by high amplitudes of first stage gear mesh frequencies harmonics – GMF1, GMF2 and GMF3 and surrounding sidebands.

Table 11 *Measured valuesof paremeters LH3, LV3, LH4*

	LH3 [mm/s]	***LV3 [mm/s]***	***LH4 [mm/s]***
1xGMF1 - 161.7Hz	4.5	4.2	2.4
1xGMF sidebands	3.8	2,6	4,4
2xGMF1 - 323.8Hz	2.1	3.9	1.6
1xGMF2 – 58.88Hz	0.3	0.5	0.4

Table 12 *Measured values of paremeters LH5, LH6, LH7*

	LH5 [mm/s]	***LH6 [mm/s]***	***LH7 [mm/s]***
1xGMF1 - 161.7Hz	3.2	6.4	4.6
1xGMF sidebands	1,2	0,8	2,1
2xGMF1 - 323.8Hz	2.1	1.1	0.4
1xGMF2 – 58.88Hz	0.6	0.5	0.3

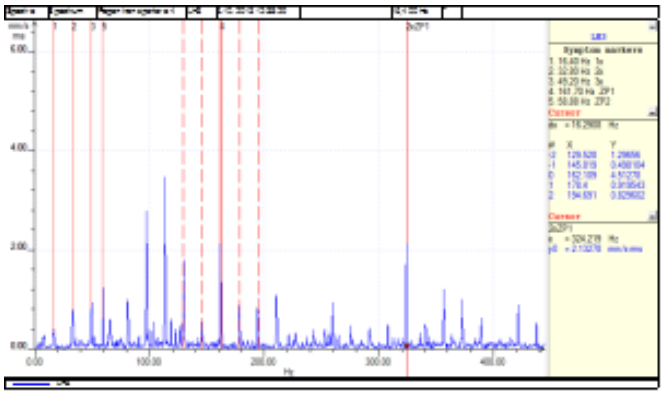

Fig. 21 *Drive unit 4 - LH3 gearbox input shaft -frequency spectrums first stage gears misalignment + gear tooth wear*

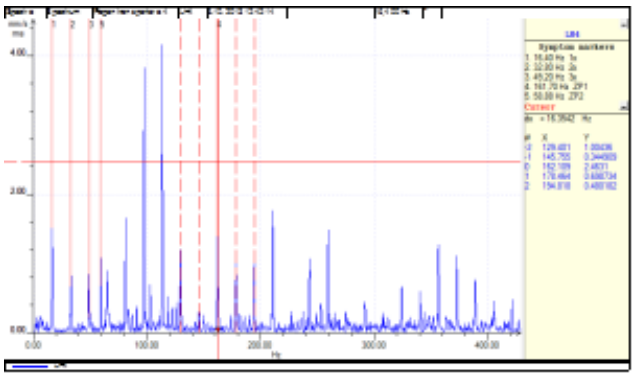

Fig. 22 *Drive unit 4 - LH4 gearbox input shaft -frequency spectrums first stage gears misalignment + gear tooth wear*

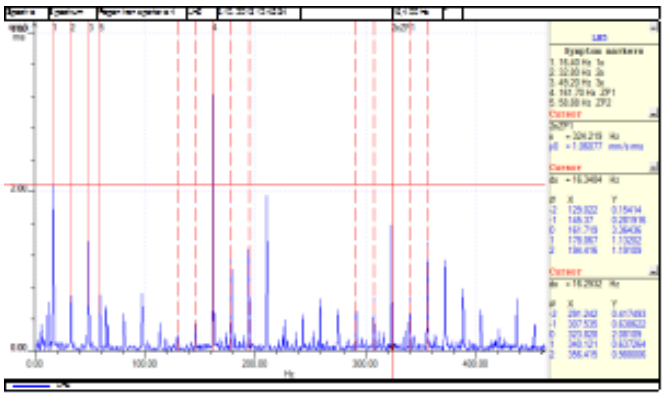

Fig. 23 *Drive unit 4 – LH5 gearbox middle and output shaft - frequency spectrums first stage gears misalignment*

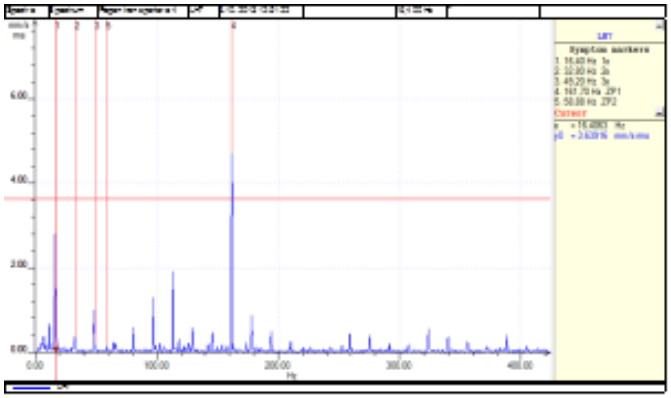

Fig. 24 *Drive unit 4 –LH7 gearbox middle and output shaft - frequency spectrums first stage gears misalignment*

Second stage gears are working properly which is indicated by low amplitudes of GMF2.

5. CONCLUSION

Excessive vibrations on drive units 1 are mainly caused by shaft misalignment between electric motors and corresponding gearboxes. Gear misalignment on drive unit 1 gearbox is noticeable but it could be fixed relatively easily without any.

Situation with drive unit 4 gearbox is much more complex. Due to unfortunate chain of events, the gearbox had been working with unpaired set of first stage gears for some time. Unpaired gears means that gear teeth are not fitted for one another, causing the load to be transferred from one gear to another with very small gear tooth surface. This small contact surface has resulted with very large contact pressure causing gear tooth wear.

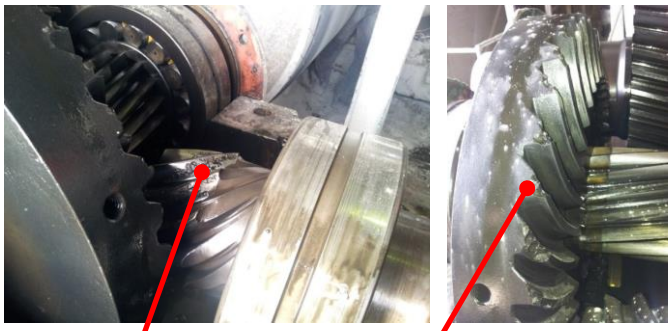

First stage pinion gear wear First stage driven gear wear

Fig. 17 *Drive unit 4 – First stage gears wear*

REFERENCES

[1.] P. Girdhar and C. Scheffer, ‘’*Practical Machinery Vibration Analysis and Predictive Maintenance’’, ISBN 0 7506 6275 1, Elsevier.*

[2.] D.S. Jovanović, N. Živković, M. Raos, Lj. Živković, M. Jovanović, M. Prašćević, *‘’Testing of level of vibration and parameters of bearings in industrial fan’’,* Applied Mechanics and Materials, Vol. 430, DOI 10.4028/www.scientific.net/AMM.430.118, pp 118-122, 2013.

[3.] ISO 10816-1:1995 Mechanical vibration - Evaluation of machine vibration by measurements on non-rotating parts -- Part 1: General guidelines

[4.] S. Jovanović, D. Jovanović, *'Dinamičko uravnoteženje kao najvažniji postupak za poboljšanje dinamičkog ponašanja ventilatora",* XXII Konferencija Buka i vibracije, Niš, ISBN 978-86-6093-019-6, pp161-164.

CIP - Каталогизација у публикацији - Народна библиотека Србије, Београд

534.83(082)
62-752(082)
614.872(082)
628.517(082)

INTERNATIONAL Conference Noise and Vibration (24th ; 2014 ; Niš)
Proceeding of Papers / 24th International Conference Noise and Vibration, Niš, October 29-31, 2014. ; [organizers University of Niš, Faculty of Occupational Safety of Niš, Department of Preventive Engineering [and] "Politechnica" University of Timisoara, Faculty of Mechanical Engineering, Department of Mechanical Engineering ; editors Dragan Cvetković ... et al.]. - Niš : Faculty of Occupational Safety, 2014 (Niš : M Kops Center). - 242 str. : ilustr. ; 29 cm

Tekst štampan dvostubačno. - Tiraž 100. - Bibliografija uz svaki rad.

ISBN 978-86-6093-062-2
1. Faculty of Occupational Safety (Niš)
a) Бука - Зборници b) Вибрације - Зборници
COBISS.SR-ID 211506188

Brüel & Kjær